GEOCHEMICAL DYNAMICS AND NITROUS OXIDE RELEASE

FROM THE HYPORHEIC ZONE OF STREAMS

by

Annika Marie Quick

A dissertation

submitted in partial fulfillment

of the requirements for the degree of

Doctor of Philosophy in Geosciences

Boise State University

May 2018

BOISE STATE UNIVERSITY GRADUATE COLLEGE

DEFENSE COMMITTEE AND FINAL READING APPROVALS

of the dissertation submitted by

Annika Marie Quick

Dissertation Title: Geochemical Dynamics and Nitrous Oxide Release from the Hyporheic Zone of Streams

Date of Final Oral Examination: 14 March 2018

The following individuals read and discussed the dissertation submitted by student Annika Marie Quick, and they evaluated her presentation and response to questions during the final oral examination. They found that the student passed the final oral examination.

Shawn Benner, Ph.D.   Chair, Supervisory Committee

Kevin Feris, Ph.D.   Member, Supervisory Committee

Daniele Tonina, Ph.D.   Member, Supervisory Committee

Jennifer Pierce, Ph.D.   Member, Supervisory Committee

The final reading approval of the dissertation was granted by Shawn Benner, Ph.D., Chair of the Supervisory Committee. The dissertation was approved by the Graduate College.

DEDICATION

This dissertation is dedicated to my parents and all of the teachers and advisors who have encouraged me to become a better person, a better scientist, and a better teacher.

ACKNOWLEDGEMENTS

While conducting my research, I completed an NSF GK-12 Fellowship and I would like to acknowledge the mentorship of program leaders Dr. Karen Viskupic and Dr. David Wilkins and the support of Cindy Busche and Aimee Hughes at the Boise WaterShed Environmental Education Center. I am also grateful for the support and guidance of Dr. Megan Frary, my mentor teacher while I was completing a Graduate Certificate in College Teaching.

Transitioning to working full time at Harvard University while trying to finish my dissertation was much more monumental a challenge than I anticipated, and would not have been possible without the patience of my advisor and committee at Boise State and the staff in the Harvard Earth and Planetary Sciences Department, in particular the "A-Team" (Chenoweth Moffatt, Sarah Colgan, Maryorie Grande, Summer Smith, Danielle Da Cruz, Joanne Choi), and faculty members Dr. John Shaw, Dr. Michael McElroy, Dr. Charles Langmuir, and Dr. James Rice. I would like to express particular gratitude to my fellow preceptor, Dr. Esther James, who has kept me moving forward and laughing the last two years.

Beyond the work that happened in the lab, I am forever grateful to the many friends who were literally my cheerleaders for the past seven years. Dr. Amanda Bremner Gilbert was truly a blessing during my Boise years and beyond, as were Katie Garland, Jill Taysom Lindstrom, Natasha Nelson, Heather Luff Uhi, Elizabeth Lefevre, Aubrey Stirling, Becky Bjorkman, and Christeena Sevy. A special shout out goes to my roommates Meranda Green and Carolyn Kay for their infinite patience. I can never adequately thank Taylor Wood, who knows better than anyone how much it means to me to complete my doctoral degree, for his loving support throughout this process.

In Boston, I am grateful to Marci Call, Rachel Boyce, Erin Rider, and Rebecca Stewart for their support and willingness to let me spend too much time at the computer instead of being a good friend; my roommates, Sarah Houghton, Jodi Cantrell, Sara Schmidt, Heather Savage, and Brittany McCready, for their understanding my unusual schedule; and my dissertation accountability partner, Chandler Hatch, for improving my writing efficiency during the final stretch.

Finally, I would like to acknowledge my family. In spite of my grumblings, my parents continually inquired after my research progress. I am grateful to my siblings and siblings-in-law, Ashley and Rich Harper, Tyler and Lisa Quick, Daniel and Susie Quick, and Lindsay Quick, for loving and supporting me through my graduate student years.

This dissertation has been one of the most challenging and rewarding experiences of my life. To my lab mates, teachers, friends, and family, THANK YOU.

ABSTRACT

The hyporheic zones of streams and rivers, consisting of the sediments beneath and immediately adjacent to the stream channel, are an important site of geochemical processing. Due to the difficulty of measuring these geochemical processes in the hyporheic zone in situ with meaningful spatial and temporal resolution, we conducted multiple column and large-scale flume experiments to model 1D and 2D hyporheic flow paths and observed important geochemical reactions, including the production and consumption of nitrous oxide (N_2O). N_2O is a significant greenhouse gas, but the controls on its emissions from streams are poorly constrained. We describe the controlling factors for hyporheic N_2O production and release, and also describe spatial and temporal trends in other geochemical processes occurring the hyporheic zone, including those relevant to pollutant remediation.

Based on the literature examining pathways for N_2O production in soils and sediments, the current understanding of physical properties of the hyporheic zone, and the existing studies of N_2O emissions from streams and rivers, it appears that production of N_2O via denitrification (and other pathways) occurs predominantly in the hyporheic zone, though production associated with suspended sediments may be significant in larger rivers or streams with high turbidity. Overall, lotic N_2O emissions increase with nitrate and ammonia concentrations, and tend to be highest in the late spring and summer and downstream of wastewater treatment plants. Observations and models combining hydromorphogical and chemical variables suggest that N_2O emissions decrease

downstream as sedimentary processes decrease relative to processes in the surface water. Downstream sites could have large N_2O emissions, however, due to inputs of dissolved inorganic nitrogen.

Observations from column and flume experiments suggest that N_2O emission from stream sediments requires subsurface residence times (and microbially mediated reduction rates) be sufficiently long (and fast reacting) to produce N_2O by nitrate reduction, but also sufficiently short (or slow reacting) to limit N_2O conversion to nitrogen gas. We also confirm previous observations that elevated nitrate and declining organic carbon reactivity increase N_2O production. These findings will aid in determining where and when streams will be a source of atmospheric N_2O emissions.

Based on measurements of additional geochemical species collected during these experiments, spatial and temporal trends reflect microbiological processes, changing redox conditions, dissolution, sorption and desorption. In general, microbial respiration causes dissolved oxygen to decrease with residence time in the hyporheic zone, leading to aerobic and anaerobic zones, nitrate reduction, and a decreasing pH gradient. Most other species concentrations increase with residence time. We propose that increases in Ca, Mg, Si, Ba, and Sr with residence time are primarily due to silicate dissolution, and increases in Fe, Mn, Co, and As with distance along flow lines are due to reductive dissolution of metal oxides and desorption in the anoxic zone. Trends over elapsed time suggest higher flow velocities (as induced by steeper bedform dune morphologies) lead to more rapid consumption of reactive carbon, larger oxic zones, and decreases in most species over elapsed time. This description of the trends of chemical species will inform future studies into the many geochemical functions of the hyporheic zone.

TABLE OF CONTENTS

LIST OF FIGURES

LIST OF TABLES

CHAPTER 1: INTRODUCTION

1.1 Background

The hyporheic zones of streams and rivers are important sites of geochemical

transformation and transportation. The hyporheic zone, which comprises the sediments

beneath and immediately adjacent to streams, is an active zone of geochemical reactions

due to the abundant surface area for the attachment and growth of microorganisms that

carry out geochemical transformations and the continual influx of reactants from surface

water moving in and out of the sediments. Stream hydrology and morphology influence

the processes taking place in the hyporheic zone and may impact surface water chemistry

and the ecosystem functions of streams and rivers. These roles include controlling

greenhouse gas production and release, serving as a sink for excess nutrients, acting as a

site for pollutant bioremediation.

1.2 Purpose/Research Goals

The purpose of this dissertation is to provide insight into the geochemical

functioning of the hyporheic zone, in particular its role in the production and

consumption of nitrous oxide (N_2O), an important greenhouse gas. Although nitrous

oxide emissions from soils have been extensively studied, the significance of nitrous

oxide production in stream sediments and subsequent emission from surface waters has

received less attention. Lotic sources of N_2O are not well constrained, and there is a

disconnect in the literature between geochemical pathways and physical settings for N_2O

production. This disconnect is often due to the difficulty in measuring the hyporheic zone in situ with meaningful spatial and temporal resolution.

In this dissertation research, multiple column and flume experiments were carried out to model one dimensional (columns) and two dimensional (flumes) hyporheic flow paths under conditions that allowed for replicates and high geochemical measurement resolution. In these experiments, we tested the role of organic carbon, nitrate loading, and streambed geomorphology on hyporheic nitrous oxide production and consumption, as well as other important processes, such as nitrification and denitrification, aerobic respiration and other redox processes, sorption, desorption, and chemical weathering. The results of this research have important implications for future studies of the hyporheic zone and potentially mitigating nitrous oxide emissions from streams and rivers.

1.3 Organization of the Dissertation

This dissertation consists of three main chapters, each of which was prepared for publication in a scientific journal. As such, each chapter varies slightly in its organization, style, and citation formats, depending on the journal to which it was submitted. Each chapter is followed by an appendix with additional explanations and data that were beyond the scope or length limitations of the journal articles.

The three chapters include an extensive literature review of nitrous oxide in the hyporheic zone (Chapter 2), a report of our column and flume experiments measuring nitrous oxide along hyporheic flow paths (Chapter 3), and a presentation of the other geochemical species in these experiments, demonstrating distinct spatial and temporal trends in the geochemical evolution of the hyporheic zone (Chapter 4).

The literature review presented in Chapter 2 came about in response to the lack of such a paper bringing together the literature on the biogeochemical pathways for nitrous oxide production and consumption (mostly from the soils literature) and the literature on the hydrology, geomorphology, and unique geochemical characteristics of the hyporheic zone (mostly from the hydrology literature). In this review, I present a compilation of many of the laboratory and in situ studies that have measured nitrous oxide emissions from streams and stream sediments, and try to connect chemical pathways to physical settings based on this information. This review was submitted to *Earth Science Reviews* in March 2018.

The results of the column and flume experiments presented in Chapter 3 lead to a conceptual model describing conditions under which nitrous oxide is most likely to be produced and consumed in the hyporheic zone, including insights into the role of exogenous nitrate and carbon availability. This chapter was published in *Environmental Science and Technology* in October 2016 (*Environ. Sci.Technol*. 2016, 50, 11491-11500. DOI: 10.1021/acs.est.6b02680).

In Chapter 4, the focus is shifted from nitrogen processing to the evolution of a wide range of geochemical species in our modeled hyporheic zones. This chapter provides some explanations for the trends observed in the extensive dataset produced by these experiments. We observed trends with residence time that reflect primarily redox reactions and silicate dissolution, and also demonstrate the significance of streambed morphology in driving temporal trends. This paper provides insight into other geochemical roles of the hyporheic zone and will be submitted to *Applied Geochemistry* in Spring 2018.

CHAPTER 2: NITROUS OXIDE FROM STREAMS AND RIVERS: A REVIEW OF

PRIMARY BIOGEOCHEMICAL PATHWAYS AND ENVIRONMENTAL

VARIABLES

Author List: Annika M. Quick,[1,4] W. Jeffery Reeder,[2] Tiffany B. Farrell, [1] Daniele Tonina,[2] Kevin P. Feris,[3] and Shawn G. Benner[1]

[1]Department of Geosciences, Boise State University, Boise, Idaho 83725, USA.
[2]Department of Civil Engineering, University of Idaho, Boise, Idaho 83702, USA.
[3]Department of Biological Sciences, Boise State University, Boise, Idaho 83725, USA.
[4]currently at Earth and Planetary Sciences Department, Harvard University, Cambridge, MA 02138, USA

Key Points:

- Denitrification, nitrification, nitrifier denitrification, and DNRA may produce lotic N_2O.
- The dominant N_2O source is likely denitrification in sediments and nitrification in surface water.
- N_2O emissions tend to increase with NO_3^- and NH_4^+ and decrease with distance downstream.
- The role of reactive carbon availability is complicated; denitrification rate generally increases with carbon reactivity, but the N_2O yield may decrease.

Abstract

Nitrous oxide (N_2O) emissions from rivers and streams may be a globally important source of this greenhouse gas. Our understanding of N_2O production, consumption, and emissions from streams and rivers is just beginning to come into focus. Nitrous oxide is produced along microbially mediated pathways: denitrification (anaerobic reduction of nitrate), nitrification (aerobic oxidation of ammonia), nitrifier denitrification (oxidation of ammonia followed by reduction of nitrite, usually at low oxygen), and anaerobic DNRA (dissimilatory nitrate reduction to ammonia). N_2O production and consumption occur in the hyporheic zone, along groundwater flow paths, and in the water column of streams. Production of N_2O via denitrification (and other pathways) occurs predominantly in the hyporheic zone, though production associated with suspended sediments (via denitrification and nitrification) may be significant in larger rivers or streams with high turbidity. Overall, lotic N_2O emissions increase with nitrate and ammonia concentrations, and tend to be highest in the late spring and summer and below wastewater treatment plants. Observations and models combining hydromorphogical and chemical variables suggest that N_2O emissions decrease downstream as sedimentary processes decrease relative to processes in the surface water. Downstream sites could have large N_2O emissions, however, due to inputs of dissolved inorganic nitrogen. Future research should include investigations into chemical pathways, and also take into account methodological biases and temporal variation.

2.1 Introduction

Nitrous oxide (N_2O) emissions are an important contributor to global climate change [Hartmann et al., 2013; IPCC, 2013] and a significant factor in the destruction of

stratospheric ozone [Ravishankara et al., 2009] Sources of this this potent greenhouse gas are poorly constrained and quantified [Sutton et al., 2007; Groffman et al., 2009]. This is particularly the case for release from rivers and streams [Hu et al., 2016; Marzadri et al., 2017]. Our uncertainty arises from the complexity of the nitrogen cycle, the difficulty of decoupling hydrologic and biogeochemical processes in riverine systems, and ever-increasing anthropogenic impacts [Stein and Klotz, 2016].

2.1.1 Motivation for This Review

The recognition of nitrous oxide as an important greenhouse gas has spurred substantial progress in our understanding of the multiple pathways that produce and release N_2O. The relative contributions of different physical settings and biogeochemical processes to nitrous oxide emissions are widely debated and this is an active area of research [e.g. Bollmann and Conrad, 1998; Garnier et al., 2009; Beaulieu et al., 2010, 2011; Yan et al., 2012; Zhu et al., 2013a; Soued et al., 2015; Turner et al., 2015, 2016; Voigt et al., 2017] and review [e.g. Wrage et al., 2001; Stein and Yung, 2003; Burgin and Hamilton, 2007; Schreiber et al., 2012; Butterbach-Bahl et al., 2013; Hu et al., 2015]. By far, the majority of studies of nitrous oxide production have focused on soils. Some researchers suggest that total indirect emissions from streams and rivers may be as large as those from agricultural soils [Mosier et al., 1998]. In rivers and streams (referred to here as lotic settings), substantial progress has been recently made toward elucidating key elements of N_2O cycling [e.g. Baulch et al., 2011; Rosamond et al., 2012; Soued et al., 2015; Gardner et al., 2016]. However, much of that work has been conducted in parallel and is often not informed by the progress that has been made in the soils community. In this review, we provide a summary of the biogeochemical pathways that produce and

consume N_2O, and synthesize our understanding of the potential relevance of those pathways to lotic settings. We review observations of N_2O generation and emissions in lotic settings, and we highlight areas of potentially productive research needed to better understand lotic N_2O emissions on the local and global scale.

2.1.2 Organization of Review

This review focuses on the elements of the nitrogen cycle needed to contextualize lotic N_2O production and emissions. The review is divided into 8 sections:

In Section 2.2, we summarize the importance of nitrous oxide as an anthropogenic atmospheric contaminant and briefly review the primary global sources of nitrous oxide. This section also introduces the basic chemistry that leads to nitrous oxide generation and provides some general observations from this chemistry that can guide understanding of nitrous oxide cycling. This section also outlines the critical influence of microbial catalysis in dictating how nitrous oxide is generated and highlights the importance of distinguishing generation and consumption of nitrous oxide from emissions.

Section 2.3 provides a detailed review of the reaction pathways that influence N_2O production and consumption; much of this section draws on research focused on soils literature and laboratory-based observations. This section is detail-oriented and will be of greatest value to researchers designing experiments and interpreting observations of nitrous oxide behavior. Further information about the reaction pathways and their influencing factors can be found in Appendix A.

In Section 2.4, we propose three distinct physical settings in lotic systems that may promote nitrous oxide generation. For each of these settings, we describe how the physical and biogeochemical characteristics of those settings can influence nitrous oxide

cycling. In Section 2.5, we review observations of N_2O concentrations and emissions in riverine field studies. Section 2.6 links biogeochemical pathways and physical settings for N_2O production and emissions from streams and rivers. Section 2.7 describes master environmental variables controlling nitrous oxide generation and consumption.

In Section 2.8, we synthesize previous sections and describe which biogeochemical and physical controls will be most significant in different types of streams and rivers. We conclude by highlighting gaps in our understanding of lotic N_2O emissions and make recommendations for future research directions.

2.2 Importance and Biogeochemistry of Nitrous Oxide Emissions

> **Section Summary**: Atmospheric concentrations of N_2O are increasing. Estimates of anthropogenic inputs of N_2O vary, but the accelerating increase of atmospheric N_2O is likely due to synthetic fertilizer use. N_2O emissions have been more carefully studied in soils, but may be significant from rivers. N_2O production and consumption are strongly microbially mediated and mostly involve oxidation and reduction of the reactive nitrogen species ammonia, nitrate and nitrite.

2.2.1 Anthropogenic Impacts on Atmospheric N_2O

The atmospheric concentration of N_2O has increased approximately 20% since 1750 [Hartmann et al., 2013] and continues to increase by 0.2-0.3% annually [Anderson et al., 2010] (Figure 2.1). While much of the N_2O emitted to the atmosphere is from natural sources, anthropogenic sources are significant, accounting for around 30% of total emissions [Wuebbles, 2009]. In addition to fossil fuel combustion and industrial processes, agricultural practices are a significant contributor to N_2O. As fertilizer runoff or wastewater treatment plant (WWTP) effluent are introduced into streams and rivers and the surrounding sediments (known as the hyporheic zone), the additional reactive nitrogen is utilized by microorganisms; N_2O emissions are a product of those processes

[Vitousek et al., 1997]. This makes the threat to climate change from N_2O distinct from that of carbon dioxide because elimination of fossil fuel consumption will only partially reduce these emissions.
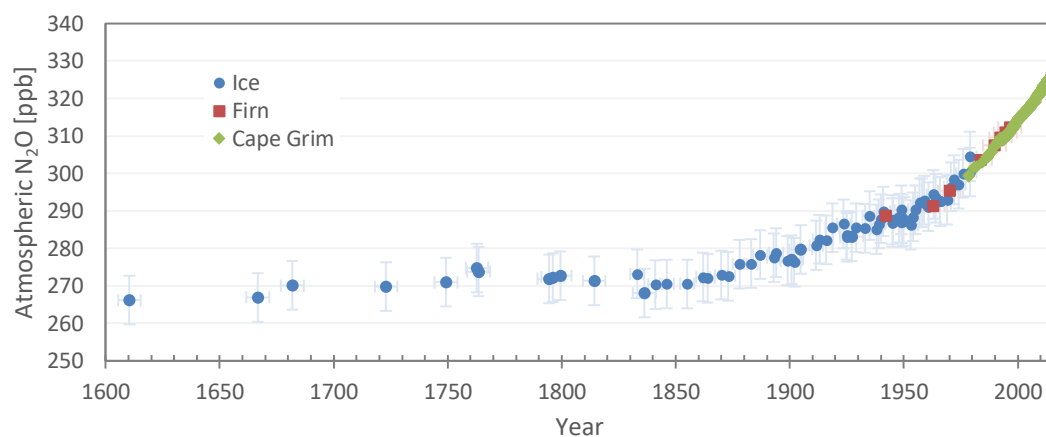
Figure 2.1.   Atmospheric nitrous oxide concentrations over time. Concentrations are from measurements of ice cores and firn from Law Dome, East Antarctica (DSS, DE08, DE08-2, DSSW20K) [MacFarling Meure et al., 2006] and the instrumental record from Cape Grim, Tasmania [CSIRO, 2016].

In the atmosphere, nitrous oxide acts as a powerful greenhouse gas, trapping longwave radiation and contributing to atmospheric warming. Although the amount of N_2O in the atmosphere is much smaller than both carbon dioxide and methane, it has approximately 300 times the warming potential of CO_2 on a 50 to 100 year time scale [Forster et al., 2007] and atmospheric concentrations are steadily increasing, as shown in Figure 2.1 [MacFarling Meure et al., 2006; CSIRO, 2016]. A molecule of N_2O persists in the atmosphere for over 100 years on average before being removed through chemical reactions [Forster et al., 2007]. While present in the atmosphere, N_2O reacts with electronically excited oxygen atoms, producing nitric oxides. The resulting nitric oxides then destroy ozone in the stratosphere [Ravishankara et al., 2009]. Nitrous oxide

emissions, therefore, contribute to both greenhouse warming and destruction of stratospheric ozone.
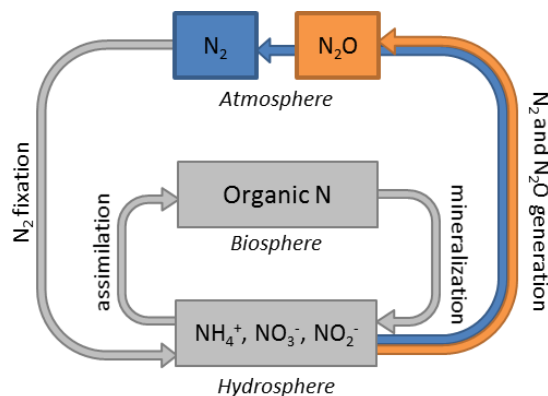
Figure 2.2.   Simplified global nitrogen cycle.

2.2.2 How Nitrous Oxide fits in the Global Nitrogen Cycle

A simplified view of the global nitrogen cycle is shown in Figure 2.2. The vast majority of Earth's atmosphere is dinitrogen (N_2) gas. Through fixation, N_2 is converted to reactive nitrogen (Nr) whose primary aqueous forms are ammonia/ammonium (NH_3/NH_4^+), nitrate (NO_3^-), and nitrite (NO_2^-), which are often collectively referred to as dissolved inorganic nitrogen (DIN). Reactive nitrogen moves in and out of biomass through assimilation and mineralization. Nitrogen returns to the atmosphere mainly as gaseous N_2 and N_2O, which are produced through multiple nitrogen cycling pathways. While each arrow on this diagram is significant to the global budget, this review focuses on nitrogen flow from the hydrosphere to the atmosphere that leads to N_2O generation. Even more specifically, we focus on the potential N_2- and N_2O-generating processes that may be occurring in streams and rivers with the specific goal of understanding when, where, and why N_2O emissions from lotic systems are significant.

2.2.3 Global Sources of Nitrous Oxide

Nitrous oxide gas emitted to the atmosphere has both natural and anthropogenic sources. Of the approximately 17.7 Tg N-N_2O emitted each year, approximately 60-70% is due to natural sources [Wuebbles, 2009]. Naturally occurring N_2O is produced during nitrogen cycling by microorganisms in soils, sediments, and the oceans. The remaining 30-40% is anthropogenic, although estimates vary [e.g. Galloway et al., 2004; Wuebbles, 2009; Anderson et al., 2010]. Industrial processes, fossil fuel combustion, and wastewater treatment contribute to human-caused N_2O emissions, but the majority of anthropogenic emissions are related to agricultural practices [Davidson, 2009], as confirmed by isotopic studies of atmospheric N_2O [Park et al., 2012]. The addition of synthetic fertilizer stimulates N_2O production by microorganisms both in soil and water bodies subjected to fertilizer runoff. The rate of atmospheric N_2O increase likely began to accelerate with more widespread synthetic fertilizer use in the 1960s [Davidson, 2009], as seen in Figure 2.1.

Soils under natural vegetation (upland and riparian) are responsible for an estimated 6.6 Tg N-N_2O yr^{-1} (of approximately 17.9 Tg N-N_2O yr^{-1} total natural and anthropogenic emissions) [Anderson et al., 2010; Ciais et al., 2013]. Fertilizer application may increase N_2O emissions from soils at the site of application [e.g. Venterea, 2007] and has been extensively examined in multitudes of studies [e.g. Butterbach-Bahl et al., 2013]. Additionally, runoff of reactive nitrogen from fertilized fields leads to emissions of N_2O from streams and rivers. Wastewater treatment plants, and their inputs to streams and rivers, are also significant sources of N_2O emissions [e.g. McMahon and Dennehy, 1999; Garnier et al., 2009; Beaulieu et al., 2010].

Far fewer studies examine N_2O production in river and stream sediments. Consequently, there is not yet consensus on how much of the N_2O emissions from streams and rivers should be considered anthropogenic (due to fertilizer runoff and wastewater treatment effluent). The EPA estimates that natural N_2O emissions from rivers are only 0.1 Tg $N-N_2O$ annually [Anderson et al., 2010], while the 2013 IPCC report suggests that 0.6 Tg $N-N_2O$ yr^{-1} from rivers, estuaries, and coastal zones is anthropogenic [Ciais et al., 2013]. Beaulieu et al. [2011] suggest that this is an underestimate, and that rivers alone account for 0.68 Tg $N-N_2O$ yr^{-1} (up to 10% of global anthropogenic N_2O emissions). Seitzinger and Kroeze [1998] suggest N_2O emissions from rivers equal 1.05 Tg $N-N_2O$ yr^{-1}, of which 90% may be considered anthropogenic. The lack of consensus on the both the magnitude of the anthropogenic contribution and the general importance of lotic systems to N_2O emissions is in part due to our incomplete understanding of the key processes leading to those emissions.

2.2.4 Basic Chemistry of Nitrous Oxide Generation

Because the processes leading to nitrous oxide generation are strongly microbially controlled, a simple chemical perspective is incomplete. However, the general chemical reactions leading to nitrous oxide generation do provide a starting point for understanding nitrous oxide generation. Nitrous oxide is produced as an intermediate reaction product during the transformation of the reactive nitrogen species ammonia, nitrate and nitrite. Nearly all of these reactions involve a series of stepwise electron transfer reactions in which nitrogen species are undergoing oxidation or reduction. From a simple chemical perspective, the majority of nitrous oxide is produced by three general reactions as shown

in Table 2.1: (1) the reduction of nitrate or nitrite to dinitrogen, (2) the oxidation of

ammonia to nitrate or nitrite, and (3) the dissimilatory reduction of nitrate to ammonia.

Table 2.1.   Basic Chemical Pathways of N₂O Production

Reduction of nitrate or nitrite to dinitrogen gas *(denitrification and nitrifier denitrification)*	NO_3^- or $NO_2^- \xrightarrow{red} NO \xrightarrow{red} N_2O \xrightarrow{red} N_2$ $\downarrow$ N_2O	N₂O is an intermediate
Oxidation of ammonia to nitrite and nitrate *(nitrification)*	$NH_3 \xrightarrow{oxid} NH_2OH \xrightarrow{oxid} NO_2^- \xrightarrow{oxid} NO_3^-$ $\downarrow oxid \qquad\quad \downarrow red$ $N_2O \qquad\qquad N_2O$	N₂O is produced from the oxidation of the intermediate NH₂OH or the reduction of intermediate NO₂⁻
Reduction of nitrate to ammonia *(DNRA)*	$NO_3^- \xrightarrow{red} NO_2^- \xrightarrow{red} NH_3$ $\downarrow$ N_2O	N₂O is produced from the reduction of intermediate NO₂⁻
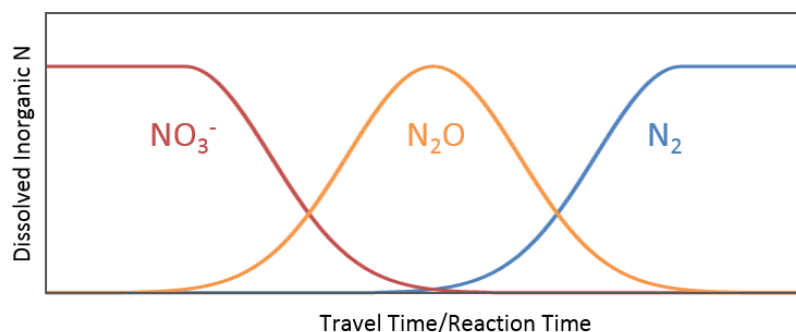
Figure 2.3.   Simplified concentration profile showing the reactant (NO₃⁻), intermediate (N₂O), and product (N₂) of denitrification over reaction time. The horizontal axis can also be conceptualized as travel time along a hyporheic or groundwater flow path.
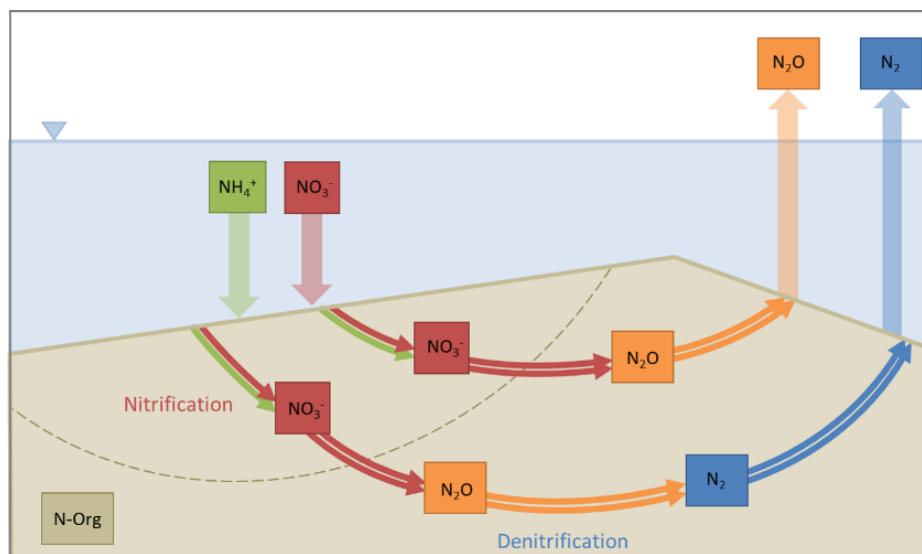
Figure 2.4. Cross sectional view of a bedform dune and overlying stream water, showing potential nitrogen transformations along hyporheic flow paths. Although multiple reactions are may produce N_2O, denitrification is shown as an example. The dashed line separates nitrification in the aerobic zone from denitrification in the anaerobic zone (intermediate species other than N_2O are not shown for simplicity). Both gaseous N_2O and N_2 can be released to the surface water and emitted to the atmosphere. Note that N_2O may be both produced and consumed along the flow paths, so not all of the N_2O that is produced is emitted. DIN (dissolved inorganic nitrogen) may be introduced to the hyporheic zone as exogenous NO_3^- and NH_4^+ (in the stream water) or as endogenous NH_4^+ (from mineralization of organic nitrogen within the sediments). Surface water flow is from left to right.

We can use these simplified reactions to make four general observations on nitrous oxide generation:

First, because nitrous oxide is produced by reactions involving reactive nitrogen species, the potential to generate nitrous oxide is greater when concentrations of ammonia, nitrite or nitrate are elevated. The dramatic increase in global anthropogenic reactive nitrogen concentrations [Galloway et al., 2008, 2013; Stein and Klotz, 2016] has led to an increase in global atmospheric nitrous oxide concentrations. This general observation applies to riverine systems; nitrous oxide generation is typically higher when concentrations of reactive nitrogen are high [e.g. García-Ruiz et al., 1999].

Second, the specific reactive nitrogen species present will dictate the specific reaction that is likely to produce nitrous oxide emissions. For example, if a system contains substantial nitrate but low levels of ammonia, nitrous oxide generation by nitrate reduction is more likely than by ammonia oxidation.

Third, all of these reactions are redox reactions; some are promoted by oxidizing conditions while others are promoted by reducing conditions. Thus, the redox status of a system will influence the likely nitrous oxide generating pathway: If a system is reducing, reduction of nitrate is a likely pathway, but oxidation of ammonia is less likely. Of course, microenvironments can provide localized conditions conducive of alternate conditions. Importantly, however, these simple chemical reactions listed above are limited predictive tools because of the dominant role that microbial catalysis plays in controlling nitrous oxide generation. Microbial communities have developed specific reaction pathways to promote these chemical reactions.

Fourth, in all of these reactions, nitrous oxide is not the primary reaction end product. During the reduction of nitrate/nitrite, nitrous oxide is an intermediate reactive species. During ammonia oxidation, nitrous oxide is produced by an alternative reaction involving the intermediate species hydroxylamine or nitrite. A similar secondary reaction is required to create nitrous oxide from the DNRA reaction. This complicates deciphering nitrous oxide generating processes because its generation is dependent on the relative rates of sequential reaction steps and/or conditions supportive of alternative reaction paths. The consumption of N_2O is also crucially important to understanding when and where N_2O will be released from streams. In biogeochemically active systems, N_2O concentrations are often transient, as its production is often followed by its consumption.

This is illustrated by the exemplified reaction sequence shown for denitrification in Figure 2.3 (note that the horizontal axis can be thought of as either time or distance along a flow path) and Figure 2.4.

2.2.5 Distinguishing N_2O production, Emissions, and Yield

When discussing N_2O in streams and rivers, it is important to distinguish between nitrous oxide production, consumption, emissions, and yield. Nitrous oxide production refers to the transformation of any other nitrogen species into N_2O. The produced N_2O may be dissolved in water according to Henry's Law, or it may escape in gaseous form to the atmosphere as nitrous oxide emissions. Importantly, however, not all of the nitrous oxide produced in soils or sediments contributes to N_2O emissions; much of the generated N_2O is consumed by conversion to N_2 before it is released to the atmosphere [Stevens and Laughlin, 1998; Quick et al., 2016]. In flowing systems, N_2O may be generated in one location but then consumed or released to the atmosphere as emissions at another location further along the flow path.

The term nitrous oxide yield, as used in this review, refers to the percentage of denitrified nitrogen released to the atmosphere as nitrous oxide instead of dinitrogen gas: $N_2O/(N_2O+N_2)$ [Beaulieu et al., 2011], though the term may also be applied to $N_2O/(N_2)$ [e.g. Silvennoinen et al., 2008b] or $N_2O/(NO_3^-)$ [e.g. Clough et al., 2007a]. In studies that don't directly measure emissions, streams are often considered N_2O sinks when the stream water is under-saturated with respect to N_2O, and are considered N_2O emission sources when the stream water is over-saturated with respect to N_2O [e.g. Soued et al., 2015].

2.2.6 Importance of Microbial Catalysis to Reaction Pathways

The reactions leading to nitrous oxide generation are strongly regulated by microbes and it is important to contextualize nitrous oxide processes in terms of microbially mediated reaction pathways. We provide a brief summary of the important role of microorganisms here; more microbially-focused reviews are available elsewhere [e.g. Stein and Yung, 2003; Jetten, 2008; Hu et al., 2015; Stein and Klotz, 2016]. Microorganisms have developed a variety of enzymatic reaction pathways to promote the sequence of electron transfer steps involving the oxidation and reduction of reactive nitrogen species. These pathways are catalyzed by diverse groups of bacteria, with the transition of reactive nitrogen species between ecosystem pools often driven by communities of microorganisms rather than only single key species [Stein and Yung, 2003; Butterbach-Bahl et al., 2013].

Microbial enzymes are large complex molecules involved in metabolic reactions and are the catalysts responsible for conversions between nitrogen species [Kirchman, 2012]. Each conversion requires a specific enzyme [Zumft, 1997]. (See Table 3 in Stein and Yung [2003] for a list of microbes involved in the nitrogen cycle and their enzymes). For example, denitrification, the sequential reduction of nitrate (NO_3^-) to dinitrogen gas (N_2), requires four different enzymes, as shown in Figure 2.5. Each enzyme is encoded for by a specific gene in a microbial genome, so genetic analysis of the microbial population aids in determining the potential for nitrogen cycling steps [e.g. Jones et al., 2013]. Although the presence of a gene indicates a microbe is capable of producing an enzyme, it does not necessarily mean that enzyme is being utilized. Identifying genes is

still, however, an important step in deducing which reactions may be taking place in streams and rivers [e.g Farrell, 2016].
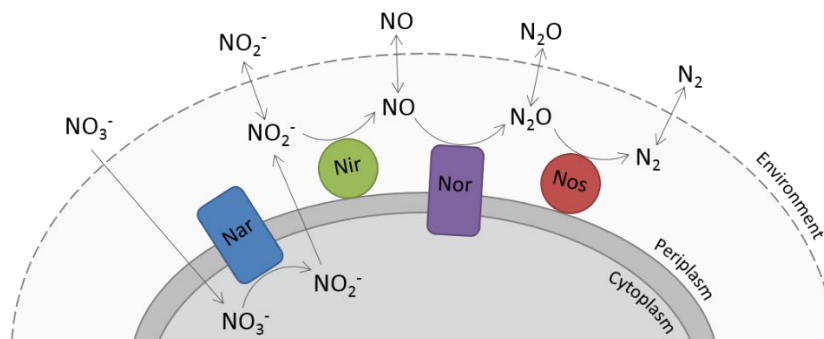
Figure 2.5. **Microbial enzymes involved in denitrification.** The enzymes, shown as circles and boxes, are nitrate reductase (Nar), nitrite reductase (Nir), nitric oxide reductase (Nor), and nitrous oxide reductase (Nos). These enzymes are encoded by the genes *nar*, *nir*, *nor*, and *nos*, respectively. A subunit of nitrite reductase (*nirS*) is often analyzed to determine denitrification enzyme activity (DEA), a measure of denitrification potential in natural systems. From [Kirchman, 2012], modified from [Zumft, 1997].

The crucial role of microorganisms in nitrogen cycling requires researchers to take into account microbial population dynamics and habitat suitability. For example, microbial population growth in surface water generally requires suspended sediments; the microbial population attached to these sediments will influence nitrogen processing rates, as will be shown [e.g. Xia et al., 2009]. It is also necessary to determine the conditions that favor different microbial groups, and within those groups, the metabolic strategies that microbes will employ based on given physicochemical conditions, substrate availability, and competition from other microbial groups. For example, the ratio of carbon to nitrate availability may determine the most likely end production of dissimilatory nitrate reduction [Megonigal et al., 2004], as will be discussed below. In this review, we do not detail the complexity of microbial metabolisms that regulate N_2O generation and

consumption but rather focus on the reaction pathways, which are strongly dictated and driven by microorganisms.

2.3 Pathways Leading to Nitrous Oxide Generation, Consumption, and Inhibition

Section Summary*: There are four main pathways leading to N_2O production in soils and sediments. Incomplete denitrification is likely the globally dominant nitrous oxide generating pathway and is favored by elevated nitrate concentrations, suboxic conditions, and sufficient organic carbon to promote reduction. The two pathways that oxidize ammonia, nitrifier denitrification and nitrification, are favored with higher concentrations of dissolved oxygen and ammonia. It is often difficult to distinguish these two pathways in field settings, but most evidence suggests that nitrifier-denitrification is likely the globally more significant of the two. The fourth reaction pathway in DNRA, in which N_2O may be produced from intermediate nitrite. This pathway is more recently discovered and its global relevance remains uncertain.

There are four distinct, microbially mediated reaction pathways that may be important to nitrous oxide generation in streams (Figure 2.6): incomplete denitrification, nitrification, nitrifier denitrification, and dissimilatory nitrate reduction to ammonium (DNRA). Importantly, these reaction pathways have primarily been described in environments other than streams and rivers, with much of our understanding coming from the soils literature. The relative importance of these pathways in lotic systems remains poorly constrained. In this section, we describe these reaction pathways and highlight factors influencing each pathway. In Section 2.5, we summarize what is known, or not known, about their occurrence in lotic systems. A more detailed overview of these pathways and the other major processes in the nitrogen cycle are presented in Appendix A, including Table A.1.

In these four pathways, microbes promote N_2O generation via the three chemical reactions described previously (Section 2.4), often coupling them in different ways. The first pathway is **incomplete denitrification** (Figure 2.6, blue line), which reductively converts nitrate (NO_3^-) to dinitrogen gas (N_2). The second pathway is **nitrification**

(Figure 2.6, red line), which involves the oxidative transformation of ammonia (NH_3) to nitrate (NO_3^-). Nitrous oxide can be produced by two reactions along this pathway, hydroxylamine oxidation and chemodenitrification. The third pathway is **nitrifier denitrification** (Figure 2.6, purple line), which converts ammonia (NH_3) to dinitrogen gas (N_2). The first steps in this pathway are oxidative, and the final steps are reductive in nature. The fourth pathway is the more recently described **incomplete dissimilatory nitrate reduction to ammonium** (**DNRA,** Figure 2.6, green line), in which organic carbon is used to reduce nitrate (NO_3^-) to ammonium (NH_4^+). In addition, we also summarize a number of additional pathways that consume, or inhibit production of, nitrous oxide, including **anammox, feammox**, **complete denitrification,** and **complete DNRA**. Biogeochemical factors relevant to N_2O production from these pathways are presented in Table 2.2. The factors listed may favor the pathway as a whole, but where information is available, the factors listed specifically favor N_2O yield (e.g. denitrification to N_2O as opposed to denitrification to N_2). Table 2.3 shows factors that favor processes that may inhibit N_2O production. A list of studies reporting the influence of environmental changes on N-cycling pathways (mostly in soils, but also in sediments) is provided in Table A.3 in Appendix A and is the basis for Tables 2.2 and 2.3.

Notes on Nomenclature: Many investigations divide N_2O production simply between nitrification and denitrification. The attribution of N_2O to "nitrification" tends to generate much confusion in the literature, since most studies do not distinguish between N_2O produced from hydroxylamine oxidation or chemodenitrification of nitrification intermediates and N_2O produced from nitrifier denitrification, which can easily be confused with nitrification. Some researchers use the terms nitrification and nitrifier denitrification interchangeably, while others group nitrifier denitrification with denitrification.
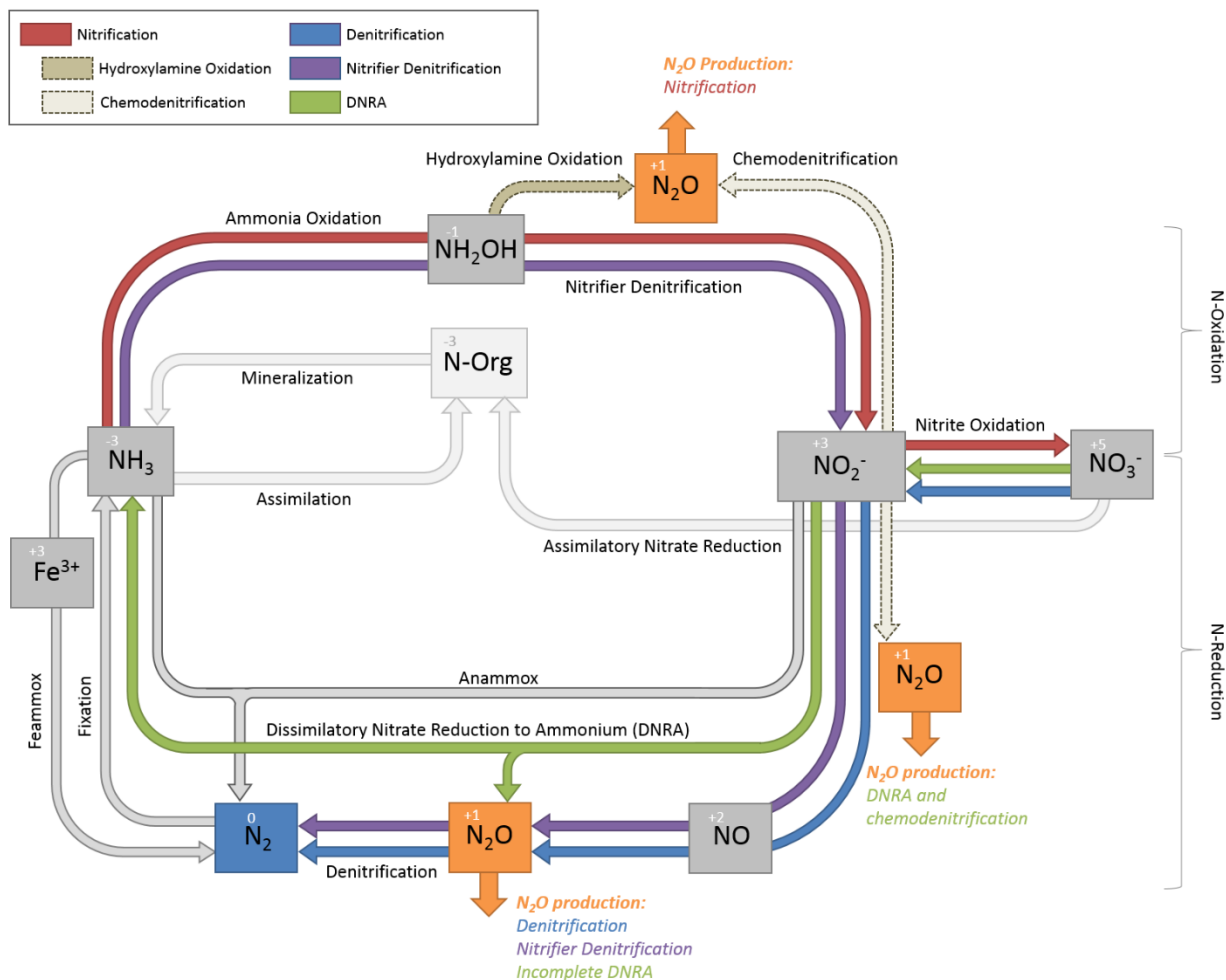
Figure 2.6.   Nitrogen cycle processes, highlighting those that produce N₂O. Processes are detailed in Table A.1 and in the text. All nitrogen species shown except dinitrogen (N₂) are considered reactive nitrogen (Nr). Note that most processes are microbially mediated. For the sake of clarity, this figure does not show all intermediate species and does not explicitly indicate the introduction of exogenous species (e.g. additional nitrate introduced via nitrogen fertilization) or the loss of gaseous species (NO, N₂) to the atmosphere. The dashed arrows for hydroxylamine oxidation and chemodenitrification indicate that all of the steps and products of these processes are not shown in detail, but that both may lead to N₂O production.

Table 2.2.   Conditions that favor N₂O Production via N-Cycling Pathways

Pathway	Oxygen Conditions	Organic Carbon Availability	Nitrogen Species Availability	pH	Groups of Microorganisms Involved	Other
Denitrification *(Incomplete)*	Anaerobic to low O_2 (boundary between aerobic and anaerobic) [Tiedje, 1988; Wrage et al., 2001]	Moderate (reduction ceases with N_2O when limited by carbon electron donors) [Tiedje, 1988; Quick et al., 2016]	High NO_3^- [Betlach and Tiedje, 1981; Beaulieu et al., 2011] High NH_4^+ (for coupled nitrification-denitrification)	Low to near neutral [Knowles, 1982; Cavigelli and Robertson, 2000; Šimek et al., 2002]	Mostly heterotrophic denitrifiers [Seitzinger, 1988; Korom, 1992] (+ ammonia- and nitrite-oxidizers for coupled nitrification-denitrification)	Lack of nitrous oxide reductase enzyme in denitrifiers [Tiedje, 1988] Low temperature [Silvennoinen et al., 2008a] Inhibition of N_2O reduction by H_2S [Sørensen et al., 1980; Dalsgaard et al., 2014]
Nitrification: *Hydroxylamine Oxidation*	Aerobic or O_2 limited [Otte et al., 1999; Sutka et al., 2006]	Low (?) [Otte et al., 1999]	High NH_4^+ [Schreiber et al., 2012] Low NO_2^- [Sutka et al., 2006]	Low [Schreiber et al., 2012]	Ammonia oxidizers [Hooper and Terry, 1979] (+ sometimes chemical) [Schreiber et al., 2012]	Oxidized metallic cations (Fe^{3+}, Mn^{4+}) [Bremner, 1997; Bengtsson et al., 2002; Schreiber et al., 2012; Zhu et al., 2013b]
Nitrification: *Chemodenitrification*	Low or fluctuating O_2 [Hynes and Knowles, 1984; Jones et al., 2015]	High (?)-phenolic compounds [Bremner, 1997]	High NH_4^+ [Stevenson and Cole, 1999] High NO_2^- [Kelso et al., 1997]	Low [Van Cleemput and Baert, 1984; Martikainen, 1985]	Chemical (after NO_2^- accumulation) [Tiedje, 1988]	Organic amines [Bremner, 1997; Stevens and Laughlin, 1998] Reduced metallic cations (e.g. Fe^{2+}) [Schreiber et al., 2012; Zhu et al., 2013b; Jones et al., 2015]
Nitrifier Denitrification	Low O_2 [Goreau et al., 1980; Poth and Focht, 1985; Zhu et al., 2013a]	Low [Wrage et al., 2001]	Moderately High NH_4^+ [Poth and Focht, 1985] High NO_2^- [Sutka et al., 2006]	Low [Wrage et al., 2001]	Heterotrophic ammonia oxidizers [Wrage et al., 2001]	
Dissimilatory Nitrate Reduction to Ammonium (DNRA) *(Incomplete)*	Mostly anaerobic [Tiedje, 1988; Fazzolari et al., 1998]	High [Tiedje et al., 1982; Lansdown et al., 2012]	Moderately high NO_3^- [Kelso et al., 1997]	High [Stevens et al., 1998]	Varies, includes obligate and facultative anaerobes [Tiedje, 1988]	High $C:NO_3^-$ High temperature (?) [Megonigal et al., 2004] High S^{2-} [Brunet and Garcia-Gil, 1996]

Table 2.3.   Conditions that inhibit N₂O Production via alternate N-removal Pathways

Pathway	Oxygen Conditions	Organic Carbon Availability	Nitrogen Species Availability	pH	Groups of Microorganisms Involved	Other
Denitrification *(Complete)*	Anaerobic [Firestone et al., 1979]	High [Firestone and Davidson, 1989; Richardson et al., 2004; Mayer et al., 2010]	High NO_3^- [Kemp and Dodds, 2002; Gardner et al., 2016]	Near neutral [Šimek et al., 2002]	Mostly heterotrophic denitrifiers [Seitzinger, 1988; Korom, 1992]	High temperature [Maag and Vinther, 1996; Silvennoinen et al., 2008a]
Dissimilatory Nitrate Reduction to Ammonium (DNRA) *(Complete)*	Mostly anaerobic [Tiedje, 1988; Fazzolari et al., 1998]	High [Tiedje et al., 1982; Lansdown et al., 2012]	Low NO_3^- [Kelso et al., 1997]	High [Stevens et al., 1998]	Varies, includes obligate and facultative anaerobes [Tiedje, 1988]	High C:NO_3^- High temperature (?) [Megonigal et al., 2004] High S^{2-} [Brunet and Garcia-Gil, 1996]
Anammox	Continuously anaerobic [Strous et al., 1997b; Kartal et al., 2011]	Low [Megonigal et al., 2004]	Low NO_3^- (?) [Thamdrup and Dalsgaard, 2002]		Anammox bacteria (chemolithotrophs) [Jetten et al., 2009]	Peak at 15°C, decreases with higher temp [Dalsgaard and Thamdrup, 2002]
Feammox	Anaerobic (periods/zones of anoxia) [Yang et al., 2012]		High NH_4^+ (?) [Clément et al., 2005]	Low [Yang et al., 2012]	Abiotic or microbial [Clément et al., 2005; Yang et al., 2012]	Requires iron oxides [Yang et al., 2012; Zhu et al., 2013b]

2.3.1 N$_2$O from Incomplete Denitrification

The process of denitrification is important to the global cycling of nitrogen because it returns nitrogen to the atmosphere in the form of N$_2$. It is also critical to the removal of reactive nitrogen (NO$_3^-$) from rivers and streams. As will be shown in section 2.5, denitrification is usually considered the predominant source of lotic N$_2$O emissions. Denitrification refers to the sequential reduction of nitrate to dinitrogen gas:

$$NO_3^- \xrightarrow{\ red\ } NO_2^- \xrightarrow{\ red\ } NO \xrightarrow{\ red\ } N_2O \xrightarrow{\ red\ } N_2$$
$$\downarrow$$
$$N_2O$$
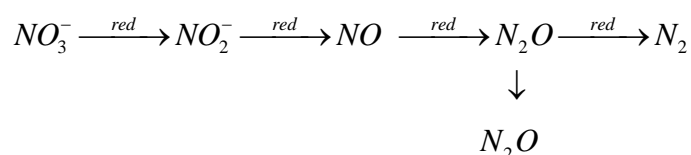
Nitrous oxide is an intermediate species along the reaction pathway. If denitrification is not carried to completion, the intermediate, nitrous oxide, may be the final product; this nitrous oxide may then be emitted to the atmosphere [Khalil et al., 2004; Laursen and Seitzinger, 2004; Čuhel et al., 2010; Baulch et al., 2011; Babbin and Ward, 2013]. Nitrous oxide may be produced during both coupled nitrification-denitrification (nitrate is supplied by nitrification of ammonia within the system) and direct denitrification involving exogenously supplied nitrate. The rate of production of nitrous oxide from denitrification, and more specifically the N$_2$O yield (N$_2$O/(N$_2$O+N$_2$)), may be controlled by a large number of factors, including the specific organisms (and enzymes) present, oxygen availability, organic carbon quality and availability, nitrate availability, temperature, and pH.

Denitrification is also significant to nitrous oxide emissions because it is the pathway through which N$_2$O is reduced to N$_2$ (whether by traditional denitrifiers or

organisms that carry out nitrifier denitrification, as explained below). N_2O is a free species [Zumft, 1997], so N_2O produced from any pathway could potentially be reduced by the last step of denitrification [Baulch et al., 2011].

2.3.1.1 Factors influencing N_2O Production from Denitrification

2.3.1.1.1 Denitrification and Oxygen. Denitrification rates increase as O_2 decreases and NO_3^- is available, because most denitrifiers are facultative aerobes and aerobic respiration is the preferred metabolic pathway when oxygen is present [Tiedje, 1988]. According to a review of freshwater and marine studies, denitrification requires DO concentrations in the water or sediment to be less than about 0.2 mg L^{-1} (6.25 µM) [Seitzinger, 1988]. Denitrification at higher levels and in well-oxygenated zones, however, has been attributed to anaerobic microsites that may not be detected in bulk samples [Edwards, 1998; Lansdown et al., 2015]. N_2O is predominantly produced at the boundary between aerobic and anaerobic zones, even though this setting is sub-optimal for both nitrifiers and denitrifiers [Wrage et al., 2001; Ji et al., 2015]. The proximity of the aerobic zone to the anaerobic zone is more important in coupled nitrification-denitrification than in direct denitrification because the nitrate is produced during aerobic nitrification.

Oxygen also inhibits denitrification enzymes. Of the four enzymes involved (see Figure 2.5), nitrous oxide reductase, which is responsible for catalyzing the reduction of N_2O to N_2, is the most strongly inhibited by O_2 [Tiedje, 1988; Otte et al., 1996; Ligi et al., 2013]. In bioreactor experiments, Dalsgaard et al. [2014] found that 50% inhibition (reversible) of N_2O production by denitrification occurred at a higher O_2 level (297 nM or 0.0095 mg L^{-1} O_2) than for N_2 production by denitrification (206 nM or 0.0066 mg L^{-1}

O_2). Therefore, denitrification may produce N_2O as an end product (higher N_2O yield) with very low O_2 concentrations [Knowles, 1982]. In soil cores, Burgin and Groffman [2012] observed that N_2O yield (as a function of total denitrification) in wet riparian soils increased from near 0% at 0% headspace O_2 to <5% at 5-10% O_2, and up to nearly 10% at 20% O_2. In soils, the activation of reduction enzymes begins within a few hours of oxygen depletion, but nitrous oxide reductase is produced after nitrate reductase [Dendooven and Anderson, 1994], which may explain why boundaries (spatial or temporal) between aerobic and anaerobic zones are hotspots for N_2O production. In laboratory experiments, denitrification decreases as O_2 increases, but N_2O yield (the proportion of the denitrified nitrogen that is reduced to N_2O instead of N_2), may increase to up to 50% at 5 kPa O_2. [Betlach and Tiedje, 1981; Jørgensen et al., 1984]. In incubations of soils, Zhu et al. [2013a] found that total N_2O production was highest at 0% O_2 in the headspace (at least 4 times higher than at 0.5% O_2), and all of the N_2O under these conditions was produced by heterotrophic denitrification.

In soils, water content strongly influences denitrification, partly due to its relationship to oxygen concentrations. N_2O emissions peak at higher soil moisture contents than for peak NO and N_2 emissions in water-saturated soils. N_2O production is favored when soils are nearly saturated, because nitrification and denitrification can occur simultaneously [Stevens et al., 1997]. Both processes can also occur simultaneously in saturated sediments if oxygenated water is continuously introduced, as is often the case in the hyporheic zone.

2.3.1.1.2 Denitrification and Carbon Availability. Because most denitrifiers are heterotrophic, denitrification, and presumably the potential for N_2O

production, increases with the availability of organic carbon that can be used for

metabolism [Wrage et al., 2001; Opdyke et al., 2006]. Organic carbon may be the

limiting factor in denitrification [Appelo and Postma, 2005], and more labile forms of

carbon support higher denitrification rates [Megonigal et al., 2004]. Tiedje [1988] points

out, however, that denitrification slows or stops with NO_2^- or N_2O when there are too few

electron donors (organic carbon) relative to electron acceptors (NO_3^-) [Firestone and

Davidson, 1989; Hutchinson and Davidson, 1993]. Thus, the balance between electron

donors and acceptors influences N_2O yield. N_2O yield is reduced at high carbon

concentrations [Quick et al., 2016].

A major role of carbon in denitrification in natural systems is creating anaerobic

zones [Tiedje, 1988; Megonigal et al., 2004; Arango et al., 2007], either in hyporheic

sediments [Quick et al., 2016], soil aggregates [Stevens et al., 1997], or suspended

particles in rivers and streams [Liu et al., 2013]. Increased organic carbon availability

encourages aerobic respiration (and oxygen consumption) by heterotrophic organisms,

leading to anaerobic zones and microsites, conditions that will generally promote N_2O

related reactions. Studies of aquifer sediments have shown that patches of organic

material in the subsurface tend to function as hotspots for microbial activity, including

denitrification [Addy et al., 1999].

2.3.1.1.3 Denitrification and Nitrogen Availability. Nitrate and ammonium

concentrations influence both potential denitrification and N_2O yield. In studies of intact

estuarine sediment cores, Meyer et al. [2008] found that N_2O production from

denitrification under low nutrient conditions was below the level of detection but

increased significantly with the addition of either NO_3^- or NH_4^+. Several sources have

reported that, in addition to increasing denitrification rates, N_2O yield increases with nitrate concentration. One explanation is that when electron donors (i.e. carbon) are limited, the more oxidized N-species, NO_3^- is a more preferred electron acceptor than N_2O, so N_2O will not be reduced to N_2 [Betlach and Tiedje, 1981; Schlegel, 1993]. As a result, increased nitrate decreases N_2O yield in carbon limited systems; in systems with abundant carbon, increased nitrate will increase denitrification rates, but will not affect N_2O yield [Betlach and Tiedje, 1981], as observed by [Beaulieu et al., 2011]. NO_3^- is provided by either nitrification or exogenous inputs (e.g. stream or groundwater advection). When NO_3^- is provided by nitrification, the substrates needed for nitrification (NH_4^+ and aerobic conditions) also become relevant to denitrification rates.

   2.3.1.1.4 <u>Denitrification and Other Factors</u>. Some organisms, including nonrespiratory denitrifiers, lack certain enzymes and tend to produce NO or N_2O instead of N_2 as the final product of denitrification [Stouthamer, 1988; Tiedje, 1988; Kolb and Horn, 2012]. The reason that some microorganisms are adapted to utilize the last step of denitrification (N_2O reduction to N_2), while others are not is not well understood, but may be related to the energetic cost versus benefit of producing the nitrous oxide reductase enzyme, particularly when NO_3^- is abundant [Zumft, 1997; Jones et al., 2008, 2013].

  Denitrification rates are also affected by other physical and chemical parameters, such as pH, temperature, and the presence of other species. Denitrification rates increase with pH [Stevens et al., 1998]. However, because Nitrous oxide reductase is less inhibited at higher pH, N_2O yield declines [Knowles, 1982; Cavigelli and Robertson, 2000]; N_2 production is favored over N_2O at circumneutral pH [Šimek et al., 2002]. Hydrogen sulfide, H_2S, also inhibits nitrification and denitrification enzymes [Sørensen et

al., 1980; Stouthamer, 1988; Brunet and Garcia-Gil, 1996]. H_2S most strongly inhibits N_2O reduction to N_2, increasing N_2O yield [Sørensen et al., 1980; Dalsgaard et al., 2014]. In sediment cores of a eutrophic river, Silvennoinen et al. [2008a] found that denitrification rates increase with temperature up to a maximum, but that N_2O yield decreases with temperature.

In summary, while denitrification rates increase with nitrate and likely with ammonia concentrations, organic carbon reactivity, pH, and temperature, N_2O yield increases with nitrate and decreases with organic carbon, pH, and temperature [Stevens and Laughlin, 1998]. Therefore, N_2O production from denitrification is predicted to be highest in suboxic to anaerobic environments with moderate organic carbon, high nitrate, and sub-neutral pH.

2.3.2 N_2O from Nitrification (via Hydroxylamine Oxidation and Chemodenitrification)

The nitrification pathway is an important process in the global nitrogen cycle and is the primary mechanism oxidizing the reduced nitrogen species ammonia [Stein and Klotz, 2016]. Nitrification is thought to be particularly important in soils, where elevated NH_4^+ concentrations from fertilizers are often coupled with oxic conditions, making this reaction energetically favorable [Butterbach-Bahl et al., 2013]. This pathway is considered a globally important source of nitrous oxide [Bremner and Blackmer, 1978; Nevison, 2000]. However, because ammonia is more reactive than nitrate, and due to its greater tendency to sorb to soil minerals, much less is exported from agricultural to lotic systems. It is also more difficult to track ammonia oxidation in streams because it rapidly sorbs to sediments [Peterson et al., 2001]. High NH_4^+ concentrations are often observed

in streams influenced by effluent from wastewater treatment plants [e.g Cébron et al., 2005].

Following denitrification, nitrification is the most often cited source of N_2O from soils. However, this pathway is often not distinguished from the nitrifier-denitrification pathway (See Notes on Nomenclature in section 2.3). This confusion makes this pathway's importance less certain and there is some evidence that much of the N_2O release from soils may be attributed to nitrifier-denitrification rather than nitrification [Goreau et al., 1980; Wrage et al., 2001; Kool et al., 2011].

The nitrification reaction pathway oxidizes ammonia to nitrite and nitrate and N_2O may be produced via alternative reaction pathways involving intermediate reaction products:

$$NH_3 \xrightarrow{\ oxid\ } NH_2OH \xrightarrow{\ oxid\ } NO_2^- \xrightarrow{\ oxid\ } NO_3^-$$

$$\downarrow oxid \qquad\qquad\quad \downarrow red$$

$$N_2O \qquad\qquad\qquad N_2O$$

$$\textit{hydroxylamine oxidation} \qquad \textit{chemodenitrification}$$
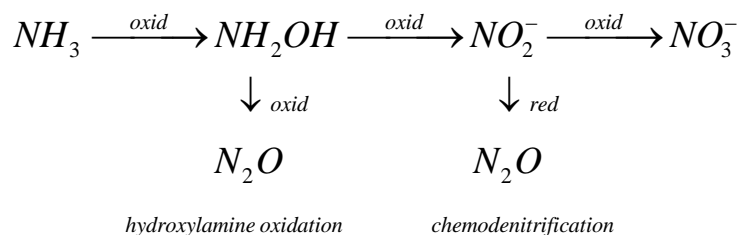
During the first step of nitrification, nitrifying bacteria oxidize ammonia and produce the intermediate species hydroxylamine (NH_2OH). Hydroxylamine is then further oxidized to nitrite (NO_2^-) and then finally to nitrate (NO_3^-). Two alternative sub-pathways can lead to nitrous oxide generation. In the first, hydroxylamine can be oxidized to nitrous oxide [Bremner, 1997; Otte et al., 1999; Bengtsson et al., 2002]. In the second, chemodenitrification, nitrite (NO_2^-) is reduced to N_2O [Tiedje, 1988;

Bremner, 1997; Stevens and Laughlin, 1998]. These sub-pathways can also lead to gaseous NO and N_2 production (see additional descriptions in Appendix A).

Notes on Nomenclature: In the literature, N_2O attributed to "nitrification" is often actually produced during nitrifier denitrification [e.g. Goreau et al., 1980], complicating the attribution of N_2O to varying pathways. The nitrifier denitrification pathway is discussed later in this section.

2.3.2.1 Hydroxylamine oxidation to produce N_2O

Hydroxylamine oxidation can occur abiotically [Bremner, 1997; Schreiber et al., 2012] and can be bacterially catalyzed. Multiple chemical NH_2OH oxidation pathways have been suggested [Schreiber et al., 2012]. Chemical hydroxylamine oxidation may involve metallic electron acceptors and produces both N_2 and N_2O [Bremner, 1997; Zhu et al., 2013b], although N_2O production is more likely under high iron(III) conditions [Bengtsson et al., 2002; Schreiber et al., 2012]. The decomposition of hydroxylamine to N_2 and N_2O has also been demonstrated with abiotic solutions in the laboratory [e.g. Bengtsson et al., 2002] and in soils [e.g. Bremner and Blackmer, 1980].

Hydroxylamine oxidation to produce NO and N_2O can be bacterially catalyzed [Hooper and Terry, 1979], including by heterotrophic ammonia oxidizers [Otte et al., 1999]. Nitric oxide (NO) and nitroxyl (HNO) have been proposed as possible intermediates. Under aerobic conditions, the HNO reacts with oxygen to give HNO_2. Under oxygen limited conditions, HNO gives N_2O and H_2O, and the N_2O may further be reduced to N_2 [Otte et al., 1999].

2.3.2.1.1 Factors Influencing N_2O Production from Hydroxylamine Oxidation. At least some oxygen is required for the ammonia monooxygenase enzyme to

oxidize ammonia to NH_2OH [Poth and Focht, 1985; Kirchman, 2012], so aerobic conditions and a supply of NH_3 are the first requirements for N_2O production from hydroxylamine oxidation. As for biologic processes, pure cultures of ammonia oxidizing bacteria produced more N_2O from hydroxylamine oxidation at high O_2 in a study by Sutka et al. [2006]. In wastewaters, Wunderlin and Mohn [2012] found that aerobic hydroxylamine oxidation of N_2O is favored under conditions of high ammonia and low nitrite. However, according to Otte et al. [1999] biologic hydroxylamine oxidation to N_2O via heterotrophic ammonia oxidizers is favored by oxygen limited conditions.

Chemical pathways of hydroxylamine oxidation involve oxidation by metallic cations (Fe^{3+} or Mn^{4+}) [Bremner, 1997; Zhu et al., 2013b], so they would be more favored at low pH, where Fe- and Mn-oxides are more soluble. Schreiber et al. [2012] suggested that chemical production of N_2O by hydroxylamine oxidation may occur in natural settings with high ammonia concentrations and low pH; both of these conditions may be present in strongly fertilized soils.

Based on the existing literature at the time, Bremner [1997] found no evidence that hydroxylamine is released by nitrifiers in soil and concluded that hydroxylamine oxidation does not produce significant amounts of N_2O in soils, although hydroxylamine oxidation does seem to produce more N_2O in soils than chemodenitrification of nitrite [Bremner and Blackmer, 1980]. Indeed, in laboratory experiments, hydroxylamine oxidation produces NO and N_2O, but in natural settings NH_2OH is rapidly converted to NO_2^-, so N_2O production from hydroxylamine oxidation is likely insignificant relative to other sources [Conrad, 1996; Whittaker et al., 2000]. However, further studies need to be carried out in natural environments.

2.3.2.2 Chemodenitrification of Nitrite to Produce N_2O

Chemodenitrification is an abiotic process in which the reduction of NO_2^- produces gaseous nitrogen, including NO, N_2O, and N_2 [Tiedje, 1988]. NO_2^- may be reduced by inorganic cations [Zhu et al., 2013b] or organic compounds [Bremner, 1997; Stevens and Laughlin, 1998]. Low pH (<5.0) favors chemodenitrification involving inorganic cations, such as iron(II) [Van Cleemput and Baert, 1984; Stevens and Laughlin, 1998; Schreiber et al., 2012], producing predominantly NO [Tiedje, 1988], but also N_2O [Schreiber et al., 2012]. The relative amount of N_2O produced may be affected by the type of electron donor used [Zhu et al., 2013b].

2.3.2.2.1 Factors influencing N_2O production from chemodenitrification. Chemodenitrification is most likely to occur in zones where redox conditions fluctuate or species from aerobic zones (NO_2^- from ammonia oxidation) and from anaerobic zones (Fe^{2+}) may interact [Jones et al., 2015]. As with coupled nitrification-denitrification, the redox requirements could also be met by advection of species from one redox zone to another. In batch experiments, Jones et al. [2015] found that the highest N_2O yields from chemodenitrification occur under excess Fe^{2+} conditions, although chemodenitrification using organic compounds would presumably be unaffected by iron concentrations. Van Cleemput and Baert [1984] found that chemodenitrification of NO_2^- is promoted by even slightly acidic conditions and conditions that increase the solubility of Fe^{3+} and promote Fe^{2+} formation, but that NO production is more significant than N_2O production.

Chemodenitrification is limited by NO_2^- concentrations. During nitrification, NO_2^- is produced from the oxidation of NH_4^+. The second step of nitrification (oxidation of NO_2^- to NO_3^-) proceeds more rapidly than the first step (oxidation of NH_3 to NO_2^-)

[Kirchman, 2012], so NO_2^- only accumulates under certain conditions. The addition of NH_3^- or NH_4^+-type fertilizers may inhibit the second step of nitrification, probably due to nitrifier sensitivity to NH_3 toxicity, allowing NO_2^- to accumulate [Stevenson and Cole, 1999]. Additionally, the low pH conditions that favor chemodenitrification, also due to nitrifier sensitivity, are caused by the conversion of NH_3 to NO_2^- and NO_3^-, and may also be enhanced by NH_3- and NH_4^+-type fertilizers [Stevenson and Cole, 1999].

Although chemodenitrification of NO_2^- from nitrification is frequently mentioned, theoretically, chemodenitrification of NO_2^- accumulated during DNRA and denitrification (see Figure 2.6 and discussion below) could also occur [Stevens and Laughlin, 1998]. During DNRA, NO_2^- may accumulate due to inhibition of nitrite reductase by NO_3^- [Kelso et al., 1997]. Although NO_2^- is also an intermediate of denitrification, it is less likely to accumulate in that process because denitrification is carried out by respiratory organisms [Kelso et al., 1997].

To summarize, N_2O is most likely to be produced from chemodenitrification of NO_2^- under fluctuating redox conditions, with low pH, and with addition of NH_3 or NH_4^+ fertilizers. Chemodenitrification may be a significant source of N_2O in soils with pH <5 [Tiedje, 1988]. Collective research in soils, however, indicates that chemodenitrification is not a major contributor to N_2O emissions [Bremner, 1997; Otte et al., 1999]. Evidence of chemodenitrification producing N_2O in streams is lacking.

2.3.3 N_2O from Nitrifier-Denitrification

The nitrifier-denitrification pathway is a multi-step redox sequence in which ammonia is first oxidized to nitrite, then the nitrite is sequentially reduced to NO, N_2O, and N_2 [Wrage et al., 2001; Stein and Yung, 2003]. This pathway is often confused with

nitrification in the literature, and may account for some of the N_2O production attributed to nitrification. It is potentially a significant source of N_2O in soils [Martikainen, 1985; Wrage et al., 2001; Kool et al., 2011; Schreiber et al., 2012; Zhu et al., 2013a]. As with denitrification, nitrifier-denitrification produces nitrous oxide as part of the regular reaction sequence. Unlike denitrification, nitrifier-denitrification involves both an oxidation and reduction step:

$$NH_3 \xrightarrow{\;oxid\;} NH_2OH \xrightarrow{\;oxid\;} NO_2^- \xrightarrow{\;red\;} NO \xrightarrow{\;red\;} N_2O \xrightarrow{\;red\;} N_2$$
$$\downarrow$$
$$N_2O$$
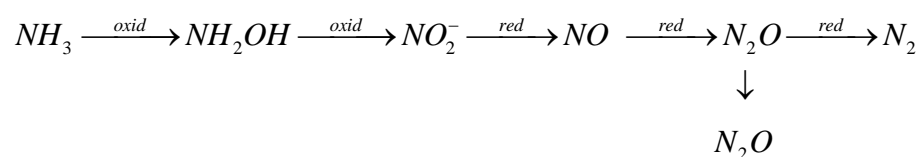
Nitrifier denitrification, as described in Appendix A, differs from traditional nitrification (compare pathways in Figure 2.6) in that the whole sequence of transformations, from NH_3 to N_2O and N_2, is carried out by ammonia-oxidizers and does not involve NO_3^- [Goreau et al., 1980; Poth and Focht, 1985]. The significance of nitrifier-denitrification to N_2O production varies widely in the literature, likely reflecting differences in the environment (e.g. soil or sediment). In a review of nitrifier denitrification studies, Wrage et al. [2001] suggested that nitrifier denitrification contributed from essentially zero to up to 30% of total N_2O production in soils. In a more recent study, however, Kool et al. [2011] observed 50 to 100% of N_2O from nitrifier denitrification in soils; this observation was made under conditions of high moisture content and no exogenous (i.e. fertilizer) nitrate loading. . With the addition or urea or ammonia, Zhu et al. [2013a] found in soil incubations with nitrate and various levels of oxygen that nitrifier denitrification accounted for 34-66% of total N_2O production at oxygen levels between 0.5 and 3% O_2, with heterotrophic denitrification accounting for

an additional 34-50% of the N_2O. While the relative importance of the nitrifier denitrification pathway in soils remains uncertain, it is plausible that this could be an important pathway in lotic settings, especially those with elevated ammonium concentrations.

> **Notes on Nomenclature**: The confusing term, nitrifier denitrification, originated from "nitrifiers" (i.e. ammonia-oxidizers) carrying out "denitrification" (i.e. reduction of nitrate or nitrite to gaseous NO, N_2O, or N_2), but multiple terms have been used in the literature to describe the production of N_2 from NO_2^-. It has also been referred to as "aerobic denitrification," "lithotrophic denitrification," or simply "nitrification" [e.g. Goreau et al., 1980; Wrage et al., 2001; Stein and Yung, 2003]. Indeed, close reading of many studies reveals that N_2O from nitrification is actually produced by nitrifier denitrification (which is not inaccurate, depending on the definition of nitrification). It is important to distinguish between nitrification and nitrifier denitrification, however, because they occur under different conditions. Many studies simply divide N_2O production between nitrification and denitrification and implicitly or explicitly assume that factors contributing to traditional nitrification will influence N_2O from "nitrification" in the same way.

2.3.3.1 Factors Influencing N_2O Production from Nitrifier Denitrification

2.3.3.1.1 Nitrifier Denitrification and Oxygen. The nitrifier-denitrification N_2O generation pathway is unique because it entails both an oxidation and reduction step. Therefore, specific O_2 concentrations are required to support nitrifier denitrification. In pure cultures, N_2O production from nitrifier denitrification and the ratio $N_2O: NO_2^-$ increase with decreasing oxygen concentrations [Goreau et al., 1980; Poth and Focht, 1985]. It is possible that ammonia oxidizing bacteria that use oxygen as a terminal electron acceptor at high oxygen concentrations (nitrification) switch to using nitrite as the terminal electron acceptor when oxygen concentrations are low (nitrifier denitrification) [Poth and Focht, 1985; Shrestha et al., 2002]. In soils, Bollman and Conrad [1996] observed that nitrifier denitrification was the main source of N_2O at soil moisture contents less than 80% maximum water holding capacity; above this threshold,

denitrification was a more important source of N_2O. In incubations of unsaturated soil aggregates, Khalil et al. [2004] found that the highest N_2O emissions resulted from denitrification under anoxic conditions, but that significant N_2O emissions also resulted from nitrifier denitrification above 0.35kPa O_2, with the highest nitrifier-derived N_2O emissions at 1.5 kPa O_2. The percentage of N converted to N_2O by denitrification (up to 11%) was higher than the percentage of N converted to N_2O by nitrifier denitrification (0.16% at 20.4 kPa O_2; 1.48% at 0.76 kPa O_2), suggesting that denitrification is likely to produce more N_2O than nitrifier denitrification. Notably, N_2O from denitrification (based on isotopic calculations) was also measured at the highest O_2 concentrations (20.4 kPa O_2) [Khalil et al., 2004]. Also in soils, Zhu et al. [2013] found that nitrifier denitrification produced as much or more N_2O than denitrification at low headspace oxygen levels (0.5 and 3% O_2). In incubations of river water collected downstream of a WWTP, the highest N_2O concentrations occurred when oxygen levels were between 1.1 and 1.5 mg L^{-1}, and this production was attributed to nitrifier denitrification [Cébron et al., 2005].

Low O_2 concentrations seem to favor nitrifier denitrification because there is a small amount of oxygen needed for NH_4^+ oxidation, but NO_2^- reduction does not require oxygen, conserving O_2 for ammonia oxidation; NO_2^- reduction also prevents nitrite accumulation, which may inhibit ammonia oxidation [Poth, 1986; Wrage et al., 2001]. Kool et al. [2011] argue that nitrifier denitrification, although it uses the same nitrite and nitric oxide reductase enzymes as denitrification, is not as inhibited by O_2 because the nitrifiers gain the same amount of energy from NH_4^+ oxidation to NO_2^- as from NO_2^- reduction with NH_4^+ as the electron source. They also observed that nitrifier

denitrification was a major contributor to N_2O emissions from soils with moisture conditions that are sub-optimal for denitrification.

2.3.3.1.2 Nitrifier Denitrification and Carbon and Nitrogen Availability. As is evident from the pathways shown in Figure 2.5, nitrifier denitrification is influenced by the addition of NH_4^+ but not NO_3^- [Poth and Focht, 1985]. In contrast, denitrification is strongly influenced by NO_3^- concentrations and only indirectly influenced by NH_4^+ concentrations in coupled nitrification-denitrification. Wrage et al. [2001] suggested that nitrifier denitrification is more likely to be a significant source of N_2O production when N content is high (nitrification may proceed) and organic carbon concentrations are low. This is consistent with the concept that anaerobic denitrification is typically carried out by heterotrophic organisms, so their influence would be less significant with lower organic carbon availability.

2.3.3.1.3 Nitrifier Denitrification and Other Factors. Based on thermodynamic calculations, nitrification and nitrifier denitrification are both more favorable (more negative ΔG) at pH 7 than at pH 4 [Wrage et al., 2001]. However, decreasing pH has a greater negative effect on nitrification, so Wrage et al. [2001] suggest that low pH favors nitrifier denitrification over nitrification, summarizing that nitrifier denitrification may be an important N_2O source with low O_2, low organic carbon, high N content, and possibly low pH.

2.3.4 N_2O from DNRA

The dissimilatory nitrate reduction to ammonium (DNRA) pathway is similar to denitrification in that nitrate undergoes reduction, but instead of producing N_2 as the final product, the nitrite is reduced to ammonia. In this way, reactive nitrogen is not consumed,

but rather is converted from an oxidized to a reduced form. DNRA occurs under conditions similar to those for denitrification and may compete with that process for nitrate. The importance of DNRA to global N_2O production could be high, but it has not been well studied.

During DNRA, bacteria use organic carbon to reduce nitrate to ammonia [e.g. Smith, 1982; Lansdown et al., 2012], with NO_2^- as an intermediate reactive species. During DNRA, nitrous oxide is not an intermediate species, but rather is only produced when NO_2^- is allowed to accumulate.

$$NO_3^- \xrightarrow{\ red\ } NO_2^- \xrightarrow{\ red\ } NH_3$$
$$\downarrow$$
$$N_2O$$
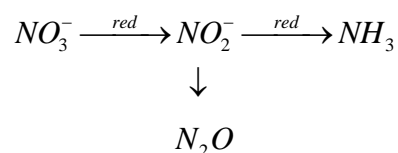
This nitrite may be reduced to N_2O via biotic or abiotic pathways (chemodenitrification, as explained previously) [Stevens and Laughlin, 1998]. The DNRA bacteria capable of the reduction of NO_2^- to N_2O may not be able to reduce the N_2O to N_2 (as in denitrification) [Kaspar, 1982; Smith, 1982]. In this way, DNRA can serve as a source for N_2O. If DNRA is carried to completion (NO_2^- to NH_4^+), however, it may serve to decrease overall N_2O production because DNRA (nitrate reduction without N_2O as an intermediate) competes with denitrification (nitrate reduction with N_2O as an intermediate) for nitrate.

2.3.4.1 Factors Influencing N_2O Production from DNRA

2.3.4.1.1 DNRA and Oxygen. DNRA is well-suited to anaerobic environments and involves mostly obligate and facultative anaerobes [Tiedje, 1988], although it can also occur in more oxidized environments [Fazzolari et al., 1998]. DNRA

and denitrification may occur simultaneously, and the relative importance of the two processes as NO_3^- sinks is a complex issue likely related to oxygen concentrations, carbon availability, temperature, and carbon: NO_3^- ratio [see Megonigal et al., 2004; Lansdown et al., 2012].

The populations of organisms present in an environment to reduce nitrate depend on the environmental conditions. Habitats that are more oxygen-rich or have periods of more oxic conditions (e.g. shallow sediments) would select for organisms that are effective competitors for carbon under aerobic respiratory conditions, such as denitrifiers. Habitats that are more continuously anoxic (e.g. deeper sediments where oxygen demand exceeds supply) have the potential to select for more fermentative or obligate anaerobes, such as DNRA reducers [Kelso et al., 1997].

2.3.4.1.2 DNRA and Carbon and Nitrogen Availability. DNRA transfers eight moles of electrons per mole of nitrate reduced, while denitrification only transfers five moles of electrons per mole of nitrate reduced. When electron donors (organic carbon) are abundant but electron acceptors (nitrate) are limited (high organic C:NO_3^- ratio), DNRA should be favored because it transfers electrons more efficiently [Tiedje et al., 1982; Tiedje, 1988; Fazzolari et al., 1998]. Although DNRA has a lower energy yield, this process may be favored in environments with abundant organic carbon but little nitrate because DNRA requires less nitrate than denitrification [Kirchman, 2012; Lansdown et al., 2012].

2.3.4.1.3 DNRA and Other Factors. There is also some evidence that DNRA might be favored at higher temperatures than denitrification, but the relationship is still unclear [Megonigal et al., 2004]. DNRA is also favored at high pH [Stevens et al.,

1998; Kolb and Horn, 2012]. In anaerobic freshwater sediment slurries, free sulfide (S^{2-}) favored nitrate reduction via DNRA instead of denitrification [Brunet and Garcia-Gil, 1996].

Although DNRA has traditionally been considered important only in marine or estuarine sediments, it may also be significant in terrestrial and freshwater systems (e.g. aquifer sediments, wet tropical forests, boreal forests, rice paddy soils, etc.; see Table 7 in Megonigal et al. [2004]). Kelso et al. [1997] found that DNRA accounted for 6-10% of nitrate reduction in river sediments.

The conditions explained above contribute to complete DNRA, with NH_4^+ as the end product. Incomplete DNRA (NO_2^- accumulation and production of N_2O) may be more likely under slightly different conditions. During DNRA, NO_2^- only accumulates (and is potentially reduced to N_2O) if NO_3^- reduction exceeds NO_2^- reduction. Kelso et al. [1997] found that sediments from warm, more anaerobic, slow-moving streams accumulated NO_2^- from DNRA, possibly due to the inhibition of nitrite reductase by NO_3^-, although Betlach and Tiedje [1981] would suggest instead that nitrite accumulation under high NO_3^- is the result of the more oxidized species (NO_3^-) being preferentially reduced over the less oxidized species (NO_2^-) when fewer electron donors are available. Thus, the C: NO_3^- ratio not only determines the prevalence of denitrification versus DNRA, but also the end product of DNRA (N_2O versus NH_4^+) [Kelso et al., 1997]. Thus, if DNRA is occurring, it is possible that higher NO_3^- concentrations will increase N_2O yield (relative to NH_4^+); however, more research is needed to support this hypothesis.

2.3.5 Other Nitrogen Cycling Processes Influencing N_2O Emissions

There are a number of reaction pathways that may limit N_2O emissions by competing for available reactive nitrogen or by consuming produced N_2O. Competitive processes include anammox and feammox. The major consumptive process is complete denitrification.

2.3.5.1 Competitive Processes

2.3.5.1.1 Anammox. Anammox, or anaerobic ammonia oxidation, is a relatively recently discovered nitrogen processing pathway [Strous et al., 1997a, 1999] that is likely a globally important alternative pathway for consumption of the reactive species ammonia, especially in oceans [Devol, 2003, 2015]. This pathway is promoted by a limited group of anaerobic bacteria that oxidize ammonia using nitrite as the terminal electron acceptor (instead of oxygen), generating N_2 [Jetten et al., 2009; Kirchman, 2012].

$$NH_3 + NO_2^- \xrightarrow{red/ox} N_2$$
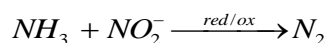
It is noteworthy that this is an oxidizing reaction that occurs under anaerobic conditions, requiring the presence of oxidized (NO_2^-) and reduced (NH_3) nitrogen species, although it can occur under conditions where the concentrations of these species are very low [Strous et al., 1999].

The anammox pathway does not include nitrous oxide as an intermediate species, and although an intermediate of anammox, NO, could serve as a substrate for N_2O formation, it has been shown to be negligible relative to denitrification, at least in soils [Hu et al., 2015]. Instead, the anammox reaction pathway could reduce overall nitrous oxide production by consuming reactive nitrogen that might otherwise follow a nitrous

oxide generating pathway [Stein and Yung, 2003]. Anammox competes with NO_2^- oxidizers for NO_2^- supplied by autotrophic ammonia oxidizers (first step of nitrification), thereby theoretically reducing N_2O production via chemodenitrification; anammox also bypasses the NO_2^- to NO to N_2O link in classic denitrification, reducing the opportunity for N_2O production.

Anammox is more likely to be a significant path for the loss of reactive nitrogen in continuously anaerobic environments when denitrification is limited by organic carbon instead of ammonia or nitrate [Thamdrup and Dalsgaard, 2002]. In anoxic incubations of marine sediment, Dalsgaard and Thamdrup [2002] observed anammox accounting for up to 62% of N_2. They also observed that: (1) the importance of anammox (relative to denitrification) decreased with increasing temperature (with an optimum rate at about 15°C); (2) anammox rates were independent of nitrite concentration, and (3) the addition of organic matter (which would favor heterotrophic denitrification) only resulted in a slight decrease in the amount of N_2 produced by anammox instead of denitrification. More recently, Lansdown et al. [2016] found that in permeable river beds (which permit longer flow paths and advection of solutes, creating a mosaic of redox microenvironments), anammox may be contribute up to half of the N_2 production (the other half being produced by denitrification).

2.3.5.1.2 Feammox. Feammox is a reactive nitrogen consuming pathway similar to anammox, but ferric iron, instead of nitrite, is used as the terminal electron acceptor for the anaerobic oxidation of ammonia to N_2 [Zhu et al., 2013b].

$$NH_3 + Fe^{3+} \xrightarrow{\;oxid\;} N_2$$
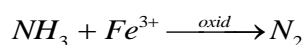
The importance of feammox to the global nitrogen cycle remains uncertain. Like anammox, feammox is an alternative pathway for consumption of reactive nitrogen that does not involve nitrous oxide production. Although the feammox pathway primarily converts ammonia all the way to N_2, feammox can also produce NO_3^- or NO_2; which could potentially be used to produce nitrous oxide production through coupling with incomplete denitrification [Yang et al., 2012]. Feammox prevents NH_4^+ accumulation when ferric iron is available, possibly reducing N_2O production rates via pathways that include NH_4^+ oxidation (nitrification and coupled nitrification-denitrification). Feammox is more likely at low pH and in iron-rich sediments or soils that experience zones or periods of anoxia, allowing both the presence of iron oxides and anaerobic ammonia oxidation [Clément et al., 2005; Yang et al., 2012; Ding et al., 2014].

2.3.5.2 Consumptive Processes

Because nitrous oxide is often produced as an intermediate species along a reaction pathway, completion of that pathway will lead to nitrous oxide consumption. Even in cases where nitrous oxide is a terminal reactant product, the further reduction of nitrous oxide to dinitrogen gas is often favored. For this reason, many systems can act as sinks for nitrous oxide and net nitrous oxide consumption has been observed in soils [Chapuis-Lardy et al., 2007], wetlands [Kolb and Horn, 2012], and lakes and rivers [Soued et al., 2015].

Most N_2O consumption in natural environments occurs due to the highly exergonic reduction of N_2O to N_2 by denitrifiers utilizing nitrous oxide reductase [Knowles, 1982; Zumft and Kroneck, 2006]. Nitrifiers that carry out nitrifier denitrification are believed to use the same enzymes as denitrifiers [Wrage et al., 2001],

so the reduction of N_2O to N_2 may also be carried out by some nitrifiers. Not all denitrifiers have the ability to complete this step [Tiedje, 1988; Hu et al., 2015], but N_2O is the sole electron acceptor for some denitrifying microorganisms [Kolb and Horn, 2012].

Other conversions of N_2O may occur abiotically or with other enzymes, including assimilatory reduction of N_2O to NH_3 [Vieten et al., 2008], but experiments have demonstrated that these alternative N_2O consumption processes play a minor role [Chapuis-Lardy et al., 2007; Vieten et al., 2008] (see review in Kolb and Horn [2012]). Complete denitrification, including reduction of N_2O to N_2, is favored by anaerobic conditions, near-neutral pH, and high carbon availability (relative to nitrogen) [Kolb and Horn, 2012]. Because denitrifiers can utilize N_2O as a free intermediate [Zumft, 1997; Baulch et al., 2011], N_2O produced along other pathways (e.g. DNRA, chemodenitrification) can also presumably be reduced to N_2 using nitrous oxide reductase. Chapuis-Lardy et al. [2007] found that N_2O consumption tends to increase with conditions that reduce N_2O diffusion, at least in soils. Beaulieu et al. [2011] suggested than N_2O consumption is lower in soils compared to aquatic sediments because N_2O can escape the denitrification zone via gaseous diffusion when soils are not fully saturated. Additionally, this is consistent with the conceptual model of Quick et al. [2016], in which longer residence times in sediments enhance N_2O consumption and reduce N_2O emissions. In summary, consumptive processes, and associated rates, can be as important as productive processes in determining if nitrous oxide emissions will be observed from streams and rivers. The relevance of all of these processes in lotic settings is the subject of the next section.

2.4 Lotic Settings for N$_2$O Generation

Section Summary: Lotic N$_2$O production and consumption may take place in the hyporheic zone, along groundwater flow paths, and in the water column of streams and rivers. Because microbial nitrogen processing requires substrate, influx of reactants, appropriate redox conditions, and intermediate residence times, the hyporheic zone is likely the site of most N$_2$O production. However, high rates of N$_2$O production may also occur associated with suspended sediments in turbid streams and rivers.

The lotic settings in which nitrous oxide is potentially generated provide a useful physical framework for discussing the details of the reaction pathways previously described. We propose N$_2$O production (and consumption) may occur in three hydrologically defined lotic settings. N$_2$O can be produced (1) in the saturated sediments beneath and immediately adjacent to streams and rivers, known as the hyporheic zone (HZ), (2) along groundwater (GW) flow paths leading to gaining streams, and (3) in the water column of a stream or river, as shown in Figure 2.7.

Physical settings for N$_2$O production/consumption
1. Hyporheic Zone
2. Groundwater flow paths
3. Water Column
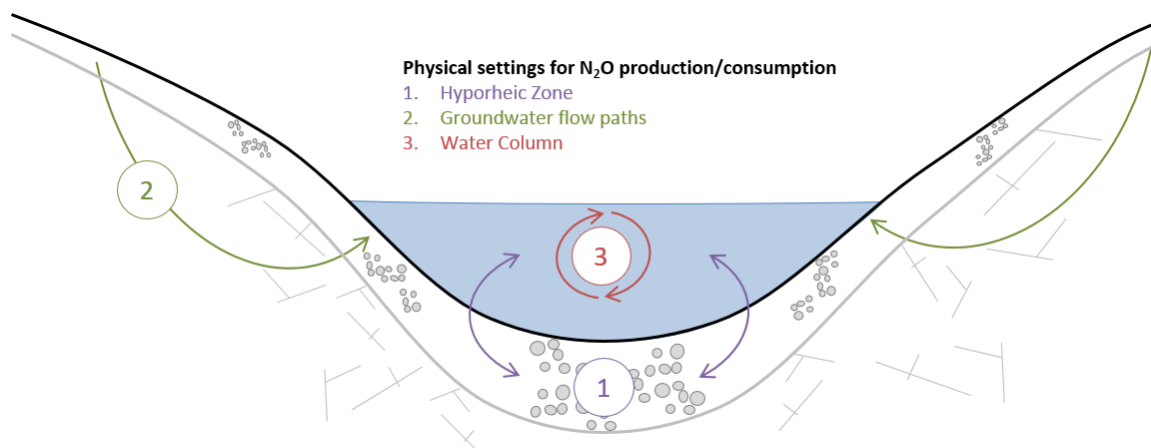
Figure 2.7. **Cross section of a stream or river showing three possible physical settings for the generation of N$_2$O.**

2.4.1 N-cycling in the Hyporheic Zone

The hyporheic zone can be defined as the saturated interstitial areas beneath the stream bed or within the stream banks where surface and groundwater interact [Winter et al., 1998]. The mixing of these waters may take place at a range of scales, from small scale bed forms, to channel bars and meanders, to large floodplains [Edwards, 1998]. The hyporheic zone is an active site of chemical and biological reactions because of the large, reactive surface area in the sediments to which microorganisms can attach, the continual introduction of solutes and long periods of sediment-water contact during which reactions can take place [Edwards, 1998; Merill and Tonjes, 2014]. In many settings, the hyporheic zone promotes rapid transformation of solutes, including nitrogen species, altering chemical concentrations of the overlying stream [Winter et al., 1998; Cardenas et al., 2004]. Groundwater and downwelling surface water supply a continuous influx of reactants (critical nutrients and dissolved gases) to microorganisms living on sediment surfaces, also known as epilithon [Edwards, 1998]. Both reactants and products are transported along flow paths in the subsurface, where more reactions may occur before the water is reintroduced into the overlying stream [e.g. Boano et al., 2010; Bardini et al., 2012]. Dissolved gases produced along these hyporheic flow paths, including nitrous oxide, may then be released from the stream water into the atmosphere (see example in Figure 2.4).

2.4.2 N-cycling Along Groundwater Flow Paths

Reactive nitrogen is introduced to the groundwater through leaching from the overlying unsaturated zone and by advection from up-gradient sources. Groundwater discharging to streams can bring dissolved N_2O that may then be emitted to the

atmosphere. The chemistry of groundwater recharge and conditions along the groundwater flow path influence the likelihood of N_2O delivery to the stream. Riparian zones that border streams can be important processing sites of nitrogen from groundwater aquifers due to the abundance of organic carbon (electron donor for N-reduction), processing by microbes, and interaction with plant roots (assimilation) [Addy et al., 1999; Groffman et al., 2000; Mayer et al., 2010; Ranalli and Macalady, 2010]. Nitrogen removal from the groundwater may be temporary (storage in plants and microbes), but denitrification of nitrate is the prominent nitrogen sink in the riparian zone [Ranalli and Macalady, 2010]. In agricultural land use areas, nitrogen inputs from soil to the groundwater may be high due to fertilizer use and livestock excretion, and may remain high due to the removal of buffering riparian vegetation [Duff et al., 2008]. Restored riparian areas can mitigate groundwater nitrate inputs to streams; however, the effect of riparian areas on N_2O emissions from streams is complex. Restored riparian zones likely shift the location of N_2O production from rivers to the riparian buffers, but may also alter the N_2O yield from denitrification of nitrate, due to differences in carbon availability and pH in the riparian zone relative to the water column of the stream or river [Groffman et al., 2000]. Denitrification, and therefore N_2O production and consumption, is most likely along groundwater flow paths with high organic matter content and permeable sediments that allow for longer residence times; little denitrification occurs along deep groundwater flow paths and those with low organic matter content and highly permeable sediments [Ranalli and Macalady, 2010].

2.4.3 N-cycling in the Water Column

Most nitrogen cycling processes, and in particular, those that produce and consume N_2O, are carried out by microorganisms. Because microbial densities are generally lower in the water column, less N-cycling (and N_2O production) often occurs in the water column than in riparian and hyporheic sediments. However, in rivers and streams with high turbidity, suspended sediments can host microorganisms and may contain microzones with redox conditions favorable for nitrogen cycling. Generally, larger rivers have less hyporheic exchange [Anderson et al., 2005], and water column processes play a relatively larger role in biogeochemical processing; it is likely this trend with scale applies to N_2O production and emissions. In the literature, however, it can be confusing to compare sediment and water-column rates of nitrogen transformations. Rates per unit volume of sediment may be much higher than rates per unit volume of water, but depending on the size of the stream or river, the volume of the water may greatly exceed the volume of sediments with active N-cycling [Seitzinger and Kroeze, 1998].

2.4.4 Important Lotic Setting Characteristics

The extent of N_2O production in these different settings depends on specific conditions, including stream geomorphology, hydrology, chemistry, and turbidity. In order to facilitate N_2O production, microbes require (1) a substrate on which to live, (2) sufficient reactants, (3) appropriate redox conditions (supply of reductant or oxidant), and (4) time for the reactions to occur. Once N_2O is produced, release to the atmosphere requires that it avoid reduction to N_2 and also be produced in large enough quantities to exceed its solubility in stream water. The release of N_2O to the atmosphere also depends

on the gas-transfer velocity for a given stream, which is a function of hydrometeorological conditions (water turbulence, wind velocity, etc.) [Raymond and Cole, 2001]. These conditions for N_2O emission are met to varying degrees in different physical settings.

2.4.4.1 Microbial Substrate and Solute Advection

Aquifer sediments, hyporheic sediments, and suspended sediments can provide a substrate for attachment and growth of microbial communities. Both microbial substrate availability and solute advection are related to grain size distribution. Typically, finer grained sediments provide more surface area for microbial growth [Deflaun and Mayer, 1983; Ranjard et al., 2000], although very fine-grained sediments limit hydraulic conductivity and decrease the rate of advection of reactants to the microbes [Schwartz and Zhang, 2003]. For example, in agricultural streams, Opdyke et al. [2006] observed that the pools and separation zones with finer-grained sediments and more organic matter had higher sediment denitrification rates than riffles and point bars with coarser-grained sediments. Sediments suspended in the water column of a stream or river are necessarily fine-grained, providing a relatively large amount of surface area for microbial habitat. Additionally, there may be less of an advection limitation for fine-grained suspended sediment because the microbes are in close physical proximity to the solutes in the surface water [Liu et al., 2013].

The necessary reactants for N_2O production may include oxygen, reactive carbon, nitrate, nitrite, and/or ammonia (see Figure 2.6 and Tables 2.2, 2.3, and A.3). As these reactants are processed in both assimilatory and dissimilatory reactions, they must by

replaced by mineralization of organic matter or advection in order for N_2O concentrations or flux to become significant.

<u>2.4.4.2 Redox Conditions</u>

As described in Section 2.3, N_2O can result from both reduction and oxidation of reactive nitrogen species. Most observed N_2O generation has been associated with low O_2 or anaerobic conditions (see Tables 2.2, A.3, and references therein). These DO conditions are most likely to be achieved when either (1) water advected into an environment is already oxygen-depleted or (2) the DO advected into an environment is consumed by aerobic respiration. In the latter case, enough reactive carbon must be present for aerobic respiration and any subsequent heterotrophic nitrogen processing, such as denitrification.

In aquifer and hyporheic sediments, the initial parts of a flow path tend to be aerobic, as water entering the flow path is often in contact with the atmosphere. The DO decreases along the flow path due to aerobic respiration, with the size of the aerobic zone increasing with lower carbon availability and decreased respiration rates [Quick et al., 2016]. The remainder of the flow path is typically anaerobic (see Figure 2.4) [Bardini et al., 2012; Trauth et al., 2014].

Redox zones may exist at multiple scales. Anaerobic microsites are frequently present in bulk aerobic zones, commonly observed in soils, and may be ideal for N_2O production for the reasons described in Section 3 [Stevens et al., 1997; Zarnetske et al., 2011]. Additionally, even when surrounded by oxygenated surface water, suspended sediments may have anaerobic cores (microzones) due to the presence of small bits of reducing organic matter [Liu et al., 2013; Reisinger et al., 2016].

2.4.4.3 Residence Time and Reaction Rate

The various nitrogen cycling processes occur at different reaction rates and along flow paths with varying residence times. Residence time is defined as the time a packet of water spends along a flow path, whether through aquifer or HZ sediments or into and out of a mass of suspended sediment in the water column. The residence time is a function of flow path length and velocity [Tonina, 2012; Harvey et al., 2013]. The velocity is a function of the hydraulic conductivity and pressure gradient (for advective flow) or concentration gradient (for diffusion). Under advective flow, high hydraulic conductivities and high pressure gradients increase flow velocities and tend to decrease residence times.

The ratio between reaction rate and residence time is critical to predicting if a certain reaction will occur along a GW or HZ flow path or within suspended particulates [e.g. Duff and Triska, 2000]. If the residence time is at least as long as the reaction rate for N_2O production, N_2O will produced. The N_2O that is produced, however, will only be released to the stream or river and potentially emitted to the atmosphere if there is not sufficient time (and the appropriate conditions) for N_2O reduction to N_2 (Figure 2.4). In other words, N_2O emission requires residence times that are longer than the reaction rates for N_2O production but shorter than the combined reaction rates for N_2O production and consumption [Quick et al., 2016], unless N_2O reduction to N_2 is otherwise inhibited. Thus, only a fraction of the N_2O produced is released to the atmosphere as N_2O emissions, and the N_2O yield is controlled by the degree to which produced N_2O is consumed.

Flow path length is dictated by the scale of the hydraulic exchange, and extends from a few centimeters at the scale of small streambed structures to kilometers associated with floodplain-scale exchange flows [Tonina, 2012; Boano et al., 2014]. In general, longer flow paths result in longer residence times; this can lead to increased N_2O production, but also increased N_2O consumption.

A useful approach when considering N_2O cycling is to explicitly couple the influence of residence time and reaction rate [e.g. Harvey et al., 2013]. Some studies employ a dimensionless Damköhler number, D_a, which relates reactant transport rates and reaction rates [Gu et al., 2007; Marzadri et al., 2012, 2017; Tonina, 2012; Zarnetske et al., 2012; Briggs et al., 2015; Lansdown et al., 2015]. For example, microbial populations, temperature, and the availability of carbon and oxygen will influence reaction rates. Geomorphology and hydrodynamics will determine flow paths and residence times. The interplay of these physical and biogeochemical processes dictates the fate of N_2O.

2.4.4.4 The Role of Geomorphology and Scale

The nature and relative importance of subsurface exchange influencing N_2O processes vary in response to stream geomorphology and scale. The amount of streamflow that moves through the HZ, termed the hyporheic exchange, depends on discharge, hydraulic conductivity, and stream geomorphology [Duff and Triska, 2000; Anderson et al., 2005; Gooseff et al., 2006; Tonina, 2012]. On a small scale, bed forms such as ripples and dunes cause head gradients that induce advective flow in and out of the HZ [Cardenas et al., 2004]. In general, heterogeneity in the surface of a streambed tends to increase exchange [Elliott and Brooks, 1997; Tonina and Buffington, 2009], and

by extension, the potential to promote N₂O related reactions. On a larger scale, the nature of the stream valley is significant to the size of the HZ and the extent of hyporheic exchange. Unconstrained river segments tend to have deeper alluvium, wider valleys, and larger hyporheic zones, producing longer flow paths and residence times. While these hyporheic zones may be larger [Kasahara and Wondzell, 2003], constrained river segments often exhibit more longitudinal variation in gradients and the strongest upwelling zones, potentially producing greater total hyporheic exchange [Baxter and Hauer, 2000]. Due to these geomorphic differences, the relative importance of hyporheic exchange generally decreases with stream order [Anderson et al., 2005]. Geomorphology and the other physical characteristics of the lotic settings described in this section ultimately dictate the conditions that support specific reaction pathways that drive N₂O cycling.

2.5 Observations from Stream-Based N₂O Studies

Section Summary: Efforts to quantify N₂O in lotic settings include mostly studies of N₂O dissolved in or emitted from surface water, with fewer studies of N₂O produced or emitted from sediments. With some exceptions and limits, N₂O emissions are generally positively correlated with nitrate concentration (and in some cases, ammonia concentration). Most studies observe more N₂O emissions with low DO. Lotic N₂O emissions were generally higher in the warmer months and at night. Most studies assume a denitrification source for N₂O, except in the case of high DO and NH_4^+, in which nitrification is assumed.

Since the late 1990s, increasing numbers of studies involving N₂O production and emission have been carried out in headwater streams, large rivers, estuaries, and surrounding sediments; these studies have included forested, grassland, agricultural, and urban catchments. The key observations of many of these studies are shown in Tables 2.4 and 2.5. The study results are separated between N₂O emissions based on measurements

of stream or river water (Table 2.4) and N_2O emissions based on measurements from sediments from the streambed, hyporheic zone, and riparian zone (Table 2.5).

A range of stream sizes and catchments have been studied, and field sites now include six continents, though most of the field sites have been in North America and Western Europe, as shown in the first columns of Tables 2.4 and 2.5. These studies can broadly be divided into

> **Reminder Definitions**:
> **Production/Generation** refers to the reaction step that creates N_2O. The produced N_2O may be then consumed or released to the atmosphere as emissions.
> **Emissions** refers to the N_2O that is not consumed and is released to the atmosphere.
> **Yield** is a metric of N_2O emission efficiency; it refers to the amount of N_2O released to the atmosphere relative to another N species, usually N_2.

in-situ measurements and studies of incubated lotic water or sediments; experimental methods are shown in the second columns of the tables. As will be explained below, these varying techniques can have a large impact on the results of the studies and implications for comparisons between studies. The range of nitrate observed in each of the studies is included due to its potential influence on N-cycling; it is also a general indicator of the amount of agricultural or urban influence on a stream or river. Where possible, nitrous oxide flux rates are shown as either N_2O emission flux per time per area of the stream/river (Table 2.4) or streambed (Table 2.5). Some studies also report N_2O production rate by volume or mass of water or sediment. The N_2O yield, when reported, is shown in the fifth columns of the tables.

While numerous studies have measured N_2O production and/or emissions in streams and rivers, there is often a disconnect between studies of chemical/microbial pathways (Section 2.3) and studies of processes in physical settings (Section 2.4). This disconnect is often due to the challenge of isolating reaction pathways from in situ

observations of naturally complex systems. Generally, studies that examine N_2O emissions in field settings are often forced to make simplifying assumptions about the reaction pathways. This disconnect also likely reflects disciplinary divides between the hydrology and soils research communities. The last decade, however, has been a period of substantial progress in quantifying N_2O and related variables. In this section, we present some of that literature with a focus of gaining insight into the controlling variables and pathways leading to lotic N_2O emissions.

2.5.1 Importance of the Experimental Approach

A variety of useful approaches have been used to investigate nitrous oxide behavior in lotic systems and each of those approaches has brought new insights to our understanding. Larger scale in-situ studies typically focus on measuring emissions from the surface of the stream, often by using floating plastic chambers from which gas is extracted and analyzed [e.g. McMahon and Dennehy, 1999; Beaulieu et al., 2010]. Other in-situ studies involve collecting samples of surface water, measuring dissolved N_2O concentrations and saturation, and then predicting N_2O emissions (flux from the stream surface) based on a gas exchange term [e.g. Baulch et al., 2011; Beaulieu et al., 2011]. This gas exchange term, whether measured or estimated from hydrologic conditions and empirical relationships, strongly influences resulting emission estimates [Hlaváčová et al., 2006; Borges et al., 2015; Schade et al., 2016; Audet et al., 2017]. Collectively, these studies likely produce the best estimates of emission rates, but are less likely to distinguish mechanisms of N_2O generation.

A second class of studies utilize sediment and water collected in the field and then analyzed in laboratory mesocosms [e.g. García-Ruiz et al., 1998b; Beaulieu et al., 2010

Kelso et al., 1997; Barnes and Owens, 1999]. This approach typically produces accurate measures of rates and flux within the experiment, and often provides insight into mechanism and process. However, these studies are less likely to provide accurate estimates of emissions because assumptions must be made about the transfer of N_2O between the sediments, stream water, and atmosphere, and experimental conditions do not necessarily replicate natural conditions. For example, studying only shallow sediments would exclude the potentially significant N_2O input from deeper sediments [Lansdown et al., 2015]. Additionally, some microcosm studies consist of columns of sediment incubated with still water. In actual systems, hyporheic or surface water moves through sediment, introducing solutes and removing products. The lack of advection in these studies could lead to incorrectly estimating nitrogen processes rates in sediments. According to Beaulieu et al.[2010], enclosure-based studies have resulted in artificially low observed biogeochemical reaction rates.

A few studies collect and analyze subsurface pore water from the hyporheic zone or surrounding aquifer, observing N_2O concentrations directly [e.g. Gardner et al., 2016; Quick et al., 2016]. These studies can inform mechanisms for N_2O production and consumption. However, these studies often struggle to constrain emissions rates and fluxes because of complexity in flow and reaction rates in natural settings, as well as the assumptions required to estimate transfer between the sediments, water, and atmosphere.

The variety of experimental approaches and complexity of controlling factors often make it difficult to directly compare values of N_2O concentrations, emissions, or yield. Two streams with identical N_2O long term emissions may have apparent differences in N_2O emissions depending on the time of day or season, hydrologic

conditions (low or high flow) during sampling, and whether the N_2O emissions were based on shallow porewater, deep porewater, or surface water concentrations of N_2O. For this reason, the N_2O flux values in Tables 2.4 and 2.5 should be used to gain a sense of observed ranges, but comparison between studies requires carefully scrutiny of collection and measurement techniques.

2.5.2 Key Observations

Although the lists of studies in Tables 2.4 and 2.5 do not include every study that has measured nitrous oxide from streams and rivers, the references provide a sense of where key observations converge and diverge, depending on the study.

2.5.2.1 N_2O emissions and nitrate concentration

There is generally consensus that N_2O emissions increase with nitrate concentrations in the surface and groundwater, up to a certain degree. Figure 2.8 shows the maximum reported N_2O production or emission rate and corresponding nitrate concentration for studies listed in Tables 2.4 and 2.5. The horizontal and vertical bars show the range of reported values for each study. Note that the maximum nitrate values do not always correspond to the highest N_2O values. The studies outlined in Tables 2.4 and 2.5 cover a wide range of types and locations of streams and rivers, and nitrate loading varies across several orders of magnitude, from nearly pristine to several thousand μg $N\text{-}NO_3^-$ L^{-1}. A positive correlation between nitrate concentrations and N_2O flux was observed in groundwater [Gardner et al., 2016], the hyporheic zone [Quick et al., 2016], and all sizes of streams, including in studies of headwaters [Mulholland and Valett, 2004; Beaulieu et al., 2011; Schade et al., 2016; Audet et al., 2017], large rivers [Borges et al., 2015; Turner et al., 2016], and studies investigating a range of stream sizes

[Stow et al., 2005]. The relationship between nitrate and N_2O was observed in all catchment types, including agricultural [García-Ruiz et al., 1998a; Hasegawa et al., 2000; Harrison and Matson, 2003], urban [Beaulieu et al., 2011], forested [Mulholland and Valett, 2004], and mixed land use [Stow et al., 2005; Baulch et al., 2012]. Additionally, N_2O consumption was observed under conditions of low nitrate [Baulch et al., 2011].

The relationship between nitrate and N_2O production and emissions is not always clear or simple, however. In a study of ten streams, Baulch et al. [2012] concluded that the relationship between nitrate and nitrous oxide may be unclear except on longer timescales. Some studies reported that N_2O flux [Turner et al., 2016] or yield [Silvennoinen et al., 2008b] increases with nitrate up to a certain point, and then levels off. In the LINX II study of 72 headwater streams, nitrate was only correlated with N_2O above 96 μg N-NO$_3^-$ L^{-1}, and there was no observed relationship between nitrate and N_2O yield [Beaulieu et al., 2011]. A clear relationship between NO_3^- and N_2O was observed in only 3 of 12 African rivers [Borges et al., 2015]. Authors have also reported on the complicated relationship between carbon and nitrate in regulating the production of N_2O, likely due to C- or N-limitation of processes such as denitrification [Mulholland and Valett, 2004]. As an example, in a study of first order streams, Schade et al. [2016] observed that N_2O increased with nitrate and decreased with DOC in one stream, while in another, N_2O decreased with nitrate and increased with DOC.
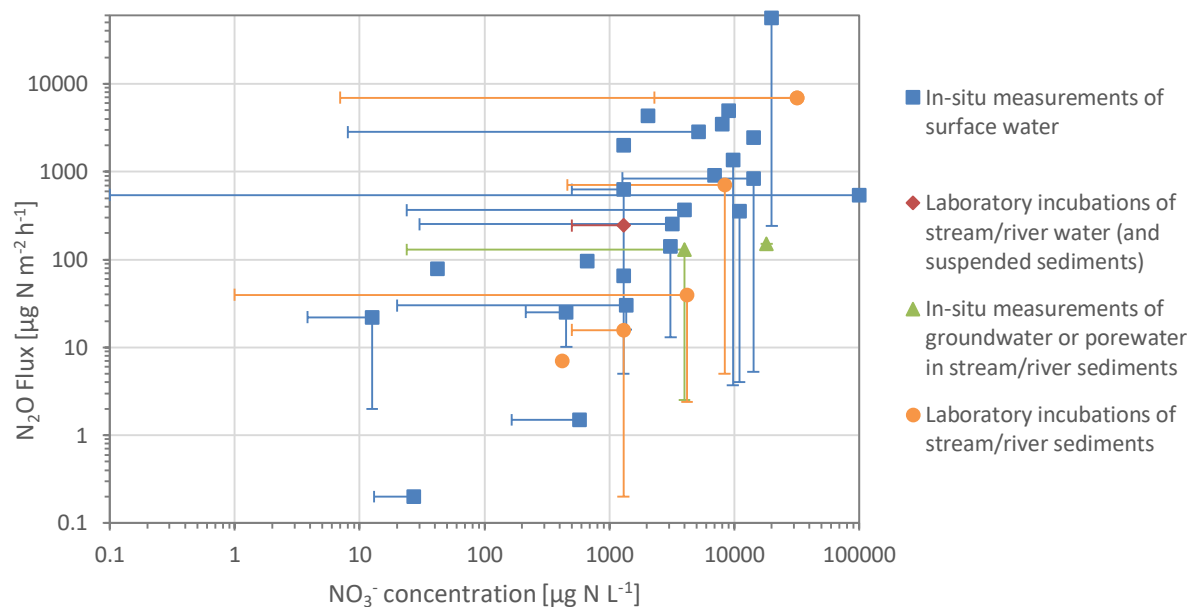
Figure 2.8. **Maximum nitrate concentrations and N₂O production rates (symbols) as reported in the studies listed in Table 2.4.** The horizontal and vertical bars show the range of values reported in each study. Note that the plotted maximum N₂O value does not necessarily occur with the maximum nitrate value.

2.5.2.2 N₂O emissions and ammonia concentration

There is also a general consensus that N₂O flux is positively correlated with NH_4^+, as reported for small agricultural streams [Harrison and Matson, 2003] and large rivers [Beaulieu et al., 2010], in both hyporheic sediments [Lansdown et al., 2015] and surface waters [Cébron et al., 2005]. Many studies observed maximum N₂O concentrations and fluxes downstream of wastewater treatment plants, most likely due to high NH_4^+ concentrations [McElroy et al., 1978; Hasegawa et al., 2000; Beaulieu et al., 2010; Rosamond et al., 2012; Borges et al., 2015; Burgos et al., 2015]. In some streams and rivers, however, no distinct relationship was observed between N₂O and NH_4^+ [Borges et al., 2015; Audet et al., 2017].

2.5.2.3 N_2O emissions and carbon

The studies outlined in Tables 2.4 and 2.5 reveal a complicated relationship between carbon and N_2O. A few studies observed a positive relationship between N_2O emissions and DOC [Harrison and Matson, 2003; Stow et al., 2005] and between N_2O concentrations and total C [García-Ruiz et al., 1998b]. In a range of lotic settings, however, Soued et al. [2015] and Baulch et al. [2011] found that N_2O consumption was more likely under conditions of high DOC. Clough et al. [2007a] observed a negative relationship between N_2O saturation and DIC (dissolved inorganic carbon) in a small rural stream. While N_2O yield was found to increase in deeper sediments with lower glucose [Kelso et al., 1997], no relationship was observed between N_2O yield and DOC by Beaulieu et al. [2011] in headwater streams.

2.5.2.4 N_2O emissions and oxygen

In the studies included in Tables 2.4 and 2.5, measurements of dissolved oxygen could provide some insight into pathways for N_2O production and consumption. An inverse relationship between DO and N_2O flux was reported for several large rivers [McElroy et al., 1978; Rosamond et al., 2012; Venkiteswaran et al., 2014], and at least for the Grand River in Canada, DO was a stronger predictor of N_2O emissions than nitrate [Rosamond et al., 2012; Venkiteswaran et al., 2014]. In incubations of river water, Cébron et al. [2005] observed peak N_2O production between 1.1 and 1.5 mg DO L^{-1}. In the hyporheic zone, hotspots of N_2O production were associated with reducing conditions, including low DO [Silvennoinen et al., 2008a; Lansdown et al., 2015; Quick et al., 2016]. Conversely, N_2O was positively correlated with DO in a 2nd order spring-fed stream [Clough et al., 2007a], an agricultural canal [Harrison and Matson, 2003], and in a

review of studies of African streams and rivers [Borges et al., 2015]. Additionally, undersaturation of N_2O was correlated with low DO and low pH in a study of high latitude rivers in Canada [Soued et al., 2015].

2.5.2.5 N_2O emissions and temporal variability

Although spatial variation in N_2O along a stream or river is likely larger than temporal variation [Cole and Caraco, 2001], several researchers report seasonal trends in N_2O production and emissions. N_2O production was reported to peak in the late spring or summer across the entire range of stream sizes [García-Ruiz et al., 1998a, 1999; Barnes and Owens, 1999; Hasegawa et al., 2000; Harrison and Matson, 2003; Garnier et al., 2009; Beaulieu et al., 2010; Rosamond et al., 2012; Burgos et al., 2015]. Some exceptions, showing the highest N_2O emissions in the colder months, were also reported [Hemond and Duran, 1989; Clough et al., 2011; Soued et al., 2015].

In ten Canadian streams, Baulch et al. [2012] found that N_2O emissions varied 2.3 fold over diel cycles, with the highest N_2O concentrations measured at night when DO, pH, and temperature were all low. Rosamond et al. [2012] and Laursen and Seitzinger [2004] also observed at least slightly higher N_2O emissions at night.

2.5.2.6 Pathways for N_2O production

A few studies have used isotopes to investigate pathways; in all of these cases denitrification was confirmed as the source of at least some of the N_2O measured in stream water [Mulholland and Valett, 2004; Baulch et al., 2011; Beaulieu et al., 2011] and sediments [Lansdown et al., 2015], with the exception of sediment cores from an estuarine river in England, in which Barnes and Owens [1999] used isotopes to infer that N_2O was produced via nitrification. Most studies of N_2O in streams, however, make

assumptions about the production pathway based on other variables that favor those pathways. For example, Hasegawa et al. [2000] assumed a denitrification source for N_2O in surface water because the high DOC and NO_3^- concentrations present would favor denitrification over nitrification.

N$_2$O production and consumption were attributed to denitrification in all of the sediment-based studies [García-Ruiz et al., 1998a, 1999; Groffman et al., 2000; Clough et al., 2007b; Silvennoinen et al., 2008a; Lansdown et al., 2015], often due to correlation with measured denitrification rates. Nitrification was more often assumed to produce N_2O in surface waters with high ammonia and/or DO [McElroy et al., 1978; McMahon and Dennehy, 1999; Harrison and Matson, 2003; Cébron et al., 2005; Guérin et al., 2008; Beaulieu et al., 2010; Burgos et al., 2015]. Although several authors acknowledged the possibility of DNRA in N_2O production, it was assumed insignificant [e.g. Turner et al., 2016], except in one study of sediment cores from rivers in Northern Ireland [Kelso et al., 1997].

2.5.2.7 Models of N$_2$O emissions

In many of the studies listed, attempts were made to predict N_2O fluxes using various models combining some of the related variables. N_2O fluxes could not be predicted by simple linear regression models of environmental variables in high latitude streams; Venkiteswaran et al. [2014] found that nonlinear models were more successful in predicting N_2O fluxes. The increasing use of regression tree analysis [Stow et al., 2005; Baulch et al., 2011; Venkiteswaran et al., 2014; Turner et al., 2016] hints at the dependence of N_2O production on interconnected variables (e.g. C, N, and DO) in multiple pathways.

Table 2.4.   N₂O Production and Yield in Lotic Settings: Water

Settings	Technique	NO$_3^-$ (µg N-NO$_3^-$ L^{-1})	N₂O Flux (µg N-N₂O m^{-2} h^{-1})	N₂O Yield (N₂O/N₂)* (N₂O/(N₂+N₂O))^ (N-N₂O/ N-NO$_3^-$)#	Source of N₂O (attributed)	Key Observations
In-situ measurements of stream/river water						
[Audet et al., 2017]						
9 3rd order and smaller streams, agricultural/ forested catchment, Sweden	Sampled surface water for dissolved N₂O, measured concentration one week later, used two empirical formulas to calculate gas exchange rate and estimate N₂O emissions.	0 to 8000	-18 to 3450 Means: 108.2 and 175.4		Denitrification (assumed, acknowledge nitrification)	▪ Two ranges of N₂O emission values depended on empirical equations for gas transfer velocity ▪ Dissolved N₂O concentration significantly correlated with NO$_3^-$, percentage arable land, and stream discharge ▪ Did not observe effect of temperature, season, DOC, oxygen, or NH$_4^+$ on N₂O concentration
[Baulch et al., 2011]						
2nd-5th order streams and rivers, Ontario, Canada	Sampled surface water for dissolved N₂O, used air-water gas exchange rate to calculate N₂O emissions (long-term)	0 to 7000	-3.7 to 905		Denitrification (isotopically confirmed)	▪ N₂O emissions positively related to nitrate concentrations ▪ N₂O consumption under very low nitrate (<2.7 uM), high DOC, high temperature, low NH$_4^+$, low SO$_4^{2-}$ ▪ Lower emissions than eutrophic tropical streams, similar to others in Midwest USA
[Baulch et al., 2012]						
10 streams draining forest, wetland, and agricultural areas Ontario, Canada	Sampled surface water for dissolved N₂O day and night, used gas exchange rate to calculate N₂O emissions.	666 (day) 615 (night)	86.8 (day) 95.2 (night)	#0.34% (day) #0.44 % (night)	Not distinguished (assume nitrification and denitrification)	▪ Mean daily fluxes related to mean NO$_2^-$+ NO$_3^-$ concentrations ▪ No single variable helped predict diel variation in N₂O ▪ N₂O flux may be underestimated by daytime sampling ▪ Stream N₂O emissions were within the range of local soil emissions
[Beaulieu et al., 2010]						
Large, impounded river, Ohio River, USA	Sampled headspace gas from floating, 20 L acrylic chambers, sampled surface water for dissolved N₂O (5 cm depth)	500 to 1300 Mean: 820	~5 to 90 Mean: 16.3 upstream WWTP: 623		Nitrification (assumed due to DO saturated surface water)	▪ High N₂O emissions in summer, low in winter; water temperature accounted for 70% of variation in N₂O saturation ▪ Maximum N₂O below WWTP ▪ Higher N₂O production in the water column than sediments
[Beaulieu et al., 2011] (LINX II)						
72 headwater streams, multiple land use types, USA	Added ^{15}NO$_3^-$ tracer, measured dissolved N₂O in surface water for 24 hours, estimated emissions from air-water gas exchange rate	~0.1 to 100,000	-25 to 541	^<1% ^(0.04 to 5.6%)	Denitrification (isotopically confirmed) Nitrification (assumed)	▪ Denitrification and N₂O production increase with nitrate above 96 µg L^{-1} N-NO$_3^-$ ▪ N₂O yield unrelated to NO$_3^-$, DOC, POC, decreases with ecosystem respiration ▪ Measured 26% of N₂O emissions due to direct denitrification, assumed 52% from nitrification *(see discussion in 6.1.2)* and the rest from coupled nitrification-denitrification and groundwater inputs

[Borges et al., 2015] includes **[Marwick et al., 2014; Teodoru et al., 2014]**						
12 streams, from headwaters to mainstem rivers, sub-Saharan Africa	Sampled surface water for dissolved N_2O, used two models of gas exchange coefficients to estimate N_2O emissions		2.3 to 32.3		Not distinguished	▪ N_2O was higher in rivers than in streams ▪ Lowest N_2O values at lowest oxygen and pCO_2 levels ▪ Positive relationship between N_2O and NO_3^- in 3 rivers ▪ No distinct relationship between N_2O and water temperatures, NO_3^-, or NH_4^+ ▪ N_2O fluxes were 1.34 times higher with basin-specific calculation for gas transfer velocity ▪ Sampled rivers were low in DIN ▪ Highest N_2O concentration due to WWTP
[Burgos et al., 2015]						
Coastal river heavily influenced by urban and agricultural discharge, Spain	Sampled surface water for dissolved N_2O, used empirically calculated gas transfer velocity to estimate N_2O emissions	23.8 to 3997 Mean: 1749	-0.12 to 365 Mean: 108		Nitrification (assumed)	▪ Highest N_2O emissions spring and summer, lowest in fall ▪ Highest N_2O concentration close to WWTP, decreases downstream ▪ N_2O fluxes are a consequence of anthropogenic inputs and wind speed variability ▪ Assume nitrification due to correlation with apparent oxygen utilization [*Bange*, 2008]
[Clough et al., 2007a]						
2nd order rural, spring-fed stream, New Zealand	N_2O flux from floating chambers and dissolved N_2O measured in surface water over 72 hours	2800 to 3100 Mean: 3000	52 to 140 Mean: 89 (Chambers) 13 to 25 (From [N_2O])	#Mean: 0.054% #Range: 0.042 to 0.065%	Not distinguished	▪ Chambers may have enhanced the measured N_2O flux, possibly due to wind speed ▪ Diurnal variation insignificant on the stream reach scale ▪ Measured N_2O flux was only 0.0006% of the NO_3^--N that moved through the reach ▪ N_2O sat. positively correlated with DO, pH, negatively with DIC ▪ Mean dissolved N_2O: 1.6 µg N-N_2O L^{-1}
[Clough et al., 2011]						
Braided gravel-bed river with mixed land use catchment, New Zealand	Sampled surface water for dissolved N_2O, used calculated gas exchange rate to calculate N_2O emissions	20 to 1360 Mean: 570	16 to 30	#Range: 0.05 to 1.69%	Denitrification or nitrification	▪ N_2O fluxes strongly, positively correlated with NO_3^--N concentrations ▪ Nitrate isotopically confirmed from agricultural, sewage sources ▪ No clear correlation between DOC and N_2O saturation ▪ Lower N_2O saturation possibly due to high turbulence and outgassing
[Cole and Caraco, 2001]						
Large, tidal freshwater river draining forest and agricultural land, New York, USA	Sampled surface water for dissolved N_2O, used gas exchange rate to calculate N_2O emissions (long-term)	3.8 to 12.6	~2 to 22 Long term average: 6.4	#Mean: 0.10%	Not distinguished	▪ Spatial variability exceeded seasonal variability. ▪ Despite high NO_3^-, nitrate was a minor source (13%) of N_2O from the watershed ▪ Either nitrification or denitrification could account for observed N_2O flux

[Gardner et al., 2016]						
Three forested and agriculturally impacted streams, Maryland, USA	Sampled surface water for dissolved N_2O, used gas exchange rate to calculate N_2O emissions	8 to 5194	-1.3 to 2828	*Range: 0 to 6.5%	Denitrification (acknowledge possibility of other pathways)	▪ A mean of 74% of stream water N_2 was from groundwater; only 12% of N_2O was from groundwater ▪ Significant positive relationship between NO_3^- and N_2O concentrations ▪ Increase in temperature caused an exponential increase in N_2O production and emission and a linear increase in N_2 production
[Garnier et al., 2009]						
1st through 8th order streams and rivers in an urban and agricultural catchment, Seine Basin, France	Sampled surface water for dissolved N_2O, used calculated gas exchange rate to calculate N_2O emissions	0 to 11,000	4 to 354		Not distinguished	▪ Highest N_2O emissions from headwater streams and polluted higher order rivers, lowest N_2O from intermediate streams ▪ Higher N_2O emissions in summer
[Guérin et al., 2008]						
2 rivers downstream of tropical reservoirs, French Guiana and Panama	Sampled N_2O emissions at the air-water interface using floating chambers		15 to 328 Means: 36-163		Not distinguished (assume nitrification due to low NO_3^- and high NH_4^+)	▪ N_2O fluxes downstream of the reservoir higher than above the reservoir.
[Harrison and Matson, 2003]						
Agricultural drainage canals, Sonora, Mexico	Suspended chambers over river surface to collect gas samples; also measured dissolved N_2O in surface water, estimated emissions using gas exchange rate	0 to 14,380	0 to 2446 Mean: 165		Nitrification and Denitrification	▪ Highest N_2O fluxes during summer, with green algae blooms and high organic carbon, nitrogen, and oxygen concentrations in surface water ▪ Positive correlation between N_2O and NH_4^+ and DO suggests importance of nitrification ▪ When nitrate was high, denitrification was C-limited
[Harrison et al., 2005]						
Agricultural drainage canal, Sonora, Mexico	Collected surface water every 2 hours for 24 hours, measured N_2O, other species and dissolved gases	0 to 1300	~400 to 2000 7 am to 10 pm 0 12 am to 8am		Not distinguished	▪ N_2O Sampling N_2O only during the day would overestimate N_2O flux 38% ▪ Denitrification during daylight, accelerate shortly after nightfall, ceased until morning ▪ N_2O likely from coupled nitrification-denitrification
[Hasegawa et al., 2000]						
Small river in agricultural area of Saitama Prefecture, Japan	Suspended chambers over river surface, collected gas samples	0 to 20,000	240 to 56,580		Denitrification (assumed due to high NO_3^- and organic matter)	▪ Dissolved concentration 7 to 407 µg N-N_2O L^{-1} ▪ Extremely high N_2O emissions; river was fed by nitrate-rich spring water and organic waste water ▪ Due to high carbon and nitrate, N_2O production attributed to denitrification

[Hemond and Duran, 1989]						
Small river just below WWTP, Massachusetts, USA	Measured dissolved N₂O in surface water, calculated flux from measured gas exchange rate; calculated benthic flux from mass balance	Mean: 810	~50 to 1300 Mean: 159		Not distinguished	▪ Sediments were a source of N₂O in the cold season and a sink in the warm season ▪ Water column rates of N₂O production were negligible
[Hlaváčová et al., 2006]						
2nd order lowland stream, agricultural catchment, Czech Republic	Measured dissolved N₂O in surface water, calculated flux from gas exchange rate; also measured N₂O emissions using floating chambers		0 to 133 Mean: 45 (Chambers) 53 to 1114 Mean: 276 (From [N₂O])		Not distinguished	▪ Values from three methods for quantifying N₂O emissions (including static chambers described below) were not correlated. ▪ Fluxes calculated from dissolved N₂O and gas transfer velocity were much higher than fluxes from floating chambers ▪ Environmental and hydrologic parameters influencing gas transfer velocity change spatially and temporally (within hours)
[Laursen and Seitzinger, 2004]						
3 small, turbid rivers draining agricultural and suburban basins, New Jersey, Illinois, and Indiana, USA	Measured net N₂O flux, oxygen consumption, and denitrification based on net changes in dissolved gas concentrations in surface water	1,274 to 14,266	5.6 to 840 Median: 96.6		Denitrification Coupled Nitrification-denitrification	▪ Rivers were consistently sources of N₂O, slightly more N₂O emissions at night ▪ Slight increases in NO₃⁻ during the day ▪ Denitrification rates were higher during the day, possibly due to increased nitrification (higher pH and temperature)
[McElroy et al., 1978; Elkins et al., 1980]						
Large, tidally-influenced river, Potomac River, USA	Measured dissolved N₂O concentrations in surface water from 0 to 10 m depth	~ 50 to 1200	(conc.) 0 to 12 μg N-N₂O L⁻¹	#Up to ~5%	Assume mostly nitrification	▪ Highest N₂O concentrations downstream of WWTP ▪ Assume nitrification source due to spatial association with nitrite ▪ N₂O is inversely correlated with DO ▪ N₂O yield higher in 1977 with low flow, low DO; N₂O lower in 1978 with higher flow and DO ▪ N₂O concentrations increase with depth, suggesting source in sediment
[McMahon and Dennehy, 1999]						
Large river impacted by WWTP and agricultural discharge, Colorado, USA	Suspended chambers over river surface, collected 10 ml gas sample every 6 minutes for 24 minutes; also measured dissolved N₂O 5 mm below the surface	0 to 9,800 in river 0 to 48,000 in alluvial aquifer	Overall median: 62.1 Range of medians: <3.7 to 1358		Denitrification and Nitrification	▪ N₂O increased downstream ▪ Total inorganic N explained 68% variance in N₂O emissions ▪ Highest emissions downstream of wastewater treatment plants, likely due to nitrification of NH₄⁺ in addition to denitrification ▪ N₂O may also be transported from soils, aquifers, and wastewater treatment plants
[Mulholland and Valett, 2004]						
1st order stream draining temperate forest, Tennessee, USA	Added ¹⁵NO₃⁻ tracer, measured dissolved N₂O in surface water for 7-8 hours, estimated emissions from air-water gas exchange and NO₃⁻ assimilation rates	27 to 13 (ambient) 166 to 580 (NO₃⁻ addition)	0.2 (ambient NO₃⁻) 1.5 (NO₃⁻ addition) (only tracer)	*0.15% (ambient NO₃⁻) *3.2% (NO₃⁻ addition)	Denitrification (isotope tracer)	▪ N₂O production was about 6x higher with NO₃⁻ addition ▪ Decrease in NO₃⁻ downstream indicates net uptake (assimilation) ▪ Carbon limitation may have contributed to denitrification decrease and N₂O yield increase with NO₃⁻ addition

[Rosamond et al., 2012]					
7th order river draining urban and agricultural land and influenced by WWTPs, Canada	Sampled surface water for dissolved N_2O, used modeled gas exchange coefficients to calculate N_2O emissions	0 to 9,000	-40.8 to 4900	Denitrification (assumed, acknowledge nitrification and DNRA)	• Highest N_2O emissions in urban areas downstream of WWTPs during summer nights with low DO • Large spatial and diel variability in emissions • DO explained more of variability in N_2O emissions than NO_3^- or DIN
[Schade et al., 2016]					
3 1st order streams with varied DOC and NO_3^-, New Hampshire, USA	Sampled surface water monthly for dissolved N_2O, used modeled and measured gas exchange coefficients to calculate N_2O emissions	~30 to 3200	Means: -28 to 252	Denitrification (assumed)	• High N_2O flux in stream with high DOC and high NO_3^-; low N_2O flux in stream with high DOC and low NO_3^- • N_2O increased with NO_3^- and decreased with DOC in one stream; decreased with NO_3^- and increased with DOC in another stream with higher nitrate • Magnitude of N_2O fluxes was higher when estimated with modeled vs measured gas transfer velocities
[Soued et al., 2015]					
321 high latitude rivers, lakes, ponds, Quebec, Canada	Measured dissolved N_2O in surface water, calculated deviation from saturation to determine flux (values shown are for rivers)	0 to 42	Mean: 0.7 Range: -27 to 79	Unspecified	• Pristine inland waters may be N_2O sinks • N_2O under-saturation most likely with low pH, high DOC, low oxygen • N_2O fluxes could not be predicted by linear regression with measured environmental variables • Highest N_2O emissions in fall
[Stow et al., 2005]					
Main stem and tributaries of river in mixed use catchment, USA	Suspended static chambers over river surface, collected gas samples; measured over species in the surface water	0 to 1300	Mean: 12.9 Range: -9.2 to 64.9	Unspecified	• Nitrate was primary driving variable for N_2O emissions, also positive relationships between N2O flux and DOC and water temperature • Highest N_2O during warmest months, but no clear seasonal pattern
[Turner et al., 2015]					
19 streams (9 stream orders) in the Corn Belt, USA	Sampled N_2O gas from flow-through, non-steady state chambers over the stream surface		<0.9 to 1739	Unspecified	• Exponential decline in N_2O flux with Strahler stream order, due to either lower concentrations or lower gas exchange downstream • Headwater streams are supersaturated, 4th order streams near equilibrium • More variability in N_2O fluxes in low order streams
[Turner et al., 2016]					
350 km reach of the Upper Mississippi River, USA	Pumped surface water (30 cm below surface) to a boat-mounted flow-through sampling system,	Mean: 339 Range: 215 to 452	Mean: 25.2 (August) 10.1 (April-October)	Acknowledge nitrification and denitrification	• Nitrate was the most important variable driving N_2O flux, followed by temperature • Secondary factors (turbidity, pH, DOM, and DO) affect the efficiency of nitrate removal • With increasing N, NO_3^- removal efficiency decreases and the relationship to N_2O flux weakens • N_2O hotspots associated with WWTP, but agriculture was a larger source of N

Setting	Technique	NO$_3^-$	N$_2$O Flux	N$_2$O Yield	Source of N$_2$O (attributed)	Key Observations
[Venkiteswaran et al., 2014]						
300 km reach of 7th-Order Grand River, Ontario Canada	Measured dissolved N$_2$O and other parameters in surface water, calculated flux using gas-exchange; also sampled groundwater	~0 to 2032	75th percentile: 90 Range: 0 to >4300		Denitrification (assume due to relationship with hypoxia)	▪ Highest N$_2$O flux in urban sections with low DO ▪ Higher N$_2$O fluxes at warmer temperatures ▪ N$_2$O production most strongly explained by DO ▪ N$_2$O fluxes are better predicted by nonlinear models (instead of linear models with NO$_3^-$)
Laboratory incubations of stream/river water (and suspended sediments)						
[Beaulieu et al., 2010]						
Large, impounded river, Ohio River, USA	Incubations of 4 L of water under river ambient conditions for 48 hours	500 to 1300	-5 to 244		Nitrification (assumed due to DO saturated surface water)	▪ Pelagic processes accounted for 26% of N$_2$O emissions in summer; production increased with NH$_4^+$ concentrations downstream of wastewater treatment effluent
[Cébron et al., 2005]						
Large river heavily influenced by WWTP, Seine River, France	Batch incubations (controlled DO, pH) and continuous cultures (vary DO, add NH$_4^+$) of river water	6500 to 12,700	(conc.) 0.036 to 5.96 µg N-N$_2$O L^{-1}		Nitrification and Nitrifier Denitrification	▪ Peak N$_2$O production rate between 1.1 and 1.5 mg L^{-1} DO ▪ N$_2$O was produced predominantly by nitrification and nitrifier denitrification ▪ N$_2$O production rate increased with NH$_4^+$ before reaching a plateau; also increased with nitrite
[García-Ruiz et al., 1999]						
Eutrophic tributary to 3rd order river, England	Incubations of 30 ml samples at 15°C for 24 hours	2254 to 31,864	0		n/a	▪ No evidence of N$_2$O production in the water column. ▪ Samples were passed through 0.45 µm filters before incubation

N$_2$O Flux is reported per square meter of stream/river area.

Table 2.5.   N$_2$O Production and Yield in Lotic Settings: Sediments

Setting	Technique	NO$_3^-$ (µg N-NO$_3^-$ L^{-1})	N$_2$O Flux (µg N-N$_2$O m^{-2} h^{-1})	N$_2$O Yield (N$_2$O/N$_2$)* (N$_2$O/(N$_2$+N$_2$O))^ (N$_2$O/ NO$_3^-$)#	Source of N$_2$O (attributed)	Key Observations
In-situ measurements of groundwater or porewaters in stream/river sediments						
[Burgos et al., 2015]						
Coastal river heavily influenced by urban	Pore water samples collected from intact sediment cores (60 cm depth)	23.8 to 3997 Mean: 1749	2.5 to 130		Denitrification (assumed)	▪ Highest N$_2$O concentrations below the surface, but depth varies by core location

and agricultural discharge, Spain						▪ Assume denitrification is the source of N_2O in the sediments; nitrification is the source in the water column
[Clough et al., 2007b]						
Groundwater in a forested riparian zone of a 2nd order tributary, Rhode Island, USA	Added labeled $^{15}N_2O$ and conservative tracers to the groundwater (65 cm depth), sampled after 4 hours to measure N_2O consumption	0	(conc.) 4.1 µg N-N_2O L^{-1}		Denitrification (assumed due to low DO, lack of NH_4^+)	▪ Denitrification responsible for depletion of $^{15}N_2O$ and overall decline in N_2O ▪ DO<1 mg L^{-1}
[Gardner et al., 2016]						
Groundwater feeding forested and agriculturally impacted streams, Maryland, USA	Pore water samples collected from piezometers screened 40-60 cm below the streambed, measured dissolved N_2O and NO_3^-.	0 to 18,200	-2.1 to 151	*Range: 0 to 0.34%	Denitrification or nitrification	▪ N_2O from groundwater only about 15% of stream water N_2O ▪ Positive, linear relationship between NO_3^- and N_2O in groundwater suggests a terrestrial nitrification source and oxic flow paths
[Hasegawa et al., 2000]						
Groundwater from an agricultural area of Saitama Prefecture, Japan	Sampled groundwater from several wells (less than 10 m depth), measured dissolved N_2O concentrations	10,000 to 70,000	(conc.) 0 to 28.2 µg N-N_2O L^{-1}		Nitrification (assumed due to high DO and low TOC)	▪ Highest dissolved N_2O in stockbreeding areas ▪ N_2O concentrations were higher in June than in November
[Hlaváčová et al., 2006]						
2nd order lowland stream, agricultural catchment, Czech Republic	Measured flux of N_2O from the streambed using static chambers, compared to fluxes from floating chambers and flux calculated from dissolved N_2O		0 to 34 Mean: 8.2		Not distinguished	▪ Values from three methods for quantifying N_2O emissions (including static chambers described below) were not correlated. ▪ N_2O fluxes from the sediment were lower than fluxes from floating chambers and fluxes calculated from dissolved N_2O ▪ Hyporheic sediments emitted N_2O on all sampling occasions
[Lansdown et al., 2015]						
Subsurface water (groundwater and hyporheic zone) of the River Leith, UK	Pore water samples collected from 10, 20, 30, 50, and 100 cm below the streambed, measured NO_3^-, N_2O, N_2, DO, DOC.	0 to >8,400		^Range: 0 to 51%, Median = 6%	Denitrification (isotopically confirmed)	▪ Hotspots of incomplete denitrification (N_2O production) most strongly correlated with reducing conditions (high NH_4^+, Fe(II), CH_4) and high microbial activity (low DO and fast denitrification rates) ▪ 80% of denitrification occurred between 10 and 100 cm depth
[McElroy et al., 1978]						
Large, tidally-influenced river, Potomac River, USA	Pore water samples collected from 0 to 42 cm depth below the streambed.		(conc.) 0 to 35 µg N-N_2O L^{-1}		Not distinguished	▪ High N_2O concentrations near the sediment-water interface, low concentrations between 8 and 30, large and increasing concentrations below 30 cm ▪ N_2O concentration minimum is evidence for consumption

[Quick et al., 2016]						
Artificial stream, similar to a headwater stream with bedform sand dunes	Pore water samples collected from artificial stream channels, measured dissolved N_2O over time and with NO_3^- additions	0 to 2,500	(conc.) 0 to 123 µg N-N_2O L^{-1}	#6.1% (potential)	Denitrification (isotopically confirmed), possibly other pathways	▪ N_2O production increases over time, presumably due to decreasing carbon availability ▪ N_2O production increases with surface water NO_3^- ▪ N_2O consumption increases with hyporheic residence time (thereby decreasing emissions)

Laboratory incubations of stream/river sediments

[Barnes and Owens, 1999]						
5 sites along the Humber river and estuary, England	Sediment cores (0-15 cm depth) incubated with river/estuary water in the dark under in situ temperatures for 4 hours, N_2O production rate based on change in concentration	462 to 8400	5 to 705		Nitrification (inferred from isotopes)	▪ Highest supersaturation of N_2O in the summer ▪ A nearby estuary with coarse sediment, low nitrate, and low turbidity was not supersaturated with N_2O ▪ The turbidity maximum in the upper reaches of the estuary (increased residence times of bacteria on particulates and elevated substrate) is the major source of N_2O

[Beaulieu et al., 2010]						
Large, impounded river, Ohio River, USA	Sediment cores (top 10 cm) incubated for 6 hours, N_2O production determined from change in dissolved N_2O in overlying water	500 to 1,300	0.2 to 15.8		Not specified	▪ Sediments accounted for 14% of N_2O emissions, may be low due to underestimation from incubation method ▪ Production increased with NO_3^- amendment, stirring of overlying water ▪ N_2O production rates not related to NO_3^- concentration, likely due to narrow range of NO_3^- concentrations ▪ N_2O production was NO_3^- limited at all but one site

[García-Ruiz et al., 1998a]						
3rd order lowland eutrophic tributary, River Wiske, England	Intact sediment cores (top 7 cm), acetylene inhibition (4 hours) and ^{15}N tracer (slurries) for N_2O and denitrification rates; slurries used for carbon test	2296 to 31,864	-175 to 6958	^Mean: 42% ^Range: 0 to 100%	Denitrification	▪ Denitrification rate decreases with depth down to 7 cm; increases with temperature ▪ N_2O production lowest during winter, increases in spring and peaks in July ▪ N_2O production accounted for an average of 42% of N gases produced by NO_3^- reduction (range: 0-100%) ▪ Addition of organic substrate decreased N_2O yield from nitrate reduction

[García-Ruiz et al., 1998b]						
50 sites from 31 rivers, 2nd to 6th order, NE England	Sediment (0-5 cm depth) mixed with river water to create 30 ml slurries, incubated at 15°C for 3 hours, N_2O production determined from change before and after incubation, denitrification determined using acetylene inhibition	3.4 to 8174 Mean: 1935	<0 to 183 µg N-N_2O kg^{-1} h^{-1} (dry)	^Mean: 18% ^Range: 0.1 to 115%	Denitrification (acknowledge nitrification and DNRA)	▪ Denitrification rate and N_2O concentration positively correlated with NO_3^- and percentage of fine particles (<100 µm) in the sediment ▪ Denitrification rate increases downstream, perhaps due to higher NO_3^-, lower velocity, and finer sediments ▪ N_2O concentration positively correlated with total C, total N; no simple or multiple relationship between N_2O yield and any analyzed variables

[García-Ruiz et al., 1999]						
Headwater to tidal river and eutrophic	Intact sediment cores (6-10 cm depth) incubated with river water for 4 hours,	7 to 31,864	Means: 1.4 to 2254		Denitrification	▪ Highest N_2O production in eutrophic river

Location	Method				Process	Findings
tributary, River Swale-Ouse and River Wiske, England	N₂O production determined from change before and after incubation		Range: -259 to 6958		(acknowledge nitrification and DNRA)	▪ No significant correlation between N₂O production with any environmental variable, but significant positive relationship with denitrification rate at each site ▪ N₂O production and NO_3^- concentration increase with distance downstream ▪ Positive relationship between NO_3^- and N₂O production at any site on annual timescale. ▪ Higher N₂O production in the late spring and summer.
[Kelso et al., 1997]						
3 rivers draining grassland and grazing areas, Northern Ireland	Sediment (5 cm sections to 15 cm depth) homogenized, amended with NH_4^+, glucose, and $^{15}NO_3^-$. Incubated at 23°C for up to 5 days	1,000 to 4,000		^Range: 2 to 75%	DNRA and Denitrification	▪ Highest N₂O yield in 6-10 cm depth on day 1, decreased by day ▪ N₂O yield higher in deeper sediments with low glucose
[Seitzinger, 1987, 1988]						
Large, tidally-influenced river, Potomac River, USA	Intact sediment cores (0-15 cm depth) incubated with aerated water in the dark at 22°C		30.8 to 280	*Range: 0.5 to 4.3%		▪ As cited in [*Seitzinger*, 1988] ▪ Higher N₂O fluxes and yields from in river sediments than in coastal and lake sediments
[Silvennoinen et al., 2008a]						
High-latitude eutrophic river draining forest, wetlands, and agricultural areas, Finland	Intact sediment cores (0-20 cm depth) incubated with circulating water at temperatures 5-20°C and a range of oxygen concentrations for 4 weeks	420	Up to 7	*Range: <0.1% to 1.7%	Denitrification (acknowledge nitrification and DNRA)	▪ N₂O efflux decreased and denitrification rates increased with temperature ▪ N₂O yield increased with low temperature ▪ Highest N₂O efflux with anoxic treatment, suggesting denitrification as the source
[Silvennoinen et al., 2008b]						
High-latitude eutrophic river draining forest, wetlands, and agricultural areas, Finland	Intact sediment cores (0-20 cm depth) incubated at 15°C with circulating water with 10-300 µM $^{15}NO_3^-$ for 1 week at a time, flux determined from difference between in- and outflowing water	<1 to 4,200	2.4 to 39.7	*Range: 1.0-3.9%	Denitrification (and some coupled nitrification-denitrification)	▪ N₂O yield increased with NO_3^- up to 100 µM, but leveled off with higher nitrate ▪ Proportion of NO_3^- denitrified decreased with additional NO_3^- ▪ NO_3^- stimulates microbial assimilation and mineralization ▪ Little evidence for DNRA
Laboratory incubations of riparian sediments						
[Groffman et al., 2000]						
Poorly-drained, forested riparian sediment, Rhode Island, USA	Intact sediment cores (15 cm diameter x 40 cm) incubated with natural groundwater enriched with 5 mg L⁻¹ N-NO3⁻	5,000		*Range: 0.2 to 4.7%	Denitrification (assumed)	▪ N₂O yield increased with low pH ▪ N₂O yield decreased with denitrification rate ▪ Large range of riparian N₂O emission rates

N₂O Flux is reported per square meter of sediment.

2.6 Linking Pathways and Settings for N_2O Production and Emissions

Section Summary: In the literature, denitrification is likely the dominant process leading to nitrous oxide emissions from streams. Denitrification occurs predominantly in sediments, resulting in the hyporheic zone and groundwater as strong contributors to N_2O emissions. Denitrification, nitrification, and nitrifier denitrification may all occur associated with suspended sediments in the water column, and nitrification is likely in surface waters high in DO and NH_4^+, though more work is required to distinguish between nitrification and nitrifier denitrification as N_2O sources. Evidence for DNRA as a source of N_2O is lacking, but more explicit studies of this pathway are needed to understand this potentially significant source.

This section describes which pathways for N_2O production are likely to contribute to lotic emissions, and where (hyporheic zone, groundwater flow paths, or water column) these pathways are most likely to occur. These interpretations are based on the requirements of the biogeochemical pathways in section 2.3, the descriptions of the physical settings in section 2.4, and the observations from multiple stream and river-based N_2O studies presented in section 2.5. While it would be ideal to rely wholly on studies that have looked specifically at settings and pathways for N_2O in streams, the research does not always exist, and related literature (in soils, for example), is extrapolated to fill the gap.

2.6.1 Lotic Settings for N_2O Production from Denitrification Pathway

N_2O generation by the denitrification pathway requires a source of nitrate and sub-oxic, reducing, conditions to promote nitrate reduction. These observations suggest sediments and subsurface flow paths associated with the hyporheic zone and groundwater discharge are most likely to support this pathway. Indeed, the vast majority of N_2O oxide generation in these groundwater and hyporheic settings is attributed to the denitrification pathway, either due to isotopic confirmation [Clough et al., 2007b; Lansdown et al., 2015], correlation with denitrification rates, or correlation with factors favoring

denitrification (NO_3^-, DOC, and low DO) [García-Ruiz et al., 1998a, 1998b, 1999; Groffman et al., 2000; Silvennoinen et al., 2008a, 2008b; Burgos et al., 2015]. When efforts have been made to evaluate reaction pathways, denitrification has often been identified as dominant. Stein and Yung [2003] reviewed multiple pathways and suggested that denitrification largely controls the rate of N_2O production in anaerobic environments, as often occurs within sediments. However, much of the lotic N_2O literature has not explicitly evaluated other reaction pathways, suggesting widespread confirmation bias.

In rivers, there is recent evidence that water column denitrification may be significant. In studies of five rivers of the Midwestern United States, Reisinger et al. [2016] measured sediment and water column denitrification rates based on samples of river water and the top 5 cm of bed sediment in laboratory mesocosms. They found that the water column could have higher biogeochemical activity rates than the sediments (accounting for 0 to 85% of the areal river denitrification rate). Per gram dry mass, water column denitrification rates were approximately 10,000 times higher than sediment denitrification rates. While this effort did not measure in-situ rates, it does suggest that water column N_2O generation by the denitrification pathway should not be discounted. The likely driver of the denitrification pathway in the water column is anaerobic microsites on suspended particles [Tiedje, 1988]. Liu et al. [2013] documented increased denitrification rates in river water with increasing turbidity and suggested that the absence of mass transport limitations (from the bulk water column into suspended particles) could produce high reaction rates.

In instances where researchers explicitly compared sediment N_2O generation with that of the overlying water column, subsurface processes typically dominate in lakes

[Seitzinger and Kroeze, 1998], oceans [Sigman et al., 2003; Devol, 2015], and estuaries [McElroy et al., 1978; Herbert, 1999; Burgos et al., 2015]. However, some of these studies observed significant water column N_2O generation, and on a global scale, nitrate reduction is partitioned 70% to sediments and 30% to the water column [DeVries et al., 2012], a ratio roughly consistent with that observed by Sigman et al. [2003].

2.6.2 Lotic Settings for N_2O Production from Nitrification

A number of studies have evoked the nitrification pathway to explain observed N_2O generation in lotic settings [McMahon and Dennehy, 1999; Harrison and Matson, 2003; Guérin et al., 2008; Beaulieu et al., 2010, 2011], often based on elevated ammonia [Guérin et al., 2008] or oxic conditions [Beaulieu et al., 2010]. However, only a few studies have collected data that directly identifies this pathway [e.g. Barnes and Owens, 1999; Cébron et al., 2005]. The nitrification pathway requires a source of the reduced nitrogen species, ammonia, and conditions supportive of its oxidation. This suggests the nitrification pathway may be an important source of N_2O in systems where ammonia is high but oxygenated conditions are maintained, likely limiting its occurrence to the water column and shallow bed sediments. Lotic systems of particular note are those with high fertilizer runoff or sewage treatment discharge or areas where significant sub-oxic organic carbon degradation produces ammonia [McMahon and Dennehy, 1999; Beaulieu et al., 2010].

There is substantial ambiguity about the prevalence of the nitrification pathway in the water column of streams. Nitrifiers require aerobic conditions to oxidize ammonia to nitrite and nitrate. However, at low NH_4^+ concentrations (<0.1 mg L^{-1} $N-NH_4^+$), nitrifiers in the water column may not compete successfully with phytoplankton for ammonium

[Farnworth et al., 1979]. On the other end of the spectrum, in highly polluted rivers, nitrification is inhibited by low oxygen concentrations [Farnworth et al., 1979]. Additionally, both NH_4^+ and NO_2^- oxidation are inhibited by light [Ryabenko, 2013], so nitrification may be restricted in clear surface waters. There is some evidence that nitrifying bacteria populations in streams are highest in the top centimeter of aerated bed sediments and attached to macrophytes [Farnworth et al., 1979]. Since nitrifiers grow slowly, they may be more likely to carry out nitrification while attached to sediments instead of in the moving water columns of streams and rivers [Pauer and Auer, 2000]. In turbid, but still oxic, rivers, nitrification rates in the water column may be high due to lack of competition for NH_4^+ from photosynthetic phytoplankton, nitrifier growth on the surface on suspended sediment particles, and lower light inhibition [Xia et al., 2009].

There is some direct evidence of N_2O generation by nitrification in the water column. Barnes and Owens [1999] concluded that the main source of N_2O emissions from the Humber River estuary in the UK was water column nitrification at the turbidity maximum. Based on incubations of river water and suspended sediments from the Ohio River, Beaulieu et al. [2010] found that water column processes accounted for 26% of N_2O emissions from the river. This study and several others [McElroy et al., 1978; Rosamond et al., 2012; Borges et al., 2015; Burgos et al., 2015] observed that emissions increased with NH_4^+ concentrations downstream of wastewater treatment plants. This trend is consistent with N_2O generation by the nitrification or nitrifier denitrification pathways. Based on the assumption of more aerobic conditions in the surface water and more anaerobic conditions in hyporheic and aquifer sediment, some authors have hypothesized that N_2O production occurs due to denitrification in sediments and

nitrification of suspended sediments in the surface water [Burgos et al., 2015; Turner et al., 2016].

<u>2.6.3 Lotic Settings for N$_2$O Production by Nitrifier-Denitrification</u>

To our knowledge, there have been no in situ observations of the nitrifier-denitrification pathway in lotic settings, however, there is also limited evidence researchers have actively attempted to measure its occurrence (Tables 2.4 and 2.5). Cébron et al. [2005], however, incubated cultures of nitrifying bacteria in water from the Seine River (France) and observed peak N$_2$O production in the narrow range of 1.1 to 1.5 mg DO L^{-1}, indicating the likelihood of nitrifier denitrification in these waters. It is likely that some of the N$_2$O broadly attributed to "nitrification" in the lotic literature may have been generated by nitrifier-denitrification. Studies that have assumed a value for the N$_2$O yield of nitrification [e.g. Beaulieu et al., 2011] may actually be using a possible value for N$_2$O yield from nitrifier denitrification [Goreau et al., 1980; as cited in Seitzinger and Kroeze, 1998]. Based on reports of hydroxylamine oxidation and chemodenitrification in the literature (see section 2.3.2), it is unlikely that the N$_2$O yield of nitrification is as high as the N$_2$O yield for nitrifier denitrification; in situ studies of N$_2$O production via nitrification are needed to constrain this potentially important source.

As with the nitrification pathway, elevated ammonia concentration is a likely prerequisite for this pathway. Elevated ammonia concentrations are most typically observed in larger order rivers impacted by human or animal waste streams; in these systems, the nitrifier-denitrification pathway may be important. Because of the coupled oxidation-reduction nature of this reaction pathway, it is less likely to occur in groundwater or deeper in the hyporheic zone where redox conditions are typically more

stable and homogeneous. Rather, this reaction pathway may be important in lotic settings characterized by micro-reductive sites in oxygenated systems, analogous to those found in soils. Such conditions may exist associated with organic carbon rich suspended material in the water column [Cébron et al., 2005] or shallow bed sediments in contact with oxic surface waters (benthic or shallow hyporheic zone). More work is required to distinguish the contribution of nitrifier denitrification to overall N_2O emissions.

It is experimentally challenging to distinguish the nitrification and nitrifier-denitrification pathways in natural lotic settings. Both require ammonia as an initial reactant and conditions supportive of its oxidation, while nitrifier-denitrification requires subsequent reductive conditions. Partitioning which pathway produces observed N_2O would likely require application of isotopic approaches and/or microbial population characterization studies.

2.6.4 Lotic Settings for N_2O Production by the DNRA

The conditions needed for the DNRA pathway to generate N_2O are similar to those for denitrification; elevated nitrate concentrations and sub-oxic conditions to promote nitrate reduction are both prerequisites. In fact, it is likely DNRA and denitrification pathways may occur simultaneously [Brunet and Garcia-Gil, 1996; Bonin et al., 1998; Stevens et al., 1998]. Intriguingly, DNRA may be favored over denitrification, especially when there is higher carbon availability [Kelso et al., 1997; Fazzolari et al., 1998; Lansdown et al., 2012] and more continuously anaerobic conditions that select for fermentative or obligate anaerobes [Kelso et al., 1997]. In homogenized sediment cores from rivers in Northern Ireland, Kelso et al. [1997] suggested that DNRA was the predominant nitrate reduction pathway because the low

flow rates, low DO, and elevated carbon from algal blooms, favored DNRA. In intact

sediment cores from a eutrophic high latitude river, however, Silvennoinen et al. [2008b]

found little evidence for DNRA. In sediment slurries from the River Leith, UK,

Lansdown et al. [2012] found that DNRA was only responsible for a small percentage of

the NO_3^- reduction (denitrification reduced the majority), probably due to low carbon

levels. While DNRA may ultimately be implicated in many instances of N_2O generation,

there is substantial uncertainty regarding the role of this new pathway in lotic systems;

studies that specifically identify the contribution of DNRA to N_2O production are needed.

2.6.5 Lotic Settings for Anammox and Feammox

The inhibitory roles of anammox and feammox in N_2O production remain poorly

constrained due to a limited understanding of how prevalent these processes may be in

different lotic settings. Because anammox is an anaerobic process, low oxygen conditions

are a prerequisite [Dalsgaard and Thamdrup, 2002]. Because both of these processes

involve the oxidation of NH_4^+, a source of ammonia is also a requirement. Finally,

anammox and feammox require an oxidizing agent, NO_2^- and Fe^{3+}, respectively. The

coupled need for both low oxygen and presence of nitrite and ferric iron suggests redox

transition zones that are rich in organic carbon but have iron oxides or nitrate present are

good candidate lotic settings. Such conditions may be found in the shallow hyporheic

zone and perhaps the water column of some more turbid, organic rich rivers. Some

evidence of anammox was observed in sediments from the River Leith [Lansdown et al.,

2012], but others have shown the process is unimportant in streams and rivers [Burgin

and Hamilton, 2007]. In contrast, [Lansdown et al., 2016] concluded that anammox is as

significant as denitrification in the hyporheic zone in some permeable river beds.

Similarly, feammox may only limit N_2O production in more restricted settings (e.g. iron-rich soils with fluctuating oxygen conditions) [Clément et al., 2005]. The feammox pathway has been observed in wetlands [Clément et al., 2005] and paddy soils [Ding et al., 2014] and tropical upland soils [Yang et al., 2012], but more research is necessary to determine its potential impact on lotic nitrogen cycling.

2.7 Master Variables Influencing N_2O Cycling in Lotic Settings

Section Summary: Key variables influencing N_2O cycling include concentrations of the primary reactants (nitrate and ammonia), organic carbon, and dissolved oxygen, which may vary temporally with season and time of day. Increasing nitrate and ammonia generally result in higher N_2O production; however, the impact on yield is more complex. Elevated organic carbon availability generally promotes denitrification. However, N_2O yield is generally higher when organic carbon is less available or less reactive. Temperature and DO vary over days and months, modulating the influence of microbial processes (mainly denitrification and nitrification) in N_2O production.

2.7.1 The Influence of Nitrate and Ammonia Concentrations

Based on the key observations in Table 2.4, Table 2.5, Table A.3 and described in section 2.5, nitrate concentration strongly influences N_2O production, yield, and emissions. With some exceptions, a positive relationship between nitrate concentration and N_2O production and/or emission was observed in lotic sediments and surface waters (Figure 2.8). Presumably, N_2O increases with NO_3^- due to incomplete denitrification. This is supported by studies that measured both denitrification rate and N_2O rates [e.g. García-Ruiz et al., 1998a, 1998b; Beaulieu et al., 2011]. Streams with low nitrate may be undersaturated with respect to N_2O, and may be a sink for nitrous oxide [Baulch et al., 2011].The relationship between nitrate and N_2O is not always simple, however. As observed in the upper Mississippi River by Turner et al. [2016], nitrate reduction by denitrification becomes less efficient as nitrate concentration increases, resulting in a

leveling off of the relationship between NO_3^- and N_2O (above about 3 mg $N\text{-}NO_3^-$ L^{-1} in the Mississippi River). Rosamond et al. [2012] found that the highest N_2O emissions occurred at moderate nitrate concentrations. These observations are consistent with the suggestion that nitrate reduction via denitrification becomes less efficient at high nitrate concentrations either because more nitrate is lost to assimilation and mineralization [Silvennoinen et al., 2008b], or the stream's nitrate reducing capacity is exceeded as all of the sedimentary denitrification "sites" are utilized [Alexander et al., 2009].

Similarly, N_2O yield was observed to increase with nitrate addition [Mulholland and Valett, 2004] or increase up to a point. Based on a eutrophic river, Silvennoinen et al. [2008b] found that N_2O yield increased with nitrate up to 1.4 mg $N\text{-}NO_3^-$ L^{-1}, but then decreased. However, some studies concluded that N_2O yield was unrelated to NO_3^- concentrations [Beaulieu et al., 2011].

Although most studies reported a much stronger relationship between nitrate and N_2O, in agricultural, urban or residential watersheds downstream of wastewater treatment plants, N_2O production was also observed to increase with NH_4^+ concentrations [Beaulieu et al., 2010]. This relationship points to N_2O production from either nitrification, coupled nitrification-denitrification, or nitrifier denitrification. In general, NH_4^+ entering streams is removed more rapidly than NO_3^- because it sorbs readily to sediments and its assimilation is more energetically favorable than NO_3^- assimilation [Peterson et al., 2001; Kemp and Dodds, 2002]. As a result, NH_4^+ concentrations tend to be high in streams and rivers only immediately downstream of exogenous sources [e.g. Beaulieu et al., 2010; Rosamond et al., 2012]; it is in these settings that N_2O is more likely to be correlated with ammonia concentrations. For example, the highest N_2O emissions in several studies were

observed downstream of wastewater treatment plants. [McElroy et al., 1978; McMahon and Dennehy, 1999; Hasegawa et al., 2000; Beaulieu et al., 2010; Rosamond et al., 2012; Borges et al., 2015; Burgos et al., 2015].

2.7.2 The Influence of Organic Carbon

In general, denitrification rates in lotic settings increase with carbon availability. García-Ruiz et al. [1998b] found that intact sediment cores for 31 streams and rivers in NE England produced N_2O in concentrations proportional to the total carbon and nitrogen in the system. More specifically, both the denitrification rate and the N_2O concentration correlated with nitrate and the percentage of fine particulate organic matter (<100 μm) in the sediment. This observation is consistent with denitrification carried out by heterotrophic microbes [Seitzinger, 1988]. Carbon also allows aerobic respiration to occur, consuming oxygen and creating anaerobic conditions favorable for denitrification [Tiedje, 1988; Stevens et al., 1997; Addy et al., 1999; Megonigal et al., 2004; Arango et al., 2007; Liu et al., 2013].

In the most general terms, organic carbon availability is positively correlated with denitrification, and therefore N_2O production. The relationship between organic carbon and N_2O emissions is complex, however. While increasing organic carbon in sediments promotes the denitrification pathway, declines in organic carbon availability have been shown to increase N_2O yields [Kelso et al., 1997; García-Ruiz et al., 1998a; Mulholland and Valett, 2004]. In sediment cores from a eutrophic river, the addition of organic substrate decreased N_2O yield [García-Ruiz et al., 1998a]. In flume experiments mimicking small streams, dissolved N_2O concentrations in pore waters increased over time as carbon reactivity decreased due to consumption by respiration [Quick et al.,

2016]. Baulch et al. [2011] found that N_2O consumption occurred with higher dissolved organic carbon (DOC), leading to reduced N_2O emissions. Similarly, in a study of 321 lakes, rivers, and ponds, Soued et al. [2015] observed that bodies of water with high DOC, low pH, and low DO were undersaturated with N_2O and acted as possible N_2O sinks. In headwater streams, Beaulieu et al. [2011] found N_2O yield to be unrelated to DOC and POC (particulate organic carbon), although N_2O yield did decrease with aerobic respiration rate, which can be a reflection of declining labile carbon availability. This may be explained by the observation that denitrification slows or stops at the intermediates NO_2^- or N_2O when there is little carbon, increasing the N_2O yield from denitrification [Tiedje, 1988; Firestone and Davidson, 1989].

2.7.3 Temporal Variations (Seasonal and Diel)

Temporal variation was observed in lotic N_2O emissions, as described in Section 2.5.2. In most studies investigating changes over time, nitrous oxide emissions tended to be higher in the spring and summer and slightly higher at night. These temporal changes in N_2O could be tied to variations in temperature, light, discharge, and turbidity; in turn, these variables influence biological activity rates, solubility of O_2 and N_2O, and pH. Additionally, inputs of carbon and nitrogen to the hyporheic zone and surface water vary temporally. For example, the input of allochthonous carbon in some streams is related to seasonal leaf fall [Bernhardt and Likens, 2011]. Inputs of nitrate and ammonia may be tied to the timing of fertilizer application in agricultural catchments [Stevenson and Cole, 1999]. Seasonally high discharge (e.g. spring runoff) may increase the wetted perimeter and extent of the hyporheic zone, as well as dilute inputs of reactive nitrogen. On a

shorter timescale, flooding events may rework particulate carbon in the sediments and/or flush nitrate from flooded soils into the stream [Audet et al., 2017].

To varying degrees, warmer temperatures tend to increase microbial processes, including those that produced N_2O. An increase in denitrification rate with temperature has been observed in laboratory [Maag and Vinther, 1996; Martin et al., 2001; Kemp and Dodds, 2002] and in-situ studies [García-Ruiz et al., 1998a; McCutchan Jr. and Lewis Jr., 2008; Gardner et al., 2016] and could explain the increase in N_2O production. Increasing temperature enhances microbial respiration rates, consuming oxygen and creating anaerobic conditions. Additionally, oxygen solubility decreases with temperature, so the rates of nitrogen cycling pathways that favor low O_2 or anaerobic conditions (including denitrification and nitrifier denitrification) would be expected to increase with temperature. Laboratory studies [Maag and Vinther, 1996; Kemp and Dodds, 2002; Strauss et al., 2004; Starry et al., 2005] have also shown an increase in nitrification rates with temperature; this may explain increases in N_2O in aerobic zones during warm seasons. However, the contribution of nitrification to N_2O is low relative to that of denitrification, particularly as high temperatures lead to more reducing conditions [Maag and Vinther, 1996]. In the large, impounded Ohio River, temperature explained approximately 70% of the seasonal variation in N_2O emissions [Beaulieu et al., 2010]. Even without clear seasonal trends, Stow et al. [2005] observed a positive relationship between N_2O flux and water temperature.

Interestingly, N_2O yield may decrease with higher temperatures, even as denitrification or nitrification rates increase. In a high latitude river, Silvennoinen et al. [2008a] observed the highest N_2O yield at low temperature. Baulch et al. [2011] observed

that more N_2O consumption occurs at high temperatures. These two observations are consistent with soil experiments, in which Maag and Vinther [1996] found that with increasing temperature, N_2 production increases more than the production of N_2O, decreasing yield. In summary, N_2O yield may decrease during warm seasons, but the overall N_2O emissions are higher due to higher overall denitrification rates.

Diel variation may be related to interrelated factors, such as light, temperature, and DO. Rosamond et al. [2012] observed the highest N_2O emissions from a 7th order river during summer nights and concluded that hypoxia could explain the higher N_2O emissions better than temperature or nitrate. In ten Canadian streams, Baulch et al. [2012] measured the highest N_2O concentrations at night when DO, pH, and temperature were all low. NO_3^- was higher during the day, and NH_4^+ was highest at night. Low nighttime nitrate could be explained by higher nighttime denitrification rates. Presumably, at night, photosynthesis (and autotrophic oxygen production) ceases, while respiration (including heterotrophic oxygen consumption) continues, so dissolved oxygen levels decrease, favoring NO_3^- conversion to N_2O during anaerobic denitrification.

Unlike Rosamond et al. [2012], which attributed most N_2O variation to changes in DO, Baulch et al. [2012] could not define a single variable that could predict the degree of diel variation in N_2O. In three small rivers, Laursen and Seitzinger [2004] observed slightly higher N_2O emissions at night, but concluded that there was not a clear diurnal pattern in their study area. The lack of a diurnal pattern may be due to the turbidity of the river, which decreased light penetration and lessened the effect of variations in photosynthesis by benthic algae. Diel variations in pH also influence N processing. As primary production increases with temperature, pH decreases, leading to the more

nitrification in the late afternoon [Warwick, 1986]; however, N_2O production from nitrification is more likely with low pH [Van Cleemput and Baert, 1984; Schreiber et al., 2012]. This is consistent with lower daytime N_2O emissions.

2.8 Synthesis

> **Section Summary:** Models that combine hydromorphogical and chemical variables are most likely to provide the best predictions of N_2O emissions. Such models and some observations suggest that N_2O emissions decrease downstream as sedimentary processes (likely denitrification) decrease relative to processes in the surface water (likely nitrification). Downstream sites could have large N_2O emissions, however, due to inputs of DIN. Future research should include investigations into chemical pathways, and also take into account methodological biases and temporal variation.

The preceding sections have discussed chemical pathways, physical settings, and actual observations of nitrous oxide from streams and rivers. Ostensibly, the power in understanding how, where, and why N_2O is produced and emitted from streams lies in being able to make predictions about lotic environments where detailed studies of N_2O emissions have yet to be conducted. Such predictions allow scientists to target their research on potential spatial and temporal N_2O hotspots and will ideally lead to strategies for mitigating future emissions. These predictions would also aid in scaling up observations from a collection of individual studies to regional or global estimates of N_2O emissions [Hu et al., 2016].

2.8.1 N_2O Emissions along the River Continuum

In recent years, attempts have been made to describe variations in N_2O emissions from headwaters to estuaries. Based on a study of 19 streams with 9 stream orders, Turner et al. [2015] observed high variability in emissions from low order streams as well as a decline with N_2O flux with stream order. The authors hypothesized this decrease was due to either lower concentrations of dissolved N_2O or lower gas exchange downstream.

In the Seine River Basin, France, Garnier et al. [2009] observed the highest N_2O emissions from headwater streams and polluted higher order rivers; intermediate streams emitted the least N_2O. Along eutrophic or highly impacted stream and river systems, McMahon and Dennehy [1999], and García-Ruiz et al. [1999] observed an increase in N_2O flux downstream.

The numerous factors that contribute to the potential for N_2O emissions vary across stream types, enabling some prediction of which process or processes will contribute most significantly to N_2O emissions from different types of streams. In line with the River Continuum concept, physical variables (and biological functionality) of a river system change predictably from headwaters to mouth and can be very broadly divided into headwaters (orders 1-3), medium-sized streams (orders 4-6), and large rivers (orders >6) [Vannote et al., 1980]. Marzadri et al. [2017] used hydromorphological data (flow velocity, hydraulic depth, mean channel width, channel slope, median grain size, and type of bed forms) and chemical data (NO_3^- and NH_4^+ concentrations) from multiple N_2O emission studies to develop a scaling relationship between stream/river parameters and N_2O emissions. Based on their work, they divided streams into three zones based on width; < 10 m (zone 1), 10-30 m (zone 2) and > 30 m (zone 3). They found that the average flux of N_2O emissions per unit area decreases from headwater streams to rivers, consistent with the observations of Turner et al. [2015].

Marzadri et al. [2017] attributed the downstream decrease in N_2O emissions to a shift in the predominant source of N_2O, from the hyporheic zone and benthic zone (sediment-water interface) in small streams (zone 1) to the water column and benthic zone and the predominant source of N_2O in rivers (zone 3) (N_2O from groundwater was

assumed to be negligible) [Marzadri et al., 2017]. This is consistent with the general observations that the percent hyporheic exchange decreases with stream order [Anderson et al., 2005] and that increasing turbidity downstream increases the potential contribution of N_2O production on suspended sediments [Xia et al., 2009; Liu et al., 2011; Reisinger et al., 2016]. As described in section 2.6, the hyporheic zone tends to produce more N_2O than the water column except in cases of high turbidity, so the shift from hyporheic processing to water column processing generally results in lower N_2O emissions. Additionally, although high order rivers may still have a large potential for biogeochemical processing in the hyporheic zone [Gomez-Velez and Harvey, 2014], longer hyporheic residence times in rivers may result in the consumption of N_2O produced in the hyporheic zone [e.g. Quick et al., 2016].

It should be noted that the Marzadri et al. [2017] study used a dimensionless flux, F^*N_2O, the ratio between the average N_2O emission flux per unit area and the total flux per unit streambed area of dissolved inorganic nitrogen (DIN) species (NO_3^- and NH_4^+). In other words, F^*N_2O decreases downstream, but the downstream decrease in actual N_2O emissions per unit area depends strongly on the DIN in the stream or river. Exogenous inputs of nitrate or ammonia from agricultural runoff or wastewater likely strongly dictate the magnitude of N_2O flux at all stream orders. This reconciles the model with observations of increasing N_2O emissions downstream in rivers affected by high DIN inputs [García-Ruiz et al., 1999; McMahon and Dennehy, 1999], high N_2O fluxes associated with urban [Venkiteswaran et al., 2014] and agricultural [Turner et al., 2016; Audet et al., 2017] areas, and N_2O undersaturation in pristine headwater streams with low DIN [Soued et al., 2015]. Point sources of reactive nitrogen, such as wastewater

treatment plants, can create 'hotspots' of N_2O production, leading to some of the largest observed lotic emissions of N_2O [McMahon and Dennehy, 1999; Hasegawa et al., 2000; Rosamond et al., 2012].

The model relating stream hydromorphological parameters and DIN flux to N_2O emissions may be able, at least qualitatively, to predict downstream trends. For example, in studies of streams and rivers in the Seine River Basin, France, Garnier et al. [2009] found that N_2O emissions were highest in 1st and 2nd order streams, decreased in intermediate streams, and then increased in higher order rivers with more urban reactive nitrogen inputs, as would be predicted by the model. In summary, headwater streams are important sources of N_2O due to high rates of hyporheic exchange and greater total streambed area and length [Gomez-Velez and Harvey, 2014; Marzadri et al., 2017], but rivers with high turbidity or DIN loading may also be important sources of N_2O emissions. Models of lotic N_2O emissions need to account for both hydrological and chemical variables.

2.8.2 Directions for Future Research

The generalizations made in the previous sections have documented exceptions, but provide a starting point for future studies. As shown in Tables 2.4, 2.5, and A.3, relatively few lotic N_2O studies have been carried out in situ, though the number is increasing. Laboratory experiments, while useful in identifying pathways and manipulating variables, may not accurately represent conditions in actual streams and rivers. In-situ studies are necessary to better quantify actual lotic N_2O emissions and develop accurate models.

The efficacy of any future mitigation efforts depends on understanding not just how much N_2O is emitted, but also where and why. In future studies, more efforts should be made, when possible, to determine the chemical pathway for N_2O production. Stable isotope tracers are useful in gaining insight into chemical pathways [e.g. Sutka et al., 2006]. Discussions of N_2O emissions should also take into account the location (shallow sediments, deep sediments, suspended sediments, etc.) of N_2O production, as the location highly influences the probability of consumption or release and emission [Meyer et al., 2008]. In-situ measurements methods, such as the USGS Mini-Point sampler [Böhlke et al., 2009; Harvey et al., 2013] for example, could aid in identifying the N_2O contribution of sediments relative to surface water.

Field-based studies of N_2O production and emission should also include measurements of carbon, oxygen, and DIN availability as much as possible, since these factors are closely tied to the predominance of the different pathways and the magnitude of the N_2O emissions.

In-situ measurements of dissolved N_2O concentrations in surface water should also be accompanied by measurement of the gas transfer velocity for each stream or river. Emission rates estimated from concentrations of dissolved N_2O in the surface water may be highly dependent on the method used to calculate the gas-transfer velocity based on empirical equations, as demonstrated by studies using multiple methods [Hlaváčová et al., 2006; Borges et al., 2015; Schade et al., 2016; Audet et al., 2017].

When collecting samples from the field or conducting in-situ studies, it is important to take into account the time of day and season, as high temporal variability may introduce sampling bias. For example, N_2O emissions at a given location in a stream

or river tend to be higher at night, so annual emissions based on in-situ studies would likely be underestimated if all sampling occurs during the day, particularly if a stream or river experiences large shifts in temperature, light, DO, and pH on a daily basis. Temporal variability may be present in temperature, DIN loading (e.g. related to the timing of fertilizer runoff or the percentage of stream flow that is wastewater treatment effluent), carbon availability (e.g. related to the timing of events that introduce particulate organic matter to the sediments, such as seasonal leaf fall or flooding), and DO (e.g. related to cycles of photosynthesis and respiration). As demonstrated by Baulch et al. [2011], certain locations may be N_2O sources or sinks depending on the time of year. Rosamond et al. [2012] and Baulch et al. [2012] observed diel variations in N_2O and suggested that sampling during the day may underestimate annual emissions.

Looking forward, a key research objective of the hydrologic community should continue to be quantifying N_2O emissions from rivers and streams. This will require both measurements of actual emissions and well-informed and calibrated scaling models such as those suggested by Marzadri et al. [2017] and Hu et al. [2016]. Better quantification of lotic N_2O emissions will inform and adjust the emission factors incorporated into IPCC greenhouse gas budgets [Nevison, 2000; Clough et al., 2011]. As the magnitude of lotic N_2O emissions are better constrained, focus should be placed on strategies for mitigation [e.g. Hasegawa et al., 2000]. Both of these objectives (quantification and mitigation) will benefit from looking more closely at the biogeochemical pathways and physical settings for N_2O production and consumption.

2.9 Acknowledgments

2.10 References

Addy, K. L., A. J. Gold, P. M. Groffman, and P. A. Jacinthe (1999), Ground water nitrate removal in subsoil of forested and mowed riparian buffer zones, *J. Environ. Qual.*, *28*(May), 962–970, doi:10.2134/jeq1999.00472425002800030029x.

Alexander, R. B., J. K. Böhlke, E. W. Boyer, M. B. David, J. W. Harvey, P. J. Mulholland, S. P. Seitzinger, C. R. Tobias, C. Tonitto, and W. M. Wollheim (2009), Dynamic modeling of nitrogen losses in river networks unravels the coupled effects of hydrological and biogeochemical processes, *Biogeochemistry*, *93*(1–2), 91–116, doi:10.1007/s10533-008-9274-8.

Anderson, B., K. Barlett, S. Frolking, K. Hayhoe, J. Jenkins, and W. Salas (2010), Methane and Nitrous Oxide Emissions From Natural Sources, , (April), 1–194, doi:EPA 430-R-10-001.

Anderson, J. K., S. M. Wondzell, M. N. Gooseff, and R. Haggerty (2005), Patterns in stream longitudinal profiles and implications for hyporheic exchange flow at the H.J. Andrews Experimental Forest, Oregon, USA, *Hydrol. Process.*, *19*(15), 2931–2949, doi:10.1002/hyp.5791.

Appelo, C. A. J., and D. Postma (2005), *Geochemistry, Groundwater and Pollution*, 2nd ed., A.A. Balkema Publishers, Leiden, The Netherlands.

Arango, C. P., J. L. Tank, J. L. Schaller, T. V. Royer, M. J. Bernot, and M. B. David (2007), Benthic organic carbon influences denitrification in streams with high nitrate concentration, *Freshw. Biol.*, *52*(7), 1210–1222, doi:10.1111/j.1365-2427.2007.01758.x.

Audet, J., M. B. Wallin, K. Kyllmar, S. Andersson, and K. Bishop (2017), Nitrous oxide emissions from streams in a Swedish agricultural catchment, *Agric. Ecosyst. Environ.*, *236*, 295–303, doi:10.1016/j.agee.2016.12.012.

Babbin, A. R., and B. B. Ward (2013), Controls on nitrogen loss processes in Chesapeake Bay sediments., *Environ. Sci. Technol.*, *47*(9), 4189–96, doi:10.1021/es304842r.

Bange, H. W. (2008), *Nitrogen in the Marine Environment*, 2nd ed., Academic Press, Burlington, MA.

Bardini, L., F. Boano, M. B. Cardenas, R. Revelli, and L. Ridolfi (2012), Nutrient cycling in bedform induced hyporheic zones, *Geochim. Cosmochim. Acta*, *84*, 47–61, doi:10.1016/j.gca.2012.01.025.

Barnes, J., and N. J. P. Owens (1999), Denitrification and nitrous oxide concentrations in the Humber estuary, UK, and adjacent coastal zones, *Mar. Pollut. Bull.*, *37*(3–7), 247–260, doi:10.1016/S0025-326X(99)00079-X.

Baulch, H. M., S. L. Schiff, R. Maranger, and P. J. Dillon (2011), Nitrogen enrichment and the emission of nitrous oxide from streams, *Global Biogeochem. Cycles*, *25*(4), 1–15, doi:10.1029/2011GB004047.

Baulch, H. M., P. J. Dillon, R. Maranger, J. J. Venkiteswaran, H. F. Wilson, and S. L. Schiff (2012), Night and day: short-term variation in nitrogen chemistry and nitrous oxide emissions from streams, *Freshw. Biol.*, *57*(3), 509–525, doi:10.1111/j.1365-2427.2011.02720.x.

Baxter, C. V, and F. R. Hauer (2000), Geomorphology, hyporheic exchange, and selection of spawning habitat by bull trout (Salvelinus confluentus), *Can. J. Fish. Aquat. Sci.*, *57*(7), 1470–1481.

Beaulieu, J. J., W. D. Shuster, and J. A. Rebholz (2010), Nitrous oxide emissions from a large, impounded river: The Ohio river, *Environ. Sci. Technol.*, *44*(19), 7527–7533, doi:10.1021/es1016735.

Beaulieu, J. J. et al. (2011), Nitrous oxide emission from denitrification in stream and river networks, *Proc. Natl. Acad. Sci. U. S. A.*, *108*(1), 214–219, doi:10.1073/pnas.1011464108.

Bengtsson, G., S. Fronæus, and L. Bengtsson-Kloo (2002), The kinetics and mechanism of oxidation of hydroxylamine by iron(iii), *J. Chem. Soc. Dalt. Trans.*, (12), 2548–2552, doi:10.1039/b201602h.

Bernhardt, E. S., and G. E. Likens (2011), Dissolved Organic Carbon Enrichment Alters Nitrogen Dynamics in a Forest Stream, *Ecology*, *83*(6), 1689–1700.

Betlach, M. R., and J. M. Tiedje (1981), Kinetic Explanation for Accumulation of Nitrite , Nitric Oxide , and Nitrous Oxide During Bacterial Denitrification, *Appl. Environ. Microbiol.*, *42*(6), 1074–1084.

Boano, F., A. Demaria, R. Revelli, and L. Ridolfi (2010), Biogeochemical zonation due to intrameander hyporheic flow, *Water Resour. Res.*, *46*(2), 1–13, doi:10.1029/2008WR007583.

Boano, F., J. W. Harvey, A. Marion, A. I. Packman, R. Revelli, L. Ridolfi, and A. Wörman (2014), Hyporheic flow and transport processes: Mechanisms, models, and biogeochemical implications, *Rev. Geophys.*, *52*, 603–679, doi:10.1002/2012RG000417.

Böhlke, J. K., R. C. Antweiler, J. W. Harvey, A. E. Laursen, L. K. Smith, R. L. Smith, and M. a. Voytek (2009), Multi-scale measurements and modeling of denitrification in streams with varying flow and nitrate concentration in the upper Mississippi River basin, USA, *Biogeochemistry*, *93*(1–2), 117–141, doi:10.1007/s10533-008-9282-8.

Bollmann, A., and R. Conrad (1998), Influence of O2 availability on NO and N2O release by nitrification and denitrification in soils, *Glob. Chang. Biol.*, *4*(4), 387–396, doi:10.1046/j.1365-2486.1998.00161.x.

Bonin, P., P. Omnes, and A. Chalamet (1998), Simultaneous occurrence of denitrification and nitrate ammonification in sediments of the French Mediterranean Coast, *Hydrobiologia*, *389*, 169–182, doi:10.1023/A:1003585115481.

Borges, A. V. et al. (2015), Globally significant greenhouse-gas emissions from African inland waters, *Nat. Geosci.*, *8*(8), 637–642, doi:10.1038/ngeo2486.

Bremner, A. J. M., and A. M. Blackmer (1978), Nitrous Oxide : Emission from Soils During Nitrification of Fertilizer Nitrogen, *Science (80-.).*, *199*(4326), 295–296.

Bremner, J. M. (1997), Sources of nitrous oxide in soils, *Nutr. Cycl. Agroecosystems*, *49*, 7–16, doi:10.1023/A:1009798022569.

Bremner, J. M., and A. M. Blackmer (1980), Mechanisms of nitrous oxide prodcution in soils, in *Biogeochemistry of Ancient and Modern Environments*, edited by P. A. Trudinger, M. R. Walter, and B. J. Ralph, pp. 279–291, Australian Academy of Science, Canberra, Australia.

Briggs, M. a, F. D. Day-Lewis, J. P. Zarnetske, and J. W. Harvey (2015), A physical explanation for the development of redox microzones in hyporheic flow, *Geophys. Res. Lett.*, *42*, 4402–4410, doi:10.1002/2015GL064200.

Brunet, R. C., and L. J. Garcia-Gil (1996), Sulfide-induced dissimilatory nitrate reduction to ammonia in anaerobic freshwater sediments, *FEMS Microbiol. Ecol.*, *21*(2), 131–138, doi:10.1016/0168-6496(96)00051-7.

Burgin, A. J., and P. M. Groffman (2012), Soil O2 controls denitrification rates and N2O yield in a riparian wetland, *J. Geophys. Res. Biogeosciences*, *117*(1), 1–10, doi:10.1029/2011JG001799.

Burgin, A. J., and S. K. Hamilton (2007), Have we overemphasized the role of denitrification in aquatic ecosystems? A review of nitrate removal pathways, *Front. Ecol. Environ.*, *5*(2), 89–96, doi:10.1890/1540-9295(2007)5.

Burgos, M., A. Sierra, T. Ortega, and J. M. Forja (2015), Anthropogenic effects on greenhouse gas (CH4 and N2O) emissions in the Guadalete River Estuary (SW Spain), *Sci. Total Environ.*, *503–504*, 179–189, doi:10.1016/j.scitotenv.2014.06.038.

Butterbach-Bahl, K., E. M. Baggs, M. Dannenmann, R. Kiese, and S. Zechmeister-Boltenstern (2013), Nitrous oxide emissions from soils: how well do we understand the processes and their controls?, *Philos. Trans. R. Soc. Lond. B. Biol. Sci.*, *368*(1621), 1–13, doi:10.1098/rstb.2013.0122.

Cardenas, M. B., J. Wilson, and V. Zlotnik (2004), Impact of heterogeneity, bed forms, and stream curvature on subchannel hyporheic exchange, *Water Resour. Res.*, *40*(8), 1–14, doi:10.1029/2004WR003008.

Cavigelli, M. A., and G. P. Robertson (2000), The Functional Significance of Denitrifier Community Composition in a Terrestrial Ecosystem, *Ecology*, *81*(5), 1402–1414, doi:10.2307/177217.

Cébron, A., J. Garnier, and G. Billen (2005), Nitrous oxide production and nitrification kinetics by natural bacterial communities of the lower Seine river (France), *Aquat. Microb. Ecol.*, *41*(1), 25–38.

Chapuis-Lardy, L., N. Wrage, A. Metay, J.-L. Chotte, and M. Bernoux (2007), Soils, a sink for N2O? A review, *Glob. Chang. Biol.*, *13*(1), 1–17, doi:10.1111/j.1365-2486.2006.01280.x.

Ciais, P. et al. (2013), Carbon and Other Biogeochemical Cycles, in Climate Change 2013: The Physical Science Basis. Contribution of Working Group I to the Fifth Assessment Report of the Intergovernmental Panel on Climate Change, edited by T. Stocker, D. Qin, G.-K. Plattner, M. Tignor, S. Allen, J. Boschung, A. Nauels, Y. Xia, V. Bex, and P. Midgley, p. 1535, Cambridge University Press, Cambridge, United Kingdom, and New York, NY, USA.

Van Cleemput, O., and L. Baert (1984), Nitrite: a key compound in N loss processes under acid conditions?, *Plant Soil*, *76*(1), 233–241.

Clément, J. C., J. Shrestha, J. G. Ehrenfeld, and P. R. Jaffé (2005), Ammonium oxidation coupled to dissimilatory reduction of iron under anaerobic conditions in wetland soils, *Soil Biol. Biochem.*, *37*(12), 2323–2328, doi:10.1016/j.soilbio.2005.03.027.

Clough, T. J., L. E. Buckthought, F. M. Kelliher, and R. R. Sherlock (2007a), Diurnal fluctuations of dissolved nitrous oxide (N2O) concentrations and estimates of N2O emissions from a spring-fed river: Implications for IPCC methodology, *Glob. Chang. Biol.*, *13*(5), 1016–1027, doi:10.1111/j.1365-2486.2007.01337.x.

Clough, T. J., K. Addy, D. Q. Kellogg, B. L. Nowicki, A. J. Gold, and P. M. Groffman (2007b), Dynamics of nitrous oxide in groundwater at the aquatic-terrestrial

interface, *Glob. Chang. Biol.*, *13*(7), 1528–1537, doi:10.1111/j.1365-2486.2007.01361.x.

Clough, T. J., L. E. Buckthought, K. L. Casciotti, F. M. Kelliher, and P. K. Jones (2011), Nitrous oxide dynamics in a braided river system, New Zealand., *J. Environ. Qual.*, *40*(5), 1532–41, doi:10.2134/jeq2010.0527.

Cole, J. J., and N. F. Caraco (2001), Emissions of nitrous oxide (N2O) from a tidal, freshwater river, the Hudson River, New York, *Environ. Sci. Technol.*, *35*(6), 991–996, doi:10.1021/es0015848.

Conrad, R. (1996), Soil microorganisms as controllers of atmospheric trace gases (H2, CO, CH4, OCS, N2O, and NO), *Microbiol. Rev.*, *60*(4), 609–640.

CSIRO, M. and A. R. and the A. B. of M. (2016), *Cape Grim Greenhouse Gas Data*.

Čuhel, J., M. Šimek, R. J. Laughlin, D. Bru, D. Chèneby, C. J. Watson, and L. Philippot (2010), Insights into the effect of soil pH on N2O and N2 emissions and denitrifier community size and activity, *Appl. Environ. Microbiol.*, *76*(6), 1870–1878, doi:10.1128/AEM.02484-09.

Dalsgaard, T., F. J. Stewart, B. Thamdrup, L. De Brabandere, N. P. Revsbech, O. Ulloa, D. E. Canfield, and E. F. Delong (2014), Oxygen at nanomolar levels reversibly suppresses process rates and gene expression in anammox and denitrification in the oxygen minimum zone off Northern Chile, *MBio*, *5*(6), doi:10.1128/mBio.01966-14.

Dalsgaard, T., and B. Thamdrup (2002), Factors Controlling Anaerobic Ammonium Oxidation with Nitrite in Marine Sediments, *Appl. Environ. Microbiol.*, *68*(8), 3802–3808, doi:10.1128/AEM.68.8.3802.

Davidson, E. A. (2009), The contribution of manure and fertilizer nitrogen to atmospheric nitrous oxide since 1860, *Nat. Geosci.*, *2*(9), 659–662, doi:10.1038/ngeo608.

Deflaun, M. F., and M. Mayer (1983), Relationships between bacteria surfaces in intertidal sediments ’, , *28*(5), 873–881.

Dendooven, L., and J. M. Anderson (1994), Dynamics of reduction enzymes involved in the denitrification process in pasture soil, *Soil Biol. Biochem.*, *26*(11), 1501–1506, doi:10.1016/j.media.2004.06.007.

Devol, A. H. (2003), Solution to a marine mystery, *Nature*, *422*(6932), 575–576, doi:10.1038/422575a.

Devol, A. H. (2015), Denitrification, anammox, and N2 production in marine sediments., *Ann. Rev. Mar. Sci.*, *7*, 403–23, doi:10.1146/annurev-marine-010213-135040.

DeVries, T., C. Deutsch, F. Primeau, B. Chang, and A. Devol (2012), Global rates of water-column denitrification derived from nitrogen gas measurements, *Nat. Geosci.*, *5*(8), 547–550, doi:10.1038/ngeo1515.

Ding, L., X. An, S. Li, G. Zhang, and Y. Zhu (2014), Nitrogen Loss through Anaerobic Ammonium Oxidation Coupled to Iron Reduction from Paddy Soils in a Chronosequence, *Environ. Sci. Technol.*, *48*(September), 10641–10647, doi:10.1021/es503113s.

Duff, J. H., and F. J. Triska (2000), Nitrogen biogeochemistry and surface-subsurface exchange in streams, in *Streams and Ground Waters*, edited by J. B. Jones and P. J. Mulholland, pp. 197–220, Academic Press, San Diego.

Duff, J. H., A. J. Tesoriero, W. B. Richardson, E. A. Strauss, and M. D. Munn (2008), Whole-Stream Response to Nitrate Loading in Three Streams Draining Agricultural Landscapes, *J. Environ. Qual.*, *37*(3), 1133–1144, doi:10.2134/jeq2007.0187.

Edwards, R. T. (1998), The Hyporheic Zone, in *River Ecology and Management*, edited by R. J. Naiman and R. E. Bilby, pp. 399–429, Springer-Verlag, New York.

Elkins, J. W., S. . Wofsy, M. B. McElroy, and W. A. Kaplan (1980), Nitrification and Production of N2O in the Potomac: Evidence for Variability, in *Estuaries and Nutrients*, edited by L. E. Neilsen, D.J, Cronin, p. 642, Humana Press, Totowa, New Jersey.

Elliott, A. H., and N. H. Brooks (1997), Transfer of nonsorbing solutes to a streambed with bed forms : Laboratory experiments, *Water Resour. Res.*, *33*(1), 137–151.

Farnworth, E. G., M. C. Nichols, C. N. Vann, L. G. Wolfson, R. W. Bosserman, P. R. Hendrix, F. B. Golley, and J. L. Cooley (1979), Impacts of Sediment and Nutrients on Biota in Surface Waters of the United States, , 315.

Farrell, T. B. (2016), Statistical Modeling to Predict N2O Production within the Hypoheic Zone by Coupling Denitrifying Microbial Community Abundance to Geochemical and Hydrological Parameters, Boise State University.

Fazzolari, É., B. Nicolardot, and J. C. Germon (1998), Simultaneous effects of increasing levels of glucose and oxygen partial pressures on denitrification and dissimilatory nitrate reduction to ammonium in repacked soil cores, *Eur. J. Soil Biol.*, *34*(1), 47–52, doi:10.1016/S1164-5563(99)80006-5.

Firestone, M. K., and E. A. Davidson (1989), Microbiological basis of NO and N2O production and consumption in soil, in *Exchange of Trace Gases between Terrstrial Ecosystems and the Atmosphere*, edited by M. Andreae and D. Schimel, pp. 7–21, John Wiley & Sons, New York.

Firestone, M. K., M. S. Smith, R. B. Firestone, and J. M. Tiedje (1979), The Influence of Nitrate, Nitrite, and Oxygen on the Composition of the Gaseous Products of Denitrification in Soil, *Soil Sci. Soc. Am. J.*, *43*(6), 1140, doi:10.2136/sssaj1979.03615995004300060016x.

Forster, P. et al. (2007), Changes in Atmospheric Constituents and in Radiative Forcing, in Climate Change 2007: The Physical Science Basis. Contribution of Working Group I to the Fourth Assessment Report of the Intergovernmental Panel of Climate Change, edited by S. Solomon, D. Qin, M. Manning, Z. Chen, M. Marquis, K. B. Averyt, M. Tignor, and H. L. Miller, Cambridge University Press.

Galloway, J. N. et al. (2004), Nitrogen Cycles: Past, Present, and Future, *Biogeochemistry*, *70*(2), 153–226.

Galloway, J. N., A. R. Townsend, J. W. Erisman, M. Bekunda, Z. Cai, J. R. Freney, L. a Martinelli, S. P. Seitzinger, and M. a Sutton (2008), Transformation of the nitrogen cycle: recent trends, questions, and potential solutions., *Science (80-.).*, *320*(5878), 889–92, doi:10.1126/science.1136674.

Galloway, J. N., A. M. Leach, A. Bleeker, and J. W. Erisman (2013), A chronology of human understanding of the nitrogen cycle, *Philos. Trans. R. Soc. Lond. B. Biol. Sci.*, *368*(1621).

García-Ruiz, R., S. N. Pattinson, and B. A. Whitton (1998a), Denitrification and nitrous oxide production in sediments of the Wiske, a lowland eutrophic river, *Sci. Total Environ.*, *210–211*, 307–320, doi:10.1016/S0048-9697(98)00020-5.

García-Ruiz, R., S. N. Pattinson, and B. A. Whitton (1998b), Denitrification in river sediments: Relationship between process rate and properties of water and sediment, *Freshw. Biol.*, *39*(3), 467–476, doi:10.1046/j.1365-2427.1998.00295.x.

García-Ruiz, R., S. N. Pattinson, and B. A. Whitton (1999), Nitrous oxide production in the river Swale-Ouse, North-East England, *Water Res.*, *33*(5), 1231–1237, doi:10.1016/S0043-1354(98)00324-8.

Gardner, J. R., T. R. Fisher, T. E. Jordan, and K. L. Knee (2016), Balancing watershed nitrogen budgets: accounting for biogenic gases in streams, *Biogeochemistry*, *127*(2–3), 231–253, doi:10.1007/s10533-015-0177-1.

Garnier, J., G. Billen, G. Vilain, A. Martinez, M. Silvestre, E. Mounier, and F. Toche (2009), Nitrous oxide (N2O) in the Seine river and basin: Observations and budgets, *Agric. Ecosyst. Environ.*, *133*(3–4), 223–233, doi:10.1016/j.agee.2009.04.024.

Gomez-Velez, J. D., and J. W. Harvey (2014), A hydrogeomorphic river network model predicts where and why hyporheic exchange is important in large basins, *Geophys. Res. Lett.*, *41*(18), 6403–6412, doi:10.1002/2014GL061099.

Gooseff, M. N., J. K. Anderson, S. M. Wondzell, J. Lanier, and R. Haggerty (2006), A modelling study of hyporheic exchange pattern and the sequence, size, and spacing of stream bedforms in mountain stream networks, Oregon, USA, *Hydrol. Process.*, *20*(11), 2443–2457, doi:10.1002/hyp.

Goreau, T. J., W. A. Kaplam, S. C. Wofsy, M. B. McElroy, F. W. Valois, and S. W. Watson (1980), Production of NO2- and N2O by nitrifying bacteria at reduced concentrations of oxygen, *Appl. Environ. Microbiol.*, *40*(3), 526–532.

Groffman, P. M., A. J. Gold, and K. Addy (2000), Nitrous oxide production in riparian zones and its importance to national emission inventories, *Chemosphere-Global Chang. Sci.*, *2*, 291–299.

Groffman, P. M., K. Butterbach-Bahl, R. W. Fulweiler, J. Arthur, J. L. Morse, E. K. Stander, C. Tague, C. Tonitto, and P. Vidon (2009), Challenges to incorporating spatially and temporally explicit phenomena (hotspots and hot moments) in denitrification models, *Biogeochemistry*, *93*(1–2), 49–77, doi:10.1007/S10533-008-9277-5.

Gu, C., G. M. Hornberger, A. L. Mills, J. S. Herman, and S. A. Flewelling (2007), Nitrate reduction in streambed sediments: Effects of flow and biogeochemical kinetics, *Water Resour. Res.*, *43*(W12413), 1–10, doi:10.1029/2007WR006027.

Guérin, F., G. Abril, A. Tremblay, and R. Delmas (2008), Nitrous oxide emissions from tropical hydroelectric reservoirs, *Geophys. Res. Lett.*, *35*(6), 2–7, doi:10.1029/2007GL033057.

Harrison, J., and P. Matson (2003), Patterns and controls of nitrous oxide emissions from waters draining a subtropical agricultural valley, *Global Biogeochem. Cycles*, *17*(3), n/a-n/a, doi:10.1029/2002GB001991.

Harrison, J. A., P. A. Matson, and S. E. Fendorf (2005), Effects of a diel oxygen cycle on nitrogen transformations and greenhouse gas emissions in a eutrophied subtropical stream, *Aquat. Sci.*, *67*(3), 308–315, doi:10.1007/s00027-005-0776-3.

Hartmann, D. L. et al. (2013), Observations: Atmosphere and Surface, in Climate Change 2013: The Physical Science Basis. Contribution of Working Group I to the Fifth Assessment Report of the Intergovernmental Panel on Climate Change, edited by T. F. Stocker, D. Qin, G.-K. Plattner, M. Tignor, S. K. Allen, J. Boschung, A. Nauels, Y. Xia, V. Bex, and P. M. Midgley, Cambridge University Press, Cambridge, United Kingdom, and New York, NY, USA.

Harvey, J. W., J. K. Böhlke, M. A. Voytek, D. Scott, and C. R. Tobias (2013), Hyporheic zone denitrification: Controls on effective reaction depth and contribution to

whole-stream mass balance, *Water Resour. Res.*, *49*(10), 6298–6316, doi:10.1002/wrcr.20492.

Hasegawa, K., K. Hanaki, T. Matsuo, and S. Hidaka (2000), Nitrous oxide from the agricultural water system contaminated with high nitrogen, *Chemosph. - Glob. Chang. Sci.*, *2*(3–4), 335–345, doi:10.1016/S1465-9972(00)00009-X.

Hemond, H. F., and A. P. Duran (1989), Fluxes of N2O at the sediment-water and water-atmosphere boundaries of a nitrogen-rich river, *Water Resour. Res.*, *25*(5), 839–846, doi:10.1029/WR025i005p00839.

Herbert, R. (1999), Nitrogen cycling in coastal marine ecosystems, *FEMS Microbiol. Ecol.*, *23*(May), 563–590.

Hlaváčová, E., M. Rulík, L. Čáp, and V. Mach (2006), Greenhouse gas (CO2, CH4, N2O) emissions to the atmosphere from a small lowland stream in Czech Republic, *Arch. für Hydrobiol.*, *165*(3), 339–353, doi:10.1127/0003-9136/2006/0165-0339.

Hooper, A. B., and K. R. Terry (1979), Hydroxylamine oxidoreductase of Nitrosomonas: Production of nitric oxide from hydroxylamine, *Biochim. Biophys. Acta-Enzymology*, *571*(1), 12–20.

Hu, H.-W., D. Chen, and J.-Z. He (2015), Microbial regulation of terrestrial nitrous oxide formation: understanding the biological pathways for prediction of emission rates, *FEMS Microbiol. Rev.*, *39*(5), 729–749.

Hu, M., D. Chen, and R. A. Dahlgren (2016), Modeling nitrous oxide emission from rivers: a global assessment, *Glob. Chang. Biol.*, *22*(11), 3566–3582, doi:10.1111/gcb.13351.

Hutchinson, G. L., and E. A. Davidson (1993), Processes for production and consumption of gaseous nitrogen oxides in soil, in *Agricultural Ecosystem Effects on Trace Gases and Global Climate Change*, edited by D. E. Rolston, L. A. Harper, A. R. Mosier, and J. M. Duxbury, pp. 79–93, American Society of Agronomy, Madison, WI.

Hynes, R. K., and R. Knowles (1984), Production of nitrous oxide by Nitrosomonas europaea: effects of acetylene, pH, and oxygen, *Can. J. Microbiol.*, *30*(11), 1397–1404.

IPCC, 2013 (2013), Summary for Policymakers, in Climate Change 2013: The Physical Science Basis. Contribution of Working Group I to the Fifth Assessment Report of the Intergovernmental Panel on Climate Change2, edited by T. F. Stocker, D. Qin, G.-K. Plattner, M. Tignor, S. K. Allen, J. Boschung, A. Nauels, Y. Xia, V. Bex, and P. M. Midgley, Cambridge University Press, Cambridge, United Kingdom, and New York, NY, USA.

Jetten, M. S. M. (2008), The microbial nitrogen cycle, *Environ. Microbiol.*, *10*(11), 2903–2909, doi:10.1111/j.1462-2920.2008.01786.x.

Jetten, M. S. M., L. Van Niftrik, M. Strous, B. Kartal, J. T. Keltjens, and H. J. M. Op den Camp (2009), Biochemistry and molecular biology of anammox bacteria., *Crit. Rev. Biochem. Mol. Biol.*, *44*(2–3), 65–84, doi:10.1080/10409230902722783.

Ji, Q., A. R. Babbin, A. Jayakumar, S. Oleynik, and B. B. Ward (2015), Nitrous oxide production by nitrification and denitrification in the Eastern Tropical South Pacific oxygen minimum zone, *Geophys. Res. Lett.*, *42*, 10755–10764, doi:10.1002/2015GL063354.

Jones, C. M., B. Stres, M. Rosenquist, and S. Hallin (2008), Phylogenetic analysis of nitrite, nitric oxide, and nitrous oxide respiratory enzymes reveal a complex evolutionary history for denitrification, *Mol. Biol. Evol.*, *25*(9), 1955–1966, doi:10.1093/molbev/msn146.

Jones, C. M., D. R. Graf, D. Bru, L. Philippot, and S. Hallin (2013), The unaccounted yet abundant nitrous oxide-reducing microbial community: a potential nitrous oxide sink, *ISME J.*, *7*(2), 417–426, doi:10.1038/ismej.2012.125.

Jones, L. C., B. Peters, J. S. Lezama Pacheco, K. L. Casciotti, and S. Fendorf (2015), Stable Isotopes and Iron Oxide Mineral Products as Markers of Chemodenitrification., *Environ. Sci. Technol.*, *49*(6), 3444–3452, doi:10.1021/es504862x.

Jørgensen, K. S., H. B. Jensen, and J. Sørensen (1984), Nitrous oxide production from nitrification and denitrification in marine sediment at low oxygen concentrations, *Can. J. Microbiol.*, *30*(8), 1073–1078, doi:10.1139/m84-167.

Kartal, B. et al. (2011), Molecular mechanism of anaerobic ammonium oxidation, *Nature*, *479*(7371), 127–130, doi:10.1038/nature10453.

Kasahara, T., and S. M. Wondzell (2003), Geomorphic controls on hyporheic exchange flow in mountain streams, *Water Resour. Res.*, *39*(1), SBH 3-1-SBH 3-14, doi:10.1029/2002WR001386.

Kaspar, H. F. (1982), Nitrite reduction to nitrous oxide by propionibacteria: Detoxicaton mechanism, *Arch. Microbiol.*, *133*(2), 126–130.

Kelso, B. H. L., R. V. Smith, R. J. Laughlin, and S. D. Lennox (1997), Dissimilatory nitrate reduction in anaerobic sediments leading to river nitrite accumulation, *Appl. Environ. Microbiol.*, *63*(12), 4679–4685.

Kemp, M. J., and W. K. Dodds (2002), The influence of ammonium, nitrate, and dissolved oxygen concentrations on uptake, nitrification, and denitrification rates associated with prairie stream substrata, *Limnol. Oceanogr.*, *47*(5), 1380–1393, doi:10.4319/lo.2002.47.5.1380.

Khalil, K., B. Mary, and P. Renault (2004), Nitrous oxide production by nitrification and denitrification in soil aggregates as affected by O2 concentration, *Soil Biol. Biochem.*, *36*(4), 687–699, doi:10.1016/j.soilbio.2004.01.004.

Kirchman, D. L. (2012), *Processes in Microbial Ecology*, 1st ed., Oxford University Press, London.

Knowles, R. (1982), Denitrification, *Microbiol. Rev.*, *46*(1), 43–70.

Kolb, S., and M. A. Horn (2012), Microbial CH4 and N2O consumption in acidic wetlands, *Front. Microbiol.*, *3*(MAR), 1–8, doi:10.3389/fmicb.2012.00078.

Kool, D. M., J. Dolfing, N. Wrage, and J. W. Van Groenigen (2011), Nitrifier denitrification as a distinct and significant source of nitrous oxide from soil, *Soil Biol. Biochem.*, *43*(1), 174–178, doi:10.1016/j.soilbio.2010.09.030.

Korom, S. F. (1992), Natural denitrification in the saturated zone: A review, *Water Resour. Res.*, *28*(6), 1657–1668, doi:10.1029/92WR00252.

Lansdown, K., M. Trimmer, C. M. Heppell, F. Sgouridis, S. Ullah, L. Heathwaite, A. Binley, and H. Zhang (2012), Characterization of the key pathways of dissimilatory nitrate reduction and their response to complex organic substrates in hyporheic sediments, *Limnol. Oceanogr.*, *57*(2), 387–400, doi:10.4319/lo.2012.57.2.0387.

Lansdown, K., C. M. Heppell, M. Trimmer, A. Binley, A. L. Heathwaite, P. Byrne, and H. Zhang (2015), The interplay between transport and reaction rates as controls on nitrate attenuation in permeable, streambed sediments, *J. Geophys. Res. G Biogeosciences*, *120*(6), 1093–1109, doi:10.1002/2014JG002874.

Lansdown, K., B. A. McKew, C. Whitby, C. M. Heppell, A. J. Dumbrell, A. Binley, L. Olde, and M. Trimmer (2016), Importance and controls of anaerobic ammonium oxidation influenced by riverbed geology, *Nat. Geosci.*, *9*(May), 357–360, doi:10.1038/ngeo2684.

Laursen, A. E., and S. P. Seitzinger (2004), Diurnal patterns of denitrification, oxygen consumption and nitrous oxide production in rivers measured at the whole-reach scale, *Freshw. Biol.*, *49*(11), 1448–1458, doi:10.1111/j.1365-2427.2004.01280.x.

Ligi, T., M. Truu, J. Truu, H. Nõlvak, A. Kaasik, W. J. Mitsch, and Ü. Mander (2013), Effects of soil chemical characteristics and water regime on denitrification genes (nirS, nirK, and nosZ) abundances in a created riverine wetland complex, *Ecol. Eng.*, doi:10.1016/j.ecoleng.2013.07.015.

Liu, T., X. Xia, S. Liu, X. Mou, and Y. Qiu (2013), Acceleration of denitrification in turbid rivers due to denitrification occurring on suspended sediment in oxic waters, *Environ. Sci. Technol.*, *47*(9), 4053–4061, doi:10.1021/es304504m.

Liu, W., H. Yang, Y. Sun, and X. Wang (2011), δ13C Values of loess total carbonate: A sensitive proxy for Asian summer monsoon in arid northwestern margin of the Chinese loess plateau, *Chem. Geol.*, *284*(3–4), 317–322, doi:10.1016/j.chemgeo.2011.03.011.

Maag, M., and F. P. Vinther (1996), Nitrous oxide emission by nitrification and denitrification in different soil types and at different soil moisture contents and temperatures, *Appl. Soil Ecol.*, *4*(1), 5–14.

MacFarling Meure, C., D. Etheridge, C. Trudinger, P. Steele, R. Langenfelds, T. van Ommen, A. Smith, and J. Elkins (2006), Law Dome CO2 , CH4 and N2O ice core records extended to 2000 years BP, *Geophys. Res. Lett.*, *33*(14), L14810, doi:10.1029/2006GL026152.

Martikainen, P. (1985), Nitrous-oxide emission associated with autotrophic ammonium oxdation in acid coniferous forest soil, *Appl. Environ. Microbiol.*, *50*(6), 1519–1525.

Martin, L. A., P. J. Mulholland, J. R. Webster, and H. M. Valett (2001), Denitrification in sediments of headwater streams in the southern Appalachian Mountains , USA, *J. North Am. Benthol. Soc.*, *20*(4), 505–519.

Marwick, T. R., F. Tamooh, B. Ogwoka, C. Teodoru, A. V. Borges, F. Darchambeau, and S. Bouillon (2014), Dynamic seasonal nitrogen cycling in response to anthropogenic N loading in a tropical catchment, Athi-Galana-Sabaki River, Kenya, *Biogeosciences*, *11*(2), 443–460, doi:10.5194/bg-11-443-2014.

Marzadri, A., D. Tonina, and A. Bellin (2012), Morphodynamic controls on redox conditions and on nitrogen dynamics within the hyporheic zone: Application to gravel bed rivers with alternate-bar morphology, *J. Geophys. Res. Biogeosciences*, *117*(3), 1–14, doi:10.1029/2012JG001966.

Marzadri, A., M. M. Dee, D. Tonina, A. Bellin, and J. L. Tank (2017), Role of surface and subsurface processes in scaling N2O emissions along riverine networks, *Proc. Natl. Acad. Sci.*, *114*(14), 4330–4335, doi:10.1073/PNAS.1617454114.

Mayer, P. M., P. M. Groffman, E. a Striz, and S. S. Kaushal (2010), Nitrogen dynamics at the groundwater-surface water interface of a degraded urban stream., *J. Environ. Qual.*, *39*(3), 810–823, doi:10.2134/jeq2009.0012.

McCutchan Jr., J. H., and W. M. Lewis Jr. (2008), Spatial and temporal patterns of denitrification in an effluent-dominated plains river, *Verhandlungen Int. Vereinigung Limnol.*, *30*(2), 323–328.

McElroy, M. B., J. W. Elkins, S. C. Wofsy, C. E. Kolb, A. P. Dura, and W. A. Kaplan (1978), Production and release of N20 from the Potomac Estuary, *Limnol. Oceanogr.*, *23*(6), 1168–1182.

McMahon, P. B., and K. F. Dennehy (1999), N2O emission from a nitrogen-enriched river, *Environ. Sci. Technol.*, *33*(303), 21–25.

Megonigal, J. P., M. E. Hines, and P. . Visscher (2004), Anaerobic Metabolism: Linkages to Trace Gases and Anaerobic Processes, in *Treatise of Geochemistry Volume 8 Biogeochemistry*, edited by W. H. Schlesinger, pp. 317–424, Elsevier, New York.

Merill, L., and D. J. Tonjes (2014), A Review of the Hyporheic Zone, Stream Restoration, and Means to Enhance Denitrification, *Crit. Rev. Environ. Sci. Technol.*, *44*(21), 2337–2379, doi:10.1080/10643389.2013.829769.

Meyer, R. L., D. E. Allen, and S. Schmidt (2008), Nitrification and denitrification as sources of sediment nitrous oxide production: A microsensor approach, *Mar. Chem.*, *110*(1–2), 68–76, doi:10.1016/j.marchem.2008.02.004.

Mosier, A., C. Kroeze, C. Nevison, O. Oenema, and S. Seitzinger (1998), Closing the global N2O budget : nitrous oxide emissions through the agricultural nitrogen cycle inventory methodology, *Nutr. Cycl. Agroecosystems*, *52*(2–3), 225–248, doi:10.1023/A:1009740530221.

Mulholland, P., and H. Valett (2004), Stream denitrification and total nitrate uptake rates measured using a field 15 N tracer addition approach, *Limnol. Oceanogr.*, *49*(3), 809–820.

Nevison, C. (2000), Review of the IPCC methodology for estimating nitrous oxide emissions associated with agricultural leaching and runoff, *Chemosph. - Glob. Chang. Sci.*, *2*(3–4), 493–500, doi:10.1016/S1465-9972(00)00013-1.

Opdyke, M. R., M. B. David, and B. L. Rhoads (2006), Influence of geomorphological variability in channel characteristics on sediment denitrification in agricultural streams., *J. Environ. Qual.*, *35*(6), 2103–2112, doi:10.2134/jeq2006.0072.

Otte, S., N. G. Grobben, L. A. Robertson, M. S. Jetten, and J. G. Kuenen (1996), Nitrous oxide production by Alcaligenes faecalis under transient and dynamic aerobic and anaerobic conditions., *Appl. Environ. Microbiol.*, *62*(7), 2421–2426.

Otte, S., J. Schalk, J. G. Kuenen, and M. S. M. Jetten (1999), Hydroxylamine oxidation and subsequent nitrous oxide production by the heterotrophic ammonia oxidizer Alcaligenes faecalis, *Appl. Microbiol. Biotechnol.*, *51*(2), 255–261, doi:10.1007/s002530051390.

Park, S. et al. (2012), Trends and seasonal cycles in the isotopic composition of nitrous oxide since 1940, *Nat. Geosci.*, *5*(4), 261–265, doi:10.1038/ngeo1421.

Pauer, J. J., and M. T. Auer (2000), Nitrification in the water column and sediment of a hypereutrophic lake and adjoining river system, *Water Res.*, *34*(4), 1247–1254, doi:10.1016/S0043-1354(99)00258-4.

Peterson, B. J. et al. (2001), Control of nitrogen export from watersheds by headwater streams., *Science*, *292*(5514), 86–90, doi:10.1126/science.1056874.

Poth, M. (1986), Dinitrogen production from nitrite by a Nitrosomonas isolate, *Appl. Environ. Microbiol.*, *52*(4), 957–959.

Poth, M., and D. D. Focht (1985), 15N Kinetic Analysis of N2O Production by Nitrosomonas europea: an Examination of Nitrifier Denitrification, *Appl. Environ. Microbiol.*, *49*(5), 1134–1141.

Quick, A. M., W. J. Reeder, T. B. Farrell, D. Tonina, K. P. Feris, and S. G. Benner (2016), Controls on nitrous oxide emissions from the hyporheic zones of streams, *Environ. Sci. Technol.*, *50*, 11491–11500, doi:10.1021/acs.est.6b02680.

Ranalli, A. J., and D. L. Macalady (2010), The importance of the riparian zone and in-stream processes in nitrate attenuation in undisturbed and agricultural watersheds - A review of the scientific literature, *J. Hydrol.*, *389*(3–4), 406–415, doi:10.1016/j.jhydrol.2010.05.045.

Ranjard, L., F. Poly, J. Combrisson, A. Richaume, F. Gourbiere, J. Thioulouse, and S. Nazaret (2000), Heterogeneous Cell Density and Genetic Structure of Bacterial Pools Associated with Various Soil Microenvironments as Determined by Enumeration and DNA Fingerprinting Approach (RISA), *Microb. Ecol.*, *39*(4), 263–272.

Ravishankara, A. R., J. S. Daniel, and R. W. Portmann (2009), Nitrous Oxide (N2O): The Dominant Ozone-Depleting Substance Emitted in the 21st Century, *Science (80-.).*, *326*(5949), 123–125, doi:10.1126/science.1176985.

Raymond, P. A., and J. J. Cole (2001), Gas Exchange in Rivers and Estuaries: Choosing a Gas Transfer Velocity, *Estuaries*, *24*(2), 312, doi:10.2307/1352954.

Reisinger, A. J., J. L. Tank, T. J. Hoellein, and R. O. Hall (2016), Sediment, water column, and open-channel denitrification in rivers measured using membrane-inlet mass spectrometry, *J. Geophys. Res. Biogeosciences*, n/a--n/a, doi:10.1002/2015JG003261.

Richardson, W. B., E. A. Strauss, L. A. Bartsch, E. M. Monroe, J. C. Cavanaugh, L. Vingum, and D. M. Soballe (2004), Denitrification in the Upper Mississippi River: Rates, controls, and contribution to nitrate flux, *Can. J. Fish. Aquat. Sci.*, *61*(7), 1102–1112, doi:10.1139/f04-062.

Rosamond, M. S., S. J. Thuss, and S. L. Schiff (2012), Dependence of riverine nitrous oxide emissions on dissolved oxygen levels, *Nat. Geosci.*, *5*(10), 715–718, doi:10.1038/ngeo1556.

Ryabenko, E. (2013), Stable Isotope Methods for the Study of the Nitrogen Cycle, in *Topics in Oceanography*, edited by E. Zambianchi.

Schade, J. D., J. Bailio, and W. H. McDowell (2016), Greenhouse gas flux from headwater streams in New Hampshire, USA: Patterns and drivers, *Limnol. Oceanogr.*, *61*, S165–S174, doi:10.1002/lno.10337.

Schlegel, H. G. (1993), *General Microbiology*, 7th ed., Cambridge University Press, New York.

Schreiber, F., P. Wunderlin, K. M. Udert, and G. F. Wells (2012), Nitric oxide and nitrous oxide turnover in natural and engineered microbial communities: Biological pathways, chemical reactions, and novel technologies, *Front. Microbiol.*, *3*(OCT), 1–24, doi:10.3389/fmicb.2012.00372.

Schwartz, F. W., and H. Zhang (2003), *Fundamentals of Groundwater*, John Wiley & Sons, New York.

Seitzinger, S. P. (1987), *The effect of pH on the release of phosphorus from Potomac River sediment*, Annapolis, Maryland.

Seitzinger, S. P. (1988), Denitrification in freshwater and coastal marine ecosystems: Ecological and geochemical significance, *Limnol. Oceanogr.*, *33*(4), 702–724, doi:10.4319/lo.1988.33.4_part_2.0702.

Seitzinger, S. P., and C. Kroeze (1998), Global distribution of nitrous oxide production and N inputs in freshwater and coastal marine ecosystems, *Global Biogeochem. Cycles*, *12*(1), 93–113.

Shrestha, N. K., S. Hadano, T. Kamachi, and I. Okura (2002), Dinitrogen production from ammonia by Nitrosomonas europaea, *Appl. Catal. A Gen.*, *237*(1–2), 33–39, doi:10.1016/S0926-860X(02)00279-X.

Sigman, D. M., R. Robinson, A. N. Knapp, A. Van Geen, D. C. McCorkle, J. A. Brandes, and R. C. Thunell (2003), Distinguishing between water column and sedimentary denitrification in the Santa Barbara Basin using the stable isotopes of nitrate, *Geochemistry, Geophys. Geosystems*, *4*(5), 1–20, doi:10.1029/2002GC000384.

Silvennoinen, H., A. Liikanen, J. Torssonen, C. F. Stange, and P. J. Martikainen (2008a), Denitrification and N2O effluxes in the Bothnian Bay (northern Baltic Sea) river sediments as affected by temperature under different oxygen concentrations, *Biogeochemistry*, *88*, 63–72.

Silvennoinen, H., A. Liikanen, J. Torssonen, C. Florian Stange, and P. J. Martikainen (2008b), Denitrification and nitrous oxide effluxes in boreal, eutrophic river sediments under increasing nitrate load: A laboratory microcosm study, *Biogeochemistry*, *91*(2–3), 105–116, doi:10.1007/s10533-008-9262-z.

Šimek, M., L. Jíšová, and D. W. Hopkins (2002), What is the so-called optimum pH for denitrification in soil?, *Soil Biol. Biochem.*, *34*(9), 1227–1234, doi:10.1016/S0038-0717(02)00059-7.

Smith, M. S. (1982), Dissimilatory reduction of NO2 to NH4 and N20 by a soil Citrobactrer sp., *Appl. Environ. Micro.*, *43*(4), 854–860.

Sørensen, J., J. M. Tiedje, and R. B. Firestone (1980), Inhibition by Sulfide of Nitric and Nitrous Oxide Reduction by Denitrifying Pseudomonas fluorescens, *Appl. Environ. Microbiol.*, *39*(1), 105–108.

Soued, C., P. A. del Giorgio, and R. Maranger (2015), Nitrous oxide sinks and emissions in boreal aquatic networks in Québec, *Nat. Geosci.*, *9*(December), 1–7, doi:10.1038/ngeo2611.

Starry, O. S., H. M. Valett, and M. E. Schreiber (2005), Nitrification rates in a headwater stream: influences of seasonal variation in C and N supply, *J. North Am. Benthol. Soc.*, *24*(4), 753–768, doi:10.1899/05-015.1.

Stein, L. Y., and M. G. Klotz (2016), The nitrogen cycle, *Curr. Biol.*, *26*(3), R94–R98, doi:10.1016/j.cub.2015.12.021.

Stein, L. Y., and Y. L. Yung (2003), Production, isotopic composition, and atmospheric fate of biologicaly produced nitrous oxide, *Annu. Rev. Earth Planet. Sci.*, *31*(1), 329–356, doi:10.1146/annurev.earth.31.110502.080901.

Stevens, R. J., and R. J. Laughlin (1998), Measurement of nitrous oxide and di-nitrogen emissions from agricultural soils, *Nutr. Cycl. Agroecosystems*, *52*(2–3), 131–139, doi:10.1023/A:1009715807023.

Stevens, R. J., R. J. Laughlin, L. C. Burns, J. R. M. Arah, and R. C. Hood (1997), Measuring the contributions of nitrification and denitrification to the flux of nitrous oxide from soil, *Soil Biol. Biochem.*, *29*(2), 139–151, doi:10.1016/S0038-0717(96)00303-3.

Stevens, R. J., R. J. Laughlin, and J. P. Malone (1998), Soil pH affects the processes reducing nitrate to nitrous oxide and di-nitrogen, *Soil Biol. Biochem.*, *30*(8–9), 1119–1126, doi:10.1016/S0038-0717(97)00227-7.

Stevenson, F. J., and M. A. Cole (1999), *Cycles of Soil: Carbon, Nitrogen, Phosphorous, Sulfur, Micronutrients*, 2nd ed., John Wiley & Sons.

Stouthamer, A. H. (1988), Dissimilatory reduction of oxidized nitrogen compounds, in *Biology of Anaerobic Microorganisms*, edited by A. J. B. Zehnder, pp. 245–305, John Wiley & Sons, New York.

Stow, C. A., J. T. Walker, L. Cardoch, P. Spece, and C. Geron (2005), N2O emissions from streams in the Neuse River Watershed, North Carolina, *Environ. Sci. Technol.*, *39*(18), 6999–7004.

Strauss, E. A., W. B. Richardson, L. A. Bartsch, J. C. Cavanaugh, D. A. Bruesewitz, H. Imker, J. A. Heinz, and D. M. Soballe (2004), Nitrification in the Upper Mississippi River: patterns, controls, and contribution to the NO3-budget, *J. North Am. Benthol. Soc.*, *23*(1), 1–14.

Strous, M., E. Van Gerven, P. Zheng, J. G. Kuenen, and M. S. M. Jetten (1997a), Ammonium removal from concentrated waste streams with the anaerobic ammonium oxidation (anammox) process in different reactor configurations, *Water Res.*, *31*(8), 1955–1962, doi:10.1016/S0043-1354(97)00055-9.

Strous, M., E. van Gerven, J. G. Kuenen, and M. Jetten (1997b), Effects of aerobic and microaerobic conditions on anaerobic ammonium-oxidizing (anammox) sludge, *Appl. Environ. Microbiol.*, *63*(6), 2446–2448.

Strous, M., J. a Fuerst, E. H. Kramer, S. Logemann, G. Muyzer, K. T. van de Pas-Schoonen, R. Webb, J. G. Kuenen, and M. S. Jetten (1999), Missing lithotroph identified as new planctomycete., *Nature*, *400*(6743), 446–449, doi:10.1038/22749.

Sutka, R. L., N. E. Ostrom, P. H. Ostrom, J. a Breznak, a J. Pitt, F. Li, and H. Gandhi (2006), Distinguishing Nitrous Oxide Production from Nitrification and Denitrification on the Basis of Isotopomer Abundances Distinguishing Nitrous Oxide Production from Nitrification and Denitrification on the Basis of Isotopomer Abundances, *Appl. Environ. Microbiol.*, *72*(1), 638–644, doi:10.1128/AEM.72.1.638.

Sutton, M. A. et al. (2007), Challenges in quantifying biosphere-atmosphere exchange of nitrogen species, *Environ. Pollut.*, *150*(1), 125–139, doi:10.1016/j.envpol.2007.04.014.

Teodoru, C. R., F. C. Nyoni, A. V. Borges, F. Darchambeau, I. Nyambe, and S. Bouillon (2014), Spatial variability and temporal dynamics of greenhouse gas (CO2, CH4, N2O) concentrations and fluxes along the Zambezi River mainstem and major tributaries.

Thamdrup, B., and T. Dalsgaard (2002), Production of N2 through Anaerobic Ammonium Oxidation Coupled to Nitrate Reduction in Marine Sediments, *Appl. Environ. Microbiol.*, *68*(3), 1312–1318, doi:10.1128/AEM.68.3.1312.

Tiedje, J. M. (1988), Ecology of Denitrification and Dissimilatory Nitrate Reduction to Ammonium, in *Biology of Anaerobic Microorganisms*, edited by A. J. B. Zehnder, pp. 179–244, John Wiley & Sons, New York.

Tiedje, J. M., A. J. Sexstone, D. D. Myrold, and J. A. Robinson (1982), Denitrification: ecological niches, competition and survival, *Antonie Van Leeuwenhoek*, *48*(6), 569–583.

Tonina, D. (2012), Surface water and streambed sediment interaction: The hyporheic exchange, in *Fluid mechanics of environmental interfaces*, edited by C. Gualtieri and D. T. Mihailović, pp. 255–294, Taylor & Francis Group, London.

Tonina, D., and J. M. Buffington (2009), Hyporheic Exchange in Mountain Rivers I: Mechanics and Environmental Effects, *Geogr. Compass*, *3*(3), 1063–1086, doi:10.1111/j.1749-8198.2009.00226.x.

Trauth, N., C. Schmidt, M. Vieweg, U. Maier, and J. H. Fleckenstein (2014), Hyporheic transport and biogeochemical reactions in pool-riffle systems under varying ambient groundwater flow conditions, *J. Geophys. Res. Biogeosciences*, *119*(5), 910–928, doi:10.1002/2013JG002586.

Turner, P. a., T. J. Griffis, X. Lee, J. M. Baker, R. T. Venterea, and J. D. Wood (2015), Indirect nitrous oxide emissions from streams within the US Corn Belt scale with

stream order, *Proc. Natl. Acad. Sci.*, *112*(32), 201503598, doi:10.1073/pnas.1503598112.

Turner, P. A., T. J. Griffis, J. M. Baker, X. Lee, J. T. Crawford, L. C. Loken, and R. T. Venterea (2016), Regional-scale controls on dissolved nitrous oxide in the Upper Mississippi River, *Geophys. Res. Lett.*, *43*, 4400–4407, doi:10.1002/2016GL068710.Received.

Vannote, R. L., G. W. Minshall, K. W. Cummins, J. R. Sedell, and C. E. Cushing (1980), The River Continuum Concept, *Can. J. Fish. Aquat. Sci.*, *37*(1), 130–137.

Venkiteswaran, J. J., M. S. Rosamond, and S. L. Schiff (2014), Nonlinear response of riverine N2O fluxes to oxygen and temperature, *Environ. Sci. Technol.*, *48*(3), 1566–1573, doi:10.1021/es500069j.

Venterea, R. T. (2007), Nitrite-driven nitrous oxide production under aerobic soil conditions: Kinetics and biochemical controls, *Glob. Chang. Biol.*, *13*(8), 1798–1809, doi:10.1111/j.1365-2486.2007.01389.x.

Vieten, B., F. Conen, B. Seth, and C. Alewell (2008), The fate of N2O consumed in soils, *Biogeosciences*, *5*, 129–132, doi:10.5194/bgd-4-3331-2007.

Vitousek, P. M., J. D. Aber, R. W. Howarth, G. E. Likens, P. A. Matson, D. W. Schindler, W. H. Schlesinger, and D. G. Tilman (1997), Human alteration of the global nitrogen cycle: sources and consequences, *Ecol. Appl.*, *7*(3), 737–750.

Voigt, C. et al. (2017), Increased nitrous oxide emissions from Arctic peatlands after permafrost thaw, *Proc. Natl. Acad. Sci.*, 201702902, doi:10.1073/pnas.1702902114.

Warwick, J. J. (1986), Diel variation of in-stream nitrification, *Water Res.*, *20*(10), 1325–1332.

Whittaker, M., D. Bergmann, D. Arciero, and A. B. Hooper (2000), Electron transfer during the oxidation of ammonia by the chemolithotrophic bacterium Nitrosomonas europaea, *Biochim. Biophys. Acta - Bioenerg.*, *1459*(2–3), 346–355, doi:10.1016/S0005-2728(00)00171-7.

Winter, T. C., J. W. Harvey, O. L. Franke, and W. M. Alley (1998), Ground water and surface water: A single resource, *USGS Publ.*, 79.

Wrage, N., G. Velthof, M. van Beusichem, and O. Oenema (2001), Role of nitrifier denitrification in the production of nitrous oxide, *Soil Biol. Biochem.*, *33*(12–13), 1723–1732.

Wuebbles, D. J. (2009), Nitrous Oxide: No Laughing Matter, *Science (80-.).*, *326*(5949), 56–57, doi:10.1126/science.1179571.

Wunderlin, P., J. Mohn, A. Joss, L. Emmenegger, and H. Siegrist (2012), Mechanisms of N 2O production in biological wastewater treatment under nitrifying and denitrifying conditions, *Water Res.*, *46*(4), 1027–1037, doi:10.1016/j.watres.2011.11.080.

Xia, X., Z. Yang, and X. Zhang (2009), Effect of suspended-sediment concentration on nitrification in river water: Importance of suspended sediment - Water interface, *Environ. Sci. Technol.*, *43*(10), 3681–3687, doi:10.1021/es8036675.

Yan, W., L. Yang, F. Wang, J. Wang, and P. Ma (2012), Riverine N2O concentrations, exports to estuary and emissions to atmosphere from the Changjiang River in response to increasing nitrogen loads, *Global Biogeochem. Cycles*, *26*(4), doi:10.1029/2010GB003984.

Yang, W. H., K. a. Weber, and W. L. Silver (2012), Nitrogen loss from soil through anaerobic ammonium oxidation coupled to iron reduction, *Nat. Geosci.*, *5*(8), 538–541, doi:10.1038/ngeo1530.

Zarnetske, J. P., R. Haggerty, S. M. Wondzell, and M. A. Baker (2011), Dynamics of nitrate production and removal as a function of residence time in the hyporheic zone, *J. Geophys. Res. Biogeosciences*, *116*(1), 1–12, doi:10.1029/2010JG001356.

Zarnetske, J. P., R. Haggerty, S. M. Wondzell, V. a. Bokil, and R. González-Pinzón (2012), Coupled transport and reaction kinetics control the nitrate source-sink function of hyporheic zones, *Water Resour. Res.*, *48*(11), 1–15, doi:10.1029/2012WR011894.

Zhu, X., M. Burger, T. A. Doane, and W. R. Horwath (2013a), Ammonia oxidation pathways and nitrifier denitrification are significant sources of N2O and NO under low oxygen availability, *Proc. Natl. Acad. Sci.*, *110*(16), 6328–6333, doi:10.1073/pnas.1219993110/-/DCSupplemental.www.pnas.org/cgi/doi/10.1073/pnas.1219993110.

Zhu, X., L. C. R. Silva, T. a. Doane, and W. R. Horwath (2013b), Iron: The Forgotten Driver of Nitrous Oxide Production in Agricultural Soil, *PLoS One*, *8*(3), 1–6, doi:10.1371/journal.pone.0060146.

Zumft, W. G. (1997), Cell Biology and Molecular Basis of Denitrification, *Microbiol. Mol. Biol. Rev.*, *61*(4), 533–616.

Zumft, W. G., and P. M. H. Kroneck (2006), Respiratory Transformation of Nitrous oxide (N2O) to dinitrogen by bacteria and archaea, *Adv. Microb. Physiol.*, *52*(6), 107–227.

CHAPTER 3: CONTROLS ON NITROUS OXIDE EMISSIONS FROM THE HYPORHEIC ZONES OF STREAMS

Author List: Annika M. Quick,[1] W. Jeffery Reeder,[2] Tiffany B. Farrell,[1] Daniele Tonina,[2] Kevin P. Feris,[3] and Shawn G. Benner[1]

[1]Department of Geosciences, Boise State University, Boise, Idaho 83725, USA.
[2]Department of Civil Engineering, University of Idaho, Boise, Idaho 83702, USA.
[3]Department of Biological Sciences, Boise State University, Boise, Idaho 83725, USA.

Key Points:
- N_2O is both produced and consumed along hyporheic flow paths.
- N_2O concentrations peak near the aerobic/anaerobic transition along flow paths.
- Elevated nitrate and declining organic carbon reactivity increase hyporheic N_2O concentrations.

Abstract

The magnitude and mechanisms of nitrous oxide (N_2O) release from rivers and streams are actively debated. The complex interactions of hydrodynamic and biogeochemical controls on emissions of this important greenhouse gas preclude

prediction of when and where N_2O emissions will be significant. We present observations from column and large-scale flume experiments supporting an integrative model of N_2O emissions from stream sediments. Our results show a distinct, replicable, pattern of nitrous oxide generation and consumption dictated by subsurface (hyporheic) residence times and biological nitrogen reduction rates. Within this model, N_2O emission from stream sediments requires subsurface residence times (and microbially mediated reduction rates) be sufficiently long (and fast reacting) to produce N_2O by nitrate reduction, but also sufficiently short (or slow reacting) to limit N_2O conversion to dinitrogen gas. Most subsurface exchange will not result in N_2O emissions; only specific, intermediate, residence times (reaction rates) will both produce and release N_2O to the stream. We also confirm previous observations that elevated nitrate and declining organic carbon reactivity increase N_2O production, highlighting the importance of associated reaction rates in controlling N_2O accumulation. Combined, these observations help constrain when N_2O release will occur, providing a predictive link between stream geomorphology, hydrodynamics, and N_2O emissions.

3.1 Introduction

Streams are an important, but poorly constrained, source of the greenhouse gas nitrous oxide (N_2O). N_2O has approximately 300 times the warming potential of CO_2 [Forster et al., 2007] and is the dominant ozone-depleting anthropogenic substance [Ravishankara et al., 2009]. Most anthropogenic emissions are related, directly or indirectly, to agricultural practices [Davidson, 2009], with nitrogen fertilizer stimulating N_2O production in soils and in downstream systems subjected to fertilizer runoff [McMahon and Dennehy, 1999; Davidson, 2009; Park et al., 2012]. The United States

Environmental Protection Agency (EPA) [Anderson et al., 2010] estimates that natural nitrous oxide emissions from rivers are 0.1 Tg N-N_2O yr^{-1}, while a recent large scale tracer study suggests that rivers account for at least 0.68 Tg N-N_2O yr^{-1}, representing up to 10% of global anthropogenic N_2O emissions [Beaulieu et al., 2011]. Despite the potential importance of streams to the global N_2O budget, there is considerable uncertainty regarding the mechanisms and controls on its release.

While nitrogen transformations can occur in the water column of a stream, many biogeochemical reactions, including denitrification, take place in the saturated sediments beneath and immediately adjacent to streams. This area of active exchange and transformation of surface and groundwater, the hyporheic zone [Findlay, 1995], operates at a range of spatiotemporal scales [Tonina, 2012; Boano et al., 2014]. It is useful to conceptualize hyporheic flow in terms of hyporheic residence time (τ_{HZ}), the time a packet of water spends in the subsurface before returning to the stream. The hyporheic residence time is a function of flow path length and flow velocity, which are dictated by stream geomorphology and hydraulics [Marzadri et al., 2014]. Stream bedform morphology influences hyporheic residence time by modulating pressure differentials that drive water into and out of the hyporheic zone [Elliott and Brooks, 1997b]; the greater the produced hydraulic gradients, the higher the flow velocities. Dissolved gases, including N_2O, produced along these hyporheic flow paths can be released to the atmosphere after returning to the stream, a process that is potentially an important global source of N_2O [Mosier et al., 1998; Mulholland et al., 2008; Beaulieu et al., 2011].

Although a variety of processes can lead to N_2O generation under varying conditions [Stevens and Laughlin, 1998; Wrage et al., 2001; Beaulieu et al., 2011], it is generally

believed that most N_2O in saturated sediments is the product of denitrification [Davidson, 1991; Bollmann and Conrad, 1998; Lansdown et al., 2012] because of the potential for favorable anaerobic conditions. Denitrification is the sequential reduction of NO_3^- to NO_2^-, NO, N_2O, and finally to N_2 [Firestone and Davidson, 1989]. This multi-step process can be simplified to two reactions:

$$2NO_3^- + 2CH_2O + 2H^+ \Rightarrow N_2O + 2CO_2 + 3H_2O \qquad (3.1)$$

$$2N_2O + CH_2O \Rightarrow 2N_2 + CO_2 + H_2O \qquad (3.2)$$

Although N_2 is the predominant end-product of denitrification, N_2O may be observed if reaction (3.2) (N_2O reduction) is decoupled from reaction (3.1) (nitrate reduction) or if the rate of nitrate reduction is greater than the rate of N_2O reduction [Betlach and Tiedje, 1981; Baulch et al., 2011]. When discussing factors that may encourage N_2O instead of N_2 as the end product of denitrification, some authors report the N_2O *yield*, the ratio of N_2O generation to (N_2O+N_2) generation [Beaulieu et al., 2011]. It is also important to distinguish between N_2O *production* (the N_2O generated due to microbial reactions along a hyporheic flow path) and N_2O *released* (the N_2O that is not reduced to N_2 and is instead returned to the stream and potentially emitted to the atmosphere).

There is general agreement that the hyporheic zone may be a globally important source of N_2O [Mosier et al., 1998; Mulholland et al., 2008; Beaulieu et al., 2011]. In addition, groundwater flow paths and riparian zones, especially in agricultural areas, are important zones of nitrate reduction and potential N_2O production [Groffman et al., 2000; Duff et al., 2008; Stelzer et al., 2011; Lansdown et al., 2015]. There is also growing recognition that nitrate reduction, which is often considered beneficial, can produce N_2O

emissions, which are considered detrimental [Burgin et al., 2013]. However, incomplete understanding of complex interactions of water flow and the biogeochemical processes leading to N_2O release currently limit our capacity to predict conditions that lead to N_2O release.

We hypothesized nitrate loading would increase N_2O production, and hyporheic flow path lengths and velocities, coupled with organic carbon reactivity, would dictate the amount of N_2O released to the stream. We evaluated this hypothesis using large-scale column and flume experiments that allowed integration and observation of coupled hydrodynamic and biogeochemical processes. Based on our observations, we propose a predictive conceptual framework for N_2O release from hyporheic stream sediments.

3.2 Materials and Methods

We conducted a series of replicated column and flume experiments (Table 3.1), scaled to approximate a natural system, in which we monitored nitrogen transformations as water followed hyporheic flow paths. We documented the conditions under which N_2O was generated and the specific hydrologic and biogeochemical conditions that led to its release or consumption.

Table 3.1.   Experimental Setup for Column and Flume Experiments

Experiment	Geometry	Sediment	Initial POM	Duration	Parameters
Columns (1D flow paths)					
Low POM			0.05%		
Intermediate POM	1 m column x10 cm diameter	• 90% sieved quarry sand • 10% inoculum sand	0.15%	16 weeks	• DO • dissolved N_2O
High POM			0.5%		
2013 Flume Experiment (2D flow paths)					
Short dune height	1 m dune x 3 cm height				• DO • dissolved N_2O
Intermediate dune height	1 m dune x 6 cm height	• 90% sieved quarry sand • 10% inoculum sand	0.15%	16 weeks	• NO_3^- • NO_2^- • NH_4^+
Tall dune height	1 m dune x 9 cm height				• Microbial DNA
2015 Flume Experiment (2D flow paths)					
Short dune length (3 rep)	0.7 m dune x 9 cm height				• DO • dissolved N_2O • NO_3^-
Long dune length (3 rep)	1 m dune x 9 cm height	• 90% sieved quarry sand • 10% inoculum sand	0.15%	13 weeks	• NO_2^- • NH_4^+ • Microbial DNA

3.2.1 Column Experiments

Column experiments evaluated nitrous oxide generation and consumption in a quasi-one-dimensional system mimicking a single hyporheic flowline. The primary variable was the initial particulate organic carbon content (Table 3.1). PVC pipes (10 cm diameter) were fitted with water-tight caps on both ends and filled with sediment. Each column was filled with a mixture of 90% quarry sand (sieved to < 2.4 mm), 10% microbial inoculum sand (wet sieved to < 2.4 mm), and <1% particulate organic matter (POM). The microbial inoculum sand was collected from the upper Boise River at Sandy Point in Lucky Peak State Park, Idaho, USA. The natural river sand provided a natural consortium of microorganisms capable of promoting nitrogen-cycling reactions, as confirmed by preliminary genetic analysis for denitrification enzyme genes.

Black cottonwood (*Populus trichocarpa*) leaves served as particulate organic matter. Fallen leaves were collected within one week of leaf fall from the banks of the Boise River, chopped to <5 mm pieces, and stored frozen until added to the sediments. These leaves were chosen to simulate a low-order natural stream in which leaf litter from the riparian zone provides POM to the hyporheic zone [Metzler and Smock, 1990; Tillman et al., 2003]. In low-order , forested streams, DOC has been shown to increase dramatically (up to 8x) following autumn leaf fall and burial [Bernhardt and Likens, 2011], so the beginning of our experiment modeled a stream system with recent input of new POM and the release of carbon from decomposition [Metzler and Smock, 1990; Tillman et al., 2003; Bernhardt and Likens, 2011]. Samples of the leaves were analyzed using a Costech ECS 4010 Elemental Analyzer. The fallen cottonwood leaves consisted of 47.7 ±1.6%

carbon on average. The columns differed in the amount of POM added (0.05, 0.15, and 0.5% crushed leaves, by dry sediment mass).

Peristaltic pumps moved water from reservoirs (filtered tap water at room temperature open to the atmosphere to allow chlorine degassing) into the bottom of each column, simulating surface water entering the subsurface at the beginning of a hyporheic flow path. Water was pumped vertically through the columns at a rate of about 5 ml min^{-1} for 16 weeks. Flow rate was monitored during the experiment to detect changes in hydraulic conditions; flow rates varied by $< 10\%$ over the duration of the experiment. Along the length of each column, eleven sampling ports were installed at intervals of 10 cm for a total monitored distance of 100 cm. Ports were used to extract pore water samples for measurement of dissolved oxygen (DO) and dissolved N_2O. Each port consisted of a rubber septum through which a 16 G, 7.5 cm stainless steel needle was inserted so that the tip of the needle was located approximately in the center of the column.

Water samples (approximately 5 ml) were analyzed for dissolved oxygen using an Optical Oxygen Meter Fibox 3 system fitted with an oxygen mini-sensor Flow-Through Cell (PreSens, Germany; DO detection limit 15 µg L^{-1}). Pore water samples were collected and transferred to gas-tight headspace vials (Agilent) using an in-line, closed sampling protocol so that any N_2O coming out of solution during the process would be collected in the sample vial and would be included in the measurement of dissolved N_2O after the water sample re-equilibrated with the headspace. The samples were passed through an in-line 0.45 micron filter and into a prepared glass headspace vial for determination of dissolved N_2O. Prior to sampling, the headspace vials were filled with

argon gas and acidified with H_2SO_4 to reduce sample pH to <2 and prevent microbial reactions prior to analysis. After the pore water samples were injected into the headspace vials and allowed to equilibrate, the headspace gas was analyzed for N_2O using an HP 7694 headspace autosampler and Agilent 6890 gas chromatograph equipped with a GS-Carbon PLOT column (30 m x 0.53 mm inner diameter) and a [63]Ni micro-electron capture detector, allowing the calculation of dissolved N_2O in the sample using Henry's Law [Hudson, 2004]. After the last sampling event, sodium chloride (NaCl) was used for a breakthrough curve experiment to determine the hydraulic properties of each column.

3.2.2 2013 Flume Experiment

The purpose of the first flume experiment, carried out in the Center for Ecohydraulics Research Stream Laboratory at the University of Idaho-Boise, was to examine the role of streambed morphology and nitrate loading on N_2O concentrations in the hyporheic zone. A large flume (approximately 20 m x 2 m) was divided into three smaller channels, each 30 cm wide, separated by narrow walkways for sampling. The sediment in each channel was identical to the mixture used in one of the columns (90% quarry sand, 10% microbial inoculum sand, and 0.15% POM). Natural sand collected a few weeks prior to the start of the experiments from the Boise River was wet sieved on site to <2.4 mm. Because microbes reside on the surfaces of sediment grains, the natural sand was not washed to remove fines. To preserve the bacterial communities over the waiting period, the natural sand was stored under aerated and dechlorinated circulating water in a large, galvanized livestock-watering trough. The sand was also turned periodically during its storage. Before running water through the channels, dunes were formed by hand to specified dimensions. All the dunes were 100 cm in length but each channel had different dune

heights (3, 6, and 9 cm). A range of dune heights was utilized to produce different subsurface flow velocities and resulting hyporheic residence times. Taller dunes created larger pressure differentials, resulting in higher hyporheic flow velocities [Elliott and Brooks, 1997b]. In addition to testing the control of geomorphology on geochemistry, the different dune sizes allowed observation of the temporal evolution of systems with different flow velocities.

The flume was equipped with a track-mounted, programmable instrument cart that traversed the length of the flume. A robotic arm attached to the instrument cart moved vertically (~60 cm) and traversed the width of the flume. The robotic system was used to take laser elevation measurements of the dune surfaces before and after the experiment; water surface elevations (Omega Engineering, Inc. CT, USA, ultrasonic sensor Model LVU30) during the experiment; and DO and N_2O concentrations along the dune surface profiles (depths of 0, 0.5, 1.2, and 4 cm at 2 cm longitudinal spacing; Unisense A/S, Aarhus, Denmark, sensor models DO500 and N2O500), also during the experiment.

Pressure differentials across the dunes produced a series of hyporheic flow paths within the subsurface [Elliott and Brooks, 1997a]. In each channel, ports (rhizon soil moisture samplers, Rhizosphere Research Products, Netherlands) were installed in the walls of two adjacent dunes to allow for sampling of subsurface pore water. Each rhizon consisted of 10 cm of porous (0.45 micron) tubing loosely surrounding a stainless steel strengthener wire and attached to 13 cm of connection tubing fitted with a luer lock adapter and plug. Rhizons were positioned so that the porous tubing was situated within the dune sediments, perpendicular to the flow direction. Adjacent to each rhizon, a fiber optic DO sensor was embedded in the sediment. The in situ DO measurement system

consisted of PreSens PSt3 sensor spots glued to the ends of fiber optic cables. The fiber optic cables were connected to an optical multiplexer (custom built by Agiltron Inc., Woburn, MA, USA) and a Fibox 3 that allowed for non-invasive automated DO measurement.

Water was pumped from a 50,000 gallon pool through a carbon filter and into a headbox at the head of the flume, from which water flowed through each channel. The first flume experiment ran for approximately 16 weeks in September 2013 through January 2014 (except for a short period of pump failure between days 20 and 21). DO measurements were obtained approximately every two days using the automated optical system (PreSens and Agiltron) and weekly using the robotic instrument cart with Unisense surface probes. DO measurements were obtained using two different techniques. The PreSens optical sensors rely upon quenching of the fluorescence of a dye that is sensitive to the presence oxygen. The Unisense surface probes are Clarke-type, ion selective sensors. When measuring in the same environment, both types of sensors were observed to yield consistent measurements. Pore water samples were regularly collected manually from the rhizons for determination of dissolved N_2O, nitrate (NO_3^-), nitrite (NO_2^-), and ammonia (NH_3), pH, alkalinity, and elemental concentrations with full sampling events on Days 49, 98, and 112. To test the impact of exogenous nitrate loading, a concentrated potassium nitrate (KNO_3) solution was added to the headbox on day 61 to bring the surface water nitrate concentration to approximately 3 mg L^{-1} NO_3^-. Nitrate concentrations in the surface water were allowed to decline due to nitrogen cycling processes for the remainder of the experiment.

During sampling, two pore water samples (approximately 10 ml) were collected from each of the rhizons using a closed sampling method. The first was a gas-tight sample collected for analysis of N_2O, as in the column experiment. During sampling, a needle was attached to the end of a rhizon. The needle was inserted into the septa cap of an evacuated vial that was submerged to prevent air contamination. Pore water moved slowly through the rhizon into the sample vial, and any dissolved gases that may have come out of solution during sampling were also transferred to the sample vial. The headspace analysis was carried out after the samples were allowed to re-equilibrate, and the original concentration of dissolved $N-N_2O$ was back calculated using Henry's Law [Hudson, 2004]. Following headspace analysis, the samples were transferred to 15 ml glass test tubes and stored at 4°C before analysis of the remaining nitrogen species. Concentrations of NH_3, NO_2^- and NO_x ($NO_3^- + NO_2^-$) were measured colorimetrically using a Lachat QuikChem 8500 Flow Injection Analysis (FIA) system (Loveland, CO). NH_3 was determined using QuikChem© method 10-107-06-1-F. Nitrite and NO_x concentrations were determined using QuikChem© method 10-107-04-1-B. NO_3^- concentrations were calculated as the difference between NO_x and NO_2^-.

The second sample collected from each rhizon was not acidified or gas tight. Half (5 ml) of this sample was acidified to 2% nitric acid (HNO_3) and stored at 4°C for elemental analysis. The remaining sample was immediately analyzed for pH (Denver Instruments) and alkalinity (Hach colorimetric method using bromocresol green methyl red solution). Elemental analysis utilized a ThermoScientific XSeries 2 ICP-MS. Following the last full sampling event, the surface water was drained slowly as to not disturb the bedforms. A final laser scan was performed, followed by sediment sampling. Approximately 10 ml of

sediment at each location were collected using autoclaved plastic scoops, transferred to sterile centrifuge tubes, and stored at -80°C prior to microbial genetic analysis (detailed in the Supporting Information).

3.2.3 2015 Flume Experiment

The second flume experiment was carried out for 13 weeks in spring 2015 and was nearly identical to the first but with triplicates of two dune sizes (1 m wavelength and 9 cm height; 0.7 m wavelength and 9 cm height), higher nitrate loading, and some differences in measurement methods. As in the 2013 experiment, multiple dune sizes were used to test the relationship between geomorphology, hyporheic residence time, and geochemistry. In situ DO measurements were taken approximately weekly, and pore water sampling events occurred on days 49, 70, and 91, with half of the ports sampled on days 15 and 55. To again test the influence of nitrate loading, a concentrated solution of KNO_3 was added to the headbox on day 62 to bring input surface water nitrate concentrations to about 10 mg L^{-1} NO_3^-. Pore water chemistry (dissolved N_2O, NO_3^-, NO_2^-, NH_3, pH, alkalinity, and elemental analysis) was analyzed as in the first flume experiment, except that a Hach TitraLab automatic titrator was used for alkalinity measurements. Sediment samples were again collected following draining of the channel and laser scan measurements of the beds. Samples were stored at -80°C for later genetic analysis.

3.3 Results and Discussion

3.3.1 Residence Time and Carbon Reactivity Constrain N_2O Release

By monitoring spatiotemporal changes within the flow systems of the columns and flume experiments, we observe distinct patterns in N_2O generation and consumption. We

can calculate hyporheic travel times for each of our sampling locations using conservative tracer tests and numerical models[*Fox et al.*, 2014] (Supporting Information), allowing observed chemistry data to be expressed as a function of hyporheic travel time (Figure 3.1, Tables B.4-B.9 in Appendix B). Chemical concentration profiles were created using Kriging in Surfer® mapping software. The search radius for the Kriging operation was set to 0.25 m and the final grid spacing was approximately 1 cm. A break line was used to set a transition between the surface water and the surface to the dune. Residence times were calculated based on geomorphology, flow characteristics, and sediment properties at the conclusion of the experiment. There is a possibility that sediment permeability may have changed during the course of the experiment due to changes in biomass. The chemical data in Figure 3.1, however, provide a snapshot from the end of the experiment that should be well correlated with the residence times calculated within a few days of water sampling. In the columns, monitored flow velocities did not change significantly over time or show a systematic increase or decrease while the pump rate remained constant, suggesting there was no significant change in permeability or residence time.

Hyporheic travel time can be conceptualized as the time available for reaction for a parcel of water as it passes through the hyporheic zone [Marzadri et al., 2012]. Within our flume hyporheic zone, DO concentrations in infiltrating waters rapidly decline from ~8 mg L^{-1} to generally less than 4 mg L^{-1} within travel times of 4 hours and less than 2 mg L^{-1} within 12 hours, presumably due to aerobic respiration [Zarnetske et al., 2011b] (Figure 3.1a). As oxygen is consumed and sub-oxic conditions are established, nitrate concentrations decline (from >1000 to <100 µg L^{-1} $N-NO_3^-$), consistent with nitrate

reduction [Marzadri et al., 2011] and reaction (3.1). The decline in nitrate is accompanied

by an increase in N$_2$O concentrations (max. >100 µg L^1 N-N$_2$O at a residence time of 9

hours). However, with longer travel times, N$_2$O concentrations decline to near zero by 12

hours. This decrease is likely driven by reaction (3.2), with N$_2$O converted to N$_2$ gas.
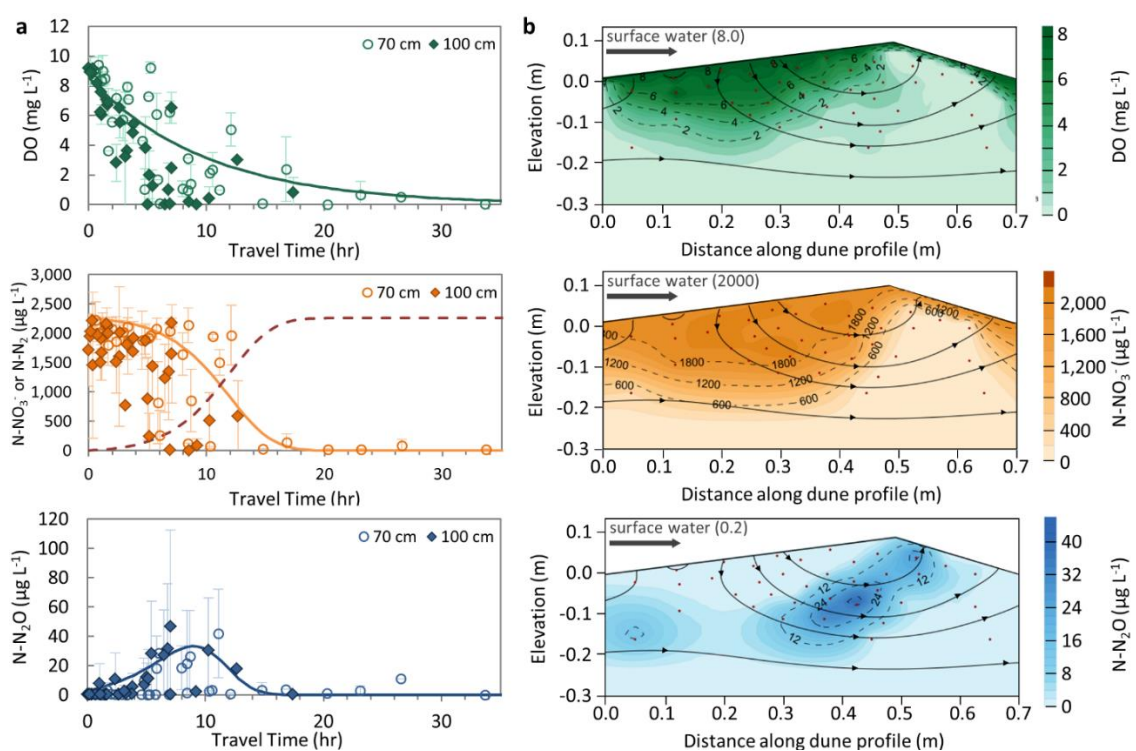
Figure 3.1.   Dissolved oxygen, N-NO$_3^-$, and N-N$_2$O concentrations in hyporheic bedform dunes. (a) Average concentrations from week 13 of the 2015 flume experiments in dunes of different dimensions (9 cm height x 70 cm length, open symbols; and 9 cm height x 100 cm length, filled symbols), with vertical bars showing the range of measurements across replicate dunes. Travel time on the horizontal axis indicates the average time for water entering the subsurface to reach the point of measurement. The solid lines show the results of a 1D reactive transport model of denitrification with typical hyporheic concentrations. The dashed red line in the middle figure shows modeled N$_2$ concentrations. (b) Species distributions in the 9 cm x 70 cm dune during week 13 of the 2015 flume experiment. Surface water flows from left to right. Black lines with arrowheads show subsurface hyporheic flow and groundwater flow (lowest flow line). Small red dots indicate sampling locations. The surface water concentrations are indicated at the top of each profile by 'surface water ( )'.

This is consistent with microbial genetic analysis of sediments, which reveals high concentrations of genes encoding for denitrifying enzymes in the region of denitrification. Specifically, *nirS*, one of the genes that encodes for nitrite reductase, an enzyme required for the pathway leading to N_2O production, is concentrated in the region of increasing N_2O concentrations and decreases in abundance as N_2O concentrations decline (Figure 3.2, Table B.7 in Appendix B).
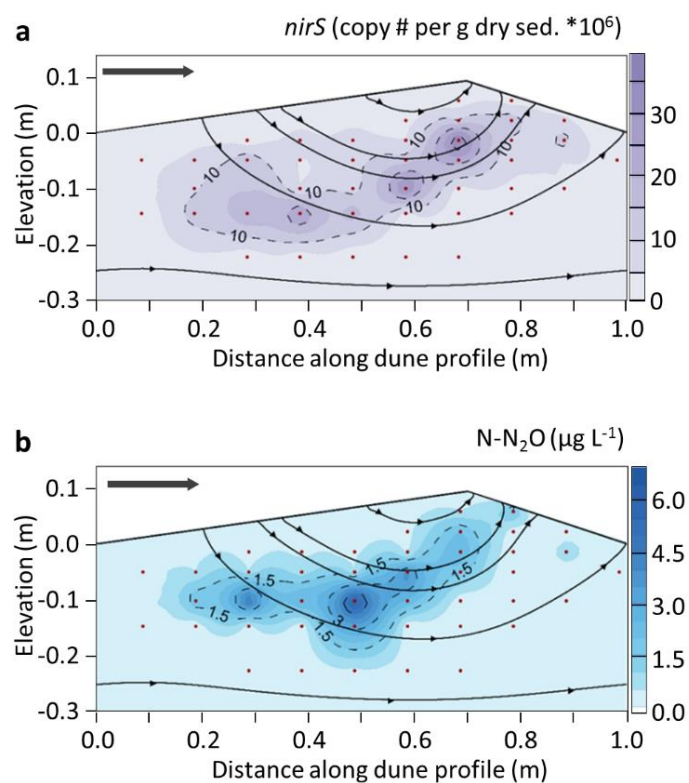
Figure 3.2.   nirS and N-N₂O from Fall 2013 flume experiment (dune 2). (a) Abundance of the *nirS* gene (encoding for nitrite reductase) in sediments collected on Day 117. Units are copy # per gram dry sediment $*10^6$. (b) Nitrous oxide concentrations in pore water on Day 112. Units are $\mu g\ L^{-1}$ N-N_2O. Water flow is from left to right. Black lines with arrowheads show subsurface hyporheic flow and groundwater flow (lowest flow line). Small red dots indicate sampling locations.

We observe the same reaction sequence in all column and flume experiments (see Tables B.4-B.9 in Appendix B): First, there is a decline in dissolved oxygen. This is followed by a decrease in nitrate and an accompanying increase in N_2O concentrations. N_2O concentrations then decline to background levels. While the observed chemical trends are strong, there is considerable variation in the data. For example, at a residence time of 5 hours in the flume experiment data (Figure 3.1), we observe a range of nitrate-N concentrations from 2.5 mg L^{-1} to near zero. This variation may be explained by flow path uncertainty, but is likely also capturing micro-site geochemical variability. It is likely that anaerobic microzones developed in association with particulate carbon in the subsurface due to higher rates of oxygen consumption [Harvey et al., 2013; Briggs et al., 2015]. Although our study was concerned with bulk trends, it is important to note that the influence of microzones with less mobile porosity may be less reflected by sampling techniques, as suggested by Briggs et al. [2015]. Theoretical work indicates that heterogeneity in aquatic sediments (as caused by organic matter) increases nitrogen processing along flow paths with the same overall travel times [Sawyer, 2015]. The presence of microzones would influence both the production and consumption of N_2O. We acknowledge this likelihood and limit our interpretation to bulk, system level trends.

Reactive transport modeling of the simplified two-step denitrification reaction sequence (solid lines in Figure 3.1a, described in Supporting Information) illustrates N_2O production by incomplete denitrification. When viewed as a snapshot within the hyporheic flow system, this reaction sequence produces a distinct band of elevated N_2O concentrations reflective of a specific range of travel times (Figure 3.1b). Importantly, the observed data highlight that the release of N_2O from the hyporheic zone requires a very

specific flow path length and residence time. Under the specific conditions of this flume experiment, maximum N_2O release to the stream occurs at flow path residence times of around 6-10 hours.
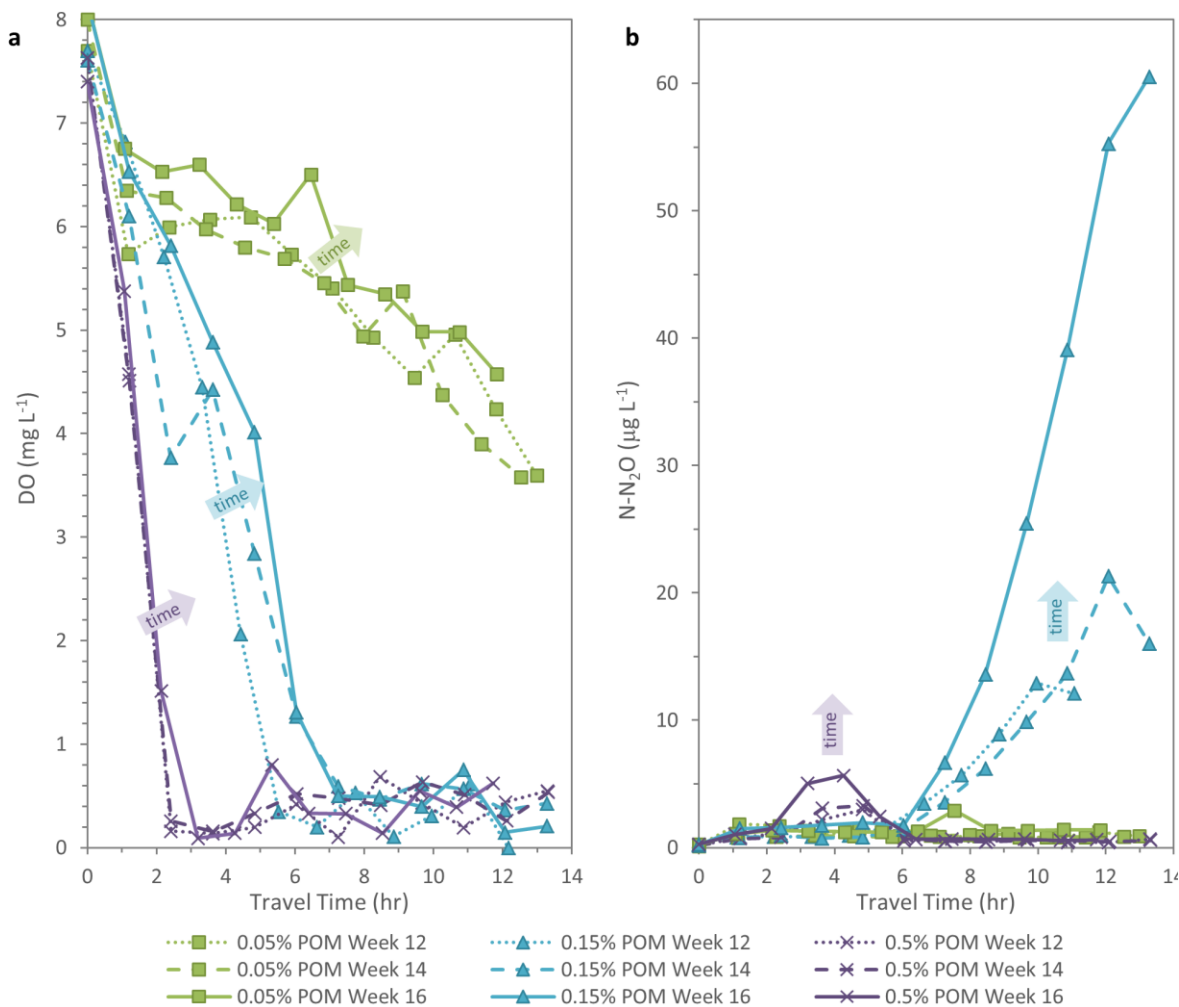
Figure 3.3. **Influence of amount and reactivity or organic carbon.** Plots of dissolved oxygen (a) and dissolved $N-N_2O$ (b) vs. travel time for three columns with different particulate organic matter (POM) content. Plots also show trends within each column over time, illustrating changes with declining organic carbon reactivity.

The location and associated travel time of the peak in N_2O concentration is modified by the rates of oxygen consumption and denitrification; carbon reactivity is a primary driver of these rates. Although our experimental design did not include direct

measurement of dissolved organic carbon or carbon reactivity, other indicators provided a proxy (through imperfect) of carbon reactivity. As carbon availability and quality decrease over time, the rate of aerobic respiration slows [Warkentin et al., 2007], less oxygen is consumed, and DO increases. We observed this trend in the column and flume experiments, as shown in Figure 3.3 and Figures B.3 and B.4 in Appendix B. The increase in DO at fixed locations in the sediments over time is best shown in the latter weeks of Figure B.3. Instability in the system is also visible in these plots, particularly early in the experiment, reflecting heterogeneity in changes in carbon reactivity (perhaps due to internal cycling) and microbial activity.

It should be noted that DO consumption rates are a proxy for carbon reactivity that does not explicitly distinguish the influence of changes in microbial populations over time. Some information about carbon reactivity and population dynamics may be gleaned from the changes in DO consumption rate over time, as shown in Figure B.4. Oxygen consumption rates in the columns increased in the first two weeks of the experiment, suggesting an increase in microbial populations and/or a release of reactive carbon from the POM. Oxygen consumption rates then decreased, likely due to decrease in carbon availability/quality, though the influence of changing microbial populations cannot be entirely ruled out. The snapshot results presented in Figures 3.1-3.3 are from the later stages of the experiments, when oxygen consumption rates are not changing as dramatically as earlier in the experiment and populations are likely stable (see Figures B.3 and B.4).

We define carbon reactivity operationally based on rates of oxygen and nitrate consumption; the greater the organic carbon reactivity, the more rapidly oxygen and

nitrate are consumed [Warkentin et al., 2007]. Trends in carbon reactivity are illustrated in results from a series of columns with different amounts of organic carbon (Figure 3.3, Table B.4 and Figures B.3 and B.4 in Appendix B). With low sediment carbon levels (0.05% POM), the rate of aerobic respiration is slower and dissolved oxygen remains high along the entire column (Figure 3.3a, Figure B.4), limiting denitrification and the associated production of N_2O (Figure 3.3b). At moderate levels of organic carbon (0.15% POM), nitrate reduction and elevated N_2O concentrations are observed, with the peak in N_2O occurring at the discharge end of the column, creating the specific reaction rates needed to release N_2O along a flow path of this length. When organic carbon content is higher (0.5% POM), the rates of oxygen consumption and nitrate reduction are even more rapid and the peak in N_2O occurs in the middle of the column. Under these conditions, sufficient additional flow path length (and travel time) exists to consume the produced N_2O, thereby limiting its release.

The accumulation and subsequent decline in N_2O concentrations over time (and flow path distance) indicates active production and then scavenging of N_2O from the pore water, a sequence analogous to that proposed for soils [Firestone et al., 1980; Chapuis-Lardy et al., 2007; Ostrom et al., 2007]. The rate of N_2O consumption relative to N_2O production via nitrate reduction dictates the amount of nitrous oxide observed in the hyporheic zone: the higher the production and the slower the consumption, the greater the resulting N_2O concentration. Thermodynamic calculations indicate N_2O reduction is highly favorable with $\Delta G = -138.7$ kJ mol N^{-1} (comparable to, or greater than, the other reduction steps in denitrification, as shown in Supporting Information), suggesting the limits on the reduction rate are not thermodynamic. Rather, this differential response is

attributable to catalytic, likely enzymatic, limitations, as recently articulated by Zheng and Doskey [2015].

3.3.2 Conceptual model summary

Nitrous oxide *emissions* from the hyporheic zone are dependent on both the magnitude of microbial N_2O *production* and on the amount of microbial N_2O *consumption* that occurs under given conditions prior to a parcel of hyporheic water returning to the stream. This can be conceptualized by three flow paths with different hyporheic residence times (τ_{HZ}, Figure 3.4a). With sufficient nitrate and organic carbon reactivity, denitrification will proceed along all of these flow paths, but the nitrogen species returned to the stream depends on the ratio between the travel time to the N_2O peak (τ_{N2O}) and the residence time of the flow path (τ_{HZ}), as shown in Figures 3.4a and 3.4b. If flow paths are too short (or reactions are too slow), $\tau_{N2O}: \tau_{HZ} > 1$ and N_2O emissions are low (compare to 0.05% POM in Figure 3.3). If flow paths are too long (or reactions are too rapid), $\tau_{N2O}: \tau_{HZ} < 1$ and N_2O emissions are low because some or all of the N_2O produced is reduced to N_2 (compare to 0.5% POM in Figure 3.3). For example, although we observed dissolved N-N_2O concentrations in the subsurface that were as high as 6.1% of the surface water N-NO_3^- concentrations in the flume, the N_2O emission yield would be reduced by conversion of N_2O to N_2. In summary: Goldilocks conditions that maximize N_2O emissions occur when the travel time to the N_2O peak is close to the flow path residence time and $\tau_{N2O}: \tau_{HZ} = 1$ (as observed for 0.15% POM profiles in Figure 3.3). Although our experiments did not allow definitive separation of the influence of internal DOC cycling and microbial population shifts from the influence of declining carbon reactivity over time on potential N_2O emissions, the conceptual model relating τ_{HZ}

and τ_{N2O} still holds. While this experimental design mimicked a hyporheic flow system, this conceptual model should be equally applicable to nitrate-rich groundwater undergoing reduction: longer residence times under reducing conditions will be more likely to consume produced nitrous oxide.
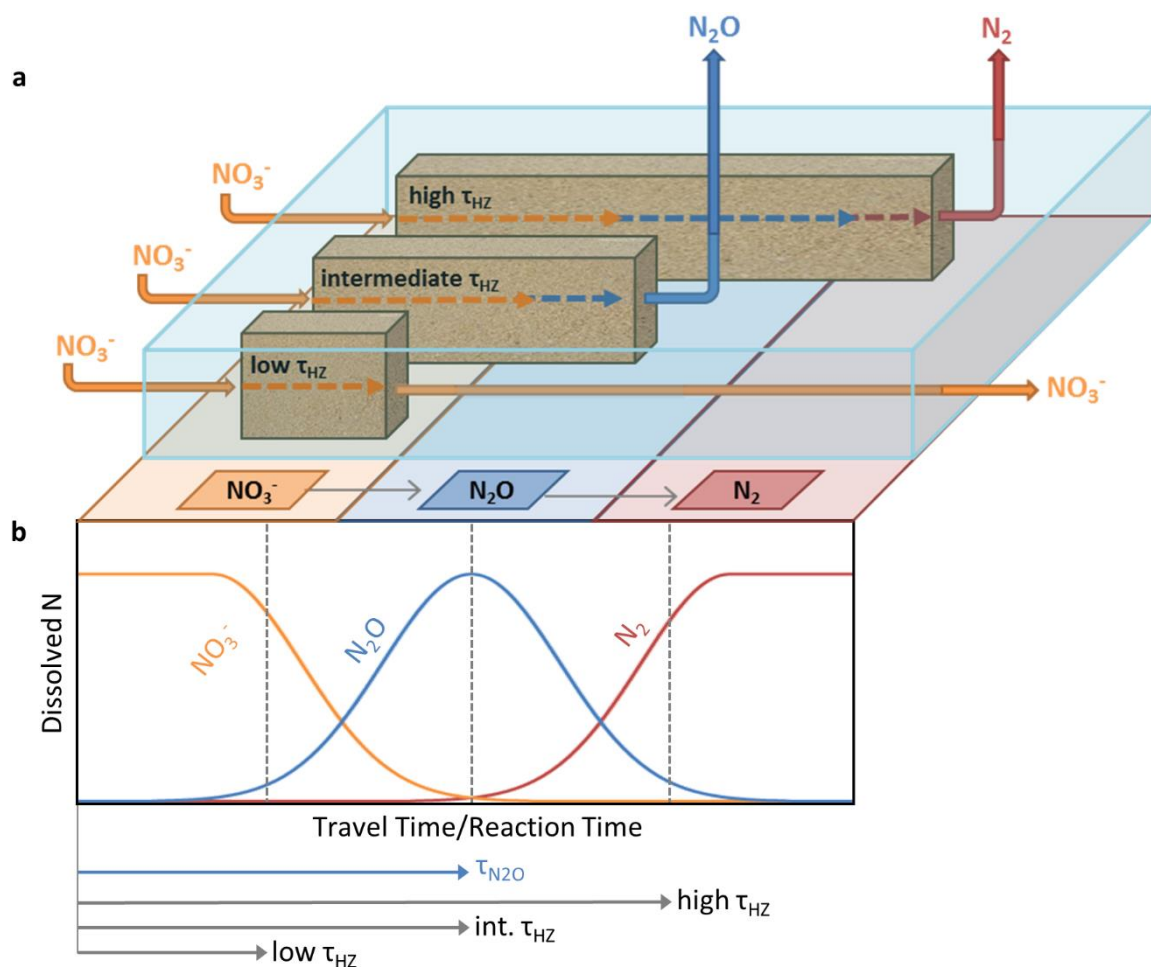
Figure 3.4.   Dissolved oxygen, N-NO₃⁻, and N-N₂O concentrations in hyporheic bedform dunes. Hyporheic residence time (and reaction rate) dictates how far denitrification will progress and which nitrogen species will be most abundant at the end of the flow path and delivered to the stream water. (a) Shown within a stream (blue box) are three idealized flow paths (tan boxes) with low, intermediate, and high hyporheic residence times (τ_{HZ}) expressing three potential release outcomes: NO_3^- (low τ_{HZ}), N_2O (intermediate τ_{HZ}), and N_2(high τ_{HZ}). (b) illustrates the reaction sequence and emphasizes the role of the travel time to the peak N_2O concentration (τ_{N2O}). In this conceptualization, a change in organic carbon reactivity would have same effect as shifting the curves in (b) and changing τ_{N2O}.

3.3.3 Potential Alternative Processes

While our conceptual model, framed around denitrification, adequately explains our observations, we cannot discount the influence of a number of alternative processes on N_2O production. Three processes of particular relevance are nitrification, dissimilatory nitrate reduction to ammonium (DNRA), and anammox (anaerobic ammonium oxidation).

Nitrification, the oxidative conversion of ammonia to nitrite and nitrate, can produce N_2O through hydroxylamine oxidation [Bremner, 1997; Stein and Yung, 2003] or chemodenitrification of NO_2^- [Bremner, 1997]. In this system, however, N_2O generation is observed only after oxygen concentrations are reduced and coincident with declining nitrate concentrations; these trends are not consistent with active nitrification. Our observations agree with Baulch et al., who found, using isotopic studies of N_2O production in streams, that N_2O was produced via denitrification instead of nitrification [2011].

It is more difficult to discard the potential for dissimilatory nitrate reduction to ammonium (DNRA) in this system. DNRA has been shown to be an important pathway for nitrate reduction with the potential to produce N_2O [Kelso et al., 1997; Stevens and Laughlin, 1998]. Maximum observed ammonium concentrations within the flume sediments were generally <100 µg/L and exhibited a trend of rising concentrations at low residence times, when oxygen was low, then gradually declining at longer residence times. Because similar trends were observed prior to nitrate addition, we attribute the majority of the observed ammonia generation to ammonification. In soil batch experiments, Smith and Zimmerman found that an average of 5-10% of nitrate reduced

by DNRA organisms was released as N_2O [1981]. Even assuming all the observed NH_3 produced in the hyporheic zone is the product of DNRA, the associated N_2O production would be a few tens of $\mu g\ L^{-1}$, a small fraction of the N_2O concentrations observed in our experiments. While the potential role of the DNRA pathway in N_2O production in streams remains an important question, there is little evidence it plays a major role in our system. Our observations are in agreement with Lansdown et al. [2012], who demonstrated that only up to 4% of $^{15}NO_3^-$ tracer in river sediment incubations underwent DNRA, while 85% underwent denitrification.

Although the 2012 Lansdown et al. study found very little evidence of anammox in sediment slurries, more recent work by Lansdown et al. documented the importance of anammox in some stream sediments [Lansdown et al., 2016]. In our system, while ammonium concentrations are generally a factor of 10 lower than input nitrate concentrations, they are elevated where active nitrate reduction is occurring. Accordingly, anammox may be acting as a sink for reactive nitrogen in this system, potentially reducing N_2O production and influencing N_2O yield. While we cannot definitively eliminate these alternative processes, we believe our proposed conceptual model provides the simplest and most plausible explanation for the observed trends.

3.3.4 Importance of Nitrate Loading

Both flume experiments demonstrated the importance of nitrate loading to N_2O generation. With no added nitrate, background surface water concentrations range from 0.1 to 2 mg L^{-1} NO_3^-, and mean peak (average of the highest 5% of measurements) subsurface dissolved N_2O concentrations remain <1 $\mu g\ L^{-1}$ $N-N_2O$ (1.0 and 0.9 $\mu g\ L^{-1}$ $N-N_2O$ in the 2013 (day 49) and 2015 (day 41) flume experiments, respectively). Nitrate

was added around Day 60 in both flume experiments to bring surface NO_3^-

concentrations to approximately 3 mg L^{-1} (2013 experiment) and 10 mg L^{-1} (2015

experiment). The nitrate addition was followed by increased mean peak N_2O

concentrations (3.4 and 77.2 µg L^{-1} N-N_2O in the 2013 (day 98) and 2015 (day 91)

experiments, respectively). This trend is consistent with multiple studies that have

demonstrated that denitrification increases with NO_3^- concentration [Mulholland et al.,

2008; Beaulieu et al., 2011; Harvey et al., 2013] and with McMahon and Dennehy

[1999], who identified a direct relationship between inorganic nitrogen loading and N_2O

emissions from rivers. Our observations demonstrate an increase in N_2O generation with

higher nitrate, consistent with the LINX II data for headwater streams presented by

Beaulieu et al [2011]. In the 2015 flume experiment, up to 6.1% of surface water N-NO_3^-

was converted to N-N_2O at the end of the experiment (molar ratio $N_2O/NO_3^- = 3\%$).

However, this value should not be compared with N_2O yield values reported in the

literature [García-Ruiz et al., 1998; Groffman et al., 2000; Silvennoinen et al., 2008;

Beaulieu et al., 2011], which reflect *emitted* N_2O. This value may represent a "potential

N_2O yield" because, as has been demonstrated, produced N_2O may be reduced to N_2

further along a flow path, reducing the amount of emitted N_2O. Additionally, N_2O may

have been produced from N sources other than exogenous nitrate.

3.3.5 Influence of Organic Carbon Reactivity

Organic carbon reactivity (reduction capacity) has been shown to strongly influence

the magnitude, and potentially yield, of observed N_2O production [Firestone and

Davidson, 1989; Soued et al., 2015]; we observe similar trends in these experiments. If

carbon levels are high enough to promote nitrate reduction and N_2O production,

decreasing carbon reactivity over time increases peak N_2O concentrations. Our column data illustrate this trend in two ways. First, the peak N_2O concentrations in the 0.15% POM column are much greater (up to 60.5 µg L^{-1} $N-N_2O$) than those in the 0.5% POM column (up to 9.7 µg L^{-1} $N-N_2O$) (Figure 3.3b). Second, increasing N_2O concentrations are also observed over time (compare the 12, 14, and 16 week plots for each column), which is interpreted to be the result of declining organic carbon reactivity; as the more reactive fractions of organic carbon are consumed, N_2O concentrations increase.

Similar trends between carbon reactivity (as described by the DO consumption rate proxy) and N_2O production are observed in the flume. In the first flume experiment, the taller dunes have greater flow velocities [Elliott and Brooks, 1997b] and higher associated respiration rates, more rapidly depleting the reactive carbon in the taller dunes as the experiment progresses. As a result, the taller dunes, with lower carbon reactivity, exhibit higher peak N_2O concentrations (6.0 µg L^{-1} $N-N_2O$ in the 9 cm dune, compared to 2.6 and 1.1 µg L^{-1} $N-N_2O$ in the 6 and 3 cm dunes on day 112, respectively).

The decline in organic carbon reactivity may differentially influence N_2O production and consumption, as recently observed by Soued et al. [2015]. Based on a large database of boreal rivers, lakes, and ponds, these authors did not find a predictive relationship between N_2O flux and reactive nitrogen and found that some freshwater environments, particularly rivers, are N_2O sinks. They also found that higher dissolved organic carbon (DOC) concentrations favored the consumption of N_2O due to stimulation of respiration, denitrification, and low DO and NO_3^- [Soued et al., 2015]. In observations of small streams, Baulch et al. [2011] also found that high DOC concentrations are correlated with

low concentrations of N_2O. Our results provide a mechanistic framework that may help explain these correlative observations of hyporheic N_2O production.

While differential rates of NO_3^- and N_2O reduction can explain the observed increases in N_2O production with declining carbon reactivity in our experiments, we cannot discount influences from other processes. One possible alternative explanation is that with lower carbon reactivity, a larger aerobic zone allows for more aerobic production of NO_3^- (nitrification), which increases the amount of NO_3^- available for denitrification in the anaerobic zone [Zarnetske et al., 2011a; Harvey et al., 2013] and increases the potential for N_2O production via ammonia oxidation [Stein and Yung, 2003; Marzadri et al., 2011]. In our flume experiments, evidence of increases in NO_3^- concentrations between the surface water and the first sampling locations suggest some modest amount of nitrification early in the flow paths. Another possible explanation is that although denitrification rates are positively correlated to organic carbon reactivity [Zarnetske et al., 2011a; Harvey et al., 2013], N_2O yield may increase with decreasing carbon reactivity relative to NO_3^- due to the relative quantities of electron donors and acceptors [Tiedje, 1988; Kolb and Horn, 2012; Senbayram et al., 2012]. Low ratios between available carbon (electron donor) and nitrate (electron acceptor) may favor N_2O over N_2 as the final product of denitrification in various environments [Firestone and Davidson, 1989; Hedin et al., 1998; Beaulieu et al., 2011]. A third alternative explanation is that decreasing carbon reactivity lowers oxygen consumption rates, allowing for inhibition by oxygen of the enzyme that catalyzes the reduction of N_2O to N_2 [Betlach and Tiedje, 1981; Tiedje, 1988].

3.4 Implications

The proposed integrative framework explicitly links hyporheic biogeochemical and hydrologic processes to predict the conditions of N_2O release. This model may be useful for improving global estimates of N_2O emissions, guiding stream restoration efforts to limit N_2O release, and informing investigations of remaining areas of uncertainty in N_2O release from streams. Previous models have determined denitrification potential of a stream or river system by establishing minimum flow paths and reactivity levels necessary for nitrate consumption [Gu et al., 2007; Boano et al., 2010; Marzadri et al., 2011; Gomez et al., 2012], and our contribution can be viewed as an extension of those models. The transience of N_2O during denitrification highly constrains N_2O emissions; when τ_{HZ} is too short (relative to τ_{N2O}), denitrification does not occur, when τ_{HZ} is too long (relative to τ_{N2O}), produced N_2O is consumed. In practice, this understanding allows elimination of the majority of hyporheic flow paths as N_2O-emitting at any given time; most are too long or too short to produce emissions. Importantly, however, temporal variations in carbon reactivity and nitrate loading (and presumably microbial populations) can alter which flow paths emit N_2O, with changing reactivity converting a hyporheic flow path to (or from) a N_2O-emitting flow path.

Stream restoration, wetland construction, and increasing hyporheic exchange are often undertaken to reduce stream nitrate levels by promoting denitrification [Kaushal et al., 2008; Klocker et al., 2009; Hester and Gooseff, 2010; Mayer et al., 2013]. Similarly, where nitrate-rich groundwater discharges to streams, riparian buffer systems are often encouraged to promote denitrification [Peter et al., 2012]. Our observations suggest such systems can potentially be designed to also limit N_2O release by extending residence

times and/or reaction rates to promote consumption of produced N_2O. The highlighted importance of the relative rates of N_2O production and reduction in controlling N_2O emissions indicates that new insights will come from research that explicitly decouples these processes. Of particular interest is the poorly understood trend, observed here and elsewhere [Firestone and Davidson, 1989; Hedin et al., 1998; Beaulieu et al., 2011], of increasing magnitudes of nitrous oxide production with declining organic carbon reactivity. In summary, our current understanding suggests that, if nitrate reduction is occurring in the hyporheic zone, less reactive organic carbon and elevated nitrate will allow greater N_2O production. However, the longer the flow path and residence time in those systems, the less likely N_2O will be released to the stream and emitted to the atmosphere.

3.5 Supporting Information

Additional explanations are found in Appendix B, including details of the hydrologic modeling and tracer tests, microbial genetic analysis, thermodynamic calculations, and reactive transport modeling.

3.6 Acknowledgements

anonymous reviewers whose detailed and thoughtful comments greatly improved this manuscript.

3.7 References

Anderson, B., K. Barlett, S. Frolking, K. Hayhoe, J. Jenkins, and W. Salas (2010), Methane and Nitrous Oxide Emissions From Natural Sources, , (April), 1–194, doi:EPA 430-R-10-001.

Baulch, H. M., S. L. Schiff, R. Maranger, and P. J. Dillon (2011), Nitrogen enrichment and the emission of nitrous oxide from streams, *Global Biogeochem. Cycles*, *25*(4), 1–15, doi:10.1029/2011GB004047.

Beaulieu, J. J. et al. (2011), Nitrous oxide emission from denitrification in stream and river networks, *Proc. Natl. Acad. Sci. U. S. A.*, *108*(1), 214–219, doi:10.1073/pnas.1011464108.

Bernhardt, E. S., and G. E. Likens (2011), Dissolved Organic Carbon Enrichment Alters Nitrogen Dynamics in a Forest Stream, *Ecology*, *83*(6), 1689–1700.

Betlach, M. R., and J. M. Tiedje (1981), Kinetic Explanation for Accumulation of Nitrite, Nitric Oxide, and Nitrous Oxide During Bacterial Denitrification, *Appl. Environ. Microbiol.*, *42*(6), 1074–1084.

Boano, F., A. Demaria, R. Revelli, and L. Ridolfi (2010), Biogeochemical zonation due to intrameander hyporheic flow, *Water Resour. Res.*, *46*(2), 1–13, doi:10.1029/2008WR007583.

Boano, F., J. W. Harvey, A. Marion, A. I. Packman, R. Revelli, L. Ridolfi, and A. Wörman (2014), Hyporheic flow and transport processes: Mechanisms, models, and biogeochemical implications, *Rev. Geophys.*, *52*, 603–679, doi:10.1002/2012RG000417.

Bollmann, A., and R. Conrad (1998), Influence of O2 availability on NO and N2O release by nitrification and denitrification in soils, *Glob. Chang. Biol.*, *4*(4), 387–396, doi:10.1046/j.1365-2486.1998.00161.x.

Bremner, J. M. (1997), Sources of nitrous oxide in soils, *Nutr. Cycl. Agroecosystems*, *49*, 7–16, doi:10.1023/A:1009798022569.

Briggs, M. a, F. D. Day-Lewis, J. P. Zarnetske, and J. W. Harvey (2015), A physical explanation for the development of redox microzones in hyporheic flow, *Geophys. Res. Lett.*, *42*, 4402–4410, doi:10.1002/2015GL064200.

Burgin, A. J., J. G. Lazar, P. M. Groffman, A. J. Gold, and D. Q. Kellogg (2013), Balancing nitrogen retention ecosystem services and greenhouse gas disservices at the landscape scale, *Ecol. Eng.*, *56*, 26–35, doi:10.1016/j.ecoleng.2012.05.003.

Chapuis-Lardy, L., N. Wrage, A. Metay, J.-L. Chotte, and M. Bernoux (2007), Soils, a sink for N2O? A review, *Glob. Chang. Biol.*, *13*(1), 1–17, doi:10.1111/j.1365-2486.2006.01280.x.

Davidson, E. A. (1991), Fluxes of nitrous oxide and nitric oxide from terrestrial ecosystems, in *Microbial production and consumption of greenhouse gases: methane, nitrogen oxides, and halomethanes*, edited by J. E. Rogers and W. B. Whitman, pp. 219–235, American Society for Microbiology, Washington D.C.

Davidson, E. A. (2009), The contribution of manure and fertilizer nitrogen to atmospheric nitrous oxide since 1860, *Nat. Geosci.*, *2*(9), 659–662, doi:10.1038/ngeo608.

Duff, J. H., A. J. Tesoriero, W. B. Richardson, E. A. Strauss, and M. D. Munn (2008), Whole-Stream Response to Nitrate Loading in Three Streams Draining Agricultural Landscapes, *J. Environ. Qual.*, *37*(3), 1133–1144, doi:10.2134/jeq2007.0187.

Elliott, A. H., and N. Brooks (1997a), Transfer of nonsorbing solutes to a streambed with bed forms: Theory, *Water Resour. Res.*, *33*(1), 123–136.

Elliott, A. H., and N. H. Brooks (1997b), Transfer of nonsorbing solutes to a streambed with bed forms : Laboratory experiments, *Water Resour. Res.*, *33*(1), 137–151.

Findlay, S. (1995), Importance of surface-subsurface exchange in stream ecosystems: The hyporheic zone, *Limnol. Oceanogr.*, *40*(1), 159–164, doi:10.4319/lo.1995.40.1.0159.

Firestone, M. K., and E. A. Davidson (1989), Microbiological basis of NO and N2O production and consumption in soil, in *Exchange of Trace Gases between Terrstrial Ecosystems and the Atmosphere*, edited by M. Andreae and D. Schimel, pp. 7–21, John Wiley & Sons, New York.

Firestone, M. K., R. B. Firestone, and J. M. Tiedje (1980), Nitrous Oxide from Soil Denitrification: Factors Controlling Its Biological Production, *Science (80-.).*, *208*(May), 749–751.

Forster, P. et al. (2007), Changes in Atmospheric Constituents and in Radiative Forcing, in Climate Change 2007: The Physical Science Basis. Contribution of Working Group I to the Fourth Assessment Report of the Intergovernmental Panel of Climate Change, edited by S. Solomon, D. Qin, M. Manning, Z. Chen, M. Marquis, K. B. Averyt, M. Tignor, and H. L. Miller, Cambridge University Press.

Fox, A., F. Boano, and S. Arnon (2014), Impact of losing and gaining streamflow conditions on hyporheic exchange fluxes induced by dune-shaped bed forms, *Water Resour. Res.*, *50*, 1895–1907, doi:10.1002/2013WR014668.

García-Ruiz, R., S. N. Pattinson, and B. A. Whitton (1998), Denitrification in river sediments: Relationship between process rate and properties of water and sediment, *Freshw. Biol.*, *39*(3), 467–476, doi:10.1046/j.1365-2427.1998.00295.x.

Gomez, J. D., J. L. Wilson, and M. B. Cardenas (2012), Residence time distributions in sinuosity-driven hyporheic zones and their biogeochemical effects, *Water Resour. Res.*, *48*(9), 1–17, doi:10.1029/2012WR012180.

Groffman, P. M., A. J. Gold, and K. Addy (2000), Nitrous oxide production in riparian zones and its importance to national emission inventories, *Chemosphere-Global Chang. Sci.*, *2*, 291–299.

Gu, C., G. M. Hornberger, A. L. Mills, J. S. Herman, and S. A. Flewelling (2007), Nitrate reduction in streambed sediments: Effects of flow and biogeochemical kinetics, *Water Resour. Res.*, *43*(W12413), 1–10, doi:10.1029/2007WR006027.

Harvey, J. W., J. K. Böhlke, M. A. Voytek, D. Scott, and C. R. Tobias (2013), Hyporheic zone denitrification: Controls on effective reaction depth and contribution to

whole-stream mass balance, *Water Resour. Res.*, *49*(10), 6298–6316, doi:10.1002/wrcr.20492.

Hedin, L. O., J. C. von Fischer, N. E. Ostrom, B. P. Kennedy, M. G. Brown, and G. P. Robertson (1998), Thermodynamic constraints on nitrogen transformations and other biogeochemical processes at soil-stream interfaces, *Ecology*, *79*(2), 684–703.

Hester, E. T., and M. N. Gooseff (2010), Moving beyond the banks: hyporheic restoration is fundamental to restoring ecological services and functions of streams., *Environ. Sci. Technol.*, *44*(5), 1521–5, doi:10.1021/es902988n.

Hudson, F. (2004), Sample preparation and calculations for dissolved gas analysis in water samples using a GC headspace equilibrium technique, RSKSOP-175, Available from: https://www.epa.gov/ne/info/testmethods/pdfs/RSKsop175v2.pdf (Accessed 1 February 2013)

Kaushal, S. S., P. M. Groffman, P. M. Mayer, E. Striz, and A. J. Gold (2008), Effects of Stream Restoration on Denitrification, *Ecol. Appl.*, *18*(3), 789–804.

Kelso, B. H. L., R. V. Smith, R. J. Laughlin, and S. D. Lennox (1997), Dissimilatory nitrate reduction in anaerobic sediments leading to river nitrite accumulation, *Appl. Environ. Microbiol.*, *63*(12), 4679–4685.

Klocker, C. A., S. S. Kaushal, P. M. Groffman, P. M. Mayer, and R. P. Morgan (2009), Nitrogen uptake and denitrification in restored and unrestored streams in urban Maryland, USA, *Aquat. Sci.*, *71*(4), 411–424, doi:10.1007/s00027-009-0118-y.

Kolb, S., and M. A. Horn (2012), Microbial CH4 and N2O consumption in acidic wetlands, *Front. Microbiol.*, *3*(MAR), 1–8, doi:10.3389/fmicb.2012.00078.

Lansdown, K., M. Trimmer, C. M. Heppell, F. Sgouridis, S. Ullah, L. Heathwaite, A. Binley, and H. Zhang (2012), Characterization of the key pathways of dissimilatory nitrate reduction and their response to complex organic substrates in hyporheic sediments, *Limnol. Oceanogr.*, *57*(2), 387–400, doi:10.4319/lo.2012.57.2.0387.

Lansdown, K., C. M. Heppell, M. Trimmer, A. Binley, A. L. Heathwaite, P. Byrne, and H. Zhang (2015), The interplay between transport and reaction rates as controls on nitrate attenuation in permeable, streambed sediments, *J. Geophys. Res. G Biogeosciences*, *120*(6), 1093–1109, doi:10.1002/2014JG002874.

Lansdown, K., B. A. McKew, C. Whitby, C. M. Heppell, A. J. Dumbrell, A. Binley, L. Olde, and M. Trimmer (2016), Importance and controls of anaerobic ammonium oxidation influenced by riverbed geology, *Nat. Geosci.*, *9*(May), 357–360, doi:10.1038/ngeo2684.

Marzadri, A., D. Tonina, and A. Bellin (2011), A semianalytical three-dimensional process-based model for hyporheic nitrogen dynamics in gravel bed rivers, *Water Resour. Res.*, *47*(W11518), 1–14, doi:10.1029/2011WR010583.

Marzadri, A., D. Tonina, and A. Bellin (2012), Morphodynamic controls on redox conditions and on nitrogen dynamics within the hyporheic zone: Application to gravel bed rivers with alternate-bar morphology, *J. Geophys. Res. Biogeosciences*, *117*(3), 1–14, doi:10.1029/2012JG001966.

Marzadri, A., D. Tonina, A. Bellin, and J. L. Tank (2014), A hydrologic model demonstrates nitrous oxide emissions depend on streambed morphology, *Geophys. Res. Lett.*, *41*(15), 5484–5491, doi:10.1002/2014GL060732.

Mayer, P. M., S. P. Schechter, S. S. Kaushal, and P. M. Groffman (2013), Effects of stream restoration on Nitrogen removal and transformation in urban watersheds: Lessons from Minebank Run, Baltimore, Maryland, *Watershed Sci. Bull.*, *2*(3), 1–9.

McMahon, P. B., and K. F. Dennehy (1999), N2O emission from a nitrogen-enriched river, *Environ. Sci. Technol.*, *33*(303), 21–25.

Metzler, G. M., and L. A. Smock (1990), Storage and Dynamics of Subsurface Detritus in a Sand-Bottomed Stream, *Can. J. Fish. Aquat. Sci.*, *47*(3), 588–594, doi:10.1139/f90-067.

Mosier, A., C. Kroeze, C. Nevison, O. Oenema, and S. Seitzinger (1998), Closing the global N2O budget : nitrous oxide emissions through the agricultural nitrogen

cycle inventory methodology, *Nutr. Cycl. Agroecosystems*, *52*(2–3), 225–248, doi:10.1023/A:1009740530221.

Mulholland, P. J. et al. (2008), Stream denitrification across biomes and its response to anthropogenic nitrate loading, *Nature*, *452*(7184), 202–205, doi:10.1038/nature06686.

Ostrom, N. E., A. Piit, R. Sutka, P. H. Ostrom, A. S. Grandy, K. M. Huizinga, and G. P. Robertson (2007), Isotopologue effects during N2O reduction in soils and in pure cultures of denitrifiers, *J. Geophys. Res. Biogeosciences*, *112*(2), 1–12, doi:10.1029/2006JG000287.

Park, S. et al. (2012), Trends and seasonal cycles in the isotopic composition of nitrous oxide since 1940, *Nat. Geosci.*, *5*(4), 261–265, doi:10.1038/ngeo1421.

Peter, S., R. Rechsteiner, M. F. Lehmann, R. Brankatschk, T. Vogt, S. Diem, B. Wehrli, K. Tockner, and E. Durisch-Kaiser (2012), Nitrate removal in a restored riparian groundwater system: Functioning and importance of individual riparian zones, *Biogeosciences*, *9*(11), 4295–4307, doi:10.5194/bg-9-4295-2012.

Ravishankara, A. R., J. S. Daniel, and R. W. Portmann (2009), Nitrous Oxide (N2O): The Dominant Ozone-Depleting Substance Emitted in the 21st Century, *Science (80-.).*, *326*(5949), 123–125, doi:10.1126/science.1176985.

Sawyer, A. H. (2015), Enhanced removal of groundwater-borne nitrate in heterogeneous aquatic sediments, *Geophys. Res. Lett.*, *42*(2), 403–410, doi:10.1002/2014GL062234.

Senbayram, M., R. Chen, A. Budai, L. Bakken, and K. Dittert (2012), N2O emission and the N2O/(N2O+N2) product ratio of denitrification as controlled by available carbon substrates and nitrate concentrations, *Agric. Ecosyst. Environ.*, *147*, 4–12, doi:10.1016/j.agee.2011.06.022.

Silvennoinen, H., A. Liikanen, J. Torssonen, C. Florian Stange, and P. J. Martikainen (2008), Denitrification and nitrous oxide effluxes in boreal, eutrophic river sediments under increasing nitrate load: A laboratory microcosm study, *Biogeochemistry*, *91*(2–3), 105–116, doi:10.1007/s10533-008-9262-z.

Smith, M. S., and K. Zimmerman (1981), Nitrous oxide production by nondenitrifying soil nitrate reducers, *Soil Sci. Soc. Am. J.*, *45*(5), 865–871.

Soued, C., P. A. del Giorgio, and R. Maranger (2015), Nitrous oxide sinks and emissions in boreal aquatic networks in Québec, *Nat. Geosci.*, *9*(December), 1–7, doi:10.1038/ngeo2611.

Stein, L. Y., and Y. L. Yung (2003), Production, isotopic composition, and atmospheric fate of biologicaly produced nitrous oxide, *Annu. Rev. Earth Planet. Sci.*, *31*(1), 329–356, doi:10.1146/annurev.earth.31.110502.080901.

Stelzer, R. S., L. A. Bartsch, W. B. Richardson, and E. A. Strauss (2011), The dark side of the hyporheic zone: depth profiles of nitrogen and its processing in stream sediments, *Freshw. Biol.*, *56*(10), 2021–2033, doi:10.1111/j.1365-2427.2011.02632.x.

Stevens, R. J., and R. J. Laughlin (1998), Measurement of nitrous oxide and di-nitrogen emissions from agricultural soils, *Nutr. Cycl. Agroecosystems*, *52*(2–3), 131–139, doi:10.1023/A:1009715807023.

Tiedje, J. M. (1988), Ecology of Denitrification and Dissimilatory Nitrate Reduction to Ammonium, in *Biology of Anaerobic Microorganisms*, edited by A. J. B. Zehnder, pp. 179–244, John Wiley & Sons, New York.

Tillman, D. C., A. H. Moerke, C. L. Ziehl, and G. A. Lamberti (2003), Subsurface hydrology and degree of burial affect mass loss and invertebrate colonisation of leaves in a woodland stream, *Freshw. Biol.*, *48*(1), 98–107, doi:10.1046/j.1365-2427.2003.00976.x.

Tonina, D. (2012), Surface water and streambed sediment interaction: The hyporheic exchange, in *Fluid mechanics of environmental interfaces*, edited by C. Gualtieri and D. T. Mihailović, pp. 255–294, Taylor & Francis Group, London.

Warkentin, M., H. M. Freese, U. Karsten, and R. Schumann (2007), New and Fast Method To Quantify Respiration Rates of Bacterial and Plankton Communities in Freshwater Ecosystems by Using Optical Oxygen Sensor Spots □, *Appl. Environ. Microbiol.*, *73*(21), 6722–6729, doi:10.1128/AEM.00405-07.

Wrage, N., G. Velthof, M. van Beusichem, and O. Oenema (2001), Role of nitrifier denitrification in the production of nitrous oxide, *Soil Biol. Biochem.*, *33*(12–13), 1723–1732.

Zarnetske, J. P., R. Haggerty, S. M. Wondzell, and M. A. Baker (2011a), Dynamics of nitrate production and removal as a function of residence time in the hyporheic zone, *J. Geophys. Res. Biogeosciences*, *116*(1), 1–12, doi:10.1029/2010JG001356.

Zarnetske, J. P., R. Haggerty, S. M. Wondzell, and M. A. Baker (2011b), Labile dissolved organic carbon supply limits hyporheic denitrification, *J. Geophys. Res. Biogeosciences*, *116*(4), 1–13, doi:10.1029/2011JG001730.

Zheng, J., and P. V Doskey (2015), Modeling nitrous oxide production and reduction in soil through explicit representation of denitrification enzyme kinetics., *Environ. Sci. Technol.*, *49*(4), 2132–9, doi:10.1021/es504513v.

CHAPTER 4: THE GEOCHEMICAL EVOLUTION OF THE HYPORHEIC ZONE

OVER TIME AND SPACE

Author List: Annika M. Quick,[1] W. Jeffery Reeder,[2] Tiffany B. Farrell,[1] Daniele Tonina,[2] Kevin P. Feris,[3] and Shawn G. Benner[1]

[1]Department of Geosciences, Boise State University, Boise, Idaho 83725, USA.
[2]Department of Civil Engineering, University of Idaho, Boise, Idaho 83702, USA.
[3]Department of Biological Sciences, Boise State University, Boise, Idaho 83725, USA.

Key Points:
- Redox sequence aerobic respiration, denitrification, Fe and Mn oxidation, and possibly sulfate reduction are observed along flow lines.
- Reductive dissolution of oxides and desorption increases metal concentrations with residence time.
- Silicate dissolution increases Si and Group II metal concentrations with residence time.
- Higher flow velocities caused by steeper dunes result in flushing of most species over time.

Abstract

The hyporheic zone is well established as an important zone of biogeochemical

activity in streams and rivers. Large-scale flume experiments were carried out to mimic

bedform-controlled hyporheic zones and observe a wide-ranging suite of chemical species over space and time. Chemical species measured in the surface water and along hyporheic flow lines included dissolved oxygen, pH, alkalinity, nitrogen species, anions, and many metals and trace elements. Observed spatial and temporal trends reflect microbiological processes, changing redox conditions, dissolution, sorption and desorption. In general, microbial respiration causes dissolved oxygen to decrease with residence time, leading to aerobic and anaerobic zones, nitrate reduction, and a decreasing pH gradient. Most other species concentrations increase with residence time. Based on observations, we propose that increases in Ca, Mg, Si, Ba, and Sr with residence time are primarily due to silicate dissolution, and increases in Fe, Mn, Co, and As with distance along flow lines are due to reductive dissolution of metal oxides and desorption in the anoxic zone. Trends over elapsed time suggest higher flow velocities (as induced by steeper dune morphologies) lead to more rapid consumption of reactive carbon, larger oxic zones, and decreases in most species over time. These results may have important implications for the remediation or storage of pollutants including mining wastes and other heavy metals.

4.1 Introduction

The hyporheic zone (HZ) of streams is well established as an important zone of biogeochemical activity in streams and rivers. Depending on the stream hydrology and morphology, the reactions that take place in the hyporheic zone may have a strong impact on surface water chemistry and the ecosystem functions of streams [Lawrence et al., 2013; Boano et al., 2014]. Significant roles of the HZ include aiding pollutant bioremediation processes [Benner et al., 1995; Harvey and Fuller, 1998; Fuller and

Harvey, 2000; Gandy et al., 2007], controlling greenhouse gas production and release

[e.g. Beaulieu et al., 2011; Gardner et al., 2016; Vidon and Serchan, 2016], influencing

aquatic habitat [e.g. Baxter and Hauer, 2000], and serving as a sink for excess nutrients

such as nitrogen [Marzadri et al., 2011; Zarnetske et al., 2012; Lansdown et al., 2015].

Most studies of the hyporheic zone focus on a few parameters, due to the difficulty and

complexity of making high spatial and temporal resolution measurements in natural

settings. There is a need for more studies of hyporheic chemistry that address a broad

range of geochemical species and provide a complete geochemical picture of the

hyporheic zone.

Due to the difficulty of controlling the conditions for hyporheic zone

measurements in the field, multiple large-scale flume experiments were carried out to

mimic bed form-controlled hyporheic zones in small streams. The laboratory setting

allowed for very high geochemical measurement resolution and replicates that would not

be possible in a natural setting. During two flume experiments, each consisting of three

small streams with variable sizes of triangular bedform dunes, chemical species were

measured in the surface water and along hyporheic flow lines in the subsurface. The

species measured include dissolved oxygen, pH, alkalinity, nitrogen species, anions, and

elemental abundances of major and trace elements.

The purpose of this paper is to provide descriptions of the spatial and temporal

evolution of geochemical species in the hyporheic zone and suggest likely mechanisms

for those trends. In general, the description of each species answers three questions: (1)

How does the species change along a hyporheic flow line (i.e. with residence time)? (2)

How does the species behave over the time elapsed since the experiment began and the

sedimentary system was "reset"? (3) How does the morphology of the bed form dune influence these changes over residence time and elapsed time?

Many of the trends described in this paper can be applied, at least qualitatively, to understanding how these species will behave in natural settings. This insight will contribute to the understanding of many of the applications of the hyporheic zone (e.g. bioremediation, habitat, etc.). For example, varying hydrological, chemical, and biological properties of the hyporheic zone may influence whether heavy metals, such as those from mining wastes, will be retained or released by streams.

4.1.1 Background

The hyporheic zone, describing the sediments beneath and adjacent to streams, is a zone of biogeochemical activity due to its high surface area for microbial populations and influx of reactants from surface water [Edwards, 1998; Winter et al., 1998]. The processes occurring as surface water and groundwater interact along hyporheic flow lines can strongly influence stream chemistry [Tonina and Buffington, 2009]. The role of dune morphology on hyporheic flow paths and velocities has been established in mathematical [Elliott and Brooks, 1997b] and physical models [Elliott and Brooks, 1997a]. Triangular dune-shaped bedforms result in a pressure gradient between the upstream and downstream sides of the dune crest, resulting in a pumping mechanism [Bardini et al., 2012; Tonina, 2012; Fox et al., 2014]. Downwelling of surface water occurs primarily on the upstream side of the dune. This water follows flow paths of varying residence time through the hyporheic sediments before being returned to the stream by upwelling, mostly on the downstream side of the dune (Figure 4.1). Steeper dunes create larger pressure differentials, resulting in overall higher downwelling (and therefore upwelling)

velocities [Fehlman, 1985; Elliott and Brooks, 1997a]. Therefore, triangular dunes with shallower slopes will have overall lower hyporheic flow velocities than those with steep slopes [Marion et al., 2002; Cardenas and Wilson, 2007].
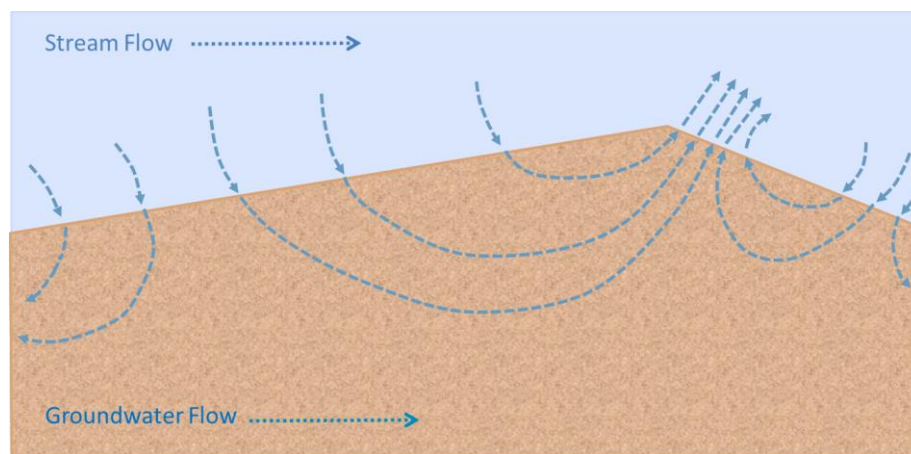
Figure 4.1. **Cross sectional view of a streambed dune.** Cross sectional view of a streambed dune. Cross section shows the downwelling of surface water and upwelling following transit through the hyporheic zone.

4.2 Methods

4.2.1 Flume overview

To study the impact of stream bed morphology on the biogeochemistry of the hyporheic zone over space and time, two long-term experiments (about 3-4 months each) were carried out in the flume at the Center for Ecohydraulics Research Stream Laboratory (CESRL) at the University of Idaho in Boise, Idaho in 2013 and 2015, as detailed by Quick et al. [2016]. The flume consists of a large tank with an adjustable slope that empties into a 50,000-gallon catch basin. To test multiple dune shapes and provide replicates, the flume (approximately 20 m long x 2 m wide) was divided into three smaller channels (each 30 cm wide) using plywood and impermeable sheeting (Figure 4.2). Pumps moved water from the catch basin through a carbon filter to a head

box at the highest end of the flume. Water moved from the head box into the three

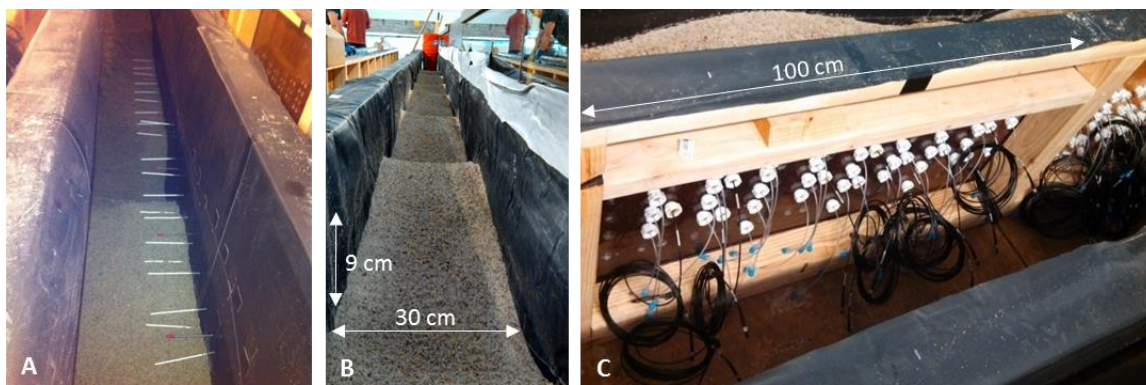smaller channels, ensuring the same initial water conditions between channels.

Figure 4.2. **Flume channel instrumentation and set up.** **(A)** Rhizons and fiber optic DO sensors (with red caps) are inserted into the wall of the flume channels as sand is added. **(B)** A view of the 9 cm dune channel in F1 before the surface water began flowing. **(C)** Rhizons (clear tubes with blue caps) and fiber optic sensor cables seen in the servicing corridor between flume channels. During the experiment, the fiber optic cables were connected to an optical multiplexer.

Table 4.1. **Sand Mixtures and Dune Geometries in F1 and F2**

Sand Mixture		Dune geometries	Channels
Flume 1 (2013)			
90%	quarry sand (sieved to < 2.4 mm)	1 m length x 3 cm height	One dune height
10%	river inoculum sand (wet sieved to < 2.4 mm)	1 m length x 6 cm height	per channel
0.15%	POM (chopped leaves)	1 m length x 9 cm height	
Flume 2 (2015)			
90%	F1 sand mix (dried) and quarry sand (sieved and rinsed)	1 m length x 9 cm height	Two dune lengths
10%	river inoculum sand (wet sieved to < 2.4 mm)	0.7 m length x 9 cm height	per channel; three replicate channels
0.15%	POM (chopped leaves)		(A, B, C)

The sand in each channel was a mixture of quarry sand, natural inoculum sand

obtained from a riverbed, and particulate organic matter (POM). The inoculum sand

provided a natural assemblage of microbes, and the POM was added to simulate the

addition of POM to a streambed following seasonal leaf fall and burial [Metzler and Smock, 1990; Bernhardt and Likens, 2011] or sediment re-working events during flooding [Wondzell and Swanson, 1999]. The quarry sand (Idaho Materials and Construction, Boise, Idaho, USA) was derived from primarily granitic source material and sieved to <2.4 mm. The sand consisted of angular to subangular grains of quartz and feldspar, with smaller amounts of magnetite and micas. The inoculum sand was obtained from a continuously submerged area of the Boise River (Lucky Peak State Park), Idaho, USA. After this sand was collected and wet sieved to < 2.4 mm, it was kept submerged in a tank with periodic mixing/aeration before being mixed with the quarry sand. The particulate organic matter consisted of freshly fallen (less than one week) leaves (47.7 $\pm$ 1.6% carbon) from Black cottonwood *(Populus trichocarpa)* trees along the banks of the Boise River. The leaves were cut into small pieces (< 5 mm) and stored in a freezer prior to being added to the sediment.

During each experiment, the sand was shaped by hand into specified dune geometries and kept moist until the stream began to "flow" from the head box (Table 4.1). Along the walls of the flume channels, sampling ports were installed to monitor subsurface conditions. A robotic cart that traversed the length of the flume was utilized before and after the experiments to make laser measurements of the sand elevation and during the experiments to measure water surface elevation (ultrasonic sensor model LVU30, Omega Engineering, Inc. CT, USA) and dissolved oxygen (DO) concentrations at the sediment-water interface (DO500 sensor, Unisense A/S, Aarhus, Denmark).

Because an additional objective of the experiment was to study nitrogen cycling, a solution of potassium nitrate (KNO_3) was added to the surface water in the middle of

each experiment. In Flume 1, KNO_3 was added on day 61 to increase the surface water nitrate concentration to about 3 mg L^{-1} NO_3^-. In Flume 2, KNO_3 was added on day 63 to increase the surface water concentration to about 10 mg L^{-1} NO_3^-.

At the conclusion of each experiment, the surface water was slowly drained and sediment samples were removed at each subsurface port location. These samples were analyzed for microbial DNA. This analysis focused on the quantification of overall bacterial density and the abundance of nitrogen-cycling microbes; results are detailed by Farrell [2016].

4.2.2 Flume 1 Experiment (2013)

In the first flume experiment in 2013 (hereafter referred to as Flume 1 or F1), all of the dunes were 1 meter long (trough-to-trough). The sand dunes consisted of 90% quarry sand, 10% river inoculum sand, and 0.15% POM. In each of the three channels, the dunes were all one meter long but shaped to different heights: 3 cm, 6 cm, and 9 cm. Two successive dunes were instrumented in the middle section of each channel; each instrumented dune was monitored with 35-41 sampling ports. Ports and samples were identified by the dune size and port location (e.g., 6.29 indicates port 29 in the channel with 6 cm tall dunes).

In Flume 1, each port consisted of a rhizon moisture sampler (Rhizosphere Research Products, Netherlands) and a fiber optic DO sensor. The rhizons, designed to collect pore water, consisted of a 10 cm length of porous tubing (0.45 µm) surrounding a small supporting wire and attached to a 13 cm length of connection tubing and Luer-Lok^{TM} plug. The permeable tube was inserted through the port and into the sand dune, perpendicular to the direction of surface water flow (Figure 4.2A). Fiber optic DO

sensors were positioned next to each rhizon. The DO measurement system, detailed by Reeder et al. [2018], consisted of a PreSens PSt3 oxygen-sensitive sensor spot (PreSens, Germany) affixed with epoxy to the end of a fiber optic cable, which was inserted into a rigid stainless steel sheath and positioned in the streambed. Connecting the cables from the individual ports to an optical multiplexer (Agiltron Inc., Woburn, Massachusetts, USA) and Fibox 3 (PreSens) allowed for automated, in-situ measurements of dissolved oxygen at frequent time points during the experiment.

Stream water flow began in the flume channels on September 9, 2013 (day 0) and continued for 16 weeks through January 2014 (day 112). In-situ DO was measured using the fiber optic sensors in the surface water and at all of the subsurface ports approximately every two days. These measurements were verified weekly with surface water and shallow sediment DO measurements made using Unisense sensors and a robotic instrument cart.

Subsurface pore water samples were collected regularly using the rhizon samplers. During each sampling event, two samples were collected from the rhizons: the first for measurement of nitrogen species (dissolved N_2O, NO_3^-, NO_2^-, and NH_3), and the second for measurement of pH, alkalinity, elemental concentrations (Li, Na, Mg, Al, Si, P, K, Ca, V, Mn, Fe, Co, Ni, Cu, Zn, As, Sr, Ba, Pb, U) and anions (NO_3^-, NO_2^-, SO_4^{2-}, P-PO_4^{3-}, Cl^-). The first sample of water (about 10 ml) was collected in a 20-mL gas-tight headspace vial with septa cap (Agilent). The vials were pre-evacuated, filled with Argon gas, and acidified with H_2SO_4 to reduce the pH to < 2 and prevent microbial processing of nitrogen following sample collection. The second sample (about 10 ml) was collected in evacuated, but not acidified, headspace vials. Half of this sample was used to

determine pH and alkalinity. The second half was transferred to a test tube and acidified to 2% nitric acid. All samples were stored at 4°C prior to analysis. Sample collection procedures are detailed in Quick et al. [2016].

4.2.3 Flume 2 Experiment (2015)

The second flume experiment in 2015 (hereafter referred to as Flume 2 or F2) differed from the first flume experiment in the dune geometries and a few procedural details (comparison shown in Table 4.1). The sand from the first flume experiment was removed, dried, and reused in Flume 2. This dried sand, together with a small amendment of more quarry sand, was rinsed to remove some of the finer clay and silt-sized sediments, and constituted 90% of the sand in F2. River inoculum sediment, collected from the same location in the Boise River as in F1, constituted 10%, and POM (chopped cottonwood leaves) again constituted 0.15% of the sand mixture in the second flume experiment.

In Flume 2, each of the three channels (A, B, and C) had identical dunes. In each channel, the upstream dunes were 70 cm in length and 9 cm in height. The downstream dunes were 100 cm in length and 9 cm in height. One 70-cm and one 100-cm dune in each channel were instrumented with 37-38 ports. The ports and samples were identified by the replicate channel, dune length, and port location (e.g., A100.25 indicates port 25 in the 100 cm long dune in the replicate channel A). In Flume 2, each port consisted of a rhizon sampler and fiber optic DO sensor, as in F1. An additional non-filtering port was inserted adjacent to the rhizon to collect pore water samples for future analysis of pore-water DNA.

Stream water flow began in the flume channels on March 17, 2015 (day 0) and continued for 13 weeks through June 2015 (day 91). Similar to F1, a solution of potassium nitrate (KNO_3) was added to the surface water on day 62 to increase the surface water nitrate concentration to about 10 mg L^{-1} NO_3^-. As in the first experiment, in-situ DO was measured regularly, and pore water samples were collected for analysis of other chemical species.

4.2.4 Chemical Analysis Methods

    4.2.4.1 Nitrogen species

Measurement of dissolved nitrous oxide (N_2O) was carried out using a headspace equilibration technique [Hudson, 2004], utilizing an Agilent 6890 gas chromatograph equipped with a GS-Carbon PLOT column, ^{63}Ni micro-electron capture detector, and HP 7694 autosampler [Quick et al., 2016]. Following N_2O measurement, samples were transferred to 15 ml test tubes for measurement of NO_2^-, NO_x (NO_3^- + NO_2^-), and NH_3 using a Lachat 8500 Flow Injection Analysis (FIA) system (QuikChem methods 10-107-04010B and 10-107-06-1-F) [Quick et al., 2016].

    4.2.4.2 pH and alkalinity

The pH and alkalinity of the non-acidified pore water samples were measured immediately after collection. The pH was measured using a pH probe (Denver Instruments) that was calibrated daily using standard buffer solutions. In Flume 1, alkalinity was determined using the Hach colorimetric method (bromocresol green and methyl red). In Flume 2, alkalinity was determined using the Hach TitraLab automatic titrator.

4.2.4.3 Elemental concentrations

Pore water samples for elemental analysis were filtered by the rhizons during collection and immediately transferred to acid-washed 15 ml glass test tubes, diluted with Milli-q water, acidified using concentrated double distilled nitric acid (HNO_3), capped, and stored at 4°C until analysis. Elemental concentrations were determined using a ThermoScientific XSeries 2 Inductively Couple Plasma Mass Spectrometer (ICP-MS) with an Elemental Scientific SC *FAST* autosampler system. The suite of elements analyzed included Li, Na, Mg, Al, Si, P, K, Ca, V, Cr, Mn, Fe, Co, Ni, Cu, Zn, Sr, Ag, Cd, Ba, Pb, and U. Three multi-element standards (1 ppm, 100 ppb, and 10 ppb for Na, Mg, Al, Si, K, and Ca; 100 ppb, 10 ppb, and 1 ppb for Li, P, V, Cr, Mn, Fe, Co, Ni, Cu, Zn, Sr, Ag, Cd, Ba, Pb, and U) were used for instrument calibration. Using the SC *FAST* autosampler system, a constant amount of internal standard solution was added to each sample and monitored during measurement runs to detect any changes in sensitivity.

4.2.4.4 Anions

Due to laboratory limitations, pore water samples were only analyzed for anions sulfate (SO_4^{2-}), orthophosphate (HPO_4^{2-}-P), bromide (Br^-), chloride (Cl^-), and fluoride (F^-) at the end of the second flume experiment (day 92). These ions were analyzed using the ion chromatography method of the Lachat QuikChem 8500 FIA instrument (QuikChem method 10-510-00-1-A).

4.2.5 Residence time modeling

Streambed dunes create pressure differentials along the sediment-water interface that drive downwelling of surface water on the upstream face of a dune and upwelling on the downstream face [Tonina, 2012]. The measurement and modeling of pressure profiles

along the dune surfaces are explained in detail by Reeder et al. [2018]. These pressure profiles, as input conditions for the flow model of Marzadri et al. [2010], were used to calculate residence times for each subsurface sampling location. The calculated residence times for each sampling location, which can also be conceptualized as travel time from the sediment-water interface to the sampling location in the subsurface, were supported by tracer tests (fluorescein dye and sodium chloride) at the end of the second flume experiment. Overall residence times were shorter in F2 than in F1 due to lower hydraulic permeability and a greater stream slope. Details are provided in the Supplementary Information of Quick et al. [2016].

4.2.6 MINTEQ geochemical modeling

To gain insight into the potential speciation and precipitation and dissolution reactions taking place in the hyporheic zone, measured species concentrations were entered into the chemical equilibrium model, Visual MINTEQ version 3.1. Details and saturation indices for selected minerals with residence time are included in Appendix C (Figures C.36-C.40).

4.3 Results

Based on residence time modeling and tracer tests, geochemical samples were collected from both the hyporheic zone (which experiences dune-scale exchange with surface water) and the groundwater zone underneath. The photograph in Figure 4.3 was taken through a Plexiglas window installed on the side of one of the 70 cm dunes in F2 and shows a grayish precipitate that formed as the second flume experiment elapsed. The streak slowly moved downstream over time and was consistent with very long residence times. The lower position of the precipitate band was fairly consistent with the assumed

boundary between the hyporheic zone (generally shorter residence times) and

groundwater zone (long residence times).

Figure 4.3. **Cross-sectional view of a 70 cm dune in F2.** The grayish streak developed over the duration (91 days) of the experiment. Surface water flow is from right to left. The black grid lines are spaced at 1 cm.

The spatial and temporal trends in each measured species in the hyporheic zone

are described in detail below and summarized in Table 4.2. Snapshot data for individual

time points during the experiment are displayed in bubble plots, in which the size of the

bubbles reflects the concentration of a species at a specific location (e.g. Figure 4.4-4.8

shows concentrations on day 112 for F1 and day 91 for F2). Bubble plots for all species

on multiple sampling days in both experiments are included in Figures C.6-C.32 in

Appendix C. Location-specific concentrations, as shown in the bubble plots, can also be

plotted with residence time (Figures 4.9-4.15). Concentrations at individual locations

were also plotted over days elapsed during the experiment to observe temporal trends.

For the sake of brevity, the majority of the data plots are included in Appendix C, and

only key plots are shown and described below. The presented residence time plots exclude measurements made from rhizons outside the hyporheic zone (i.e. those rhizons sampling sub-hyporheic groundwater flow) and from rhizons in recirculating zones with unreliable modeled residence times (see Figures C.1 and C.2 in Appendix C for rhizon locations). The full dataset is available online through the Boise State University ScholarWorks data repository.

To facilitate discussion, following descriptions of DO, pH, alkalinity, nitrogen species and anions, most of the remaining species will be discussed as groups of elements showing similar trends, as apparent when plotting relative concentrations (Groups A, B, and C).

Table 4.2. **Trends in Geochemical Species**

|	Spatial	Temporal	Geomorphological
	Over Residence Time	Over Elapsed Time (relative to surface water)	Difference in dunes at end of experiment
DO	Decrease	Increase	Higher in steeper dune
pH	Decrease	Increase (F2 only)	Higher in steeper dune
Alkalinity	Increase (F1 only)	unclear	Lower in steeper dune (F1 only)
$N\text{-}NH_3$	Increase	unclear	Lower in steeper dune (F2 only)
$N\text{-}NO_3^-$	Decrease	unclear	Higher in steeper dune
$N\text{-}NO_2^-$	Increase then decrease (hotspot) (F2)	Increase following KNO_3 addition (F2)	unclear
$N\text{-}N_2O$	Increase then decrease (hotspot)	Increase following KNO_3 addition	Higher in steeper dune (F1 only)
Cl^-, Br^-, F^-	unclear	--	Higher in steeper dune
SO_4^{2-}	Decrease	--	unclear
$P\text{-}PO_4^{3-}$	Increase then decrease	--	unclear
Mn, Fe, Co, As	Increase	Decrease	Lower in steeper dune
Ni, Zn	Increase (F1 only)	unclear	Lower in steeper dune (F1 only)
P	Increase (except 100 cm in F2)	Decrease (less clear)	Lower in steeper dune
Cu, U	Decrease	unclear	unclear
Pb	Decrease (F1 only)	unclear	unclear
V	Increase then decrease (hotspot)	unclear	unclear
Mg, Ca, Si, Sr, Ba, (Li)	Increase	Decrease	Lower in steeper dune (F1 only)
Na	unclear	unclear	unclear
Al, K	unclear	unclear	unclear
Cr, Ag, Cd	Concentrations too low to determine trends		
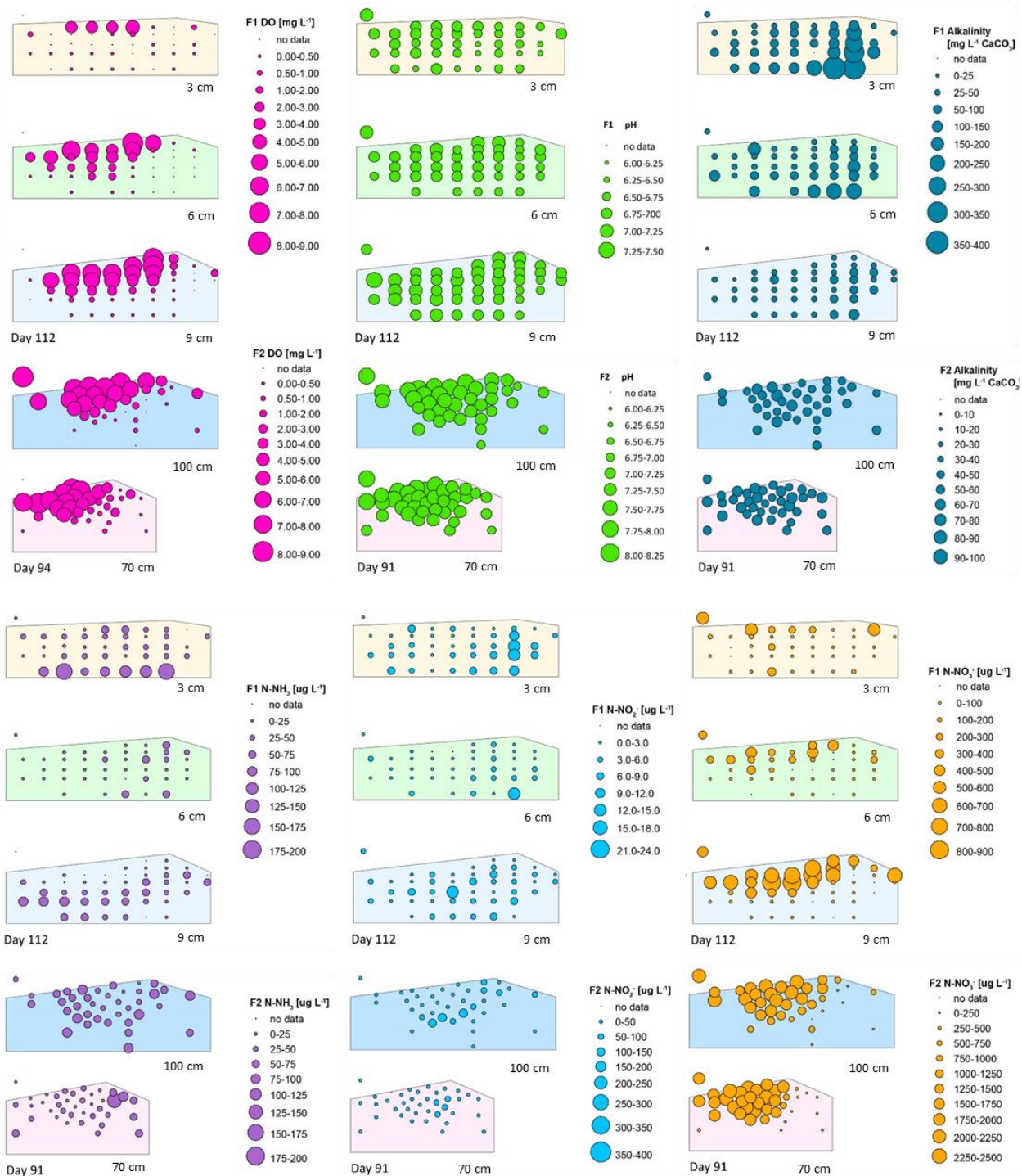
Figure 4.4.   Species concentrations in the hyporheic zone (DO, pH, Alkalinity, NH₃, NO₂⁻, NO₃⁻). Concentrations (as represented by bubble size) are displayed at the measurement locations on shapes representing the dune cross sections. The species name is shown above the bubble scale. The top three dunes for each species show the 3 cm, 6 cm, and 9 cm dunes at the end of F1 (day 112). The bottom two dunes for each species show the 100 cm and 70 cm dunes at the end of F2 (day 91).

Figure 4.5. **Species concentrations in the hyporheic zone (N₂O, Mn, Fe, Co, As, V).** Concentrations (as represented by bubble size) are displayed at the measurement locations on shapes representing the dune cross sections. The species name is shown above the bubble scale. The top three dunes for each species show the 3 cm, 6 cm, and 9 cm dunes at the end of F1 (day 112). The bottom two dunes for each species show the 100 cm and 70 cm dunes at the end of F2 (day 91).
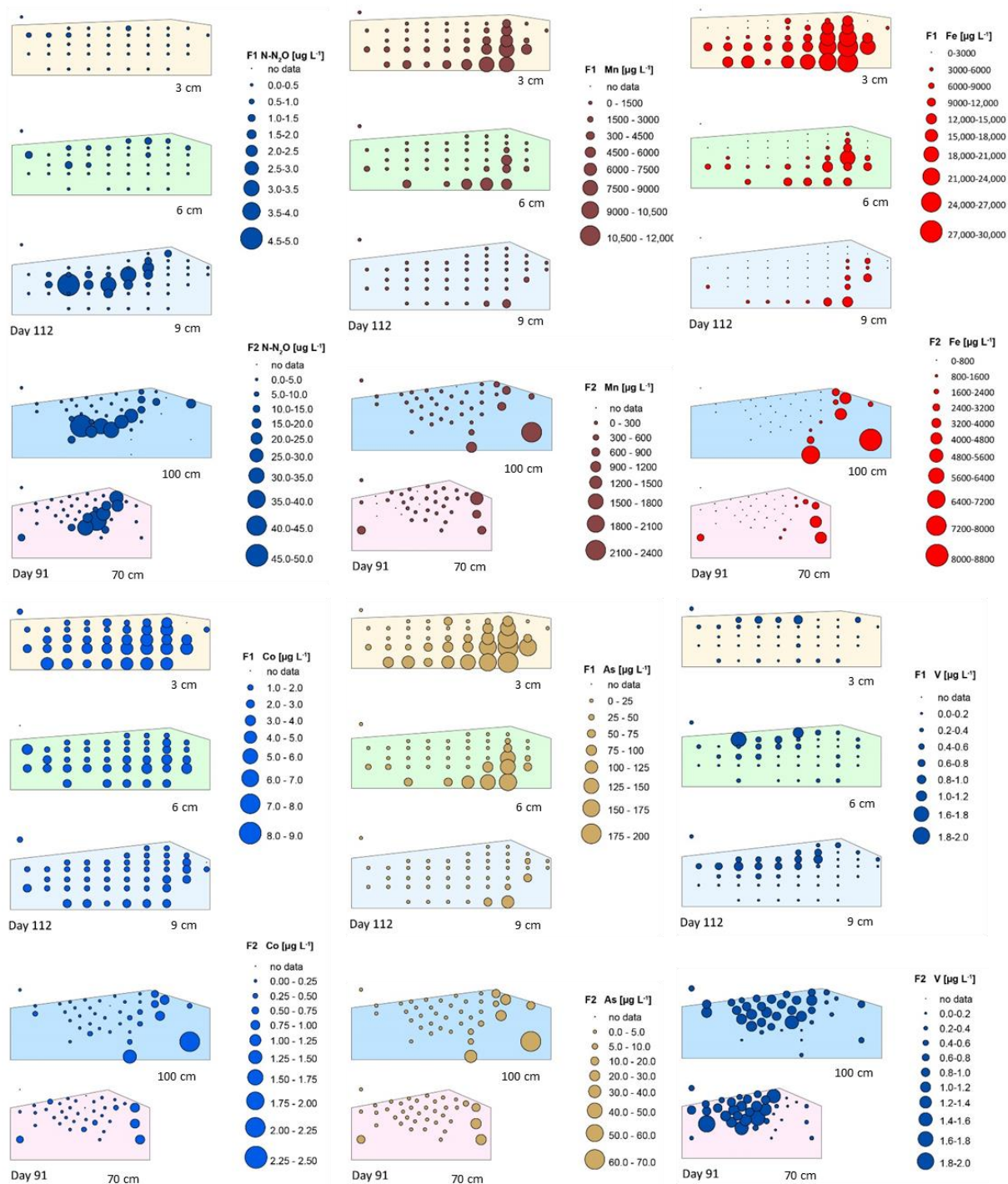
Figure 4.6.   Species concentrations in the hyporheic zone (Cu, Pb, U, Ni, Zn, Na). Concentrations (as represented by bubble size) are displayed at the measurement locations on shapes representing the dune cross sections. The species name is shown above the bubble scale. The top three dunes for each species show the 3 cm, 6 cm, and 9 cm dunes at the end of F1 (day 112). The bottom two dunes for each species show the 100 cm and 70 cm dunes at the end of F2 (day 91).
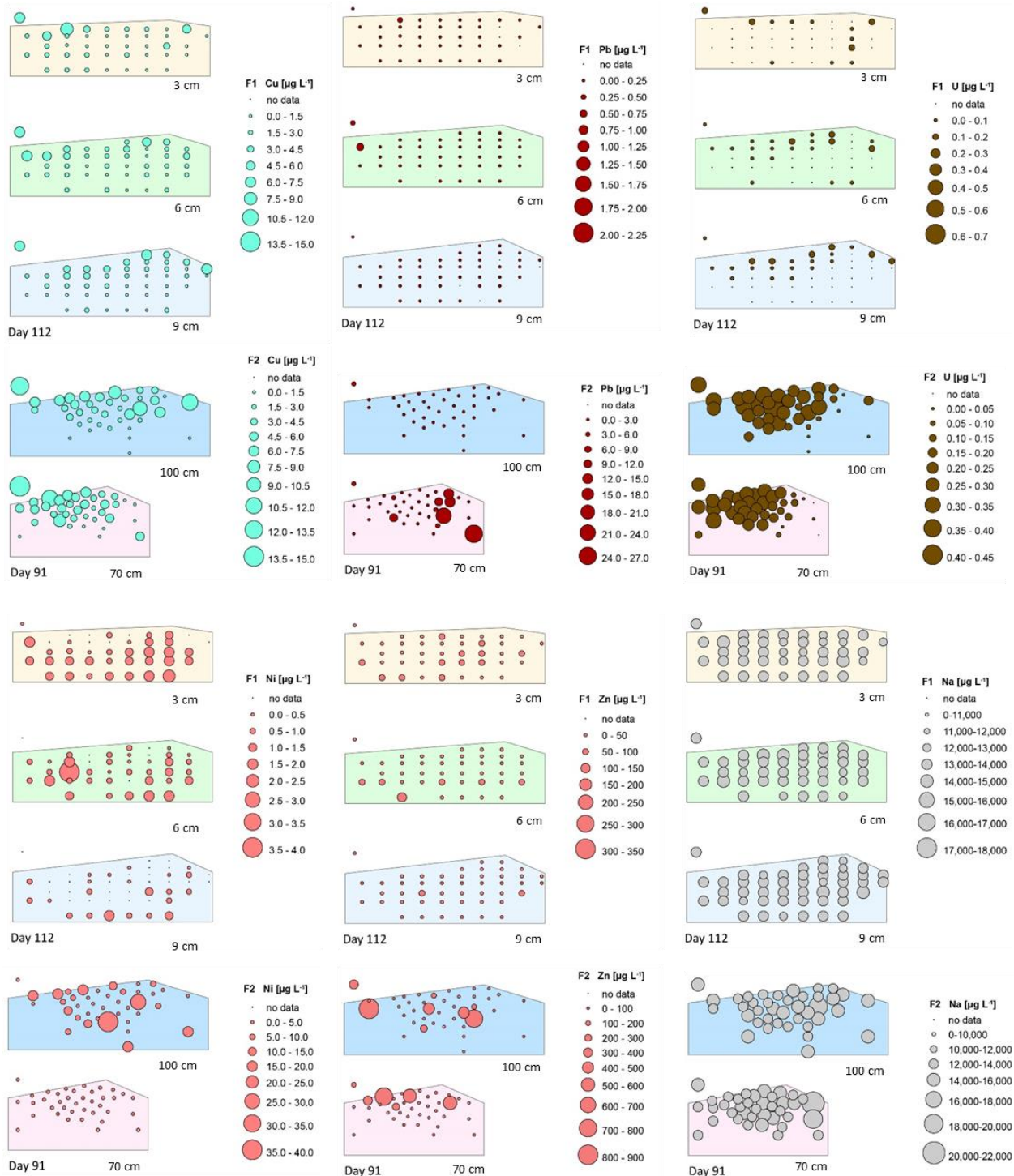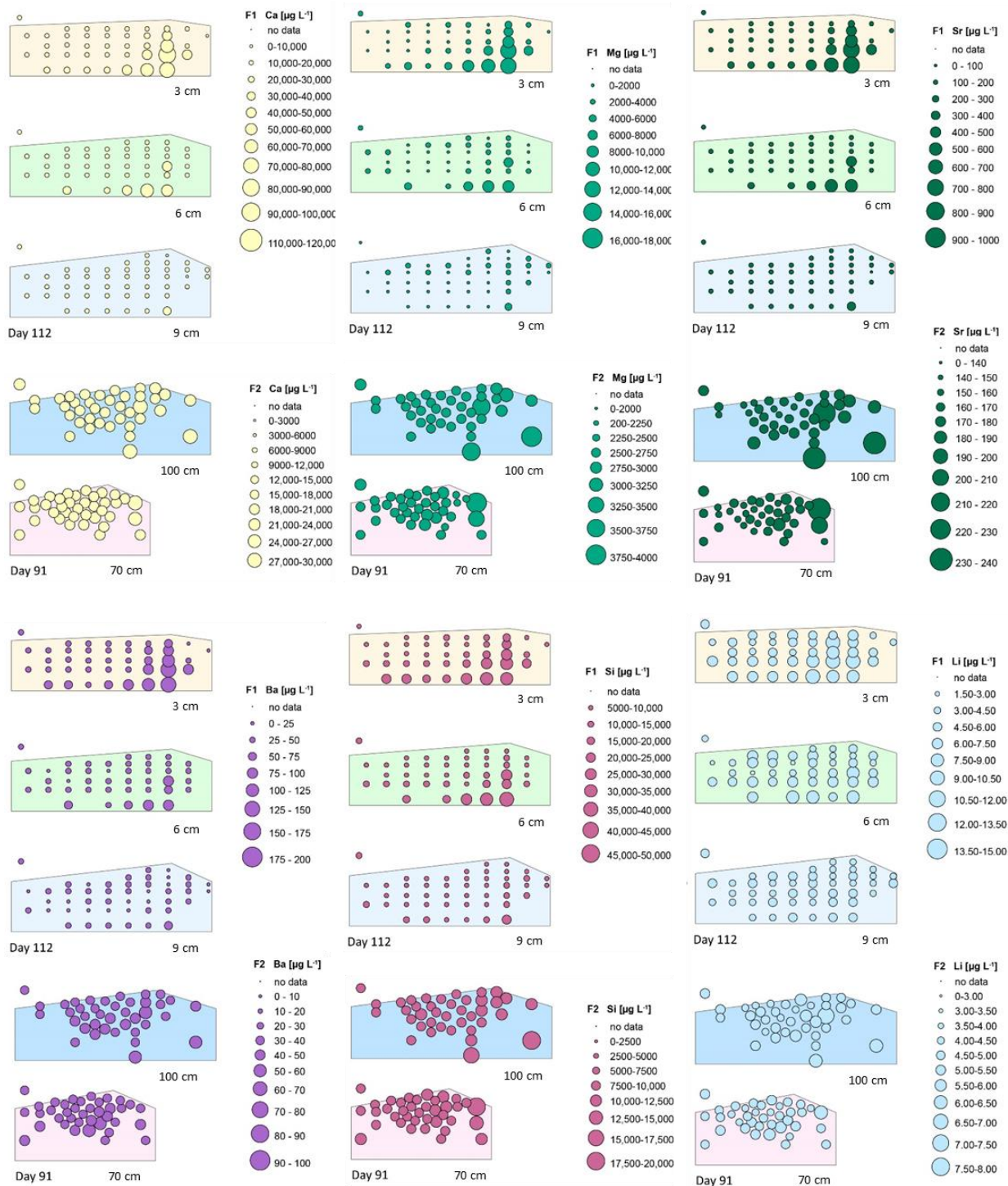
Figure 4.7. **Species concentrations in the hyporheic zone (Ca, Mg, Sr, Ba, Si, Li).** Concentrations (as represented by bubble size) are displayed at the measurement locations on shapes representing the dune cross sections. The species name is shown above the bubble scale. The top three dunes for each species show the 3 cm, 6 cm, and 9 cm dunes at the end of F1 (day 112). The bottom two dunes for each species show the 100 cm and 70 cm dunes at the end of F2 (day 91).

Figure 4.8. **Species concentrations in the hyporheic zone (P, K, Al).** Concentrations (as represented by bubble size) are displayed at the measurement locations on shapes representing the dune cross sections. The species name is shown above the bubble scale. The top three dunes for each species show the 3 cm, 6 cm, and 9 cm dunes at the end of F1 (day 112). The bottom two dunes for each species show the 100 cm and 70 cm dunes at the end of F2 (day 91).
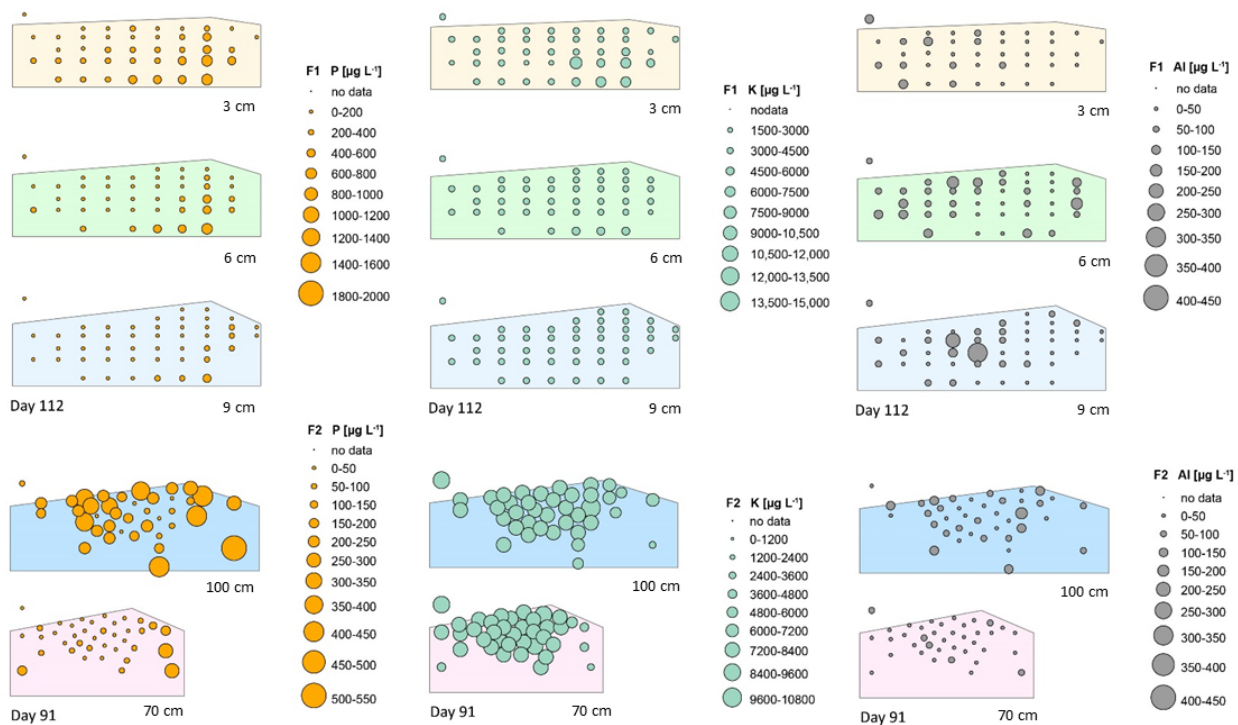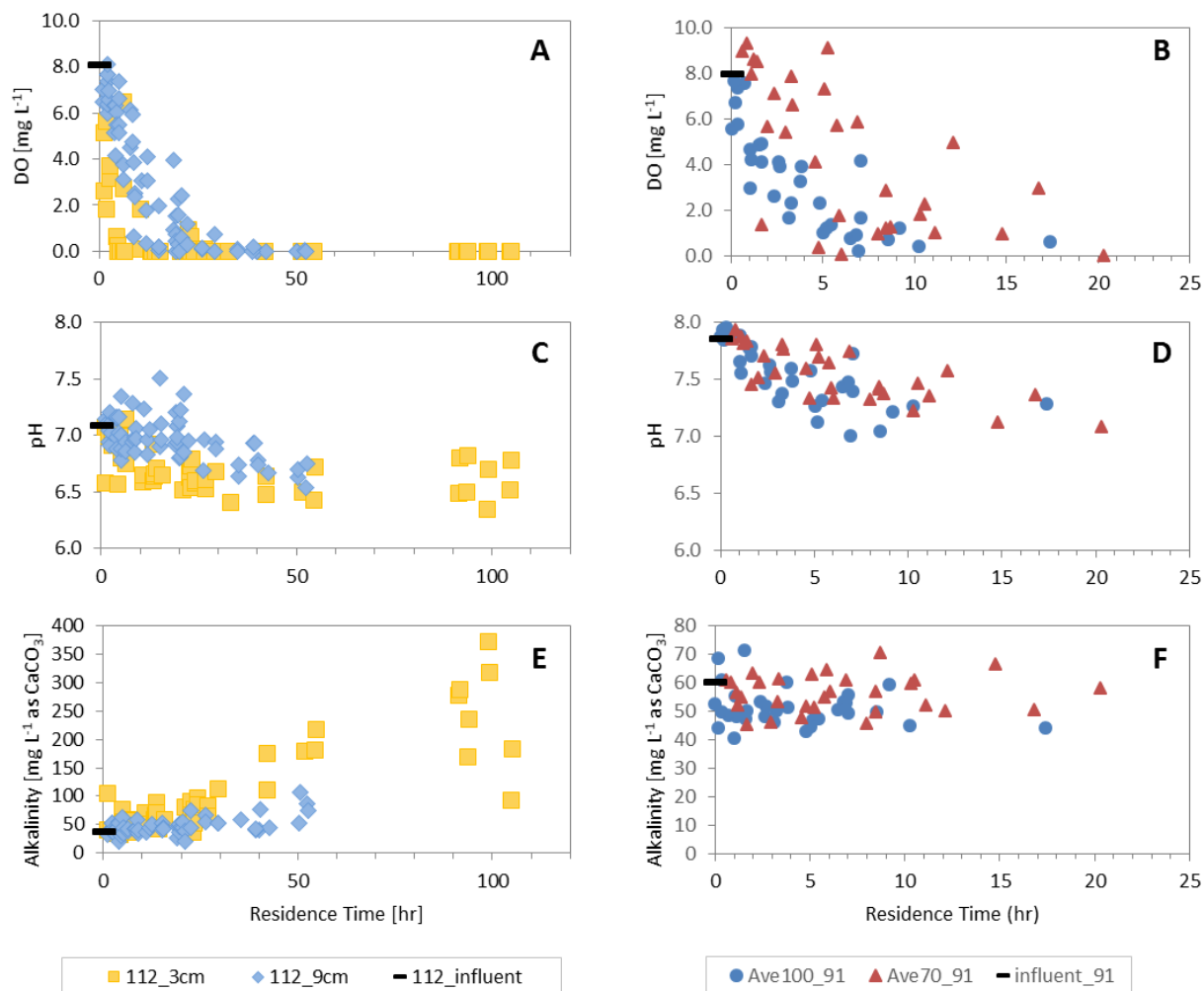
Figure 4.9.   Dissolved oxygen concentrations, pH, and alkalinity versus residence time. Measurements are shown for the 3 cm, 6 cm, and 9 cm dunes (A, C, E) at the end of F1 (day 112) and in the 100 cm and 70 cm dunes (B, D, F) at the end of F2 (day 91). In the plots for F2, the values shown are the averages of three replicates.
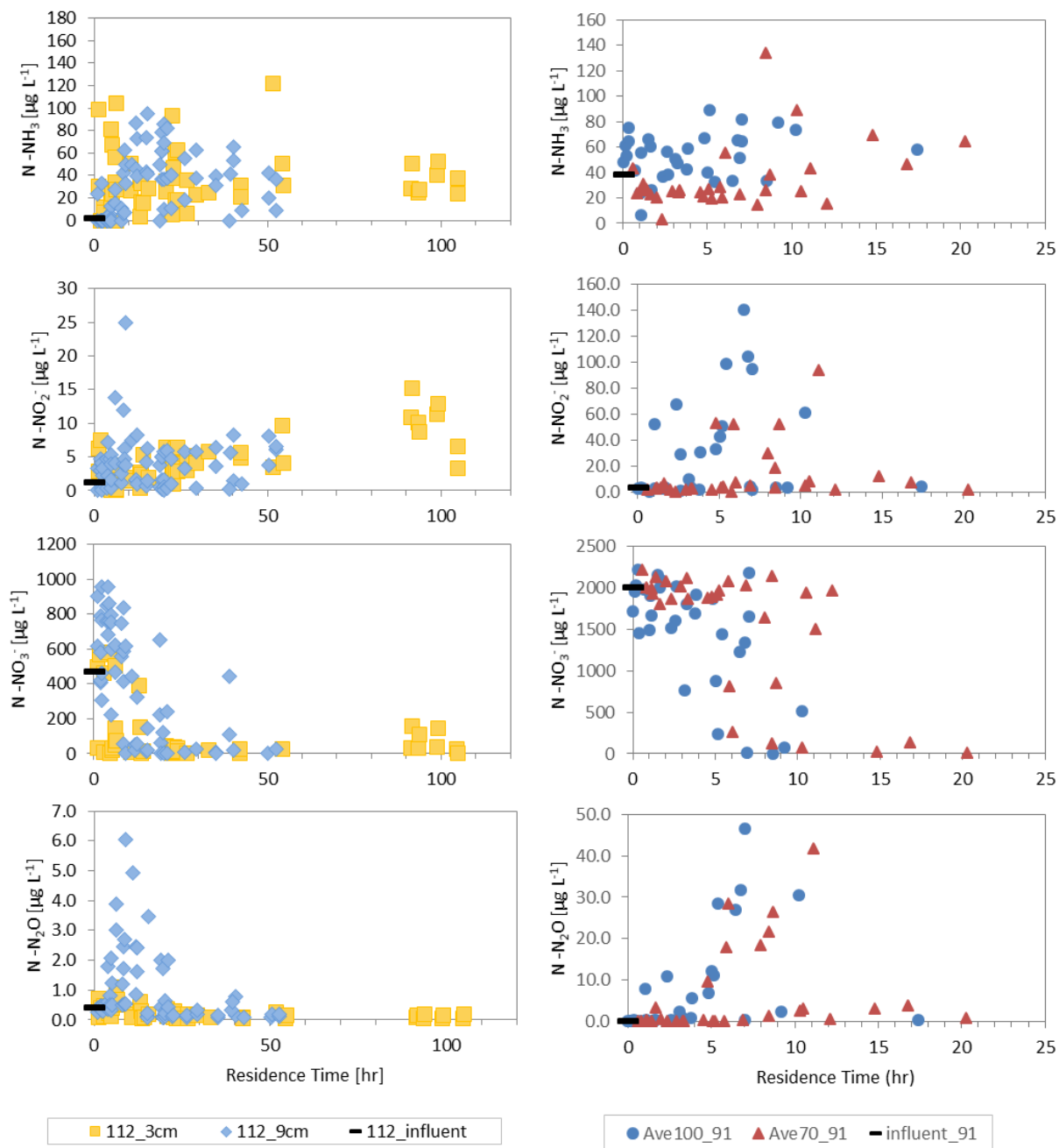
Figure 4.10. Nitrogen species concentrations residence time. Measurements are shown for the 3 cm, 6 cm, and 9 cm dunes (A, C, E, G) at the end of F1 (day 112) and in the 100 cm and 70 cm dunes (B, D, F, H) at the end of F2 (day 91). In the plots for F2, the values shown are the averages of three replicates.
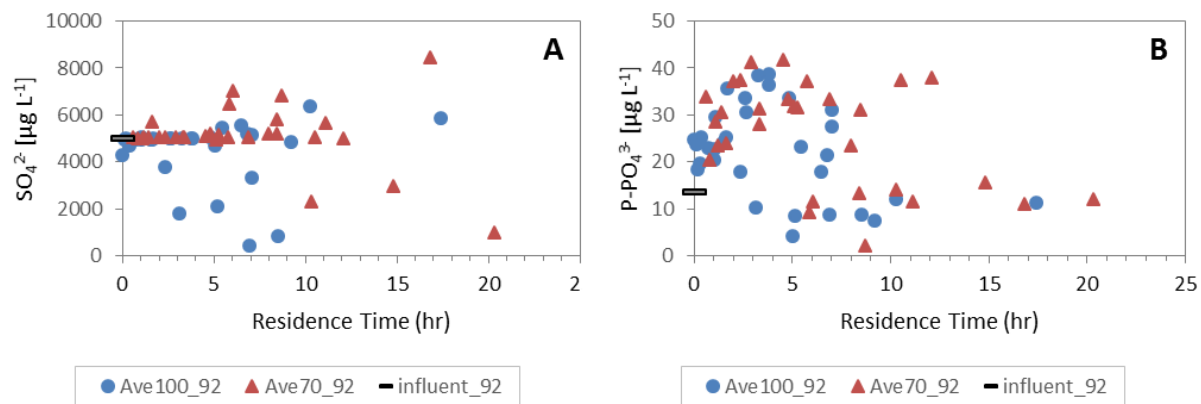
Figure 4.11.   Sulfate and orthophosphate-P concentrations versus residence time. Measurements are from F2 on day 91. The measurements of sulfate below about 2000 µg L^{-1} correspond to hyporheic locations on the downstream side of the dune crest.
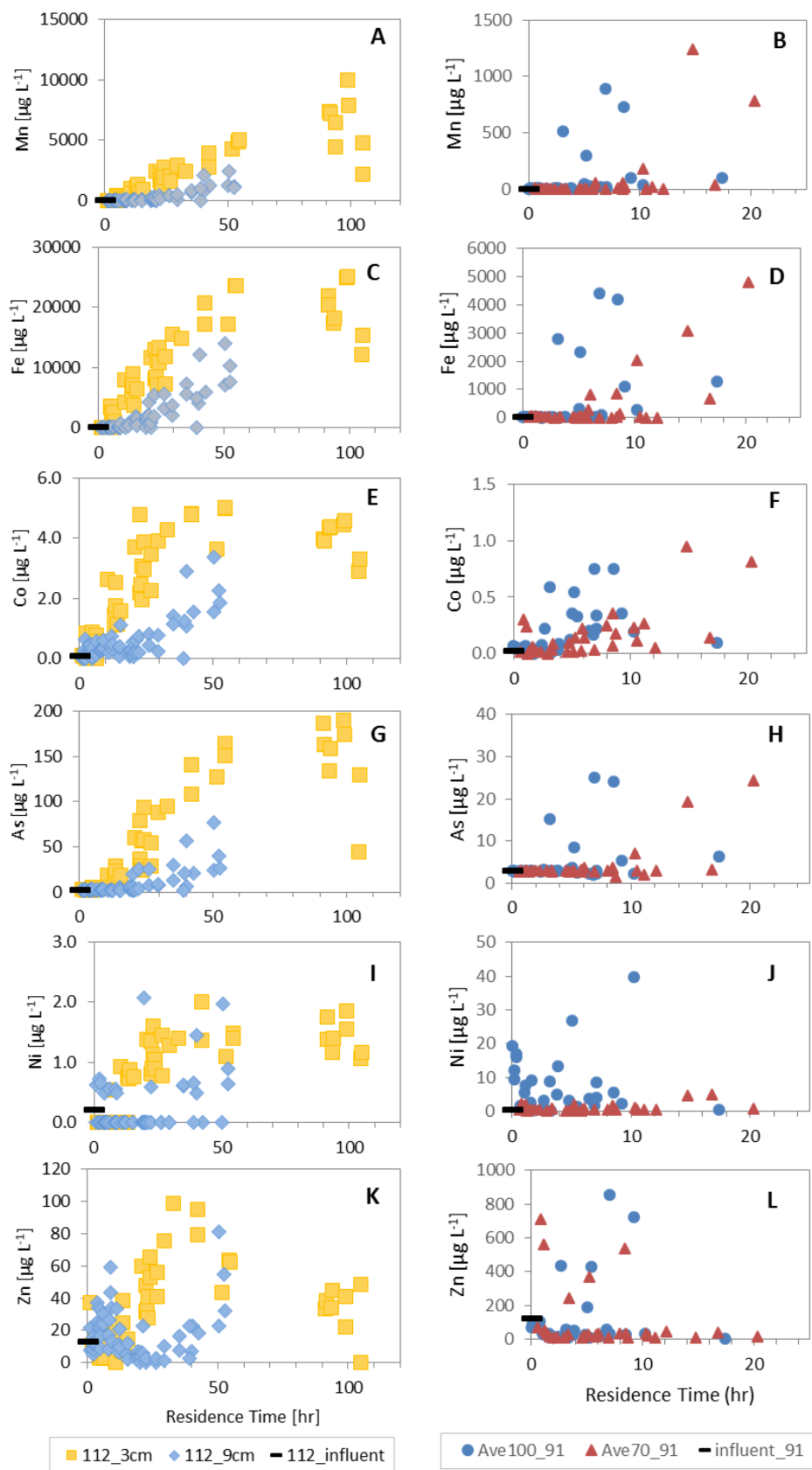
Figure 4.12. Hyporheic species concentrations versus residence time (Mn, Fe, Co, As, Ni, Zn). Measurements are for day 112 for F1 (left panels) and day 91 for F2 (right panels).
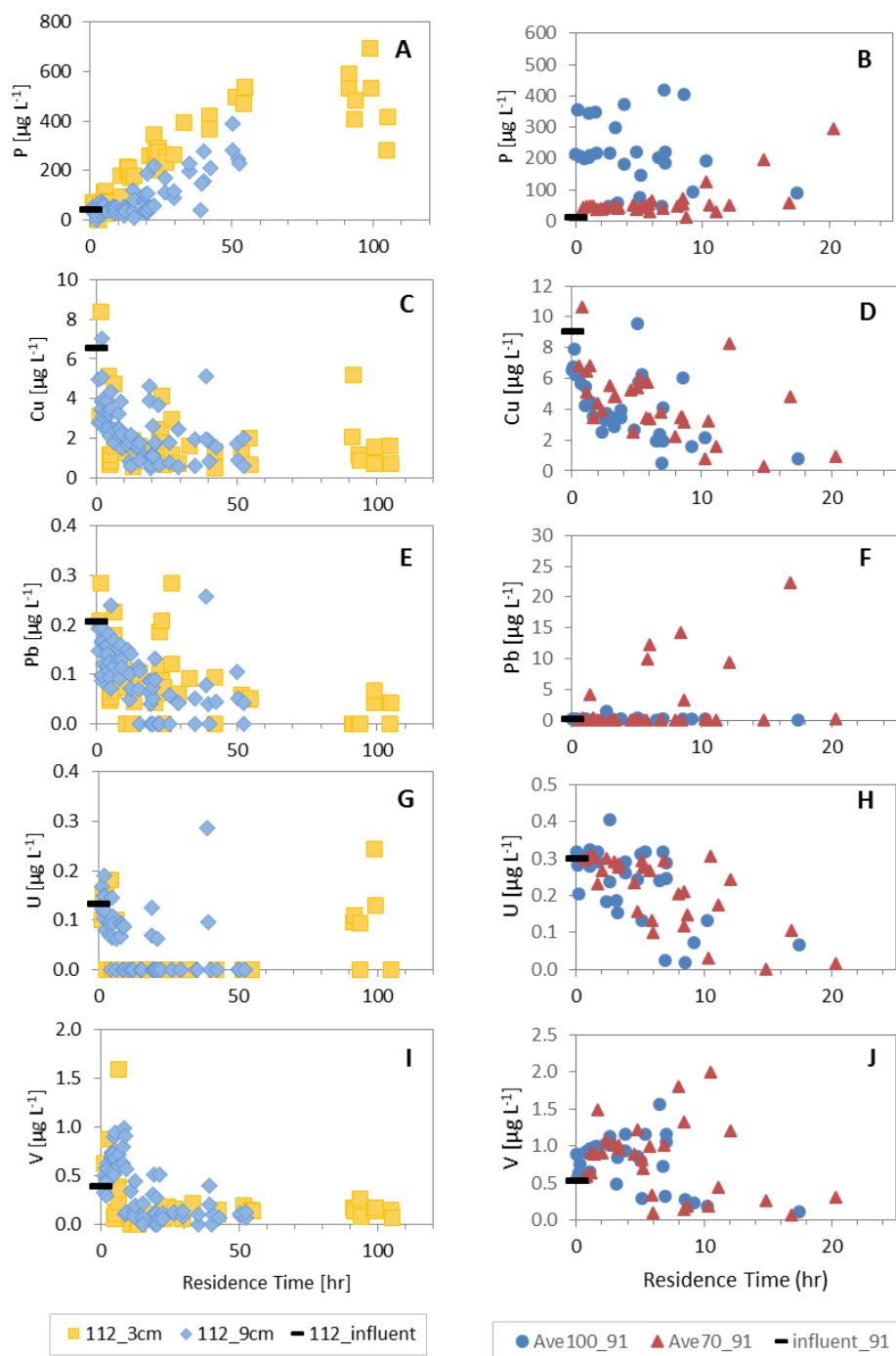
Figure 4.13. Hyporheic species concentrations versus residence time (P, C, Pb, U, V). Measurements are for day 112 for F1 (left panels) and day 91 for F2 (right panels).
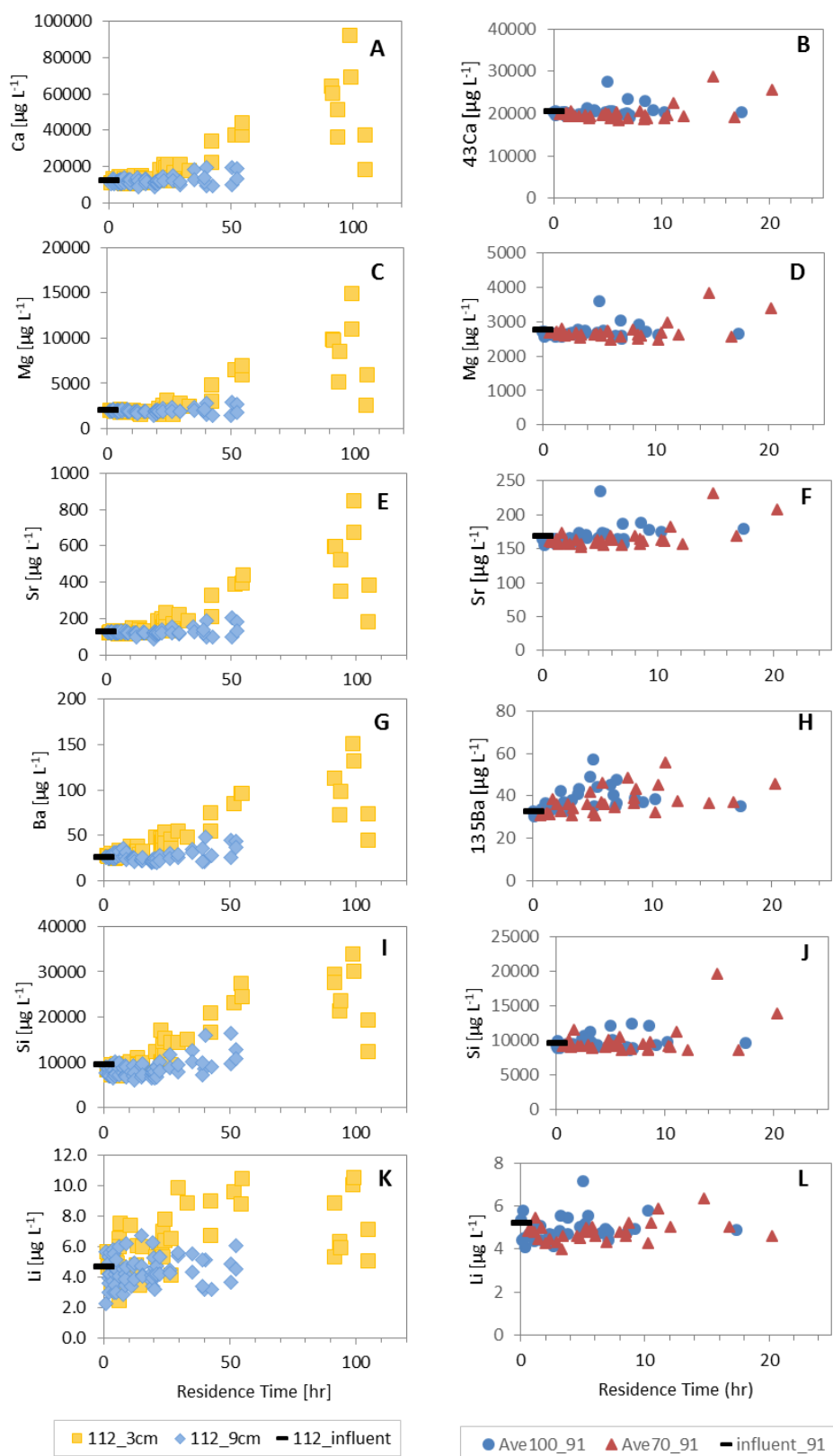
Figure 4.14. Hyporheic species concentrations versus residence time (Ca, Mg, Sr, Ba, Si, Li). Measurements are for day 112 for F1 (left panels) and day 91 for F2 (right panels).
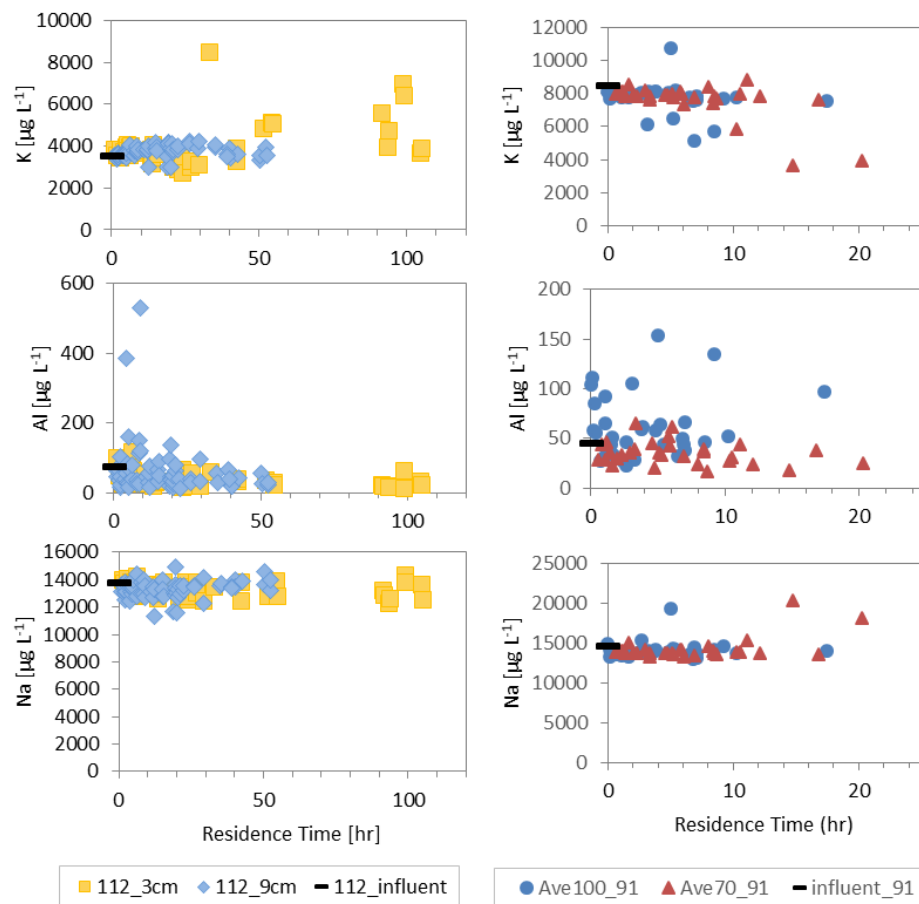
Figure 4.15. Hyporheic species concentrations versus residence time (K, Al, Na). Measurements are for day 112 for F1 (left panels) and day 91 for F2 (right panels).

4.3.1 Dissolved Oxygen

The surface water feeding into the stream channels is open to the atmosphere and saturated with oxygen (7-9 mg/L, depending on atmospheric temperature and pressure). As DO-saturated surface water moves into the hyporheic zone, the oxygen concentration decreases along flow paths, as shown in Figure 4.4. The decrease in DO along flow path is also apparent when DO is plotted versus residence time, as in Figure 4.9. During both experiments, DO concentrations increased over elapsed time, as shown at multiple individual sampling locations in Figures C.3 and C.4, resulting in larger aerobic zones and smaller anaerobic zones as the experiment progressed. As shown in Figure 4.9, the

steeper dunes in each experiment (9 cm in F1 and 70 cm in F2) have lower rates of oxygen consumption, and as a result, these steeper dunes also have larger aerobic zones than the more shallowly sloped dunes (3 cm in F1 and 100 cm in F2). For example, on day 112 of the first flume experiment, the DO drops to below 1 mg L^{-1} within approximately 10 hours in the 3 cm dune, 20 hours in the 6 cm dune, and 30 hours in the 90 cm dune. On day 91 of the second flume experiment, DO drops to below 1 mg L^{-1} within about 10 hours in the 100 cm dune and about 20 hours for the 70 cm dune. The spatial and temporal evolution of DO in the flume experiments is described in further detail in Reeder et al. [2018].

4.3.2 pH

Across both experiments, hyporheic pH remained in the range 6.0-8.0. The pH decreased with residence time for all of the dunes, as shown in Figure 4.9. Over elapsed time, the overall pH increased (this trend is uncertain in F1, clear in F2), while maintaining the decreasing trend with residence time. The overall change in pH over the 13-16 weeks of the experiments was 1.0 or less. The rate of pH decrease is lower in the steeper (higher velocity) 9 cm and 70 cm dunes. In a given dune, pH was lower at the deeper rhizons.

4.3.3 Alkalinity

As measured at the subsurface rhizons, alkalinity (as mg L^{-1} $CaCO_3$) increased relative to the surface water and over residence time in F1 (Figure 4.9). The increase with residence time is not clear in F2, and the range of alkalinity is 36-92 mg L^{-1} as $CaCO_3$, which is significantly lower than the range in F1 (0-373 mg L^{-1} as $CaCO_3$). There is not an obvious trend over days elapsed during the experiment. In F1, the alkalinity is highest

in the dunes with shallower leeward slopes and lower flow velocities (ranges are approximately 32-373 in the 3 cm dune and 0-106 in the 9 cm dune).

4.3.4 Nitrogen species

4.3.4.1 Ammonia

In general, Ammonia concentrations in the subsurface are much higher than in the surface water, and increase with residence time in both F1 and F2, though there is considerable noise in the data (Figure 4.10). Over elapsed time, NH_3 concentrations generally increase, but the trend is not clear due to noise in the data and difficulty comparing calibration curves across measurement days. Between the dunes, the shallower-sloped dune with lower flow velocity (100 cm in F2) has higher concentrations than the higher flow velocity (70 cm in F2), although this is only obvious in F2.

4.3.4.2 Nitrate

Along a flow path, $[NO_3^-]$ first increases somewhat from surface water concentrations and then decreases sharply, with low concentrations after about 10 hours in the subsurface (Figure 4.10). Temporal trends are unclear due to the addition of concentrated KNO_3 solution about 60 days into each experiment. Overall concentrations are higher in the higher velocity dunes (9 cm in F1 and 70 cm in F2).

4.3.4.4 Nitrite

Subsurface concentrations of nitrite are higher than in the surface water (Figure 4.10). Particularly in F2, it appears that there is an increase in nitrite followed by a decrease along flowlines. This is apparent in the plots of concentrations with residence time, and shows up as a nitrite hotspot on the bubble plots (Figure C.11). Trends over

elapsed time are not clear, at least partially due to the addition of KNO_3. Trends between different dune morphologies are unclear.

4.3.4.5 Nitrous Oxide

Like nitrite, nitrous oxide concentrations appear to increase and then decrease with residence time (Figure 4.10). The resulting hotspot is most apparent in the bubble plots for both F1 and F2 (Figure C.12). N_2O concentrations in both experiments are higher after the addition of KNO_3 to the system. Between dunes, the highest concentrations are found in the steeper 9 cm dune, followed by the 6 cm and 3 cm dunes. There was not a significant difference between the concentrations in the 70 cm and 100 cm dunes in F2.

4.3.5 Anions

4.3.5.6 Chloride, bromide, and fluoride

Concentrations of chloride, bromide, and fluoride anions, as shown by bubble plots and residence time plots in Figures C.33 and C.34 did not show clear trends in the hyporheic zone. Anions were only measured at the end of the second flume experiment, so trends over time are unavailable. Concentrations of F^-, Cl^-, and Br^- were generally higher in the faster velocity, 70 cm dune.

4.3.5.7 Phosphate-P (and total P)

Based on the measurements taken at the end of F2, orthophosphate-P concentrations, ranging from below the level of detection to 54 µg L^{-1}, show an increase followed by a decrease with residence time (Figure 4.11), which is somewhat apparent as a "hotspot" in the bubble plot for the 100 cm dune (Figure C33). There is not a clear difference in $[P\text{-}PO_4^{3-}]$ between the 70 cm and 100 cm dunes. While orthophosphate

concentrations were only measured once, total P was measured via ICPMS with the other elemental abundances throughout both experiments (Figures 4.8, 4.13, C.18). Interestingly, total P increases with residence time in both F1 and F2 (except for the anomalous decreasing trend in the 100 cm dune on day 91 in Figure 4.13). Over elapsed time, overall concentrations of P decreased, at least in F1. At the end of the experiments, P ranged from 0 to 695 µg L^{-1} in F1 (day 112) and from 0 to 857 µg L^{-1} in F2 (day 91). Concentrations are lower in the higher velocity dunes (9 cm and 70 cm).

4.3.5.8 Sulfate

Sulfate concentrations measured at the end of F2 show an overall decrease with residence time when considering all measurement locations in the hyporheic zone (range: 19-9820 µg $L^{-1}SO_4^{2-}$) (Figure 4.11). Sulfate concentrations lower than the surface water (4990 µg L^{-1}) were mostly measured at hyporheic locations on the downstream side of the dune crest (rhizons 33, 34, 36 in the 100 cm dune and rhizons 34, 35, 36 in the 70 cm dune in Figure C.2). Between the dunes, sulfate concentrations were lower in the lower velocity 100 cm dune. Sulfate concentrations in the higher velocity 70 cm dune are constant through residence times of 5 hours and the only measurements that are lower than those in the surface water occur after residence times of 10 hours.

4.3.6 Group A Species: Manganese, Iron, Cobalt, Arsenic

Hyporheic concentrations of manganese, iron, cobalt, and arsenic, referred to here as Group A species, all show very similar spatial and temporal trends (Figures 4.12, 4.16, 4.17). Hyporheic concentrations are higher than in surface water and increase with residence time (Figure 4.12). Group A species concentrations are negatively correlated with dissolved oxygen (Figure 4.17). Concentrations are higher in F1 than in F2. For

example, at the end of the experiments, [Fe] ranges from 7 to 25,610 µg L^{-1} in F1 and ranges from 0 to 10,440 µg L^{-1} in F2 (average of replicates) (Figure 4.12). Particularly in F2, the highest concentrations are observed at subsurface locations on the downstream side of the dune crest.

Overall, concentrations decrease over elapsed time, while surface water concentrations remain very low and fairly constant. The largest temporal decrease occurred in the 3 cm dune, where the maximum measured [Fe] decreased from 41,142 to 25,610 µg L^{-1} between days 9 and 112. Between dunes, the highest concentrations were observed in the lower velocity 3 cm dune in F1. The two dunes in F2 showed similar concentrations.

4.3.7 Group B Species: Copper, Lead, Uranium

In contrast to the species in Group A, copper, lead, and uranium showed decreases with residence time (Figures 4.13 and 4.16). Copper concentrations decreased with hyporheic residence time in all dunes and were lower than in the surface water. Temporal and geomorphological trends in [Cu] are unclear. In most dunes at most time points, [Pb] is very low and trends are not obvious. However, in F1, there is an apparent decrease in [Pb] with residence time, particularly in the 9 cm dune. An exception to this trend are the very high, decreasing [Pb] only in the 70 cm dune on day 91 of F2. The decrease in [U] with residence time is most clear in both dunes in F2 and the 9 cm dune in F1. Trends in [U] between dunes and over elapsed time are unclear.

4.3.8 Group C Species: Calcium, Magnesium, Strontium, Barium, Silicon, and Lithium

Calcium, magnesium, strontium, barium, and silicon show similar spatial and temporal trends in both experiments (Figures 4.14, 4.16, 4.17). Lithium concentrations

show similar trends to Ca, Mg, Sr, Ba, and Si, but with less distinct temporal trends in surface water and hyporheic concentrations. These species are here referred to as Group C species. Concentrations of these elements increase with residence time. Increasing concentrations with residence time are more apparent in F1 than in F2, and the hyporheic concentrations are higher in F1 (Figures 4.14 and 4.16). For example, [Mg] ranges from 1421 to 14,950 μg L^{-1} in F1 and ranges from 2469 to 3936 μg L^{-1} in F2 (average of replicates) (Figure 4.14).

Surface water concentrations of these species generally increase over time (Figures C.13, C.15, C.17, C.20, C.29, C.30). For example, surface water [Mg] increased from 1675 to 2076 μg L^{-1} between days 49 and 112 of F1 and from 2314 to 2777 μg L^{-1} between days 9 and 91 of F2. Over elapsed time, hyporheic concentrations at specific locations tend to decrease relative to the surface water concentrations in both dunes. Though both dunes have similar concentrations in F2, the influence of dune shape is clear in F1; the highest concentrations of Ca, Mg, Sr, Ba, and Si are found at the lower rhizons of the 3 cm dune, with low concentrations at all of the 9 cm rhizons.

Although species in both Group A and Group C increase with residence time, Group C species are grouped separately based on their relationship to DO, as shown in Figure 4.17. Group A species concentrations are more highly (negatively) correlated with dissolved oxygen than those in Group C.

4.3.9 Additional Species

4.3.9.1 Nickel, Zinc

Hyporheic concentrations of Ni and Zn were consistently higher than in the surface water (Figure 4.12) but the data (Figures C.25 and C.27) do not show consistent

trends. In F1, it appears that Ni and Zn may increase with residence time and that concentrations are higher in the lower velocity 3 cm dune, similar to the Group A species. Temporal trends, however, are not clear.

4.3.9.2 Vanadium

In both F1 and F2, concentrations of vanadium increase and then decrease with residence time, so hyporheic concentrations are both higher and lower than in the surface water (Figure 4.13 and 4.16). Vanadium is grouped with the Group B species in Figure 4.16 because it shows a decrease in concentration with residence time (although it differs from those species in first showing an increase in concentration). A concentration hotspot is most apparent in the bubble plots for the 9 cm dune and 100 cm dune (Figure C.21). Temporal trends are unclear. Concentration differences between the dune sizes are not apparent.

4.3.9.3 Sodium

Measurements of sodium in the hyporheic zone do not show an obvious increase or decrease with residence time (except for perhaps a slight increase in some rhizons in F2) (Figure 4.15). Surface water concentration increased between days 49 and 112 in F1 (12.5 to 13.8 mg L^{-1}) and between days 9 and 91 in F2 (11.7 to 14.6 mg L^{-1}). Subsurface concentrations increase over time with the increase in surface water, but do not show a clear temporal trend relative to the surface water. Sodium concentrations were about the same across all the dune sizes.

4.3.9.4 Potassium and Aluminum

Trends in potassium concentrations are rather inconsistent, and complicated by the addition of KNO_3 around day 60 in both experiments. Due to this addition, [K] is not

discussed in detail in this study. Additionally, due to noise in the data, trends are not apparent in the aluminum concentrations (Figure 4.15).
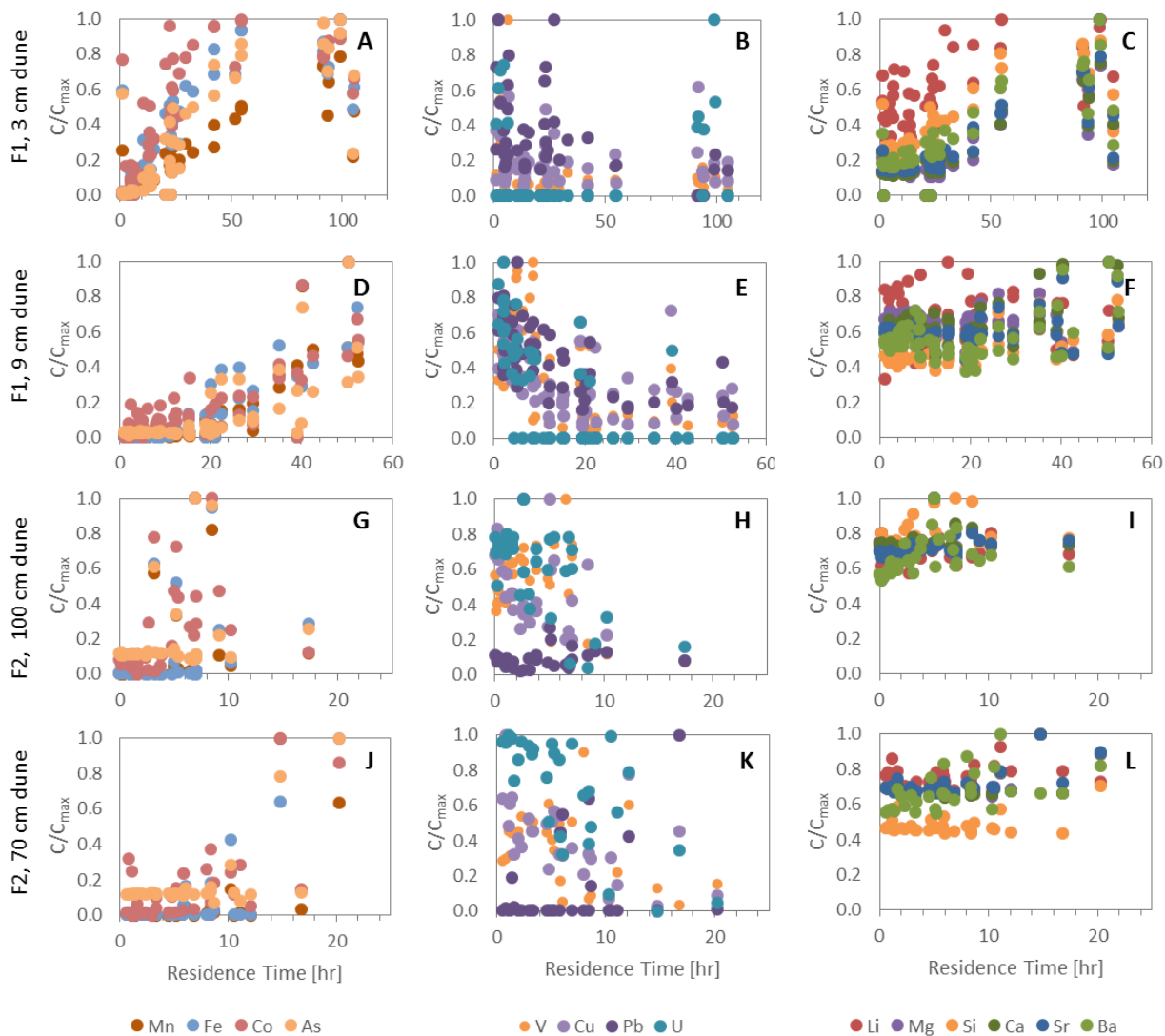
Figure 4.16. Relative species concentrations versus residence time. Group A (left), Group B (center), and Group C (right) relative species concentrations in the hyporheic zone are shown on day 112 (F1, panels A-F) and day 91 (F2, panels G-L). The dune shape is indicated on the far left. Concentrations shown are relative to each dune on the last day of the experiment.
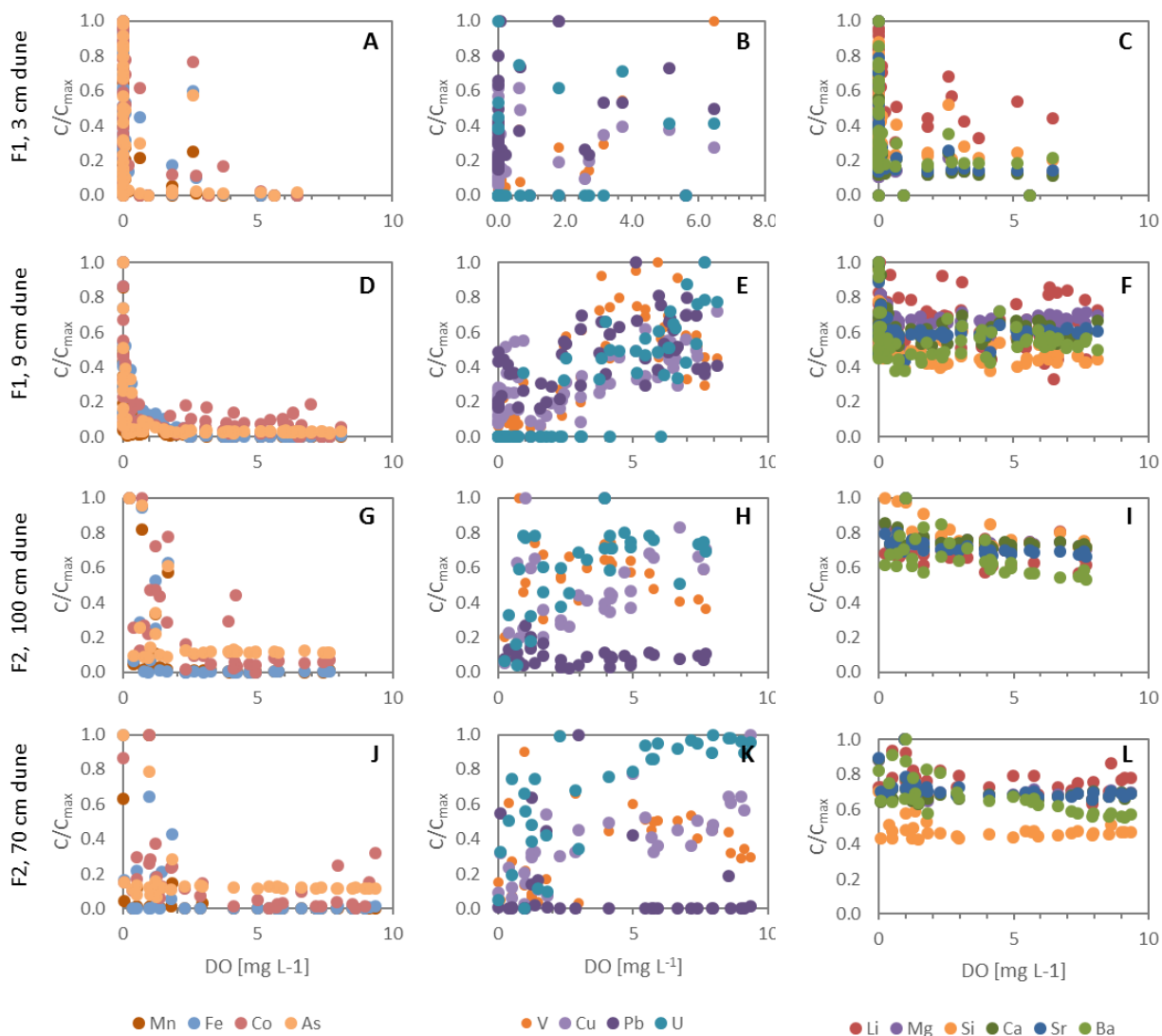
Figure 4.17.   Relative species concentrations versus dissolved oxygen. Group A (left), Group B (center), and Group C (right) relative species concentrations in the hyporheic zone are shown on day 112 (F1, panels A-F) and day 91 (F2, panels G-L). The dune shape is indicated on the far left. Concentrations shown are relative to each dune on the last day of the experiment.
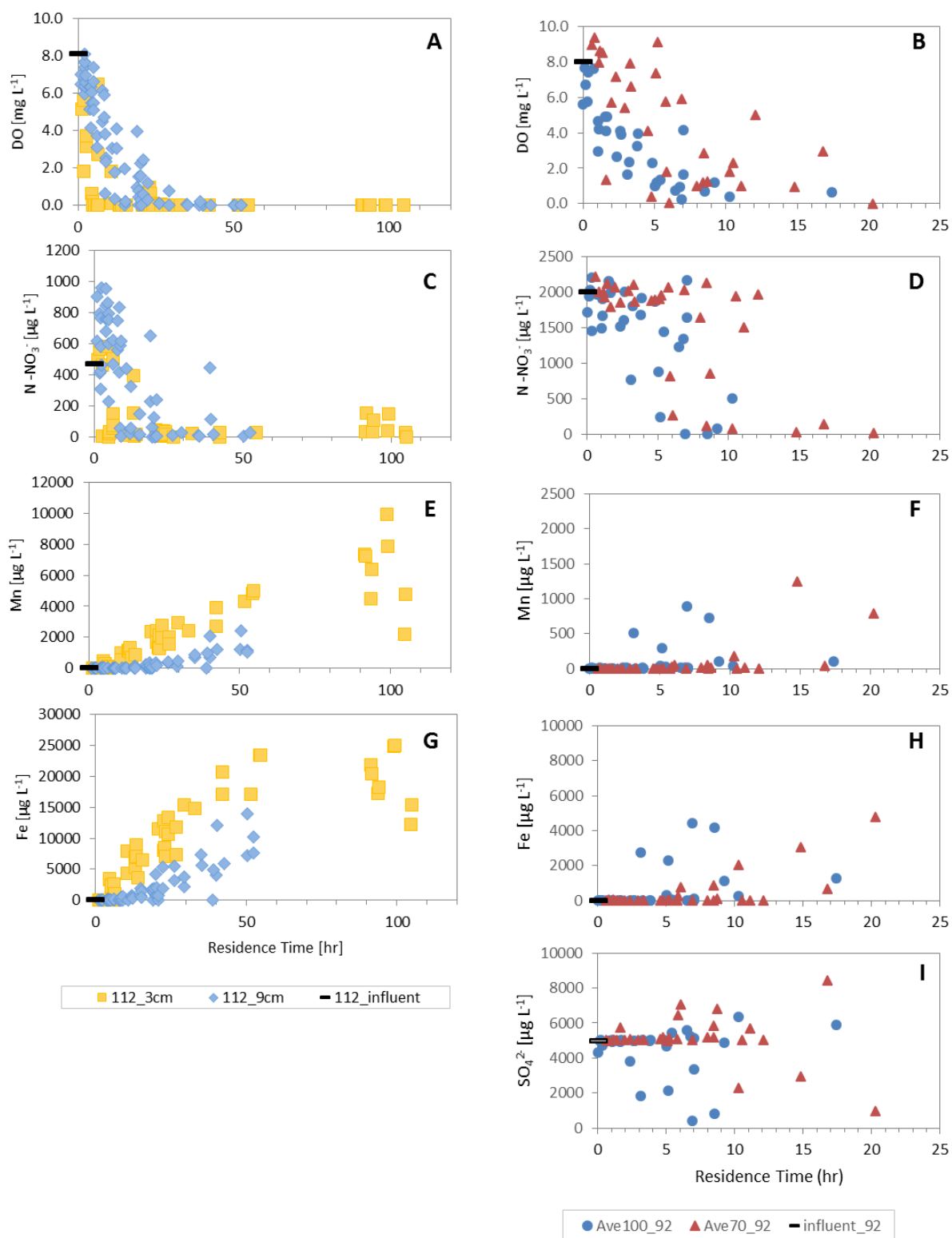
Figure 4.18. Hyporheic concentrations versus residence time for key redox-sensitive species. Panels on the left are from F1 (day 112) and panels on the right are from F2 (day 91, day 92 for sulfate).

4.4 Discussion

In this discussion, we attempt to provide baseline explanations for (1) how geochemistry changes along flow lines (spatially), (2) how these trends evolve over elapsed time, and (3) how flow velocity and geomorphology influence the spatial and temporal trends.

<u>4.4.1 Geochemical processes along flow lines</u>

Changes in geochemical species in the hyporheic zone over space and time could result from many different biogeochemical processes. Species that show both increases and decreases with residence time, such as N_2O, NO_2^-, PO_4^{3-}, NO_3^-, and V, indicate the importance of at least two chemical processes just in relation to those individual species. In this discussion, we do not attempt to explain every possible process for every measured species; rather, we present a few of the most likely and most important processes. These include redox reactions, related sorption and desorption, and dissolution reactions (weathering).

Modulating all of these biogeochemical processes are flow velocity and residence time (specifically in relation to reaction rates), and elapsed time since the directional evolution of the system has been reset by additional inputs of fresh sediment or carbon. Residence times are determined by the geomorphology of the streambed sediments and hydraulic properties of the sediments and stream [Kasahara and Wondzell, 2003; Harvey et al., 2013]. The influence of these factors on *temporal* trends will be presented following discussion of the key processes controlling the *spatial* trends: redox reactions (and associated impacts on sorbed species) and weathering.

4.4.1.1 Redox Reactions

Redox reactions and associated sorption and desorption are likely processes explaining the spatial trends in most of the species measured in the flume experiments. Concentrations of some of the redox-related species measured in this study are plotted versus residence time in Figure 4.18. Redox reactions have been shown to occur in a fairly consistent sequence in saturated sediments [Stumm and Morgan, 1996; Appelo and Postma, 2005; Fitts, 2013]. In natural systems, heterotrophic microorganisms utilize different electron acceptors and redox reactions, typically (though not always) in order of decreasing energy yield (aerobic respiration, denitrification, Mn-reduction, Fe-reduction, sulfate reduction, and methanogenesis) [e.g. Berner, 1981].

4.4.1.1.1 Aerobic respiration. Dissolved oxygen (DO) is likely the most important factor directly or indirectly controlling other species within the hyporheic zone, due to the dependence of microbial processes on oxygen and the resulting changes in redox conditions, pH, and solubility. Aerobic respiration (Equation 4.1) consumes both dissolved oxygen and organic carbon, producing CO_2. In our system, the surface water entering the hyporheic zone was well oxygenated. The decrease in DO with residence time (Figure 4.18) is most likely explained by aerobic respiration (free energy of -119.0 kJ mol^{-1}) [Fitts, 2013].

$$CH_2O + O_2 \Rightarrow H_2O + CO_2 + energy \qquad (4.1)$$
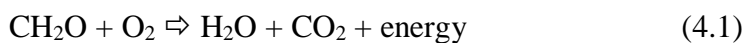
At the end of F2, the sand downstream of the dune crest (i.e. from the anaerobic zone) had higher total carbon than sand from the upstream side of the dune crest (i.e. from the aerobic zone) (Figure C.35), supporting aerobic respiration as a major process in the decrease in DO with residence time.

The spatial and temporal trends in pH are very similar to those observed for DO (decrease with residence time, increase over elapsed time) (see Figure 4.9), most likely reflecting the influence of microbial aerobic respiration on pH. As organic carbon is oxidized by DO, CO_2 is produced (Equation 4.1), which reacts with water to release H_3O^+ to the solution (Equations 4.2 and 4.3), decreasing pH [Cole and Prairie, 2010].

$$CO_2 + H_2O \Rightarrow H_2CO_3 \hspace{4cm} (4.2)$$

$$H_2CO_3 + H_2O \Rightarrow HCO_3^- + H_3O^+ \hspace{3cm} (4.3)$$
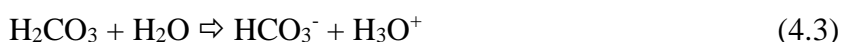
As will be shown, spatial and temporal changes in pH are significant to other chemical elements whose speciation and solubility are pH-dependent.

4.4.1.1.2 Denitrification. Following respiration, denitrification (free energy of -113.0 kJ mol^{-1}) is the most energetically favorable redox reaction [*Fitts*, 2013]. During denitrification, nitrate (NO_3^-) is sequentially reduced to nitrite (NO_2^-), nitric oxide (NO), nitrous oxide (N_2O), and finally dinitrogen (N_2) as shown in Equation 4.4 [Fitts, 2013].

$$0.25\ CH_2O + 0.2\ NO_3^- + 0.2\ H^+ \Rightarrow 0.25\ CO_2\ (g) + 0.1\ N_2(g) + 0.35\ H_2O \hspace{1cm} (4.4)$$
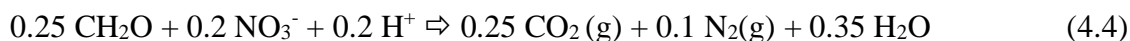
Denitrification enzymes are inhibited by oxygen, so anaerobic conditions are required for this process [Madigan et al., 2003]. Comparing the residence time plots of DO and NO_3^- in Figure 4.18, notice that in F2, NO_3^- concentrations only begin to decrease after 5-10 hours residence time, and that nitrate reduction begins later in the steeper dune because it has a larger oxic zone. In both experiments, the decrease in nitrate (and presumably denitrification) begins before DO is completely consumed. Denitrification occurring in bulk oxic zones is likely occurring at anaerobic microsites,

possibly associated with particulate organic matter [Lansdown et al., 2012; Liu et al., 2013].

In this study, denitrification explains the decrease in $[NO_3^-]$ as well as production and consumption of intermediate N_2O (as indicated by the increase and decrease with residence time). It also appears that nitrification (production of nitrite and nitrate from ammonia) occurs in the very shallow oxic zone, resulting in an increase in $[NO_3^-]$ from surface water concentrations at very short residence times. Two of the species that increase and then decrease with residence time can be explained by multiple nitrogen cycling reactions: NO_3^- increases due to nitrification and decreases due to denitrification; N_2O increases due to reduction of NO_3^- to N_2O and decreases with the subsequent reduction of N_2O to N_2.

4.4.1.1.3 Mn- and Fe-reduction. At circumneutral pH, oxidized forms of iron and manganese (Fe^{3+} and Mn^{4+}) form insoluble oxides, oxyhydroxides, and hydroxides [Giblin, 2010; Lawrence et al., 2013], so the dissolved Fe and Mn measured in this study were very likely the reduced forms (Fe^{2+} and Mn^{3+}). The increase in aqueous Fe and Mn with residence time can be explained by the reduction of insoluble forms of these elements and release of soluble forms. Fe and Mn in oxides are reduced by organic matter via microbial catalysis (Equations 4.5 and 4.6) [Giblin, 2010; Fitts, 2013].

$$0.25\ CH_2O + 0.5\ MnO_2\ (s) + H^+ \Rightarrow 0.25\ CO_2\ (g) + 0.5\ Mn^{2+} + 0.75\ H_2O \qquad (4.5)$$

$$0.25\ CH_2O + Fe(OH)_3\ (s) + H^+ \Rightarrow 0.25\ CO_2\ (g) + Fe^{2+} + 2.75\ H_2O \qquad (4.6)$$
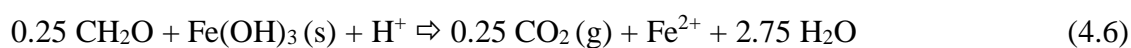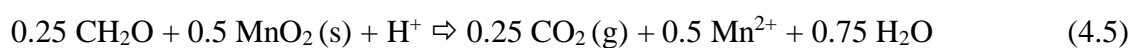
The energy yields of $MnO_2(s)$ and $Fe(OH)_3$ reduction (-96.7 and -46.7 kJ mol^{-1}, respectively) are lower than those for respiration and denitrification [Fitts, 2013]. As

shown in Figure 4.18 Fe and Mn concentrations begin to decline after DO is consumed, which is further along the flow paths (higher residence time) in the steeper dunes (9 cm and 70 cm). Mn and Fe reduction along hyporheic flow lines is evidenced by the crust of oxides that formed on the downstream sides of the dunes where upwelling water from the anaerobic zone of the hyporheic zone came in contact with the oxygenated surface water. The crust became more pronounced over time and is shown in Figure 4.19.
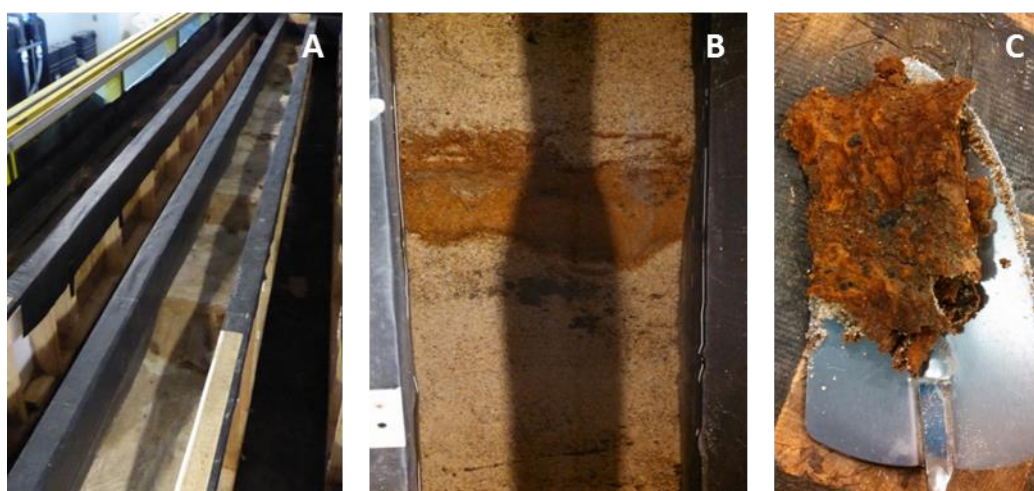
Figure 4.19.   Precipitate crust on the downstream dune faces. In panel A, each dune (1 m in length) can be distinguished by the darker colored crust that developed over time (close-up in panel B, 30 cm across). Panel C shows a piece of the crust removed with a small trowel at the end of the experiment.

4.4.1.1.4 Sulfate reduction. Based on pore water measurements, there was little evidence for sulfate reduction (free energy of -20.5 kJ mol^{-1}), which typically only occurs under very reducing conditions after respiration, denitrification, and Mn- and Fe-reduction [Berner, 1981; Fitts, 2013]. Only a few rhizon measurements of sulfate were lower than surface water concentrations; these were all located in the zone downstream of the dune crest where residence times were very high. However, sulfate measurements were only made on one day of the second experiment. Additionally, we observed a gray

streak in the subsurface that became more pronounced over time (Figure 4.3). Although this streak was not directly sampled, it possibly indicates sulfate reduction and precipitation of iron sulfides in that narrow region. This probable sulfide accumulation zone is indicative of very slow residence times and the most reducing conditions observed in the hyporheic zone.

4.4.1.1.5 Other redox reactions

While they are not major energy sources to microbes due to their typically low reactant concentrations, additional redox reactions may be used to explain the trends in species such as uranium, which decreased with residence time and showed a positive correlation with DO (Figure 4.17). For Fe and Mn, the oxidized species formed insoluble solids, while the reduced forms were soluble. For uranium, the opposite is true. The most soluble form of uranium is U(VI). Less soluble U(IV) is stable in reducing environments [Rosenberg et al., 2016] and precipitates out of solution [Drever, 1997].

4.4.1.2 Sorption and Desorption

The increase in aqueous iron and manganese concentrations with residence time can be explained by reduction and dissolution of oxides. The other Group B species that behave similarly, cobalt and arsenic, are likely explained by redox-related sorption and desorption. The behavior of trace metals in the hyporheic zone was summarized by Gandy et al. [2007] in Figure 4.20. Under oxic conditions, with high DO and high pH, Mn and Fe precipitate as oxides, and many other metals, including arsenic, nickel, and zinc, either co-precipitate with Fe and Mn oxides or adsorb to them [Harvey and Fuller, 1998; Fuller and Harvey, 2000; Gandy et al., 2007; Giblin, 2010]. However, along the hyporheic flow lines, respiration leads to low DO and low pH. Under these reducing

conditions, there is reductive dissolution of Mn and Fe oxides, and the other metals that were co-precipitated or adsorbed are released into solution. This process explains the increase in aqueous Fe, Mn, Co, and As (and probably Ni and Zn) with residence time as DO and pH decrease.
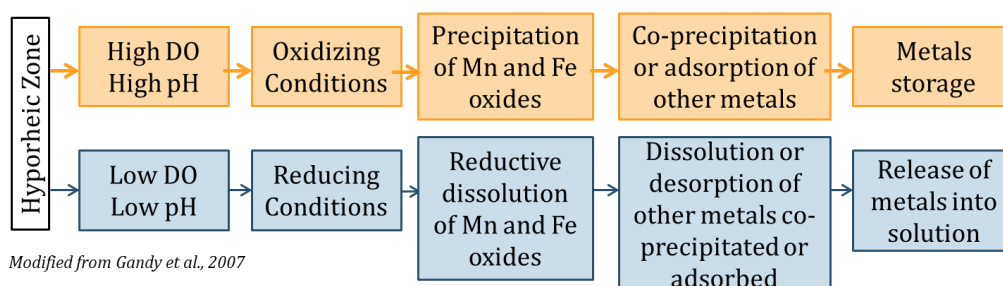
Figure 4.20.   Conceptual model of the storage and release of metals in the hyporheic zone. Modified from Gandy et al. [2007].

4.4.1.2.1 Combined effects of sorption and complexation. Species that showed decreased concentrations with residence time (copper, lead, vanadium and phosphate) also likely experienced some combination of adsorption and complexation. Adsorption to oxides may have occurred in the oxic zone, but complexation with organic matter prevented increases in these species under reducing conditions.

In our system, copper concentrations were very low (< 15 µg L^{-1}) and decreased along hyporheic flow lines, likely due to adsorption and complexation. Like the other trace metals, under oxic conditions, copper is strongly adsorbed by iron and manganese oxyhydroxides [Drever, 1997]. Even under reducing conditions, however, copper is not measured in solution in our system. Copper is insoluble as a native metal under reducing conditions in the absence of sulfur [Drever, 1997], and also tends to form complexes at lower pH that attach to organic matter and are not measured in solution [Drever, 1997; Goldman, 2010]. Complexation with organic matter would explain the decrease in [Cu]

with residence time and the slight increase over time as organic matter is depleted (see the temporal trends section below). However, copper exists in multiple oxidation states and due to the complexity of the copper system [Mann and Deutscher, 1977], the mechanism responsible for Cu scavenging by sediments deserves more study.

Like copper, lead appears to be scavenged from the water. Lead concentrations were mostly very low in this study and decreased from the surface water concentrations (with the exception of the 70 cm dune on day 91 in F2, which suggests some type of contamination). Lead behaves similarly to copper in that it is adsorbed onto Fe- and Mn-oxyhydroxides across the pH range in our experiment and is strongly complexed by organic matter [Drever, 1997]. MINTEQ results for F1 (3 cm) and F2 (both dunes) indicated positive saturation indices for plumbgummite, a lead phosphate mineral (Figure C.40) that increased with residence time, so it is also likely that lead was removed from solution by precipitation of phosphates.

Vanadium concentrations in the flume experiments increased and then decreased with residence time. Similarly to uranium, the decrease in [V] could theoretically be explained by the precipitation of vanadium oxides of V(III) or V(IV) following the reduction of more soluble V(V) [Brookins, 1988]. However, more recent studies of vanadium speciation in natural systems suggest that nearly all vanadium in natural systems is V(V) except at pH <2 [Pyrzyńska and Wierzbicki, 2004]. The decrease in concentration is therefore more likely to attributable to adsorption to Fe-oxides (in the oxic zone) or complexation with organic substances [Wällstedt et al., 2010] in the anoxic zone, similar to the behavior of lead and copper. The initial increase in [V] in the oxic

zone is unique among the trace metal species measured and must be attributable to a different process.

Phosphate also strongly adsorbs to iron oxides [Giblin, 2010]. The initial increase in $[PO_4^{3-}]$ within the oxic zone in F2 (Figure 4.11) is as of yet unexplained, but the decrease in $[PO_4^{3-}]$ could be due to adsorption to Fe-oxides [Wällstedt et al., 2010], binding to siliceous clays resulting from silicate dissolution [Caraco, 2010], or precipitation of phosphate minerals (such as Ca-, Al-, and Fe-phosphates). MINTEQ modeling (Figure C.40) shows increasing saturation indices for iron-, manganese- and lead phosphates with residence time and supports the latter hypothesis.

4.4.1.3 Weathering/Dissolution

Group C species concentrations (Mg, Ca, Sr, Ba, Si, Li) are not as correlated with redox conditions, as indicated by their poor correlations with DO (Figure 4.17), but can likely be explained primarily by mineral dissolution. In the process of silicate dissolution, aluminosilicate minerals react with hydrogen and water to form clay minerals, releasing cations and silica, as shown by the sample silicate weathering reactions in Equations 4.7-4.10 [Appelo and Postma, 2005]. These reactions, which are listed in order of decreasing weatherability [Goldich, 1938] are just examples; many similar reactions and different types of silicate and clay minerals may be involved. For most minerals, silicate dissolution rates are lowest at near neutral pH and increase exponentially with hydrogen ion concentration (decreasing pH) and also increase at high pH [Drever, 1997]. This would suggest that as pH decreases with aerobic respiration along flowlines, more weathering occurs. However, because silicate weathering consumes hydrogen ions, it is possible that silicate weathering has a buffering effect on the acidification that results

from respiration. We observed an increase in the cation elements, silicon, and alkalinity, which supports the hypothesis that silicate dissolution occurred along hyporheic flow paths, leading to increases in kaolinite ($Al_2Si_2O_5(OH)_4$), other clays, and elements such as Ca, Mg, and Si. Positive saturation indices that slightly increase with residence time for kaolinite and greenalite (an iron-bearing member of the kaolinite group) in the MINTEQ modeling results support the weathering hypothesis (Figure C.36). Depending on the minerals present in the sediment, species such as Fe, Mn, and trace metals may also be released by dissolution.

Anorthite (calcic feldspar):

$$Ca(Al_2Si_2)O_8 + 2H^+ + H_2O \Rightarrow \text{kaolinite} + Ca^{2+} \tag{4.7}$$

Albite (sodic feldspar):

$$2Na(AlSi_3)O_8 + 2H^+ + 9H_2O \Rightarrow \text{kaolinite} + 2Na^+ + 4H_4SiO_4 \tag{4.8}$$

Biotite:

$$2K(Mg_2Fe)(AlSi_3)O_{10}(OH)_2 + 10H^+ + 0.5O_2 + 7H_2O \rightarrow \text{kaolinite} + 2K^+$$
$$+ 4Mg^{2+} + 2Fe(OH)_3 + 4H_4SiO_4 \tag{4.9}$$

K-feldspar:

$$2K(AlSi_3)O_8 + 2H^+ + 9H_2O \Rightarrow \text{kaolinite} + 2K^+ + 4H_4SiO_4 \tag{4.10}$$
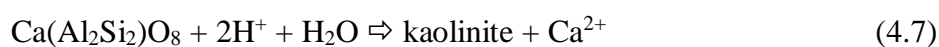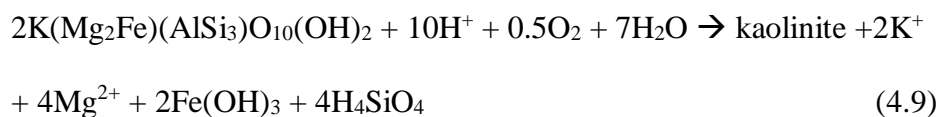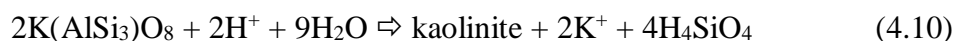
Bicarbonate also results from the weathering of silicates [Appelo and Postma, 2005], which would help explain the increase in alkalinity in the hyporheic zone with residence time. The alkalinity measured is likely the result of both silicate dissolution and the reaction of CO_2 from respiration to give HCO_3^- (Equations 4.2 and 4.3). In comparing the concentrations of major cationic species, the range of [Ca] (up to about 120 mg L^{-1}) is much higher than the ranges of [Na], [K], [Mg], and [Si] (up to about 18, 15, 18, and 50

mg L^{-1}, respectively). This suggests that Ca-bearing silicates were either more abundant

in the sand or weathered more rapidly. The latter explanation is consistent with the

observation that anorthite (Ca-feldspar) weathers about 700 times as rapidly as albite

(Na-feldspar) [Lasaga, 1984]. It is also possible that calcite was present in the original

sand. Calcite dissolution would also help explain the increase in alkalinity and Ca with

residence time.

4.4.2 Temporal trends

The processes discussed in the previous sections may explain the general spatial

trends in geochemical species in the hyporheic zone. These trends evolved over time and

varied between dunes with different velocities. Our flume system was essentially closed

to the addition of sediments and carbon, so for the reactions considered, the only

continuously replenished reactant to the hyporheic zone was dissolved oxygen (due to gas

exchange between the surface water and atmosphere). This had important implications

for the temporal evolution of the geochemical system.

Temporal trends in redox-related species (Groups A and B) are related to

temporal trends in DO. We observed that over time, the rate of aerobic respiration

decreases, as indicated by the slope of the DO concentration versus residence time. This

could be explained by the consumption of the more reactive carbon over time, decreasing

the rate of respiration. This allows DO to move further into the hyporheic zone and

results in larger oxic zones over time (assuming no replenishment of reactive carbon). As

a result, the locations of other redox-sensitive reactions may also move farther into the

hyporheic zone over time. The observed increase in pH over elapsed time is consistent

with the rate of aerobic respiration and CO_2 production decreasing as reactive carbon in

consumed. Like respiration, the most likely processes for denitrification and Mn- and Fe-reduction require organic carbon [Giblin, 2010]. As a result, these reaction rates (and the associated product concentrations) decreased over elapsed time.

The decrease in dissolution rates and species concentrations (especially for group C elements) over elapsed time may be the result of the increase in pH. It may also likely related to the "freshness" of the sediment. Mineral dissolution rates vary widely for silicates [Goldich, 1938; Lasaga, 1984; Appelo and Postma, 2005]. In fresh sediment (e.g. sand from a quarry), more surfaces of more-easily weathered minerals are available for dissolution. When this sediment is subjected to continuous water flow, the more easily weathered minerals are dissolved, leaving behind the less easily weathered minerals, decreasing the overall weathering rate. The key difference between F1 and F2 was that the sand from the first flume experiment was reused in the second flume experiment. We observed that the magnitudes of nearly all species were higher in F1 than in F2. For many elements, the concentrations in F2 are about the same as the lowest concentrations in F1 (see box plots in Figures C.2 through C.32). This can be explained by the higher weathering rates in F1 when the sand was fresh.

4.4.3 Influence of geomorphology and flow velocity

The flume experiments were designed to test the influence of geomorphologic and hydrologic conditions on hyporheic zone geochemistry. Due to a higher stream slope and higher hydraulic conductivity, overall surface and hyporheic flow velocities were higher in F2. Within each experiment, the velocities also differed between dunes. The steeper dunes (9 cm dune in F1 and 70 cm dune in F2) induced larger pressure gradients, resulting in faster hyporheic flow rates and longer residence times than in the shallower

dunes (3 cm dune in F1 and 100 cm dune in F2), even with the same surface water velocities in each experiment [e.g. Marion et al., 2002; Cardenas and Wilson, 2007; Tonina, 2012]. We will discuss the influence of flow velocities on the geochemical trends in different dunes, but the same explanations might be used for hyporheic zones that have different velocities for reasons other than different bedform morphology.

We observed that spatial trends in species concentrations (i.e. increases or decreases with residence time) are more pronounced earlier in the experiments and in the lower velocity dunes. For the most part, spatial trends were also more pronounced in F1 than in F2. The range of flow velocities modeled in these experiments helps explain the rates of the redox and dissolution processes described above, where they occur spatially, how the rates change over elapsed time, and why the magnitudes of concentrations vary between dunes and experiments.

Looking at the DO consumption rates on a given day of the experiment (e.g. Figures 4.9 and 4.18), the rates are higher in the lower velocity dunes (i.e. DO is completely consumed at lower residence times). As explained in detail in Quick et al. [2016], we hypothesize that the different rates of DO consumption across dunes are a result of faster flow rates and more carbon consumption in the steeper dunes. Assuming that all of the dunes begin with the same amount and quality of reactive carbon, the reactive carbon will be consumed more quickly in the higher velocity dunes. As a result, at the end of the experiment, the steeper, faster dunes have less remaining high quality reactive carbon in the subsurface, aerobic respiration and carbon consumption rates are lower, and the boundary between the aerobic and anaerobic zones has moved farther into the hyporheic zone. Unfortunately, carbon reactivity was not measured in these

experiments, but this hypothesis is supported by lower total carbon measured in sand

recovered from the steeper, higher velocity dune at the end of F1 (see section 3.3.5,

section C.5, and Figure C.35).

At the end of the experiments, nitrate concentrations were higher in the steeper

dunes with higher flow velocities. This trend can be explained by the lower carbon

reactivity (more has been consumed by respiration), lower respiration rate, lower DO

consumption, more aerobic nitrification (producing NO_3^-), and less anaerobic

denitrification (consuming NO_3^-) in the higher velocity dunes. An extensive discussion of

the nitrogen cycling processes observed in this study is presented in chapter three and

Quick et al. [2016].

Concentrations of group A (Mn, Fe, Co, As) and group C (Mg, Ca, Si, Sr, Ba, Li)

elements were lower in the higher velocity dunes. Fe- and Mn- reduction rates decrease

with the more oxidizing conditions and lower carbon availability at later time points and

in the higher velocity dunes. This explains why measured Mn and Fe concentrations

decrease over time and are lower in the steeper dunes, as are the concentrations of the

associated Co, As, Ni, and Zn. With more flow, as in the steeper dunes, there is also more

dissolution and removal of cations. As a result, species that are released by dissolution

(such as Mg, Ca, Si, Sr, Ba, and Li) have lower concentrations in the steeper dunes at the

end of the experiment.

4.4.3.1 Conceptual Model

The observed influence of velocity on the evolution of hyporheic geochemistry

can be generalized with a conceptual model. When flow velocities in a hyporheic zone

are high, rates of redox reactions, dissolution, etc. occur rapidly at the beginning of the

experiment (or, in a natural system, when a system is "reset" by the addition of reactants such as carbon and sediment). Later in the experiment, more of the reactants for these processes have been consumed, and reaction rates are lower (more reactant-limited). With lower hyporheic flow velocities, initial rates of redox and dissolution reactions are slower (more transport-limited) than in hyporheic zones with higher velocities. Later in the experiment, more reactants are still available in the lower velocity hyporheic zones, and the redox and dissolution reaction rates may be relatively higher than those in the higher velocity hyporheic zones at the same time point. Note that this hypothesis applies to a system in which the reactants (carbon, silicate minerals, etc.) are not continuously replenished.

This conceptual model is illustrated in Figure 4.21. Early in the experiment, a similar amount of water has flowed through the high and low velocity systems (panel A). Later in the experiment, more water has flowed through the higher velocity system. The difference in the amount of water that has flowed through the two systems increases over time. In panel B, the dashed line represents how the concentration of a reaction product decreases with the amount of water that has flowed past a given point, based on the assumptions that reaction rates are related to flow rates, the products of a reaction are advected from the hyporheic zone (as is generally the case with most of the species measured in this study), and that the requirements for redox conditions and microbial catalysis are met. The rate of decreasing product concentration declines because the reactants become less available as more water flows past, causing a decline in the reaction rate. The symbols on the line show how species concentrations at a given point in time vary between high and low velocity systems. In the simplest terms, species

concentrations decrease with the amount of "flushing," and more flushing occurs in the higher velocity hyporheic zones. Eventually, concentrations between low and high velocity systems will be similar. This may help explain the similarity in species concentrations between dune sizes in F2, which used sand that had effectively already been "flushed" in the first flume experiment.
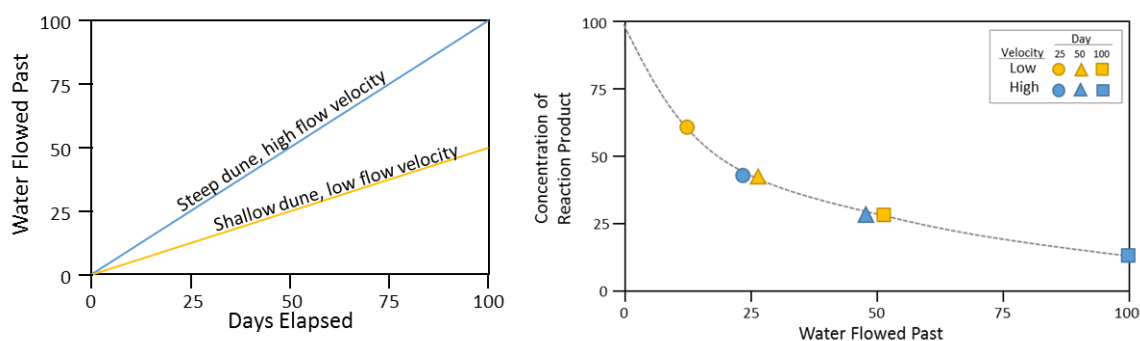
Figure 4.21. Conceptual model of the influence of flow velocity on temporal trends in the hyporheic zone. Hypothetical concentrations are shown for species that are removed by "flushing." Time and concentration scales are arbitrary.

4.5 Conclusion

This paper provides a comprehensive picture of spatial and temporal trends in the hyporheic zone geochemistry of a small stream. The observed trends reflect redox reactions (aerobic respiration, denitrification, Fe- and Mn-oxide reduction, and possibly sulfate reduction), associated changes in sorption and solubility, complexation, and chemical weathering.

Spatially, we observed the decrease in dissolved oxygen along flowlines, resulting in distinct oxic and anoxic zones, as well as a related decrease in pH. We also observed increases in metals (Fe, Mn, Co, As) with residence time, suggesting that the reducing conditions in the anoxic zone dissolve Fe and Mn oxides and release associated metals. We observed increases in cation-forming species (including Ca, Mg, Sr, Ba, Li, Si) with

residence time that are likely attributable to mineral dissolution. We observed decreases in Cu, U, and Pb with residence time, suggesting the hyporheic zone could be a sink for these species.

Our flume experiments modeled a system with an initial influx of fresh sediments and carbon and allowed us to observe changes in the spatial trends over time. Temporally, we observed that as the reactive carbon available for aerobic respiration was consumed, the boundary between the oxic and anoxic zones moved farther into the dune, shifting the locations of other redox reactions. Our results are mostly consistent with the traditional view of redox sequencing in saturated sediments. Over time, most species concentrations decreased.

In our second flume experiment, we used sand from the prior experiment but replenished the solid phase organic carbon. Because organic carbon was replenished (a process that is likely to occur when bedforms are reworked), we observed similar rates of oxygen consumption and the onset of reducing conditions in both experiments. However, concentrations of many constituents were lower, even at early times, compared to the first experiment. These observations suggest fresh sediments deposited into streams will promote higher rates of hyporheic reactions, particularly silicate dissolution, and associated higher concentrations and loading of associated reaction products to the overlying stream.

A key observation of our study is that geomorphologically dictated differences in hyporheic flow velocity produce distinct temporal trajectories in chemical evolution. Larger bed structures that produce higher hyporheic flow velocities have higher oxygen flux rates, which produce initially higher redox and dissolution reaction rates. However,

because the higher flux rates more rapidly consume organic carbon and remove reaction products, solid phase reactants (organic carbon, fresh mineral surfaces) are more rapidly expended. This results in a more rapid decline in reaction rates as well as a more rapid decline in the concentrations of associated reaction products. In contrast, smaller bedform structures produce lower flow velocities and associated lower reaction rates and product concentrations at early times. These lower velocity systems consume reactive materials more slowly, however, and therefore maintain elevated associated reaction products longer. This means that larger bed structures produce higher product concentrations at early times, but smaller bed structures can exhibit higher product concentrations at later times.

Collectively, these observations have the following implications: First, researchers should carefully consider their sampling techniques in the field. Sampling from different depths in the hyporheic zone will yield very different species concentrations, which could skew interpretations of overall conditions in the subsurface.

Second, researchers should consider when measurements are taken, since concentrations change over time in response to the depletion of reactive carbon and the addition of fresh sediment. The often dynamic nature of stream beds (due to high discharge events, landslides or mass wasting, stream restoration activities, seasonal organic carbon input, etc.) likely imparts a strong transient influence on the biogeochemistry of shallow bedform hyporheic processes.

Third, the morphology of the streambed can strongly affect the storage or release of species in the hyporheic zone. More heterogeneity and steeper bedforms that lead to more and faster hyporheic flow result in more "flushing" of most species from the

system. The shapes of the dunes also dictate the shapes and positions of the oxic and anoxic zones, where different species may be stored or released under varying redox conditions. Understanding the role of dune morphology will be very useful in the potential mitigation of contaminants in stream water and other roles of the hyporheic zone. This research has potentially significant implications for the management of remnant mining contamination and heavy metals in aquatic systems. As an example, we observed that adjusting the geomorphology to increase flow rates resulted in more removal and flushing of arsenic from the sediments. This removal of arsenic was also controlled by the carbon reactivity and redox conditions in the hyporheic zone. Depending on whether it is more favorable to flush arsenic from a system or prevent movement of arsenic from a given sedimentary system, the hydrological and chemical parameters of the hyporheic zone could be adjusted accordingly.

This study provides a "survey level" view of many different species, but future work could use the observations from these flume experiments to inform studies of particular species of interest (e.g. elements resulting from mining waste) or functions of the hyporheic zone (e.g. denitrification and removal of nitrate). It would be very useful to apply reactive transport modeling and mass balance to future studies. If possible, future studies should include careful measurements of carbon reactivity, flow velocities, and residence times.

<div align="center">

4.6 Acknowledgements

</div>

4.7 Supplementary Information and Data

Supplementary information and data related to this chapter can be found in Appendix C and online at the Boise State University ScholarWorks data repository.

4.8 References

Appelo, C. A. J., and D. Postma (2005), *Geochemistry, Groundwater and Pollution*, 2nd ed., A.A. Balkema Publishers, Leiden, The Netherlands.

Bardini, L., F. Boano, M. B. Cardenas, R. Revelli, and L. Ridolfi (2012), Nutrient cycling in bedform induced hyporheic zones, *Geochim. Cosmochim. Acta*, *84*, 47–61, doi:10.1016/j.gca.2012.01.025.

Baxter, C. V, and F. R. Hauer (2000), Geomorphology, hyporheic exchange, and selection of spawning habitat by bull trout (Salvelinus confluentus), *Can. J. Fish. Aquat. Sci.*, *57*(7), 1470–1481.

Beaulieu, J. J. et al. (2011), Nitrous oxide emission from denitrification in stream and river networks, *Proc. Natl. Acad. Sci. U. S. A.*, *108*(1), 214–219, doi:10.1073/pnas.1011464108.

Benner, S. G., E. W. Smart, and J. N. Moore (1995), Metal Behavior during Surface-Groundwater Interaction, Silver Bow Creek, Montana, *Environ. Sci. Technol.*, *29*(7), 1789–1795, doi:10.1021/es00007a015.

Berner, R. A. (1981), A New Geochemical Classification of Sedimentary Environments, *SEPM J. Sediment. Res.*, *Vol. 51*(2), 359–365, doi:10.1306/212F7C7F-2B24-11D7-8648000102C1865D.

Bernhardt, E. S., and G. E. Likens (2011), Dissolved Organic Carbon Enrichment Alters Nitrogen Dynamics in a Forest Stream, *Ecology*, *83*(6), 1689–1700.

Boano, F., J. W. Harvey, A. Marion, A. I. Packman, R. Revelli, L. Ridolfi, and A. Wörman (2014), Hyporheic flow and transport processes: Mechanisms, models, and biogeochemical implications, *Rev. Geophys.*, *52*, 603–679, doi:10.1002/2012RG000417.

Brookins, D. G. (1988), *Eh-pH Diagrams for Geochemistry*, Springer-Verlag, Berlin.

Caraco, N. F. (2010), Phosphorous, in *Biogeochemistry of Inland Waters*, edited by G. E. Likens, pp. 408–413, Elsevier Academic Press, Amsterdam.

Cardenas, M. B., and J. L. Wilson (2007), Hydrodynamics of coupled flow above and below a sediment-water interface with triangular bedforms, *Adv. Water Resour.*, *30*(3), 301–313, doi:10.1016/j.advwatres.2006.06.009.

Cole, J. J., and Y. T. Prairie (2010), Dissolved CO2, in *Biogeochemistry of Inland Waters2*, edited by G. E. Likens, pp. 3434–347, Elsevier Academic Press, Amsterdam.

Drever, J. I. (1997), *The Geochemistry of Natural Waters Surface and Groundwater Environments*, 3rd ed., Prentice-Hall, Inc., Upper Saddle River, NJ.

Edwards, R. T. (1998), The Hyporheic Zone, in *River Ecology and Management*, edited by R. J. Naiman and R. E. Bilby, pp. 399–429, Springer-Verlag, New York.

Elliott, A. H., and N. Brooks (1997a), Transfer of nonsorbing solutes to a streambed with bed forms: Theory, *Water Resour. Res.*, *33*(1), 123–136.

Elliott, A. H., and N. H. Brooks (1997b), Transfer of nonsorbing solutes to a streambed with bed forms : Laboratory experiments, *Water Resour. Res.*, *33*(1), 137–151.

Farrell, T. B. (2016), Statistical Modeling to Predict N2O Production within the Hypoheic Zone by Coupling Denitrifying Microbial Community Abundance to Geochemical and Hydrological Parameters, Boise State University.

Fehlman, H. M. (1985), Resistance component and velocity distributions of open channel flows over bedforms, Colorado State University.

Fitts, C. R. (2013), *Groundwater Science*, 2nd ed., Academic Press, Waltham, MA.

Fox, A., F. Boano, and S. Arnon (2014), Impact of losing and gaining streamflow

conditions on hyporheic exchange fluxes induced by dune-shaped bed forms, *Water Resour. Res.*, *50*, 1895–1907, doi:10.1002/2013WR014668.

Fuller, C. C., and J. W. Harvey (2000), Reactive uptake of trace metals in the hyporheic zone of a mining- contaminated stream, Pinal Creek, Arizona, *Environ. Sci. Technol.*, *34*(7), 1150–1155, doi:10.1021/es990714d.

Gandy, C. J., J. W. N. Smith, and A. P. Jarvis (2007), Attenuation of mining-derived pollutants in the hyporheic zone: A review, *Sci. Total Environ.*, *373*(2–3), 435–446, doi:10.1016/j.scitotenv.2006.11.004.

Gardner, J. R., T. R. Fisher, T. E. Jordan, and K. L. Knee (2016), Balancing watershed nitrogen budgets: accounting for biogenic gases in streams, *Biogeochemistry*, *127*(2–3), 231–253, doi:10.1007/s10533-015-0177-1.

Giblin, A. E. (2010), Iron and Manganese, in *Biogeochemistry of Inland Waters*, edited by G. E. Likens, pp. 368–377, Elsevier Academic Press, Amsterdam.

Goldich, S. S. (1938), A Study in Rock Weathering, *J. Geol.*, *46*, 17–58.

Goldman, C. R. (2010), Micronutrient Elements (Co, Mo, Mn, Zn, Cu), in *Biogeochemistry of Inland Waters*, edited by G. E. Likens, pp. 378–382, Elsevier Academic Press, Amsterdam.

Harvey, J. W., and C. C. Fuller (1998), Effect of enhanced manganese oxidation in the hyporheic zone on basin-scale geochemical mass balance, *Water Resour. Res.*, *34*(4), 623–636, doi:10.1029/97WR03606.

Harvey, J. W., J. K. Böhlke, M. A. Voytek, D. Scott, and C. R. Tobias (2013), Hyporheic zone denitrification: Controls on effective reaction depth and contribution to whole-stream mass balance, *Water Resour. Res.*, *49*(10), 6298–6316, doi:10.1002/wrcr.20492.

Hudson, F. (2004), Sample preparation and calculations for dissolved gas analysis in water samples using a GC headspace equilibrium technique, RSKSOP-175, Available from: https://www.epa.gov/ne/info/testmethods/pdfs/RSKsop175v2.pdf (Accessed 1 February 2013)

Kasahara, T., and S. M. Wondzell (2003), Geomorphic controls on hyporheic exchange flow in mountain streams, *Water Resour. Res.*, *39*(1), SBH 3-1-SBH 3-14, doi:10.1029/2002WR001386.

Lansdown, K., M. Trimmer, C. M. Heppell, F. Sgouridis, S. Ullah, L. Heathwaite, A. Binley, and H. Zhang (2012), Characterization of the key pathways of dissimilatory nitrate reduction and their response to complex organic substrates in hyporheic sediments, *Limnol. Oceanogr.*, *57*(2), 387–400, doi:10.4319/lo.2012.57.2.0387.

Lansdown, K., C. M. Heppell, M. Trimmer, A. Binley, A. L. Heathwaite, P. Byrne, and H. Zhang (2015), The interplay between transport and reaction rates as controls on nitrate attenuation in permeable, streambed sediments, *J. Geophys. Res. G Biogeosciences*, *120*(6), 1093–1109, doi:10.1002/2014JG002874.

Lasaga, A. (1984), Chemical Kinetics of Water-Rock Interaction, *J. Geophys. Res. Solid Earth (...*, *89*(4), 4009–4025.

Lawrence, J. E., M. E. Skold, F. A. Hussain, D. R. Silverman, V. H. Resh, D. L. Sedlak, R. G. Luthy, and J. E. McCray (2013), Hyporheic Zone in Urban Streams: A Review and Opportunities for Enhancing Water Quality and Improving Aquatic Habitat by Active Management, *Environ. Eng. Sci.*, *30*(8), 480–501, doi:10.1089/ees.2012.0235.

Liu, T., X. Xia, S. Liu, X. Mou, and Y. Qiu (2013), Acceleration of denitrification in turbid rivers due to denitrification occurring on suspended sediment in oxic waters, *Environ. Sci. Technol.*, *47*(9), 4053–4061, doi:10.1021/es304504m.

Madigan, M. T., J. M. Martinko, and J. Parker (2003), *Brock Biology of Microorganisms*, 10th ed., Pearson Education, Upper Saddle River, NJ.

Mann, A. W., and R. L. Deutscher (1977), Solution geochemistry of copper in water containing carbonate, sulphate and chloride ions, *Chem. Geol.*, *19*, 253–265.

Marion, A., M. Bellinello, I. Guymer, and A. Packman (2002), Effect of bed form geometry on the penetration of nonreactive solutes into a streambed, *Water Resour. Res.*, *38*(10), 1–12, doi:10.1029/2001WR000264.

Marzadri, A., D. Tonina, A. Bellin, G. Vignoli, and M. Tubino (2010), Semianalytical analysis of hyporheic flow induced by alternate bars, *Water Resour. Res.*, *46*(W07531), 1–14, doi:10.1029/2009WR008285.

Marzadri, A., D. Tonina, and A. Bellin (2011), A semianalytical three-dimensional process-based model for hyporheic nitrogen dynamics in gravel bed rivers, *Water Resour. Res.*, *47*(W11518), 1–14, doi:10.1029/2011WR010583.

Metzler, G. M., and L. A. Smock (1990), Storage and Dynamics of Subsurface Detritus in a Sand-Bottomed Stream, *Can. J. Fish. Aquat. Sci.*, *47*(3), 588–594, doi:10.1139/f90-067.

Pyrzyńska, K., and T. Wierzbicki (2004), Determination of vanadium species in environmental samples, *Talanta*, *64*(4), 823–829, doi:10.1016/j.talanta.2004.05.007.

Quick, A. M., W. J. Reeder, T. B. Farrell, D. Tonina, K. P. Feris, and S. G. Benner (2016), Controls on nitrous oxide emissions from the hyporheic zones of streams, *Environ. Sci. Technol.*, *50*, 11491–11500, doi:10.1021/acs.est.6b02680.

Reeder, W. J., A. M. Quick, T. B. Farrell, S. G. Benner, K. P. Feris, and D. Tonina (2018), Spatial and Temporal Dynamics of Dissolved Oxygen Concentrations and Bioactivity in the Hyporheic Zone, *Water Resour. Res.*, *54*(3), 2112–2128, doi:10.1002/2017WR021388.

Rosenberg, E., G. Pinson, R. Tsosie, H. Tutu, and E. Cukrowska (2016), Uranium Remediation by Ion Exchange and Sorption Methods: A Critical Review, *Johnson Matthey Technol. Rev.*, *60*(1), 59–77, doi:10.1595/205651316X690178.

Stumm, W., and J. J. Morgan (1996), *Aquatic Chemistry: Chemical Equilibria and Rates in Natural Waters*, 3rd ed., John Wiley & Sons, Inc., New York.

Tonina, D. (2012), Surface water and streambed sediment interaction : the hyporheic exchange, in *Fluid Mechanics of Environmental Interfaces, Second Edition*, edited by C. Gualtieri and D. Mihailovic, pp. 1–44, Taylor & Francis/Balkema, Leiden, The Netherlands.

Tonina, D., and J. M. Buffington (2009), Hyporheic Exchange in Mountain Rivers I: Mechanics and Environmental Effects, *Geogr. Compass*, *3*(3), 1063–1086, doi:10.1111/j.1749-8198.2009.00226.x.

Vidon, P., and S. Serchan (2016), Impact of Stream Geomorphology on Greenhouse Gas Concentration in a New York Mountain Stream, *Water. Air. Soil Pollut.*, *227*(12), doi:10.1007/s11270-016-3131-5.

Wällstedt, T., L. Björkvald, and J. P. Gustafsson (2010), Increasing concentrations of arsenic and vanadium in (southern) Swedish streams, *Appl. Geochemistry*, *25*(8), 1162–1175, doi:10.1016/j.apgeochem.2010.05.002.

Winter, T. C., J. W. Harvey, O. L. Franke, and W. M. Alley (1998), Ground water and surface water: A single resource, *USGS Publ.*, 79.

Wondzell, S. M., and F. J. Swanson (1999), Floods, channel storage and the hyporheic zone, *Water Resour. Res.*, *35*(2), 555–567.

Zarnetske, J. P., R. Haggerty, S. M. Wondzell, V. a. Bokil, and R. González-Pinzón (2012), Coupled transport and reaction kinetics control the nitrate source-sink function of hyporheic zones, *Water Resour. Res.*, *48*(11), 1–15, doi:10.1029/2012WR011894.

CHAPTER 5: CONCLUSION

The purpose of this dissertation was to examine the geochemical processing in the hyporheic zone of streams and rivers, particularly as it pertains to the production and potential release of nitrous oxide. The literature review and research presented in this dissertation advance our understanding of the specific biogeochemical reactions taking place in the hyporheic zone and how they are related to nitrogen cycling, redox reactions, and chemical weathering.

In chapter 2, I described multiple pathways leading to N_2O production in stream sediments. These microbially-mediated pathways include denitrification (anaerobic reduction of nitrate), nitrification (aerobic oxidation of ammonia), nitrifier denitrification (oxidation of ammonia followed by reduction of nitrite), and DNRA (the anaerobic dissimilatory nitrate reduction to ammonia). These processes may occur in the hyporheic zone, along groundwater flow paths, and in the water columns of streams. Based on the current literature, most lotic N_2O emissions result from denitrification in the hyporheic zone. However, there is also evidence that N_2O production via denitrification and nitrification in the water column may be more important in turbid streams and rivers with high suspended sediments. Other pathways may be significant under conditions of high ammonia (such as increased nitrification downstream of wastewater treatment plants). In general, models and some studies suggest that N_2O emissions decrease downstream, except in cases of large inputs of DIN.

The experiments described in chapter 3 provided an opportunity to add to the literature reviewed in the proceeding chapter. In column and flume experiments, we observed that peak nitrous oxide concentrations increased with exogenous nitrate loading. However, not all of the N_2O measured in the hyporheic zone was delivered to the surface water and emitted to the atmosphere. We observed that nitrous oxide first increased with residence time (i.e. along hyporheic flow paths) and then decreased. We attributed this pattern to N_2O production (most likely by denitrification), followed by N_2O consumption due to reduction to N_2 in the last step of denitrification. In our conceptual model, N_2O release from stream sediments is only likely to occur if the reaction rate for N_2O production is similar to the hyporheic residence time. In other words, in order to be released to the surface water and potentially emitted to the atmosphere, N_2O must be produced and then exit the hyporheic zone before being reduced to N_2.

Organic carbon played an important role in promoting aerobic respiration and the creation of anaerobic zones in the subsurface. The N_2O "hotspot" occurred near the boundary between the aerobic and anaerobic zones in the subsurface. We also observed that N_2O concentrations increased with declining organic carbon reactivity.

In addition to the nitrogen cycling processes described in chapter 3, redox-related sorption and desorption and silicate dissolution processes along hyporheic flow paths were described in chapter 4. Concentrations of most of these reaction products increase spatially (along flow paths) but decrease over elapsed time.

The importance of the streambed morphology was presented in both chapters 3 and 4. Streambed features that created higher pressure gradients experienced higher

overall hyporheic flow velocities. This lead to a more rapid depletion of reactive carbon, and more flushing of reaction products in the steeper, higher velocity dunes over time.

In conclusion, the hyporheic zone is an important site of nitrogen processing and potentially a source of N_2O release to the surface water under specific hydrological and chemical conditions. The geochemistry of the hyporheic zone evolves over time as reactants are consumed, but the system can be reset by events that introduce new sediments and carbon. In future investigations of the hyporheic zone, researchers should take into account spatial and temporal variability in these systems. When possible, experiments should be designed to examine specific geochemical pathways; these pathways, together with hydrological and geomorphological factors, are important to understanding hyporheic processes, such as N_2O production and emissions, at all scales.

APPENDIX A

Supporting Information for Chapter Two

A.1 General Descriptions of Processes in the Nitrogen Cycle

The simplest, traditional view of the nitrogen cycle consists of fixation, nitrification, and denitrification [Stein and Klotz, 2016]. During fixation, the triple N-N bond in dinitrogen gas (N_2) is broken, creating reactive nitrogen (Nr) that can be used by all forms of life. Fixation is carried out by lightning, certain microorganisms, and industrial processes, such as the Haber-Bosch process, resulting in mostly ammonia (NH_3). Ammonia is oxidized to hydroxylamine (NH_2OH), nitrite (NO_2^-) and then nitrate during nitrification, an aerobic process. During denitrification, a generally anaerobic process, nitrate is reduced to nitrite, nitric oxide (NO), nitrous oxide, and then dinitrogen. Nitrogen is also cycled into and out of biomass through assimilation and mineralization. During assimilation or assimilatory nitrate reduction, ammonia or nitrate (NO_3^-) is incorporated into biomass. The assimilated organic nitrogen may later be released and converted back to inorganic ammonium (NH_4^+) during mineralization. Additional processes, including dissimilatory nitrate reduction to ammonia (DNRA) and anaerobic ammonia oxidation (anammox) complicate this simple cycle.

Table A.1. **Processes in the Nitrogen Cycle**

Process	N_2O produced	Aerobic/ Anaerobic	Description
Fixation	No	Anaerobic (may occur in aerobic conditions with heterocysts)	N_2 gas transformed to Nr (NO or NH_3). High energetic costs due to N-N triple bond. **Lightning**: $N_2 + O_2$ + electrical energy $\Rightarrow$ 2NO **Fossil Fuel Combustion**: $N_2 + O_2$ + fossil energy $\Rightarrow$ 2NO **Biological Nitrogen Fixation**: $2N_2 + 6H_2O \Rightarrow 4NH_3 + 3O_2$ **Haber Bosch Process**: $N_2 + 3H_2 \Rightarrow 2NH_3$
Assimilation	No	Aerobic or Anaerobic	NH_4^+ is assimilated into amino acids and then converted into other forms of organic-N: $NH_4^+ \Rightarrow$ N-org
Assimilatory Nitrate Reduction	No	Aerobic or Anaerobic	Nitrate uptake by organisms, conversion to ammonia, incorporation into biomass: $NO_3^- \Rightarrow NH_4^+ \Rightarrow$ N-org
Mineralization/ Regeneration	No	Aerobic or Anaerobic	Detrital protein/organic-N compounds produce NH_4^+ during decomposition N-org $\Rightarrow NH_4^+$
Nitrification	No*	Aerobic	NH_3 is oxidized to NO_2^- and NO_3^- with oxygen as the terminal electron acceptor and hydroxylamine (NH_2OH) as an intermediate. Ammonia oxidation: $NH_3 + 1.5O_2 \Rightarrow NO_2^- + H_2O$ Nitrite oxidation: $NO_2^- + 0.5O_2 \Rightarrow NO_3^-$
Hydroxylamine Oxidation	Yes	Likely Low O_2 to Anaerobic	Following enzymatic production of NH_2OH as an intermediate in NH_4^+ oxidation, NH_2OH may be oxidized to NO, N_2O, or N_2
Chemodenitrification	Yes	Likely Low O_2 to Anaerobic	Abiotic reduction of NO_2^- to NO, N_2O, or N_2 with organic compounds or inorganic cations
Nitrifier Denitrification	Yes	Aerobic or Anaerobic	NH_4^+ oxidation to NO_2^- , followed by reduction to NO, N_2O, and N_2: $NH_4^+ \Rightarrow NO_2^- \Rightarrow NO \Rightarrow N_2O \Rightarrow N_2$
Denitrification	Yes	Low O_2 to Anaerobic	NO_3^- is reduced to NO_2, then NO, N_2O, and N_2 $5C_6H_{12}O_6 + 24NO_3^- + 24H^+ \longrightarrow 30 CO_2 + 12N_2 + 42H_2O$
Dissimilatory Nitrate Reduction to Ammonium	Yes	Low O_2 to Anaerobic	Bacteria use organic carbon to reduce NO_3^- to NH_4^+ : glucose $+ 3NO_3^- + 6H^+ \longrightarrow 6 CO_2 + 3NH_4^+ + 3H_2O$ Nitrate respiration: $NO_3^- + H_2 \Rightarrow NO_2^- + H_2O$ Nitrite reduction: $NO_2^- + 3H_2 + 2H^+ \Rightarrow NH_4^+ + 2H_2O$

Anammox	No	Anaerobic	Ammonia is oxidized with nitrite as the terminal electron acceptor to produce N_2. $NH_4^+ + NO_2^-$ --> $N_2 + 2H_2O$
Feammox	No*	Anaerobic	Ammonia is oxidized with ferric iron is used as the terminal electron acceptor instead of nitrite, produces predominantly N_2, but also NO_3^- or NO_2^- Feammox to N_2: $NH_4^+ + 5H^+ + 3Fe(OH)_3 \Rightarrow 3Fe^{2+}\ 0.5N_2 + 9H_2O$

*These processes do not produce N_2O directly, but their products or intermediates may be used by other processes that do produce N_2O.

A.1.1 Nitrogen Fixation and Reactive Nitrogen

Nitrogen fixation is crucial to life because it converts a mostly unusable form of nitrogen, dinitrogen gas (N_2) to reactive nitrogen (Nr) that can then be used by all other forms of life. Large amounts of energy are required to break the triple bond in N_2 (226 kcal mol-1). As a result, fixation only occurs through a few pathways, converting N_2 to either ammonia, NH_3, or nitric oxide, NO [Galloway, 2003]. NO is produced naturally by lightning ($N_2 + O_2$ + electrical energy $\Rightarrow$ 2NO) or anthropogenically during fossil fuel combustion ($N_2 + O_2$ + fossil energy $\Rightarrow$ 2NO). About 11% of N_2 fixation results in NO [Galloway, 2003].

NH_3 creation from N_2 can occur during both natural and anthropogenic processes. In biological nitrogen fixation (BNF), specialized bacteria and some cyanobacteria called diazotrophs convert N_2 to NH_3 using the *nitrogenase* enzyme in an anaerobic environment [Galloway, 2003]. The *nitrogenase* enzyme is strongly inhibited by oxygen, but fixation may occur in aerobic environments in specialized structures (e.g. heterocysts) that isolate the process from the environment [Megonigal et al., 2004]. Nitrogen-fixing organisms must have a ready supply of energy to compensate for the high energetic cost of breaking the N triple bond. Many diazotrophs gain energy from symbiotic relationships with plants (e.g. rhizobia bacteria in the root nodules of legumes) [Chapelle, 1993] or from photosynthesis (e.g. anaerobic purple and green bacteria) [Madigan et al., 2003].

The cultivation of legumes and rice (rice paddies create anaerobic environments for diazotrophs) leads to the creation of Nr and is sometimes termed cultivated biological nitrogen fixation (C-BNF) to distinguish it from non-anthropogenic BNF [Watanabe,

1986; Galloway et al., 2004]. In addition to C-BNF, humans have developed alternative means of creating Nr. The Haber-Bosch process, developed in 1909, fixes dinitrogen gas through reaction with hydrogen gas at high temperature to create ammonia ($N_2 + 3H_2 \Rightarrow 2NH_3$) [Galloway et al., 2004; Stein and Klotz, 2016]. The development of industrial processes to fix N_2 led to the development of synthetic fertilizers that have been critical to a growing world population. Other anthropogenic sources of new and mobilized Nr are biomass burning and fossil fuel combustion. Human activity has doubled the amount of Nr creation in the last 150 years [Vitousek et al., 1997]. Galloway et al. [2008] indicate that the creation of Nr increased from approximately 15 Tg N yr^{-1} in 1860 to 156 Tg N yr^{-1} in 1995, and 187 Tg N yr^{-1} in 2005. The fate of this reactive nitrogen is largely unknown, but could cause environmental damage as excess nitrate (NO_3^-) or N_2O gas [e.g. Seitzinger and Kroeze, 1998], leading to eutrophication, greenhouse warming, and multiple indirect effects due to coupling with the carbon cycle [Gruber and Galloway, 2008].

Table A.2.   Natural and Anthropogenic Nitrogen Fixation, 1997

	Fixation Process (Nr Creation)	**Global Rate (Tg N yr^{-1})**
Natural (120)	Terrestrial BNF	100
	Marine BNF	15
	Lightning (NO)	5
Anthropogenic (144)	Haber-Bosch	80
	Cultivation BNF	40
	Fossil Fuel Combustion (NO)	24
	Total Global	**264**

From [Schlesinger, 1997] as cited in [Galloway, 2003].

A.1.2 Assimilation and Assimilatory Nitrate Reduction

During assimilation, microorganisms and some macroorganisms (plants) uptake inorganic NH_3 or NH_4^+ into their biomass as organic nitrogen compounds [Galloway,

2003]. Many organisms use N in the -3 oxidation state (NH_3 or NH_4^+) for amino acids (containing NH_2^- amine groups) in proteins, although some organisms may also uptake NO_3^- and reduce it to ammonia for incorporation into biomass during assimilatory nitrate reduction [Andrews et al., 2004]. During this process, nitrate is transported to a receptor within the organism where it is reduced o NH_4^+ and then incorporated into the cell. This process is inhibited by NH_4^+ or organic N, but is not regulated by O_2 [Rice and Tiedje, 1989].
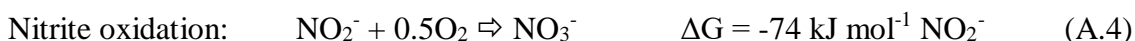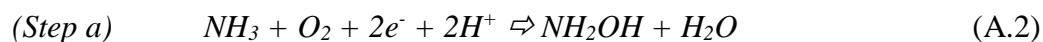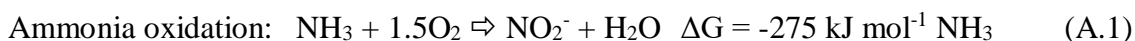
A.1.3 Mineralization/regeneration

During decomposition, heterotrophic (require organic carbon) organisms reduce organic nitrogen from decay or excretion to NH_4^+. This process (sometimes also referred to as ammonification) [Stein and Klotz, 2016], is carried out by both aerobic and anaerobic organisms [Canfield et al., 2005]. The terms mineralization and regeneration (referring to conversion of an organic species to an inorganic species) may be used to describe the decomposition of organic material to produce ammonia. NH_4^+ produced by mineralization is cationic and may be easily adsorbed onto negatively charged organic material or clay particles, making it readily available for uptake into other organisms (assimilation). The NH_4^+ may also be oxidized to nitrite (NO_2^-) and NO_3^- during nitrification [Andrews et al., 2004].

A.1.4 Nitrification

Nitrification is an aerobic process in which microorganisms derive energy from the oxidation of ammonia to nitrate. Ammonia is transformed to nitrite (NO_2^-) and nitrate (NO_3^-) in two steps by two separate groups of microbes, often collectively referred to as nitrifiers. The oxidation of NH_3 is usually coupled with inorganic carbon reduction (CO_2

fixation via the Calvin Cycle) because most nitrifying bacteria are obligate chemolithotrophs [Madigan et al., 2003]. Nitrification occurs in two main steps, ammonia oxidation and nitrite oxidation [Kirchman, 2012].

Ammonia oxidation: $NH_3 + 1.5O_2 \Rightarrow NO_2^- + H_2O$ $\Delta G = -275$ kJ mol^{-1} NH$_3$ (A.1)

    (Step a) $NH_3 + O_2 + 2e^- + 2H^+ \Rightarrow NH_2OH + H_2O$ (A.2)

    (Step b) $NH_2OH + H_2O + O_2 \Rightarrow NO_2^- + 2H_2O + H^+$ (A.3)

Nitrite oxidation: $NO_2^- + 0.5O_2 \Rightarrow NO_3^-$ $\Delta G = -74$ kJ mol^{-1} NO$_2^-$ (A.4)

The first step, ammonia oxidation (Equation A.1), is usually carried out by chemolithotrophic ammonia-oxidizing bacteria (AOB) or archaea (AOA) termed nitrosifyers (though often called nitrifiers) (e.g. *Nitrosomonas*) that utilize the *ammonia monooxygenase* (AMO) enzyme to oxidize NH$_3$ to the intermediate hydroxylamine (NH$_2$OH) (Equation A.2). The same organisms use the *hydroxylamine oxidoreductase enzyme* (HAO) to oxidize the hydroxylamine to NO$_2^-$ (Equation A.3) [Madigan et al., 2003]. For chemolithotrophic ammonia-oxidizers, ammonia oxidation is a dissimilatory process, meaning that the organisms do not incorporate the nitrogen species into their cells, but use the process for energy.

Ammonia oxidation requires oxygen and is usually considered to be the limiting step of nitrification. Ammonia oxidizing microbes generally have low cell yields, likely due to the low energy yield and low ammonia concentrations in most oxic environments where the first step of nitrification occurs. Additionally, ammonia oxidation is inhibited by light and extremes in pH. At lower pH, NH$_3$ gains a proton to produce NH$_4^+$. Since NH$_3$ is the actual substrate used by ammonia oxidizers, ammonia oxidation rates decrease with acidity [Kirchman, 2012]. Conditions for ammonia oxidation are optimal at the

interface between environments that provide oxygen (oxic) and environments with higher ammonium concentrations (usually anoxic) [Kirchman, 2012].

The second step of nitrification (Equation A.4), nitrite oxidation, is carried out rapidly by a separate group of microorganisms called nitrifying bacteria (e.g. *Nitrobacter*) that utilize the *nitrite oxidoreductase* enzyme [Madigan et al., 2003]. Nitrite oxidation is less well studied because it is not the rate-limiting step of nitrification.

Methane-oxidizing bacteria (methanotrophs) and heterotrophic ammonia oxidizers are also capable of oxidizing NH_3 to NO_3^- via NH_2OH, but do not gain energy from the reaction [Stein and Yung, 2003]. Heterotrophic nitrification is sometimes attributed to fungi; these heterotrophs may also carry out nitrifier denitrification (explained below) in conditions of high oxygen and organic carbon and low pH [Wrage et al., 2001].

A.1.5 Hydroxylamine oxidation

During the first step of nitrification, nitrifying bacteria oxidize ammonia to nitrite with hydroxylamine (NH_2OH) as an intermediate. Instead of being oxidized to nitrate, alternate biological or nonbiological processing of hydroxylamine (sometimes with nitrite) may produce nitrogen gases.

The chemical oxidation of hydroxylamine generates N_2O and N_2 [Bremner, 1997]. Multiple possible pathways for NH_2OH oxidation with production of N_2O exist [Schreiber et al., 2012]. One oxidation process involves metallic electron acceptors including iron(III) [Schreiber et al., 2012; Zhu et al., 2013b] and manganese(VI) [Bremner, 1997]. N_2O is more likely to be produced than N_2 when iron(III) is in excess of hydroxylamine [Bengtsson et al., 2002].
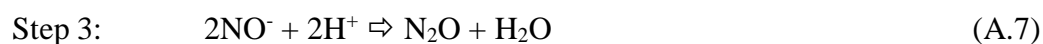
Biological hydroxylamine oxidation may also be carried out enzymatically, including by heterotrophic ammonia oxidizers [Otte et al., 1999]. Multiple pathways have been suggested. Hooper and Terry [1979] suggested that hydroxylamine oxidoreductase oxidize NH_2OH to give NO, which is then reduced to N_2O. It is also possible that N_2O is formed directly without NO reduction [Schreiber et al., 2012]. Alternatively, nitroxyl (HNO) may be an intermediate of the enzymatic oxidation of hydroxylamine [Schreiber et al., 2012]. Under aerobic conditions, the HNO reacts with oxygen to give HNO_2. Under oxygen limited conditions, HNO gives N_2O and H_2O, and the N_2O may further be reduced to N_2 [Otte et al., 1999]. Otte et al. [1999] observed that N_2O emitted from cultures of the heterotrophic ammonia oxidizer *Alcaligenes faecalis* in carbon-limited systems was produced by NH_2OH oxidation instead of nitrifier denitrification. Most heterotrophic organisms, however, do not gain any energy from hydroxylamine oxidation.

A.1.6 Chemodenitrification

Chemodenitrification is an abiotic process in which the reduction of NO_2^- produces gaseous nitrogen, including NO, N_2O, and N_2 [Tiedje, 1988]. NO_2^- may be reduced by inorganic cations [Zhu et al., 2013b] or organic compounds [Bremner, 1997; Stevens and Laughlin, 1998]. Low pH (<5.0) favors chemodenitrification involving inorganic cations, such as iron(II) [Van Cleemput and Baert, 1984; Stevens and Laughlin, 1998], producing predominantly NO [Tiedje, 1988]. The relative amount of N_2O produced may be affected by the type of electron donor used [Zhu et al., 2013b].

Ferrous iron (Fe^{2+}) can reduce nitrite to NO and then to N_2O [Schreiber et al., 2012]. NO_2^- reduction by metallic cations produces oxide minerals, as shown in the

example chemodenitrification sequence in Equations A.5-7, and also causes the accumulation of NO [Jones et al., 2015]. Chemodenitrification is most likely to occur in zones where redox conditions fluctuate or species from aerobic zones (NO_2^-) and from anaerobic zones (Fe^{2+}) may interact. Jones et al. [2015] found that the highest N_2O yields from chemodenitrification occur under excess Fe^{2+} conditions, although chemodenitrification using organic compounds would presumably be unaffected by iron concentrations.

$$\text{Step 1:} \qquad Fe^{2+} + NO_2^- + H_2O \Rightarrow FeOOH + NO + H^+ \qquad\qquad \text{(A.5)}$$

$$\text{Step 2:} \qquad NO + Fe^{2+} + 2H_2O \Rightarrow NO^- + FeOOH + 3H^+ \qquad\qquad \text{(A.6)}$$

$$\text{Step 3:} \qquad 2NO^- + 2H^+ \Rightarrow N_2O + H_2O \qquad\qquad\qquad\qquad \text{(A.7)}$$

Chemodenitrification is limited by NO_2^- concentrations. Although NO_2^- is an intermediate in nitrification, denitrification, and DNRA, N_2O production from chemodenitrification is more often discussed in the literature in relation to nitrification, although it could occur during DNRA and denitrification if NO_2^- is allowed to accumulate.

During nitrification, NO_2^- is produced from the oxidation of NH_4^+. The second step of nitrification (oxidation of NO_2^- to NO_3^-) proceeds more rapidly than the first step (oxidation of NH_3 to NO_2^-), so NO_2^- only accumulates under certain conditions. The addition of NH_3^-- or NH_4^+-type fertilizers may inhibit the second step of nitrification, probably due to nitrifier sensitivity to NH_3 toxicity, allowing NO_2^- to accumulate [Stevenson and Cole, 1999]. The low pH conditions that favor chemodenitrification, also due to nitrifier sensitivity, are caused by the conversion of NH_3 to NO_2^- and NO_3^-, and may also be enhanced by NH_3- and NH_4^+-type fertilizers [Stevenson and Cole, 1999].

A.1.7 Nitrifier denitrification

Nitrifiers are metabolically diverse and are often capable of carrying out reactions other than ammonia oxidation (the first step in nitrification). Some nitrifiers, including chemolithotrophic ammonia-oxidizers, methanotrophs and heterotrophic ammonia-oxidizers oxidize NH_4^+ to NO_2^- and then proceed to reduce the NO_2^- to NO, N_2O, and N_2 [Wrage et al., 2001; Stein and Yung, 2003]. The oxidation of NH_4^+ likely provides the electron source for NO_2^- reduction [Poth and Focht, 1985; Kool et al., 2011]. This pathway is often referred to as nitrifier denitrification because it is carried out by ammonia-oxidizers and results in loss of nitrogen from the system (denitrification) [Kirchman, 2012]. It may also be referred to as aerobic or lithotrophic denitrification [Stein and Yung, 2003]. It is different from coupled nitrification-denitrification in that it can be carried out by a single group of organisms and occurs under different conditions. The enzymes used in nitrifier denitrification, however, are considered to be the same as those for coupled autotrophic nitrification-heterotrophic denitrification [Wrage et al., 2001]. An important distinction between nitrifier denitrification and coupled nitrification-denitrification is that NO_3^- is not produced in nitrifier denitrification.

Nitrifier denitrification may be aerobic or anaerobic. It is possible that ammonia oxidizing bacteria that use oxygen as a terminal electron acceptor at high oxygen concentrations (nitrification) switch to using nitrite as the terminal electron acceptor when oxygen concentrations are low (nitrifier denitrification) [Poth and Focht, 1985; Shrestha et al., 2002]. Using NO_2^- as an electron acceptor conserves O_2 for ammonia oxidation and prevents the accumulation of nitrite, which may inhibit the *ammonia monooxygenase* enzyme (necessary for ammonia oxidation) under both aerobic and

anaerobic conditions [Poth and Focht, 1985; Kool et al., 2011]. Nitrifier denitrification is favored at low oxygen, low carbon, and possibly low pH conditions [Wrage et al., 2001].

A.1.8 Denitrification

Denitrification is one of two dissimilatory nitrate reduction pathways in the nitrogen cycle. Through a series of redox reactions, denitrifying bacteria (as well as some archaea and fungi) convert NO_3^- to NO_2^-, NO, N_2O, and finally back to N_2 [Tiedje, 1988; Korom, 1992; Kirchman, 2012]. Nitrate serves as the terminal electron acceptor for the oxidation of organic material when little to no O_2 is available. An overall denitrification reaction using glucose is shown in Equation A.8, although other species may be involved.

$$5C_6H_{12}O_6 + 24NO_3^- + 24H^+ \rightarrow 30CO_2 + 12N_2 + 42H_2O \qquad (A.8)$$

$$\Delta G^{\circ'} = -2657 \text{ kJ mol}^{-1} \text{ } C_6H_{12}O_6$$

Each step of denitrification requires a specific enzyme to catalyze the reaction [Zumft, 1997]. Each of the required enzymes is repressed, by varying degrees, by O_2, so denitrification occurs primarily in anaerobic conditions [Tiedje, 1988; Körner and Zumft, 1989; Madigan et al., 2003; Kirchman, 2012]. Denitrification products may also be observed from oxic environments that contain anaerobic microzones [Lansdown et al., 2012; Liu et al., 2013]. Most denitrifying bacteria are facultative aerobes and are metabolically diverse. In other words, they will carry out aerobic respiration if oxygen is present (due to higher energy yield) even in the presence of nitrate, but will switch to anaerobic metabolism when oxygen availability decreases [Tiedje, 1988; Megonigal et al., 2004].
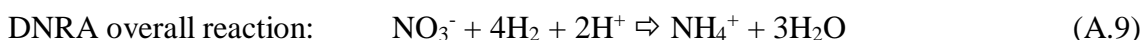
The dominant and best-described denitrifiers are heterotrophs (e.g. *Pseudomonas*) that use organic carbon as an electron donor and nitrate or nitrite as the terminal electron acceptor. Some denitrifiers can reduce other electron acceptors, such as ferric iron, in addition to nitrate [Madigan et al., 2003] or use other electron donors (e.g. ferrous iron) [Appelo and Postma, 2005]. For most denitrifiers, a single organism can complete the entire reduction of NO_3^- to N_2, although some lack the ability to reduce NO_3^- to NO_2^- or N_2O to N_2 [Tiedje, 1988]. Some denitrifiers, including those that carry out nonrespiratory nitrogen reduction, tend to produce N_2O instead of N_2 [Tiedje, 1988]. Several intermediates are produced during the stepwise reduction of NO_3^- to N_2O, including NO_2^-, NO, and N_2O. These intermediates may be used in other processes, or these intermediates may be introduced to denitrifiers from other processes, thus complicating the view of denitrification as four linear reduction steps between NO_3^- and N_2.

Because denitrification requires nitrate, denitrification is often coupled to nitrification as a source of nitrate. This may be termed endogenous nitrate or coupled nitrification-denitrification. In rivers, lakes, and coastal sediments, nitrification is the most important source of NO_3^- for denitrification [Seitzinger, 1988]. These coupled processes must be separated in time or space because nitrification requires aerobic conditions, while denitrification is generally an anaerobic process. A typical setting for coupled nitrification-denitrification is an oxic sediment layer that provides the nitrate for denitrification to lower anoxic sediments. Along a hyporheic flow path, nitrate from nitrification in the aerobic zone is advected into the anaerobic zone, where denitrification can occur. Nitrate for denitrification may also be supplied exogenously. Instead of using nitrification-derived nitrate, denitrifiers may use nitrate introduced by advection of
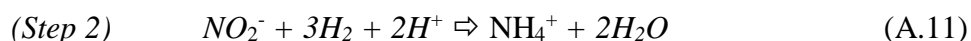
surface water or groundwater or by atmospheric deposition. Nitrogen-based fertilizers can greatly increase nitrate availability in surface water and groundwater [e.g. Megonigal et al., 2004].

A.1.9 Dissimilatory nitrate reduction to ammonium (DNRA)

An alternative fate for nitrate is dissimilatory nitrate reduction to ammonium (DNRA), as opposed to denitrification, which is dissimilatory reduction to gaseous nitrogen. This process generally occurs in two steps, shown in Equations A.9-11 [Megonigal et al., 2004]. The first step produces energy for the cell and is called nitrate respiration. Some microorganisms that complete nitrate respiration also complete the second step in DNRA. The second step does not generate energy, but is ecologically important because it generates ammonium that is more readily available for plant and microorganism assimilation and is easily adsorbed [Megonigal et al., 2004].

DNRA overall reaction: $NO_3^- + 4H_2 + 2H^+ \Rightarrow NH_4^+ + 3H_2O$ (A.9)

$$\Delta G = -6000 \text{ kJ mol}^{-1} NO_3^-$$

(Step 1) $NO_3^- + H_2 \Rightarrow NO_2^- + H_2O$ (A.10)

(Step 2) $NO_2^- + 3H_2 + 2H^+ \Rightarrow NH_4^+ + 2H_2O$ (A.11)

If the second step does not occur immediately or at the same rate as the first step, NO_2^- may accumulate. Some fermentative DNRA bacteria are capable of reducing the accumulated NO_2^- to N_2O in addition to NH_4^+ [Kaspar, 1982; Smith, 1982]. Additionally, the accumulated NO_2^- may also be reduced to N_2O abiotically through chemodenitrification (explained above) [Stevens and Laughlin, 1998]. In soil batch experiments, between 5 and 10% and up to 35% of nitrate reduced by DNRA organisms was released as N_2O [Smith and Zimmerman, 1981].

The bacteria that carry out DNRA can be aerobic, facultatively anaerobic, or obligately anaerobic, but most species are fermentative [Tiedje, 1988]. These bacteria can compete for carbon and nitrate, so DNRA and denitrification can occur simultaneously. DNRA mostly occurs under anaerobic conditions, although there is now evidence that DNRA organisms are less sensitive to oxygen than denitrifying bacteria, so DNRA may occur in relatively oxidized environments as well as in anaerobic conditions [Fazzolari et al., 1998].

There is also evidence of abiotic reactions that are capable of reducing nitrate to ammonium, possibly at rates similar to DNRA. These abiotic reactions may involve chemical reduction by Fe (II) with trace metal catalysts such as Cu(II) [Ottley et al., 1997] or Fe(II)-Fe(III) precipitates known as green rusts that occur in nonacid, iron-rich sediments and soils [Hansen and Koch, 1998].

A.1.10 Anammox

Anammox is the anaerobic oxidation of NH_4^+ and NO_2^- to N_2 with NO and hydrazine (N_2H_4) as intermediates, shown in Equations A.12-15 [Kartal et al., 2011]. Anammox organisms are not as well-described as denitrifiers, but evidence suggests that anammox organisms are slow-growing chemolithoautotrophs [Jetten et al., 2009]. Like nitrifiers than carry out aerobic ammonia oxidation, anammox organisms can use inorganic CO_2 as a carbon source to produce cell material [Madigan et al., 2003]. Anammox takes place within a specialized cellular structure with a highly impermeable membrane, called an anammoxosome, likely to protect the cell from toxic intermediates. Anammox is completely inhibited by oxygen [Strous et al., 1997] and even low levels of nitrite (20 mM) [Jetten et al., 1998].

Anammox overall reaction:

$$NH_4^+ + NO_2^- \Rightarrow N_2 + 2H_2O \qquad \Delta G' = -357 \text{ kJ mol}^{-1} \text{ NH}_4^+ \qquad (A.12)$$

Intermediate redox reactions:

$$NO_2^- + 2H^+ + e^- \Rightarrow NO + H_2O \qquad (E_0' = +0.38 \text{ V}) \qquad (A.13)$$

$$NO + NH_4^+ + 2H^+ + 3e^- \Rightarrow N_2H_4 + H_2O \qquad (E_0' = +0.06 \text{ V}) \qquad (A.14)$$

$$N_2H_4 \Rightarrow N_2 + 4H^+ + 4e^- \qquad (E_0' = -0.75 \text{ V}) \qquad (A.15)$$

Like denitrification, anammox consumes nitrate, although the nitrate is first reduced to nitrite [Thamdrup and Dalsgaard, 2002]. Per mole of NO_3^- consumed, anammox produces twice as much N_2 as denitrification (compare Equations A.8 and A.12). If nitrification rates limit nitrate production, anammox may increase N loss from the system because half of its nitrogen is from ammonia [Megonigal et al., 2004]. Studies have suggested that the contribution of anammox to Nr loss (through N_2 production) varies greatly with the environment. Anammox may account for 50% or more of global N loss in the oceans [Dalsgaard et al., 2005; Jetten et al., 2009] and has been demonstrated in freshwater lakes [Schubert et al., 2006] and rivers [Lansdown et al., 2016]. Most denitrifiers are heterotrophic, while anammox bacteria are autotrophic, so anammox is more likely to be a significant pathway for Nr loss in systems where denitrification is limited by organic carbon instead of availability of ammonia or nitrate [Megonigal et al., 2004].

A.1.11 Feammox

In another anaerobic ammonia oxidation process, termed Feammox, ferric iron is used as the terminal electron acceptor instead of nitrite [Zhu et al., 2013b]. This process could occur abiotically or be microbially mediated. Feammox produces predominantly
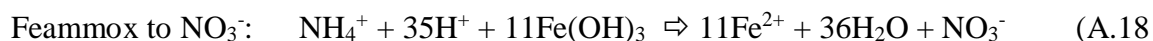
N_2, but also NO_3^- or NO_2^- (Equations 16-18) [Clément et al., 2005; Yang et al., 2012]. If this process is microbially-mediated, dissimilatory reducing bacteria could use this process as an energy source [Clément et al., 2005].

Feammox to N_2: $\qquad NH_4^+ + 5H^+ + 3Fe(OH)_3 \Rightarrow 3Fe^{2+}\ 0.5N_2 + 9H_2O \qquad$ (A.16)

$\qquad\qquad\qquad\qquad \Delta G = -245 \text{ kJ mol}^{-1}\ NH_4^+$

Feammox to NO_2^-: $\qquad NH_4^+ + 10H^+ + 6Fe(OH)_3 \Rightarrow 6Fe^{2+} + 16H_2O + NO_2^- \qquad$ (A.17)

$\qquad\qquad\qquad\qquad \Delta G = -164 \text{ kJ mol}^{-1}\ NH_4^+$

Feammox to NO_3^-: $\qquad NH_4^+ + 35H^+ + 11Fe(OH)_3 \Rightarrow 11Fe^{2+} + 36H_2O + NO_3^- \qquad$ (A.18

$\qquad\qquad\qquad\qquad \Delta G = -207 \text{ kJ mol}^{-1}\ NH_4^+$

Of the three Feammox processes, Feammox to N_2 seems to be the dominant pathway. Feammox to N_2 is thermodynamically favorable over a wide pH range, but Feammox to NO_2^- or NO_3^- only occurs at pH below 6.5. Because iron oxides become less reactive at higher pH, rates for all Feammox process decrease with increasing pH, with very low rates at circumneutral pH [Yang et al., 2012]. Feammox processes are thermodynamically feasible and likely in acidic soils rich in iron that experience anoxic conditions, either at anoxic microsites or during periods of anoxia [Yang et al., 2012]. Feammox has at least been observed in intertidal wetlands [Li et al., 2015], tropical upland soils [Yang et al., 2012], and paddy soils [Ding et al., 2014].

A.1.12 Abiotic and autotrophic denitrification

Denitrification is usually supported by the oxidation of organic carbon, but other electron donors, such as Fe(II), Mn(II), and H_2S may also be used as electron donors along abiotic and biotic pathways. At pH 2-7, abiotic Fe(II) oxidation may be coupled with NO_3^- oxidation to N_2. This reaction occurs at low rates and is sensitive to

temperature and could be relevant in aquifers with low nitrate loads or long residence times [Postma, 1990; Megonigal et al., 2004]. Manganese has been observed to provide alternate N-cycling pathways in Mn-rich seawater and coastal sediments through NH_3 and N-org oxidation with MnO_2 under aerobic conditions, and reduction of NO_3^- to N_2 by Mn^{2+} under anaerobic conditions [Luther et al., 1997]. In marine sediments with high sulfur, some bacteria may carry out chemoautotrophic denitrification of NO_3^- coupled to H_2S, S^0, or $S_2O_3^{2-}$ [Megonigal et al., 2004].

A.2 Effects of environmental factors on nitrogen cycle processes

Table A.3. Effects of environmental factors on nitrogen cycle processes and N₂O production

Environmental Change	Process Affected	Reference	Experimental Setting	Change in Process Rate	Effects on N₂O Yield*	Effects on N₂O Production
Increased nitrate	Denitrification	[Arango et al., 2007]	**Laboratory**-sediment slurries (top 5 cm) from agricultural streams	Increase		
		[Beaulieu et al., 2010]	**In-stream-**measurements of N₂O emissions from the water surface **Laboratory**-sediment core (10 cm) incubations	Increase		Increase
		[Beaulieu et al., 2011]	**In-stream**-water samples from 72 headwater streams	Increase	No effect	Increase (above 0.09 mg/L threshold)
		[Betlach and Tiedje, 1981]	**Laboratory**-resting cell suspensions of denitrifiers isolated from soils		No effect (with high carbon availability)	
		[Böhlke et al., 2009]	**In-stream-**measurements in hyporheic sediments, benthic chambers, stream waters **Laboratory**-sediment core microcosms	Increase		
		[Duff and Triska, 1990]	**Laboratory**-sediment slurries (top 6-10 cm) from the pristine 3rd order stream and **In-stream**-nitrate injection into stream sediments	Increase		
		[Firestone et al., 1979, 1980]	**Laboratory**-soil slurries with addition of NO₃$^-$ and/or O₂.	Increase	Increase	
		[García-Ruiz et al., 1998]	**Laboratory**-sediment cores and slurries from a lowland eutrophic river	Increase	Possible decrease[#]	Possible increase[#]
		[García-Ruiz et al., 1999]	**Laboratory**-sediment cores and slurries from headwater and eutrophic rivers	Increase		Increase
		[Gardner et al., 2016]	**In-stream**-water samples, tracer test in forested and agricultural streams and groundwater	Increase		
		[Guentzel et al., 2014]	**Laboratory**-sediment cores (top 15 cm) from streams in agricultural and undeveloped watersheds	Decrease (due to associated low DOC)		
		[Inwood et al., 2005]	**Laboratory**-sediment slurries (top 5 cm) from 1st order headwater streams	Increase (above 0.4 mg/L threshold)		
		[Kemp and Dodds, 2002]	**Laboratory**-substrata incubations from prairie stream	Increase		
		[Martin et al., 2001]	**Laboratory**-sediment slurries (top 4-10 cm) from headwater streams	Increase		
		[Mulholland and Valett, 2004]	**In-stream**-water samples, tracer test in forested stream	Decrease (stimulate assimilation)	Increase	
		[Richardson et al., 2004]	**Laboratory**-sediment slurries (top 5 cm) from the Upper Miss. River	Increase		

		[Royer et al., 2004]	**Laboratory**-sediment slurries (top 5 cm) of small agricultural streams	Increase (below 5 mg N- NO_3^-/L)		
		[Silvennoinen et al., 2008b]	**Laboratory**-sediment cores (top 20 cm) from high latitude eutrophic river	Increase to maximum	Increase to maximum, then decrease	Increase to maximum
		[Weier et al., 1993]	**Laboratory**-repacked soil cores		Increase	
Increased ammonium	Nitrification	[Beaulieu et al., 2010]	**In-stream**-measurements of N_2O emissions from the water surface **Laboratory**-sediment core (10 cm) incubations	Increase		Increase
		[Duff et al., 2008]	**Laboratory**-sediment cores (top 5 cm) from small agricultural streams	Increase		
		[Kemp and Dodds, 2002]	**Laboratory**-substrata incubations from prairie stream	Increase		
		[Strauss and Lamberti, 2000]	**Laboratory**-sediment slurries from 3rd order temperate stream	Increase		
		[Strauss et al., 2002]	**Laboratory**-sediment slurries from temperate streams	Increase		Possible increase
		[Strauss et al., 2004]	**Laboratory**-sediment cores (top 5 cm) from the Upper Miss. River	No effect (due to excessive N loading, decrease in organic-poor sediment)		
	Nitrifier Denitrification	[Jiang and Bakken, 1999]	**Laboratory**-cultures of ammonia-oxidizing bacteria from soil and wastewater		Decrease, or no effect (N_2O/NO_2^-)	
Increased Carbon	Denitrification	[Addy et al., 1999]	**Laboratory**-sediment cores (40 cm) from riparian zones	Increase		
		[Arango et al., 2007]	**Laboratory**-sediment slurries (top 5 cm) from agricultural streams	Increase or increase when [NO_3^-] > 1 mg N/L		
		[Beaulieu et al., 2010]	**In-stream**-measurements of N_2O emissions from the water surface **Laboratory**-sediment core (10 cm) incubations			Increase (sediment organic matter)
		[Beaulieu et al., 2011]	**In-stream**-water samples from 72 headwater streams		Decrease[#] with aerobic respiration (labile carbon availability)	
		[Bernhardt and Likens, 2011]	**Laboratory**-intact benthic sediment cores (<20 cm) from a second order forested stream	No effect or some increase		
		[Duff and Triska, 1990]	**Laboratory**-sediment slurries (top 6-10 cm) from the pristine 3rd order stream	No effect or increase		
		[Firestone and Davidson, 1989]	**Literature review**	Increase	Decrease	
		[García-Ruiz et al., 1998]	**Laboratory**-sediment cores and slurries from a lowland eutrophic river	No effect	Decrease	Decrease

		[Inwood et al., 2005]	**Laboratory**-sediment slurries (top 5 cm) from 1st order headwater streams	Some increase, more associated with sediment organic content		
		[Lansdown et al., 2015]	**In-stream-**measurements of porewater chemistry from river sediments (0-100 cm)	Increase		
		[Martin et al., 2001]	**Laboratory**-sediment slurries (top 4-10 cm) from headwater streams	No effect (DOC or % organic matter)		
		[Mayer et al., 2010]	**In-stream-**measurements of NO₃⁻ and DOC in surface water and groundwater **Laboratory**-sediment incubations from urban stream	Increase		
		[Opdyke et al., 2006]	**Laboratory**-sediment slurries (top 5 cm) from small agricultural streams	Increase (benthic organic matter)		
		[Richardson et al., 2004]	**Laboratory**-sediment slurries (top 5 cm) from the Upper Miss. River	Increase, no effect		
		[Weier et al., 1993]	**Laboratory**-repacked soil cores	Increase	Decrease	
	Nitrification	[Bernhardt and Likens, 2011]	**In stream**-water samples from a second order forested stream	Decrease (initially)		
		[Starry et al., 2005]	**Laboratory**-sediment slurries from temperate streams (top 10 cm)	Decrease		
		[Strauss and Lamberti, 2000]	**Laboratory**-sediment slurries from 3rd order temperate stream	Decrease		
		[Strauss et al., 2002]	**Laboratory**-sediment slurries from temperate streams	Decrease		
		[Strauss et al., 2002]	**Laboratory**-sediment slurries from temperate streams	No effect		
		[Strauss et al., 2004]	**Laboratory**-sediment cores (top 5 cm) from the Upper Miss. River	No effect (low ambient C:N ratio) Decrease# (high organic matter-low oxygen)		
	DNRA	[Kelso et al., 1997]	**Laboratory**-sediment slurries from N. Ireland rivers (5 cm sections down to 15 cm)	Increase		
Increased temperature	Denitrification	[Firestone and Davidson, 1989]	**Literature review**	Increase	Decrease	
		[García-Ruiz et al., 1998]	**Laboratory**-sediment cores and slurries from a lowland eutrophic river	Increase	Possible increase#	Possible increase#
		[García-Ruiz et al., 1999]	**Laboratory**-sediment cores and slurries from headwater and eutrophic rivers	Increase		Increase
		[Gardner et al., 2016]	**In-stream**-measured dissolved N₂O in forested and agricultural rivers	Increase	Possible increase#	Exponential increase
		[Kemp and Dodds, 2002]	**Laboratory**-substrata incubations from prairie stream	No effect		

	Process	Reference	Description			
		[Maag and Vinther, 1996]	**Laboratory**-incubations of multiple soils at different temperatures	Increase	Decrease	
		[Martin et al., 2001]	**Laboratory**-sediment slurries (top 4-10 cm) from headwater streams	Increase or no effect		
		[McCutchan Jr. and Lewis Jr., 2008]	**In-stream**-measured dissolved N_2 in effluent-dominated plains river	Increase		
		[Silvennoinen et al., 2008a]	**Laboratory**-sediment cores (top 20 cm) from high latitude eutrophic river	Increase to maximum	Decrease	Decrease
		[Venkiteswaran et al., 2014]	**In-stream**-measured dissolved N_2O in a seventh-order river	Increase		Increase
	Nitrification	[Kemp and Dodds, 2002]	**Laboratory**-substrata incubations from prairie stream	No effect		
		[Maag and Vinther, 1996]	**Laboratory**-incubations of multiple soils at different temperatures	Increase	Decrease	
		[Starry et al., 2005]	**Laboratory**-sediment slurries from temperate streams (top 10 cm)	Increase		
		[Strauss et al., 2004]	**Laboratory**-sediment cores (top 5 cm) from the Upper Miss. River	Increase, up to 30°C		
		[Warwick, 1986]	**Model**-mass balance model based on in-stream measurements	Increase		
Increased oxygen	Denitrification	[Betlach and Tiedje, 1981]	**Laboratory**-resting cell suspensions of denitrifiers isolated from soils	Decrease	Increase	
		[Bollmann and Conrad, 1998]	**Laboratory**-incubations of soil	Decrease		
		[Cavigelli and Robertson, 2000]	**Laboratory**-incubations of agricultural soil (10 cm depth)	Decrease	Increase	
		[Cavigelli and Robertson, 2001]	**Laboratory**-bacterial isolates from agricultural soil		Increase	
		[Firestone et al., 1979, 1980]	**Laboratory**-soil slurries with addition of NO3- and/or O_2.	Decrease	Increase	
		[Kemp and Dodds, 2002]	**Laboratory**-substrata incubations from prairie stream	Decrease		
		[Jørgensen et al., 1984]	**Laboratory**-suspensions of marine sediments	Decrease	Increase	
		[Khalil et al., 2004]	**Laboratory**-incubations of soil aggregates	Decrease		Likely decrease
		[Rosamond et al., 2012]	**In-stream**-measured dissolved N_2O, NO_3^- and DO in a large river			Decrease
		[Silvennoinen et al., 2008a]	**Laboratory**-sediment cores (top 20 cm) from high latitude eutrophic river	Decrease	Decrease (depends on temperature)	Decrease (depends on temperature)
		[Weier et al., 1993]	**Laboratory**-repacked soil cores		Increase	
	Nitrification	[Goreau et al., 1980] *likely nitrifier denitrification*	**Laboratory**-cultures of nitrifying bacteria	Increase	Decrease (Max at 0.5 kPa /0.18 mg/L O_2)	
		[Kemp and Dodds, 2002]	**Laboratory**-substrata incubations from prairie stream	Increase		

		[Strauss et al., 2004]	**Laboratory**-sediment cores (top 5 cm) from the Upper Miss. River, in-situ DO with microsensor	Increase (potential)		
	Nitrifier Denitrification	[Bollmann and Conrad, 1998]	**Laboratory**-incubations of soil	Decrease (max at 0.1-0.5% O_2)		
		[Khalil et al., 2004]	**Laboratory**-incubations of soil aggregates	Increase (up to max)	Max at 1.5 kPa O_2	Likely decrease; Main source of N_2O above 0.35 kPa O_2, but lower N_2O yield (1.5%) than denitrification (11%)
		[Kool et al., 2011]	**Laboratory**-incubations of soil with added NO_3^- and NH_4^+	Increase		
		[Stevens et al., 1998]	**Laboratory**-incubations of pasture soil (10 cm depth)	Increase (up to max)		
		[Zhu et al., 2013a]	**Laboratory**-incubations of soil	Decrease (max at 0.5-3% O_2)		
Increased pH	Denitrification	[Cavigelli and Robertson, 2000]	**Laboratory**-incubations of agricultural soil (10 cm depth)	Increase#	Decrease	
		[Firestone et al., 1980]	**Laboratory**-soil slurries with addition of NO_3^- and/or O2.	Increase	Decrease (pH influence only when NO_3^--N > 10 mg/L)	
		[Groffman et al., 2000]	**Laboratory**-incubations of riparian sediments (40 cm horizontal sections)	Increase (mostly)	Decrease	
		[Martin et al., 2001]	**Laboratory**-sediment slurries (top 4-10 cm) from headwater streams	Decrease		
		[Müller et al., 1980]	**Laboratory**-incubations of non-agricultural soil	Increase		
		[Šimek et al., 2002]	**Laboratory**-incubations of five mineral soils (15 cm depth)	Peak at neutral pH, not simple relationship	Decrease, above 7	
		[Stevens et al., 1998]	**Laboratory**-incubations of pasture soil (10 cm depth)	Increase	Max at pH 6.5	
	Nitrification	[Strauss et al., 2002]	**Laboratory**-sediment slurries from temperate streams	Max at pH 7.5, inhibited at low pH		
		[Warwick, 1986]	**Model**-mass balance model based on in-stream measurements	Increase, max at pH 8.5		
		[Wrage et al., 2001]	**Thermodynamic calculations**-N cycling pathways from published values	Increase		
	Nitrifier Denitrification	[Firestone and Davidson, 1989]	**Literature review**	Increase	Decrease	
		[Jiang and Bakken, 1999]	**Laboratory**-cultures of ammonia-oxidizing bacteria from soil and wastewater		Decrease (N_2O/NO_2^-)	
		[Martikainen, 1985]	**Laboratory**-incubations of forest soil with and without urea fertilizer application	Increase	Decrease	Increase

		[Wrage et al., 2001]	**Thermodynamic calculations**-N cycling pathways from published values	Increase (decrease relative to nitrification)		Possible decrease (Less nitrifier denitrification than nitrification at higher pH)
	DNRA	[Stevens et al., 1998]	**Laboratory**-incubations of pasture soil (10 cm depth)	Increase	Increase, max at pH 8.0	
	Chemodenitrification	[Martikainen, 1985]	**Laboratory**-incubations of forest soil with and without urea fertilizer application	Decrease	Decrease	Decrease
		[Van Cleemput and Baert, 1984]	**Laboratory**-incubations of soil and solutions	Decrease		

*adapted and updated from [Baulch et al., 2011]; [#] implied; *for denitrification: $N_2O/(N_2+ N_2O)$; for nitrification: N_2O/NO_3^-*

A.3 References

Addy, K. L., A. J. Gold, P. M. Groffman, and P. A. Jacinthe (1999), Ground water nitrate removal in subsoil of forested and mowed riparian buffer zones, *J. Environ. Qual.*, *28*(May), 962–970, doi:10.2134/jeq1999.00472425002800030029x.

Andrews, J. E., P. Brimblecombe, T. D. Jickells, P. S. Liss, and B. J. Reid (2004), *An Introduction to Environmental Chemistry*, 2nd ed., Blackwell Science Ltd, Malden, MA.

Appelo, C. A. J., and D. Postma (2005), *Geochemistry, Groundwater and Pollution*, 2nd ed., A.A. Balkema Publishers, Leiden, The Netherlands.

Arango, C. P., J. L. Tank, J. L. Schaller, T. V. Royer, M. J. Bernot, and M. B. David (2007), Benthic organic carbon influences denitrification in streams with high nitrate concentration, *Freshw. Biol.*, *52*(7), 1210–1222, doi:10.1111/j.1365-2427.2007.01758.x.

Baulch, H. M., S. L. Schiff, R. Maranger, and P. J. Dillon (2011), Nitrogen enrichment and the emission of nitrous oxide from streams, *Global Biogeochem. Cycles*, *25*(4), 1–15, doi:10.1029/2011GB004047.

Beaulieu, J. J., W. D. Shuster, and J. A. Rebholz (2010), Nitrous oxide emissions from a large, impounded river: The Ohio river, *Environ. Sci. Technol.*, *44*(19), 7527–7533, doi:10.1021/es1016735.

Beaulieu, J. J. et al. (2011), Nitrous oxide emission from denitrification in stream and river networks, *Proc. Natl. Acad. Sci. U. S. A.*, *108*(1), 214–219, doi:10.1073/pnas.1011464108.

Bengtsson, G., S. Fronæus, and L. Bengtsson-Kloo (2002), The kinetics and mechanism of oxidation of hydroxylamine by iron(iii), *J. Chem. Soc. Dalt. Trans.*, (12), 2548–2552, doi:10.1039/b201602h.

Bernhardt, E. S., and G. E. Likens (2011), Dissolved Organic Carbon Enrichment Alters Nitrogen Dynamics in a Forest Stream, *Ecology*, *83*(6), 1689–1700.

Betlach, M. R., and J. M. Tiedje (1981), Kinetic Explanation for Accumulation of Nitrite , Nitric Oxide , and Nitrous Oxide During Bacterial Denitrification, *Appl. Environ. Microbiol.*, *42*(6), 1074–1084.

Böhlke, J. K., R. C. Antweiler, J. W. Harvey, A. E. Laursen, L. K. Smith, R. L. Smith, and M. a. Voytek (2009), Multi-scale measurements and modeling of denitrification in streams with varying flow and nitrate concentration in the upper Mississippi River basin, USA, *Biogeochemistry*, *93*(1–2), 117–141, doi:10.1007/s10533-008-9282-8.

Bollmann, A., and R. Conrad (1998), Influence of O2 availability on NO and N2O release by nitrification and denitrification in soils, *Glob. Chang. Biol.*, *4*(4), 387–396, doi:10.1046/j.1365-2486.1998.00161.x.

Bremner, J. M. (1997), Sources of nitrous oxide in soils, *Nutr. Cycl. Agroecosystems*, *49*, 7–16, doi:10.1023/A:1009798022569.

Canfield, D. E., E. Kristensen, and B. Thamdrup (2005), *Aquatic Geomicrobiology*, Elsevier Academic Press, San Diego.

Cavigelli, M. A., and G. P. Robertson (2000), The Functional Significance of Denitrifier Community Composition in a Terrestrial Ecosystem, *Ecology*, *81*(5), 1402–1414, doi:10.2307/177217.

Cavigelli, M. A., and G. P. Robertson (2001), Role of denitrifier diversity in rates of nitrous oxide consumption in a terrestrial ecosystem, *Soil Biol. Biochem.*, *33*(3), 297–310, doi:10.1016/S0038-0717(00)00141-3.

Chapelle, F. (1993), *Ground-Water Microbiology and Geochemistry*, John Wiley & Sons, Inc., New York.

Clément, J. C., J. Shrestha, J. G. Ehrenfeld, and P. R. Jaffé (2005), Ammonium oxidation coupled to dissimilatory reduction of iron under anaerobic conditions in wetland soils, *Soil Biol. Biochem.*, *37*(12), 2323–2328, doi:10.1016/j.soilbio.2005.03.027.

Dalsgaard, T., B. Thamdrup, and D. E. Canfield (2005), Anaerobic ammonium oxidation (anammox) in the marine environment, *Res. Microbiol.*, *156*(4), 457–464, doi:10.1016/j.resmic.2005.01.011.

Ding, L., X. An, S. Li, G. Zhang, and Y. Zhu (2014), Nitrogen Loss through Anaerobic Ammonium Oxidation Coupled to Iron Reduction from Paddy Soils in a Chronosequence, *Environ. Sci. Technol.*, *48*(September), 10641–10647, doi:10.1021/es503113s.

Duff, J. H., and F. J. Triska (1990), Denitrification in sediments from the hyporheic zone adjacent to a small forested stream, *Can. J. Fish. Aquat. Sci.*, *47*(6), 1140–1147, doi:10.1139/f90-133.

Duff, J. H., A. J. Tesoriero, W. B. Richardson, E. A. Strauss, and M. D. Munn (2008), Whole-Stream Response to Nitrate Loading in Three Streams Draining Agricultural Landscapes, *J. Environ. Qual.*, *37*(3), 1133–1144, doi:10.2134/jeq2007.0187.

Fazzolari, É., B. Nicolardot, and J. C. Germon (1998), Simultaneous effects of increasing levels of glucose and oxygen partial pressures on denitrification and dissimilatory nitrate reduction to ammonium in repacked soil cores, *Eur. J. Soil Biol.*, *34*(1), 47–52, doi:10.1016/S1164-5563(99)80006-5.

Firestone, M. K., and E. A. Davidson (1989), Microbiological basis of NO and N2O production and consumption in soil, in *Exchange of Trace Gases between Terrstrial Ecosystems and the Atmosphere*, edited by M. Andreae and D. Schimel, pp. 7–21, John Wiley & Sons, New York.

Firestone, M. K., M. S. Smith, R. B. Firestone, and J. M. Tiedje (1979), The Influence of Nitrate, Nitrite, and Oxygen on the Composition of the Gaseous Products of Denitrification in Soil, *Soil Sci. Soc. Am. J.*, *43*(6), 1140, doi:10.2136/sssaj1979.03615995004300060016x.

Firestone, M. K., R. B. Firestone, and J. M. Tiedje (1980), Nitrous Oxide from Soil Denitrification: Factors Controlling Its Biological Production, *Science (80-.).*, *208*(May), 749–751.

Galloway, J. N. (2003), The Global Nitrogen Cycle, in *Treatise of Geochemistry Volume 8 Biogeochemistry*, edited by W. H. Schlesinger, pp. 557–583, Sevier, El, New York.

Galloway, J. N. et al. (2004), Nitrogen Cycles: Past, Present, and Future, *Biogeochemistry*, *70*(2), 153–226.

Galloway, J. N., A. R. Townsend, J. W. Erisman, M. Bekunda, Z. Cai, J. R. Freney, L. a Martinelli, S. P. Seitzinger, and M. a Sutton (2008), Transformation of the nitrogen cycle: recent trends, questions, and potential solutions., *Science (80-.).*, *320*(5878), 889–92, doi:10.1126/science.1136674.

García-Ruiz, R., S. N. Pattinson, and B. A. Whitton (1998), Denitrification and nitrous oxide production in sediments of the Wiske, a lowland eutrophic river, *Sci. Total Environ.*, *210–211*, 307–320, doi:10.1016/S0048-9697(98)00020-5.

García-Ruiz, R., S. N. Pattinson, and B. A. Whitton (1999), Nitrous oxide production in the river Swale-Ouse, North-East England, *Water Res.*, *33*(5), 1231–1237, doi:10.1016/S0043-1354(98)00324-8.

Gardner, J. R., T. R. Fisher, T. E. Jordan, and K. L. Knee (2016), Balancing watershed nitrogen budgets: accounting for biogenic gases in streams, *Biogeochemistry*, *127*(2–3), 231–253, doi:10.1007/s10533-015-0177-1.

Goreau, T. J., W. A. Kaplam, S. C. Wofsy, M. B. McElroy, F. W. Valois, and S. W. Watson (1980), Production of NO2- and N2O by nitrifying bacteria at reduced concentrations of oxygen, *Appl. Environ. Microbiol.*, *40*(3), 526–532.

Groffman, P. M., A. J. Gold, and K. Addy (2000), Nitrous oxide production in riparian zones and its importance to national emission inventories, *Chemosphere-Global Chang. Sci.*, *2*, 291–299.

Gruber, N., and J. N. Galloway (2008), An Earth-system perspective of the global nitrogen cycle., *Nature*, *451*(7176), 293–6, doi:10.1038/nature06592.

Guentzel, K. S., M. Hondzo, B. D. Badgley, J. C. Finlay, M. J. Sadowsky, and J. L. Kozarek (2014), Measurement and modeling of denitrification in sand-bed streams under various land uses, *J. Environ. Qual.*, *43*(3), 1013–1023, doi:10.2134/jeq2013.06.0249.

Hansen, H. C. B., and C. B. Koch (1998), Reduction of nitrate to ammonium by sulphate green rust: activation energy and reaction mechanism, *Clay Miner.*, *33*, 87–101.

Hooper, A. B., and K. R. Terry (1979), Hydroxylamine oxidoreductase of Nitrosomonas: Production of nitric oxide from hydroxylamine, *Biochim. Biophys. Acta-Enzymology*, *571*(1), 12–20.

Inwood, S. E., J. L. Tank, and M. J. Bernot (2005), Patterns of denitrification associated with land use in 9 midwestern headwater streams, *J. North Am. Benthol. Soc.*, *24*(2), 227–245, doi:10.1899/04-032.1.

Jetten, M. S. M., M. Strous, K. T. Van De Pas-Schoonen, J. Schalk, U. G. J. M. Van Dongen, A. A. Van De Graaf, S. Logemann, G. Muyzer, M. C. M. Van Loosdrecht, and J. G. Kuenen (1998), The anaerobic oxidation of ammonium, *FEMS Microbiol. Rev.*, *22*(5), 421–437, doi:10.1016/S0168-6445(98)00023-0.

Jetten, M. S. M., L. Van Niftrik, M. Strous, B. Kartal, J. T. Keltjens, and H. J. M. Op den Camp (2009), Biochemistry and molecular biology of anammox bacteria., *Crit. Rev. Biochem. Mol. Biol.*, *44*(2–3), 65–84, doi:10.1080/10409230902722783.

Jiang, Q. Q., and L. R. Bakken (1999), Nitrous oxide production and methane oxidation by different ammonia-oxidizing bacteria, *Appl. Environ. Microbiol.*, *65*(6), 2679–84.

Jones, L. C., B. Peters, J. S. Lezama Pacheco, K. L. Casciotti, and S. Fendorf (2015), Stable Isotopes and Iron Oxide Mineral Products as Markers of Chemodenitrification., *Environ. Sci. Technol.*, *49*(6), 3444–3452, doi:10.1021/es504862x.

Jørgensen, K. S., H. B. Jensen, and J. Sørensen (1984), Nitrous oxide production from nitrification and denitrification in marine sediment at low oxygen concentrations, *Can. J. Microbiol.*, *30*(8), 1073–1078, doi:10.1139/m84-167.

Kartal, B. et al. (2011), Molecular mechanism of anaerobic ammonium oxidation, *Nature*, *479*(7371), 127–130, doi:10.1038/nature10453.

Kaspar, H. F. (1982), Nitrite reduction to nitrous oxide by propionibacteria: Detoxicaton mechanism, *Arch. Microbiol.*, *133*(2), 126–130.

Kelso, B. H. L., R. V. Smith, R. J. Laughlin, and S. D. Lennox (1997), Dissimilatory nitrate reduction in anaerobic sediments leading to river nitrite accumulation, *Appl. Environ. Microbiol.*, *63*(12), 4679–4685.

Kemp, M. J., and W. K. Dodds (2002), The influence of ammonium, nitrate, and dissolved oxygen concentrations on uptake, nitrification, and denitrification rates associated with prairie stream substrata, *Limnol. Oceanogr.*, *47*(5), 1380–1393, doi:10.4319/lo.2002.47.5.1380.

Khalil, K., B. Mary, and P. Renault (2004), Nitrous oxide production by nitrification and denitrification in soil aggregates as affected by O2 concentration, *Soil Biol. Biochem.*, *36*(4), 687–699, doi:10.1016/j.soilbio.2004.01.004.

Kirchman, D. L. (2012), *Processes in Microbial Ecology*, 1st ed., Oxford University Press, London.

Kool, D. M., J. Dolfing, N. Wrage, and J. W. Van Groenigen (2011), Nitrifier denitrification as a distinct and significant source of nitrous oxide from soil, *Soil Biol. Biochem.*, *43*(1), 174–178, doi:10.1016/j.soilbio.2010.09.030.

Körner, H., and W. G. Zumft (1989), Expression of Denitrification Enzymes in Response to the Dissolved Oxygen Level and Respiratory Substrate in Continuous Culture of Pseudomonas stutzeri, *Appl. Environ. Microbiol.*, *55*(7), 1670–1676.

Korom, S. F. (1992), Natural denitrification in the saturated zone: A review, *Water Resour. Res.*, *28*(6), 1657–1668, doi:10.1029/92WR00252.

Lansdown, K., M. Trimmer, C. M. Heppell, F. Sgouridis, S. Ullah, L. Heathwaite, A. Binley, and H. Zhang (2012), Characterization of the key pathways of dissimilatory nitrate reduction and their response to complex organic substrates in hyporheic sediments, *Limnol. Oceanogr.*, *57*(2), 387–400, doi:10.4319/lo.2012.57.2.0387.

Lansdown, K., C. M. Heppell, M. Trimmer, A. Binley, A. L. Heathwaite, P. Byrne, and H. Zhang (2015), The interplay between transport and reaction rates as controls on nitrate attenuation in permeable, streambed sediments, *J. Geophys. Res. G Biogeosciences*, *120*(6), 1093–1109, doi:10.1002/2014JG002874.

Lansdown, K., B. A. McKew, C. Whitby, C. M. Heppell, A. J. Dumbrell, A. Binley, L. Olde, and M. Trimmer (2016), Importance and controls of anaerobic ammonium oxidation influenced by riverbed geology, *Nat. Geosci.*, *9*(May), 357–360, doi:10.1038/ngeo2684.

Li, X., L. Hou, M. Liu, Y. Zheng, G. Yin, X. Lin, L. Cheng, Y. Li, and X. Hu (2015), Evidence of Nitrogen Loss from Anaerobic Ammonium Oxidation Coupled with Ferric Iron Reduction in an Intertidal Wetland, *Environ. Sci. Technol.*, *49*(19), 11560–11568, doi:10.1021/acs.est.5b03419.

Liu, T., X. Xia, S. Liu, X. Mou, and Y. Qiu (2013), Acceleration of denitrification in turbid rivers due to denitrification occurring on suspended sediment in oxic waters, *Environ. Sci. Technol.*, *47*(9), 4053–4061, doi:10.1021/es304504m.

Luther, G. W., B. Sundby, B. L. Lewis, P. J. Brendel, and N. Silverberg (1997), Interactions of manganese with the nitrogen cycle: Alternative pathways to dinitrogen, *Geochim. Cosmochim. Acta*, *61*(19), 4043–4052, doi:10.1016/S0016-7037(97)00239-1.

Maag, M., and F. P. Vinther (1996), Nitrous oxide emission by nitrification and denitrification in different soil types and at different soil moisture contents and temperatures, *Appl. Soil Ecol.*, *4*(1), 5–14.

Madigan, M. T., J. M. Martinko, and J. Parker (2003), *Brock Biology of Microorganisms*, 10th ed., Pearson Education, Upper Saddle River, NJ.

Martikainen, P. (1985), Nitrous-oxide emission associated with autotrophic ammonium oxdation in acid coniferous forest soil, *Appl. Environ. Microbiol.*, *50*(6), 1519–1525.

Martin, L. A., P. J. Mulholland, J. R. Webster, and H. M. Valett (2001), Denitrification in sediments of headwater streams in the southern Appalachian Mountains , USA, *J. North Am. Benthol. Soc.*, *20*(4), 505–519.

Mayer, P. M., P. M. Groffman, E. a Striz, and S. S. Kaushal (2010), Nitrogen dynamics at the groundwater-surface water interface of a degraded urban stream., *J. Environ. Qual.*, *39*(3), 810–823, doi:10.2134/jeq2009.0012.

McCutchan Jr., J. H., and W. M. Lewis Jr. (2008), Spatial and temporal patterns of denitrification in an effluent-dominated plains river, *Verhandlungen Int. Vereinigung Limnol.*, *30*(2), 323–328.

Megonigal, J. P., M. E. Hines, and P. . Visscher (2004), Anaerobic Metabolism: Linkages to Trace Gases and Anaerobic Processes, in *Treatise of Geochemistry Volume 8 Biogeochemistry*, edited by W. H. Schlesinger, pp. 317–424, Elsevier, New York.

Mulholland, P., and H. Valett (2004), Stream denitrification and total nitrate uptake rates measured using a field 15 N tracer addition approach, *Limnol. Oceanogr.*, *49*(3), 809–820.

Müller, M. M., V. Sundman, and J. Skujins (1980), Denitrification in Low pH Spodosols and Peats Determined with the Acetylene Inhibition Method, *Appl. Environ. Microbiol.*, *40*(2), 235–239.

Opdyke, M. R., M. B. David, and B. L. Rhoads (2006), Influence of geomorphological variability in channel characteristics on sediment denitrification in agricultural streams., *J. Environ. Qual.*, *35*(6), 2103–2112, doi:10.2134/jeq2006.0072.

Otte, S., J. Schalk, J. G. Kuenen, and M. S. M. Jetten (1999), Hydroxylamine oxidation and subsequent nitrous oxide production by the heterotrophic ammonia oxidizer Alcaligenes faecalis, *Appl. Microbiol. Biotechnol.*, *51*(2), 255–261, doi:10.1007/s002530051390.

Ottley, C. J., W. Davison, and W. M. Edmunds (1997), Chemical catalysis of nitrate reduction by iron (II), *Geochim. Cosmochim. Acta*, *61*(9), 1819–1828, doi:10.1016/S0016-7037(97)00058-6.

Postma, D. (1990), Kinetics of nitrate reduction by detrital Fe (II)-silicates, *Geochim. Cosmochim. Acta*, *54*(3), 903–908.

Poth, M., and D. D. Focht (1985), 15N Kinetic Analysis of N2O Production by Nitrosomonas europea: an Examination of Nitrifier Denitrification, *Appl. Environ. Microbiol.*, *49*(5), 1134–1141.

Rice, C. W., and J. M. Tiedje (1989), Regulation of ntirate assimilation by ammonium in soils and in isolated soil microorganisms, *Soil Biol. Biochem.*, *21*(4), 597–602.

Richardson, W. B., E. A. Strauss, L. A. Bartsch, E. M. Monroe, J. C. Cavanaugh, L. Vingum, and D. M. Soballe (2004), Denitrification in the Upper Mississippi River: Rates, controls, and contribution to nitrate flux, *Can. J. Fish. Aquat. Sci.*, *61*(7), 1102–1112, doi:10.1139/f04-062.

Rosamond, M. S., S. J. Thuss, and S. L. Schiff (2012), Dependence of riverine nitrous oxide emissions on dissolved oxygen levels, *Nat. Geosci.*, *5*(10), 715–718, doi:10.1038/ngeo1556.

Royer, T. V, J. L. Tank, and M. B. David (2004), Transport and fate of nitrate in headwater agricultural streams in Illinois, *J. Environ. Qual.*, *33*(4), 1296–1304, doi:10.2134/jeq2004.1296.

Schlesinger, W. H. (1997), *Biogeochemistry: An Analysis of Global Change*, 2nd ed., Academic Press, San Diego.

Schreiber, F., P. Wunderlin, K. M. Udert, and G. F. Wells (2012), Nitric oxide and nitrous oxide turnover in natural and engineered microbial communities: Biological pathways, chemical reactions, and novel technologies, *Front. Microbiol.*, *3*(OCT), 1–24, doi:10.3389/fmicb.2012.00372.

Schubert, C. J., E. Durisch-kaiser, B. Wehrli, B. Thamdrup, P. Lam, and M. M. M. Kuypers (2006), Anaerobic ammonium oxidation in a tropical freshwater system (Lake Tanganyika), *Env. Microbiol*, *8*(10), 1857–1863, doi:10.1111/j.1462-2920.2006.001074.x.

Seitzinger, S. P. (1988), Denitrification in freshwater and coastal marine ecosystems: Ecological and geochemical significance, *Limnol. Oceanogr.*, *33*(4), 702–724, doi:10.4319/lo.1988.33.4_part_2.0702.

Seitzinger, S. P., and C. Kroeze (1998), Global distribution of nitrous oxide production and N inputs in freshwater and coastal marine ecosystems, *Global Biogeochem. Cycles*, *12*(1), 93–113.

Shrestha, N. K., S. Hadano, T. Kamachi, and I. Okura (2002), Dinitrogen production from ammonia by Nitrosomonas europaea, *Appl. Catal. A Gen.*, *237*(1–2), 33–39, doi:10.1016/S0926-860X(02)00279-X.

Silvennoinen, H., A. Liikanen, J. Torssonen, C. F. Stange, and P. J. Martikainen (2008a), Denitrification and N2O effluxes in the Bothnian Bay (northern Baltic Sea) river sediments as affected by temperature under different oxygen concentrations, *Biogeochemistry*, *88*, 63–72.

Silvennoinen, H., A. Liikanen, J. Torssonen, C. Florian Stange, and P. J. Martikainen (2008b), Denitrification and nitrous oxide effluxes in boreal, eutrophic river sediments under increasing nitrate load: A laboratory microcosm study, *Biogeochemistry*, *91*(2–3), 105–116, doi:10.1007/s10533-008-9262-z.

Šimek, M., L. Jíšová, and D. W. Hopkins (2002), What is the so-called optimum pH for denitrification in soil?, *Soil Biol. Biochem.*, *34*(9), 1227–1234, doi:10.1016/S0038-0717(02)00059-7.

Smith, M. S. (1982), Dissimilatory reduction of NO2 to NH4 and N20 by a soil Citrobactrer sp., *Appl. Environ. Micro.*, *43*(4), 854–860.

Smith, M. S., and K. Zimmerman (1981), Nitrous oxide production by nondenitrifying soil nitrate reducers, *Soil Sci. Soc. Am. J.*, *45*(5), 865–871.

Starry, O. S., H. M. Valett, and M. E. Schreiber (2005), Nitrification rates in a headwater stream: influences of seasonal variation in C and N supply, *J. North Am. Benthol. Soc.*, *24*(4), 753–768, doi:10.1899/05-015.1.

Stein, L. Y., and M. G. Klotz (2016), The nitrogen cycle, *Curr. Biol.*, *26*(3), R94–R98, doi:10.1016/j.cub.2015.12.021.

Stein, L. Y., and Y. L. Yung (2003), Production, isotopic composition, and atmospheric fate of biologicaly produced nitrous oxide, *Annu. Rev. Earth Planet. Sci.*, *31*(1), 329–356, doi:10.1146/annurev.earth.31.110502.080901.

Stevens, R. J., and R. J. Laughlin (1998), Measurement of nitrous oxide and di-nitrogen emissions from agricultural soils, *Nutr. Cycl. Agroecosystems*, *52*(2–3), 131–139, doi:10.1023/A:1009715807023.

Stevens, R. J., R. J. Laughlin, and J. P. Malone (1998), Soil pH affects the processes reducing nitrate to nitrous oxide and di-nitrogen, *Soil Biol. Biochem.*, *30*(8–9), 1119–1126, doi:10.1016/S0038-0717(97)00227-7.

Stevenson, F. J., and M. A. Cole (1999), *Cycles of Soil: Carbon, Nitrogen, Phosphorous, Sulfur, Micronutrients*, 2nd ed., John Wiley & Sons.

Strauss, E. A., and G. A. Lamberti (2000), Regulation of nitrification in aquatic sediments by organic carbon, *Limnol. Oceanogr.*, *45*(8), 1854–1859, doi:10.4319/lo.2000.45.8.1854.

Strauss, E. A., N. L. Mitchell, and G. A. Lamberti (2002), Factors regulating nitrification in aquatic sediments: effects of organic carbon, nitrogen availability, and pH, *Can. J. Fish. Aquat. Sci.*, *59*(3), 554–563, doi:10.1139/f02-032.

Strauss, E. A., W. B. Richardson, L. A. Bartsch, J. C. Cavanaugh, D. A. Bruesewitz, H. Imker, J. A. Heinz, and D. M. Soballe (2004), Nitrification in the Upper Mississippi River: patterns, controls, and contribution to the NO3-budget, *J. North Am. Benthol. Soc.*, *23*(1), 1–14.

Strous, M., E. van Gerven, J. G. Kuenen, and M. Jetten (1997), Effects of aerobic and microaerobic conditions on anaerobic ammonium-oxidizing (anammox) sludge, *Appl. Environ. Microbiol.*, *63*(6), 2446–2448.

Thamdrup, B., and T. Dalsgaard (2002), Production of N2 through Anaerobic Ammonium Oxidation Coupled to Nitrate Reduction in Marine Sediments, *Appl. Environ. Microbiol.*, *68*(3), 1312–1318, doi:10.1128/AEM.68.3.1312.

Tiedje, J. M. (1988), Ecology of Denitrification and Dissimilatory Nitrate Reduction to Ammonium, in *Biology of Anaerobic Microorganisms*, edited by A. J. B. Zehnder, pp. 179–244, John Wiley & Sons, New York.

Van Cleemput, O., and L. Baert (1984), Nitrite: a key compound in N loss processes under acid conditions?, *Plant Soil*, *76*(1), 233–241.

Venkiteswaran, J. J., M. S. Rosamond, and S. L. Schiff (2014), Nonlinear response of riverine N2O fluxes to oxygen and temperature, *Environ. Sci. Technol.*, *48*(3), 1566–1573, doi:10.1021/es500069j.

Vitousek, P. M., J. D. Aber, R. W. Howarth, G. E. Likens, P. A. Matson, D. W. Schindler, W. H. Schlesinger, and D. G. Tilman (1997), Human alteration of the global nitrogen cycle: sources and consequences, *Ecol. Appl.*, *7*(3), 737–750.

Warwick, J. J. (1986), Diel variation of in-stream nitrification, *Water Res.*, *20*(10), 1325–1332.

Watanabe, I. (1986), Nitrogen fixation by non-legumes in tropical agriculture with special reference to wetland rice, *Plant Soil*, *90*(1–3), 343–357.

Weier, K. L., J. W. Doran, J. F. Power, and D. T. Walters (1993), Denitrification and the dinitrogen/nitrous oxide ratio as affected by soil water, available carbon, and nitrate, *Soil Sci. Soc. Am. J.*, *57*(1), 66–72, doi:10.2136/sssaj1993.03615995005700010013x.

Wrage, N., G. Velthof, M. van Beusichem, and O. Oenema (2001), Role of nitrifier denitrification in the production of nitrous oxide, *Soil Biol. Biochem.*, *33*(12–13), 1723–1732.

Yang, W. H., K. a. Weber, and W. L. Silver (2012), Nitrogen loss from soil through anaerobic ammonium oxidation coupled to iron reduction, *Nat. Geosci.*, *5*(8), 538–541, doi:10.1038/ngeo1530.

Zhu, X., M. Burger, T. A. Doane, and W. R. Horwath (2013a), Ammonia oxidation pathways and nitrifier denitrification are significant sources of N2O and NO under low oxygen availability, *Proc. Natl. Acad. Sci.*, *110*(16), 6328–6333, doi:10.1073/pnas.1219993110/-/DCSupplemental.www.pnas.org/cgi/doi/10.1073/pnas.1219993110.

Zhu, X., L. C. R. Silva, T. a. Doane, and W. R. Horwath (2013b), Iron: The Forgotten Driver of Nitrous Oxide Production in Agricultural Soil, *PLoS One*, *8*(3), 1–6, doi:10.1371/journal.pone.0060146.

Zumft, W. G. (1997), Cell Biology and Molecular Basis of Denitrification, *Microbiol. Mol. Biol. Rev.*, *61*(4), 533–616.

APPENDIX B

Supporting Information for Chapter Three

B.1 Hydrologic modeling and tracer tests.

Bed surface pressure profiles were modeled using ANSYS Fluent computational

dynamics software (ANSYS Inc., Canonsburg, PA, USA). The surface pressure modeling

procedure was validated using the measured data of Fehlman [1985]. The modeled

pressure profiles were used as input conditions for the hypothetical flow model of

Mazadri et al. [2010], which was modified to enable back particle tracking from the

sensor locations. The back particle data was used to calculate travel time to the sensor

locations. The Mazadri model was cross-validated using a conservative test, described

below. Following the final pore water sampling events, visual tracer tests were conducted

on one of the 70 cm dunes using fluorescein dye. The dye was injected at multiple points

in the dune and photographed, at ten minute intervals, under black light through a glass

window. A conservative tracer test was also conducted in one of the channels using a

sodium chloride solution and forty embedded conductivity sensors. The sensors were

designed and developed at the Center for Ecohydraulics Research (CERSL) and built by

Rapid Creek Research, Boise, ID, USA. Electrical conductivity (EC) was logged for each

of the sensors, at five minute intervals, for approximately seven days. EC sensor channels

were switched using Model AM16/32 multiplexers and data was logged using Model

CR1000 data loggers (Campbell Scientific, Logan, UT, USA).

B.2 Microbial genetic analysis

Sediment samples collected at the conclusion of the 2013 flume experiment were

subsampled from sterile 15 mL culture tubes. Total microbial DNA was extracted from

approximately 1 gram of sediment using the FastDNA™ SPIN Kit for Soil (MP

Biomedical LLC, Solon, OH) according to the manufacturer's instructions. DNA

concentrations were quantified using a NanoDrop3300 Fluorospectrometer (Thermo-Scientific, Waltham, MA). DNA quality was visually confirmed on a 1.5% (wt./vol) agarose gel. SYBR quantitative PCR (qPCR) was used to determine bacterial densities. Concentrations of *nirS*, the gene encoding for nitrite reductase, were quantified using primer pairs nirSCd3aF (5'-AACGYSAAGGARACSGG-3') and nirSR3cd (5'-GASTTCGGRTGSGTCTTSAYGAA-3') [Kandeler et al., 2006].

B.3 Thermodynamic calculations

Thermodynamic calculations presented in this paper were based on the four sequential reduction steps of denitrification (NO_3^- to NO_2^-, NO_2^- to NO, and NO to N_2O, and N_2O to N_2), using H_2 as an electron donor [Alter and Steiof, 2005]. The standard state Gibbs free energy for each step (ΔG°_{rxn}) was calculated using standard enthalpies of formation [Stumm and Morgan, 1996] and the following equation [Appelo and Postma, 2005]:

$$\Delta G^{\circ}_{rxn} = \Sigma\ \Delta G^{\circ}_{f\,(products)} - \Sigma\ \Delta G^{\circ}_{f\,(reactants)} \qquad (B1)$$

The following equation was used determine Gibbs free energy values for non-standard state conditions in the hyporheic zone (ΔG_{rxn}), where R is the gas constant (0.00831 kJ mol^{-1} K^{-1}), T is the temperature (K), and Q is the reaction quotient [Appelo and Postma, 2005].

$$\Delta G_{rxn} = \Delta G^{\circ}_{rxn} + RT\ lnQ \qquad (B2)$$

The reaction quotient was based on the observed average range of conditions in the flume experiment and dissolved organic carbon (DOC) concentrations observed in a natural sandy streambed [Stelzer et al., 2011].

Table B.1. **Gibbs Free Energy for Steps of Denitrification**

Reaction	$\Delta G°_{rxn}$	ΔG_{rxn} (HZ conditions)
NO_3^- to NO_2^-	-180.7	-130.3
NO_2^- to NO	-122.2	-68.1
NO to N_2O	-161.8	-106.4
N_2O to N_2	-179.5	-138.7
Denitrification (NO_3^- to N_2)	-644.2	-443.5

B.4 Reactive transport modeling

We utilized reactive transport modeling to evaluate our conceptual model. Our approach was to express our conceptual model of nitrogen dynamics along a flow path as a series of reactions with associated rate expressions. This model is spatially expressed within a one-dimensional flow domain approximating a hyporheic flow path within a dune within our flume experiment. Rate expressions were formulated to be consistent with our conceptual model and observed chemical trends within our experiment. While the model is constrained by transport physics and reaction stoichiometry, the system is under-constrained by the high number of unknown parameters. Accordingly, there are likely multiple combinations of parameter values that could produce similar model results. The model output match to observed concentrations, therefore, provides an evaluation of the plausibility of the conceptual model within the context of spatiotemporal distributions of reactants and products along an idealized hyporheic flow path.

Simulations were performed using MIN3P [Mayer et al., 2002], a general purpose reactive transport code that has previously been used for the investigation of a variety of reactive transport problems in saturated and unsaturated porous media [Mayer et al.,

2002; Jurjovec et al., 2004]. The MIN3P code couples advective-diffusive flow, solute transport, intra-aqueous reactions and solid phase transformations.

The model domain was idealized within the model as a one-dimensional (2 m long) flow system of unit height and width (Table B.2). Flow velocity was fixed at 0.0514 m hour^{-1}, flowing from left to right. The left hand boundary was specified as constant third type boundary condition with specified input concentrations (Table B.2). The right hand boundary was specified as a free exit type boundary.

The reaction network was developed from the conceptual model with three reactions utilizing organic carbon as electron donor: oxygen reduction, nitrate reduction to nitrous oxide and nitrous oxide reduction to dinitrogen. These reactions are formulated as heterogeneous reactions with aqueous species reacting with solid phase organic carbon. Rate expressions were formulated for each of these reactions:

Oxygen reduction by organic carbon reaction

Oxygen reduction is expressed as:

$$O_{2(aq)} + CH_2O_{(s)} \Rightarrow CO_{2(aq)} + H_2O \qquad\qquad \text{(B3)}$$

The rate expression for oxygen reduction by organic carbon is simply expressed as first order dependency on oxygen concentration and an effective rate constant:

$$R_{O_{2(aq)}-H_2O} = -k_{O_{2(aq)}-H_2O}\left[O_{2(aq)}\right] \qquad\qquad \text{(B4)}$$

Nitrate reduction to nitrous oxide by organic carbon reaction

Nitrate reduction is expressed as:

$$2NO_3^- + 2CH_2O_{(s)} \Rightarrow N_2O_{(aq)} + 2CO_3^{2-} + 2H^+ \qquad\qquad \text{(B5)}$$
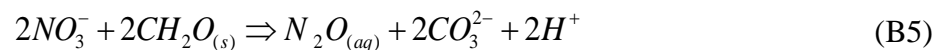
The rate expression for nitrate reduction to nitrous oxide is also expressed as first order dependency on nitrate concentration and an effective rate constant but also includes an inhibition term to limit nitrate reduction when oxygen concentrations are high:

$$R_{NO_3^- - N_2O_{(aq)}} = -k_{NO_3^- - N_2O_{(aq)}} \left[NO_3^- \right] \left[\frac{K_{NO_3^- - N_2O_{(aq)}}^{inhib\, O_{2(aq)}}}{K_{NO_3^- - N_2O_{(aq)}}^{inhib\, O_{2(aq)}} + \left[O_{2(aq)} \right]} \right]^{X_{NO_3^- - N_2O_{(aq)}}^{inhib\, O_{2(aq)}}} \tag{B6}$$

Nitrous oxide reduction to di-nitrogen gas by organic carbon reaction

Nitrous oxide reduction is expressed as:

$$2N_2O_{(aq)} + CH_2O_{(s)} \Rightarrow 2N_{2(aq)} + CO_3^{2-} + 2H^+ \tag{B7}$$
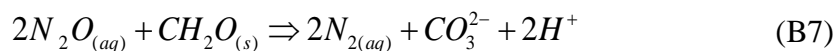
The rate expression for nitrous oxide reduction to di-nitrogen gas by organic carbon oxide is also expressed as first order dependency on nitrate concentration and an effective rate constant but also includes an inhibition term to limit nitrate reduction when oxygen concentrations are high. Note that the inhibition concentration for nitrous oxide reduction is established at a value lower than that used in the nitrate reduction rate expression to reflect a higher sensitivity to oxygen:

$$R_{N_2O_{(aq)} - N_{2(aq)}} = -k_{N_2O - N_{2(aq)}} \left[N_2O_{(aq)} \right] \left[\frac{K_{N_2O - N_{2(aq)}}^{inhib\, O_{2(aq)}}}{K_{N_2O - N_{2(aq)}}^{inhib\, O_{2(aq)}} + \left[O_{2(aq)} \right]} \right]^{X_{N_2O - N_{2(aq)}}^{inhib\, O_{2(aq)}}} \tag{B8}$$

Table B.2.   **Initial and Boundary Conditions**

Physical Parameters and Initial Conditions	
Domain dimensions	2 m
Flow velocity	0.0514 m hour^{-1}
Domain residence time	39.9 hours
Organic carbon content	0.15% by wt. POM
Input Concentrations (left boundary)	
Dissolved oxygen	8.8 mg L^{-1}
Nitrate	10 mg L^{-1}
Nitrous oxide	1 x 10^{-12} mg L^{-1}
Dinitrogen gas	1 x 10^{-12} mg L^{-1}

Table B.3.Rate Expression Terms

Reaction, *Term name*	Rate Expression Term	Term Value
Oxygen reduction, *Rate Constant*	$-k_{O_{2(aq)}-H_2O}$	1.0×10^{-5} *mol m^{-3}* sec^{-1}
Oxygen reduction, *Oxygen concentration*	$\left[O_{2(aq)}\right]$	model variable
Nitrate reduction to nitrous oxide, *Rate constant*	$k_{NO_3^- - N_2O_{(aq)}}$	5.0×10^{-3} *mol m^{-3}* sec^{-1}
Nitrate reduction by nitrous oxide, *Nitrate conc. dependency*	$\left[NO_3^-\right]$	model variable
Nitrate reduction by nitrous oxide, *Inhibition constant*	$K_{NO_3^- - N_2O_{(aq)}}^{inhib\ O_{2(aq)}}$	3.0×10^{-5} *mol^{-1}L*
Nitrate reduction by nitrous oxide, *Oxygen concentration*	$\left[O_{2(aq)}\right]$	model variable
Nitrate reduction by nitrous oxide, *Inhibition, exponential*	$X_{NO_3^- - N_2O_{(aq)}}^{inhib\ O_{2(aq)}}$	4.0
Nitrous oxide reduction to di-nitrogen, *Rate constant*	$k_{N_2O_{(aq)}-N_{2(aq)}}$	3.0×10^{-2} *mol m^{-3}* sec^{-1}
Nitrous oxide reduction to di-nitrogen, *Nitrous oxide conc. dependency*	$\left[N_2O\right]$	model variable
Nitrous oxide reduction to di-nitrogen, *Inhibition constant*	$K_{N_2O_{(aq)}-N_{2(aq)}}^{inhib\ O_{2(aq)}}$	1.0×10^{-5} *mol^{-1}L*
Nitrous oxide reduction to di-nitrogen, *Oxygen concentration*	$\left[O_{2(aq)}\right]$	model variable
Nitrous oxide reduction to di-nitrogen, *Inhibition, exponential*	$X_{N_2O_{(aq)}-N_{2(aq)}}^{inhib\ O_{2(aq)}}$	2.0

Table B.4.   Column data for weeks 12, 14, and 16

Distance* (cm)	Week:	Travel Time (hours			DO (mg L⁻¹)			N-N2O (µg L⁻¹)		
		12	14	16	12	14	16	12	14	16
-10	0.05 % POM	0.0	0.0	0.0	7.7	8.0	8.2	0.2	0.1	0.2
0	Column	1.2	1.1	1.1	5.7	6.3	6.8	1.9	0.8	1.1
10		2.4	2.3	2.2	6.0	6.3	6.5	1.7	0.9	1.4
20		3.5	3.4	3.2	6.1	6.0	6.6	0.9	1.0	1.3
30		4.7	4.6	4.3	6.1	5.8	6.2	1.5	0.9	1.3
40		5.9	5.7	5.4	5.7	5.7	6.0	0.9	0.8	1.2
50		7.1	6.8	6.5	5.4	5.5	6.5	0.8	0.9	1.3
60		8.3	8.0	7.5	4.9	4.9	5.4	0.9	1.0	2.9
70		9.4	9.1	8.6	4.5	5.4	5.4	0.8	1.1	1.3
80		10.6	10.3	9.7	5.0	4.4	5.0	0.8	0.8	1.3
90		11.8	11.4	10.8	4.2	3.9	5.0	1.2	0.8	1.4
100		13.0	12.5	11.8	3.6	3.6	4.6	0.9	0.9	1.4
-10	0.15% POM	0.0	0.0	0.0	7.7	7.6	8.2	0.2	0.2	0.2
0	Column	1.1	1.2	1.2	6.8	6.1	6.5	0.8	0.8	1.5
10		2.2	2.4	2.4	5.7	3.8	5.8	0.9	0.9	1.6
20		3.3	3.6	3.6	4.5	4.4	4.9	0.8	0.7	1.8
30		4.4	4.8	4.8	2.1	2.8	4.0	0.9	0.8	2.0
40		5.5	6.0	6.0	0.3	1.3	1.3	1.6	1.4	1.8
50		6.6	7.2	7.2	0.2	0.6	0.5	3.5	3.6	6.7
60		7.7	8.5	8.5	0.5	0.5	0.5	5.7	6.2	13.6
70		8.8	9.7	9.7	0.1	0.6	0.4	8.9	9.9	25.5
80		10.0	10.9	10.9	0.3	0.6	0.8	12.9	13.7	39.1
90		11.1	12.1	12.1	0.6	0.4	0.1	12.1	21.3	55.3
100		12.2	13.3	13.3		0.4	0.2		16.0	60.5
-10	0.50% POM	0.0	0.0	0.0	7.6	7.6	7.4	0.2	0.2	0.3
0	Column	1.2	1.2	1.1	4.6	4.5	5.4	0.8	0.7	1.0
10		2.4	2.4	2.1	0.2	0.3	1.5	1.1	0.8	1.5
20		3.6	3.6	3.2	0.1	0.2	0.1	2.2	3.1	5.0
30		4.8	4.8	4.3	0.2	0.3	0.1	3.0	3.3	5.7
40		6.0	6.1	5.3	0.4	0.5	0.8	0.6	0.7	2.4
50		7.3	7.3	6.4	0.1	0.5	0.3	0.5	0.5	0.6
60		8.5	8.5	7.5	0.7	0.4	0.3	0.4	0.5	0.7
70		9.7	9.7	8.5	0.4	0.6	0.1	0.7	0.6	0.6
80		10.9	10.9	9.6	0.2	0.5	0.5	0.4	0.6	0.7
90		12.1	12.1	10.7	0.4	0.3	0.4	0.4	0.5	0.6
100		13.3	13.3	11.7	0.5	0.5	0.6	0.7	0.6	0.6

Distance from the first sampling port in the direction of flow.

Table B.5. 2013 flume data for 100 cm x 3 cm dunes, day 112

Port*	X	Y	Travel Time	*nirS*	DO	N-N$_2$O	N-NO$_3^-$	N-NH$_3$	N-NO$_2^-$	pH
	cm	cm	hours	copy #/ gram sed *10^6	mg L^{-1}	µg L^{-1}	µg L^{-1}	µg L^{-1}	µg L^{-1}	
3.01	8.5	-5	8	43.5	1.8	0.5	65	44	1	6.9
3.02	8.5	-14.4	39	2.0	0.5	0.2	14	10	3	6.6
3.03	18.5	-5	7	7.9	0.0	0.7	73	27	0	6.9
3.04	18.5	-10	16	2.6	0.0	0.2	0	28	2	6.7
3.05	18.5	-14.4	27	1.4	0.1	0.2	1	35	3	6.5
3.06	28.5	-1.5	2	6.3	1.8	0.4	568	0	8	7.0
3.07	28.5	-5	6	15.4	0.0	0.5	84	56	2	6.8
3.08	28.5	-14.4	23	1.3	0.6	0.1	11	61	3	6.8
3.09	28.5	-22.1	55	1.6	0.2	0.2	11	169	5	6.5
3.10	38.5	-1.5	3	11.7	3.2	0.5	462	12	2	6.9
3.11	38.5	-5	5		0.0	0.4	22	67	1	6.8
3.12	38.5	-10	13	2.0	0.0	0.3	151	36	3	6.6
3.13	38.5	-14.4	23	1.6	0.0	0.2	14	93	4	6.6
3.14	38.5	-22.1	49	1.5	0.0	0.1	30	105	5	6.6
3.15	48.5	-1.5	1	7.8	5.1	0.7	498	31	3	7.1
3.16	48.5	-5	5	5.1	0.2	0.1	3	81	2	7.1
3.17	48.5	-10	14	1.5	0.0	0.1	4	33	2	6.6
3.18	48.5	-14.4	24	0.8	0.1	0.2	30	63	6	6.6
3.19	48.5	-22.1	52	0.8	0.0	0.3	0	122	3	6.5
3.20	58.5	-1.5	6	6.5	2.7	1.1	53	104	0	6.8
3.21	58.5	-5	11	2.5	0.1	0.2	12	50	2	6.6
3.22	58.5	-10	21	2.3	0.0	0.3	16	35	5	6.5
3.23	58.5	-22.1	63	2.3	0.0	0.1	17	106	9	6.5
3.24	68.5	-1.5	23	4.5	0.0	0.3	0	47	3	6.5
3.25	68.5	-5	29	3.1	0.0	0.2	0	23	4	6.7
3.26	68.5	-10	42	4.8	0.0	0.1	1	31	5	6.6
3.27	68.5	-14.4	55	1.7	0.0	0.2	0	31	4	6.7
3.28	68.5	-22.1	88	0.9	0.0	0.1	15	120	7	6.6
3.29	78.5	-1.5	105	2.5	0.0	0.2	1	23	3	6.8
3.30	78.5	-5	94	1.6	0.0	0.2	110	28	9	6.8
3.31	78.5	-10	92	2.3	0.0	0.2	156	51	15	6.8
3.32	78.5	-14.4	99	0.9	0.0	0.2	148	52	13	6.7
3.33	78.5	-22.1	150	0.8	0.0	0.1	103	151	9	6.6
3.34	88.5	-10	55	3.1	0.4	0.1	135	24	9	6.6
3.35	88.5	-14.4	185	2.2	0.0	0.1	110	53	10	6.7
3.36	98.5	-5	15	2.6	0.0	0.1	55	44	5	7.0
3.37	108.5	-5	8	11.5	0.0	0.6	192	40	4	6.8
3.38	108.5	-14.4		1.9	0.0	0.1	0	18	7	6.7
3.39	118.5	-5		13.3	0.0	1.0	69	37	2	6.8
3.40	118.5	-10		3.0	0.0	0.1	0	18	6	6.9
3.41	118.5	-14.4	27	1.2	0.0	0.1	0	6	5	6.6
3.42	118.5	-22.1	80	0.6	0.0	0.1	57	80	8	6.6
3.43	128.5	-1.5	2	11.9	5.6					

3.44	128.5	-5	6	13.2	0.0	0.8	147	34	4	6.9
3.45	128.5	-10	14	3.5	0.0	0.1	14	15	5	6.7
3.46	128.5	-14.4	23	3.0	0.0	0.1	36	18	6	
3.47	128.5	-22.1	55	0.7	0.0	0.1	0	152	6	6.5
3.48	138.5	-1.5	3	10.5	3.7	0.1	6	7	2	7.1
3.49	138.5	-5	5	4.7	0.0	0.6	32	24	1	6.9
3.50	138.5	-10	13	1.3	0.0	0.6	393	3	0	6.9
3.51	138.5	-14.4	23	1.1	0.0	0.1	2	5	2	6.8
3.52	138.5	-22.1	49	0.3	0.0	0.3	618	0	0	7.2
3.53	148.5	-1.5	1	12.0	2.6	0.1	31	99	6	6.6
3.54	148.5	-5	5	9.5	0.0	0.1	0	17	0	7.0
3.55	148.5	-10	14	2.4	0.0	0.1	3	16	2	6.7
3.56	148.5	-14.4	24	2.9	0.0	0.1	15	18	3	6.6
3.57	148.5	-22.1	52	1.4	0.0	0.1	12	76	3	
3.58	158.5	-1.5	6	11.8	6.5	0.5	504	0	1	7.1
3.59	158.5	-5	11	10.4	1.8	0.1	11	26	1	6.7
3.60	158.5	-10	21	4.1	0.0	0.1	46	26	6	
3.61	158.5	-14.4	33	2.9	0.0	0.1	20	25	6	6.4
3.62	168.5	-1.5	23	15.6	0.9	0.2	35	38	1	6.7
3.63	168.5	-10	42	2.3	0.0	0.1	27	21	6	6.5
3.64	168.5	-14.4	54	1.1	0.0	0.1	28	51	10	6.4
3.65	178.5	-1.5	105	2.0	0.0	0.1	24	37	7	6.5
3.66	178.5	-5	94	4.6	0.0	0.1	31	25	10	6.5
3.67	178.5	-10	91	3.7	0.0	0.1	34	28	11	6.5
3.68	178.5	-14.4	99	2.0	0.0	0.1	41	40	11	6.4
3.69	188.5	-1.5	4	16.2	0.6	0.2	583	0	1	6.6
3.70	188.5	-10	180	2.4	0.0	0.0	26	14	6	6.2
3.71	188.5	-14.4	184	1.1	0.0	0.1	16	35	5	6.1

* See Figure S1 for the layout of ports. X and Y coordinates are given from the trough upstream of the first dune.

Table B.6.   2013 flume data for 100 cm x 6 cm dunes, day 112

Port*	X	Y	Travel Time	*nirS*	DO	N-N$_2$O	N-NO$_3^-$	N-NH$_3$	N-NO$_2^-$	pH
	cm	cm	hours	copy #/gram sed *10^6	mg L^{-1}	µg L^{-1}	µg L^{-1}	µg L^{-1}	µg L^{-1}	
6.01	8.5	-5	9	2.7	0.1	2.6	99	35	5	6.8
6.02	8.5	-14.4	39	1.3	0.0	0.2	6	19	1	6.5
6.03	18.5	-5	9	8.7	1.2	0.2	0	22	0	6.9
6.04	18.5	-10	17	3.6	0.0	0.2	0	15	0	
6.05	18.5	-14.4	28	1.8	0.0	0.2	6	15	1	6.6
6.06	28.5	-1.5	4	20.5	6.1	0.7	430	13	1	6.9
6.07	28.5	-5	8	22.3	0.8	0.3	0	27	0	6.9
6.08	28.5	-14.4	25	2.2	0.1	0.2	7	19	1	6.7
6.09	28.5	-22.1	61	1.3	0.0	0.2	0	20	1	6.5
6.10	38.5	-1.5	6	14.0	4.1	0.6	226	12	0	7.1
6.11	38.5	-5	9		0.9	0.2	0	21	0	7.0
6.12	38.5	-10	16	3.2	0.0	0.2	0	22	0	6.6
6.13	38.5	-14.4	26	1.5	0.0	0.2	0	10	1	6.7
6.14	48.5	-1.5	5	13.1	3.6	0.6	173	7	0	6.7
6.15	48.5	-5	11	14.1	0.4	0.5	30	32	0	6.9
6.16	48.5	-10	19	3.2	0.0	0.1	0	16	0	6.8
6.17	48.5	-14.4	29	3.1	0.0	0.2	33	24	1	6.6
6.18	48.5	-22.1	66	13.0	0.0	0.2	19	17	2	6.6
6.19	58.5	2	4	19.8	7.9	1.0	332	17	1	7.1
6.20	58.5	-1.5	10	20.1	5.4	0.6	63	20	0	6.8
6.21	58.5	-5	18	2.4	2.6	0.1	1	14	0	6.7
6.22	58.5	-10	29	1.3	0.2	0.2	0	22	3	6.8
6.23	58.5	-22.1	92	1.0	0.1	0.4	0	51	5	6.6
6.24	68.5	2	37	36.2	3.3	1.3	432	4	4	7.0
6.25	68.5	-5	47	35.2	0.0	0.7	0	55	4	6.8
6.26	68.5	-10	58	3.6	0.0	0.2	0	29	3	6.7
6.27	68.5	-14.4	72	1.6	0.0	0.2	13	21	5	6.6
6.28	68.5	-22.1	214	0.5	0.0	0.2	0	20	3	6.7
6.29	78.5	2	9	21.7	0.1	1.0	42	30	2	6.8
6.30	78.5	-1.5	203	5.2	0.0	0.1	2	56	2	6.8
6.31	78.5	-5	134	2.6	0.0	0.2	0	48	3	6.6
6.32	78.5	-14.4	133	0.7	0.0	0.2	2	18	4	6.6
6.33	78.5	-22.1		1.2	0.0	0.4	41	55	12	6.7
6.34	88.5	-1.5	28	28.7	0.0	0.7	159	36	2	6.8
6.35	88.5	-5	246	6.0	0.0	0.2	0	1	2	6.9
6.36	88.5	-10		2.0	0.0	0.2	0	1	5	6.6
6.37	88.5	-14.4		1.0	0.0	0.2	19	12	4	6.7
6.38	98.5	-5	25	21.9	0.0	0.2	0	25	1	6.8
6.39	108.5	-5	9	7.2	5.4	0.3	429	11	1	7.0
6.40	108.5	-14.4	39	1.2	0.0	0.1	11	26	1	6.9
6.41	118.5	-5	9	10.8	7.1	0.3	740	0	1	7.1
6.42	118.5	-10	17	47.2	2.5	0.8	125	20	2	6.9
6.43	118.5	-14.4	28	2.2	0.2	0.1	0	25	3	7.0

6.44	128.5	-5	8	8.4	1.4	0.3	454	0	3	7.0
6.45	128.5	-10	15	26.4	1.5	1.2	369	11	3	7.0
6.46	128.5	-14.4	25	1.8	0.9	0.1	0	22	2	6.9
6.47	128.5	-22.1	61	1.9	0.1	0.1	0	0	11	6.9
6.48	138.5	-5	9	10.2	6.2	0.4	365	0	0	7.0
6.49	138.5	-10	16	18.5	4.2	1.1	364	12	4	7.1
6.50	138.5	-14.4	26	4.1	2.6	0.1	9	15	2	7.1
6.51	148.5	-5	11	7.3	6.4	0.4	555	28	2	7.1
6.52	148.5	-10	19	45.5	3.8	0.1	0	17	3	7.0
6.53	148.5	-14.4	29	2.0	2.0	0.1	0	1	1	7.0
6.54	148.5	-22.1	66	1.9	0.3	0.1	16	6	3	6.8
6.55	158.5	-1.5	10	6.2	4.7	0.3	796	0	2	7.2
6.56	158.5	-5	18	13.7	1.8	0.2	308	15	2	7.1
6.57	158.5	-10	29	15.1	0.1	0.1	0	20	3	7.0
6.58	158.5	-14.4	43	2.8	0.0	0.1	7	0	3	6.9
6.59	168.5	2		18.6	7.0	1.5	499	3	3	7.2
6.60	168.5	-1.5	41	1.2	0.9	0.1	0	13	1	7.0
6.61	168.5	-5	46	2.7	0.0					
6.62	168.5	-10	58	0.9	0.0	0.0	25	17	5	6.6
6.63	168.5	-14.4	72	0.6	0.0	0.0	27	33	7	6.6
6.64	178.5	2	9	17.7	0.2	0.3	46	90	3	6.7
6.65	178.5	-1.5	203	4.3	0.0	0.0	17	23	3	6.7
6.66	178.5	-5	134	5.2	0.0	0.1	11	14	2	6.6
6.67	178.5	-10	120	2.4	0.0	0.1	5	22	2	6.6
6.68	188.5	-5	244	22.8	0.0	0.5	502	4	0	6.9
6.69	188.5	-10		12.0	0.0	0.1	7	16	3	6.7
6.70	188.5	-14.4		1.9	0.0	0.0	6	18	3	6.6

* See Figure S1 for the layout of ports. X and Y coordinates are given from the trough upstream of the first

dune.

Table B.7. **2013 flume data for 100 cm x 9 cm dunes, day 112**

Port*	X	Y	Travel Time	*nirS*	DO	N-N$_2$O	N-NO$_3^-$	N-NH$_3$	N-NO$_2^-$	pH
	cm	cm	hours	copy #/gram sed *10^6	mg L^{-1}	µg L^{-1}	µg L^{-1}	µg L^{-1}	µg L^{-1}	
9.01	8.5	-5		4.0	0.3	0.7	352	83	5	6.9
9.02	8.5	-14.4	249	0.9	0.0	0.2	19	54	6	6.8
9.03	18.5	-5	16	12.3	4.5	1.2	559	11	2	6.9
9.04	18.5	-10	42	5.9	0.6	0.4	2	82	0	6.9
9.05	18.5	-14.4	345	0.3	0.0	0.4	0	47	2	6.9
9.06	28.5	-1.5	4	32.8	6.4	0.5	581	33	4	6.9
9.07	28.5	-5	10	17.6	5.1	1.2	226	0	2	6.9
9.08	28.5	-14.4	41	3.3	0.0	0.2	1	69	0	6.8
9.09	28.5	-22.1	277	1.2	0.0	0.2	0	6	2	6.7
9.10	38.5	-1.5	4	13.1	6.0	0.4	410	0	5	6.9
9.11	38.5	-5	8		4.2	1.8	955	4	7	6.9
9.12	38.5	-10	17	28.4	0.6	0.5	55	63	5	6.9
9.13	38.5	-14.4	30	2.9	0.0	0.1	12	43	4	6.9
9.14	38.5	-22.1	382	1.1	0.0	0.1	18	11	6	6.7
9.15	48.5	-1.5	5	2.8	7.0	0.3	959	0	3	
9.16	48.5	-5	9	18.0	6.0	0.8	861	5	5	7.0
9.17	48.5	-10	18	21.4	2.4	0.5	3	50	4	7.0
9.18	48.5	-14.4	31	2.7	0.2	0.2	146	42	6	7.0
9.19	48.5	-22.1	128	0.5	0.0	0.1	21	17	5	6.7
9.20	58.5	2	2	6.0	7.0	0.3	904	24	3	7.1
9.21	58.5	-1.5	8	4.4	6.3	0.3	848	0	5	7.0
9.22	58.5	-5	13	28.4	3.1	3.0	468	27	4	6.9
9.23	58.5	-10	24	63.0	0.3	0.9	19	46	2	6.8
9.24	58.5	-14.4	39	1.8	0.0	0.1	0	37	5	7.0
9.25	58.5	-22.1	364	1.6	0.0	0.1	14	16	5	7.0
9.26	68.5	5.5	4	7.9	8.1	0.3	766	0	4	7.2
9.27	68.5	2	10	0.9	7.4	0.3	793	2	4	7.4
9.28	68.5	-1.5	17	18.8	5.9	1.7	836	6	4	7.0
9.29	68.5	-5	25	26.3	4.1	2.4	323	39	8	
9.30	68.5	-10	39	12.8	0.4	1.7	64	61	5	6.9
9.31	68.5	-14.4	59	1.3	0.0	0.3	26	37	6	6.9
9.32	68.5	-22.1	308	2.3	0.0	0.3	0	0	8	6.9
9.33	78.5	5.5	38	6.4	4.0	0.5	650	0	4	7.2
9.34	78.5	2	40	19.0	2.3	0.7	123	10	6	7.1
9.35	78.5	-1.5	45	7.1	1.2	0.1	0	11	5	7.0
9.36	78.5	-5	53	2.2	0.1	0.2	11	18	6	7.0
9.37	78.5	-10	71	2.2	0.0	0.1	5	31	6	6.7
9.38	78.5	-14.4	105	3.1	0.0	0.2	0	9	7	6.8
9.39	88.5	2	78	8.1	0.2	0.6	111	42	6	6.9
9.40	88.5	-1.5	80	10.2	0.0	0.2	18	53	8	6.7
9.41	88.5	-10	101	3.3	0.0	0.2	0	20	8	6.7
9.42	98.5	-5	139	8.7	0.0	0.3	6	69	4	6.9
9.43	108.5	-5		4.4	0.2	0.3	826	0	3	7.6

9.44	108.5	-14.4	444	1.8	0.0	0.1	3	124	5	7.0
9.45	118.5	-5	16	6.4	6.1	0.5	748	0	1	7.3
9.46	118.5	-10	42	9.0	2.4	2.0	239	37	6	7.4
9.47	118.5	-14.4	568	12.7	0.2	0.2	6	128	1	7.3
9.48	128.5	-1.5	4	1.7	7.4	0.4	419	0	0	
9.49	128.5	-5	10	14.5	5.5	0.5	753	0	0	6.8
9.50	128.5	-10	22	14.1	3.1	4.9	441	49	7	7.2
9.51	128.5	-14.4	41	19.5	1.6	0.3	0	85	1	7.2
9.52	128.5	-22.1	452	1.2	0.2	0.2	20	97	3	7.2
9.53	138.5	-1.5	4	8.3	7.7	0.5	793	0	3	7.0
9.54	138.5	-5	8	4.5	6.3	0.6	682	0	2	7.2
9.55	138.5	-10	17	4.6	3.8	2.7	587	7	6	7.0
9.56	138.5	-14.4	30	26.1	2.0	0.1	0	74	1	7.5
9.57	138.5	-22.1	602	1.5	0.3	0.1	4	93	1	7.4
9.58	148.5	-1.5	5	8.2	6.6	0.4	465	0	2	7.0
9.59	148.5	-5	9	8.0	5.5	0.5	762	0	1	7.2
9.60	148.5	-10	18	7.3	2.5	6.0	616	33	25	7.1
9.61	148.5	-14.4	31	17.7	0.2	3.5	18	95	1	7.1
9.62	148.5	-22.1	128	0.6	0.0	0.4	0	80	5	7.0
9.63	158.5	2	2	3.5	6.5	0.4	617	0	0	7.1
9.64	158.5	-1.5	8	4.5	5.1	0.4	760	0	0	7.2
9.65	158.5	-5	13	12.0	3.7	3.9	624	16	14	6.9
9.66	158.5	-10	24	32.4	1.8	2.4	51	86	1	7.0
9.67	158.5	-14.4	39	2.5	0.8	0.1	0	78	2	7.1
9.68	158.5	-22.1	564	1.1	0.0	0.3	7	49	3	7.0
9.69	168.5	5.5	4	2.4	7.7	0.3	309	0	0	7.1
9.70	168.5	2	10	9.6	6.6	2.1	601	13	5	7.0
9.71	168.5	-1.5	17	37.7	4.7	2.4	415	42	12	
9.72	168.5	-5	25	22.4	3.1	1.6	56	73	1	7.1
9.73	168.5	-10	39	2.4	1.5	0.1	0	62	0	7.1
9.74	168.5	-14.4	59	1.9	0.8	0.2	0	62	0	6.9
9.75	168.5	-22.1	476	1.3	0.1					
9.76	178.5	5.5	38	2.4	1.0	2.0	226	50	1	6.9
9.77	178.5	2	40	13.8	0.3	0.1	0	36	2	6.8
9.78	178.5	-1.5	45	8.8	0.3	0.1	0	41	1	
9.79	178.5	-5	53	6.1	0.1	0.1	0	55	3	6.7
9.80	178.5	-10	70	4.2	0.1	0.1	9	39	4	6.6
9.81	178.5	-14.4	105	1.9	0.0	0.1	28	37	6	6.5
9.82	178.5	-22.1	455	0.7	0.0	0.1	8	17	3	6.6
9.83	188.5	2	78	6.3	0.0	0.3	444	0	0	6.9
9.84	188.5	-1.5	80	12.4	0.0	0.8	0	65	1	6.8
9.85	188.5	-5	85	4.7	0.0	0.1	0	9	1	6.7
9.86	188.5	-10	101	4.4	0.0	0.1	4	42	4	6.6
9.87	198.5	-1.5		2.5	1.1	0.3	633	0	1	6.8

See Figure S1 for the layout of ports. X and Y coordinates are given from the trough upstream of the first dune.

Table B.8. 2015 flume data for 100 cm x 9 cm dunes (ave. of three replicates), day 91

Port*	X	Y	Travel Time	DO	N-N$_2$O	N-NO$_3^-$	N-NH$_3$	N-NO$_2^-$	pH
	cm	cm	hours	mg L^{-1}	µg L^{-1}	µg L^{-1}	µg L^{-1}	µg L^{-1}	
100.01	12.5	1	0	9.2	0.3	1718	48	2	7.9
100.02	12.5	-3	7	6.5	0.4	2178	64	2	7.7
100.03	25	2	0	9.2	0.3	1458	65	2	7.9
100.04	27.5	-2	2	6.7	0.3	2108	60	2	7.8
100.05	30	3	0	9.0	0.2	1950	61	2	7.9
100.06	32.5	0	1	7.6	0.2	1906	55	3	7.9
100.07	30	-6.5	4	5.4	5.7	1917	59	31	7.5
100.08	30	-17		0.4	14.0	868	78	33	7.4
100.09	37.5	4	0	8.8	0.3	2216	75	-3	8.0
100.10	35	-4	3	6.5	0.4	1602	57	29	7.6
100.11	35	-10	7	2.5	46.6	1649	82	95	7.4
100.12	40	0	2	7.1	0.3	2156	66	3	7.8
100.13	40	-8	5	3.8	6.9	1867	67	33	7.6
100.14	40	-13		0.5	24.7	1014	65	147	7.5
100.15	42.5	-3	3	5.5	0.3	2013	38	1	7.6
100.16	45	3.5	1	8.2	0.3	1974	42	0	7.9
100.17	47.5	-5	4	4.9	1.0	1686	42	2	7.6
100.18	44.74	-10.27	7	1.0	31.7	1343	65	104	7.5
100.19	52.5	6	0	8.9	0.2	2030	53	3	7.9
100.20	50	1	2	6.9	0.4	2002	27	3	7.7
100.21	50	-12	10	0.4	30.5	508	73	61	7.3
100.22	57.5	3	1	6.1	0.3	1671	7	2	7.6
100.23	55	-2	3	3.6	1.1	1806	47	3	7.4
100.24	55	-8	6		27.0	1230	33	140	7.4
100.25	60	-5	5	1.2	28.4	1440	32	99	7.3
100.26	60	-12	17	0.8	0.3	0	58	4	7.3
100.27	60	-17		1.0	0.0	758	70	7	7.2
100.28	60	-24.5			0.0	0	83	5	7.0
100.29	65	7	1	6.2	7.9	1497	24	53	7.7
100.30	65	3	2	2.8	10.9	1515	37	68	7.5
100.31	65	-2	5		12.3	881	40	42	7.3
100.32	65	-8	9		2.4	80	79	3	7.2
100.33	72.5	7	3	3.2	2.5	768	51	10	7.3
100.34	72.5	2	5	2.0	11.3	242	89	51	7.1
100.35	75	-4	9	0.2	0.0	2	34	3	7.0
100.36	77.5	4	7	0.0	0.0	6	52	4	7.0
100.37	90	1	13	3.0	17.7	586	76	59	7.3
100.38	90	-17	44	0.6	0.0	8	67	11	6.8

See Figure S2 for the layout of ports. X and Y coordinates are given from the trough upstream of the dune.

Table B.9. 2015 flume data for 70 cm x 9 cm dunes (ave. of three replicates), day 91

Port*	X	Y	Travel Time	DO	N-N$_2$O	N-NO$_3^-$	N-NH$_3$	N-NO$_2^-$	pH
	cm	cm	hours	mg L^{-1}	µg L^{-1}	µg L^{-1}	µg L^{-1}	µg L^{-1}	
70.01	5	-2	5	7.3	0.2	1914	27	3	7.8
70.02	5	-16		0.3	14.2	449	66	50	7.1
70.03	12	1	5	9.2	0.2	1962	20	4	7.7
70.04	12.5	-2.5		8.6	0.2	1928	22	3	7.7
70.05	12.5	-9	11	2.3	3.2	1942	25	8	7.5
70.06	20	3	1	9.4	0.2	2007	23	-5	7.9
70.07	18	-1	3	7.9	0.2	2113	24	3	7.8
70.08	22	-5	7	6.2	0.3	2034	23	5	7.7
70.09	25	2	1	8.5	0.2	2126	27	4	7.8
70.10	26	-2	3	7.1	0.2	1869	26	2	7.8
70.11	28	-5	6	6.1	0.3	2074	29	0	7.6
70.12	25	-8	12	5.1	0.7	1968	15	2	7.6
70.13	29	4.5	1	8.9	0.3	2224	43	2	7.9
70.14	30	0	2	7.2	0.3	1863	3	0	7.7
70.15	32	-7	8	3.1	1.5	2137	26	3	7.4
70.16	30	-11		1.2	12.0	1786	24	19	7.5
70.17	33	3.5	1	8.3	0.4	1998	26	3	7.9
70.18	34	-3	5	4.3	0.3	1882	24	2	7.6
70.19	38	6	1	9.0	0.2	1933	31	3	7.8
70.20	37.5	0	3	5.7	0.3	2016	25	2	7.6
70.21	38	-6	8	1.1	18.5	1643	15	30	7.3
70.22	37	-11		0.8	34.9	1467	35	50	7.3
70.23	42	3	2	5.6	0.6	2076	21	1	7.5
70.24	42	-1.8	5	1.0	9.8	1891	21	53	7.3
70.25	42.5	-7.5	11	1.0	41.9	1502	43	94	7.4
70.26	46	5	2	3.6	3.4	1798	23	7	7.5
70.27	47.5	0	6	1.7	18.1	816	20	52	7.4
70.28	46	-4	9	1.4	26.5	855	38	52	7.4
70.29	50	-7	17	2.4	3.9	143	46	7	7.4
70.30	47	-12	27	0.5	11.1	82	38	2	7.2
70.31	45	-16	23	0.7	2.9	19	48	1	7.2
70.32	52.5	4	6	0.1	28.4	264	55	7	7.3
70.33	53	0	8	1.0	21.6	123	134	18	7.4
70.34	57.5	2	10	2.1	2.8	74	89	5	7.2
70.35	62.5	0	15	0.1	3.2	31	69	12	7.1
70.36	62.5	-8	20	0.0	1.0	18	64	1	7.1
70.37	65	-16	34	0.1	0.0	15	69	2	7.0

* See Figure S2 for the layout of ports. X and Y coordinates are given from the trough upstream of the dune.

Table B.10.   2013 Flume data statistics, day 112

Dune	Statistic	*nirS* copy#/ gram sed $*10^6$	DO mg L^{-1}	N-N$_2$O µg L^{-1}	N-NO$_3^-$ µg L^{-1}	N-NH$_3$ µg L^{-1}	N-NO$_2^-$ µg L^{-1}	pH
100 cm x 3 cm	Mean	5.0	0.5	0.2	86	44	5	6.7
	StDev	6.3	1.4	0.2	154	38	3	0.2
	Maximum	43.5	6.5	1.1	618	169	15	7.2
	Median	2.5	0.0	0.1	27	33	4	6.7
	Minimum	0.3	0.0	0.0	0	0	0	6.1
100 cm x 6 cm	Mean	9.7	1.4	0.4	113	20	2	6.8
	StDev	10.9	2.2	0.4	197	16	2	0.2
	Maximum	47.2	7.9	2.6	796	90	12	7.2
	Median	4.2	0.1	0.2	9	18	2	6.8
	Minimum	0.5	0.0	0.0	0	0	0	6.5
100 cm x 9 cm	Mean	9.2	2.3	0.8	271	34	4	7.0
	StDev	10.4	2.7	1.1	325	32	4	0.2
	Maximum	63.0	8.1	6.0	959	128	25	7.6
	Median	5.9	0.8	0.3	53	33	4	7.0
	Minimum	0.3	0.0	0.1	0	0	0	6.5
Surface	Inflow		8.1	0.5	548	0	1	7.1
	3 cm channel			0.7	547	1	1	7.1
	6 cm channel			0.8	396	7	0	7.2
	9 cm channel			0.7	402	0	3	7.0
	Outflow			0.7	375	0	0	7.1

Table B.9.   2015 Flume data statistics, day 91

Dune	Statistic	DO	N-N$_2$O	N-NO$_3^-$	N-NH$_3$	N-NO$_2^-$	pH
		mg L^{-1}	µg L^{-1}	µg L^{-1}	µg L^{-1}	µg L^{-1}	
100 cm x 9 cm	Mean	3.9	7.6	1268	56	30	7.5
	StDev	3.5	18.9	877	42	70	0.3
	Maximum	9.9	122.7	2476	232	365	8.0
	Median	4.0	0.3	1604	56	3	7.5
	Minimum	0.0	0.0	0	0	0	6.6
70 cm x 9 cm	Mean	4.1	7.1	1392	37	13	7.5
	StDev	3.5	16.5	859	46	30	0.3
	Maximum	10.2	83.7	2483	321	159	8.0
	Median	3.8	0.3	1862	23	2	7.5
	Minimum	0.0	0.0	0	0	0	6.8
Surface	Inflow	8.9	0.2	2006	38	3	7.9
	above 100 cm		0.3	2056	43	4	7.9
	above 70 cm		0.2	1785	12	5	8.0
	Outflow		0.3	2045	40	0	7.8
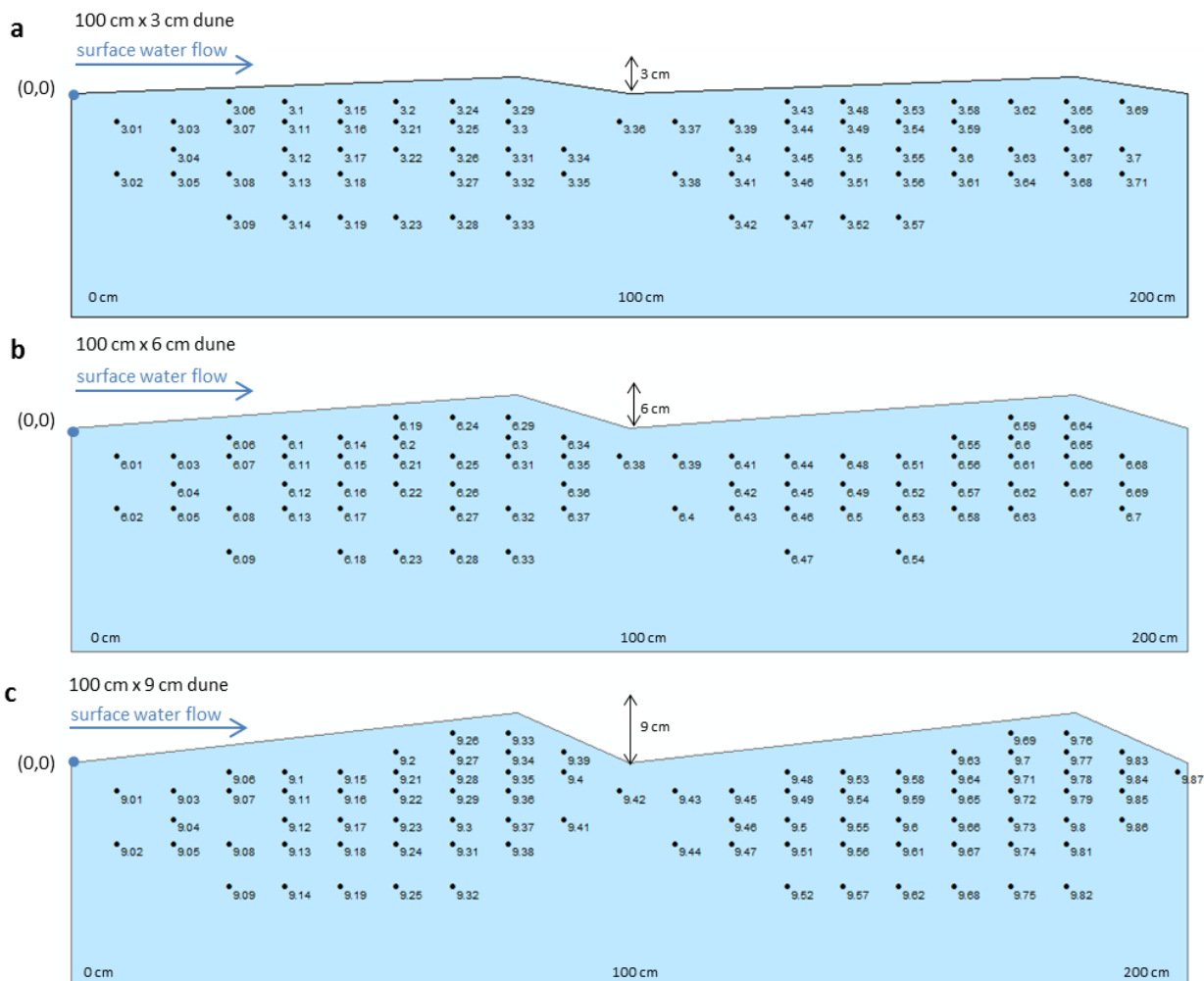
Figure B.1. **Sampling port locations for the 2013 flume experiment for the (a) 3 cm dune height, (b) 6 cm dune height, and (c) 9 cm dune height.** Colored areas represent the instrumented sand dunes. Black dots show rhizon sampling ports. Surface water flow above the dunes was from left to right. The coordinates given in the data tables are measured from the origins indicated by (0,0).
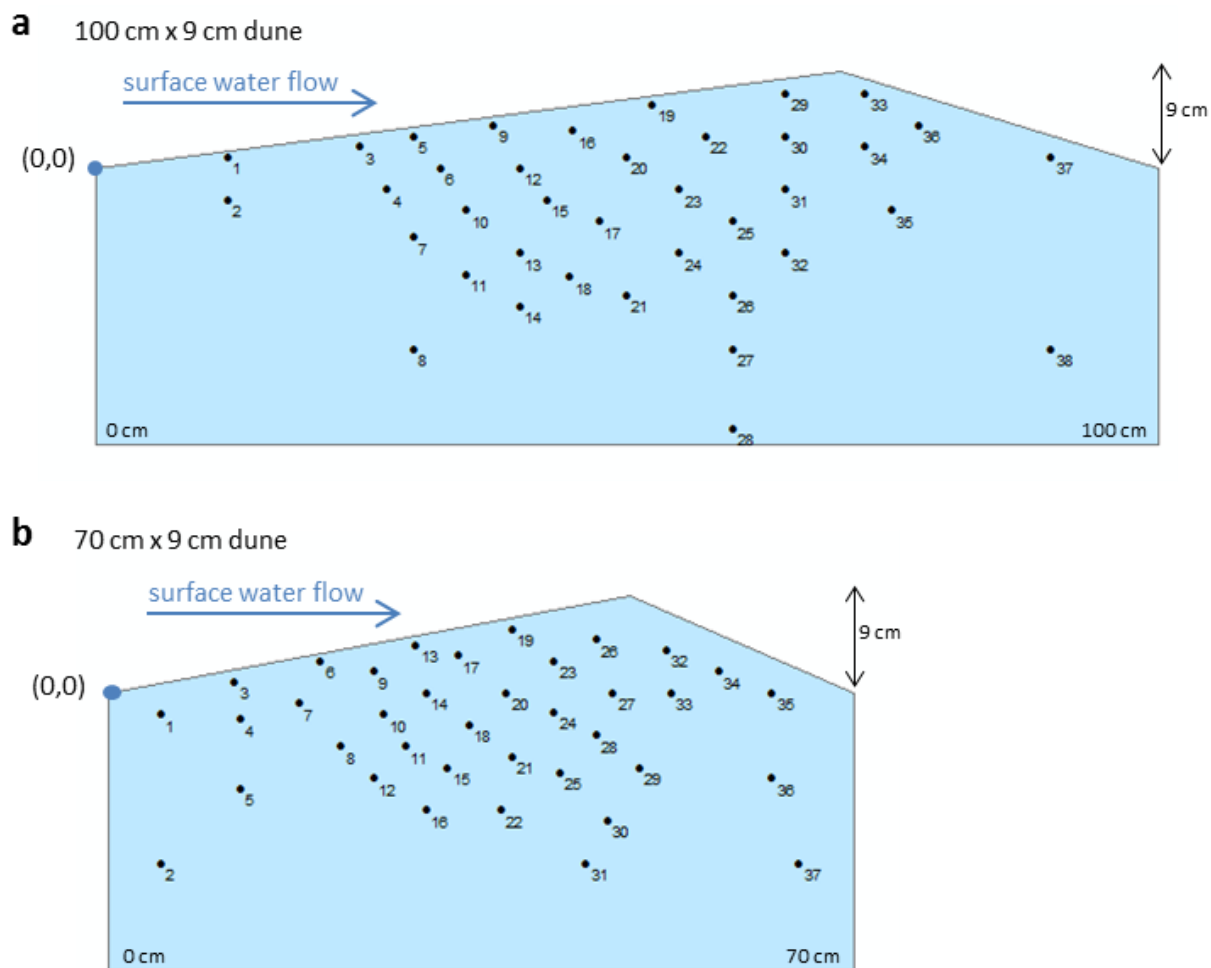
Figure B.2.   Sampling port locations for the 2015 flume experiment for the (a) 100 cm dune length, and (b) 70 cm dune length. Colored areas represent the instrumented sand dunes. Black dots show rhizon sampling ports. Surface water flow above the dunes was from left to right. The coordinates given in the data tables are measured from the origins indicated by (0,0).
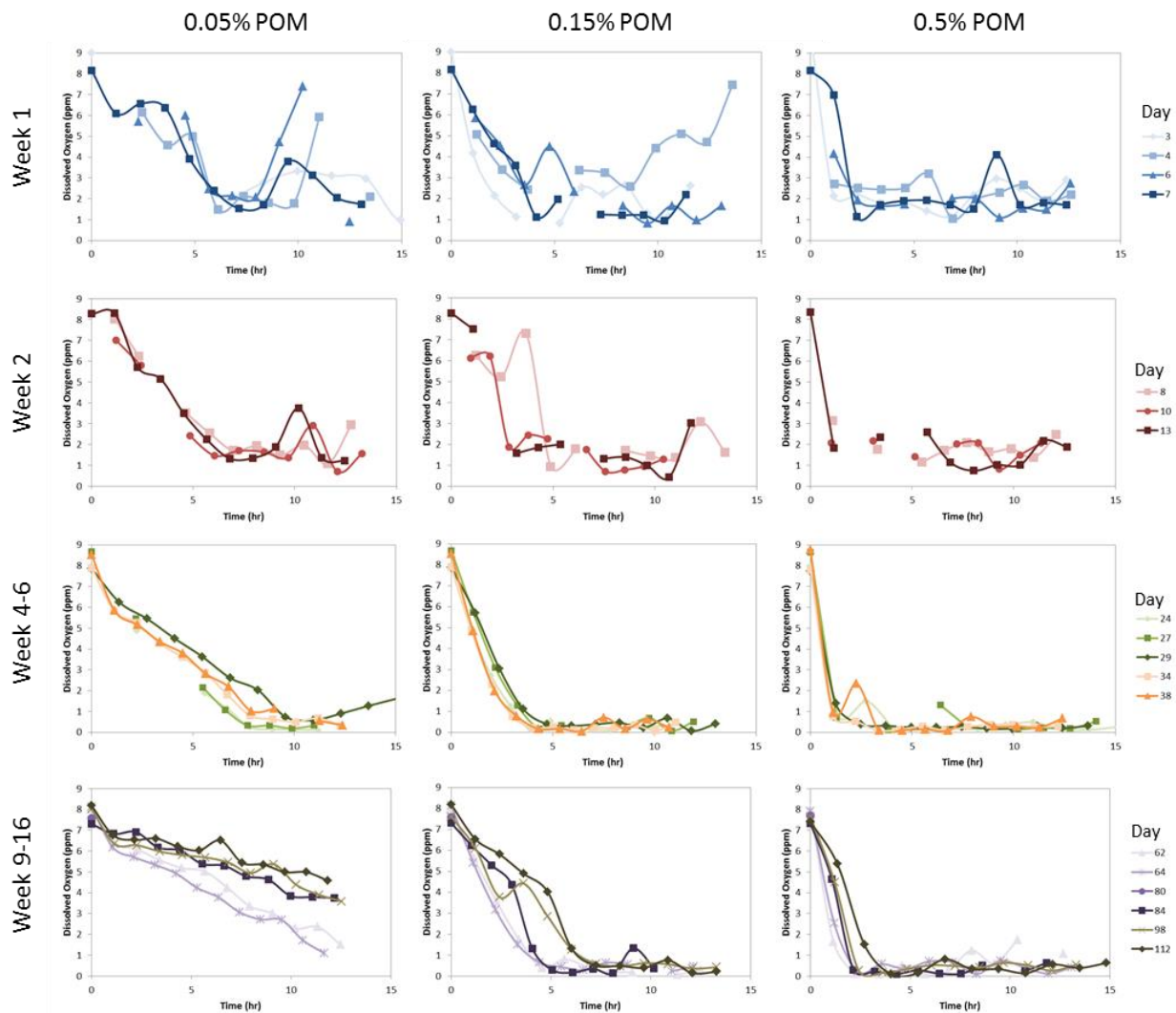
Figure B.3. **Dissolved oxygen concentrations plotted over travel time in the column experiment.** Each column of plots is for a different level of initial POM (0.05%, 0.15%, and 0.5% by dry weight). The colored lines indicate days elapsed during the experiment. Periods of time are displayed in multiple plots for the sake of clarity.
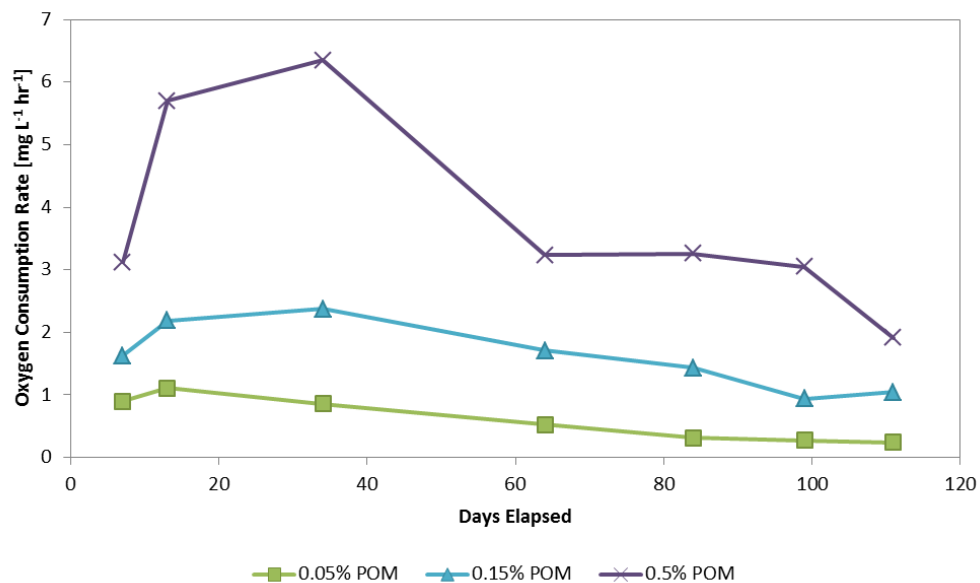
Figure B.4. **Dissolved oxygen consumption rates over time in the column experiment.** Rates were calculated from the slope of DO concentrations over travel time over the travel time interval during which DO was decreasing.
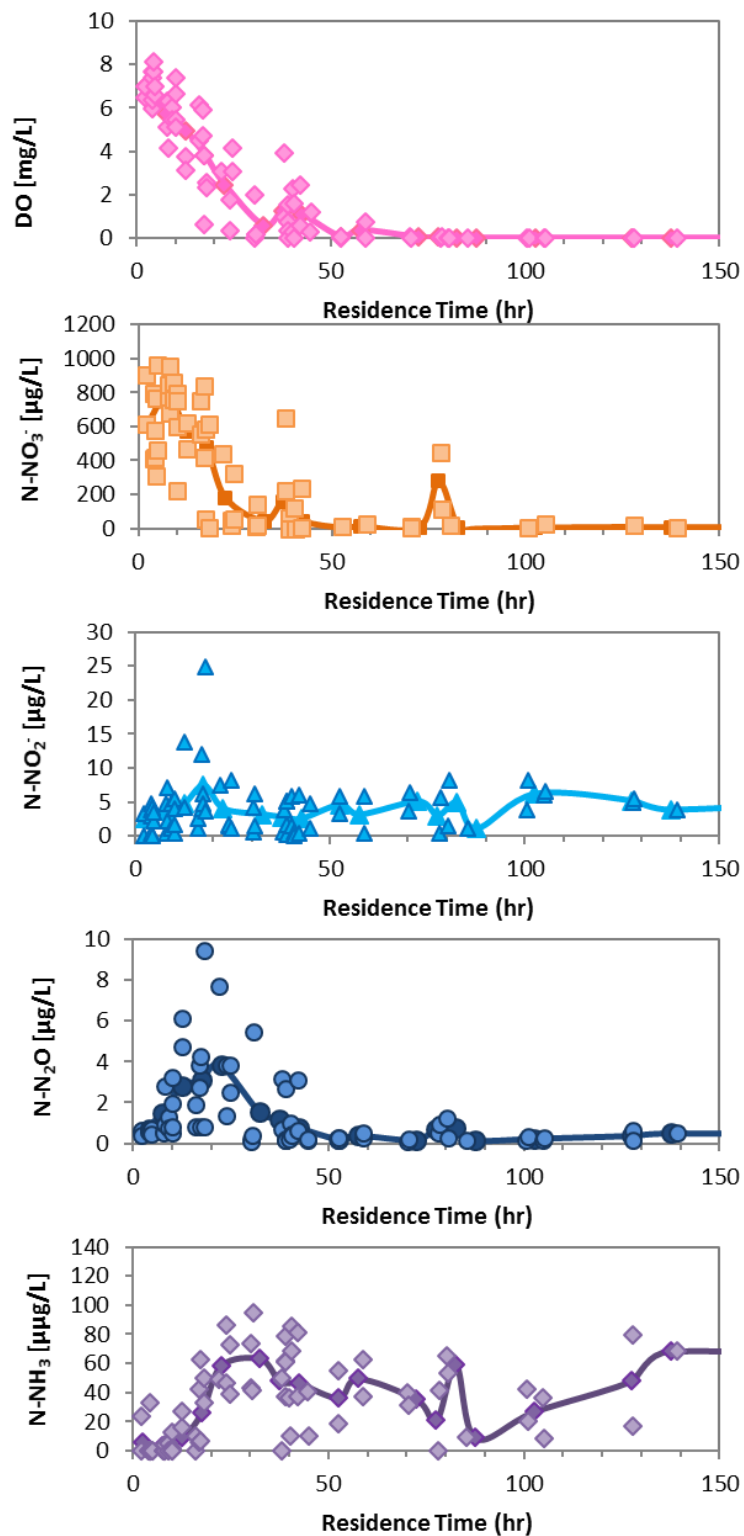
Figure B.5. **Dissolved oxygen and nitrogen concentrations with residence time in the 9 cm dune on day 112 pf F1.** The darker symbols and lines show concentrations for residence time bins.
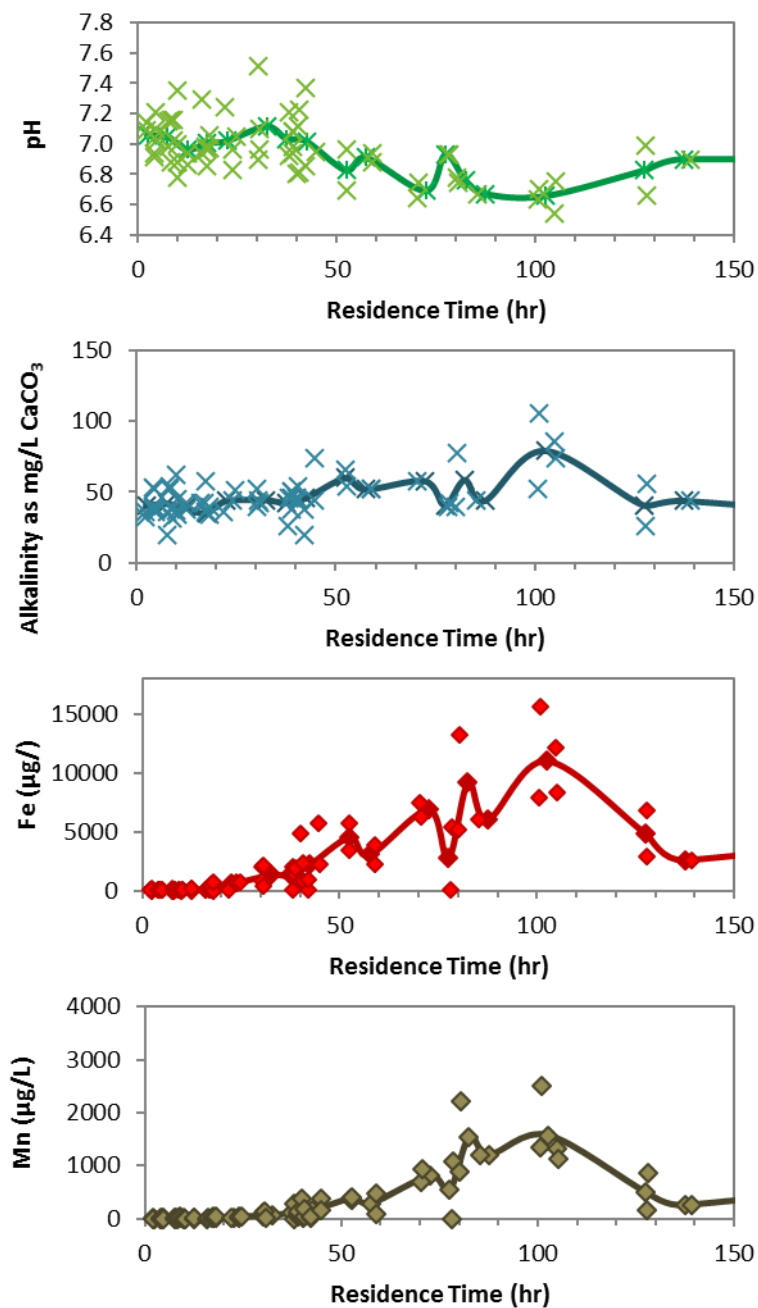
Figure B.6. **pH, alkalinity, Fe, and Mn concentrations with residence time in the 9 cm dune on day 112 pf F1.** The darker symbols and lines show concentrations for residence time bins.
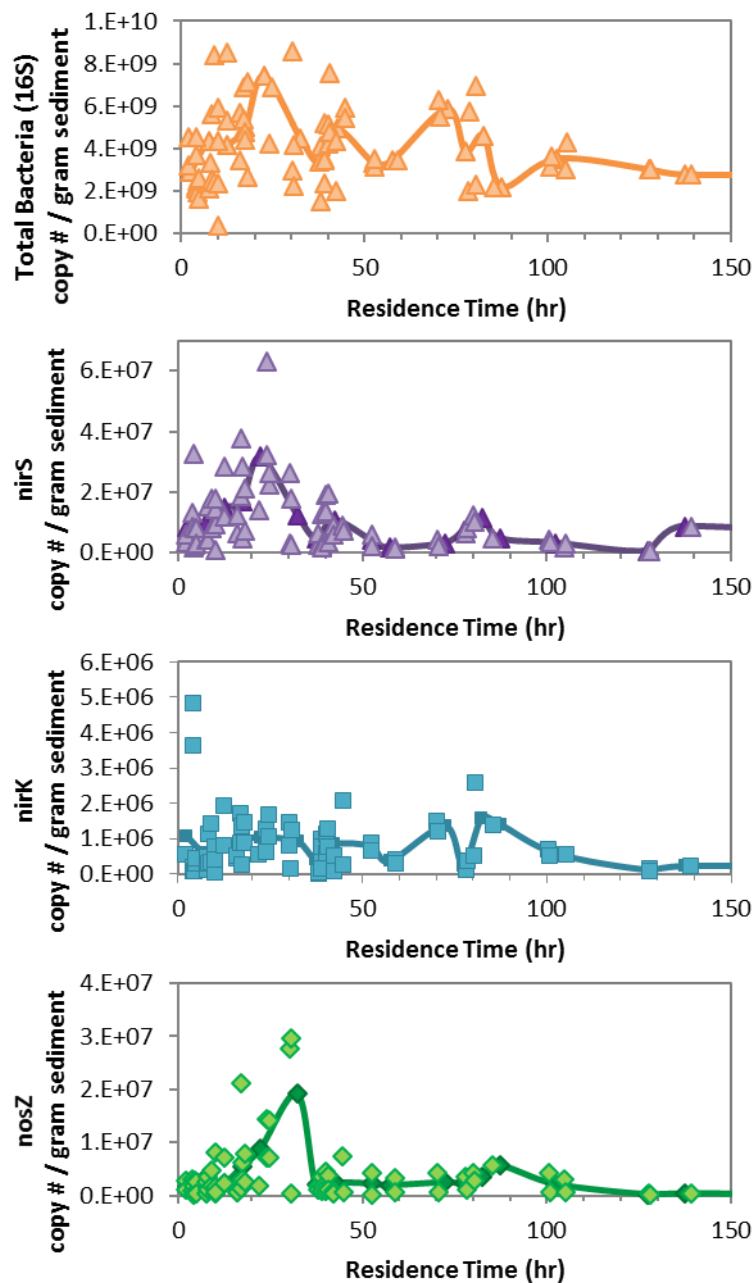
Figure B.7. **Total bacteria and gene abundances with residence time in the 9 cm dune on day 112 pf F1.** The darker symbols and lines show concentrations for residence time bins.

B.5 References

Alter, M. D., and M. Steiof (2005), Optimized method for dissolved hydrogen sampling in groundwater, *J. Contam. Hydrol.*, *78*(1–2), 71–86, doi:10.1016/j.jconhyd.2005.03.002.

Appelo, C. A. J., and D. Postma (2005), *Geochemistry, Groundwater and Pollution*, 2nd ed., A.A. Balkema Publishers, Leiden, The Netherlands.

Fehlman, H. M. (1985), Resistance component and velocity distributions of open channel flows over bedforms, Colorado State University.

Jurjovec, J., D. W. Blowes, C. J. Ptacek, and K. U. Mayer (2004), Multicomponent reactive transport modeling of acid neutralization reactions in mine tailings, *Water Resour. Res.*, *40*(11), 1–17, doi:10.1029/2003WR002233.

Kandeler, E., K. Deiglmayr, D. Tscherko, D. Bru, and L. Philippot (2006), Abundance of narG, nirS, nirK, and nosZ genes of denitrifying bacteria during primary successions of a glacier foreland, *Appl. Environ. Microbiol.*, *72*(9), 5957–5962, doi:10.1128/AEM.00439-06.

Marzadri, A., D. Tonina, A. Bellin, G. Vignoli, and M. Tubino (2010), Semianalytical analysis of hyporheic flow induced by alternate bars, *Water Resour. Res.*, *46*(W07531), 1–14, doi:10.1029/2009WR008285.

Mayer, K. U., E. O. Frind, and D. W. Blowes (2002), Multicomponent reactive transport modeling in variably saturated porous media using a generalized formulation for kinetically controlled reactions, *Water Resour. Res.*, *38*(9), 1174, doi:10.1029/2001WR000862.

Stelzer, R. S., L. A. Bartsch, W. B. Richardson, and E. A. Strauss (2011), The dark side of the hyporheic zone: depth profiles of nitrogen and its processing in stream sediments, *Freshw. Biol.*, *56*(10), 2021–2033, doi:10.1111/j.1365-2427.2011.02632.x.

Stumm, W., and J. J. Morgan (1996), *Aquatic Chemistry: Chemical Equilibria and Rates in Natural Waters*, 3rd ed., John Wiley & Sons, Inc., New York.

APPENDIX C

Supporting Information for Chapter Four

C.1 Rhizon Locations

Locations of the rhizon sampling locations for F1 and F2 are shown in Figures C.1 and C.2. The circled rhizon locations were excluded from the plots in Chapter 3 and Appendix C. Rhizons along ground water flow paths were excluded, as were those in areas of the hyporheic zone where recirculation effects prevented high-confidence residence time calculations. A few locations were included due to missing or anomalous residence times.
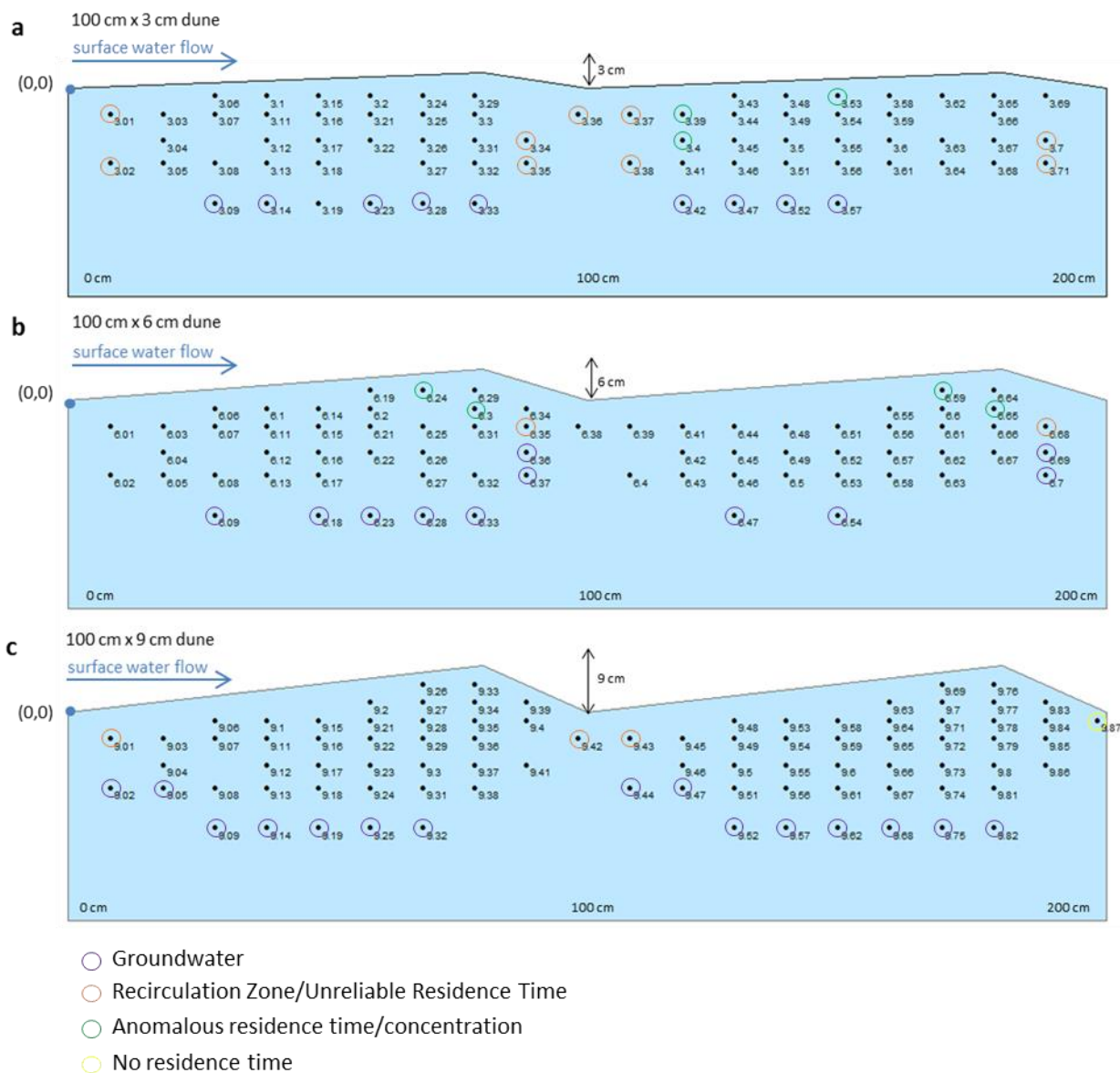
Figure C.1.   Sampling port locations for F1. Panels A, B, and C show the rhizon locations in the 3 cm, 6 cm, and 9 cm dunes, respectively, in F1.
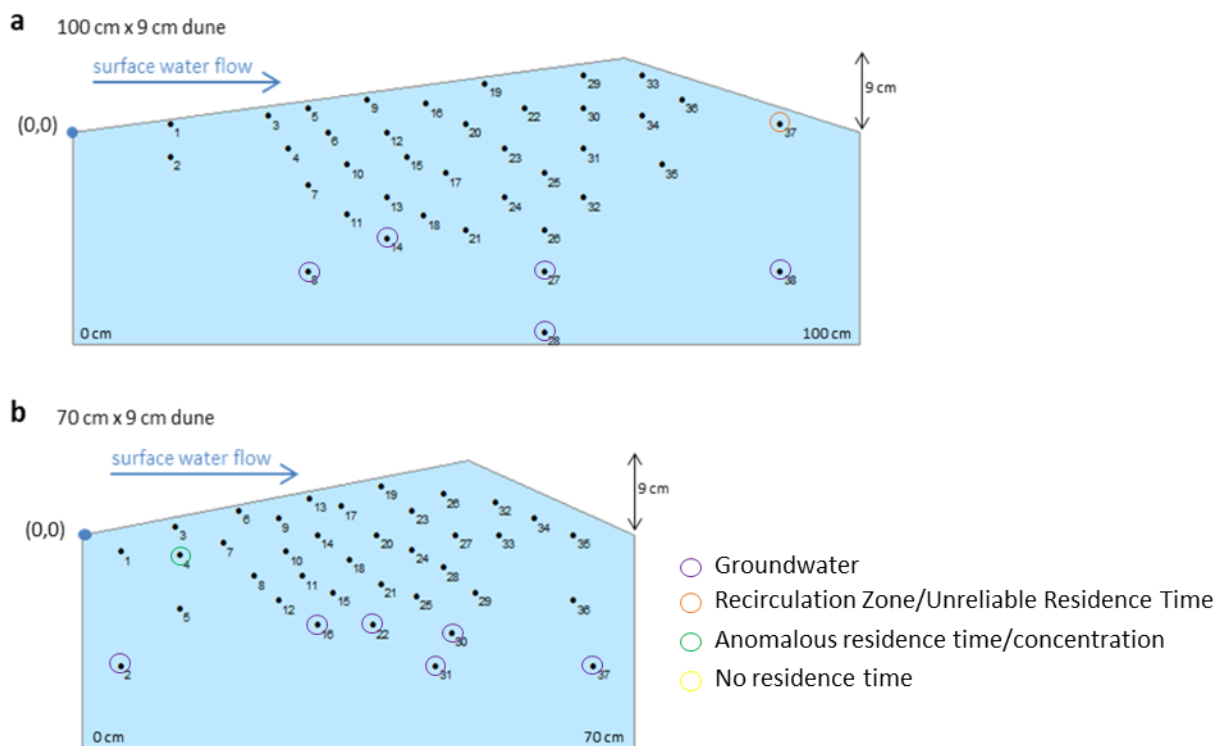
Figure C.2. **Sampling port locations for F2.** Panels A and B show the rhizon locations in the 100 cm and 70 cm dunes, respectively, in F2.

C.2 Dissolved Oxygen over Elapsed Time
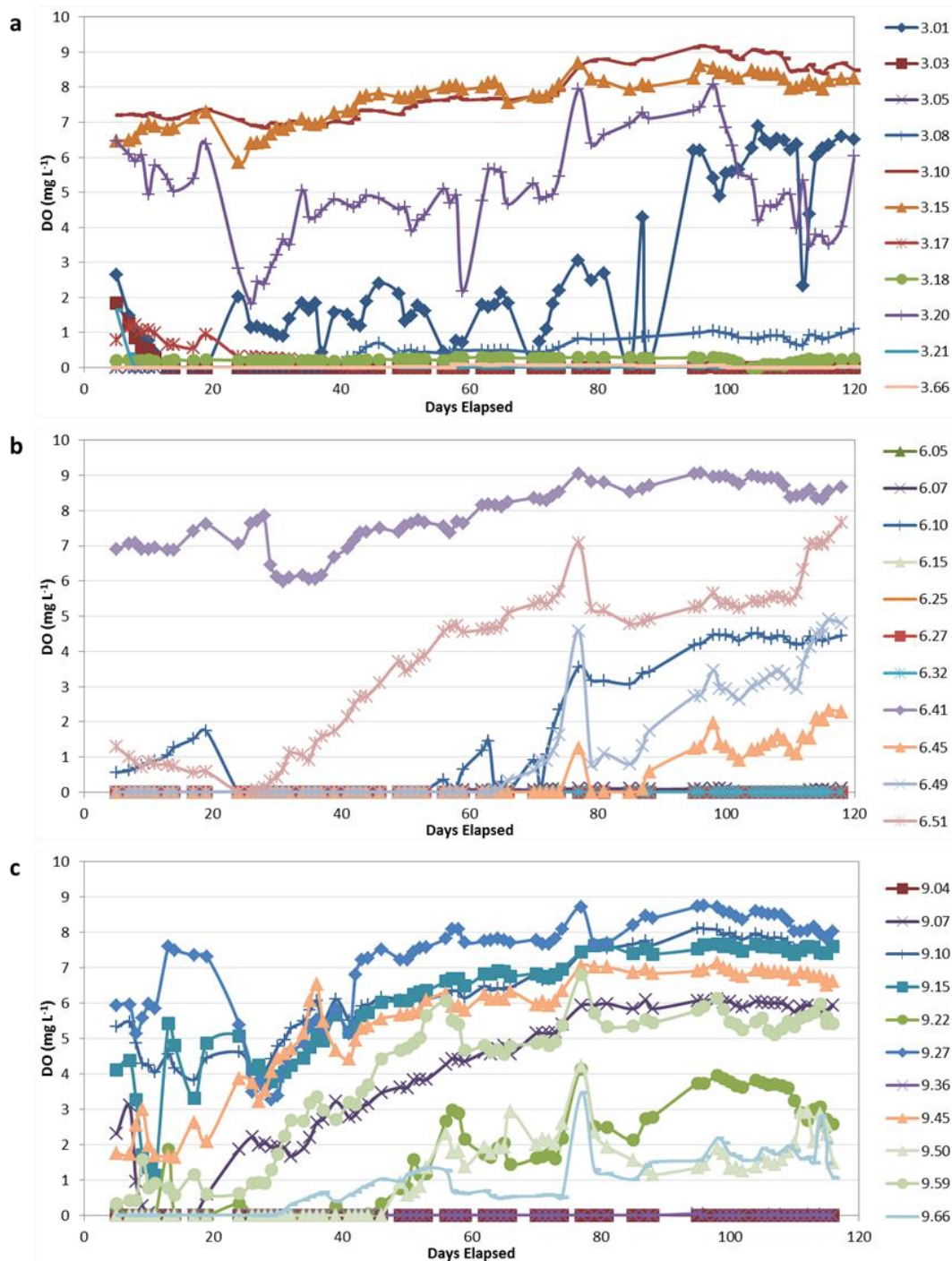
Figure C.3. **Dissolved oxygen concentrations over time in F1.** Measurements are from the PreSens instrument at selected subsurface rhizon locations in the 3 cm dunes (A), 6 cm dunes (B), and 9 cm dunes (C). Individual lines correspond to sampling locations in Figure C.1. Note that a pump failure around day 20-12 caused systems to shift temporarily towards anaerobic conditions.
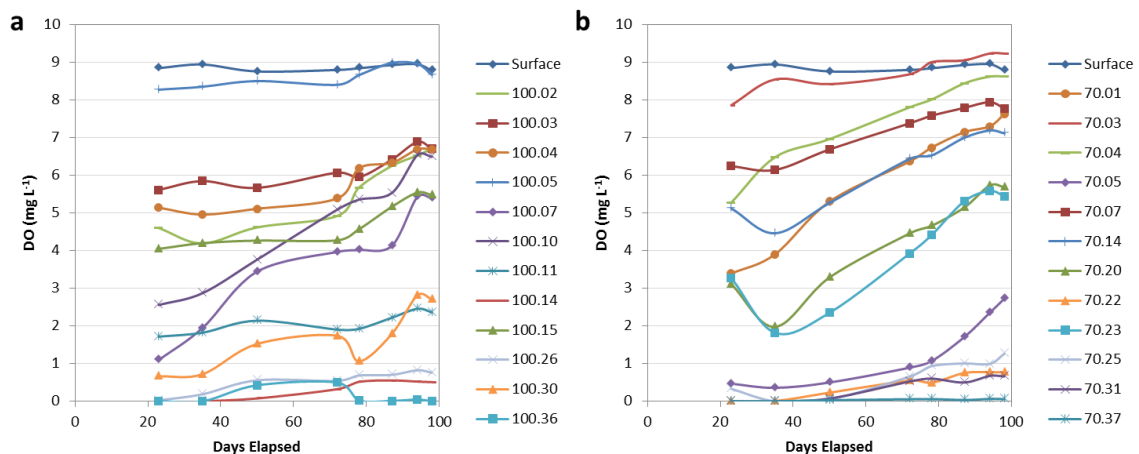
Figure C.4. **Dissolved oxygen concentrations over time in F2.** Measurements are from the surface water and selected subsurface locations in the 100 cm dunes (average of three replicates (A) and in the 70 cm dunes (average of three replicates) (B). See Figure C.2 for sampling locations.

C.3 pH and Dissolved Oxygen in F2
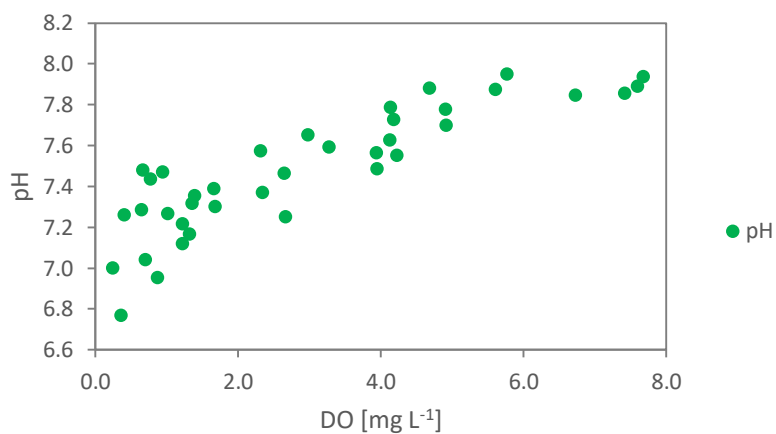
Figure C.5. **pH versus dissolved oxygen.** Measurements are from the 100 cm dune on day 91 of F2.

C.4 Concentrations of Individual Species

Concentrations of species in the hyporheic zone were measured across two experiments, at multiple surface and subsurface locations, and at multiple time points. These data can be presented in different ways to focus on spatial trends (with residence time), temporal trends (over elapsed time), and between dunes with different morphologies. In this section of the appendix, two pages of plots are presented for each measured species, with four different types of plots. The first page (A and B) shows bubble plots for each dune on three sampling days (top of the page) and box plots of species concentrations distributions over time (bottom of page). The second page (C and D) for each species shows hyporheic concentrations versus residence time (left side of page) and over elapsed time at selected hyporheic locations (right side of page). Explanations of the four types of plots are below:

A. **Bubble Plots for F1 (Days 49, 98, 112) and F2 (Days 41, 70, 91).** For F1, bubbles show the average of two consecutive dunes. For F1, bubbles show average of three replicate dunes across channels. Surface water flow is from left to right. The bubbles about the dune outline show surface water concentrations. Notice the different scales between F1 and F2. Within each experiment, the scales are the same across days for each species.

B. **Box Plots of species concentration distributions over time.** For each dune, the distribution of concentrations is shown over days elapsed during each experiment. Mean concentrations are shown by the diamond-shaped symbols. Note the difference in scales between F1 (3 cm, 6 cm, and 9 cm dunes) and F2 (100 cm and 70 cm dunes).

C. **Concentrations versus residence time.** Concentrations of chemical species [$\mu g\ L^{-1}$ unless otherwise specified] at locations in the hyporheic zone (and some groundwater locations) are plotted versus residence time for Flume 1 (top) and Flume 2 (bottom). Concentrations are distinguished based on dune

size (3 cm, 6 cm, 9 cm in Flume 1, 70 cm and 100 cm in Flume 2) and day of the experiment (days 49 and 112 in Flume 1, days 41 and 91 in Flume 2). For Flume 2, the values shown are the average of three replicates.

D. Hyporheic concentrations over elapsed time at selected locations.

Concentrations of chemical species [μg L^{-1}] measured at selected rhizons are plotted on sampling days over the duration of the experiments. For Flume 1, measurements for the 3 cm, 6 cm, and 9 cm dunes are shown in subpanels A, B, and C, respectively. For Flume 2, measurements for the 70 cm and 100 cm dunes are shown in subpanels D and E, respectively. Rhizon locations are shown in Figures C.1 and C.2. Shallower rhizon locations are represented with lighter symbols, deeper rhizon locations with darker symbols. The bright red lines show surface water concentrations.

The following species are presented (with figure numbers):

C.6 Dissolved Oxygen
C.7 pH
C.8 Alkalinity
C.9 Ammonia (N-NH$_3$)
C.10 Nitrate (N-NO$_3^-$)
C.11 Nitrite (N-NO$_2^-$)
C.12 Nitrous oxide (N-N$_2$O)
C.13 Lithium (^{7}Li)
C.14 Sodium (^{23}Na)
C.15 Magnesium (^{24}Mg)
C.16 Aluminum (^{27}Al)
C.17 Silicon (^{29}Si)
C.18 Phosphorous (^{31}P)
C.19 Potassium (^{39}K)

C.20 Calcium (^{43}Ca)
C.21 Vanadium (^{51}V)
C.22 Manganese (^{55}Mn)
C.23 Iron (^{57}Fe)
C.24 Cobalt (^{59}Co)
C.25 Nickel (^{60}Ni)
C.26 Copper (^{65}Cu)
C.27 Zinc (^{66}Zn)
C.28 Arsenic (^{75}As)
C.29 Strontium (^{88}Sr)
C.30 Barium (^{135}Ba)
C.31 Lead (^{206}Pb)
C.32 Uranium (^{238}U)

The following anions are presented for day 92, Flume 2 (in Figures C.33 and C.34):

Chloride (Cl$^-$)
Fluoride (F$^-$)
Bromide (Br$^-$)

Sulfate (SO$_4^{2-}$)
Phosphate-P (P-PO$_4^{3-}$)
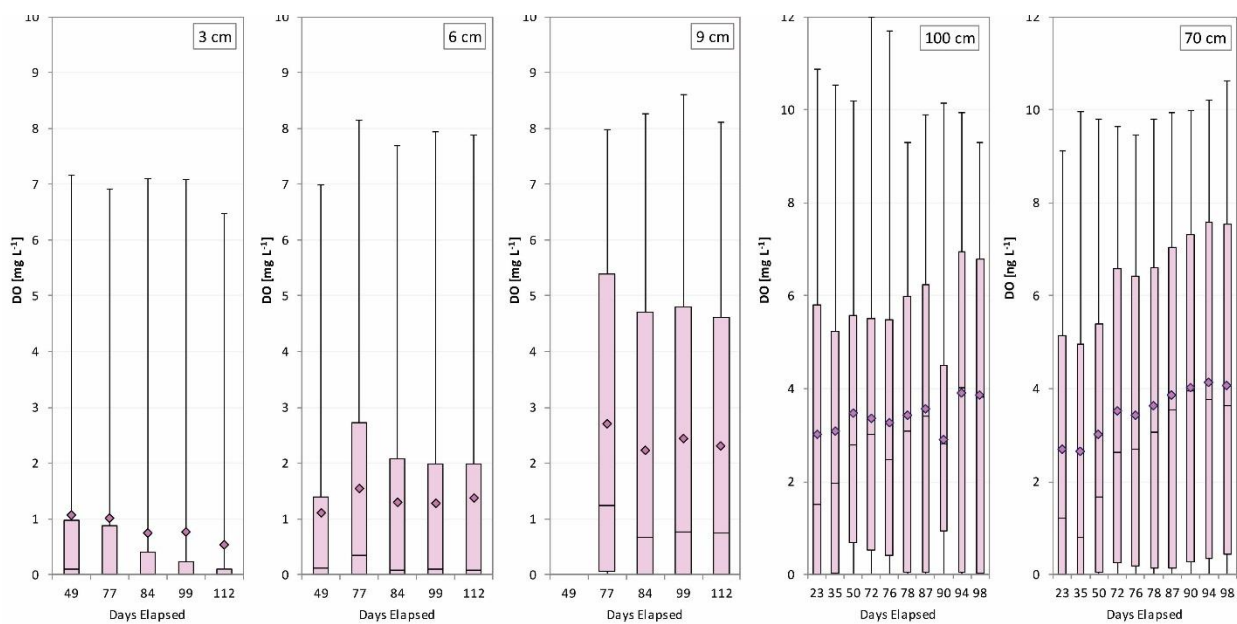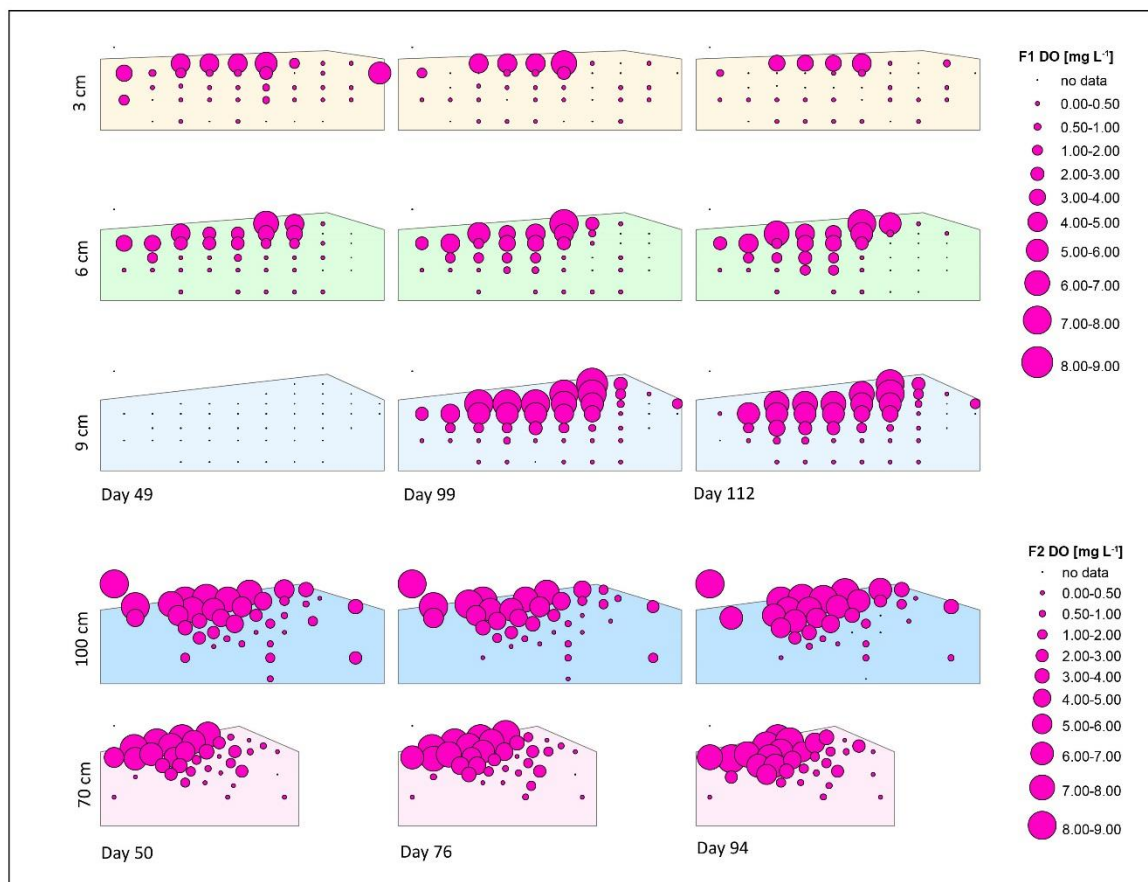
Figure C.6. Dissolved oxygen concentrations. (Top) Concentrations at rhizon locations; (Bottom) concentrations over elapsed time.
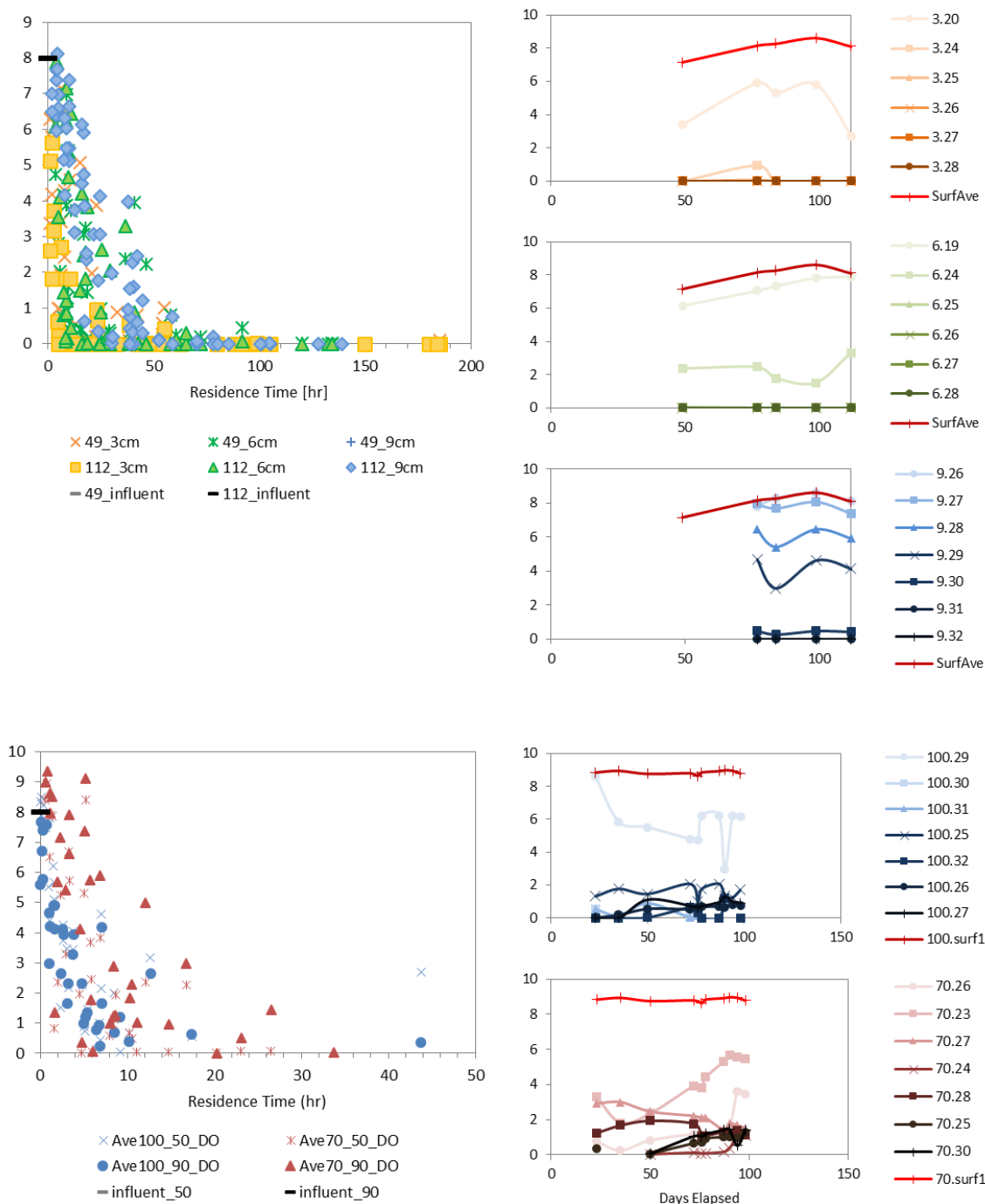
Figure C.6. (cont.)   Dissolved oxygen concentrations. (Left) concentrations versus residence time on days 49 and 112 (F1) and days 50 and 90 (F2); (Right) concentrations over elapsed time at selected locations. All concentrations are [mg L^{-1}].
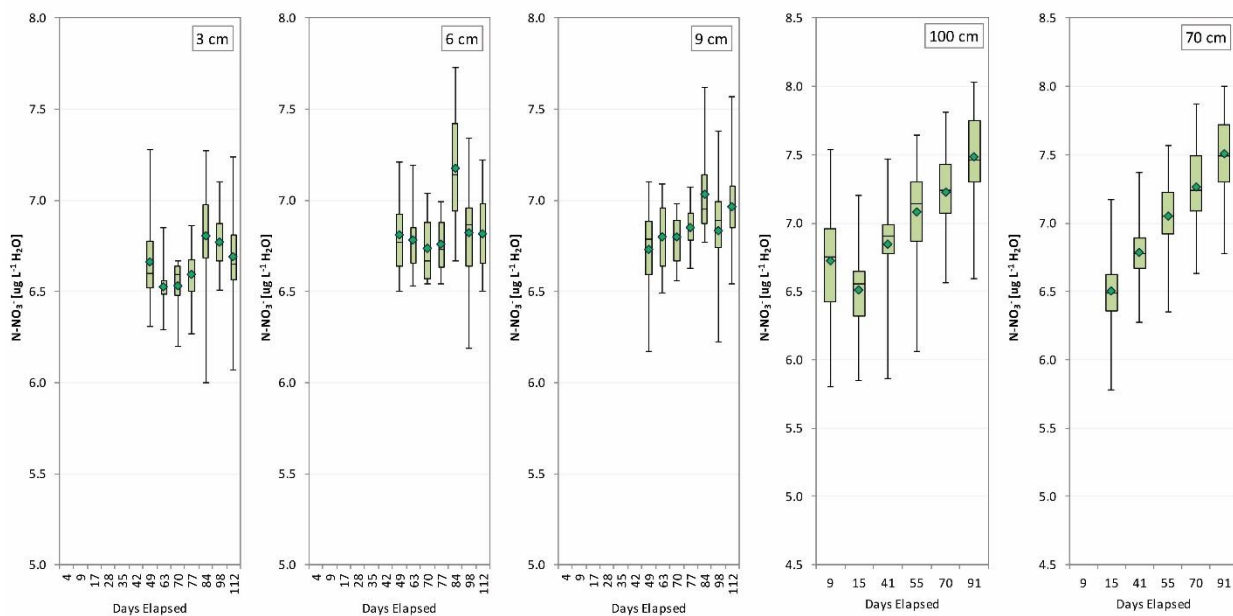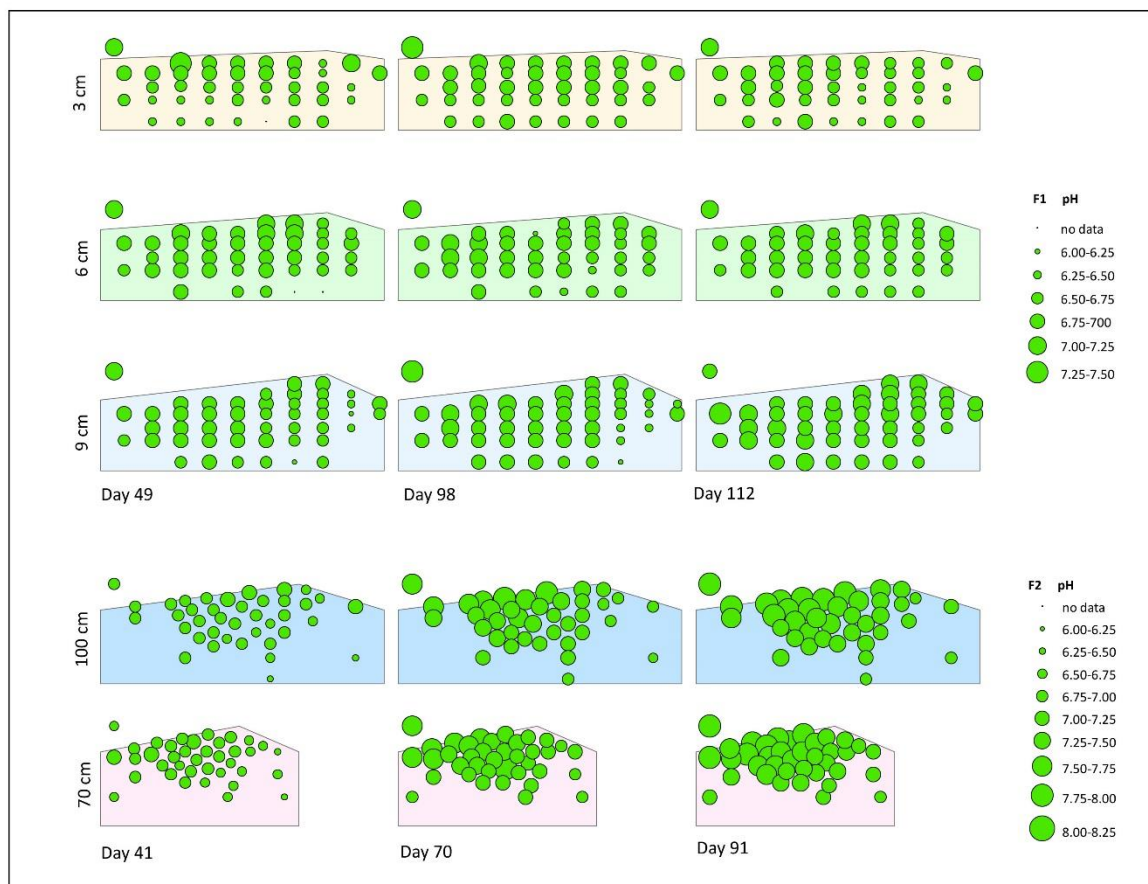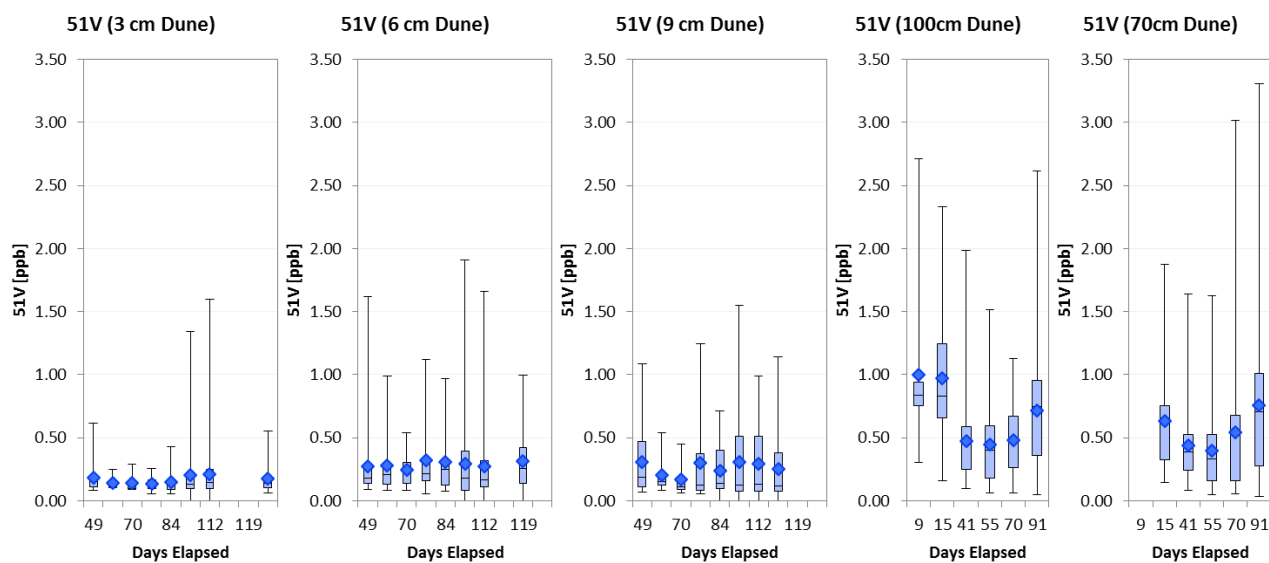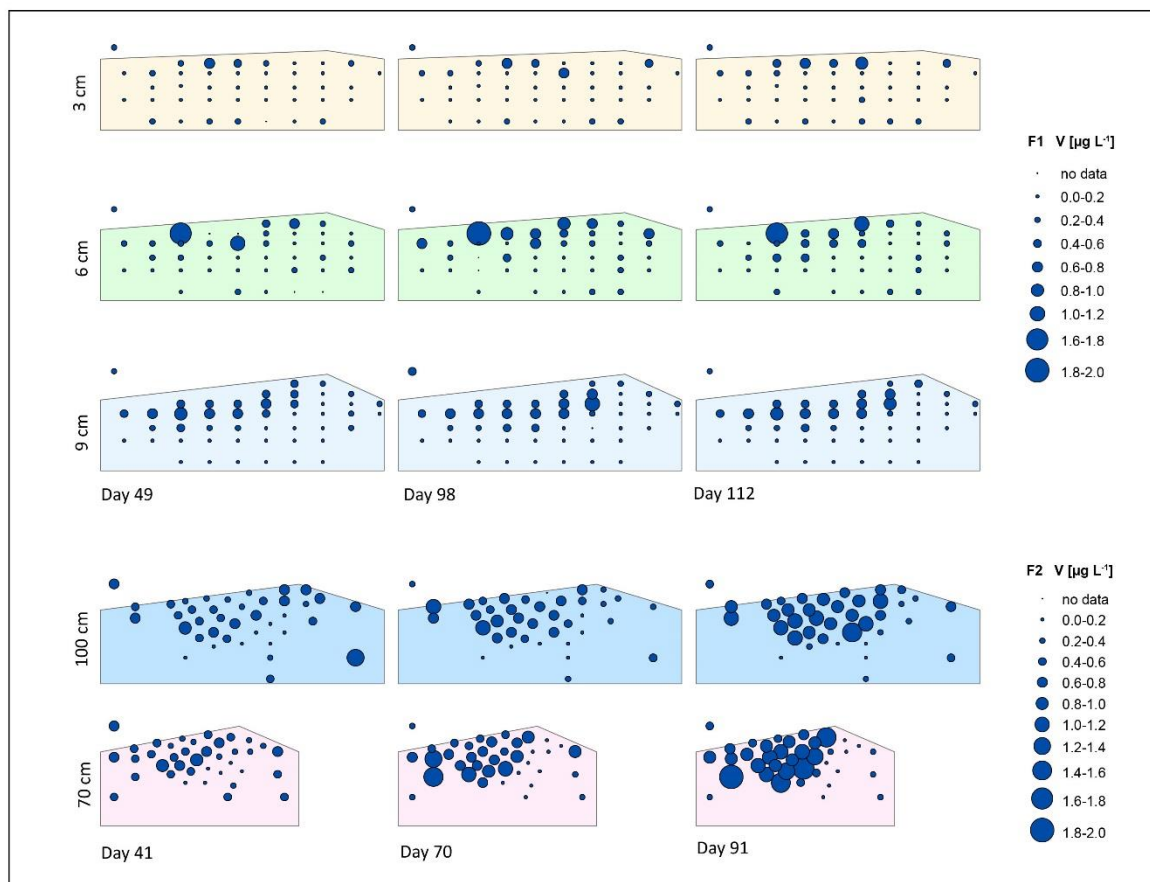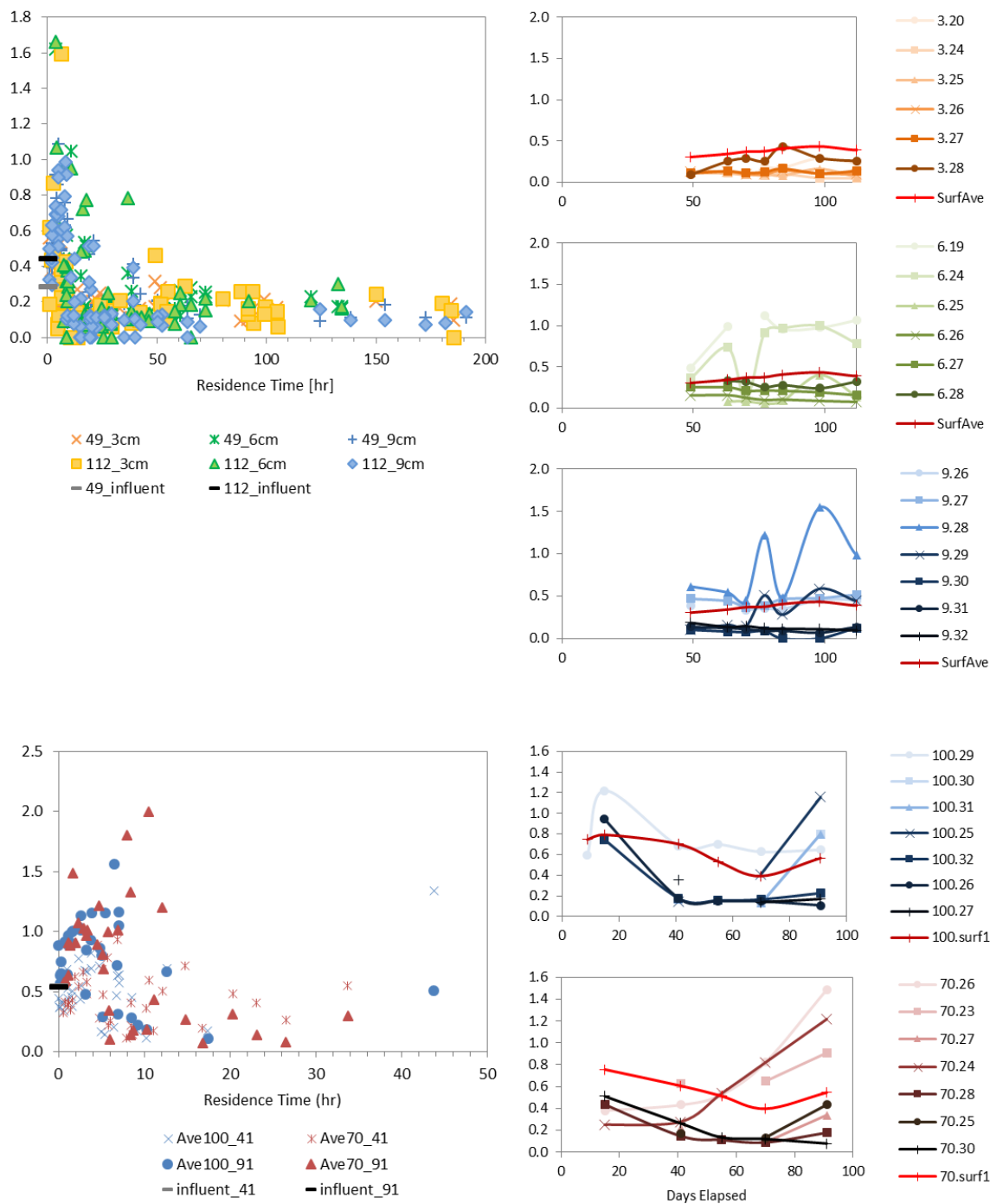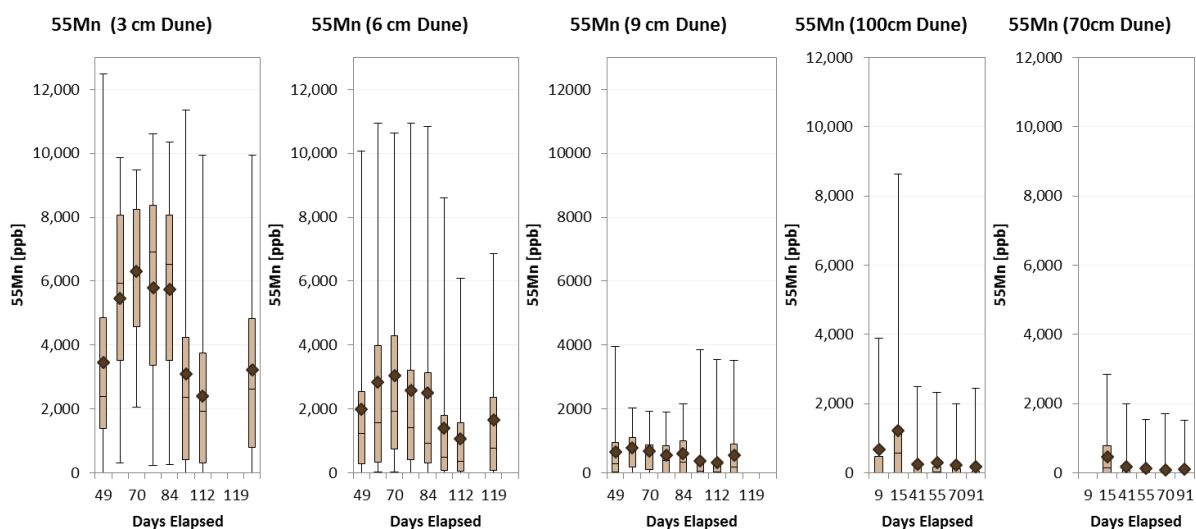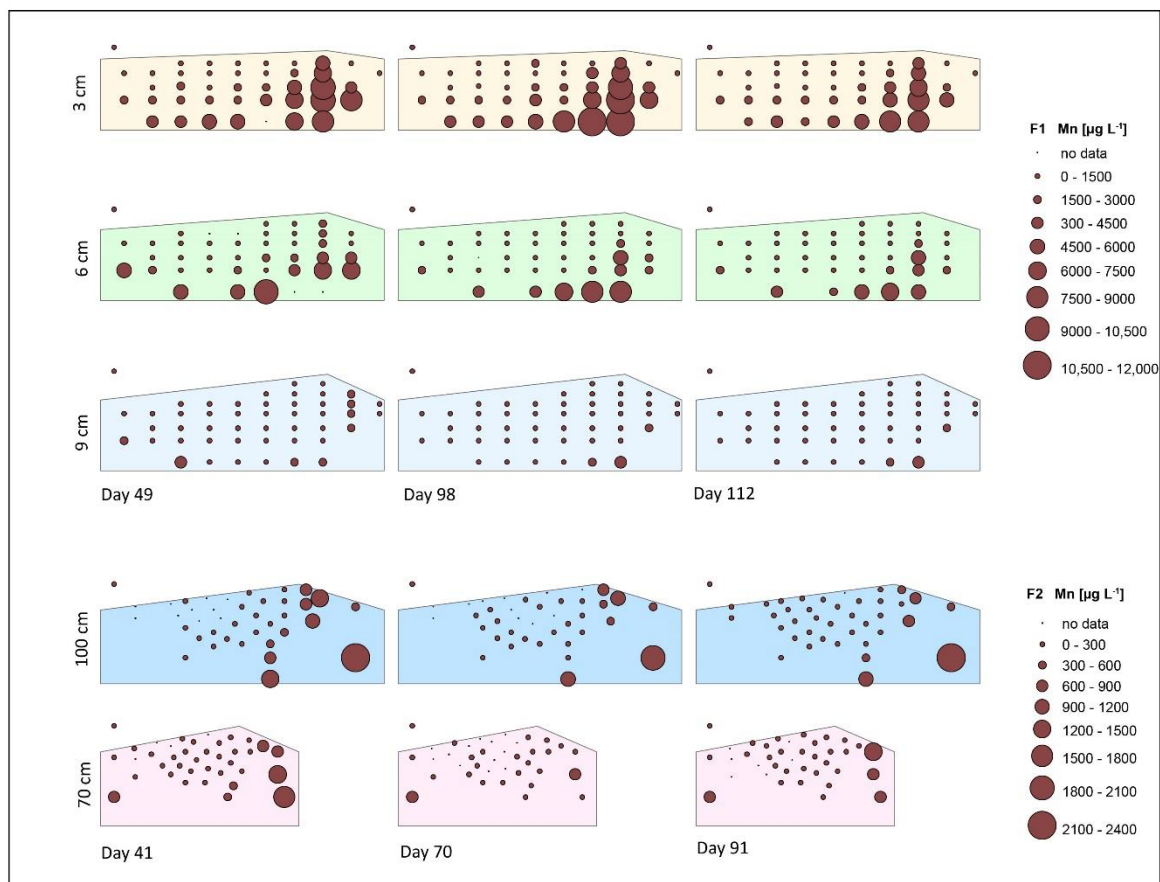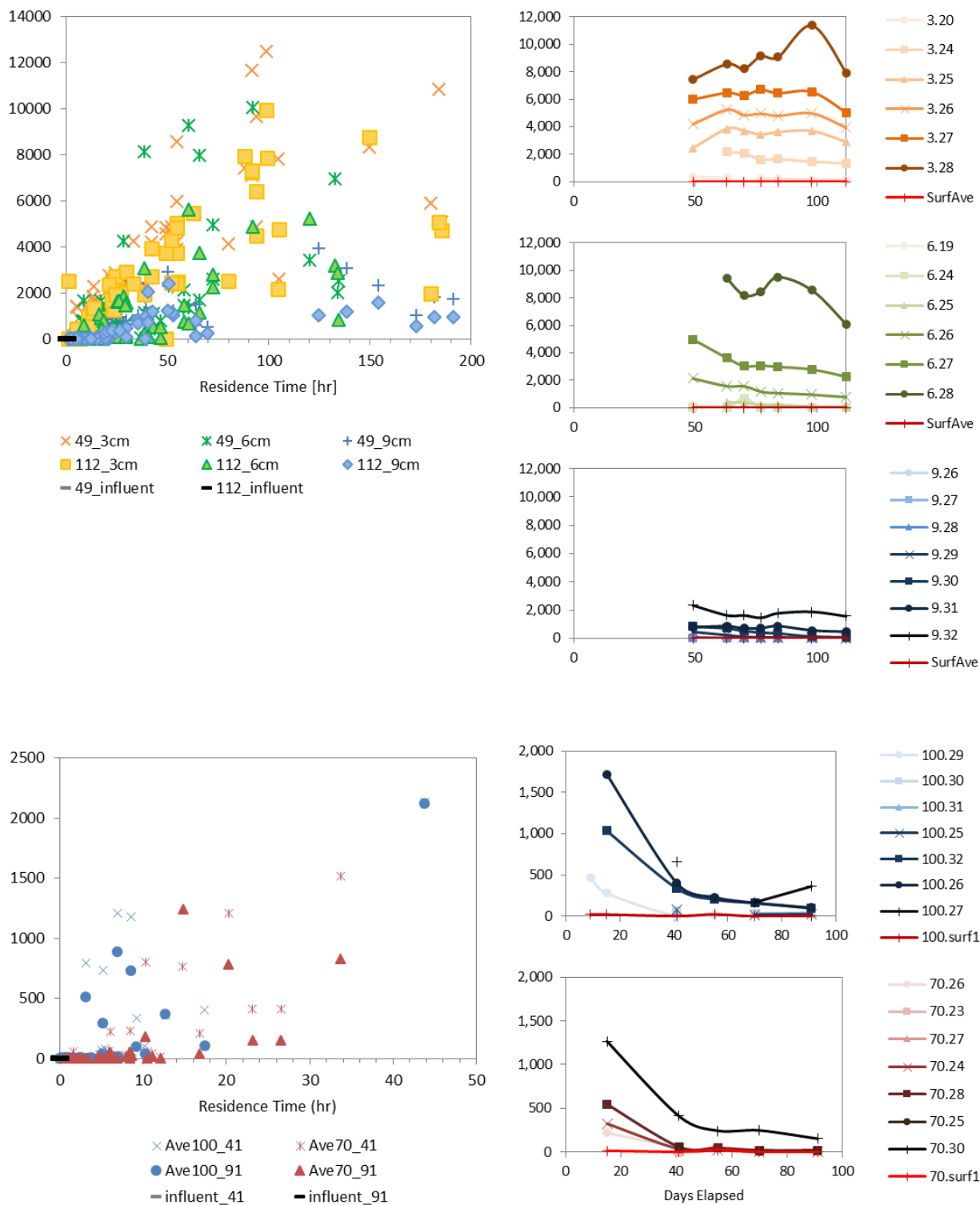
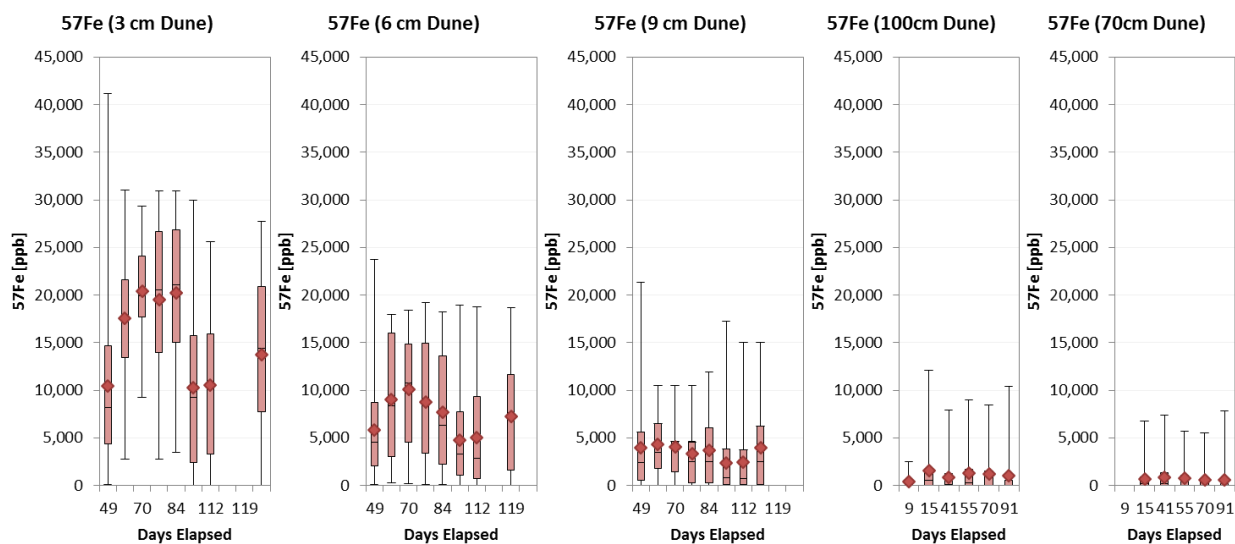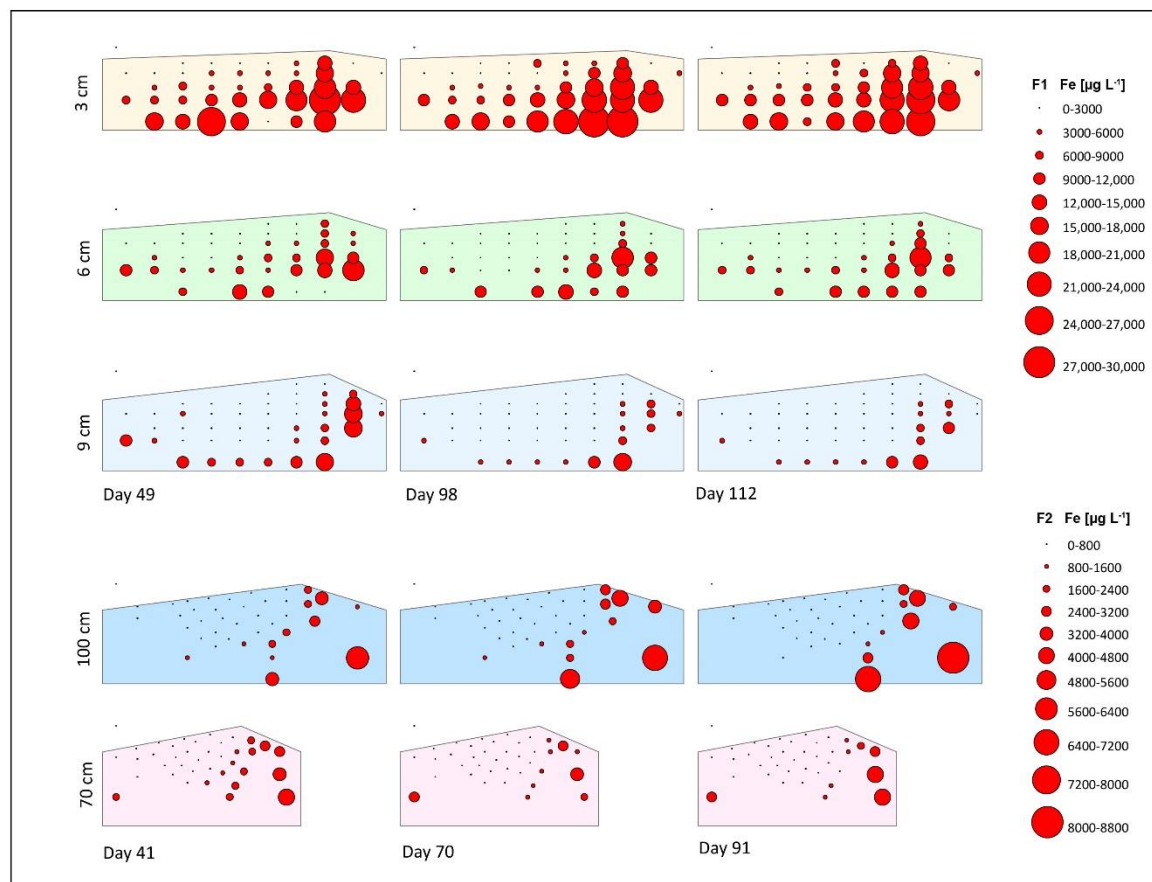**Figure C.7. pH.** (Top) pH at rhizon locations; (Bottom) pH over elapsed time.
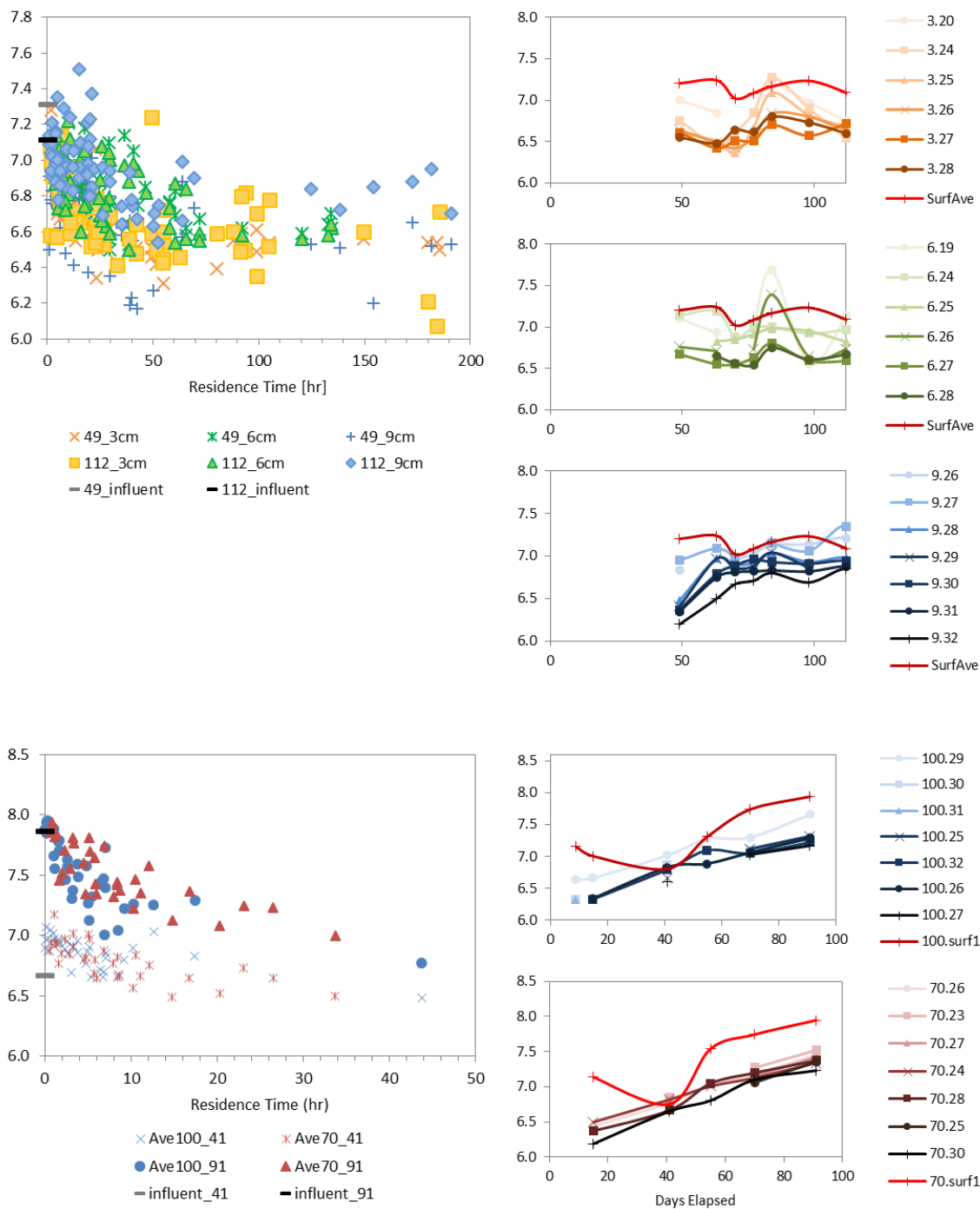
Figure C.7. (cont.) **pH.** (Left) pH versus residence time on days 49 and 112 (F1) and days 41 and 91 (F2); (Right) pH over elapsed time at selected locations.
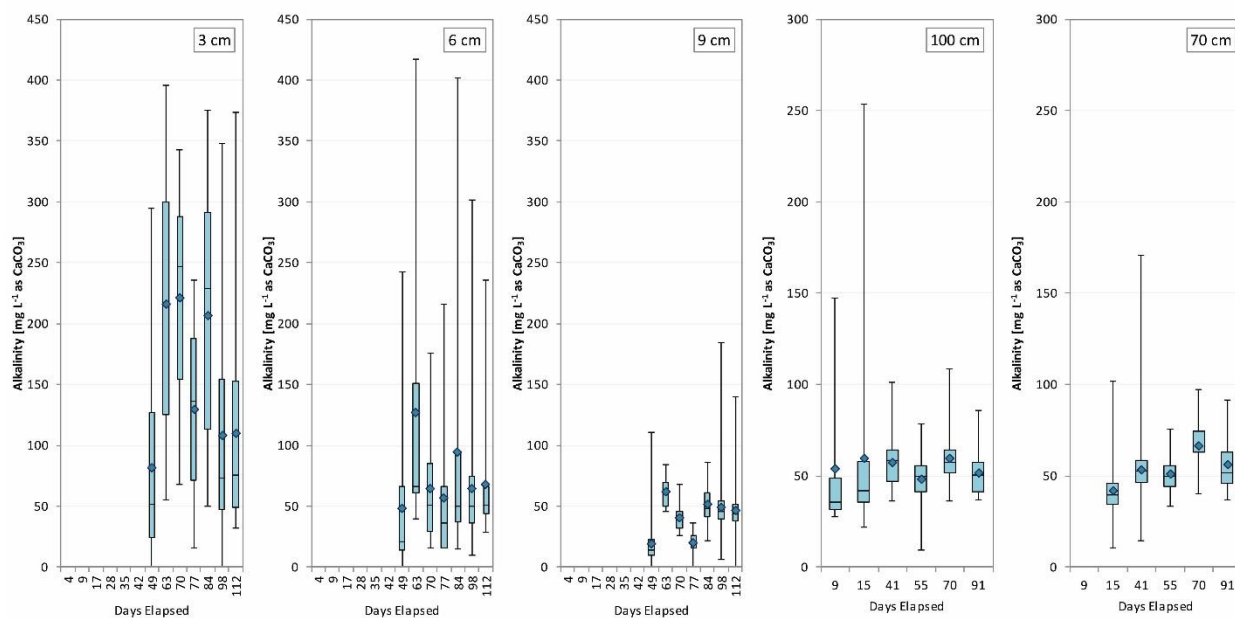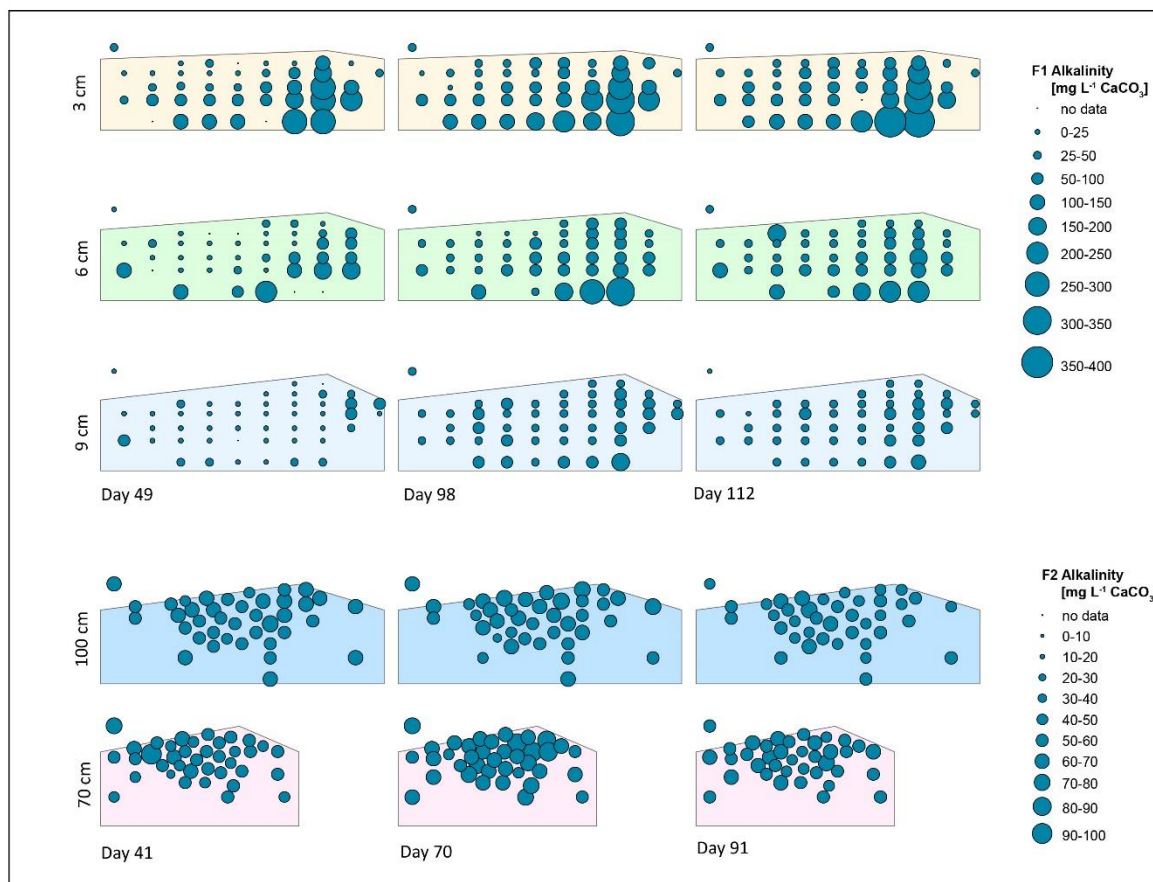
Figure C.8. Alkalinity. (Top) Concentrations at rhizon locations; (Bottom) concentrations over elapsed time. All concentrations are [µg L^{-1}].
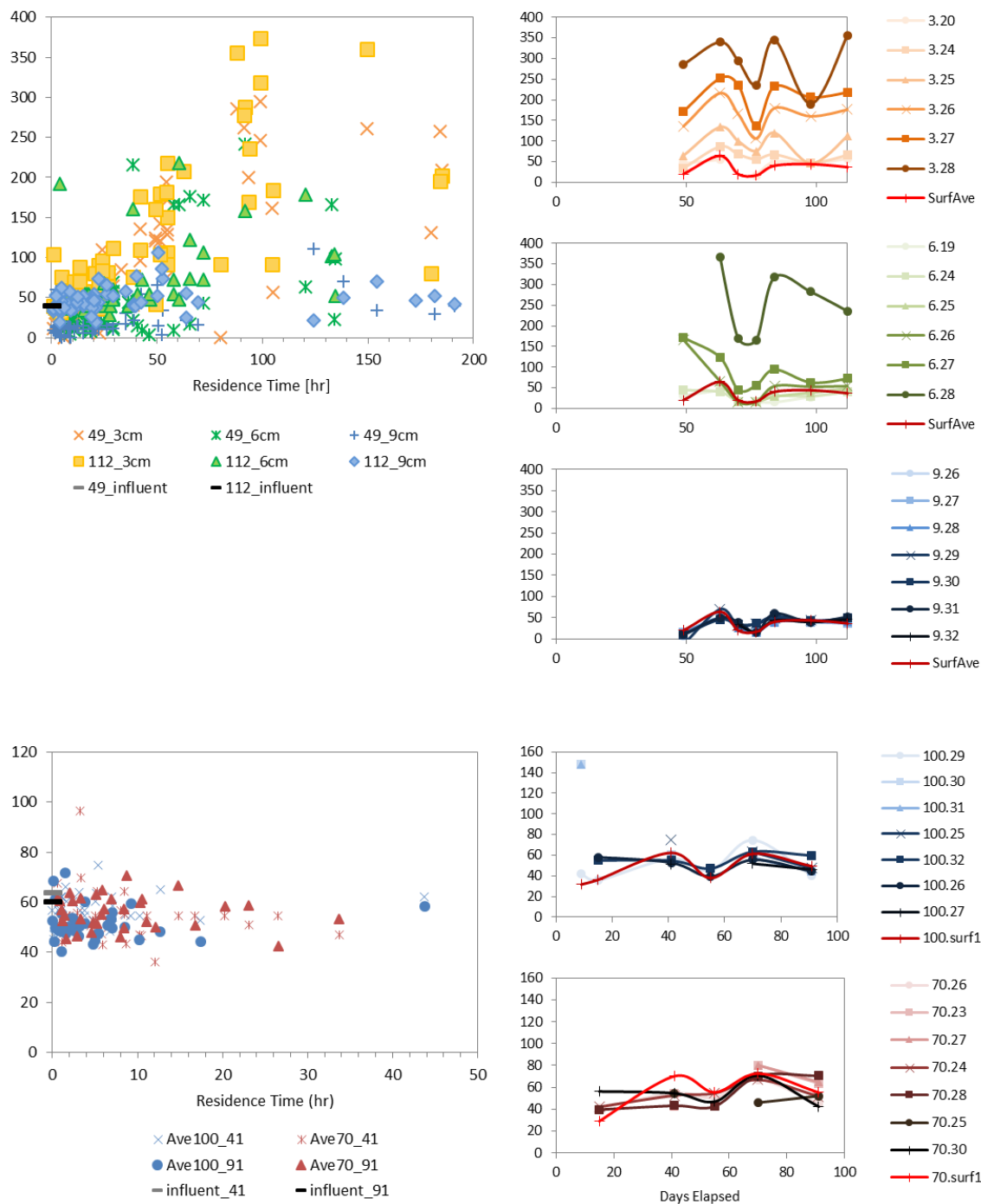
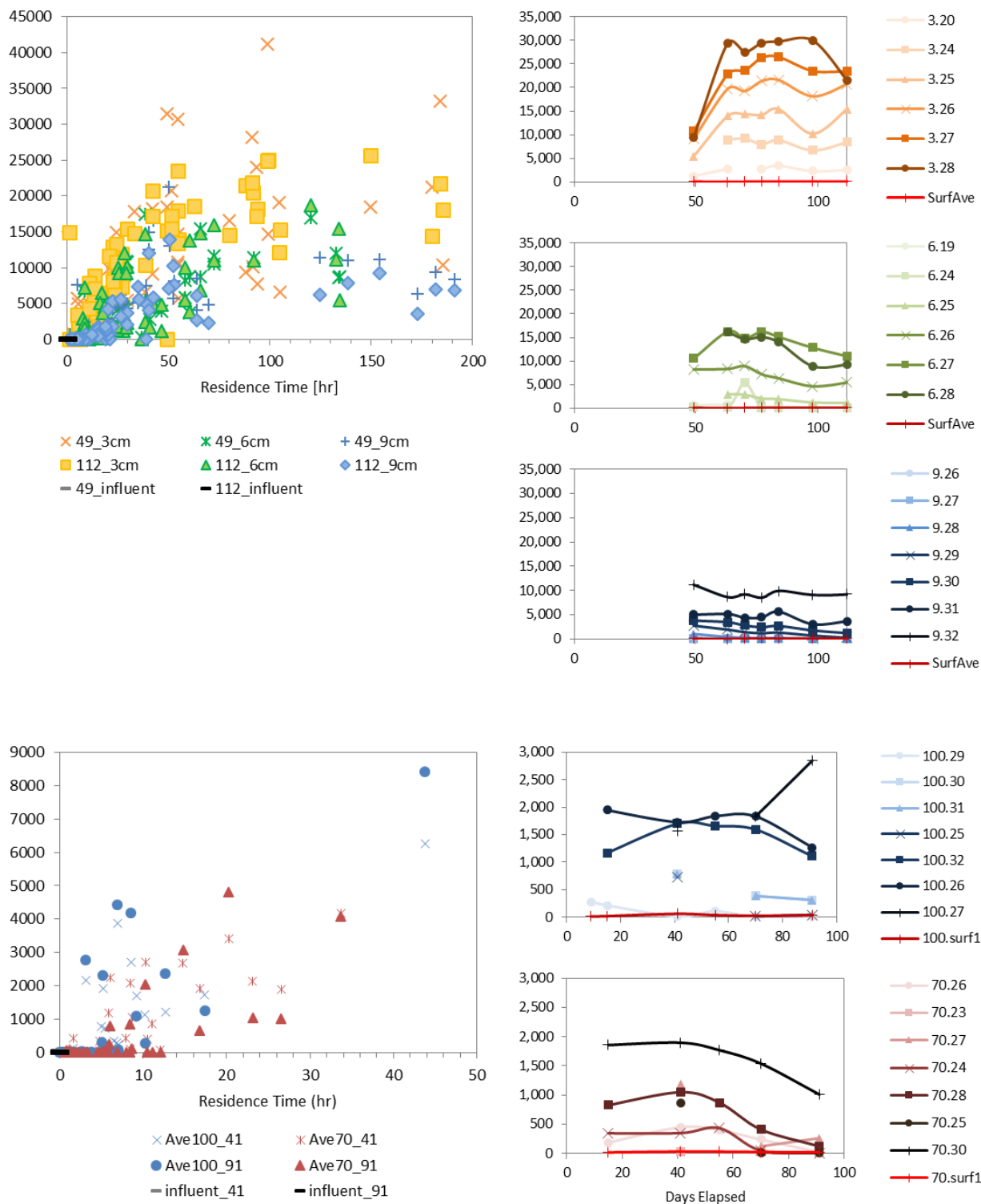**Figure C.8. (cont.)   Akalinity.** (Left) concentrations versus residence time on days 49 and 112 (F1) and days 41 and 91 (F2); (Right) concentrations over elapsed time at selected locations. All concentrations are [µg L-1].
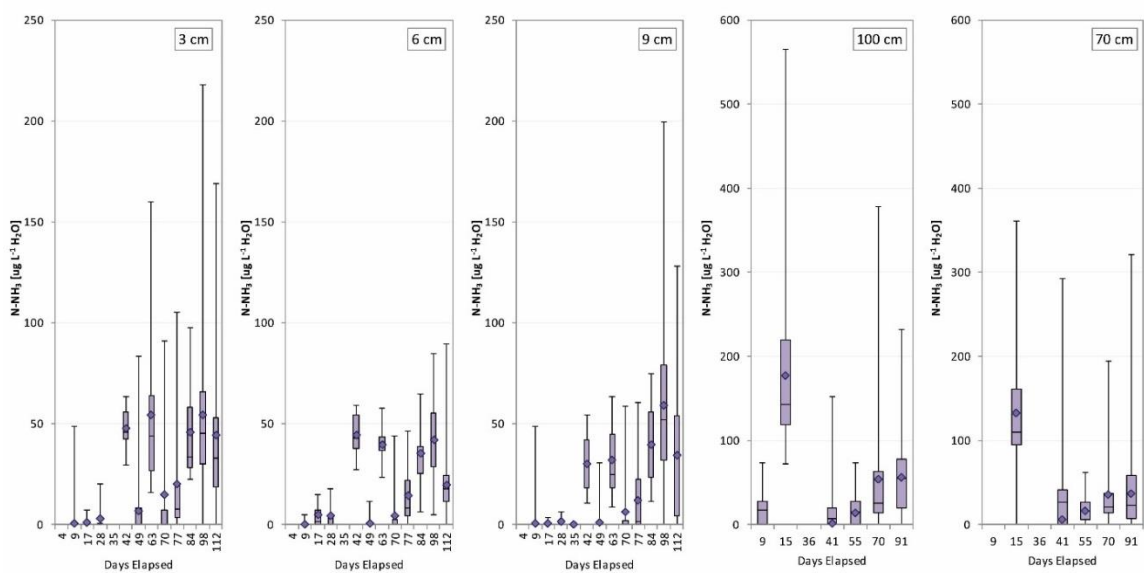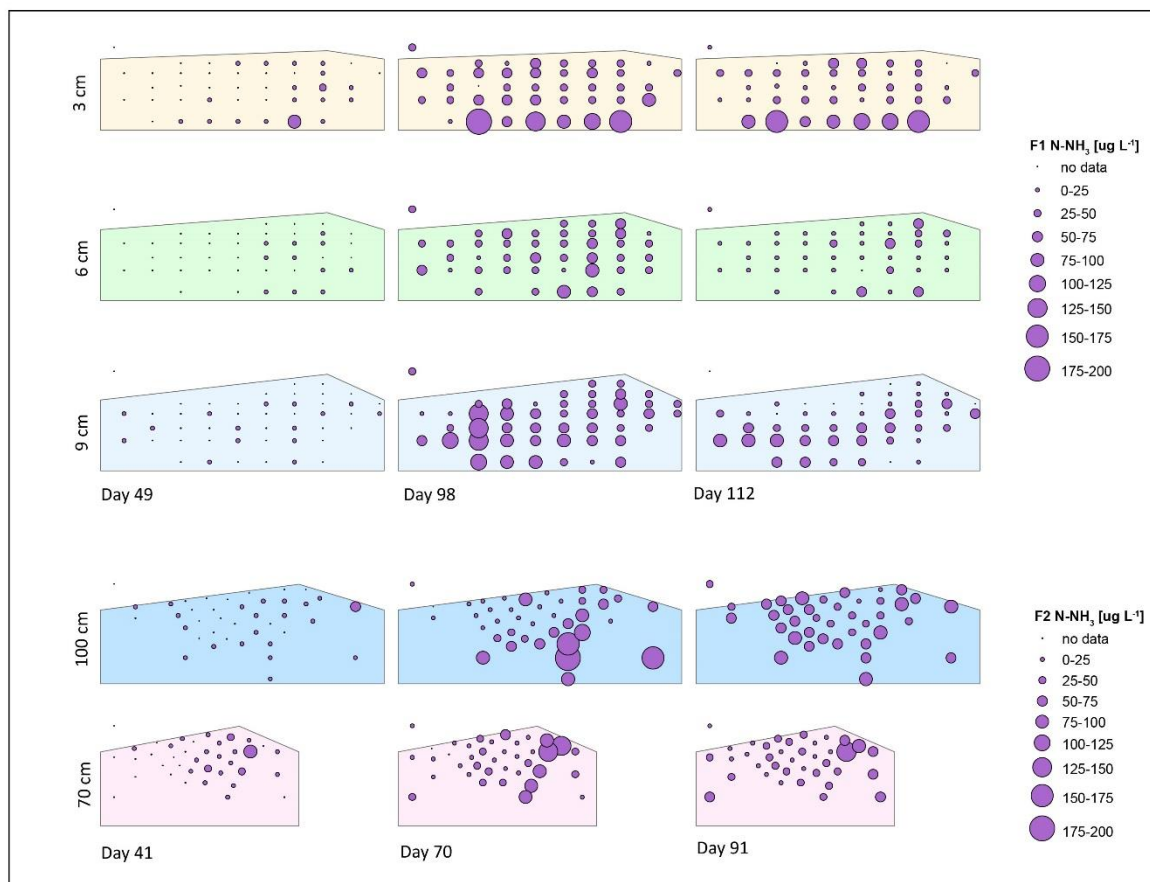
Figure C.9. Ammonia (N-NH₃) concentrations. (Top) Concentrations at rhizon locations; (Bottom) concentrations over elapsed time. All concentrations are [µg L⁻¹].
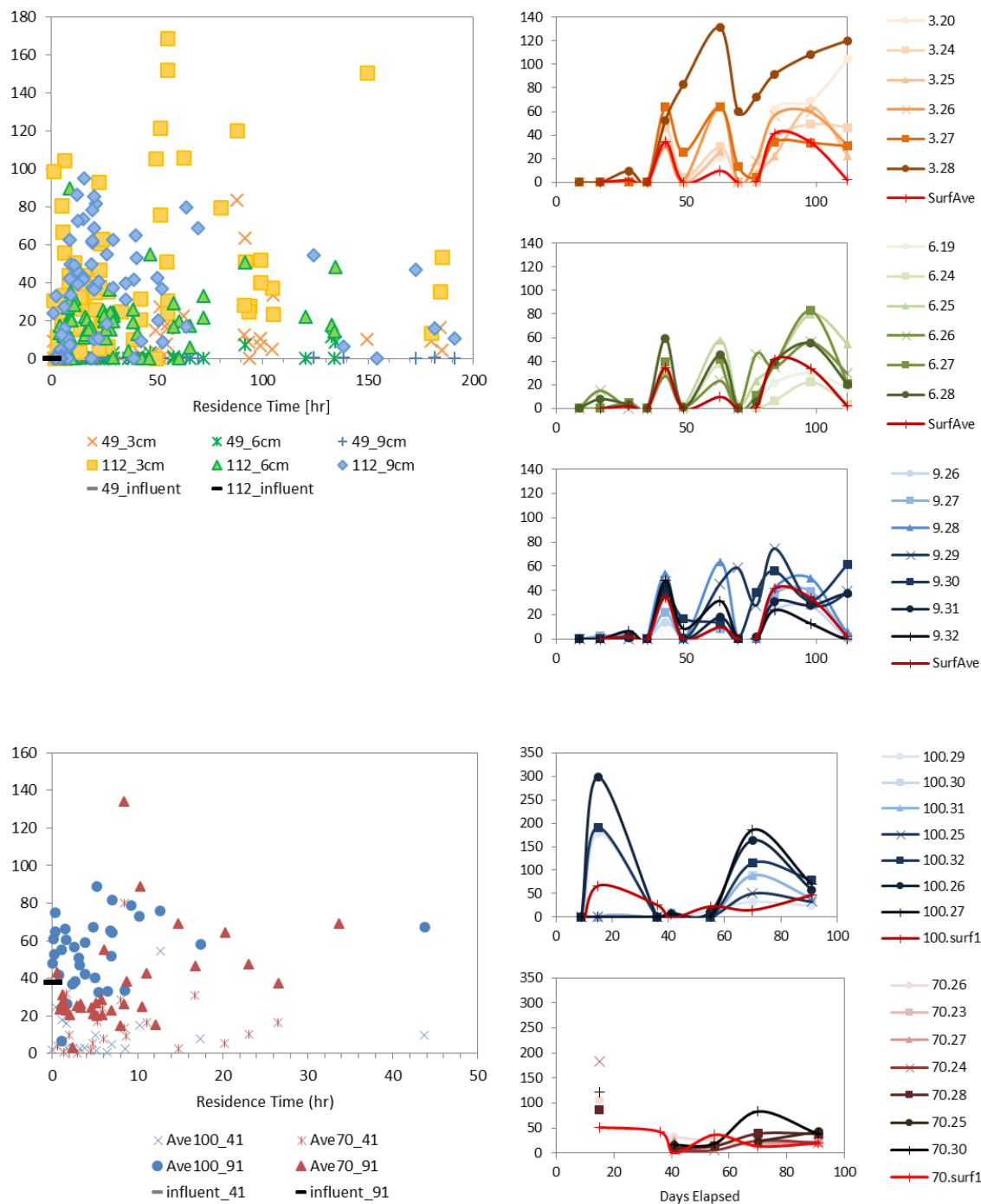
Figure C.9. (cont.) **Ammonia (N-NH₃) concentrations.** (Left) concentrations versus residence time on days 49 and 112 (F1) and days 41 and 91 (F2); (Right) concentrations over elapsed time at selected locations. All concentrations are [µg L⁻¹].
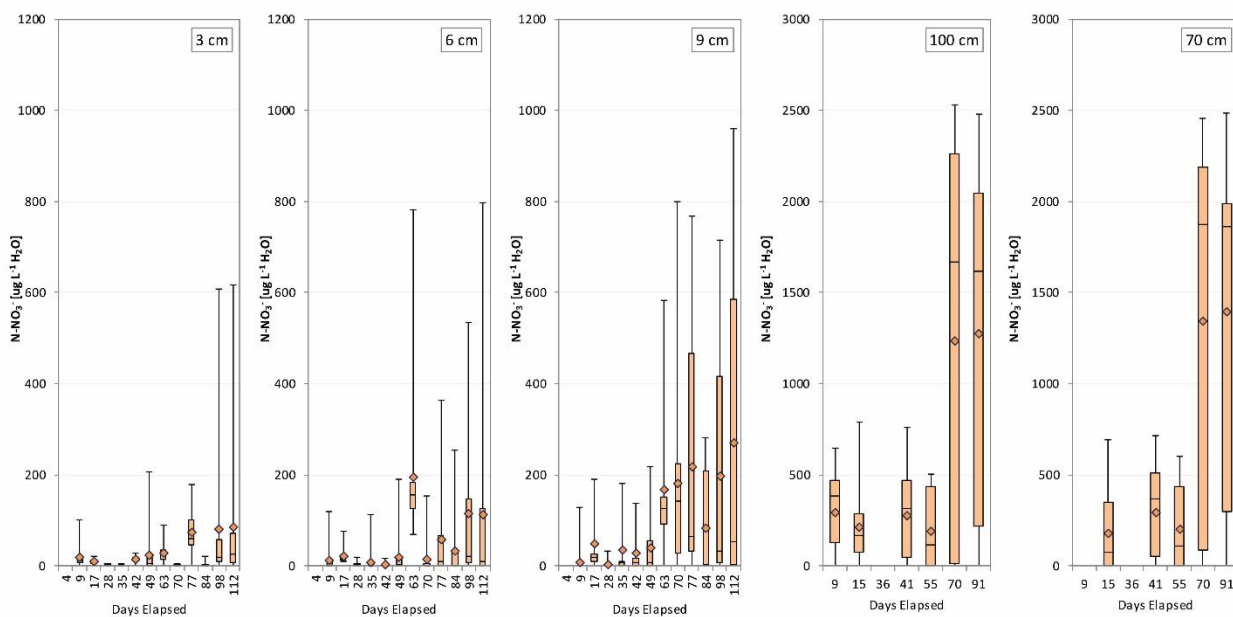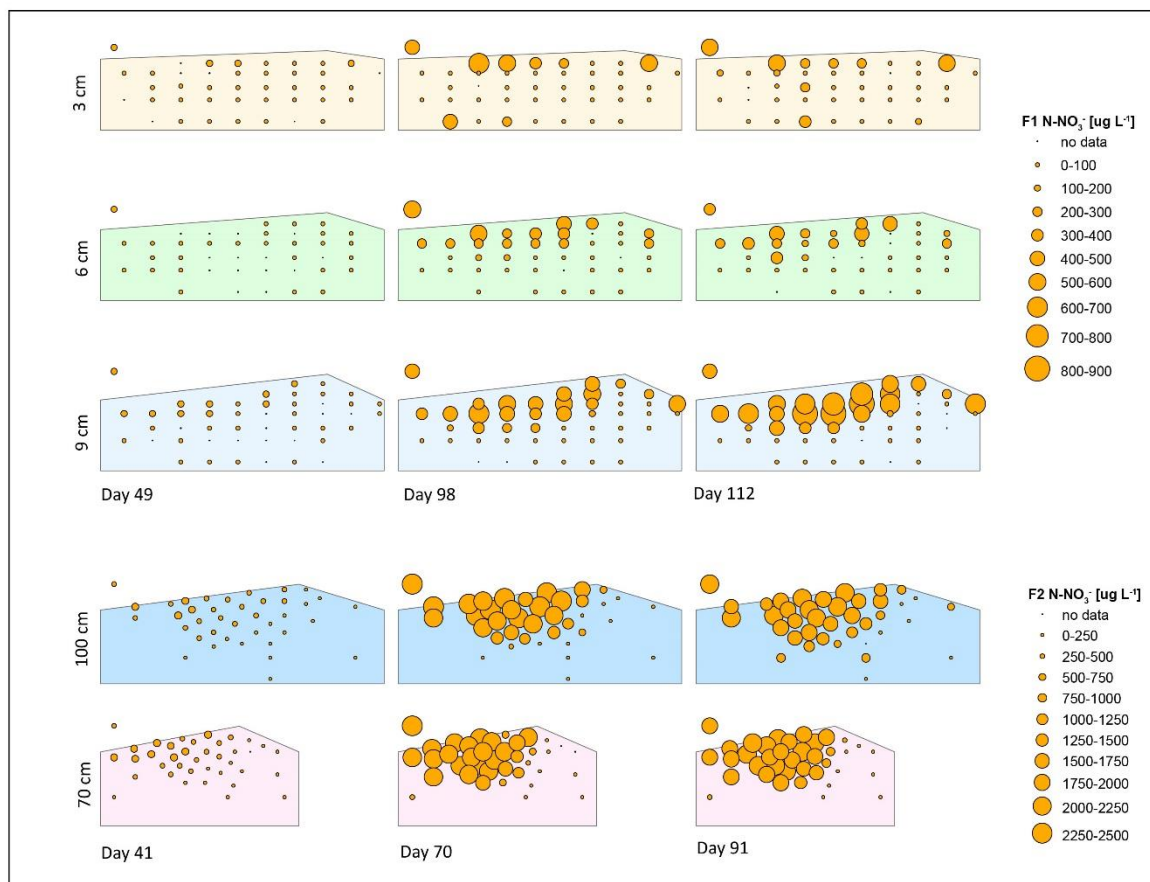
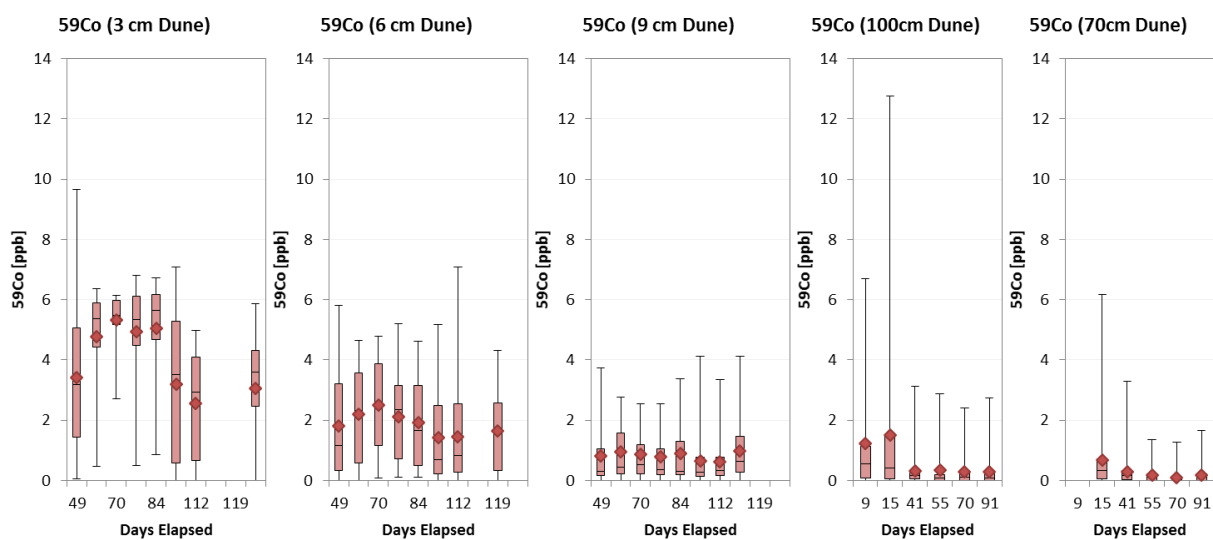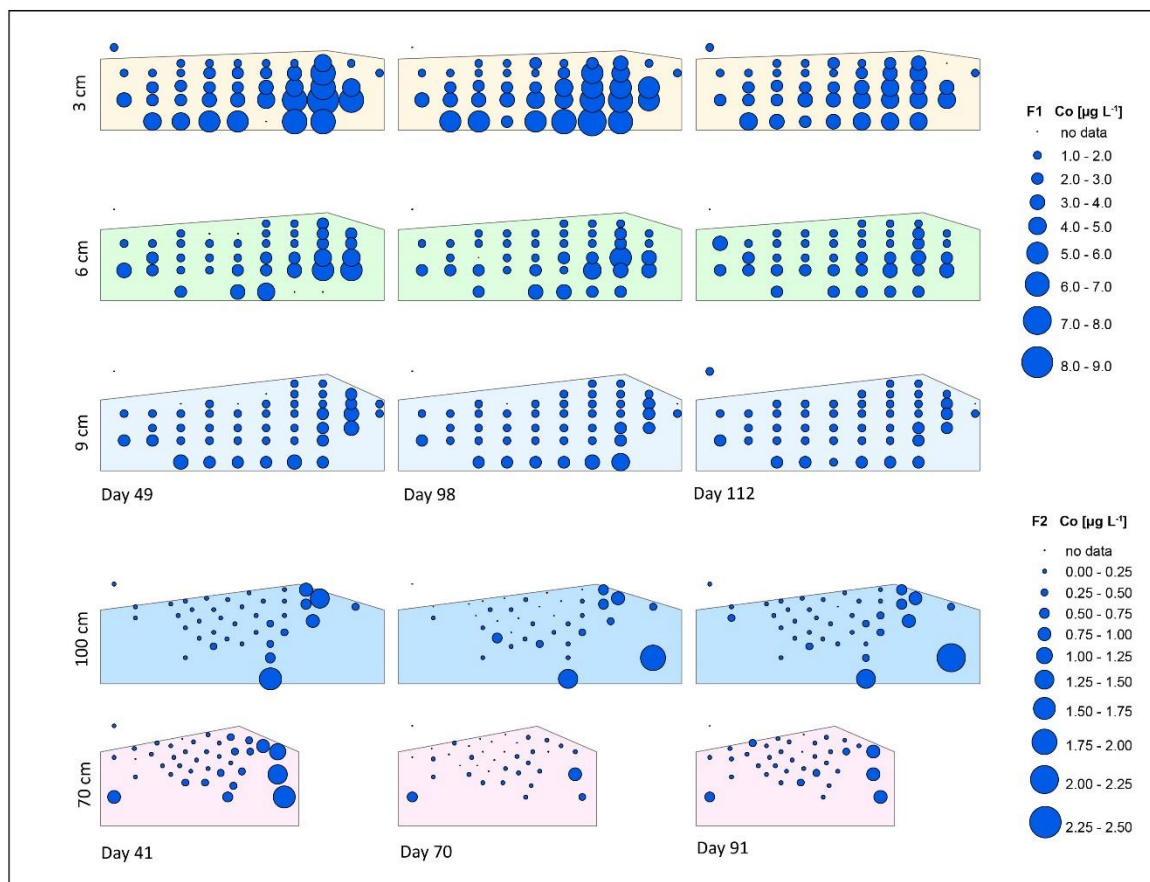**Figure C.10. Nitrate (N-NO₃⁻) concentrations.** (Top) Concentrations at rhizon locations; (Bottom) concentrations over elapsed time. All concentrations are [µg L⁻¹]. KNO³ was added to the system around day 60 in both experiments.

Figure C.10. (cont.) Nitrate (N-NO₃⁻) concentrations. (Left) concentrations versus residence time on days 49 and 112 (F1) and days 41 and 91 (F2); (Right) concentrations over elapsed time at selected locations. All concentrations are [μg L⁻¹]. KNO³ was added to the system around day 60 in both experiments.
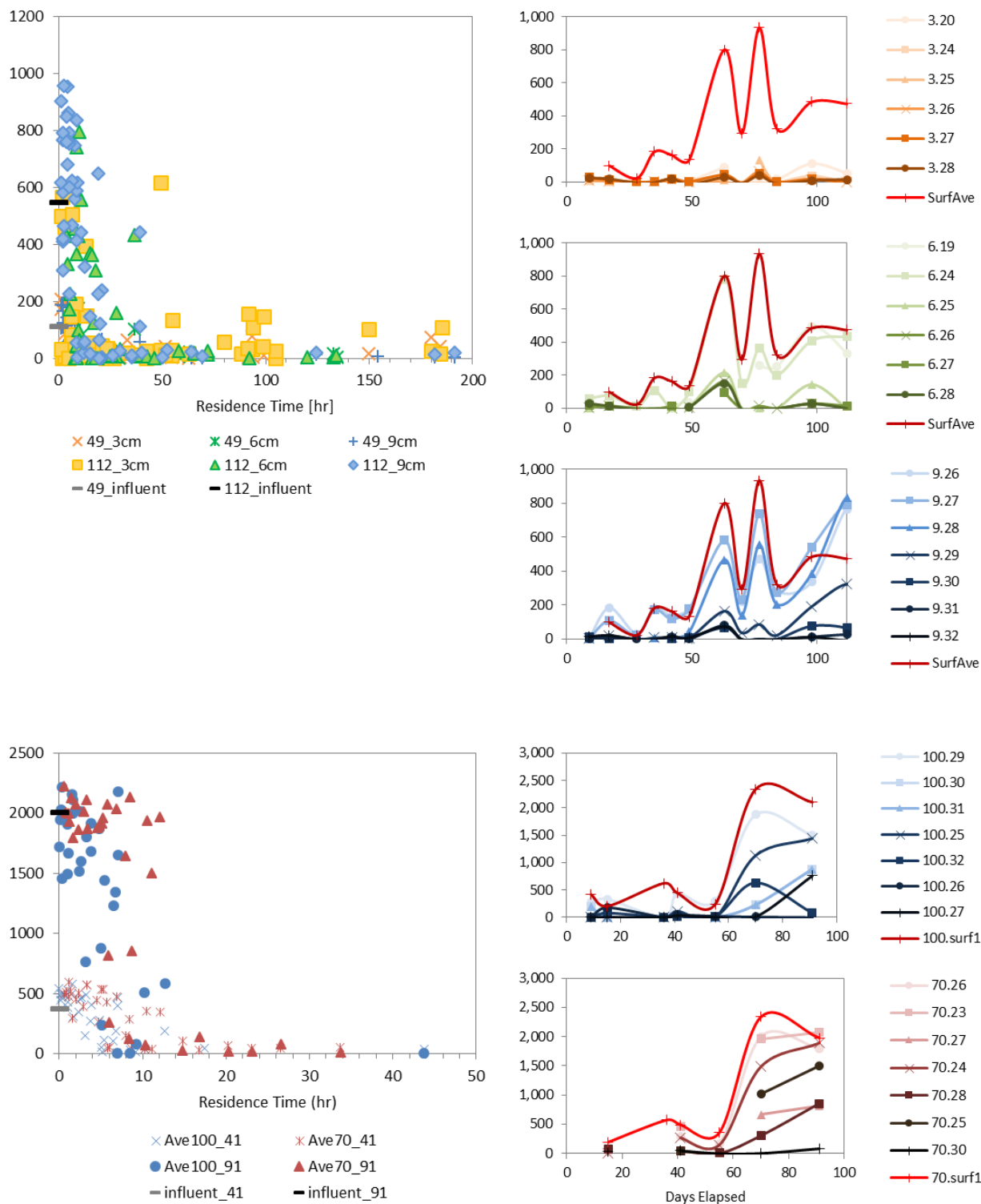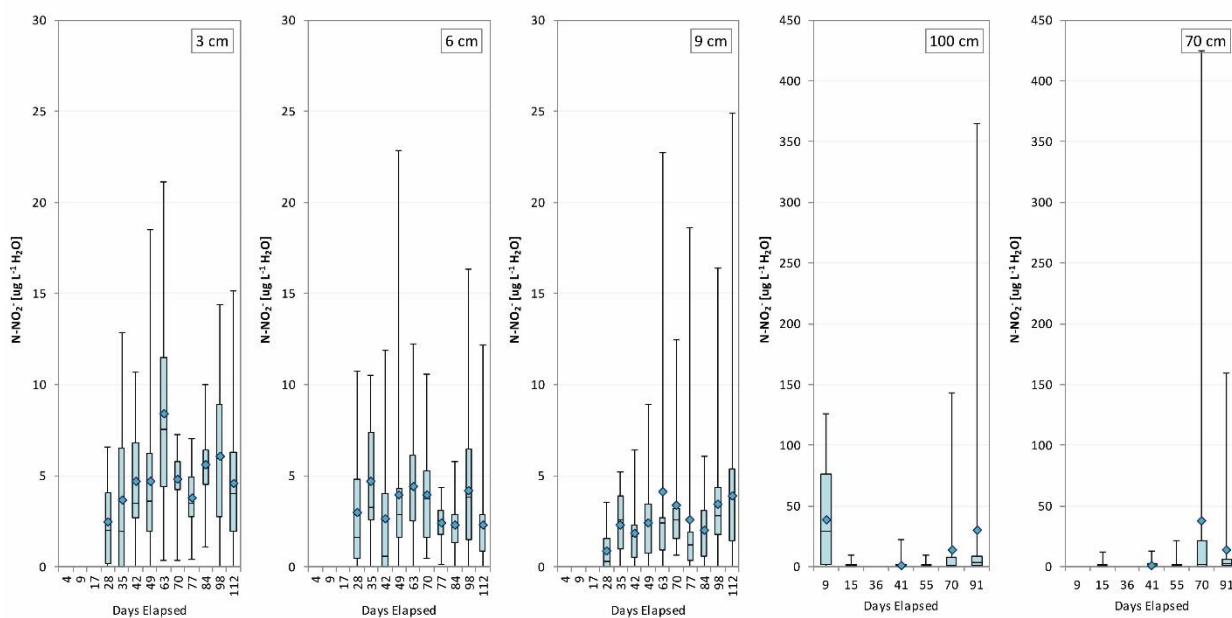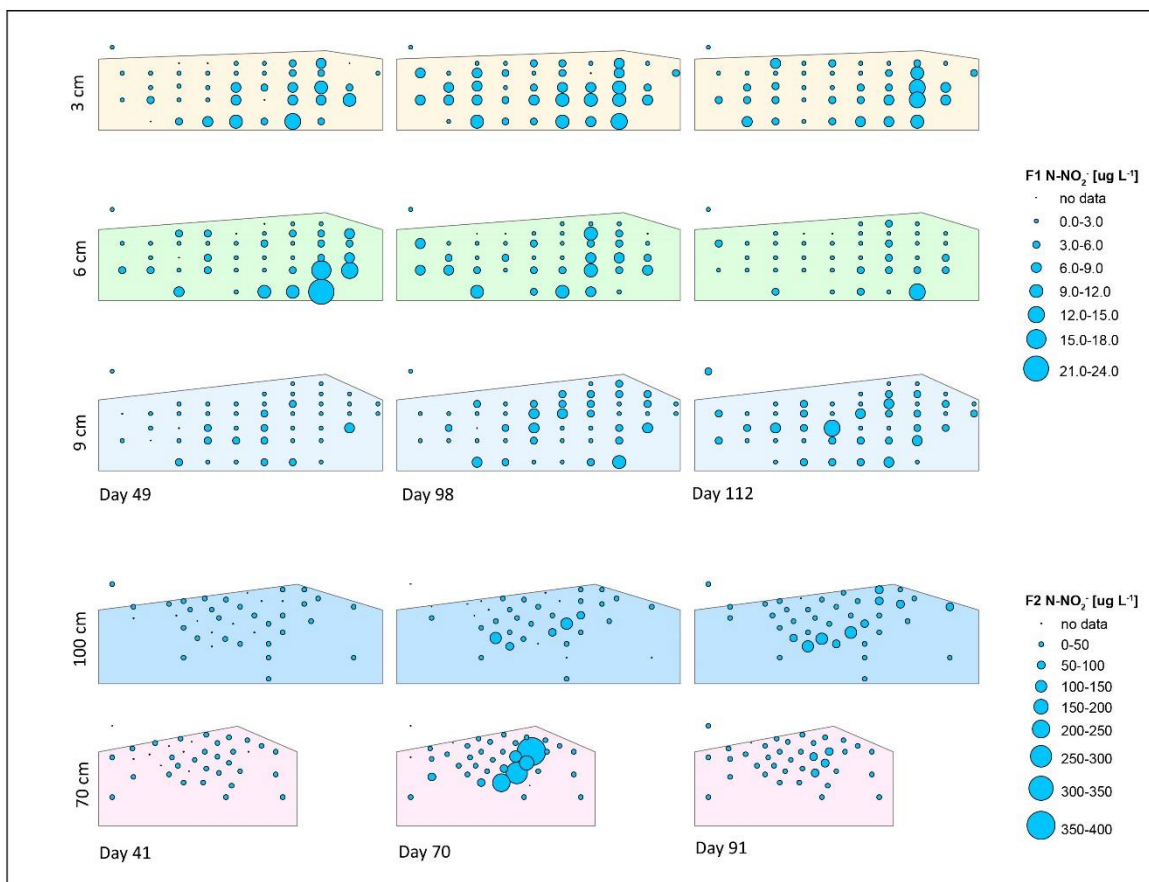
Figure C.11. Nitrite (N-NO$_2^-$) concentrations. (Top) Concentrations at rhizon locations; (Bottom) concentrations over elapsed time. All concentrations are [μg L^{-1}]. KNO^3 was added to the system around day 60 in both experiments.
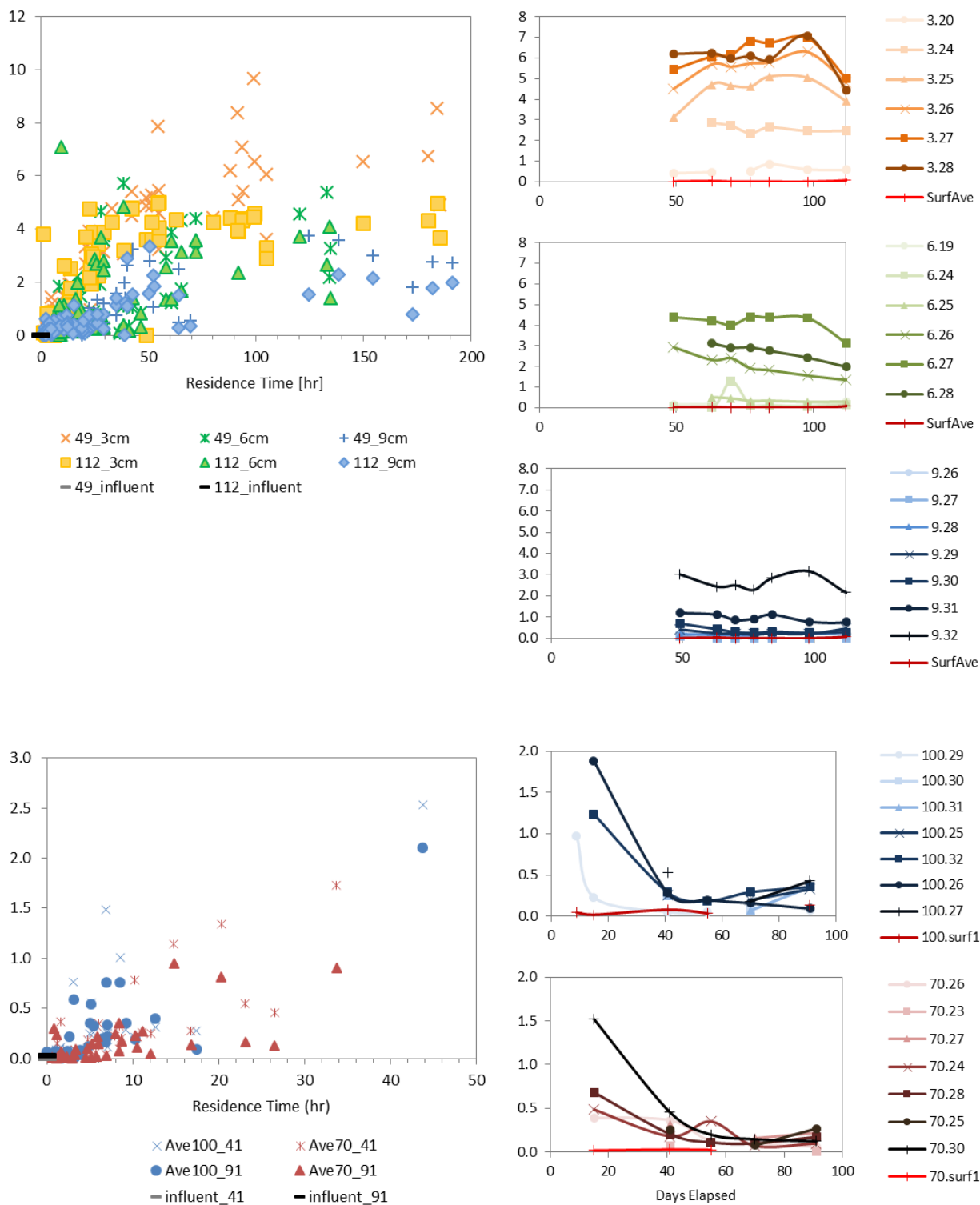
Figure C.11. (cont.) Nitrite (N-NO₂⁻) concentrations. (Left) concentrations versus residence time on days 49 and 112 (F1) and days 41 and 91 (F2); (Right) concentrations over elapsed time 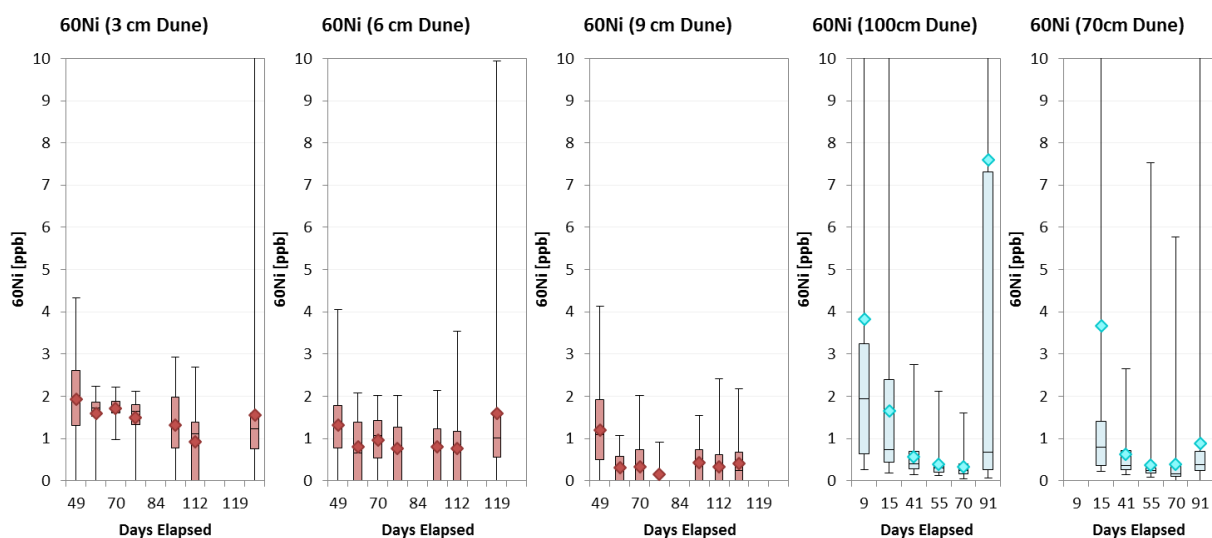at selected locations. All concentrations are [μg L^{-1}]. KNO^3 was added to the system around day 60 in both experiments.
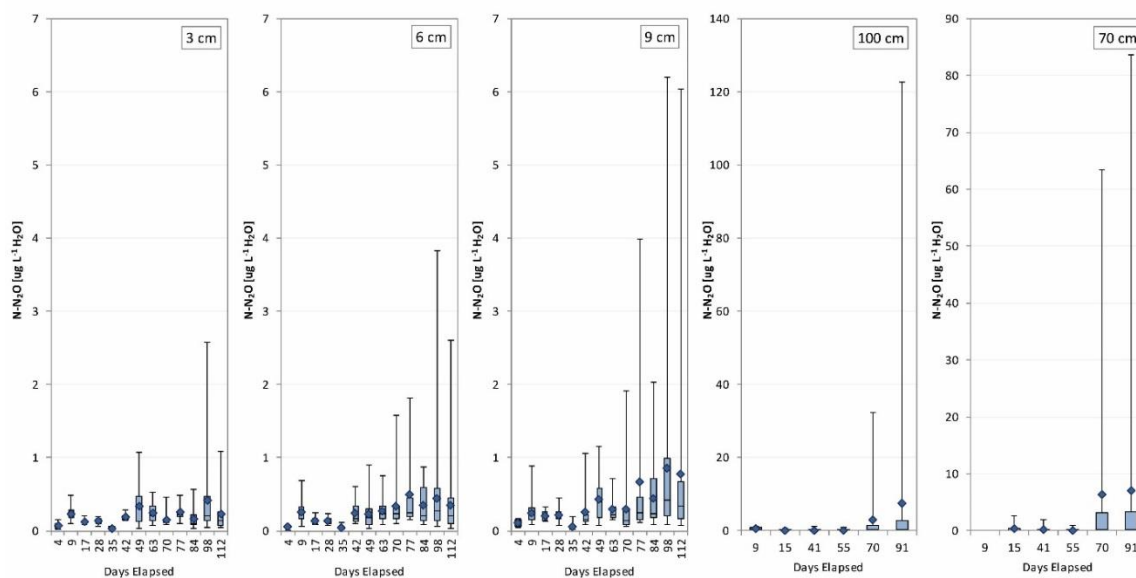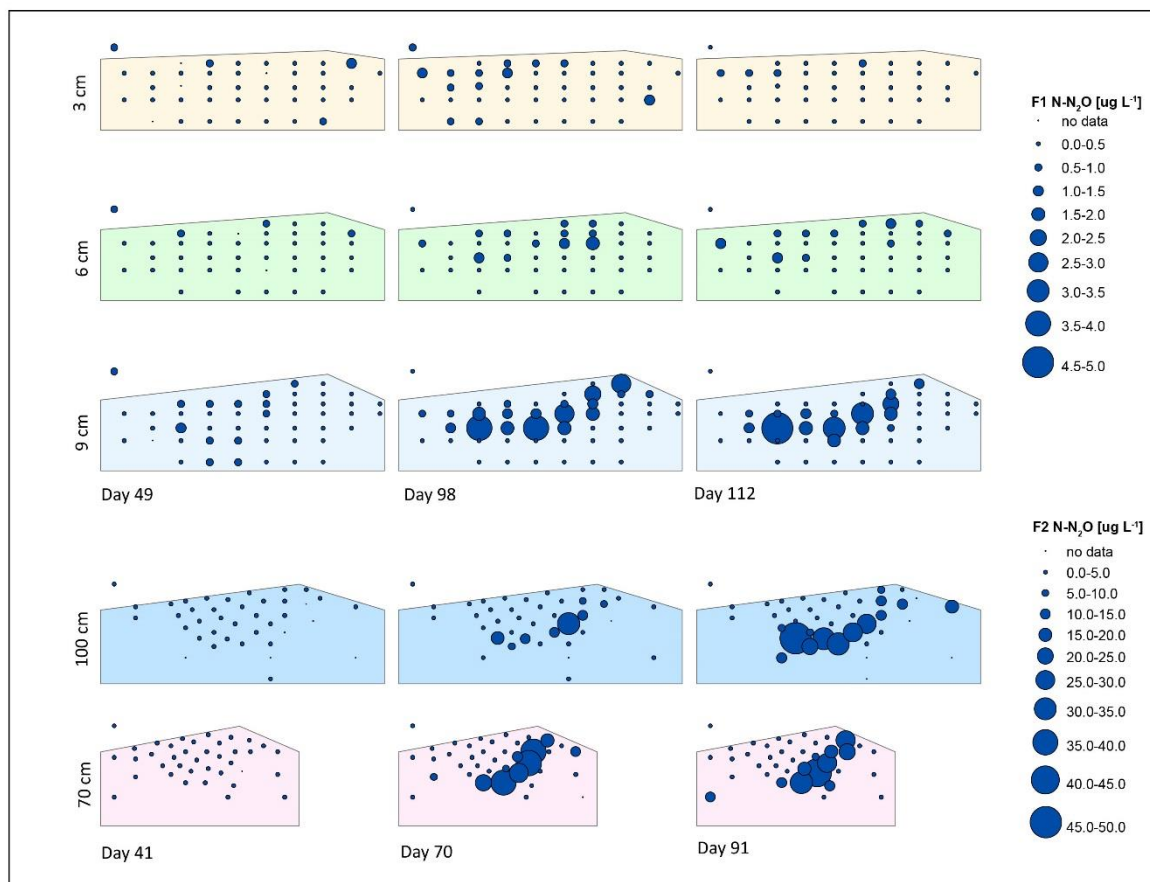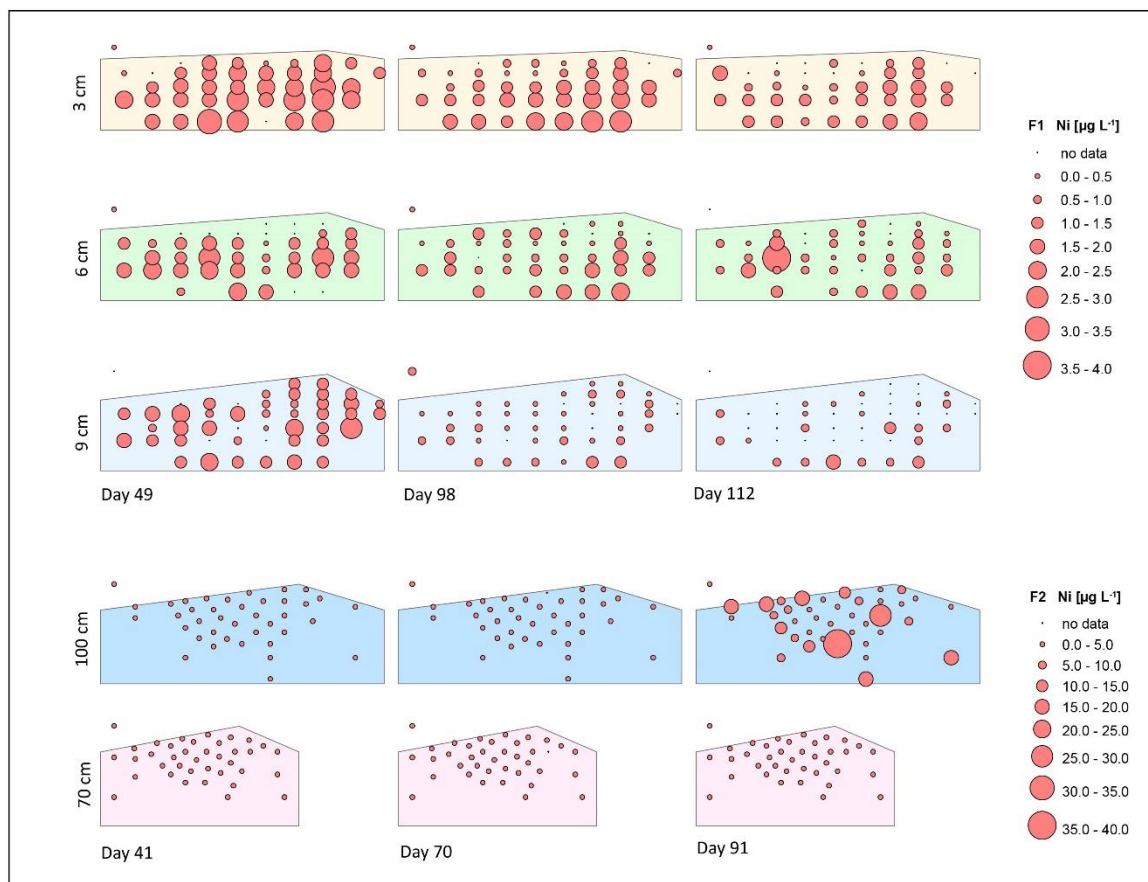
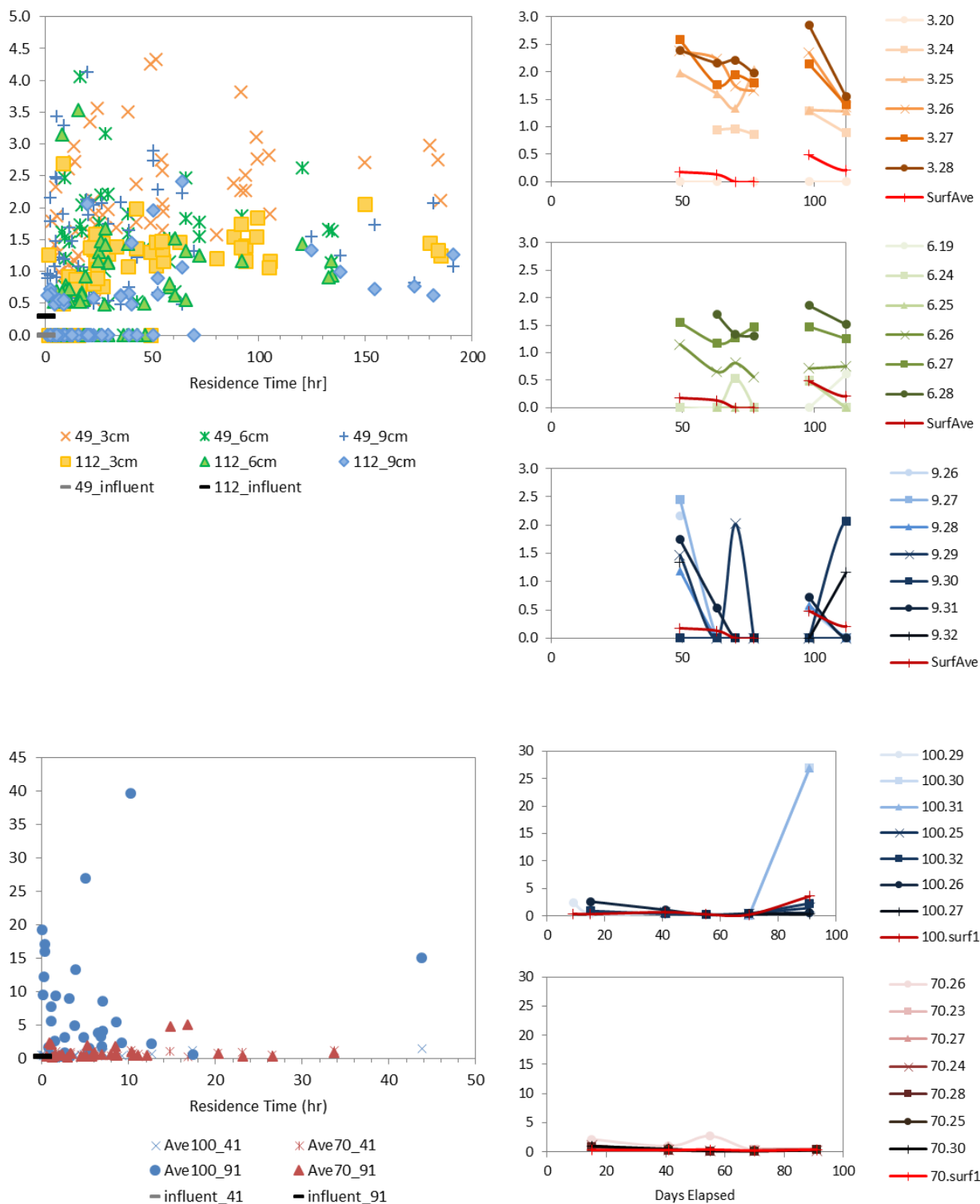**Figure C.12. Nitrous oxide (N-N₂O) concentrations.** (Top) Concentrations at rhizon locations; (Bottom) concentrations over elapsed time. All concentrations are [μg L⁻¹]. KNO₃ was added to the system around day 60 in both experiments.
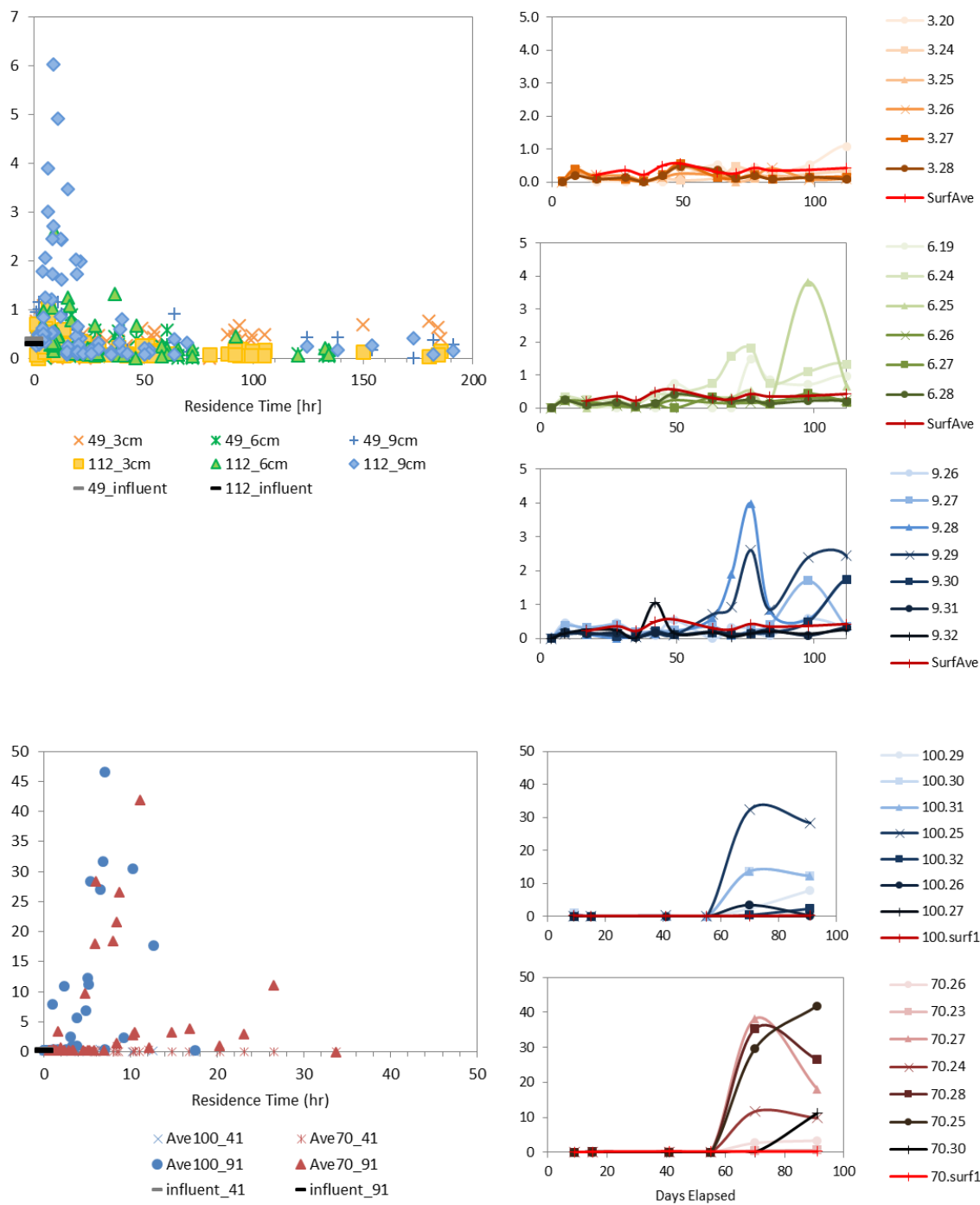
Figure C.12. (cont.) Nitrous oxide (N-N₂O) concentrations. (Left) concentrations versus residence time on days 49 and 112 (F1) and days 41 and 91 (F2); (Right) concentrations over elapsed time at selected locations. All concentrations are [µg L-1]. KNO3 was added to the system around day 60 in both experiments.
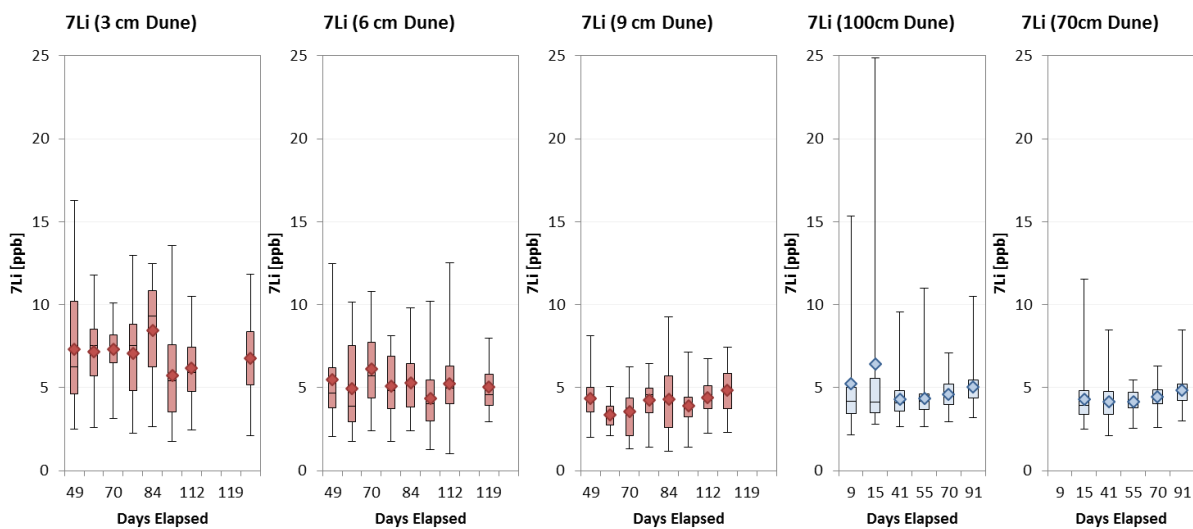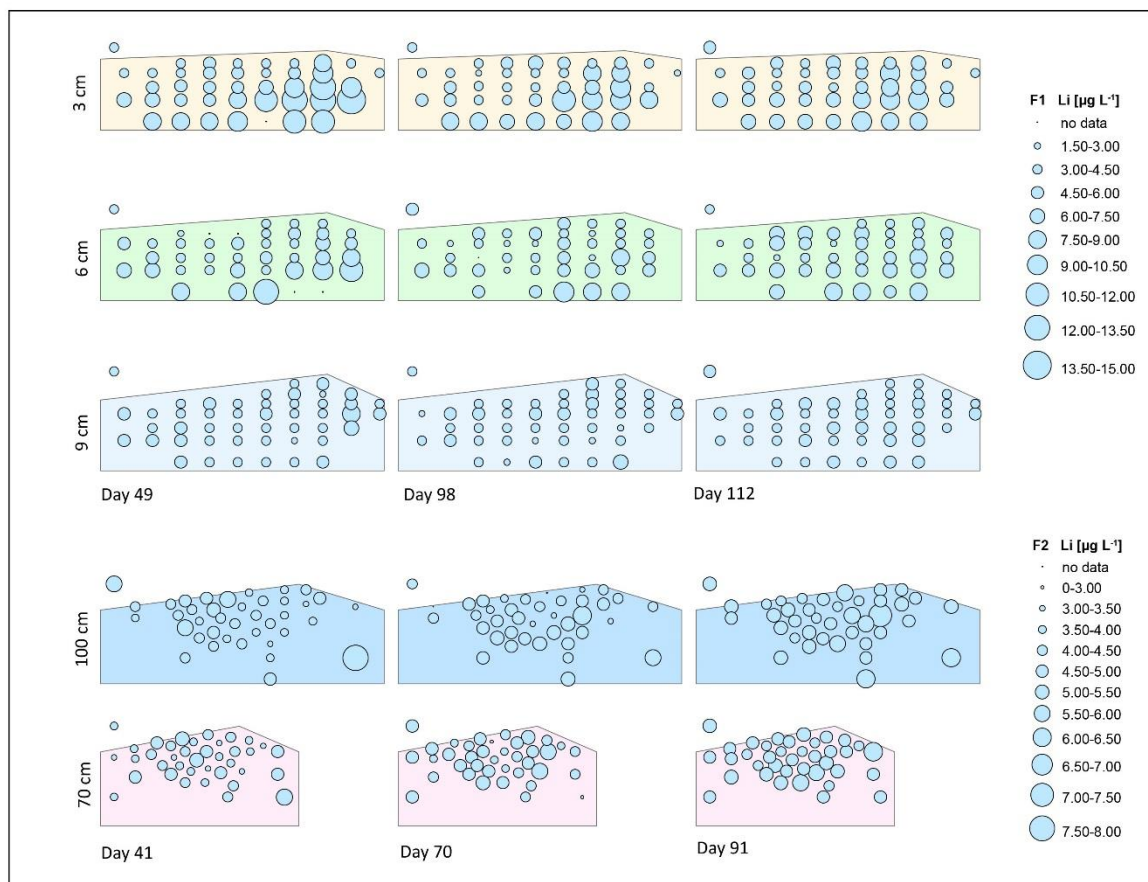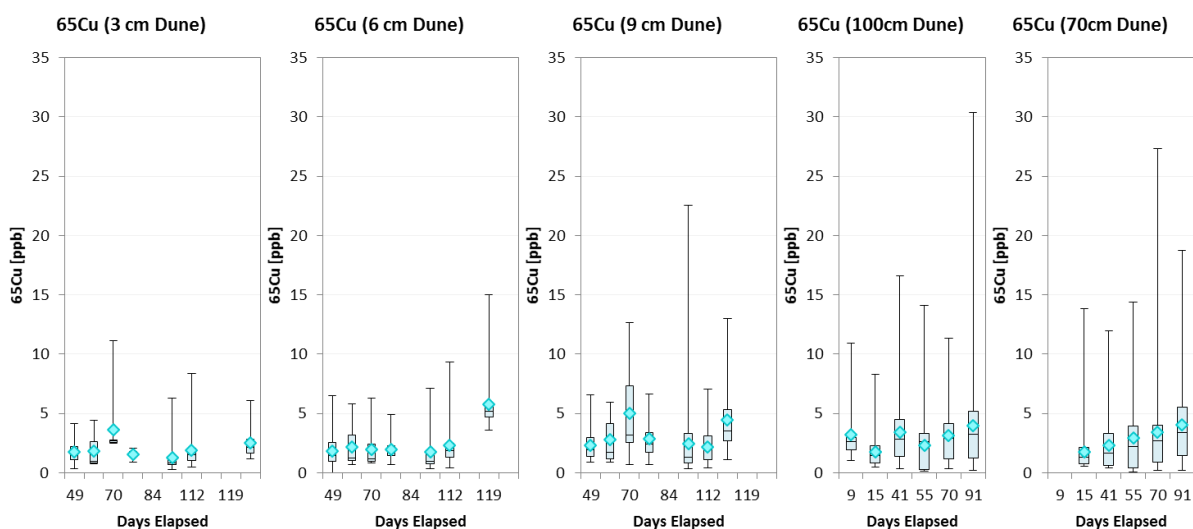
Figure C.13. Lithium (^{7}Li) concentrations. (Top) Concentrations at rhizon locations; (Bottom) concentrations over elapsed time. All concentrations are [μg L^{-1}].
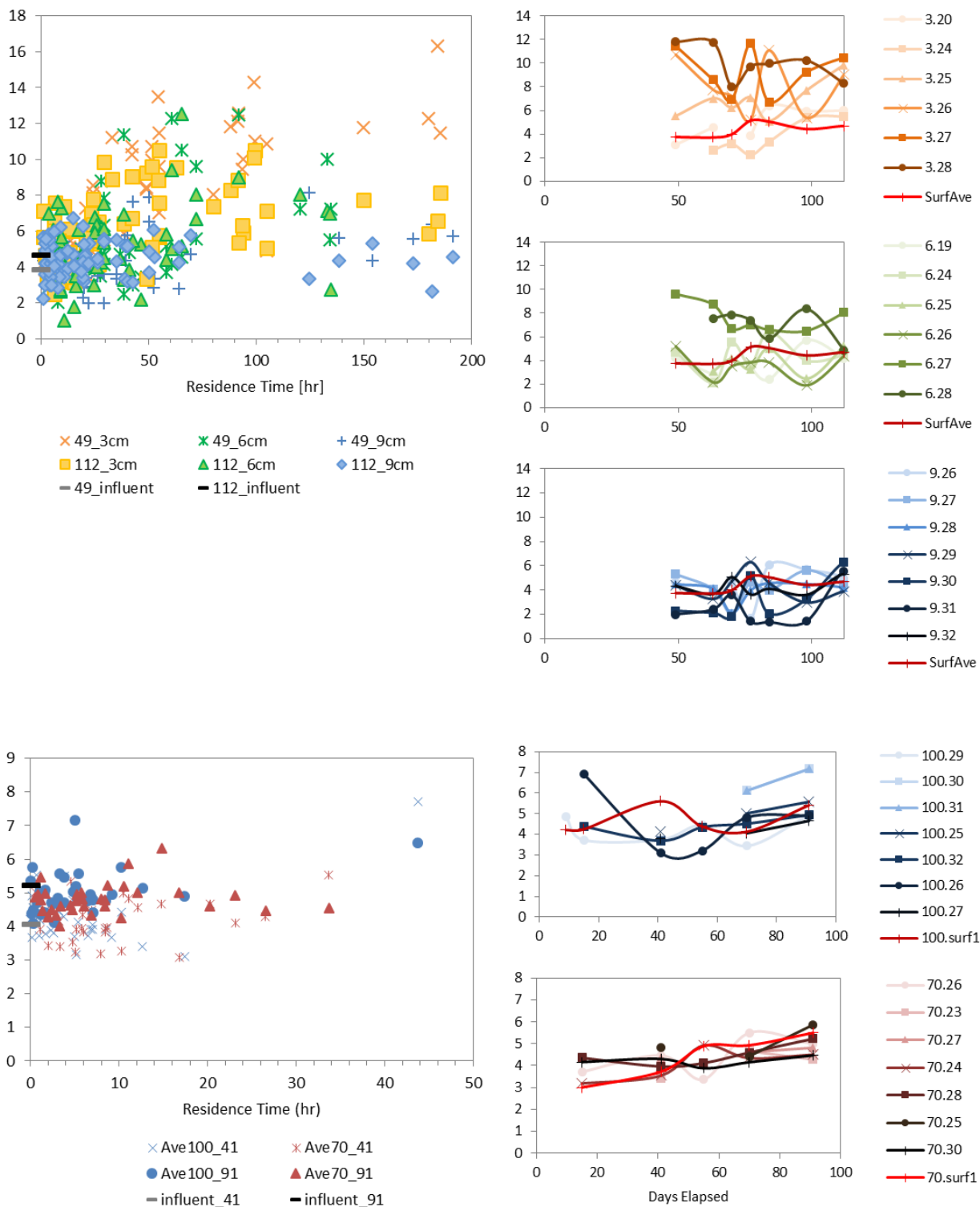
Figure C.13. (cont.) Lithium (^{7}Li) concentrations. (Left) concentrations versus residence time on days 49 and 112 (F1) and days 41 and 91 (F2); (Right) concentrations over elapsed time at selected locations. All concentrations are [μg L-1].
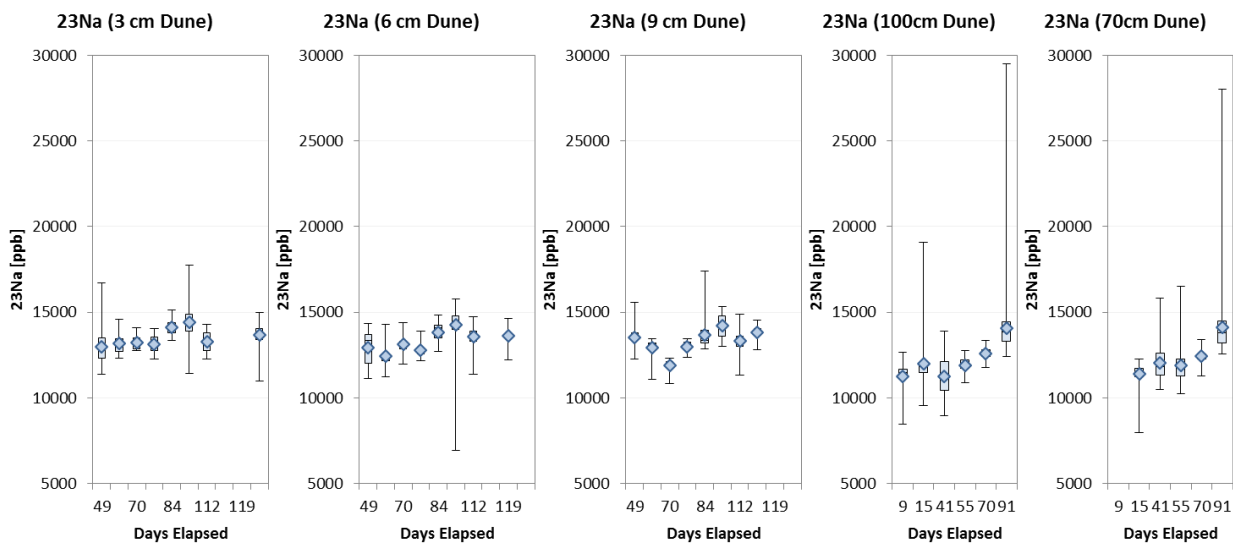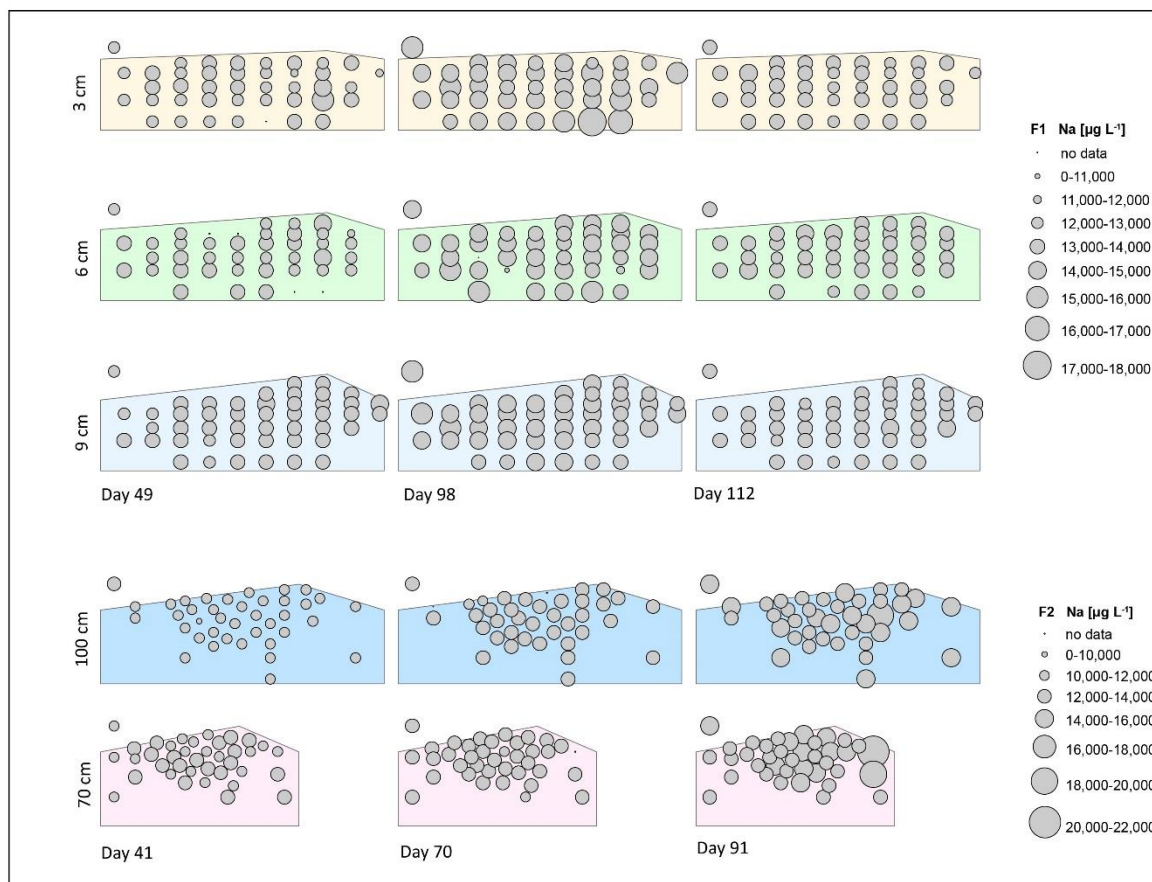
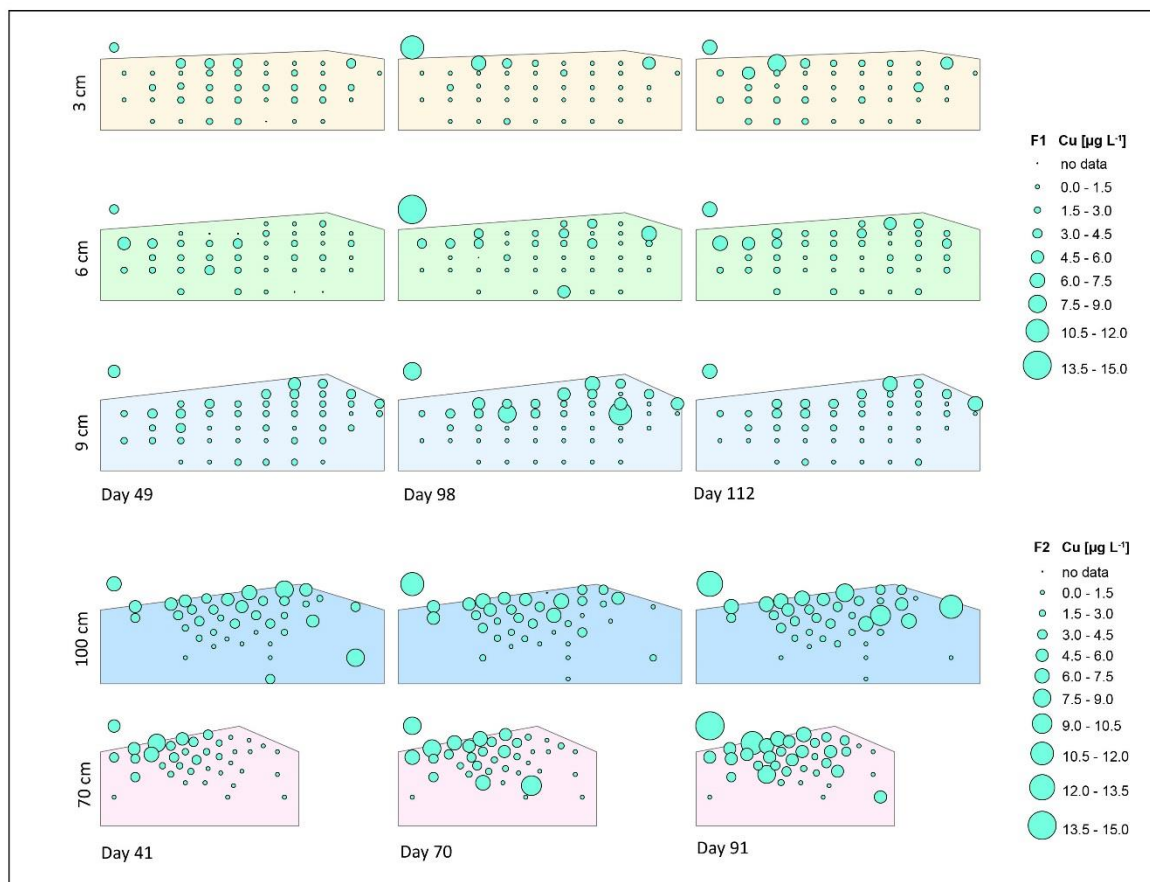**Figure C.14. Sodium (^{23}Na) concentrations.** (Top) Concentrations at rhizon locations; (Bottom) concentrations over elapsed time. All concentrations are [µg L^{-1}].
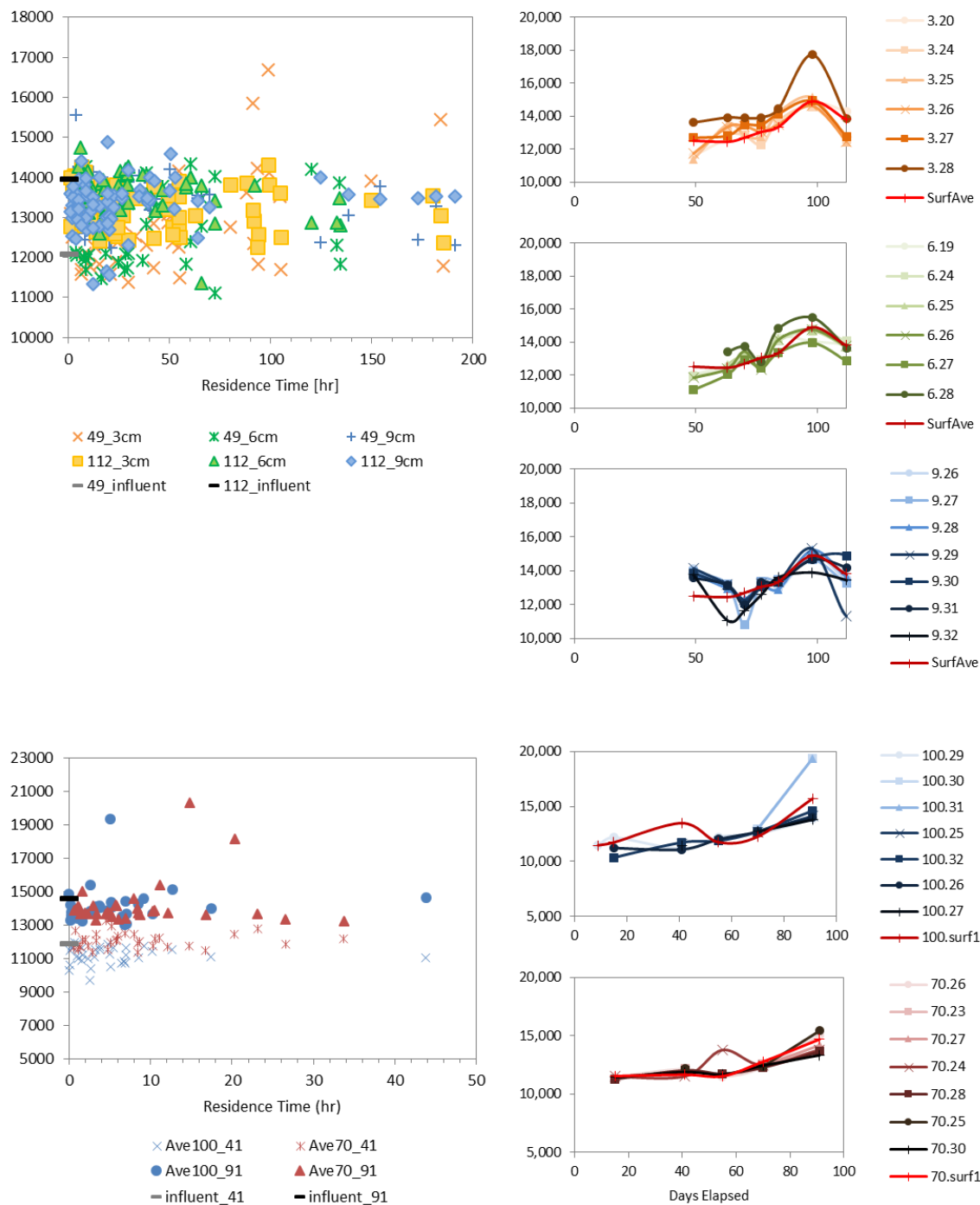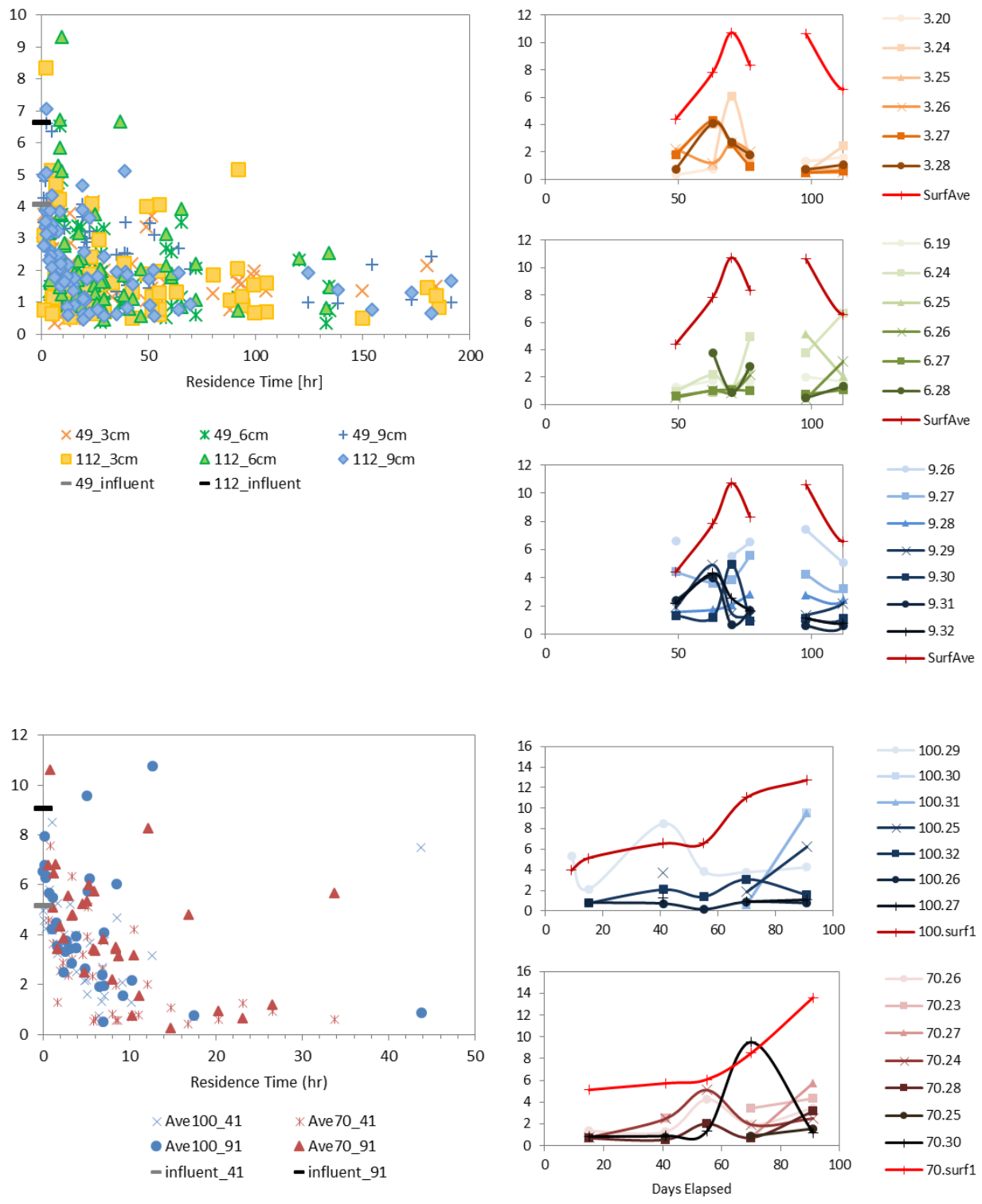
Figure C.14. (cont.) Sodium (²³Na) concentrations. (Left) concentrations versus residence time on days 49 and 112 (F1) and days 41 and 91 (F2); (Right) concentrations over elapsed time at selected locations. All concentrations are [µg L⁻¹].
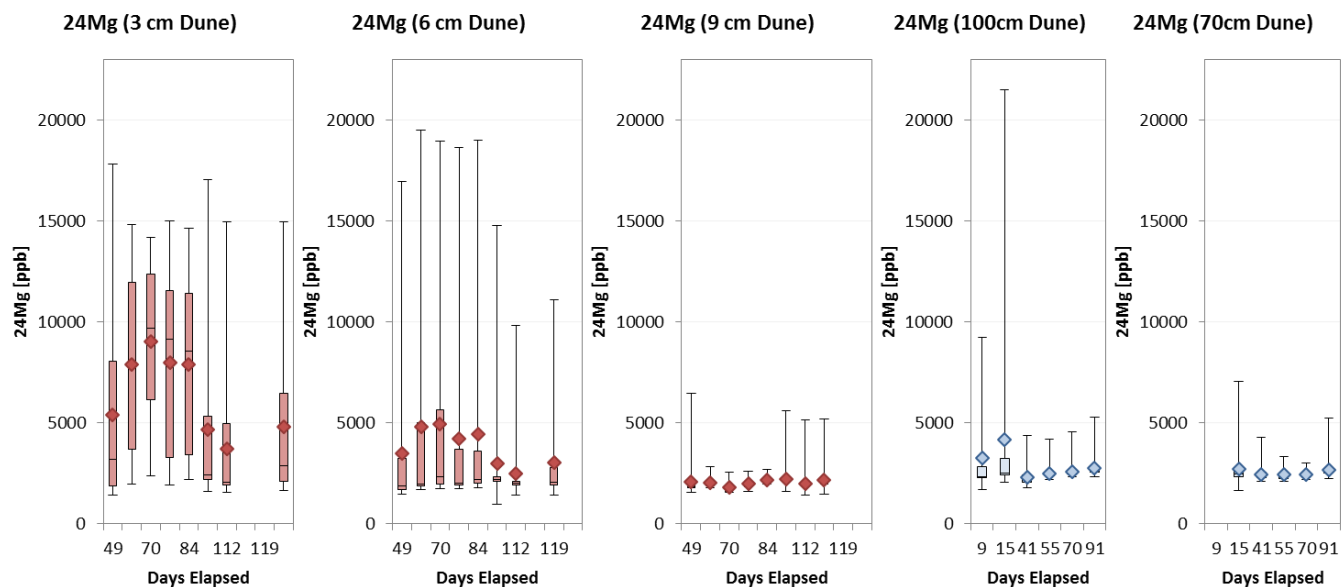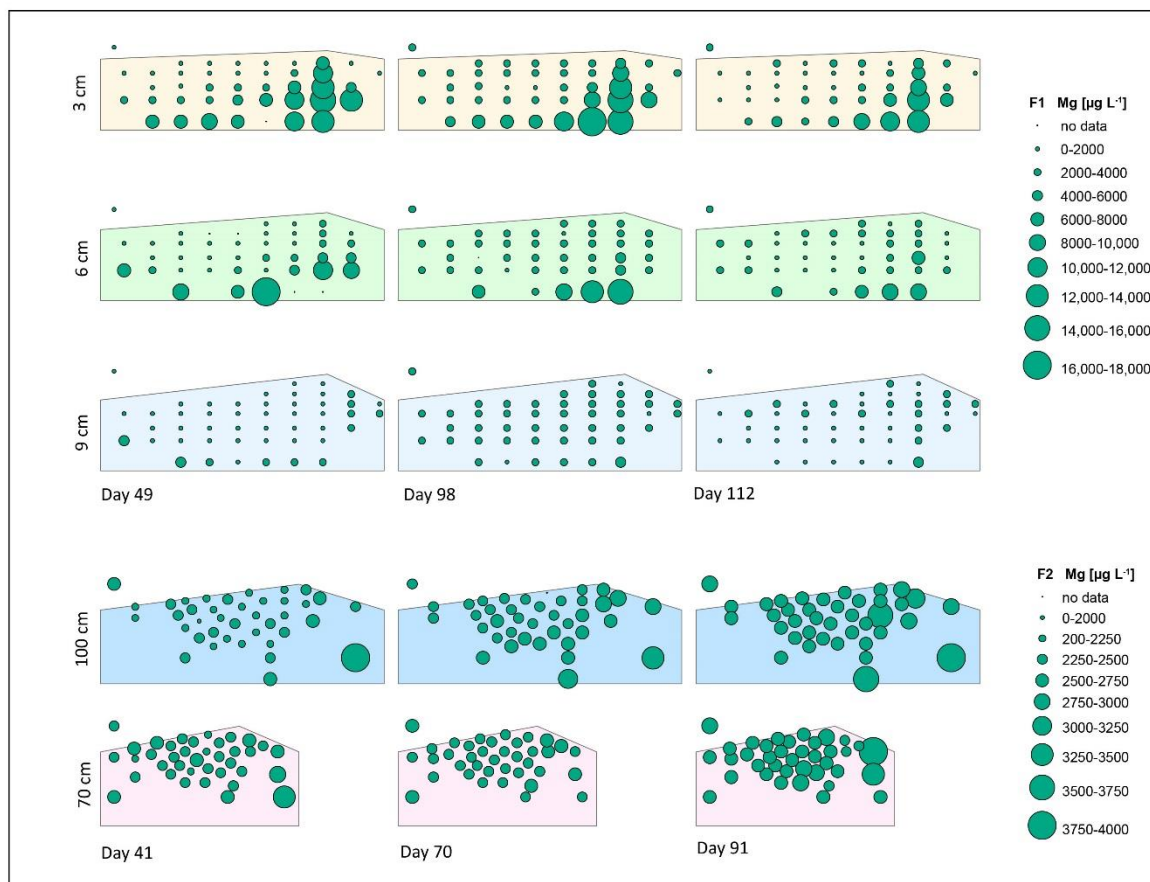
Figure C.15. Magnesium (^{24}Mg) concentrations. (Top) Concentrations at rhizon locations; (Bottom) concentrations over elapsed time. All concentrations are [µg L^{-1}].
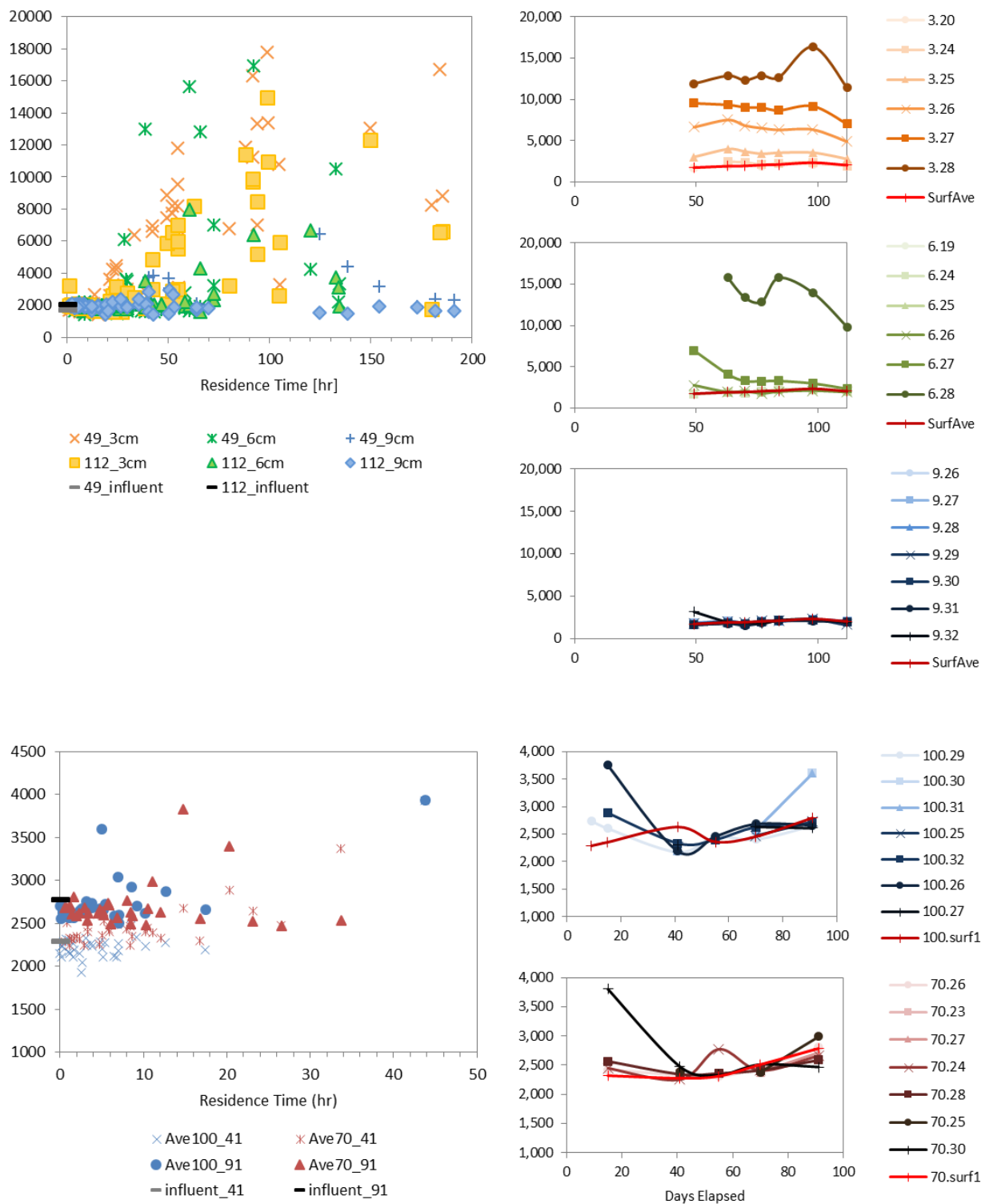
Figure C.15. (cont.) Magnesium (^{24}Mg) concentrations. (Left) concentrations versus residence time on days 49 and 112 (F1) and days 41 and 91 (F2); (Right) concentrations over elapsed time at selected locations. All concentrations are [µg L^{-1}].
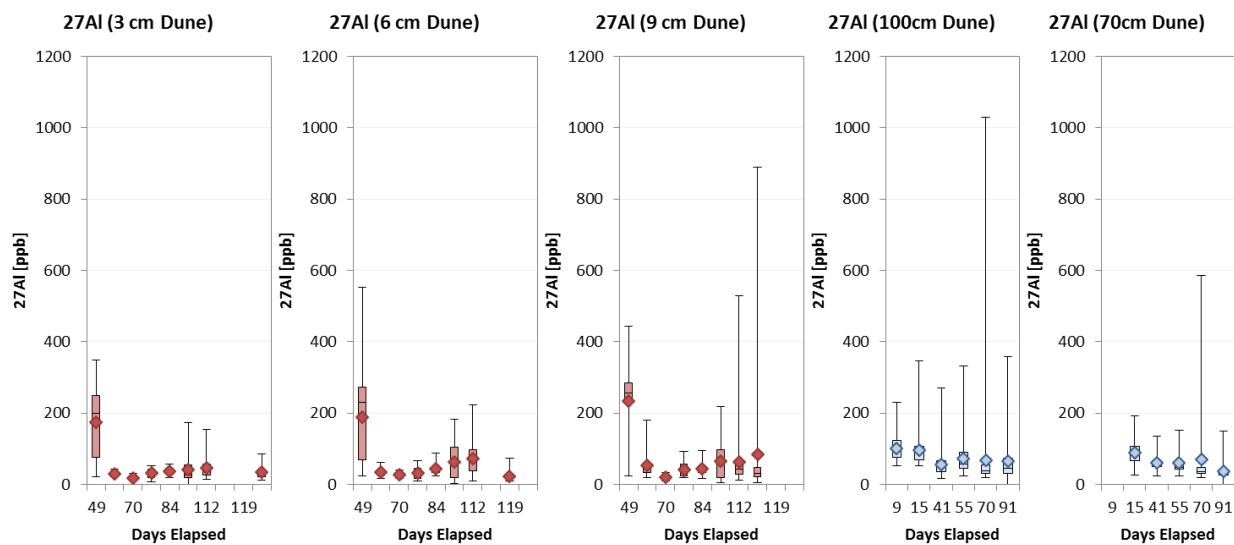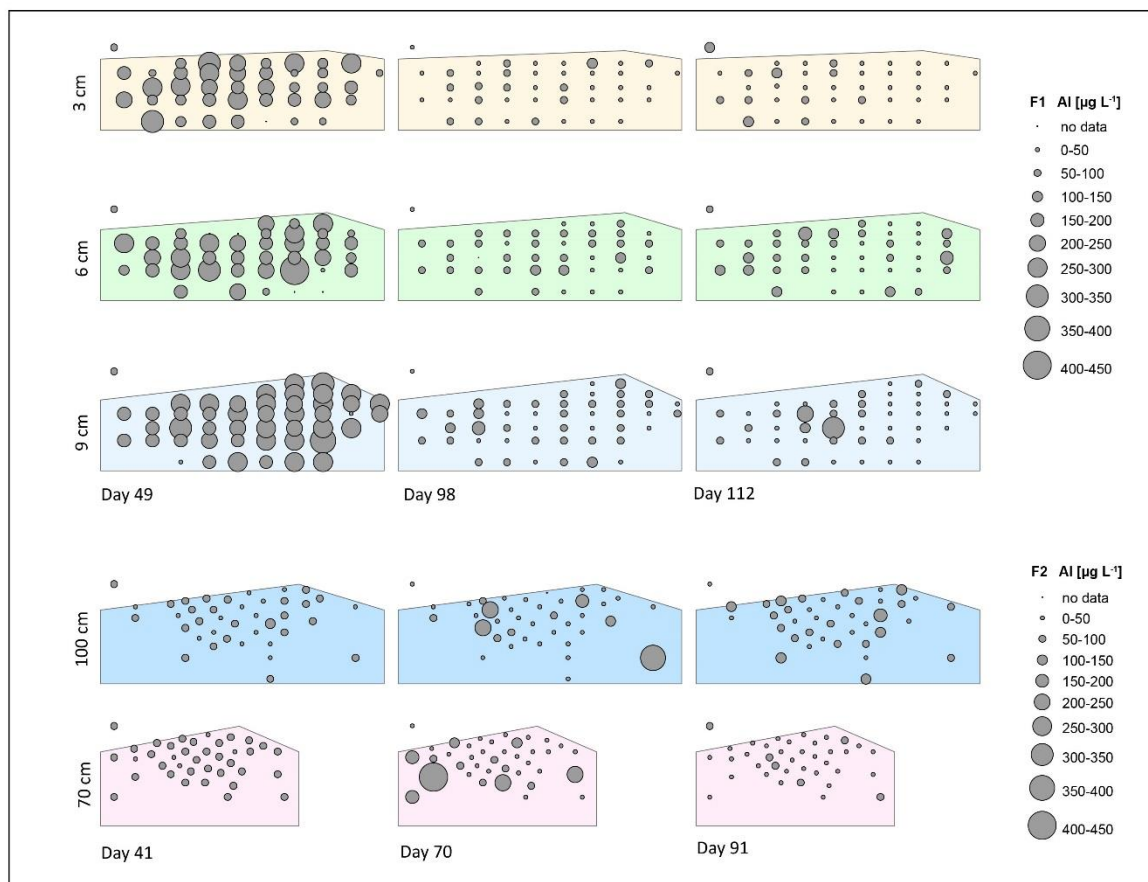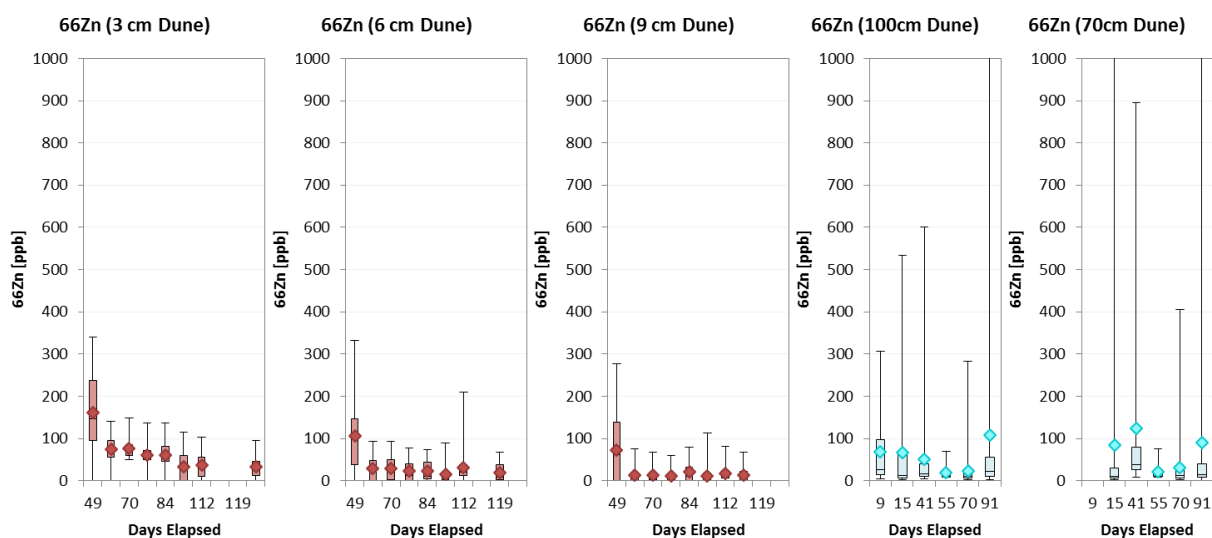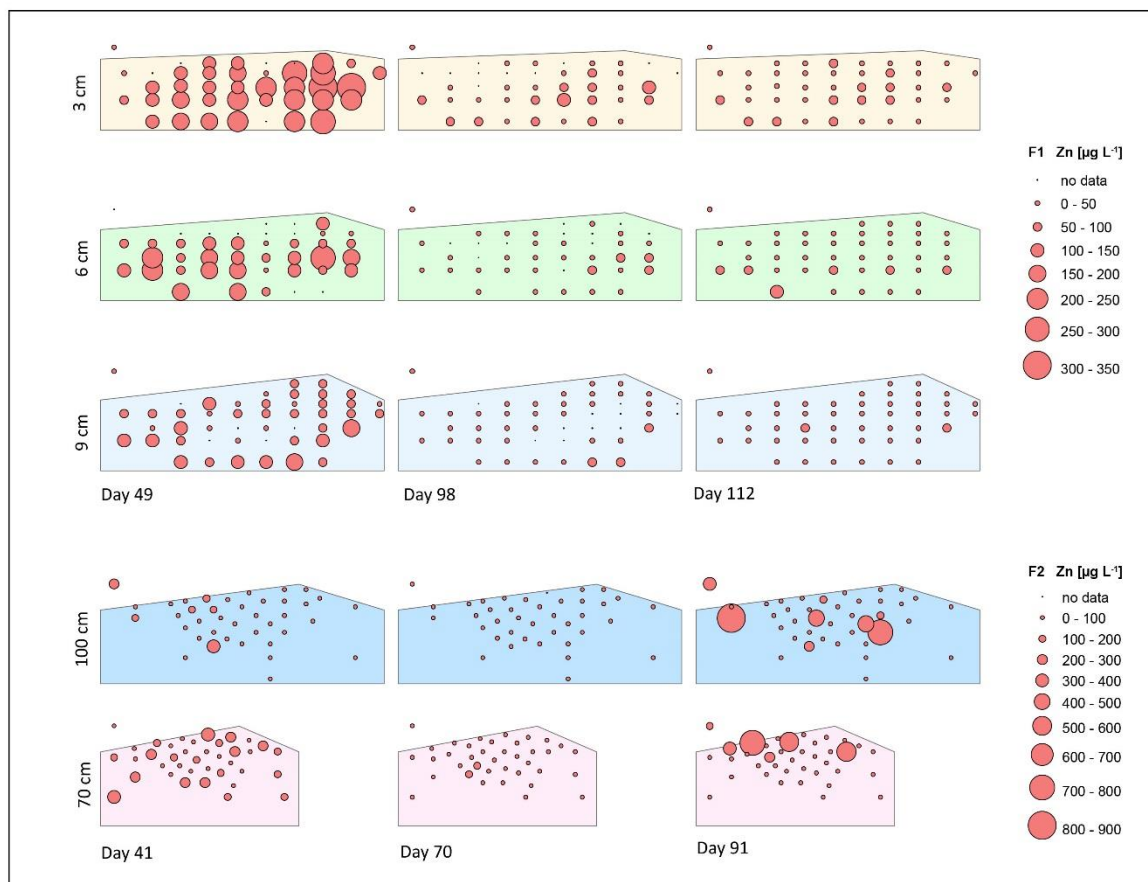
Figure C.16. Aluminum (^{27}Al) concentrations. (Top) Concentrations at rhizon locations; (Bottom) concentrations over elapsed time. All concentrations are [µg L^{-1}].
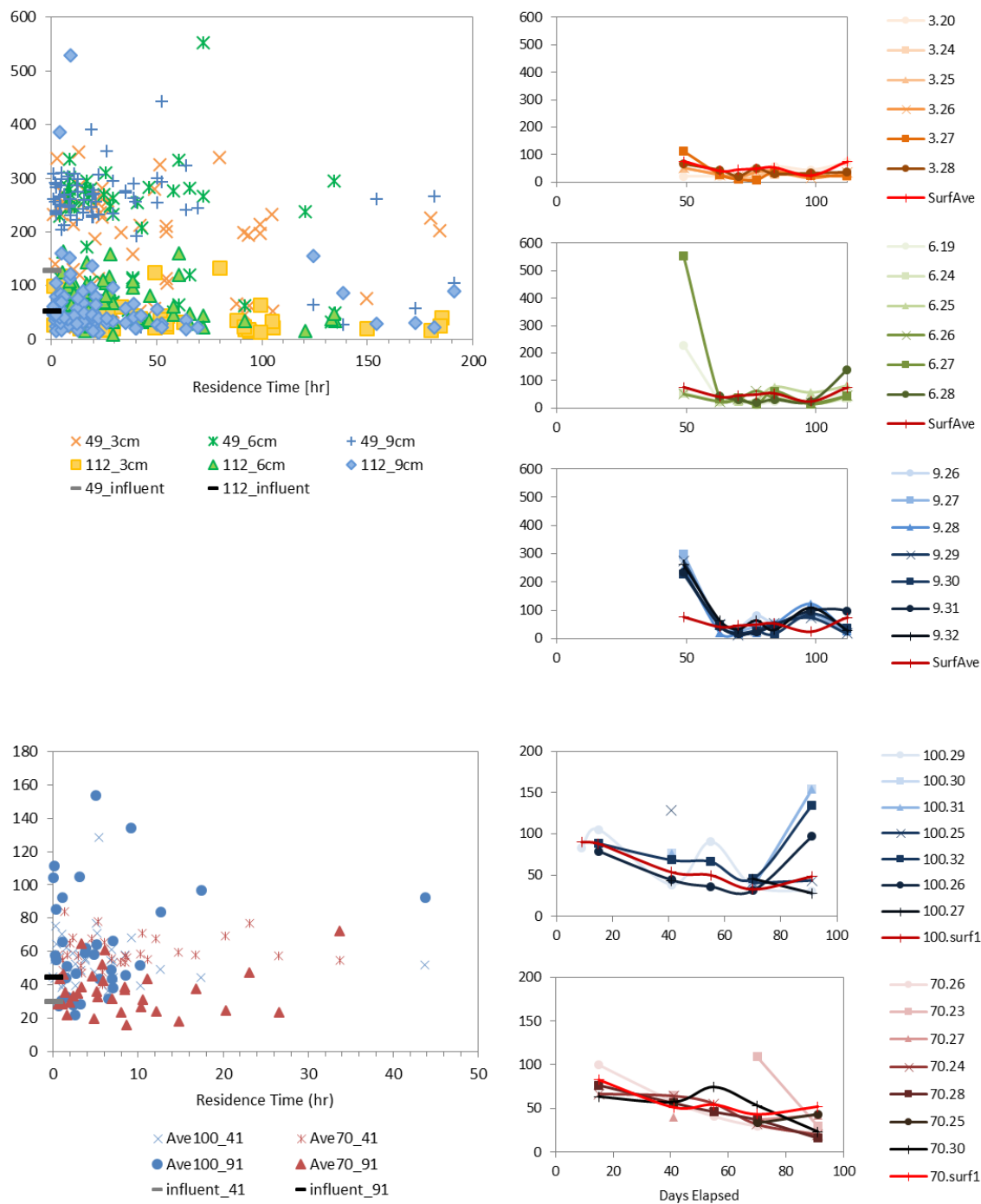
Figure C.16. (cont.) Aluminum (^{27}Al) concentrations. (Left) concentrations versus residence time on days 49 and 112 (F1) and days 41 and 91 (F2); (Right) concentrations over elapsed time at selected locations. All concentrations are [µg L-1].
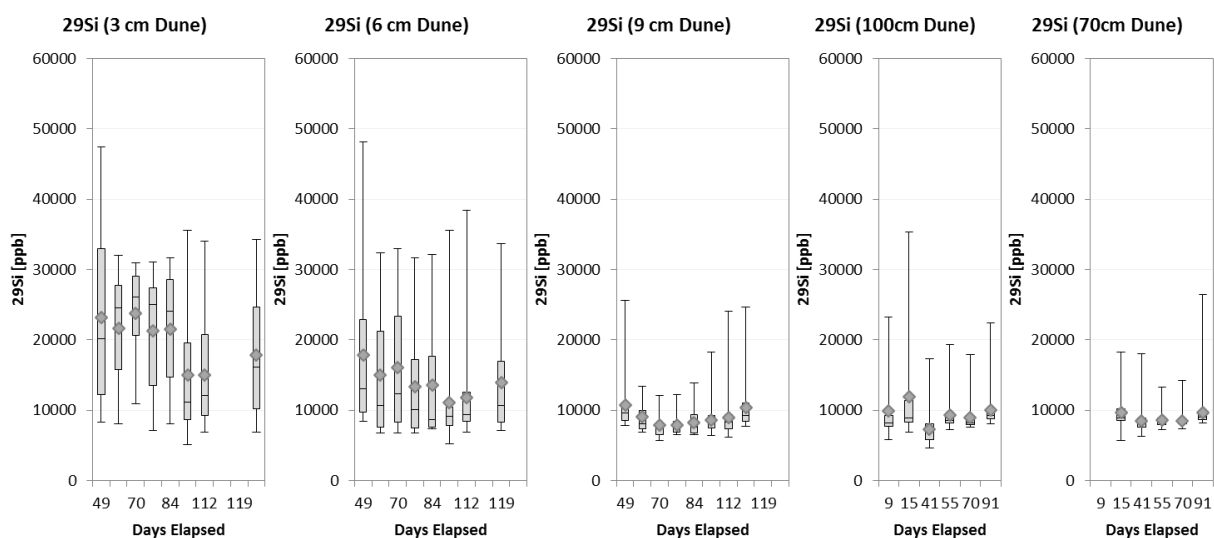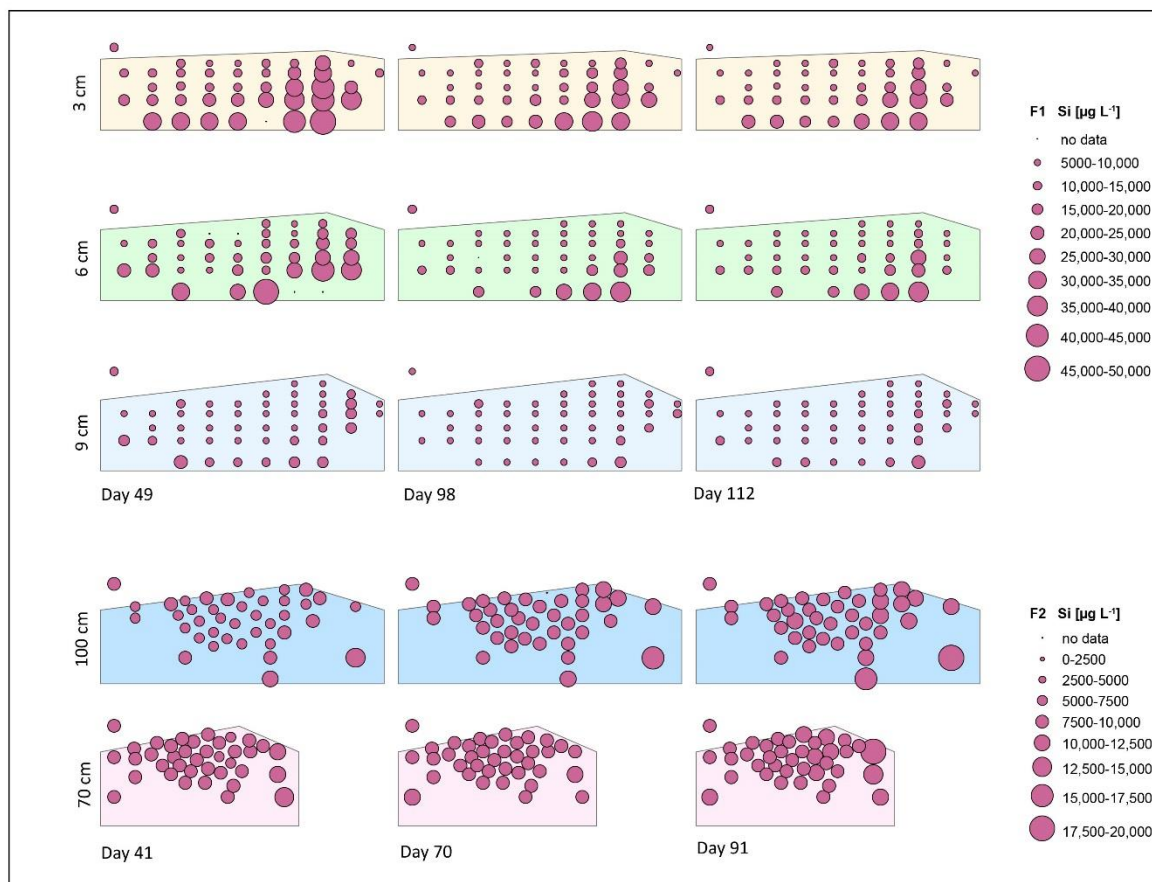
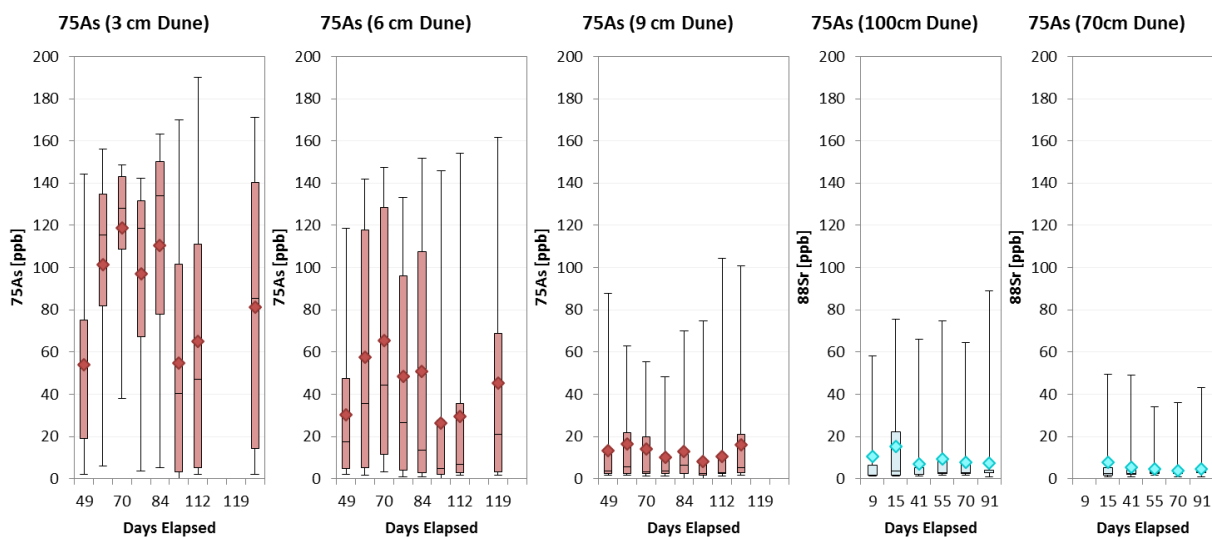**Figure C.17. Silicon (²⁹Si) concentrations.** (Top) Concentrations at rhizon locations; (Bottom) concentrations over elapsed time. All concentrations are [µg L⁻¹].
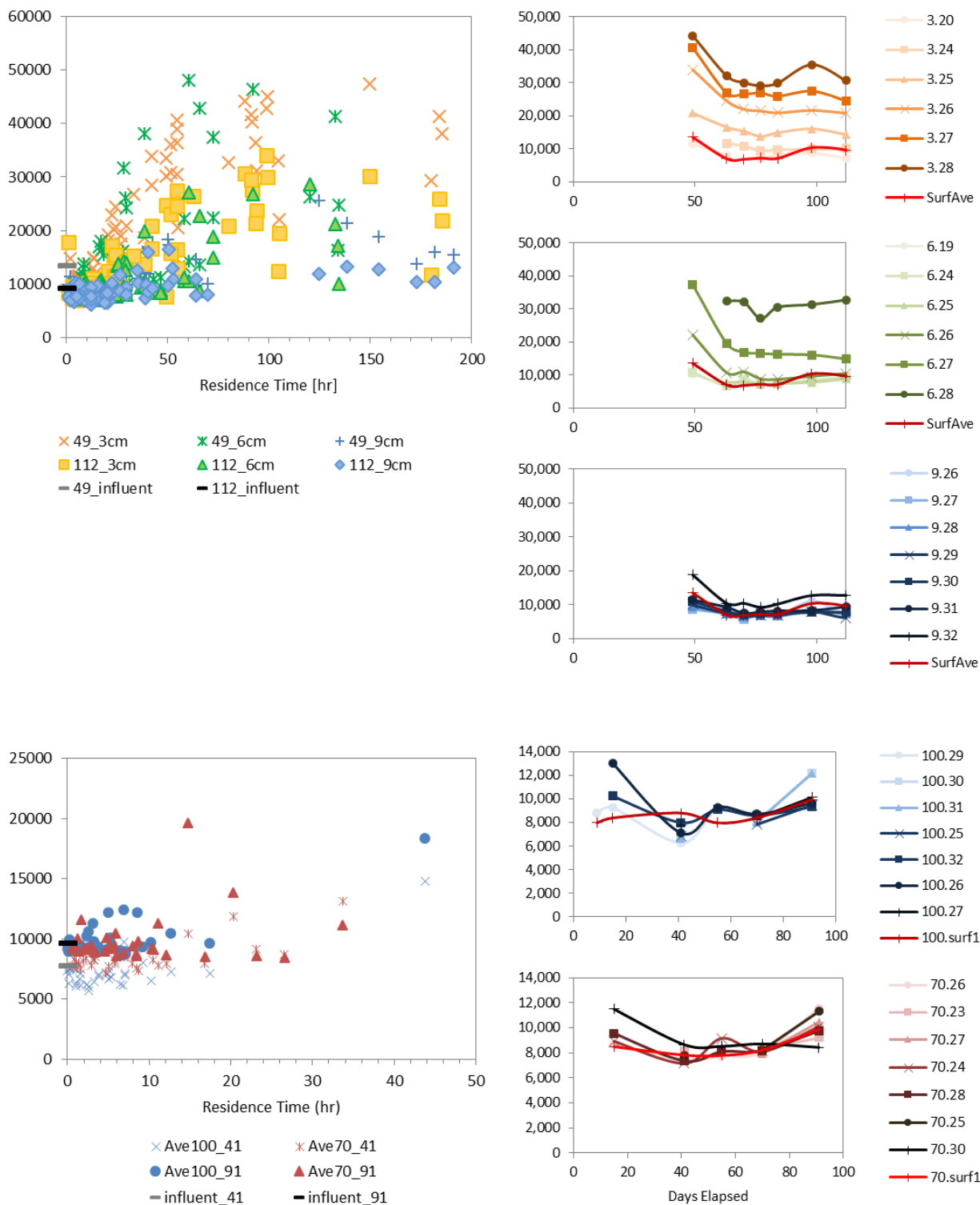
Figure C.17. (cont.) Silicon (29Si) concentrations. (Left) concentrations versus residence time on days 49 and 112 (F1) and days 41 and 91 (F2); (Right) concentrations over elapsed time at selected locations. All concentrations are [µg L-1].
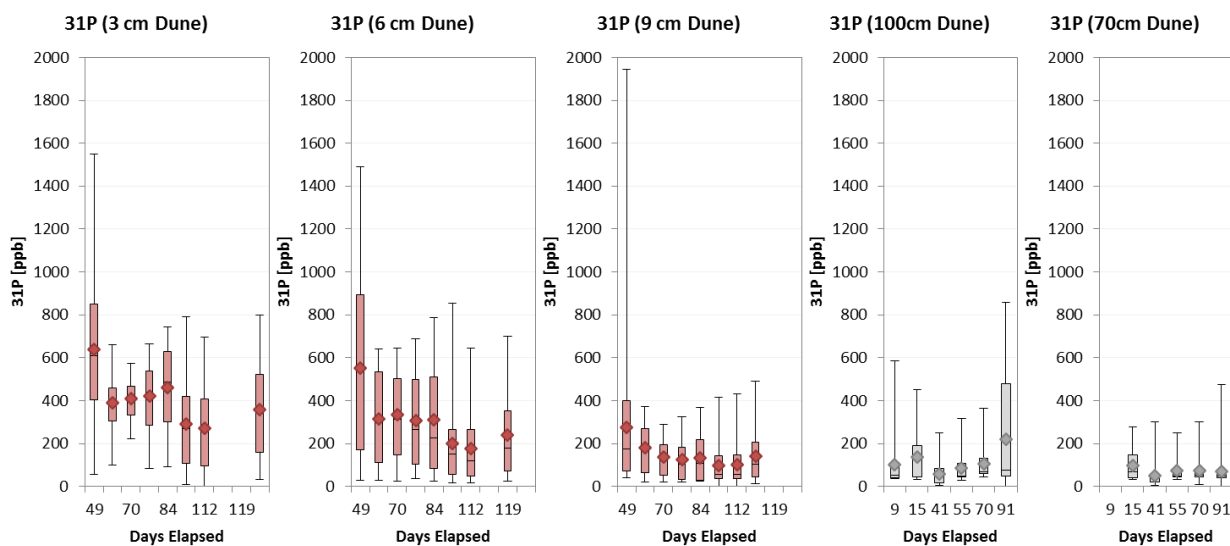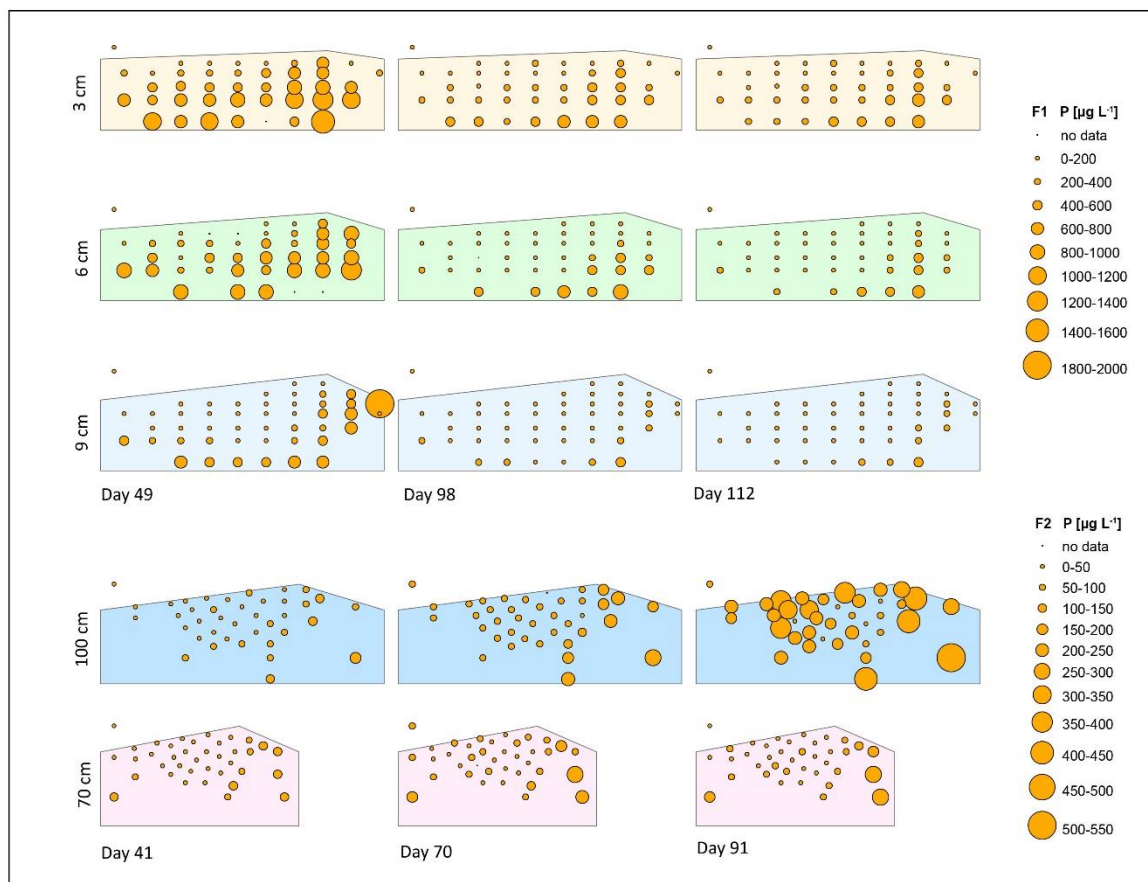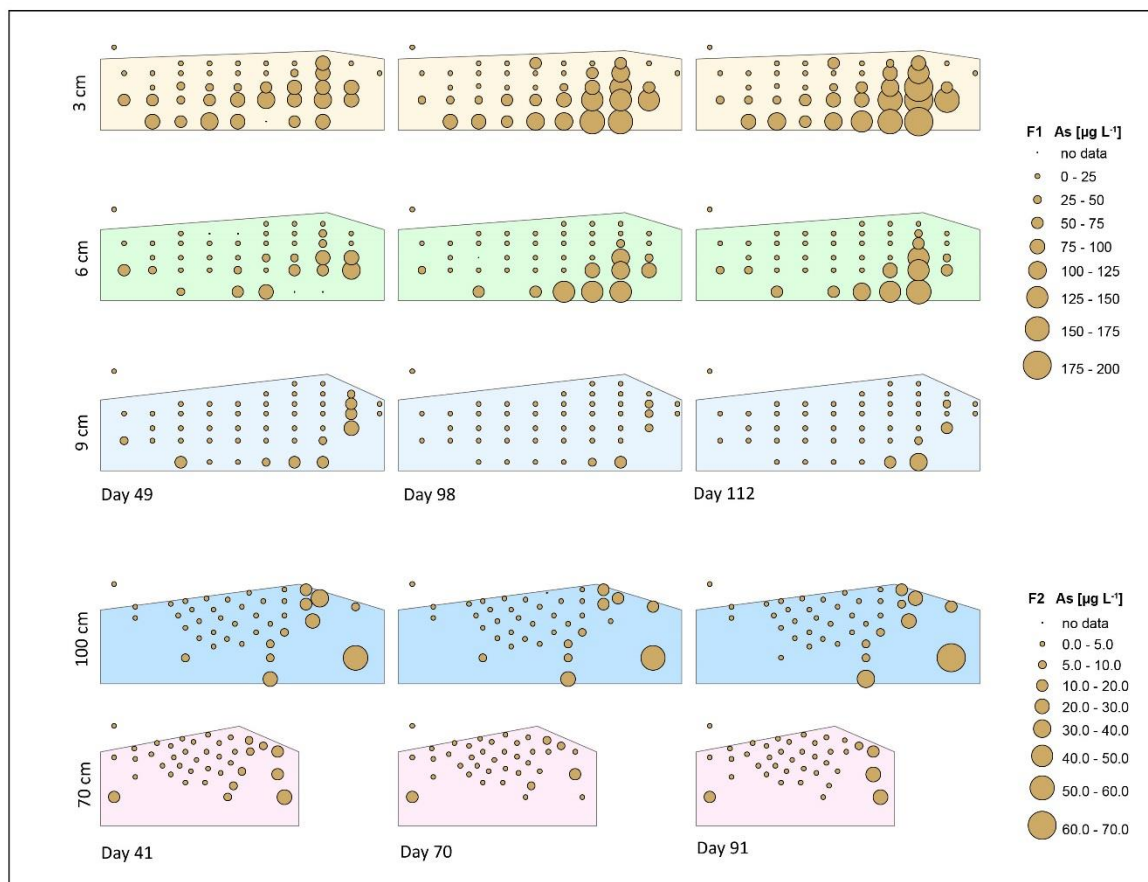
Figure C.18. Phosphorous (^{31}P) concentrations. (Top) Concentrations at rhizon locations; (Bottom) concentrations over elapsed time. All concentrations are [µg L^{-1}].
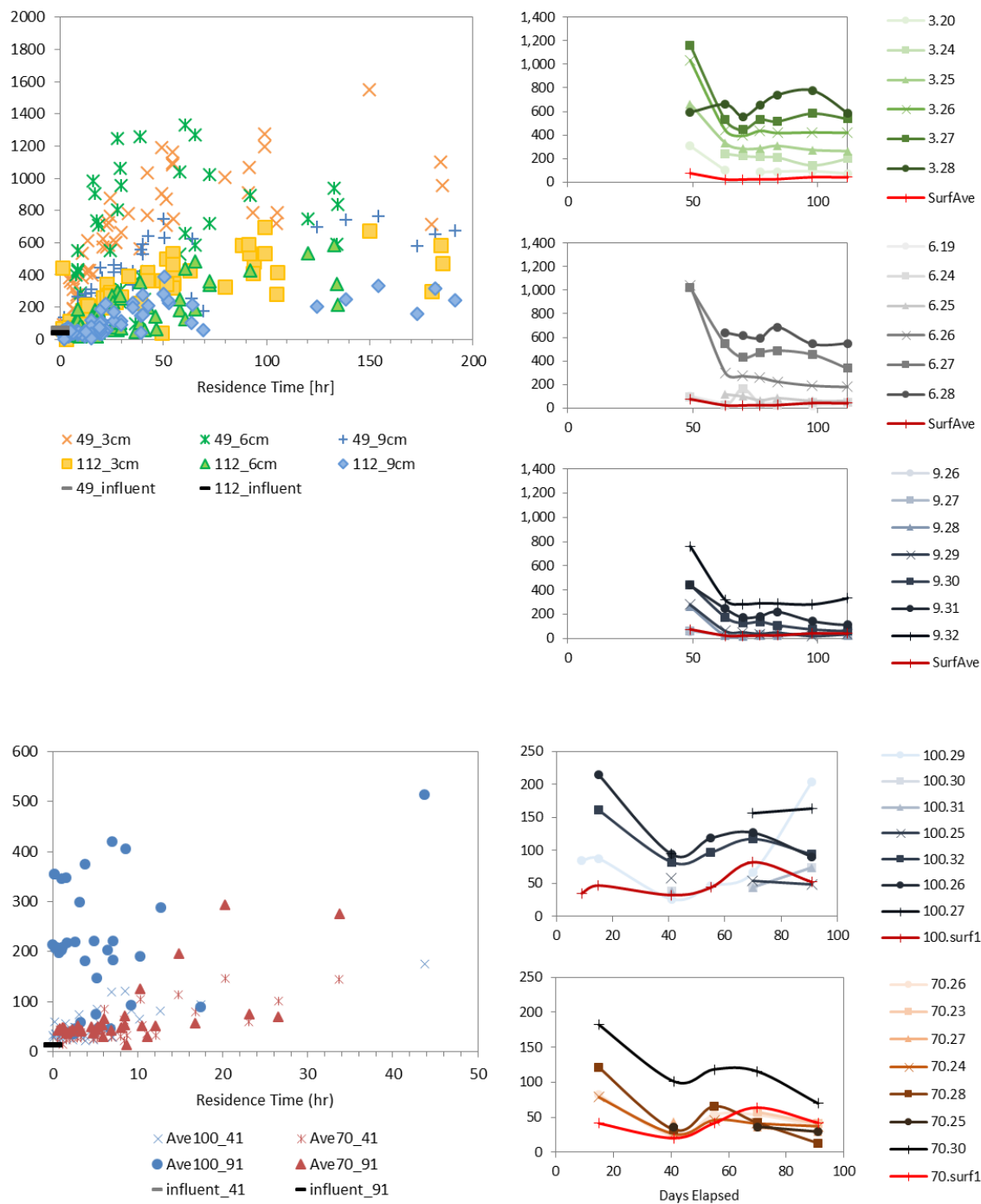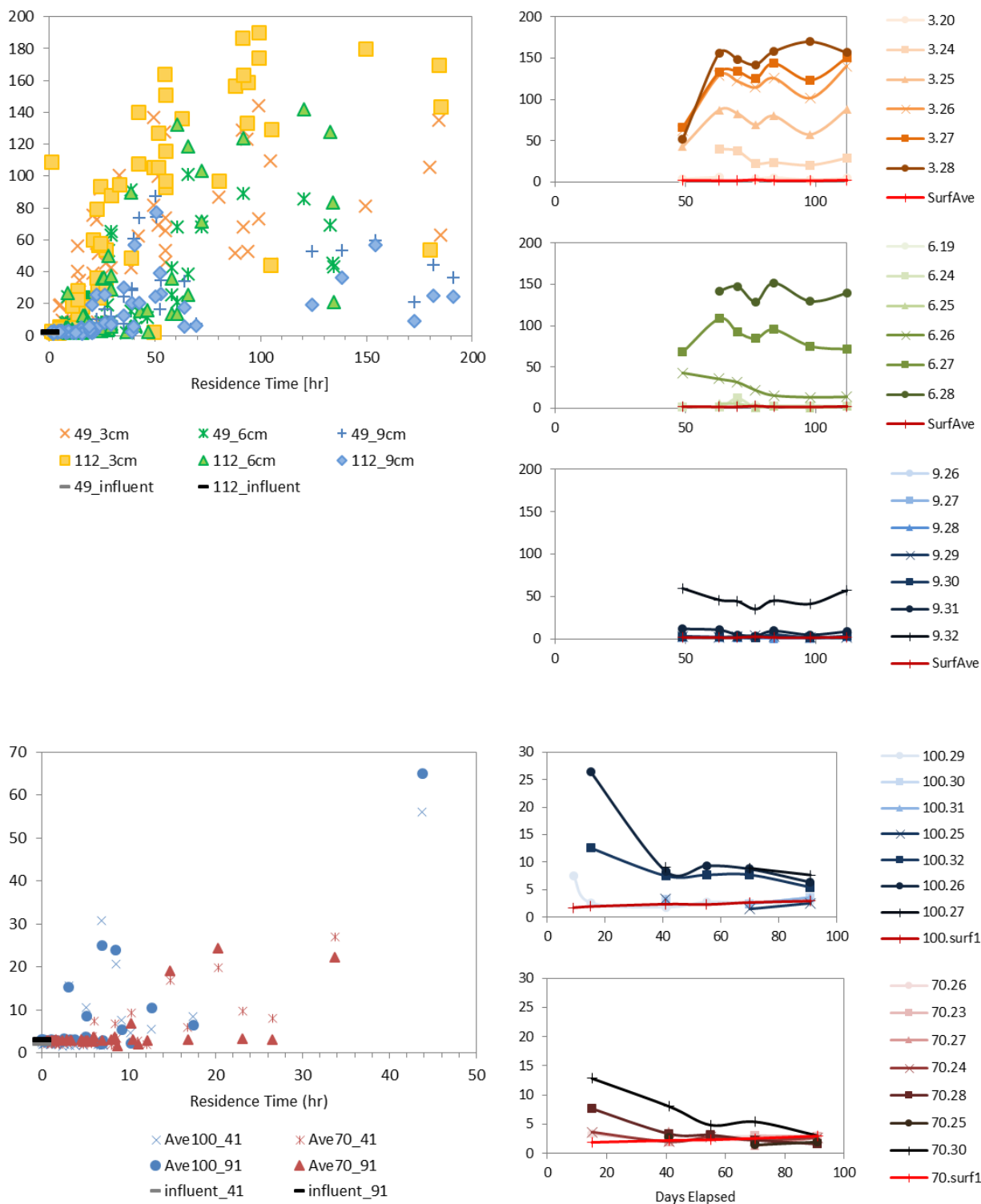
Figure C.18. (cont.) Phosphorous (31P) concentrations. (Left) concentrations versus residence time on days 49 and 112 (F1) and days 41 and 91 (F2); (Right) concentrations over elapsed time at selected locations. All concentrations are [µg L-1].
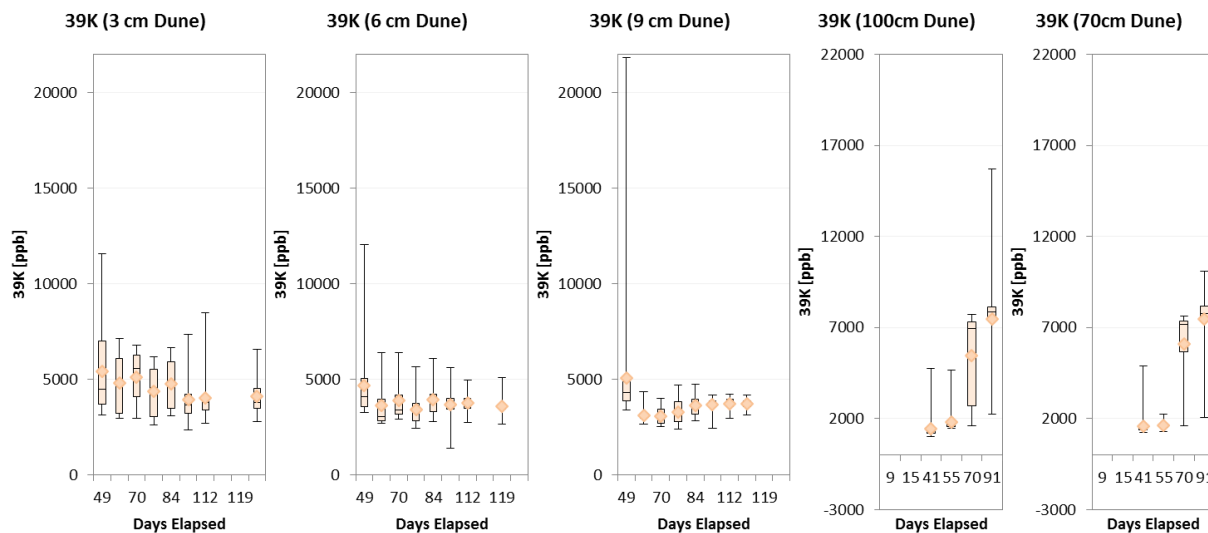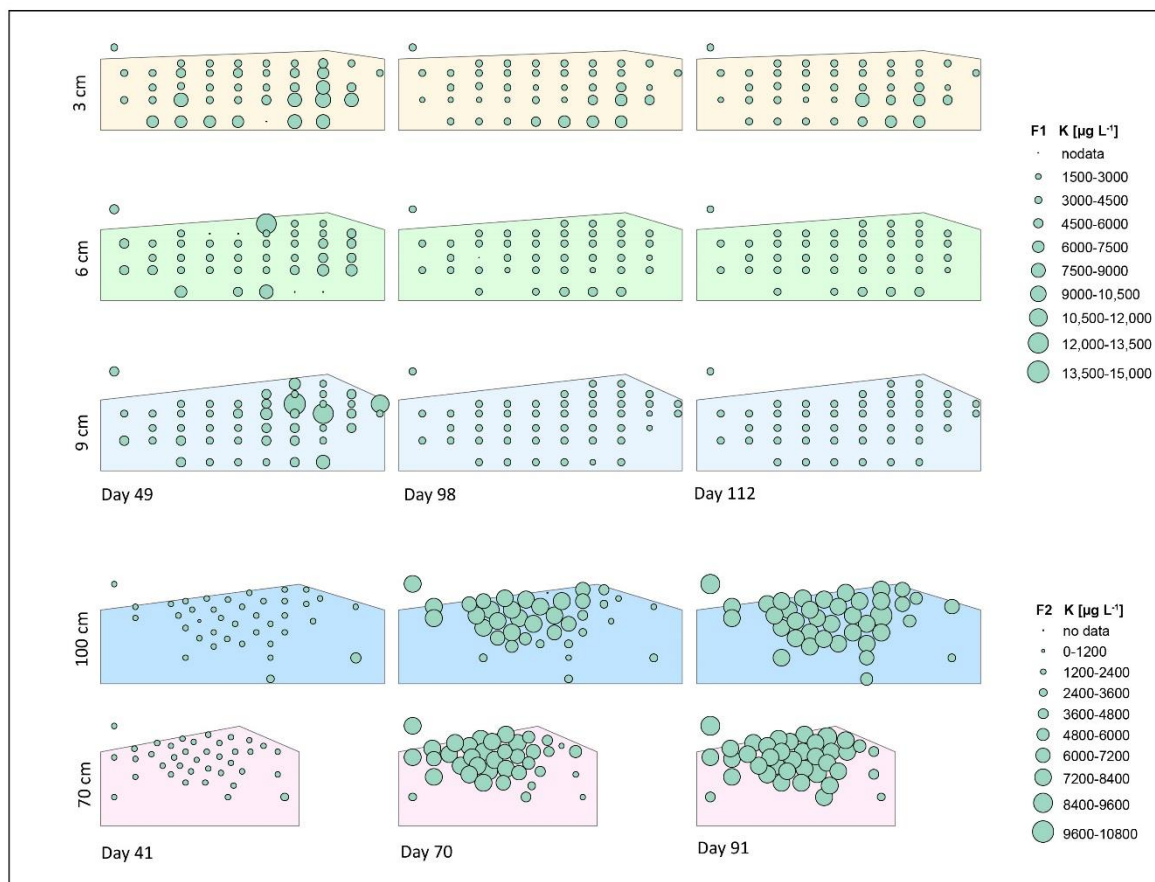
Figure C.19. Potassium (^{39}K) concentrations. (Top) Concentrations at rhizon locations; (Bottom) concentrations over elapsed time. All concentrations are [µg L^{-1}]. KNO^3 was added to the system around day 60 in both experiments.
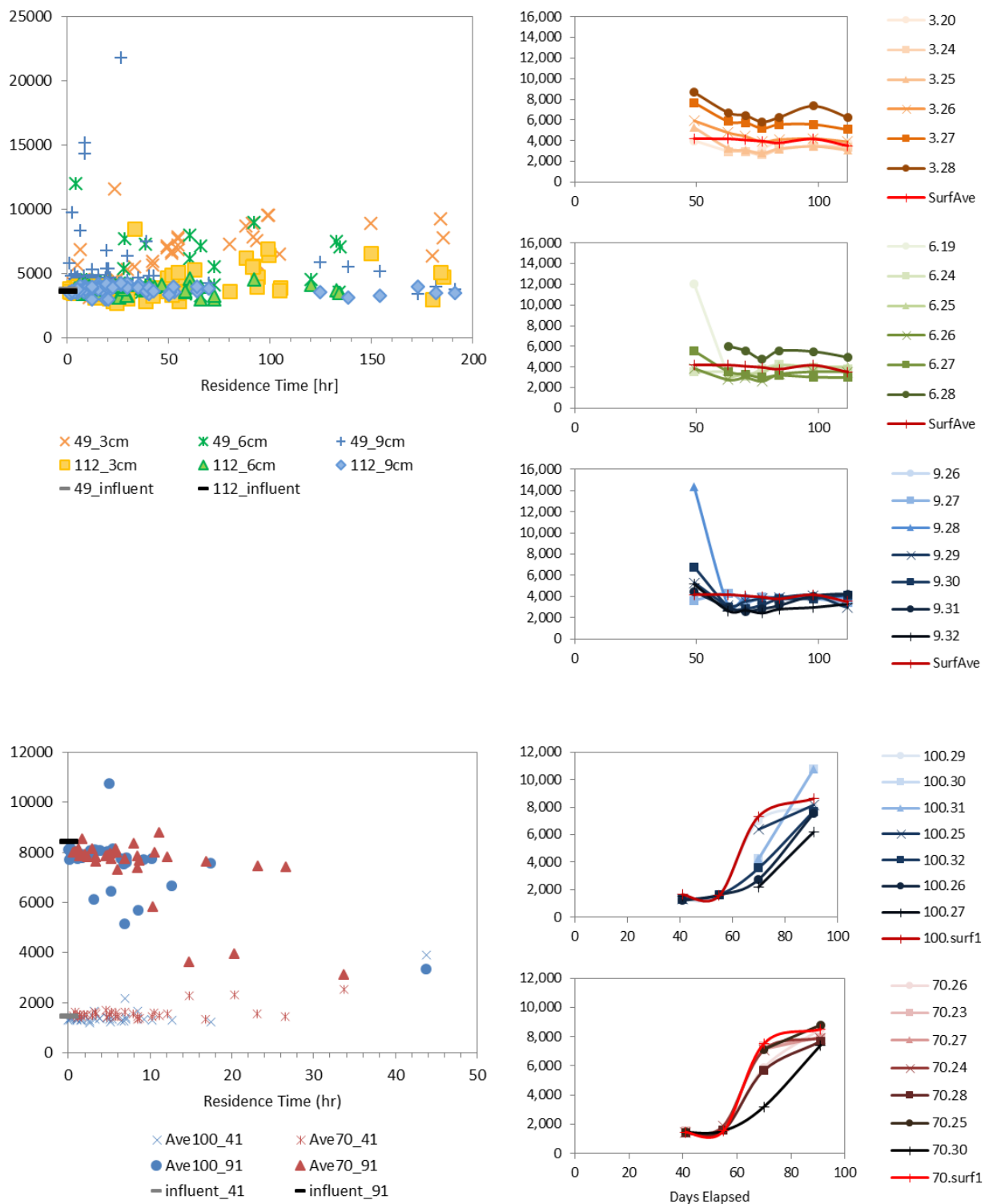
Figure C.19. (cont.) Potassium (^{39}K) concentrations. (Left) concentrations versus residence time on days 49 and 112 (F1) and days 41 and 91 (F2); (Right) concentrations over elapsed 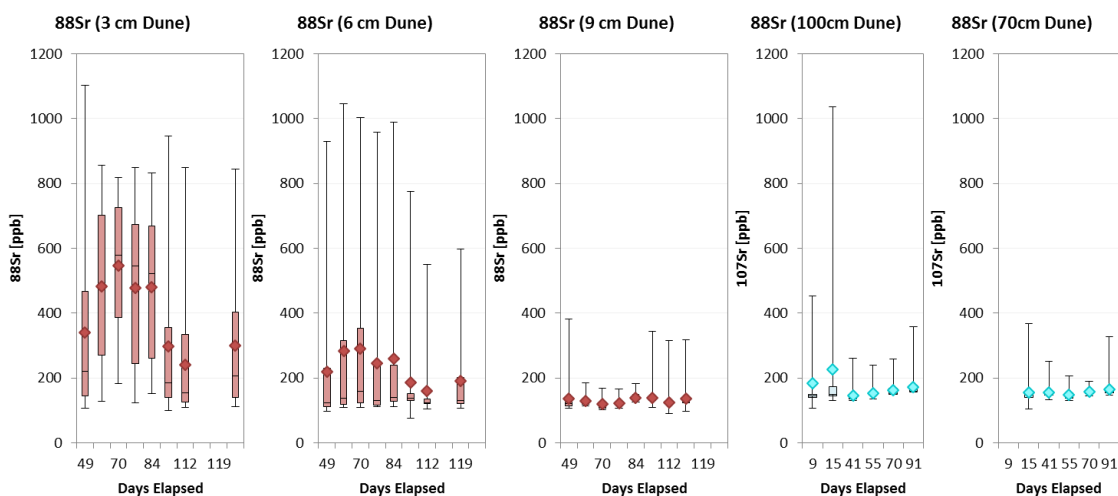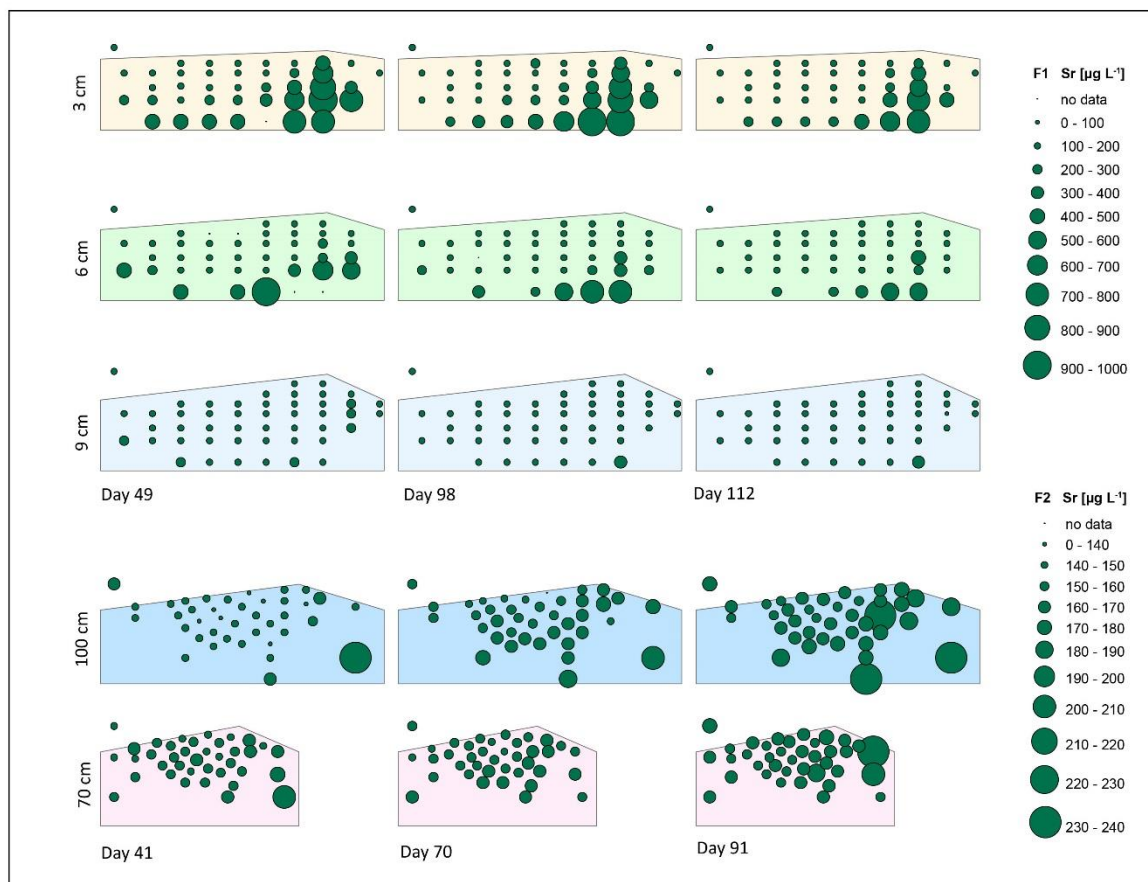time at selected locations. All concentrations are [µg L-1]. KNO3 was added to the system around day 60 in both experiments.
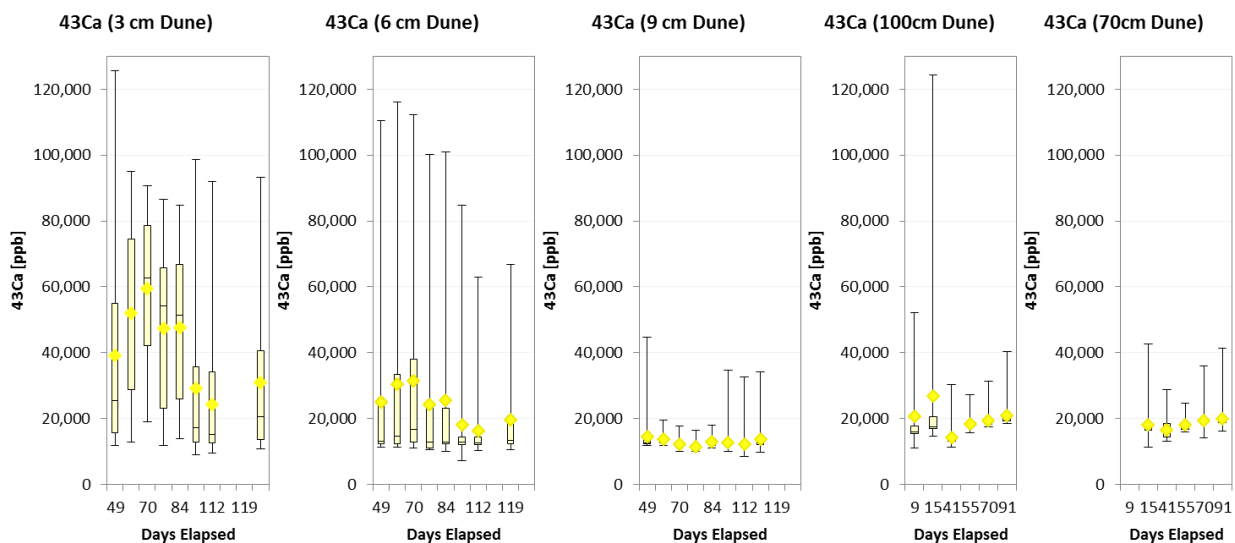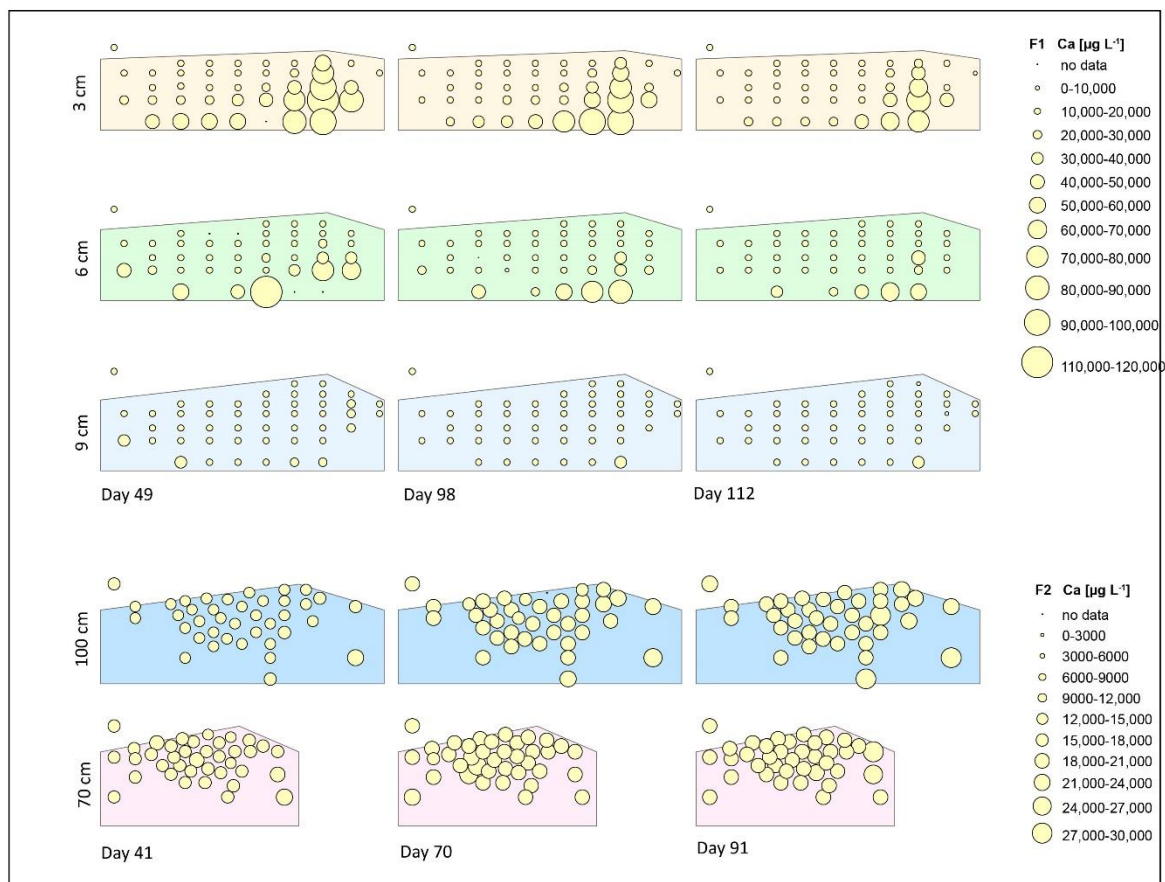
Figure C.20.   Calcium (^{43}Ca) concentrations. (Top) Concentrations at rhizon locations; (Bottom) concentrations over elapsed time. All concentrations are [µg L^{-1}].
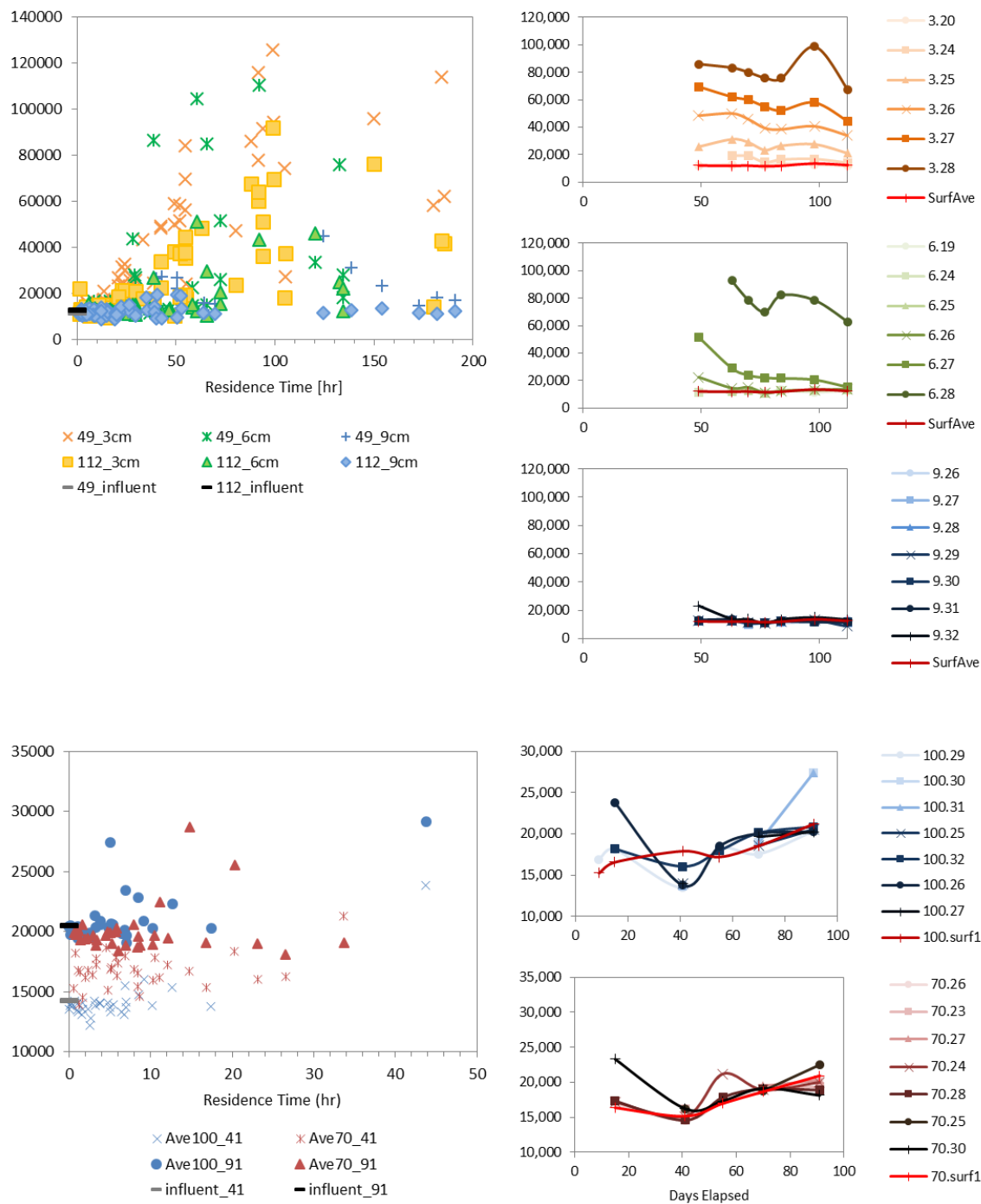
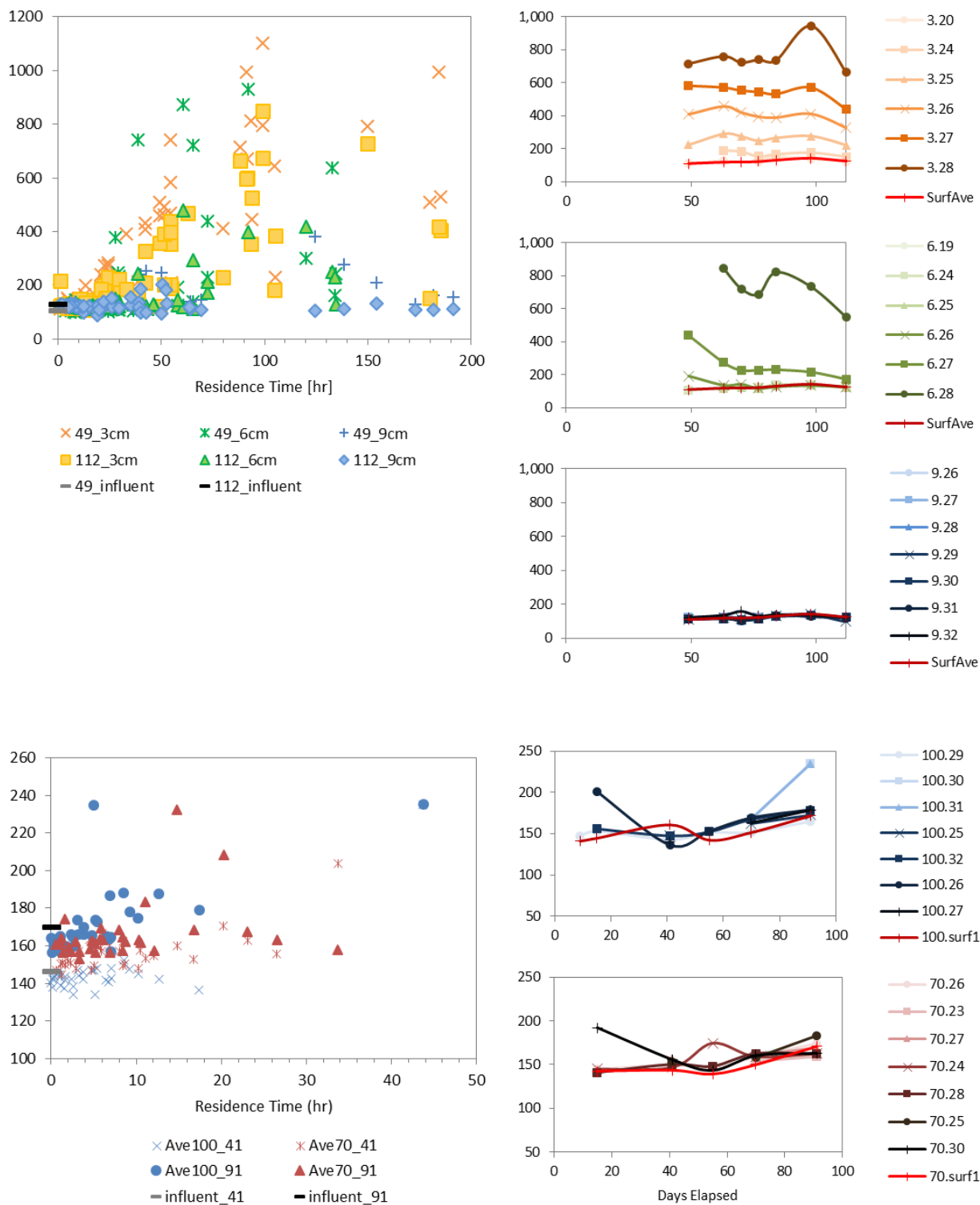**Figure C.20. (cont.) Calcium (^{43}Ca) concentrations.** (Left) concentrations versus residence time on days 49 and 112 (F1) and days 41 and 91 (F2); (Right) concentrations over elapsed time at selected locations. All concentrations are [µg L-1].

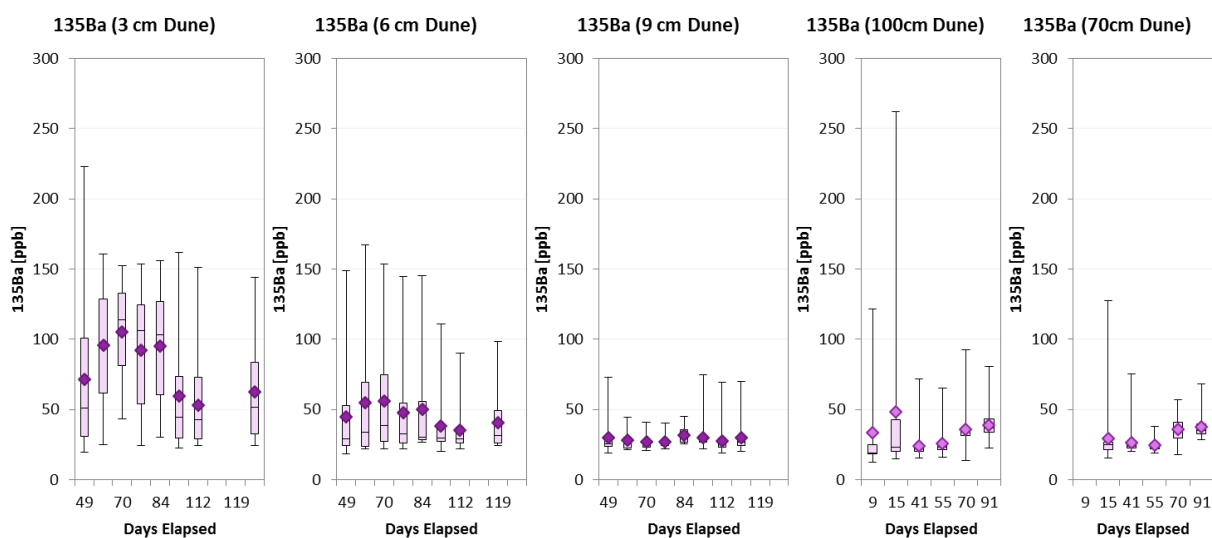**Figure C.21.   Vanadium (^{51}V) concentrations.** (Top) Concentrations at rhizon locations; (Bottom) concentrations over elapsed time. All concentrations are [µg L^{-1}].

Figure C.21. (cont.) Vanadium (^{51}V) concentrations. (Left) concentrations versus residence time on days 49 and 112 (F1) and days 41 and 91 (F2); (Right) concentrations over elapsed time at selected locations. All concentrations are [µg L-1].

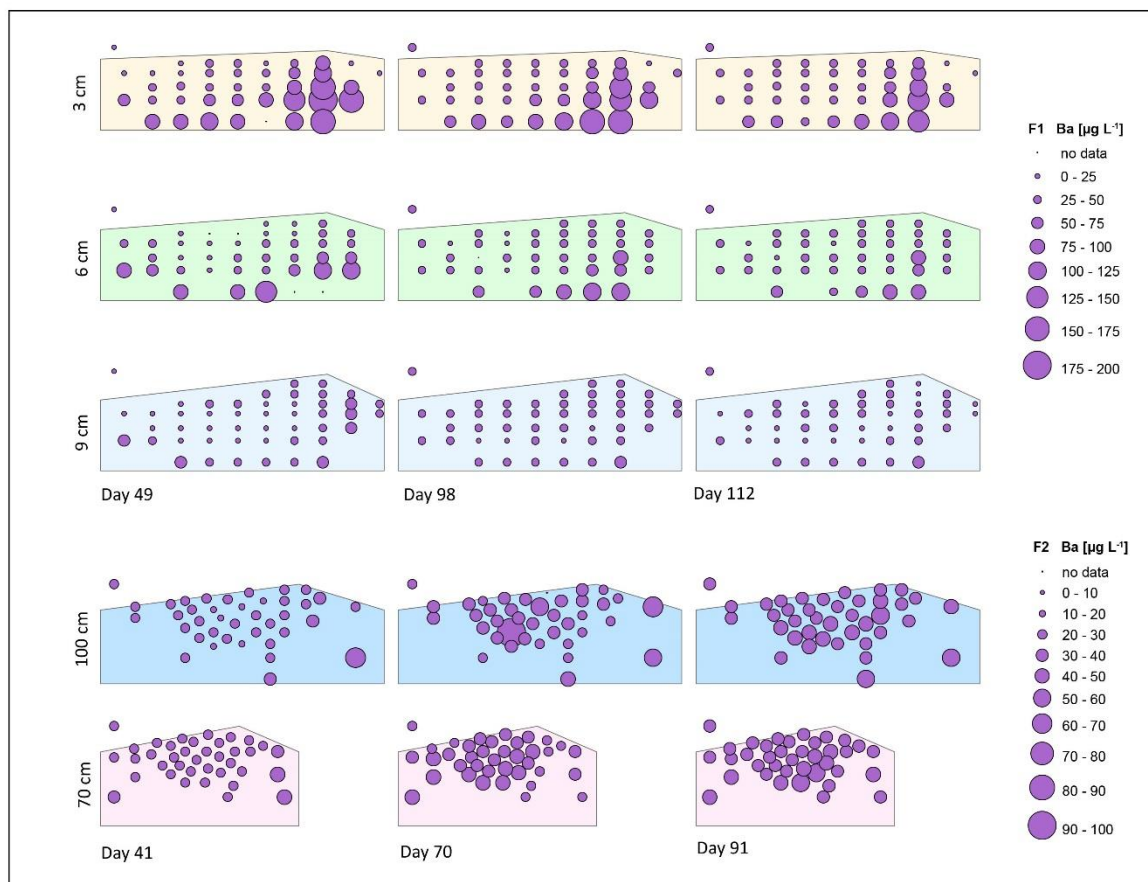**Figure C.22. Manganese (^{55}Mn) concentrations.** (Top) Concentrations at rhizon locations; (Bottom) concentrations over elapsed time. All concentrations are [µg L^{-1}].

Figure C.22. (cont.) Manganese (^{55}Mn) concentrations. (Left) concentrations versus residence time on days 49 and 112 (F1) and days 41 and 91 (F2); (Right) concentrations over elapsed time at selected locations. All concentrations are [µg L-1].
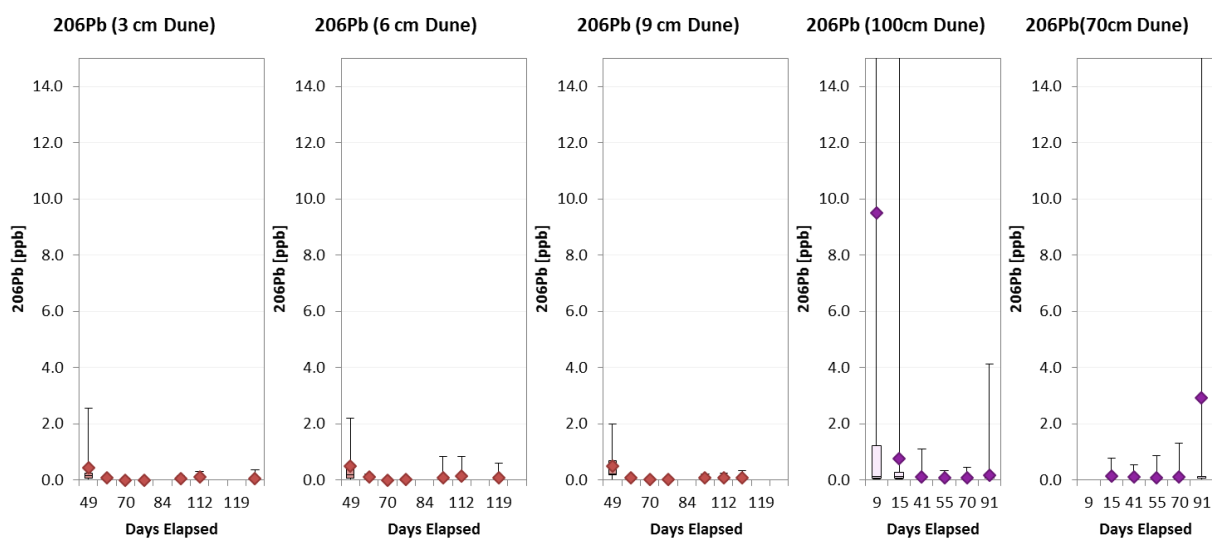
Figure C.23. Iron (^{57}Fe) concentrations. (Top) Concentrations at rhizon locations; (Bottom) concentrations over elapsed time. All concentrations are [µg L^{-1}].

Figure C.23. (cont.)   Iron (^{57}Fe) concentrations. (Left) concentrations versus residence time on days 49 and 112 (F1) and days 41 and 91 (F2); (Right) concentrations over elapsed time at selected locations. All concentrations are [µg L-1].

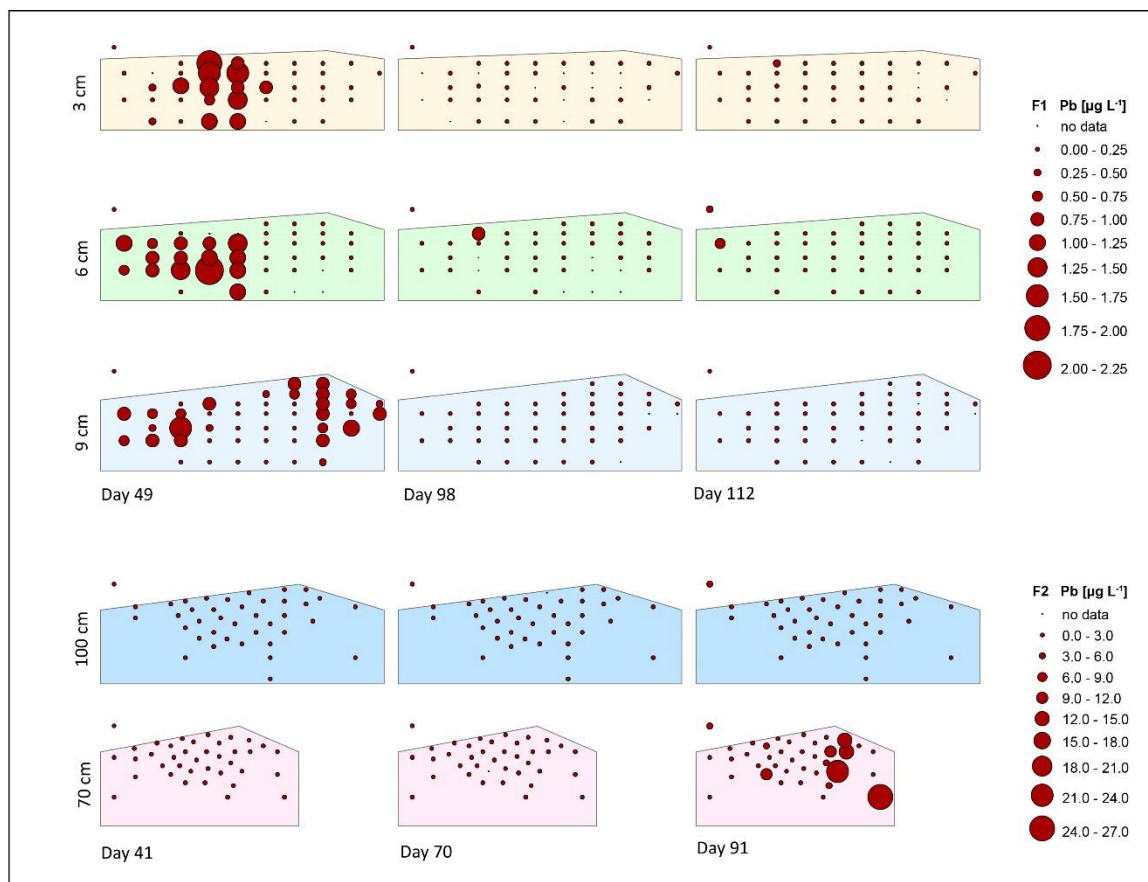**Figure C.24. Cobalt (^{59}Co) concentrations.** (Top) Concentrations at rhizon locations; (Bottom) concentrations over elapsed time. All concentrations are [µg L^{-1}].
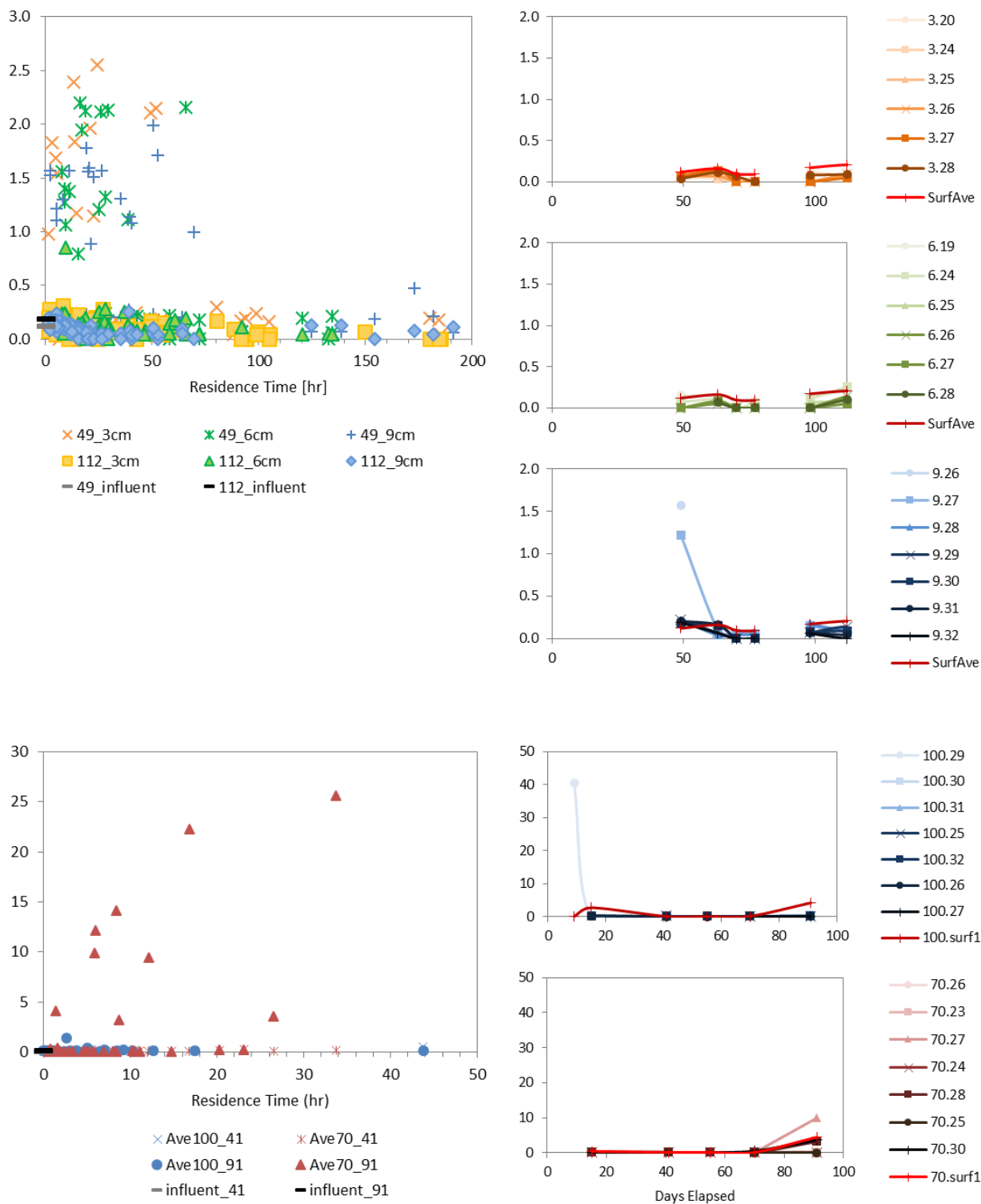
Figure C.24. (cont.) Cobalt (^{59}Co) concentrations. (Left) concentrations versus residence time on days 49 and 112 (F1) and days 41 and 91 (F2); (Right) concentrations over elapsed time at selected locations. All concentrations are [µg L-1].

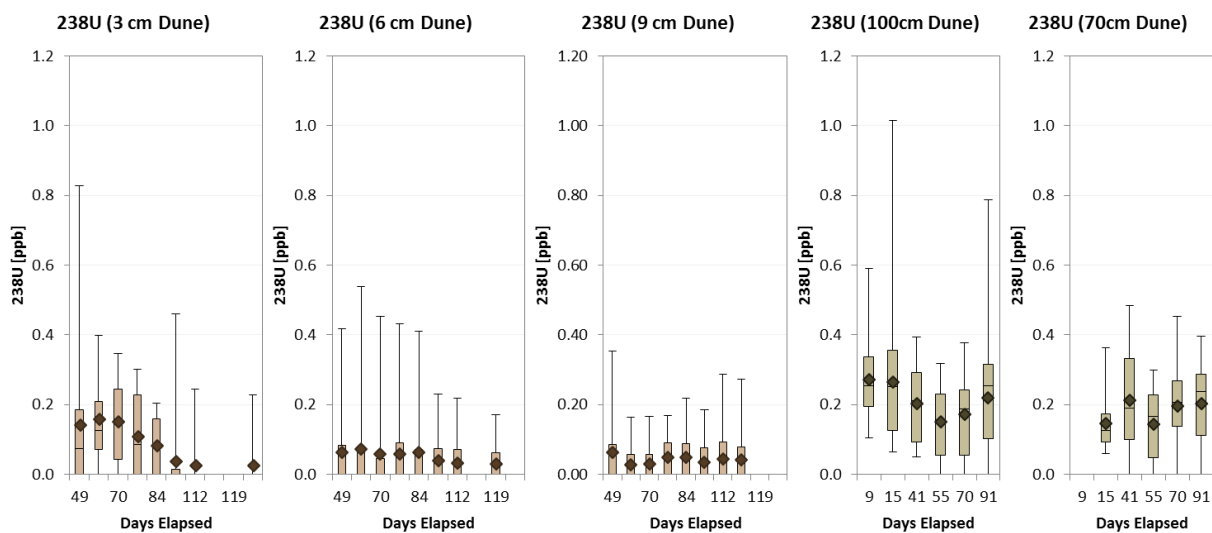**Figure C.25. Nickel (^{61}Ni) concentrations.** (Top) Concentrations at rhizon locations; (Bottom) concentrations over elapsed time. All concentrations are [µg L^{-1}].

Figure C.25. (cont.) Nickel (⁶¹Ni) concentrations. (Left) concentrations versus residence time on days 49 and 112 (F1) and days 41 and 91 (F2); (Right) concentrations over elapsed time at selected locations. All concentrations are [µg L-1].

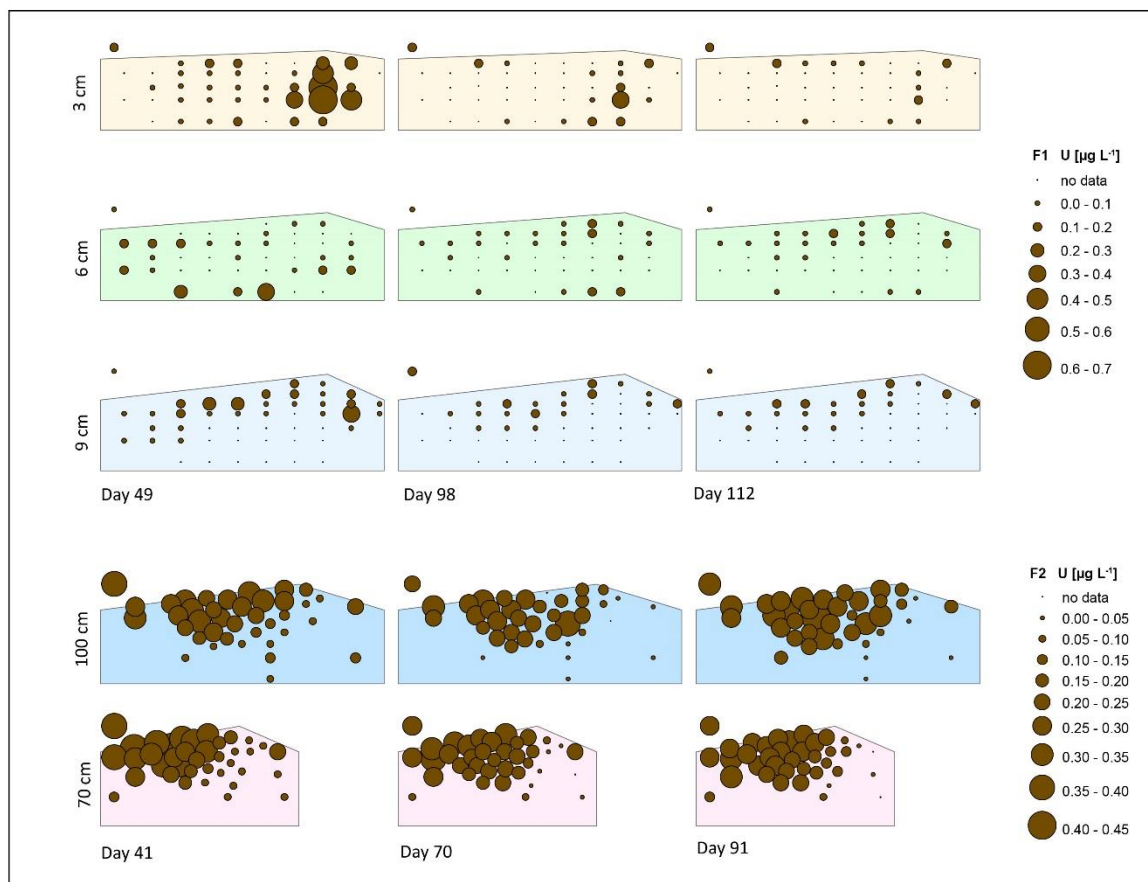**Figure C.26. Copper (^{65}Cu) concentrations.** (Top) Concentrations at rhizon locations; (Bottom) concentrations over elapsed time. All concentrations are [µg L^{-1}].
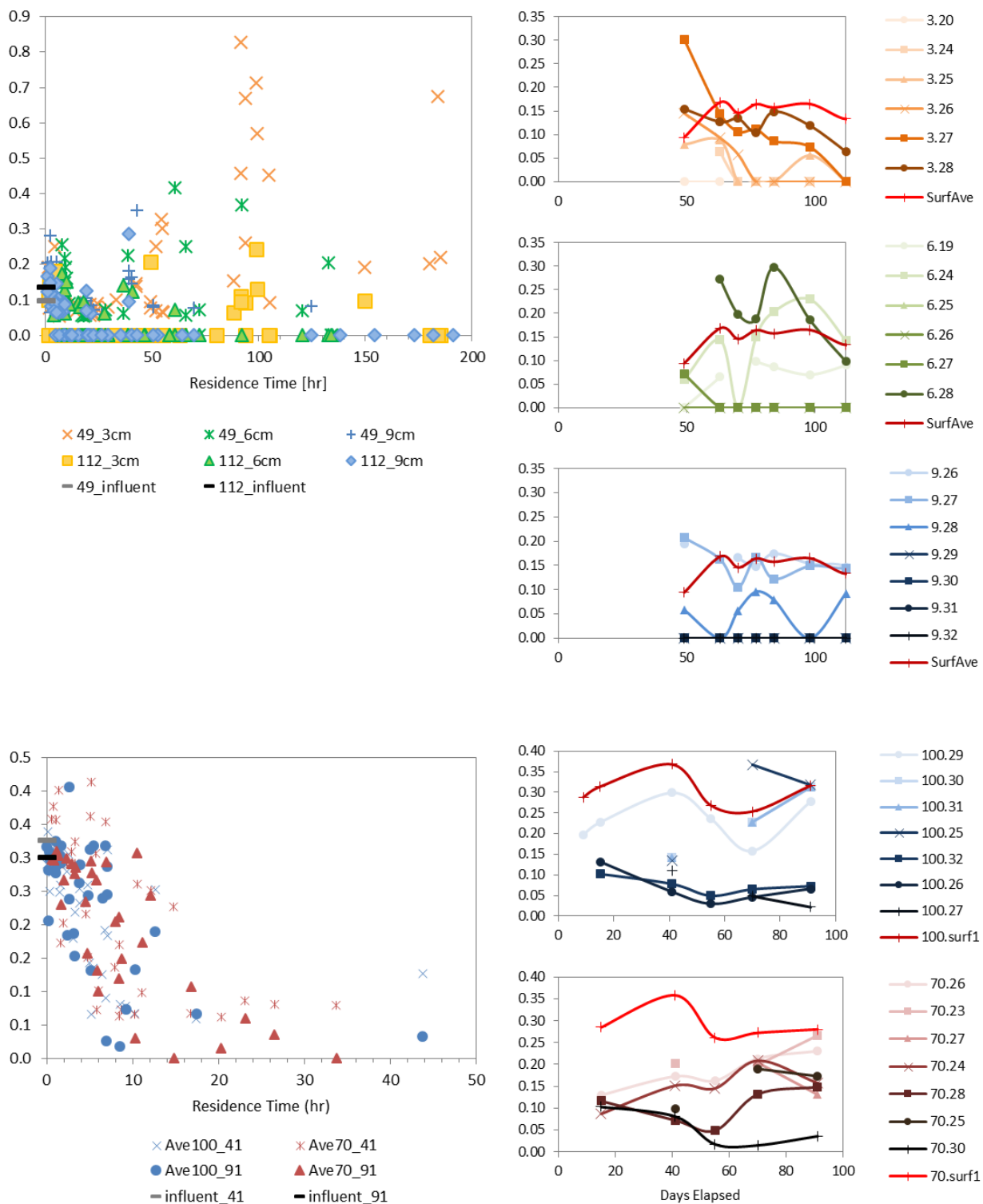
Figure C.26. (cont.) Copper (^{65}Cu) concentrations. (Left) concentrations versus residence time on days 49 and 112 (F1) and days 41 and 91 (F2); (Right) concentrations over elapsed time at selected locations. All concentrations are [µg L-1].

Figure C.27. Zinc (^{66}Zn) concentrations. (Top) Concentrations at rhizon locations; (Bottom) concentrations over elapsed time. All concentrations are [µg L^{-1}].

Figure C.27. (cont.)   Zinc (^{66}Zn) concentrations. (Left) concentrations versus residence time on days 49 and 112 (F1) and days 41 and 91 (F2); (Right) concentrations over elapsed time at selected locations. All concentrations are [µg L-1].

Figure C.28. Arsenic (^{75}As) concentrations. (Top) Concentrations at rhizon locations; (Bottom) concentrations over elapsed time. All concentrations are [µg L^{-1}].

Figure C.28. (cont.) Arsenic (^{75}As) concentrations. (Left) concentrations versus residence time on days 49 and 112 (F1) and days 41 and 91 (F2); (Right) concentrations over elapsed time at selected locations. All concentrations are [µg L-1].

Figure C.29. Strontium (^{88}Sr) concentrations. (Top) Concentrations at rhizon locations; (Bottom) concentrations over elapsed time. All concentrations are [µg L^{-1}].

Figure C.29. (cont.) Strontium (88Sr) concentrations. (Left) concentrations versus residence time on days 49 and 112 (F1) and days 41 and 91 (F2); (Right) concentrations over elapsed time at selected locations. All concentrations are [µg L-1].

Figure C.30. Barium (¹³⁵Ba) concentrations. (Top) Concentrations at rhizon locations; (Bottom) concentrations over elapsed time. All concentrations are [µg L⁻¹].

Figure C.30. (cont.) Barium (^{135}Ba) concentrations. (Left) concentrations versus residence time on days 49 and 112 (F1) and days 41 and 91 (F2); (Right) concentrations over elapsed time at selected locations. All concentrations are [µg L-1].

Figure C.31. Lead (^{206}Pb) concentrations. (Top) Concentrations at rhizon locations; (Bottom) concentrations over elapsed time. All concentrations are [µg L^{-1}].

Figure C.31. (cont.) Lead (^{206}Pb) concentrations. (Left) concentrations versus residence time on days 49 and 112 (F1) and days 41 and 91 (F2); (Right) concentrations over elapsed time at selected locations. All concentrations are [µg L-1].

Figure C.32. Uranium (^{238}U) concentrations. (Top) Concentrations at rhizon locations; (Bottom) concentrations over elapsed time. All concentrations are [µg L^{-1}].

Figure C.32. (cont.) Uranium (^{238}U) concentrations. (Left) concentrations versus residence time on days 49 and 112 (F1) and days 41 and 91 (F2); (Right) concentrations over elapsed time at selected locations. All concentrations are [µg L-1].
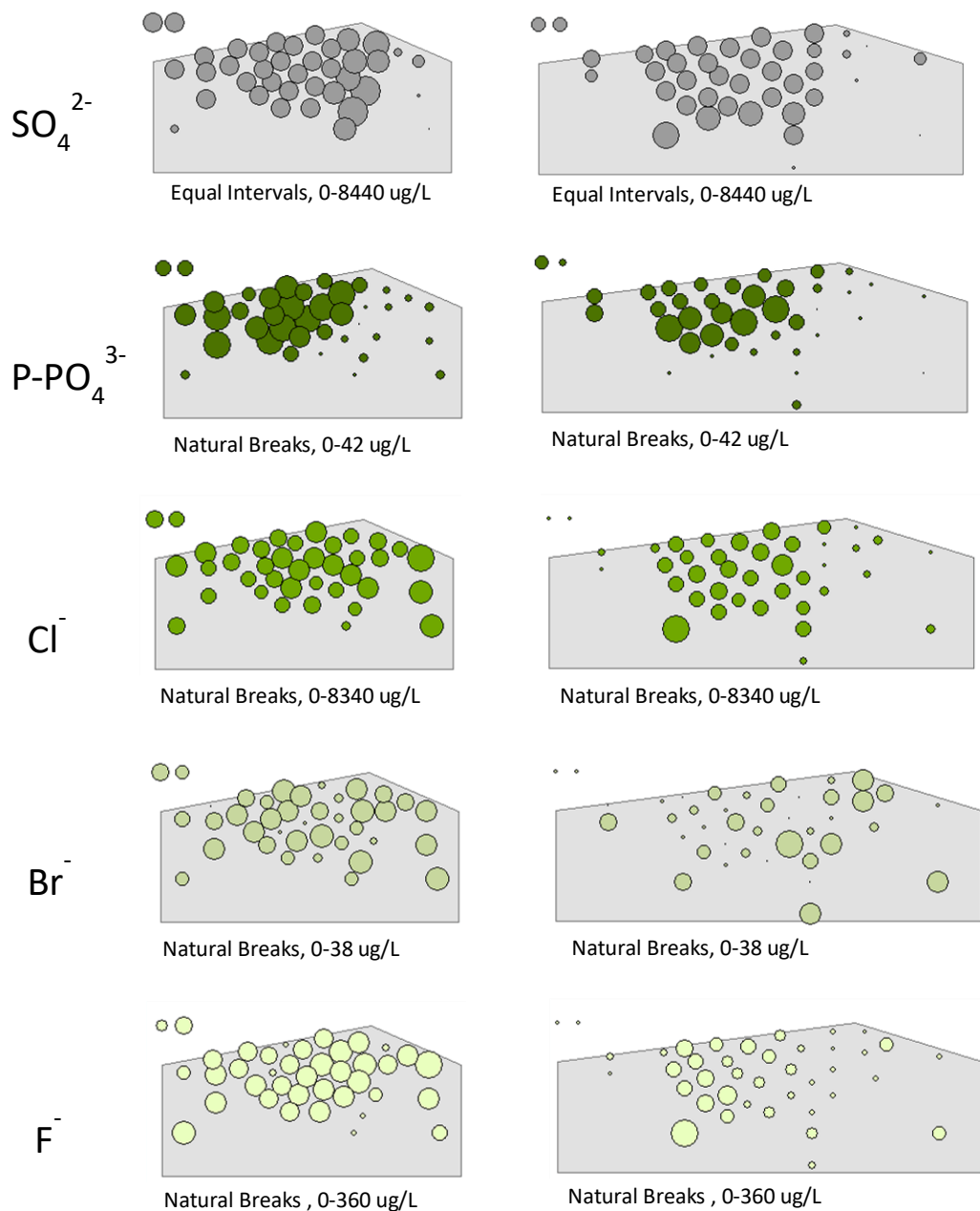
Figure C.33. Bubble plots of anion concentrations in F2. The measurements are the averages of three replicates for the 70 cm dunes (left) and 100 cm dunes (right) on day 92 of F2. Surface water flow is from left to right. The bubbles about the dune outline show surface water concentrations. All concentrations are [$\mu g\ L^{-1}$].
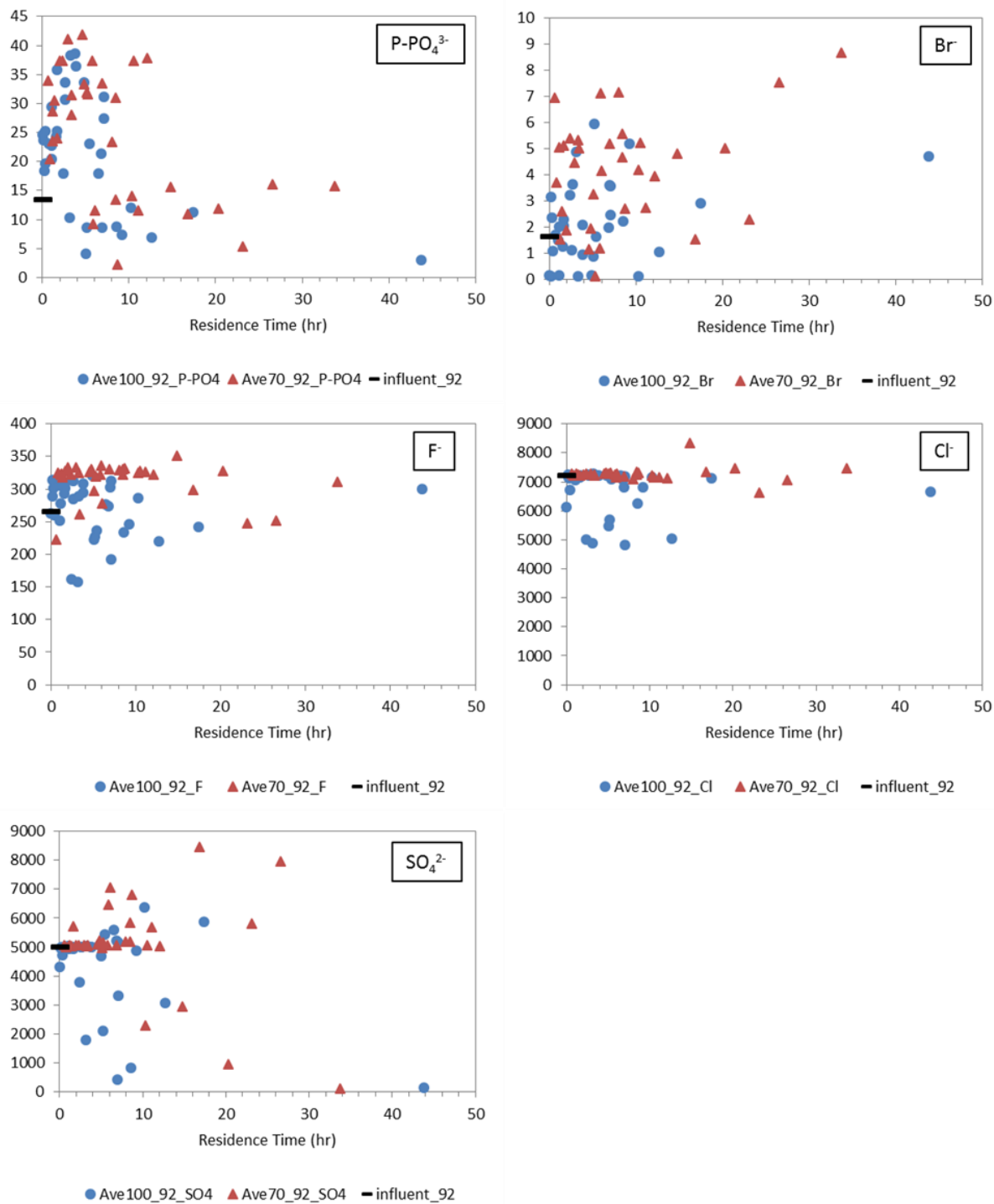
Figure C.34.   Anion concentrations versus residence time in F2. The measurements are the averages of three replicates for the 70 cm dunes (red triangle symbols) and 100 cm dunes (blue circle symbols) on day 92 of F2. All concentrations are [μg L^{-1}].

C.5 Total Carbon

Total carbon was measured at the conclusion of the first flume experiment, prior to the second experiment, and on days 62 and 99/100 in F2. Samples were ground on a ball mill for 48 hours and then dried in a 50C over overnight. Approximately 55 mg of each sample was packed into 5 x 9 mm aluminum tins. Samples were then analyzed for percent carbon and nitrogen using a Thermo Electron Flash EA 1112 CN analyzer (CE Elantech, Inc., Lakewood, New Jersey). Measurements are shown in Figure C.35.

While total carbon was not measured prior to F1, an initial total C value can be estimated by adding the % carbon in the sand purchased from the quarry (0.033%) and the carbon contributed by POM. The sand mixture in the flume was calculated to have 0.15% POM, which was 47% C, resulting in an overall contribution of 0.072% C. We can roughly estimate the original carbon in F1 to be 0.105%. As shown in Figure C.35, panel A, the carbon was lower at the end of the experiment, with the lowest values in the steepest, higher velocity 9 cm dune.

The total carbon in the sand before after F2 is shown in Figure C.35, panel B. The was not much difference in the total % C between the two dunes at the end of the experiment, but we did observe that more carbon remained in the sand on the downstream sides of the dune troughs. This supports the conclusion that aerobic respiration consumed more carbon on the upstream side of the dune. In both experiments, the carbon content was also found to be high in the precipitate crust on the downstream dune face.
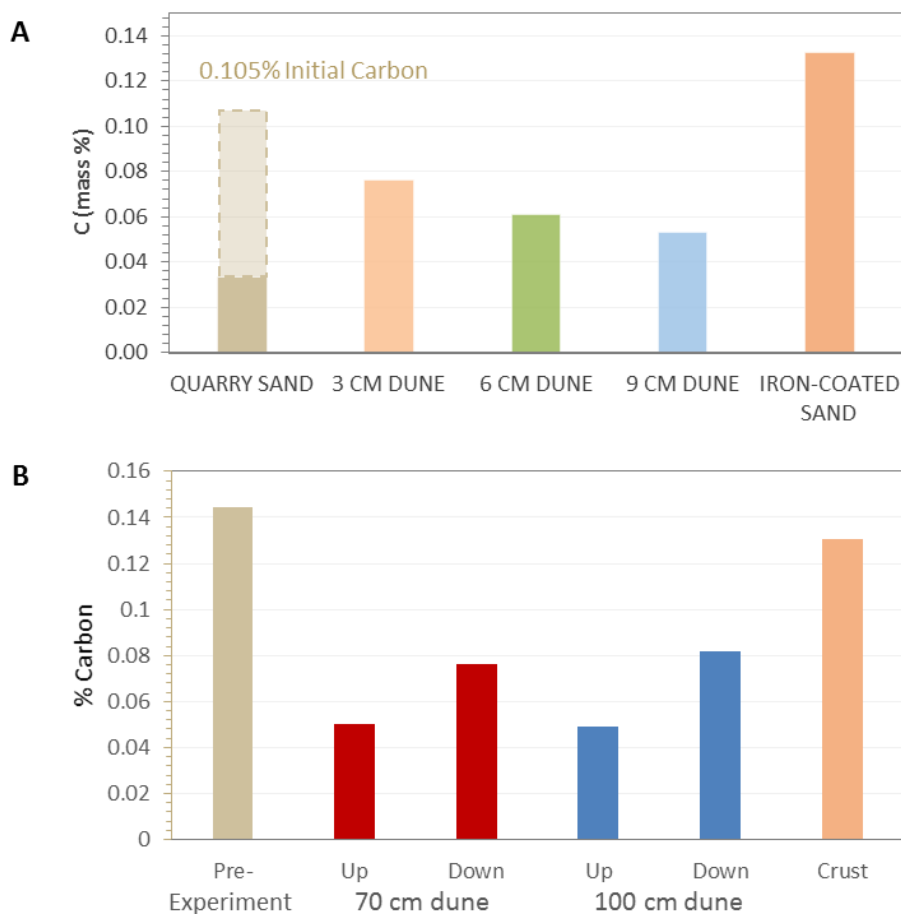
Figure C.35. Total carbon in the flume sand. Panel A shows the initial total carbon in the dune sand (estimated, see explanation above), and the total carbon in the 3 cm, 6 cm, and 9 cm dunes at the end of the F1 experiment. Panel B shows the measured total carbon before in the dune sand mixture before the experiment and the total carbon percentages in the 70 cm and 100 cm dunes at the end of the F2 experiments. Samples were collected upstream and downstream of the dune crests. For F2, the values shown are averages of the replicate channels. The crust of precipitate on the downstream face of the dunes was also analyzed at the end of both experiments.

C.6 MINTEQ Geochemical Modeling

In order to gain insight into the geochemical conditions along hyporheic flow paths, selected concentration data were entered into an equilibrium speciation model (Visual MINTEQ version 3.1). Rhizon locations were binned by residence time to estimate an "average" flow path through the hyporheic zone. The average species concentrations for each residence time bin were entered into MINTEQ. Saturation indices (SI) were determined with the fixed, measured pH. For F2, plots of SI versus residence time for a range of minerals are shown in Figures C.36-C.40. For F1, plots of SI versus residence time are shown in Figures C.41-C.44.
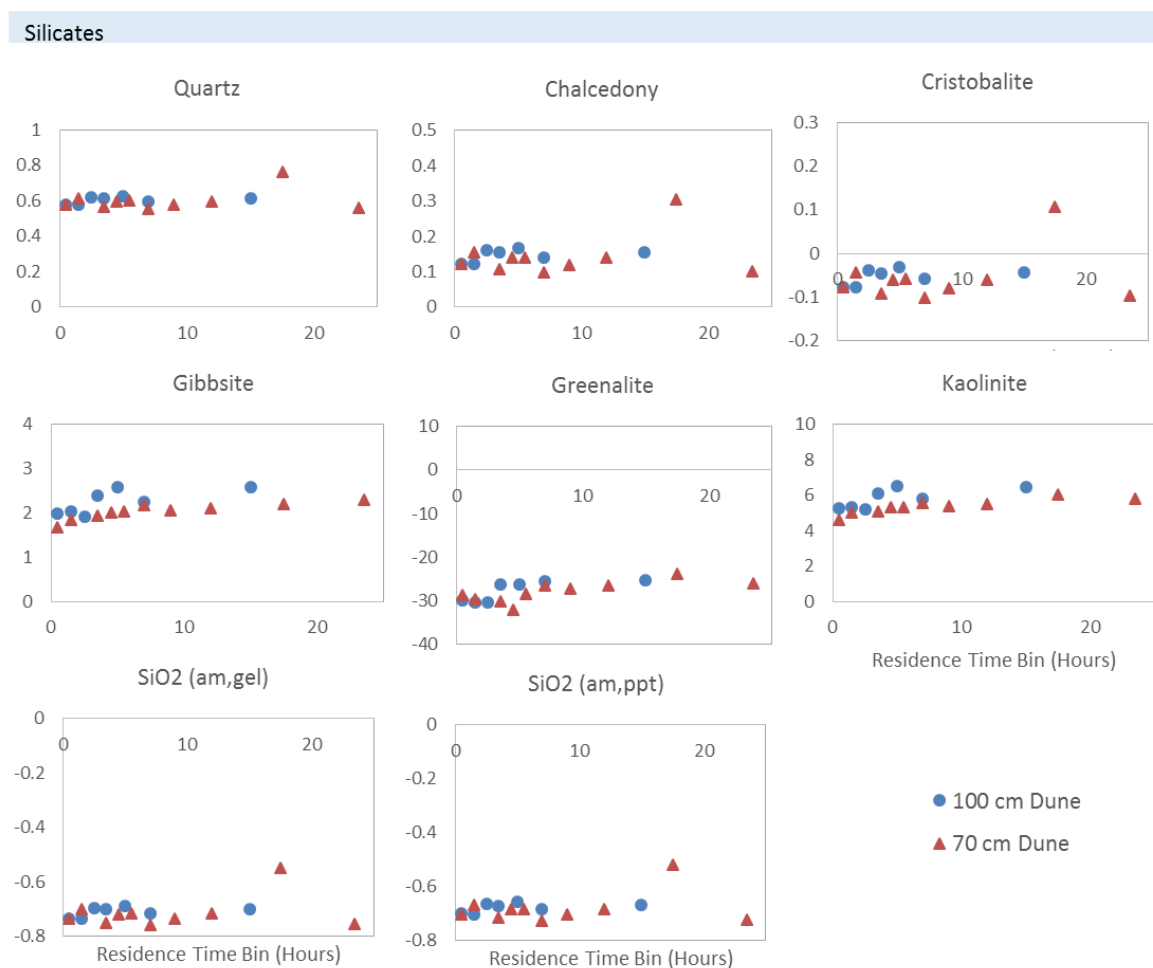
Figure C.36.   Saturation indices for F2, day 91 (silicates).
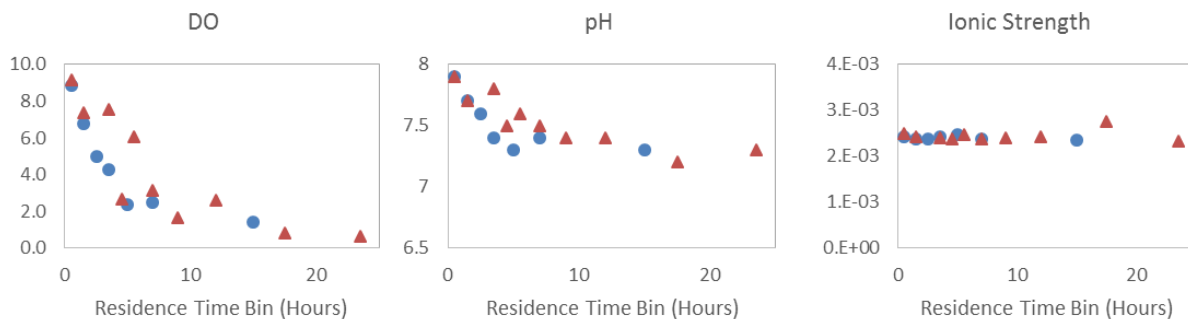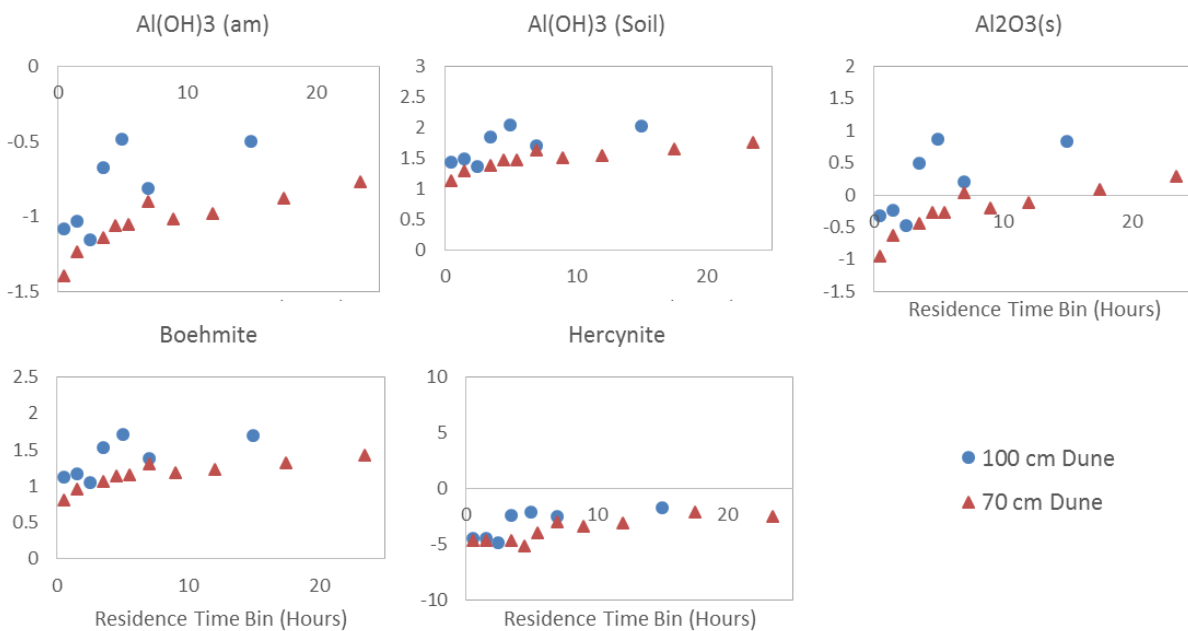
Figure C.37. Saturation indices for F2, day 91 (Al oxides and hydroxides, sulfates).
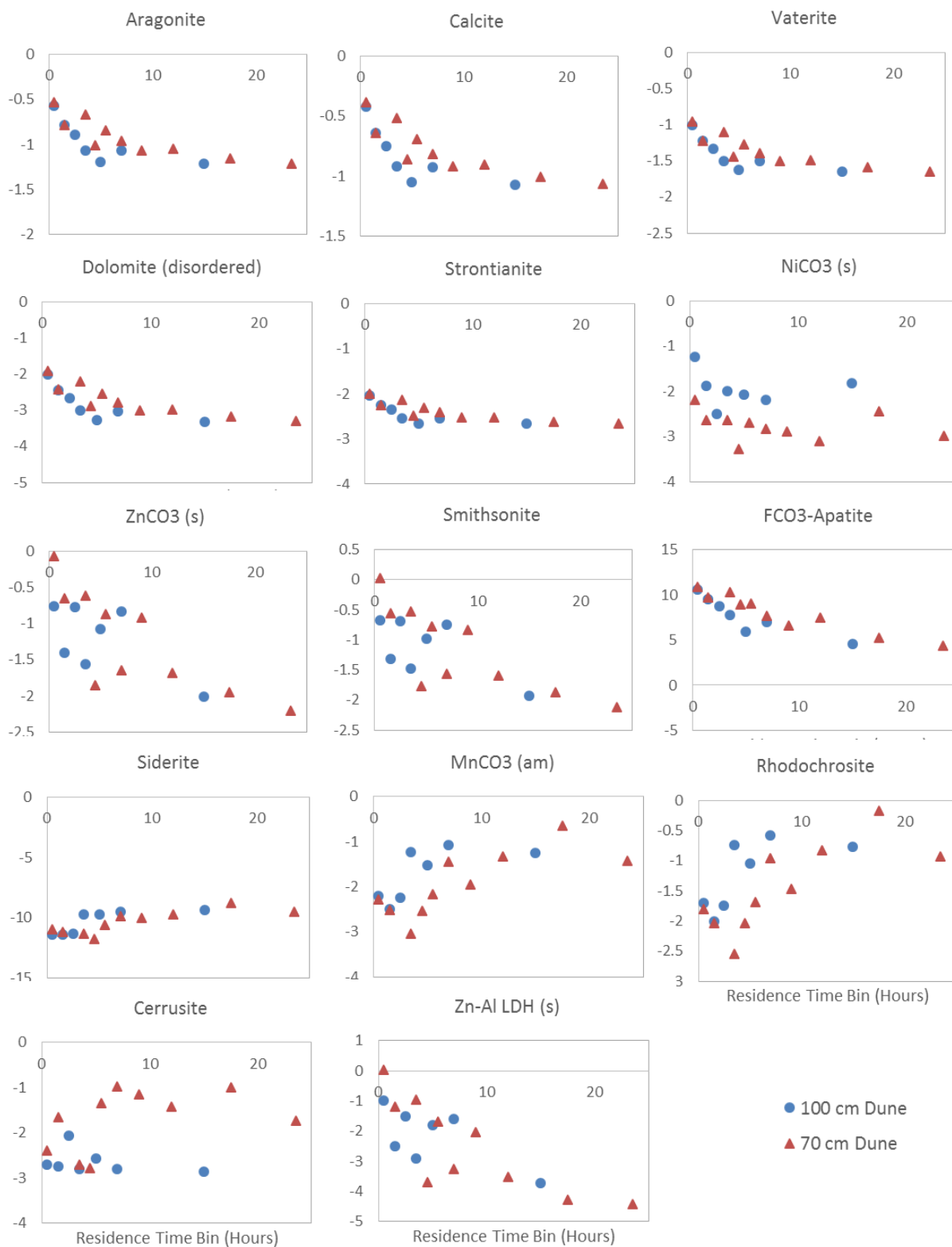
Figure C.38.   Saturation indices for F2, day 91 (carbonates).
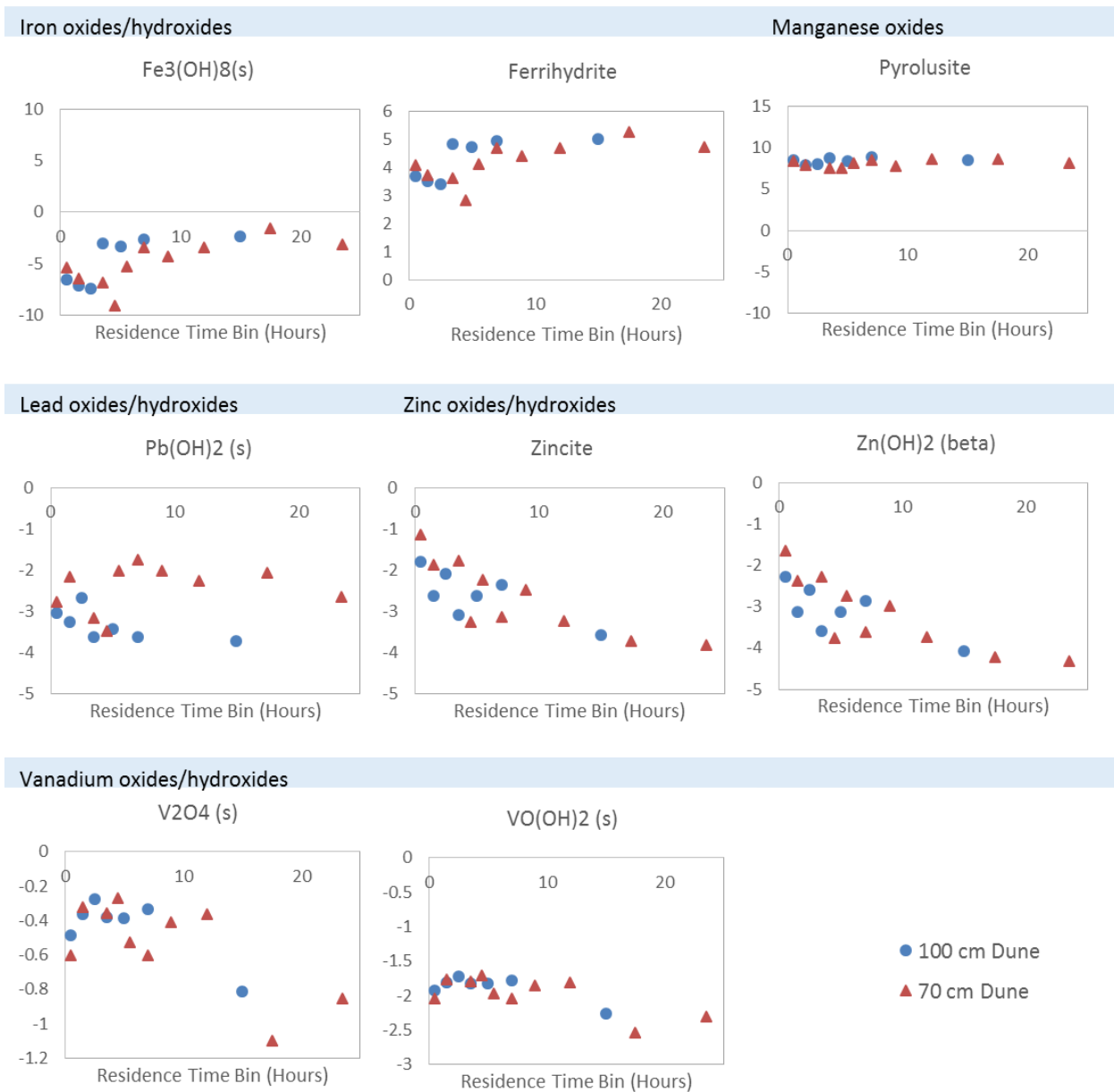
Figure C.39. Saturation indices for F2, day 91 (Iron oxides/hydroxides, manganese oxides, lead oxides/hydroxides, zinc oxides/hydroxides, vanadium oxides/hydroxides).
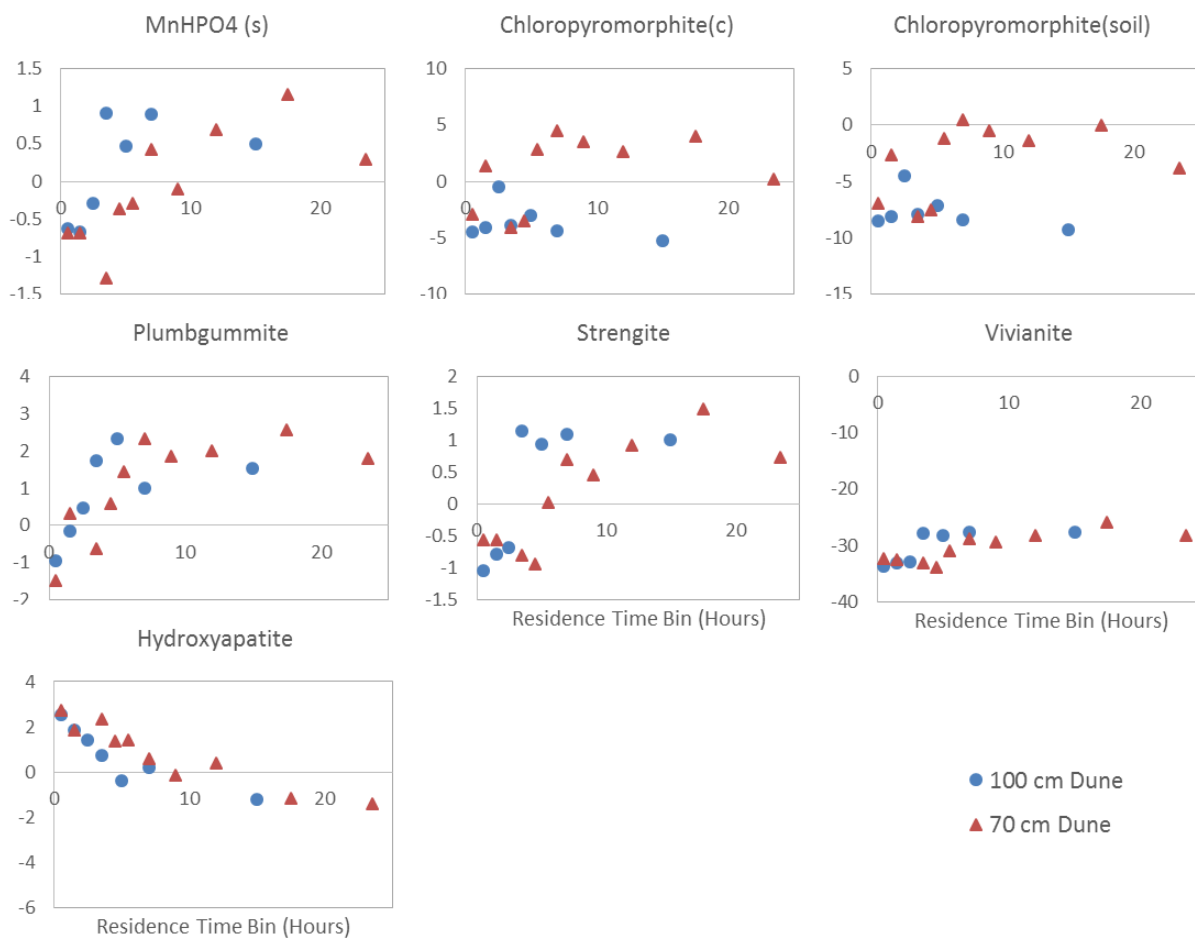
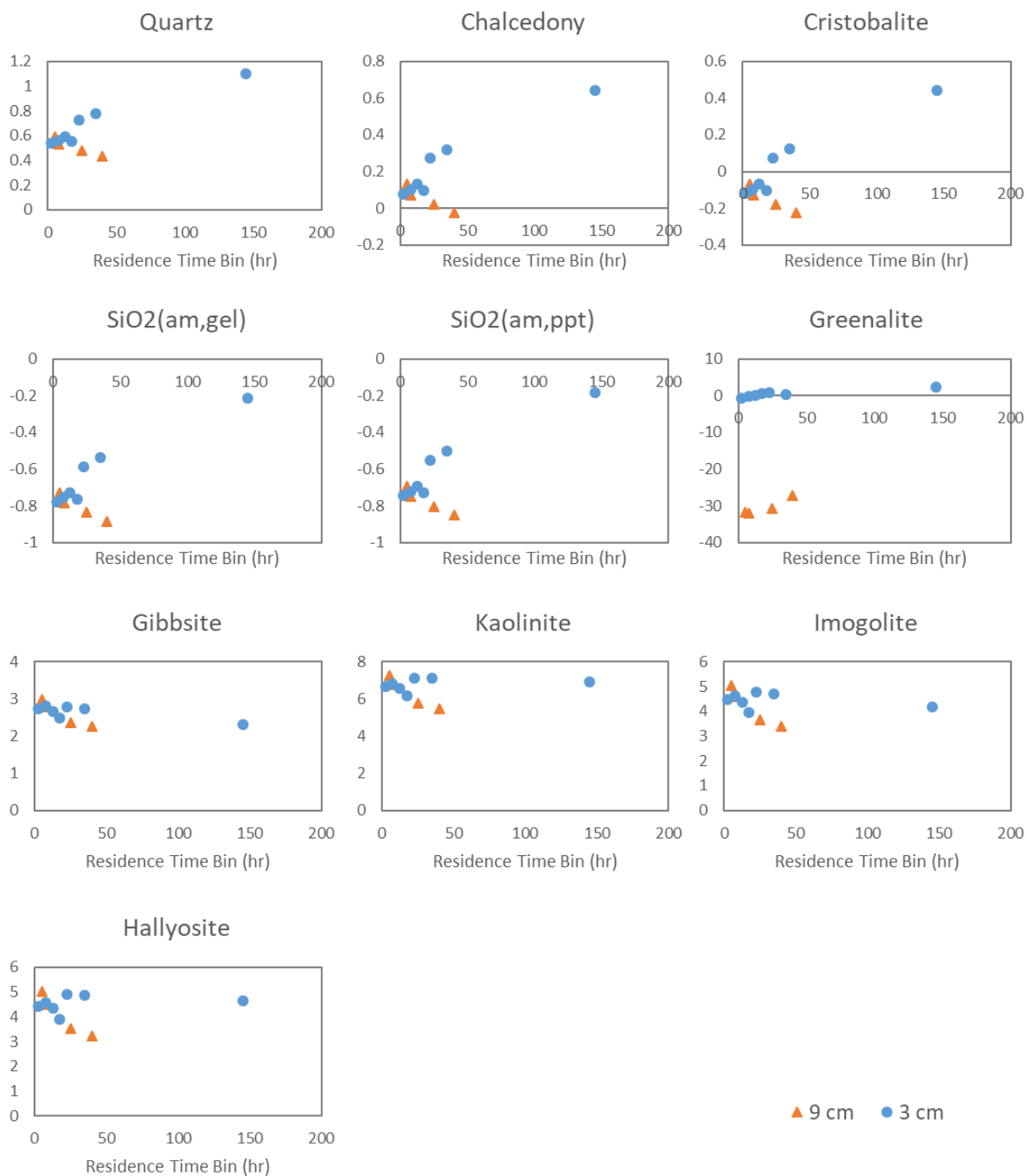**Figure C.40.   Saturation indices for F2, day 91 (phosphates).**

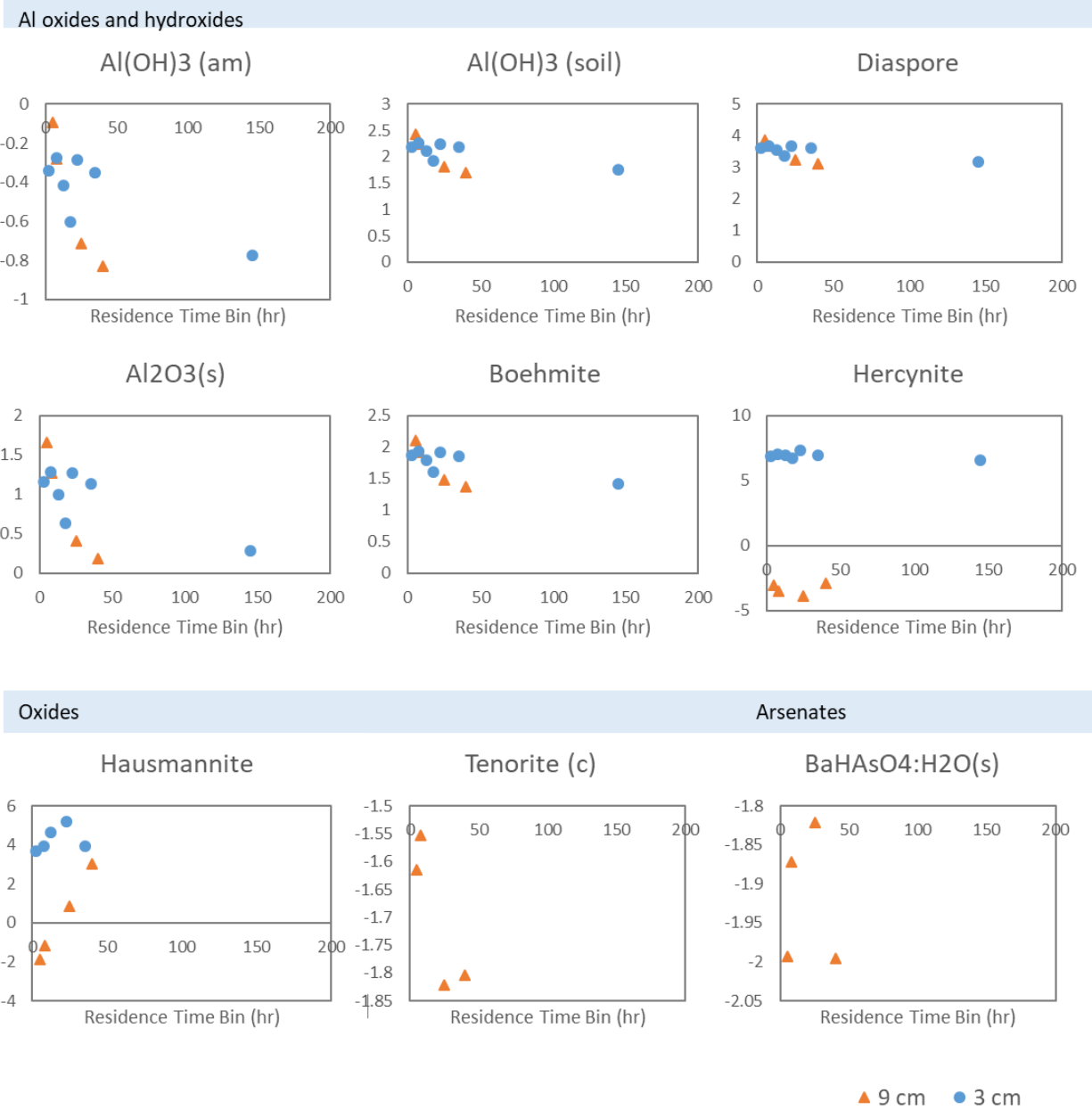**Figure C.41. Saturation indices for F1, day 112 (silicates).**

Figure C.42. Saturation indices for F1, day 112 (oxides and hydroxides).
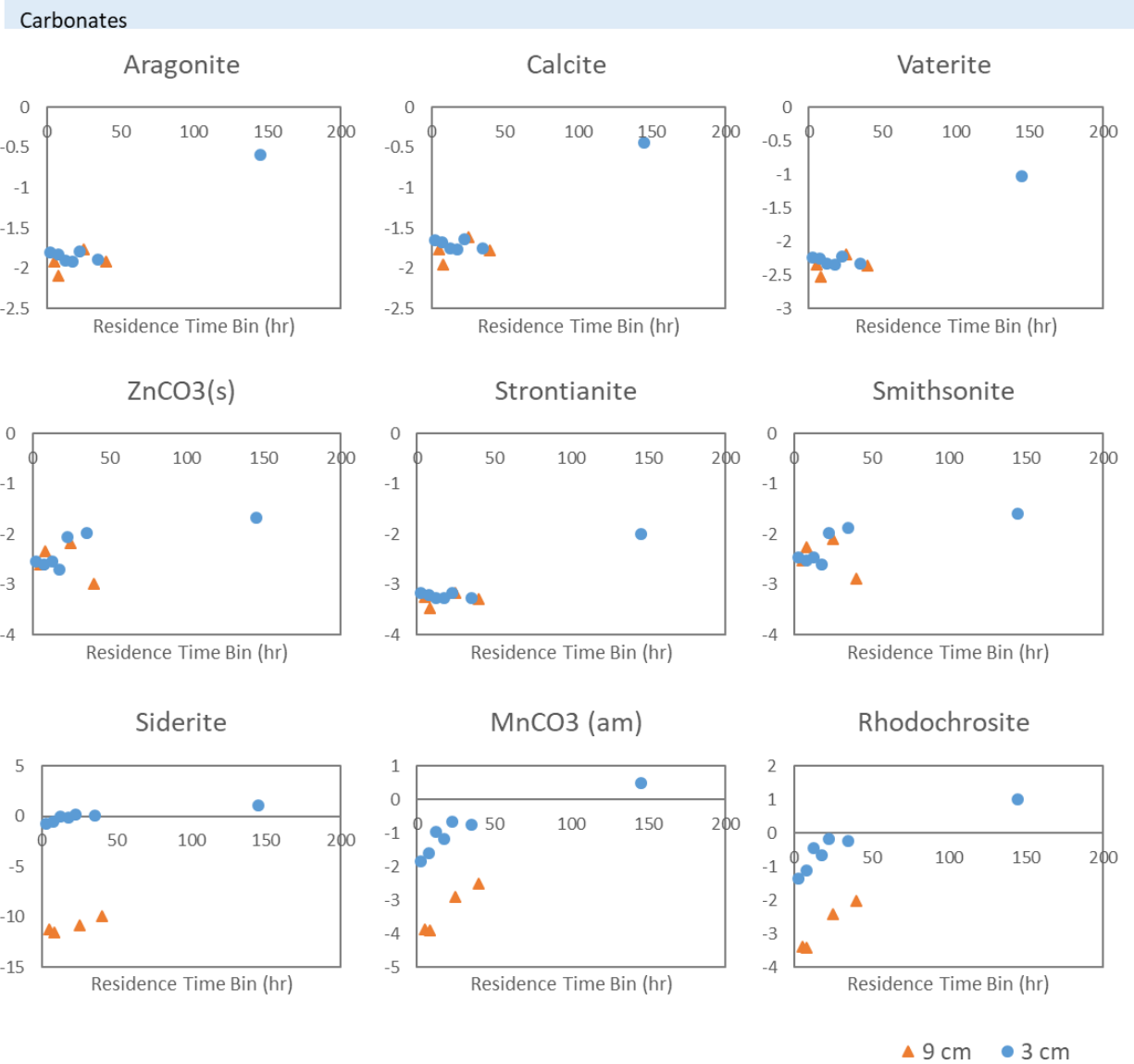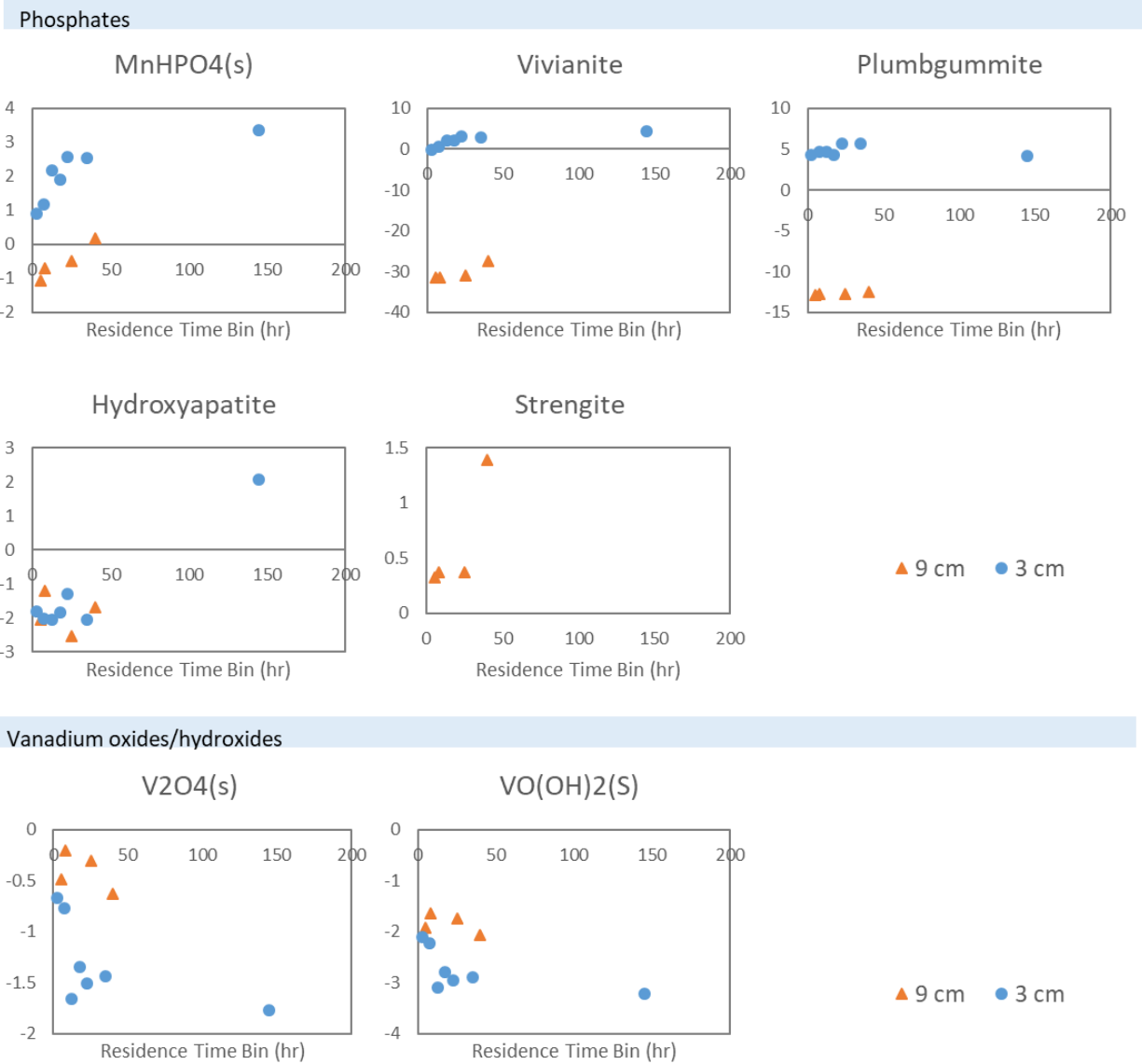
Figure C.43. **Saturation indices for F1, day 112 (carbonates).**

Figure C.44. Saturation indices for F1, day 112 (phosphates and vanadium oxides/hydroxides).

APPENDIX D

Permission letters and copyright permissions

Annika Quick
20 Oxford St.
Cambridge, MA 02478
(859) 321-9944

Shawn G. Benner, Ph.D.
1910 University Drive
Boise, ID 83725
(208) 850-9033

March 3, 2018

Dear Dr. Benner:

I am writing to request permission to use the article "Controls on nitrous oxide emissions from the hyporheic zone of streams," which was published in *Environmental Science and Technology*, volume 50, on October 3, 2016, for which you were a contributing author, in my dissertation.

I will include acknowledgements and/or appropriate citations to the work and copyright and reprint rights in the appendices. The bibliographic citation will appear in the References list at the end of the manuscript as typed below. Please advise me of any changes you require.

Please indicate your approval of this request by signing in the space provided, attaching any forms or instructions necessary to confirm permission. If you charge a reprint fee for use of you material, please indicate that as well. If you have questions, please call me at the number above.

Thank you for your cooperation,

Annika Quick

I hereby give permission to Annika Quick to reprint the following material in her dissertation.

Quick, A.M., Reeder, W.J., Farrell, T.B., Tonina, D., Feris, K.P., Benner, S.G., 2016.
Controls on nitrous oxide emissions from the hyporheic zones of streams. Environ.
Sci. Technol. 50, 11491–11500. doi:10.1021/acs.est.6b02680

Signed: _____

Date: 3/16/18

Annika Quick
20 Oxford St.
Cambridge, MA 02478
(859) 321-9944

Kevin Feris, Ph.D.
1910 University Drive
Boise, ID 83725
(208) 426-5498

March 3, 2018

Dear Dr. Feris:

I am writing to request permission to use the article "Controls on nitrous oxide emissions from the hyporheic zone of streams," which was published in *Environmental Science and Technology*, volume 50, on October 3, 2016, for which you were a contributing author, in my dissertation.

I will include acknowledgements and/or appropriate citations to the work and copyright and reprint rights in the appendices. The bibliographic citation will appear in the References list at the end of the manuscript as typed below. Please advise me of any changes you require.

Please indicate your approval of this request by signing in the space provided, attaching any forms or instructions necessary to confirm permission. If you charge a reprint fee for use of you material, please indicate that as well. If you have questions, please call me at the number above.

Thank you for your cooperation,

Annika Quick

I hereby give permission to Annika Quick to reprint the following material in her dissertation.

Quick, A.M., Reeder, W.J., Farrell, T.B., Tonina, D., Feris, K.P., Benner, S.G., 2016. Controls on nitrous oxide emissions from the hyporheic zones of streams. Environ. Sci. Technol. 50, 11491–11500. doi:10.1021/acs.est.6b02680

Signed: _____

Date: 3-6-18 _____

Annika Quick
20 Oxford St.
Cambridge, MA 02478
(859) 321-9944

William Jeffery Reeder, Ph.D.
322 E. Front St. Suite 340
Boise, ID 83702
(208) 841-1934

March 3, 2018

Dear Dr. Reeder:

I am writing to request permission to use the article "Controls on nitrous oxide emissions from the hyporheic zone of streams," which was published in *Environmental Science and Technology*, volume 50, on October 3, 2016, for which you were a contributing author, in my dissertation.

I will include acknowledgements and/or appropriate citations to the work and copyright and reprint rights in the appendices. The bibliographic citation will appear in the References list at the end of the manuscript as typed below. Please advise me of any changes you require.

Please indicate your approval of this request by signing in the space provided, attaching any forms or instructions necessary to confirm permission. If you charge a reprint fee for use of you material, please indicate that as well. If you have questions, please call me at the number above.
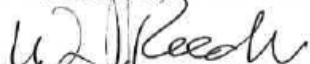
Thank you for your cooperation,

Annika Quick

I hereby give permission to Annika Quick to reprint the following material in her dissertation.

Quick, A.M., Reeder, W.J., Farrell, T.B., Tonina, D., Feris, K.P., Benner, S.G., 2016. Controls on nitrous oxide emissions from the hyporheic zones of streams. Environ. Sci. Technol. 50, 11491–11500. doi:10.1021/acs.est.6b02680

Signed: _____
Date: 3/12/2018

Annika Quick
20 Oxford St.
Cambridge, MA 02478
(859) 321-9944

Daniele Tonina, Ph.D.
322 E. Front St. Suite 340
Boise, ID 83702
(208) 364-6194

March 3, 2018

Dear Dr. Tonina:

I am writing to request permission to use the article "Controls on nitrous oxide emissions from the hyporheic zone of streams," which was published in *Environmental Science and Technology*, volume 50, on October 3, 2016, for which you were a contributing author, in my dissertation.

I will include acknowledgements and/or appropriate citations to the work and copyright and reprint rights in the appendices. The bibliographic citation will appear in the References list at the end of the manuscript as typed below. Please advise me of any changes you require.

Please indicate your approval of this request by signing in the space provided, attaching any forms or instructions necessary to confirm permission. If you charge a reprint fee for use of you material, please indicate that as well. If you have questions, please call me at the number above.

Thank you for your cooperation,

Annika Quick

I hereby give permission to Annika Quick to reprint the following material in her dissertation.

Quick, A.M., Reeder, W.J., Farrell, T.B., Tonina, D., Feris, K.P., Benner, S.G., 2016. Controls on nitrous oxide emissions from the hyporheic zones of streams. Environ. Sci. Technol. 50, 11491–11500. doi:10.1021/acs.est.6b02680

Signed: _____

Date: 03/05/2018

Annika Quick
20 Oxford St.
Cambridge, MA 02478
(859) 321-9944

Tiffany Farrell
1910 University Drive
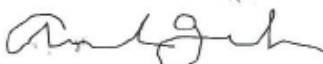Boise, ID 83725
(361) 774-6402

March 3, 2018

Dear Tiffany:

I am writing to request permission to use the article "Controls on nitrous oxide emissions from the hyporheic zone of streams," which was published in *Environmental Science and Technology*, volume 50, on October 3, 2016, for which you were a contributing author, in my dissertation.

I will include acknowledgements and/or appropriate citations to the work and copyright and reprint rights in the appendices. The bibliographic citation will appear in the References list at the end of the manuscript as typed below. Please advise me of any changes you require.

Please indicate your approval of this request by signing in the space provided, attaching any forms or instructions necessary to confirm permission. If you charge a reprint fee for use of you material, please indicate that as well. If you have questions, please call me at the number above.
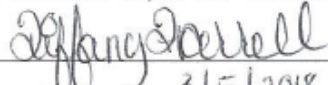
Thank you for your cooperation,

Annika Quick

I hereby give permission to Annika Quick to reprint the following material in her dissertation.

Quick, A.M., Reeder, W.J., Farrell, T.B., Tonina, D., Feris, K.P., Benner, S.G., 2016. Controls on nitrous oxide emissions from the hyporheic zones of streams. Environ. Sci. Technol. 50, 11491–11500. doi:10.1021/acs.est.6b02680

Signed: _Tiffany Farrell_

Date: _3 | 5 | 2018_

Rightslink® by Copyright Clearance Center

Copyright Clearance Center

RightsLink®

Home | Create Account | Help | ✉

ACS Publications
Most Trusted. Most Cited. Most Read.

Title:	Controls on Nitrous Oxide Emissions from the Hyporheic Zones of Streams
Author:	Annika M. Quick, W. Jeffery Reeder, Tiffany B. Farrell, et al
Publication:	Environmental Science & Technology
Publisher:	American Chemical Society
Date:	Nov 1, 2016

Copyright © 2016, American Chemical Society

PERMISSION/LICENSE IS GRANTED FOR YOUR ORDER AT NO CHARGE

This type of permission/license, instead of the standard Terms & Conditions, is sent to you because no fee is being charged for your order. Please note the following:

- Permission is granted for your request in both print and electronic formats, and translations.
- If figures and/or tables were requested, they may be adapted or used in part.
- Please print this page for your records and send a copy of it to your publisher/graduate school.
- Appropriate credit for the requested material should be given as follows: "Reprinted (adapted) with permission from (COMPLETE REFERENCE CITATION). Copyright (YEAR) American Chemical Society." Insert appropriate information in place of the capitalized words.
- One-time permission is granted only for the use specified in your request. No additional uses are granted (such as derivative works or other editions). For any other uses, please submit a new request.

BACK | CLOSE WINDOW